16 March 2007 | S10

Science

POLAR SCIENCE

AAAS

Dare to be Different

We customize your oligo plate orders

without sacrificing your patience *or* your piggy bank.

Your research is unique and now your plate orders can be as well:

- **Select yield, concentration or volume**
- **Select from a variety of plate types**
- **Choose from columns, rows or custom-defined loading schemes**
- **Benefit from a consistent turnaround time for all orders.**
- **Receive documentation of scheduled shipments for large volume orders.**

All the choices you need with the confidence of industry-leading quality.
Go to www.idtdna.com for more information and to place your order.

IDT®
INTEGRATED DNA TECHNOLOGIES, INC.

Innovation and Precision in Nucleic Acid Synthesis

www.idtdna.com **800.328.2661**

BSI REGISTERED
ISO 9001:2000
FM88954

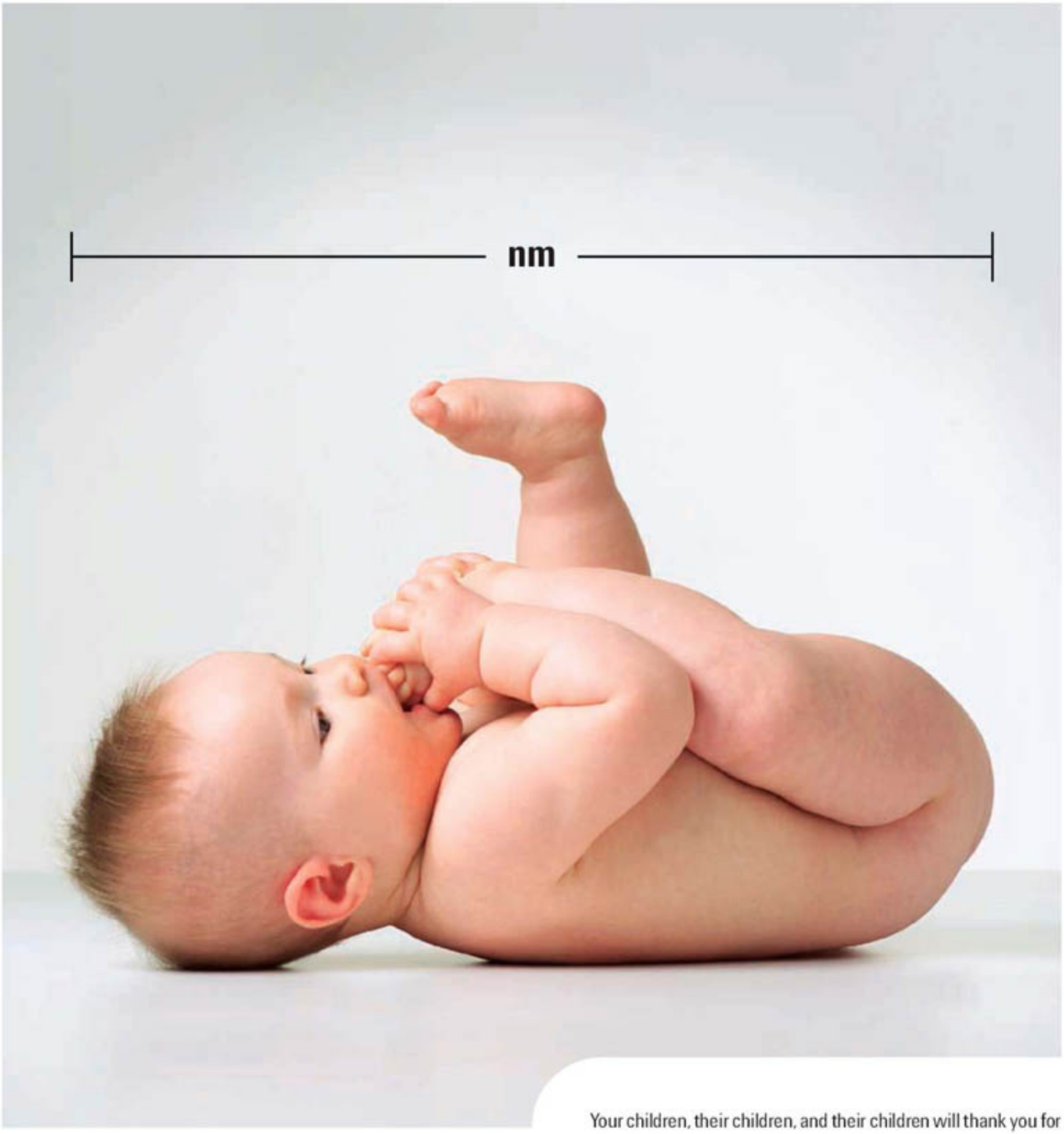

Your children, their children, and their children will thank you for the work you do in nanotechnology today. Agilent instruments for electronics, bioanalysis, chemical analysis, and microscopy make it possible for you to explore, be novel, and be first.

www.agilent.com/find/nanotechnology

Agilent Technologies

GE Healthcare

Bringing protein analysis to life with Ettan DIGE and Amersham ECL

When it comes to life sciences, GE Healthcare is setting the standard. Tens of thousands of scientists worldwide rely on our products and proven expertise in protein analysis and detection every day. But we're never content to stand still. We're constantly striving for innovations that boost accuracy and deliver quantitative data.

The result is new fluorescence platforms like the Ettan™ DIGE Imager and Amersham ECL Plex™ for quantitative protein analysis.

By continually developing technology that can turn your scientific ideas into reality, we're bringing science to life and helping to transform drug discovery and healthcare.

We call it Protein Analysis Re-imagined.

Discover the full power of Ettan DIGE and the Amersham ECL™ family of Western blotting systems.

www.gehealthcare.com/protein_analysis

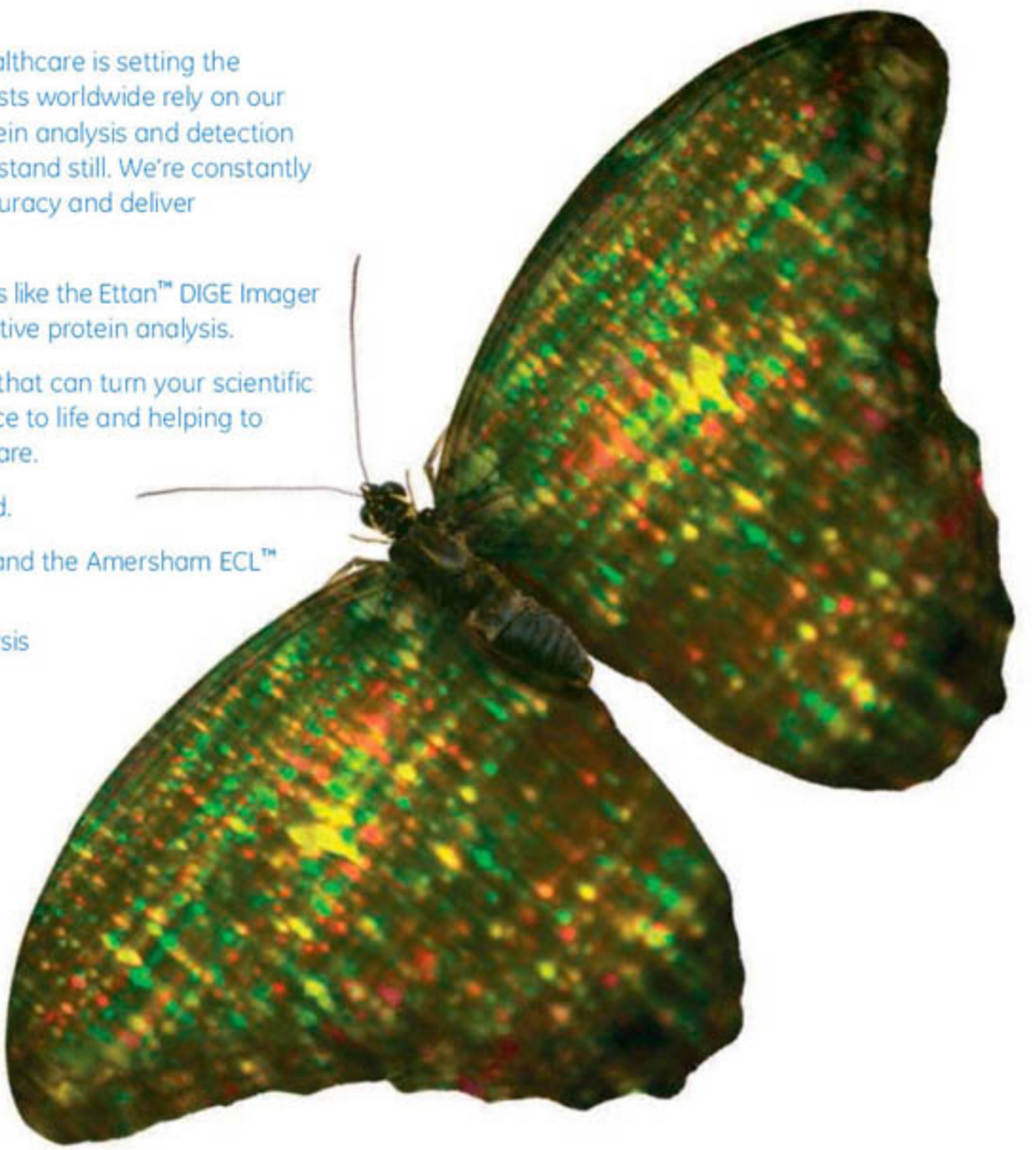

imagination at work

GE Healthcare Bio-Sciences AB, a General Electric Company.
Björkgatan 30, 751 84 Uppsala, Sweden.

GE08-06

Volume 315, Issue 5818

COVER

Sunset along the Graham Coast of the Antarctic Peninsula. In both the Arctic and Antarctica, melting ice and disrupted ecosystems have sounded the alarm on global warming. These regions also offer exciting research opportunities. To ring in the International Polar Year, a special section beginning on page 1513 explores the many dimensions of polar science.

Photo: Kim Heacox/Peter Arnold Inc.

DEPARTMENTS

EDITORIAL

SPECIAL SECTION

Polar Science

INTRODUCTION

NEWS

REVIEWS

>> Editorial p. 1465; Perspectives pp. 1503 and 1508; Research Article p. 1544; Report p. 1559
For related online content, see page 1459 or go to www.sciencemag.org/sciext/polarscience/

1514

1482

NEWS OF THE WEEK

NEWS FOCUS

CONTENTS continued >>

QIAcube — pure efficiency

New

- Free up your time with automated sample preparation
- Continue to use proven QIAGEN spin-column kits
- Purify DNA, RNA, or proteins from up to 12 samples per run
- Standardize your results
- Increase your productivity

Contact QIAGEN today or visit www.qiagen.com/MyQIAcube .

QIAGEN®

Sample & Assay Technologies

Science

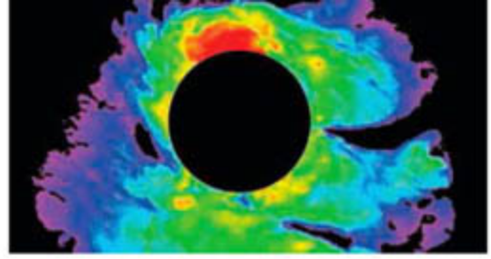

SCIENCE EXPRESS

www.sciencexpress.org

IMMUNOLOGY

Promotion of Lymphocyte Egress into Blood and Lymph by Distinct Sources of Sphingosine-1-Phosphate
R. Pappu et al.
Immune cells move into the bloodstream in response to a lipid signal made in red blood cells and move into the lymphatic system when the same signal is made elsewhere.
10.1126/science.1139221

GENETICS

Strong Association of De Novo Copy Number Mutations with Autism
J. Sebat et al.
Individuals with autism are more likely to show variations in the number of copies of certain genomic regions than are their unaffected relatives.
10.1126/science.1138659

PLANETARY SCIENCE

Subsurface Radar Sounding of the South Polar Layered Deposits of Mars
J. J. Plaut et al.
Radar mapping of layered deposits at Mars' south pole shows that they are pure water ice, sitting on cratered terrain, with a volume equivalent to a global water layer 11 meters thick.
10.1126/science.1139672

ASTROPHYSICS

Early Optical Polarization of a Gamma-Ray Burst Afterglow
C. G. Mundell et al.
Light emitted within a few minutes of a gamma-ray burst is not strongly polarized, implying that an aligned magnetic field near the dying source star is not driving the burst.
10.1126/science.1138484

LETTERS

BOOKS *ET AL.*

POLICY FORUM

PERSPECTIVES

TECHNICAL COMMENT ABSTRACTS

GENETICS

BREVIA

CLIMATE CHANGE

RESEARCH ARTICLES

CLIMATE CHANGE

STRUCTURAL BIOLOGY

CONTENTS continued >>

“Combining live imaging with high resolution electron microscopy is a real challenge.”

“With the introduction of Green Fluorescent Protein (GFP) technology, cell biology and life sciences in general have entered a whole new exciting era of research. [...] In some instances however, the resolution of the light microscope is the limiting factor in answering our scientific questions. In these cases, the higher resolution of the electron microscope is essential. Combining both light and electron microscopy is my field of interest. By performing so-called Correlative Light Electron Microscopy (CLEM) experiments one has the advantage of live cell imaging in the confocal microscope and afterwards have high resolution results from the transmission electron microscope of the same cell. The Leica EM RTS was specifically developed to be used in such experiments in conjunction with EM PACT2. It provides a high time resolution between the light and electron microscope, allowing excellent preservation of the ultrastructure close to the natural state, an essential prerequisite for electron microscopy. It allows us to decide upon the exact moment of interest and study that particular event at high resolution.”

Dr. Paul Verkade, Max Planck Institute for Molecular Cell Biology and Genetics, Dresden, Germany
Dr. Verkade works with the Leica EM PACT2 & RTS High Pressure Freezer.

www.leica-microsystems.com

Leica
MICROSYSTEMS

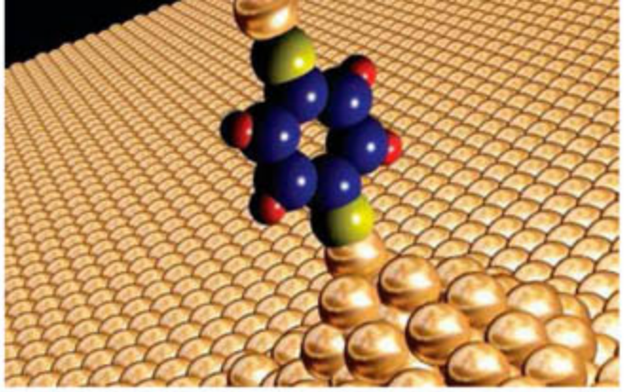

1568

REPORTS

1574

AAAS

ADVANCING SCIENCE, SERVING SOCIETY

SCIENCE (ISSN 0036-8075) is published weekly on Friday, except the last week in December, by the American Association for the Advancement of Science, 1200 New York Avenue, NW, Washington, DC 20005. Periodicals Mail postage (publication No. 484460) paid at Washington, DC, and additional mailing offices.

Domestic individual membership and subscription (51 issues): $142 ($74 allocated to subscription). Domestic institutional subscription (51 issues): $710; Foreign postage extra: Mexico, Caribbean (surface mail) $55; other countries (air assist delivery) $85. First class, airmail, student, and emeritus rates on request. Canadian rates with GST available upon request, GST #1254 88122. Publications Mail Agreement Number 1069624. **Printed in the U.S.A.**

Change of address: Allow 4 weeks, giving old and new addresses and 8-digit account number. **Postmaster:** Send change of address to AAAS, P.O. Box 96178, Washington, DC 20090–6178. **Single-copy sales:** $10.00 current issue, $15.00 back issue prepaid includes surface postage; bulk rates on request.

CONTENTS continued >>

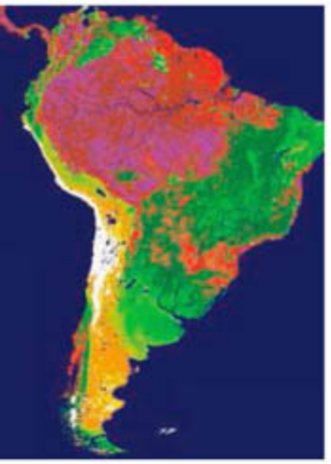

Time of the season.

SCIENCE**NOW**

www.sciencenow.org DAILY NEWS COVERAGE

Turn, Turn: The Amazon Gets Seasons
Changes in leaf cover reveal rainforest not so monotonous.

I Don't Want to Grow Up
Modern humans have always developed slowly.

A Lag Before Dying
Massive extinctions may take longer than previously believed.

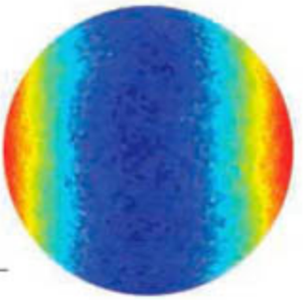

Simulation of lipid accumulation.

SCIENCE'S **STKE**

www.stke.org SIGNAL TRANSDUCTION KNOWLEDGE ENVIRONMENT

PROTOCOL: A Simulation Environment for Directional Sensing as a Phase Separation Process
A. de Candia et al.
DirSens software allows you to explore how polarization in membrane lipids occurs in response to chemotactic stimuli.

FORUM: Can Mesoscopic Models Test Spatial Mechanisms of Cell Signaling?
J. Shillcock
Share your thoughts on the feasibility of constructing spatiotemporal models of a signaling network on micrometer-length and millisecond time scales.

CREDIT (SCIENCE NOW): BOSTON UNIVERSITY; NASA

Careers in the cold.

SCIENCE **CAREERS**

www.sciencecareers.org CAREER RESOURCES FOR SCIENTISTS

GLOBAL: Special Feature—Research at the Poles
A. Fazekas
In time for the International Polar Year, Science Careers focuses on scientists doing polar research.

US: Cruising Frozen Seas
A. Fazekas
Biological oceanographers share their experiences doing science on Antarctic seas.

EUROPE: Polar Research in Portugal—Breaking the Ice
E. Pain
Physical geographer Gonçalo Vieira gets warm, sunny Portugal involved in the International Polar Year.
>> Polar Science special section p. 1513

US: Employment Due Diligence, Part 2
D. Jensen
After getting a job offer, it is tempting to just say "yes," but that can have serious risks.

SCIENCE**PODCAST**

Listen to the 16 March *Science* Podcast to hear about new insights into HIV evolution, developments in the field of polar science, attention in fruit flies, and more.
www.sciencemag.org/about/podcast.dtl

Separate individual or institutional subscriptions to these products may be required for full-text access.

EDITED BY STELLA HURTLEY AND PHIL SZUROMI

<< From Ecology to Evolution

Although the time scales of ecological and evolutionary processes can be quite different, the opportunities for the interplay of the two are increasingly evident. **Pelletier *et al.*** (p. 1571) show how the feedback between ecological variation and evolutionary change can be estimated using individual contributions to population growth. In a long-term detailed study of a population of Soay sheep living on the remote Scottish island of St. Kilda, variation in size-related traits of individual animals influenced population growth and fluctuates with the environment. It was also possible to estimate the contribution of additive genetic variation to population growth, which provides a measure of how evolutionary processes influence ecological change. Finally, an assessment could be made of how ecological variation influences selection pressures.

Insights into Ice Stream Discharge

How quickly sea level will rise as climate warms depends mainly on how much the ocean expands from warming, how fast the polar ice sheets melt, and how fast the ice sheets discharge frozen ice into the ocean. This third process is by far the most poorly constrained, but in recent years large and rapid increases have occurred in the discharge rates of some of these outlet glaciers—as much as doubling in less than 1 year (see the Perspectives by **Vaughan and Arthern** and by **Truffer and Fahnestock**). **Fricker *et al.*** (p. 1544, published online 15 February) analyzed ice-surface elevations obtained from satellite laser altimetry in the vicinity of two important Antarctic ice streams and found rapid, local changes in the height of the ice on annual time scales. They interpret these results as the signatures of subglacial water movement between lakes at the base of the ice sheet. **Howat *et al.*** (p. 1559, published online 8 February) show that glacial discharge from ice streams in Greenland can decrease as suddenly as it can increase. Their findings illustrate the difficulty of extrapolating short-term trends in ice mass balance to longer intervals.

Resonantly Depinning Domain Walls

In conventional magnetic-storage media, changes in magnetization of localized regions are produced with a magnetized head. In efforts to decrease the bit size, reduce power consumption, and develop new active magnetoelectronic technology, the possibility of using electrical pulses to directly manipulate magnetization is being explored. The injection of a sufficiently large current pulse through a domain wall (which separates regions of different polarity) is known to cause domain walls to move. **Thomas *et al.*** (p. 1553) now show that a train of well-timed current pulses can also depin the domain wall, but at much lower pulse amplitudes. The subthreshold depinning, which is explained in terms of a resonant amplification of the domain-wall motion within its confining potential, could have implications in addressing magnetoelectronic devices.

Energy Management

Chemical reactions are often modeled with reference to an energy landscape comprised of activation barriers and potential wells and, in general, any excess energy in the system is expected to spread evenly across this landscape like an overflowing stream. **Kim *et al.*** (p. 1561) observe a surprising exception to this trend. Through a combination of theory and experiments, they find that two conformations of the propanal cation, separated by ~1 kilocalorie per mole, dissociate to form very different product distributions upon absorption of light energy ~100 times greater than for the small barrier to their interconversion. The calculations suggest that molecular rearrangements in the excited electronic state funnel each distinctly configured structure toward an isolated portion of the ground state surface, after which dissociation outpaces conformational equilibration.

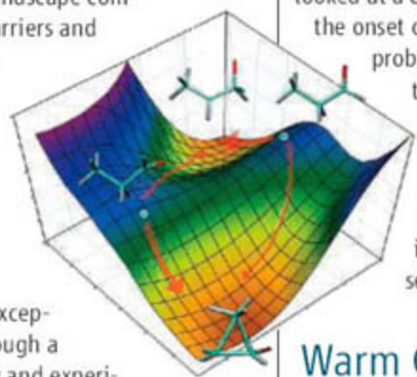

Following Fluctuations

Near a second-order, or continuous, phase transition, fluctuations of the order parameter (such as for magnetization or superfluidity) completely govern the behavior of the system on all length scales and exhibit a universal scaling behavior that can be characterized by critical exponents. However, probing the actual phase transition at the critical region itself and extracting these critical exponents has proven experimentally challenging. **Donner *et al.*** (p. 1556; see the Perspective by **Altman**) looked at a cloud of cold atoms (bosons) near the onset of Bose-Einstein condensation and probed the spatial correlations between the atoms as the temperature was varied around the critical point. As these results can carry over to a multitude of other systems, they should provide an important testing ground for the general theory of second-order phase transitions.

Warm Currents

Most studies of electron transport through molecules have focused on currents generated by applied voltages, but many details about the electronic structure of molecular junctions can be gleaned from measuring voltage changes

Continued on page 1463

CREDITS (TOP TO BOTTOM): OWEN R. JONES; KIM *ET AL.*

www.roche-applied-science.com

Introducing Our Second Generation Genome Sequencing System

Genome Sequencer FLX

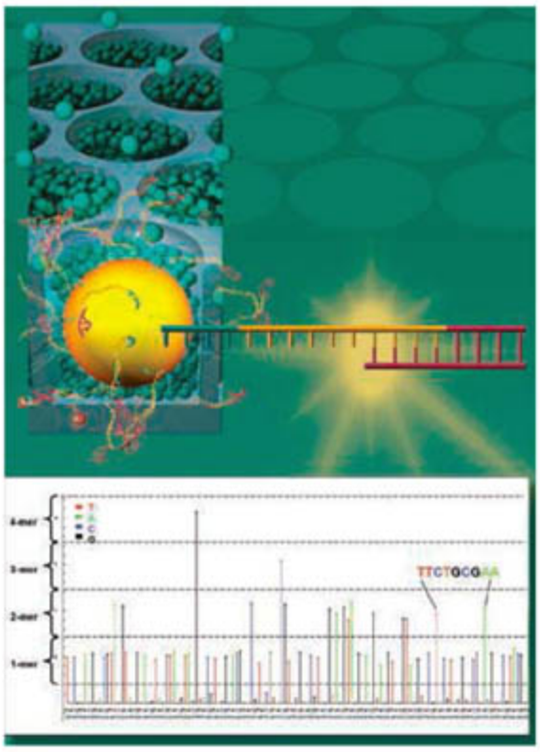

Be First to the Finish with...

- Increased read lengths averaging 200 to 300 bases per read
- Throughput of more than 400,000 reads per run
- High single-read accuracy greater than 99.5% over 200 bases
- Consensus-read accuracy greater than 99.99%

...more Flexibility and more Applications.

Visit ***www.genome-sequencing.com*** to learn about the expanding number of peer-reviewed publications appearing weekly.

454 LIFE SCIENCES

Roche Diagnostics

Roche Diagnostics GmbH
Roche Applied Science
68298 Mannheim
Germany

Continued from page 1461

when there is a temperature differential between the two electrodes. For example, the sign of the corresponding Seebeck coefficient *S* will reflect the position of the Fermi levels relative to the highest occupied and lowest unoccupied orbitals of the molecules. **Reddy *et al.*** (p. 1568, published online 15 February) measured *S* values for several conjugated organic dithiols on gold surfaces. The molecules were in contact with a gold scanning tunneling microscope tip that was kept at constant temperature; the substrate was then heated. The positive sign of *S* indicates that these molecules are hole conductors.

New Look at an Old Problem

A ribozyme that can catalyze RNA assembly is central to the RNA-world hypothesis. No known existing ribozyme catalyzes the required template-dependent 5′ to 3′ phosphodiester bond ligation, but proof of principle has been provided by laboratory-created nucleotide triphosphate ribozymes. **Robertson and Scott** (p. 1549; see the Perspective by **Joyce**) have determined the structure of such a ligase ribozyme at 2.6 angstrom resolution. The structure of the active site suggests that the ligase ribozyme uses strategies of transition-state stabilization and acid-base catalysis well known in natural ribozymes and protein enzymes.

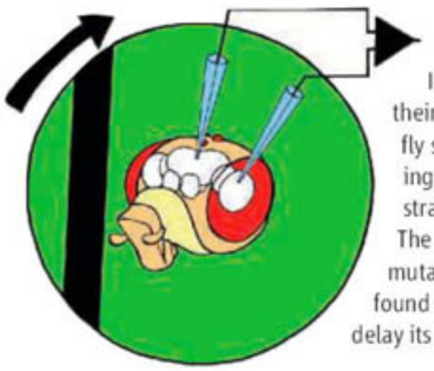

CREDIT: BRUNO VAN SWINDEREN

Attention in Fruit Flies

Insect brains compare favorably with vertebrate brains in their levels of sophistication. However, can insects like the fruit fly show selective attention? Using local field potential recordings during visual fixation, **van Swinderen** (p. 1590) demonstrated attention-like processes in *Drosophila* brain activity. The author also examined the effect of the short-term learning mutants *dunce* and *rutabaga* on novelty-evoked responses and found that these mutations attenuate selective attention and delay its onset.

Not-So-Hot Tropical Diversification

What causes the latitudinal gradient in species diversity, with greater species richness in the tropics? **Weir and Schluter** (p. 1574) present data and simulations that together point to high speciation rates, not in the tropics as often assumed, but rather at temperate latitudes and low extinction rates in the tropics. This finding contradicts the hypothesis that the tropics have an elevated speciation rate relative to the temperate zones, as previously suggested.

From MicroRNA to Carcinogenesis

Misregulation of microRNA (miRNA) function has been implicated in cancer. However, the precise role of miRNAs in tumorigenesis has been unclear. High Mobility Group A2 protein (Hmga2) is a small, nonhistone, chromatin-associated protein found in a number of benign and malignant tumors, where the gene is often truncated at the 3′ end. **Mayr *et al.*** (p. 1576, published online 22 February) now show that it is the loss of the noncoding 3′ untranslated region of the Hmga2 messenger RNA, and specifically regulator sites for the let-7 miRNA, which cause the overexpression of Hmga2, and that this overexpression contributes to the progression of carcinogenesis both in a tissue culture assay and in nude mice.

HIV Evolution: Host or Virus?

During infection, the human immunodeficiency virus (HIV) is under pressure to mutate in order to escape immune detection. A population-level study has suggested that polymorphisms in genes that encode the major histocompatibility complex (MHC) proteins responsible for presenting viral antigens to cytotoxic T cells have a strong influence on how the virus evolves. However, **Bhattacharya *et al.*** (p. 1583; see the Perspective by **Klenerman and McMichael**) now present an analysis that takes into account other confounding effects of viral phylogeny and reveals that the majority of such associations result from effects of viral lineages, rather than immune escape. Although MHC polymorphism is still likely to have some influence on viral evolution, this effect could be significantly less than previously suggested.

ISI Web of Knowledge℠

You should be in control of your research experience…
sounds ideal, but what does it mean? With *ISI Web of Knowledge*,
it means options. Options that let you personalize your search …
cross search as wide or as targeted a selection of content as you wish …
and analyze your search results.

What research options do you require? It's up to you —
take control of your research with *ISI Web of Knowledge*.

THE POWER OF TEN
10 YEARS OF WEB OF SCIENCE®
100 YEARS OF DISCOVERY

Take the next step
isiwebofknowledge.com

THOMSON

Alan I. Leshner is chief executive officer of AAAS and executive publisher of *Science*.

Celebrating Polar Science

AS WE ENTER THE FOURTH INTERNATIONAL POLAR YEAR (IPY), WE HONOR THE FACT THAT although the poles are among the most desolate places on Earth, they are also among the most scientifically rich and important to the future of the planet. The first of these "geophysical years" was 1882–1883; the most recent was 1957–1958. By now, most people know that the poles are ideal places to study the effects of global climate change. Indeed, some have called polar glaciers and ice sheets the "canaries in the mine" of climate change.

Because the impacts of climate change are disproportionately felt at high latitudes, polar ecosystems will continue to bear careful watching. Cores through the polar ice shelves into the underwater sediment provide a record of Earth's biological and geological history over millions of years. The Arctic has also given us a history of human settlement and associated climate records that span thousands of years and offer an outstanding base for integrated research on global systems and human adaptation. The poles are also home to some of the most unusual species, living successfully in incredibly cold and dark water hundreds of meters under the ice.

The air is so pristine that scientists at the Amundsen-Scott South Pole Station, poised atop a constantly shifting ice sheet several miles thick, give out little vials labeled "cleanest air on earth." That air provides a matchless environment in which cosmologists and astronomers can study the origins and evolution of the universe. Their work will be accelerated by a brand-new 10-meter telescope, transported to the South Pole in sections on turboprop freight planes and assembled outside at –60°C. Work also continues on the world's largest neutrino detector, called IceCube, which after 6 years of work will occupy a cubic kilometer of ice beneath the South Pole Station. Antarctic polar ice turns out to be an ideal medium for detecting neutrinos because it is exceptionally pure, transparent, and free of radioactivity.

The IPY epitomizes the globalization of science. Organized by the International Council for Science (ICSU) and the World Meteorological Organization, over 60 nations will contribute thousands of scientists to it to work together on over 200 projects. According to the organizers, "The fundamental concept of the IPY 2007–2008 is of an intensive burst of internationally coordinated, interdisciplinary, scientific research and observations focused on the Earth's polar regions." The IPY focuses on new ways to both understand the polar regions and develop enhanced, long-lasting observational facilities and infrastructure. It also aims to recruit a new generation of polar scientists and engineers. The IPY offers the scientific community a superb opportunity to reach out to citizens around the world with the wonders of science and its applicability to crucial issues affecting them and generations to come.

IPY research projects will include mathematical, physical, biological, behavioral, and social scientists and a wide range of engineering researchers. This mix of disciplines makes this polar year initiative unique, because the earlier ones were strictly geophysical. This IPY specifically includes research directed at the human elements of polar regions "to investigate the cultural, historical, and social processes that shape the sustainability of circumpolar human societies." Its multidisciplinary character underscores how much society depends on the full array of sciences—mathematics; the physical, life, and social sciences; and engineering—to fully understand the natural world, how to preserve it, and how to make sure humans will continue to have a secure, productive, and fulfilling place in it.

Reaping the benefits of this grand IPY initiative is not only up to the global scientific community. It also will depend on the wisdom of policymakers around the world to provide enough resources to ensure its success. The recent budget frenzies in the United States came dangerously close to compromising, or at least substantially delaying, this country's participation. We all need to be vigilant and make certain that the great opportunities inherent in the IPY are not forsaken.

– Alan I. Leshner

10.1126/science.1141969

CREDIT: ALAN LESHNER

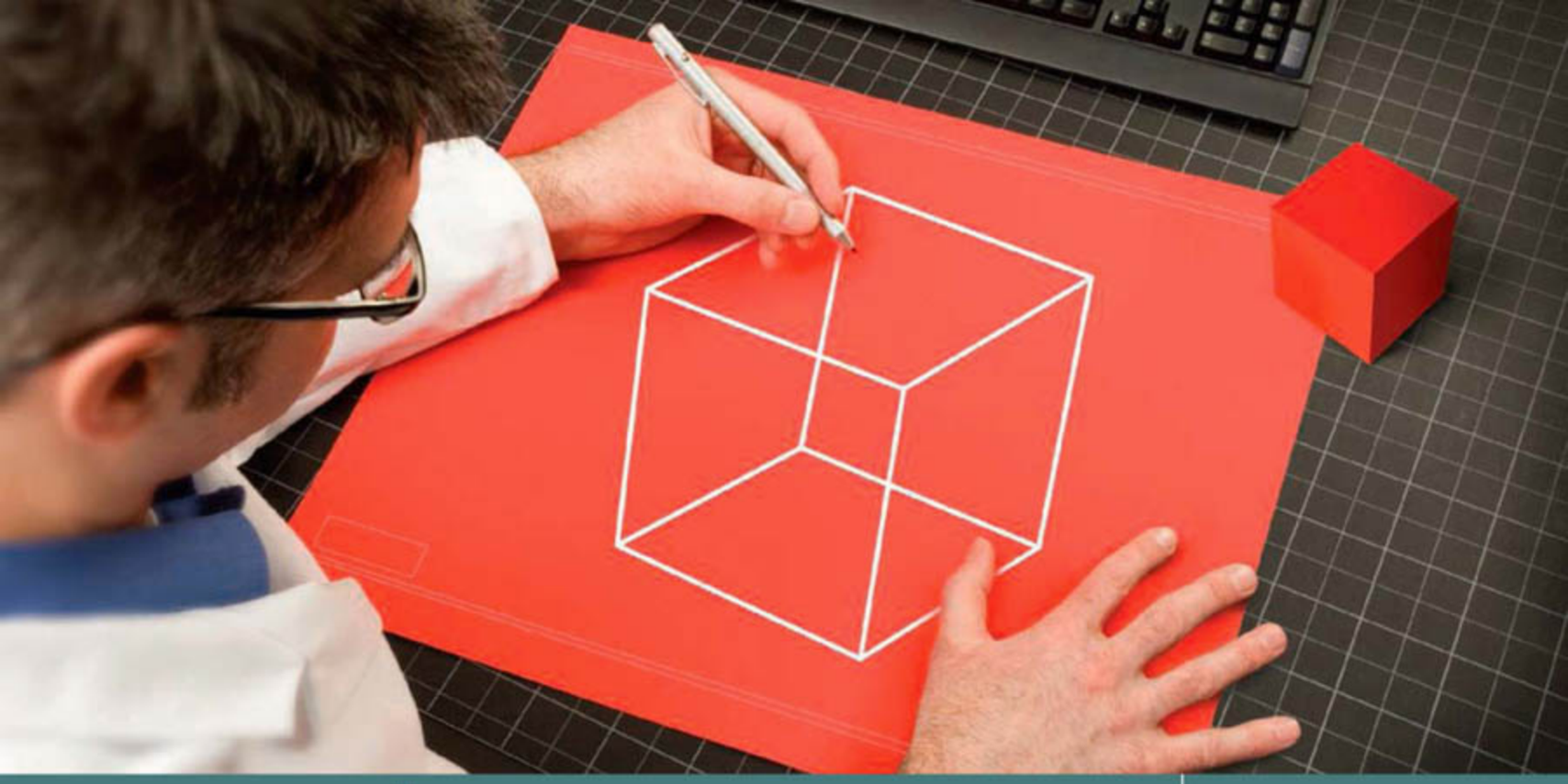

Design!

INNOVATION @ WORK

With MISSION® siRNA – It's About Design!

Sigma and Rosetta Inpharmatics, a recognized leader in Bioinformatics, have partnered to bring you the best siRNA design to improve your RNAi results.

Current studies suggest that the rules used to design gene-specific siRNAs have a direct effect on how well your siRNA will perform in a given RNAi experiment. Using an siRNA designed with a best-in-class algorithm saves time and money, enabling you to focus on downstream applications, not up-front siRNA design work.

Better siRNA Design, Better RNAi Performance

The MISSION siRNA Druggable Genome Libraries designed with Rosetta algorithm provide:

- Efficient knockdown for low abundance message
- Improved target specificity
- Flexible gene family sets, pre-arrayed for a range of applications
- Optimum products from highest quality, experienced manufacturing
- Freedom to operate for research use

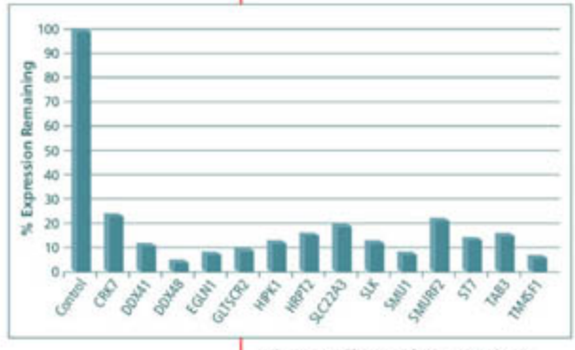

Silencing Efficacy of representative MISSION siRNAs designed using the Rosetta algorithm. Target mRNA levels were measured by the QuantiGene® Reagent System from samples harvested 24 hours after transfection into HeLa cells.

The MISSION siRNA Performance Guarantee

Sigma guarantees that 2 out of 3 siRNA duplexes per target gene will achieve knockdown efficiencies of greater than or equal to 75%

For more information on MISSION siRNA Druggable Genome Libraries, please visit us on the Web at sigma.com/missionsirna.

POWERED BY ROSETTA INPHARMATICS

Accelerating Customers' Success through **Leadership** in **Life Science, High Technology** and **Service**

SIGMA-ALDRICH CORPORATION • BOX 14508 • ST. LOUIS • MISSOURI 63178 • USA

SIGMA®

MOLECULAR BIOLOGY

Facing in Two Directions

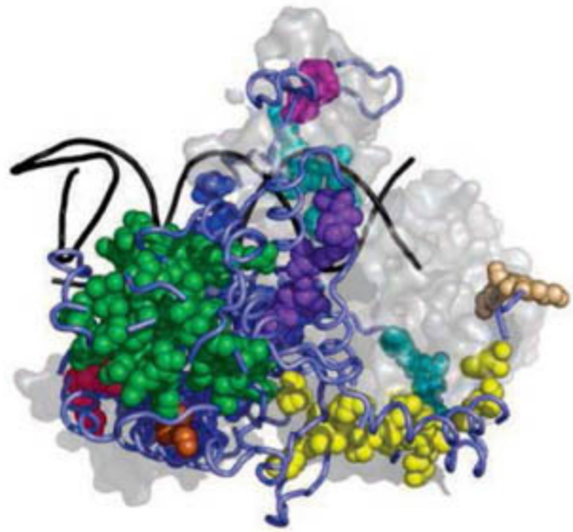

The inward-facing domain (green) of Ku80; DNA, black strands.

The ends of DNA molecules can be extremely dangerous to a cell because of their potential to recombine with other DNA sequences, which would cause large-scale disruption of genome integrity. Double-stranded DNA ends are found naturally at the termini (called telomeres) of linear eukaryotic chromosomes and also at sites of spontaneous genomic damage. Exposed ends at both locations are recognized by the evolutionarily conserved Ku heterodimer, which is required for the nonhomologous end-joining (NHEJ) repair of broken DNA as well as for the silencing of genes at telomeres. How does Ku orchestrate such distinct functions? The Ku heterodimer consists of the structurally and evolutionarily related Ku70 and Ku80 proteins, which together form a ring that wraps around DNA ends. The N-terminal domains of the two subunits face in opposite directions when bound to DNA, with Ku70 oriented toward the DNA ends. Ribes-Zamora *et al.* have carried out a mutagenesis study of yeast Ku and show that an α helix in the Ku70 N-terminal domain is required for DNA repair, possibly as a surface to which NHEJ factors are recruited. The equivalent helix in Ku80 is required for telomeric silencing, which is consistent with its facing toward the bulk of the telomeric structure when Ku is bound at telomeres. Prokaryotes contain a single Ku gene that is involved in DNA repair, and most lack telomeres, having circular genomes. The advent of linear chromosomes and telomeres in eukaryotes probably favored the duplication of the Ku gene and the subsequent functional differentiation of the Ku70 and Ku80 subunits. — GR

Nat. Struct. Mol. Biol. 10.1038/nsmb1214 (2007).

CHEMISTRY

Lactide Loops...

Selective routes to cyclic polymers must overcome the dual challenges of enthalpic strain and unfavorable entropy. Culkin *et al.* have found that an N-heterocyclic carbene substituted with two bulky mesityl groups can catalyze the polymerization of lactide to yield macrocycles with molecular weights on the order of 20 kD and polydispersities of ~1.2 to 1.3. The authors had previously shown the effectiveness of this catalyst for generating linear poly(lactide) in the presence of alcohol initiators; the cyclic products result when the initiators are omitted. Polymerization of optically pure lactide proceeds with retention of stereochemistry. The narrow polydispersities and observation of a product molecular weight increase with reaction time suggest that propagation outpaces the macrolactonization step that liberates the carbene catalyst. — JSY

Angew. Chem. Int. Ed. **46**, 10.1002/anie.200604740 (2007).

CHEMISTRY

...and Peptoid Polygons

The potential therapeutic usefulness of peptides is often limited by their degradation via proteolysis, and a number of peptide mimics have been developed that avoid degradation by using a different backbone linkage. Peptoids, which are composed of glycine monomers substituted at the nitrogen atom, can develop helical secondary structure if they bear bulky chiral side chains, but in solution they often exhibit some disordering and conformational heterogeneity.

Octapeptoid structure.

Shin *et al.* show that the use of the peptide coupling agent PyBOP led to remarkably efficient head-to-tail cyclization of peptoids with methoxyethyl, phenylmethyl, and azidopropyl side chains. Products ranging from cyclic pentamers up to cyclic 20-mers could be prepared with yields of ~90% or greater. These compounds have sufficient conformational ordering that several could be crystallized for structural analysis by x-ray diffraction. — PDS

J. Am. Chem. Soc. **129**, 10.1021/ja066960o (2007).

CELL BIOLOGY

Capturing Immature Components

The γ-secretase complex catalyzes proteolytic cleavage of a variety of membrane proteins, including the amyloid precursor protein that is implicated in Alzheimer's disease. The complex contains several components, including presenilin, anterior pharynx defective-1 (APH-1), and nicastrin. Spasic *et al.* have examined the intracellular assembly path of this complex and have found that a protein involved in recycling within the early secretory pathway, Rer1p, interacts with immature nicastrin either in the Golgi or in the endoplasmic reticulum (ER): the entry portal to the secretory pathway. It seems that Rer1p effectively binds to a site within the transmembrane domain of nicastrin that can also interact with APH-1 in the mature γ-secretase complex. Rer1p-binding competes with the assembly of APH-1 and nicastrin and also returns to the ER any immature nicastrin that has escaped into the Golgi. — SMH

J. Cell Biol. **176**, 629 (2007).

CLIMATE SCIENCE

Eye of the Beholder

One of the most contentious issues in the debate about the impact of global warming on hurricanes is the accuracy of hurricane records;

Continued on page 1469

CREDITS (TOP TO BOTTOM): RIBES-ZAMORA *ET AL.*, *NAT. STRUCT. MOL. BIOL.* 10.1038/NSMB1214 (2007); SHIN *ET AL.*, *J. AM. CHEM. SOC.* **129**, 10.1021/JA066960O (2007)

A Challenge from Dow

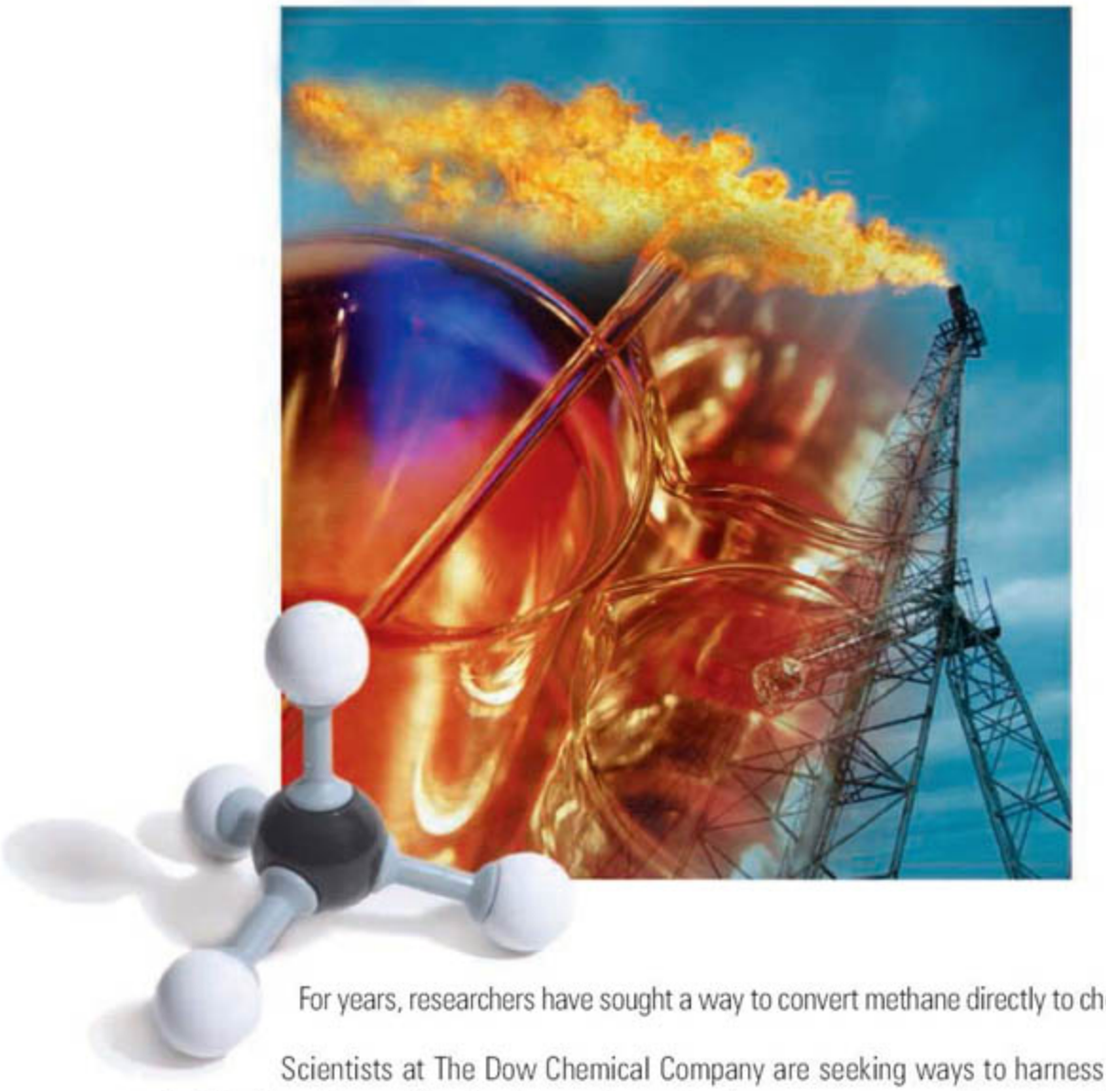

For years, researchers have sought a way to convert methane directly to chemicals.

Scientists at The Dow Chemical Company are seeking ways to harness the full potential of methane without using costly synthesis gas processes. We are so intent on discovering these technologies that we want to identify and collaborate with colleagues from around the world to find a solution.

Are you interested in working with us?

Dow will award one or more grants of up to $2 million each for three years, with an option to be renewed depending upon progress. These grants will go to collaborators who have a desire, like us, to develop more effective ways of converting methane. Our ultimate goal is to use this chemistry to produce ethylene and propylene, avoiding synthesis gas processes.

Maybe your team has ideas on how to find an answer. We would like to hear from you – non-confidential proposals will be accepted by Dow until May 31, 2007.

For complete details, go to www.dowmethane.com.

DOW®

Continued from page 1467

it is important for hurricane intensity measurements to be evaluated in a consistent manner, so that methodological differences do not introduce spurious trends. Kossin *et al.* take a step in that direction by constructing a homogeneous global record of hurricane intensity between 1983 and 2005, using the available satellite data archive of nearly 170,000 observations of more than 2000 tropical storms. After standardizing the spatial and temporal resolution of the images, they treat all the data (from the Atlantic, Pacific, and Indian Oceans) with a single algorithm for estimating hurricane intensity, based on the infrared brightness temperatures of the storms measured by satellites. Their analysis reveals a rise in storm intensity and the power dissipated by storms in the North Atlantic over the period of investigation, but no significant trends in the global averages. These findings would seem to contradict the assertion that hurricanes are becoming more intense as climate warms, because sea surface temperatures, the factor generally believed to have the greatest impact on hurricane strength, have risen in all ocean basins over the same period. — HJS

Geophys. Res. Lett. **34**, L04815 (2007).

CELL BIOLOGY

Turning Right or Left

During transport from the cell center to the periphery, organelles are carried long distances along microtubules by kinesin and then locally along actin tracks by myosin Va (myoVa). What do these motors do when confronted with enmeshed cytoskeletal elements, and how do they pass their cargoes onward?

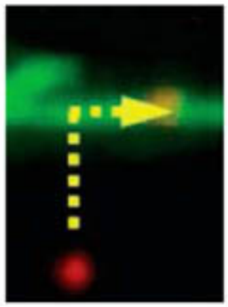

MyoVa (red dot) turning right onto an actin filament (green).

Ali *et al.* have addressed these questions by watching the movement of single molecules of myoVa (labeled with quantum dots) as they encountered intersecting filaments: either actin or microtubules. At actin-actin intersections, myoVa either stepped over the crossing filament, stopped moving altogether, or turned left or right, with the direction determined by the polarity of the second filament. The ratio of stepping versus turning events correlated with the ratio of binding sites within reach of a flexible myoVa head that samples actin monomers within a target zone defined by its 50- to 95-nm stepping range. Despite a tendency to switch tracks, myoVa has a high probability of reaching the cell periphery because of the strong bias for actin filaments to be oriented with their barbed ends aimed at the plasma membrane. At actin-microtubule intersections, myoVa could not step over the obstructing element (microtubules are significantly larger than actin filaments); however, in a few cases, myoVa turned onto the microtubule and diffused randomly along it, mimicking the search it would undertake for a cargo that was being delivered to the periphery by kinesin. — VV

Proc. Natl. Acad. Sci. U.S.A. **104**, 10.1073/pnas.0611471104 (2007).

CREDIT: ALI *ET AL.*, *PROC. NATL. ACAD. SCI. U.S.A.* **104**, 10.1073/PNAS.0611471104 (2007)

Science STKE AAAS

www.stke.org

<< Antipsychotics and Weight Gain

Although atypical antipsychotic drugs (AAPDs) are currently the most commonly used treatments for schizophrenia, some of them stimulate a substantial weight gain—largely associated with increased food intake—that can lead to the development of diabetes and cardiovascular disease. Noting that activation of hypothalamic adenosine 5′-monophosphate–activated protein kinase (AMPK) is associated with increased food intake, Kim *et al.* explored the effects of AAPDs on the phosphorylation of AMPK, which enhances its kinase activity. Clozapine and olanzapine, two AAPDs that elicit weight gain, stimulated phosphorylation of AMPK in mouse hypothalamic slices, as did quetiapine, whereas antipsychotic drugs with less effect on appetite did not. Furthermore, clozapine stimulated the phosphorylation and catalytic activity of hypothalamic AMPK in intact mice. After confirming earlier reports that that the potency of AAPDs in blocking the histamine H_1 receptor (H1R) correlated with their tendency to stimulate weight gain, the authors showed that clozapine blocked the ability of histamine to decrease the phosphorylation of AMPK in hypothalamic slices. Moreover, clozapine failed to stimulate AMPK phosphorylation in mice lacking the H1R. Thus, they conclude that the orexigenic effects of AAPDs probably involve blockade of the H1R and an associated activation of hypothalamic AMPK. — EMA

Proc. Natl. Acad. Sci. U.S.A. **104**, 3456 (2007).

www.sciencemag.org

Science

1200 New York Avenue, NW
Washington, DC 20005
Editorial: 202-326-6550, FAX 202-289-7562
News: 202-326-6500, FAX 202-371-9227

Bateman House, 82-88 Hills Road
Cambridge, UK CB2 1LQ
+44 (0) 1223 326500, FAX +44 (0) 1223 326501

Subscription Services For change of address, missing issues, new orders and renewals, and payment questions: 866-434-AAAS (2227) or 202-326-6417, FAX 202-842-1065. Mailing addresses: AAAS, P.O. Box 96178, Washington, DC 20090-6178 or AAAS Member Services, 1200 New York Avenue, NW, Washington, DC 20005

Institutional Site Licenses please call 202-326-6755 for any questions or information

Reprints: Author Inquiries 800-635-7181
Commercial Inquiries 803-359-4578
Corrections 202-326-6501

Permissions 202-326-7074, FAX 202-682-0816

Member Benefits Bookstore: AAAS/BarnesandNoble.com bookstore www.aaas.org/bn; Car purchase discount: Subaru VIP Program 202-326-6417; Credit Card: MBNA 800-847-7378; Car Rentals: Hertz 800-654-2200 CDP#343457, Dollar 800-800-4000 #AA1115; AAAS Travels: Betchart Expeditions 800-252-4910; Life Insurance: Seabury & Smith 800-424-9883; Other Benefits: AAAS Member Services 202-326-6417 or www.aaasmember.org.

science_editors@aaas.org (for general editorial queries)
science_letters@aaas.org (for queries about letters)
science_reviews@aaas.org (for returning manuscript reviews)
science_bookrevs@aaas.org (for book review queries)

Published by the American Association for the Advancement of Science (AAAS), *Science* serves its readers as a forum for the presentation and discussion of important issues related to the advancement of science, including the presentation of minority or conflicting points of view, rather than by publishing only material on which a consensus has been reached. Accordingly, all articles published in *Science*—including editorials, news and comment, and book reviews—are signed and reflect the individual views of the authors and not official points of view adopted by the AAAS or the institutions with which the authors are affiliated.

AAAS was founded in 1848 and incorporated in 1874. Its mission is to advance science and innovation throughout the world for the benefit of all people. The goals of the association are to: foster communication among scientists, engineers and the public; enhance international cooperation in science and its applications; promote the responsible conduct and use of science and technology; foster education in science and technology for everyone; enhance the science and technology workforce and infrastructure; increase public understanding and appreciation of science and technology; and strengthen support for the science and technology enterprise.

Information for Authors

See pages 120 and 121 of the 5 January 2007 issue or access www.sciencemag.org/feature/contribinfo/home.shtml

EDITOR-IN-CHIEF **Donald Kennedy**
EXECUTIVE EDITOR **Monica M. Bradford**
DEPUTY EDITORS **R. Brooks Hanson, Barbara R. Jasny, Katrina L. Kelner**
NEWS EDITOR **Colin Norman**

Editorial supervisory senior editor Phillip D. Szuromi; **senior editor/perspectives** Lisa D. Chong; **senior editors** Gilbert J. Chin, Pamela J. Hines, Paula A. Kiberstis (Boston), Marc S. Lavine (Toronto), Beverly A. Purnell, L. Bryan Ray, Guy Riddihough, H. Jesse Smith, Valda Vinson, David Voss; **associate editors** Jake S. Yeston, Laura M. Zahn; **online editor** Stewart Wills; **associate online editor** Tara S. Marathe; **book review editor** Sherman J. Suter; **associate letters editor** Etta Kavanagh; **editorial manager** Cara Tate; **senior copy editors** Jeffrey E. Cook, Cynthia Howe, Harry Jach, Barbara P. Ordway, Jennifer Sills, Trista Wagoner; **copy editors** Lauren Kmec, Peter Mooreside; **editorial coordinators** Carolyn Kyle, Beverly Shields; **publications assistants** Ramatoulaye Diop, Chris Filiatreau, Joi S. Granger, Jeffrey Hearn, Lisa Johnson, Scott Miller, Jerry Richardson, Brian White, Anita Wynn; **editorial assistants** Maris M. Bish, Emily Guise, Patricia M. Moore, Jennifer A. Seibert; **executive assistant** Sylvia S. Kihara; **administrative support** Maryrose Police

News senior correspondent Jean Marx; **deputy news editors** Robert Coontz, Eliot Marshall, Jeffrey Mervis, Leslie Roberts; **contributing editors** Elizabeth Culotta, Polly Shulman; **news writers** Yudhijit Bhattacharjee, Adrian Cho, Jennifer Couzin, David Grimm, Constance Holden, Jocelyn Kaiser, Richard A. Kerr, Eli Kintisch, Andrew Lawler (New England), Greg Miller, Elizabeth Pennisi, Robert F. Service (Pacific NW), Erik Stokstad; John Simpson (intern); **contributing correspondents** Barry A. Cipra, Jon Cohen (San Diego, CA), Daniel Ferber, Ann Gibbons, Robert Irion, Mitch Leslie, Charles C. Mann, Evelyn Strauss, Gary Taubes, Ingrid Wickelgren; **copy editors** Linda B. Felaco, Rachel Curran, Sean Richardson; **administrative support** Scherraine Mack, Fannie Groom; **bureaus** Berkeley, CA: 510-652-0302, FAX 510-652-1867, New England: 207-549-7755, San Diego, CA: 760-942-3252, FAX 760-942-4979, Pacific Northwest: 503-963-1940

Production director James Landry; **senior manager** Wendy K. Shank; **assistant manager** Rebecca Doshi; **senior specialists** Jay Covert, Chris Redwood; **specialist** Steve Forrester; **Preflight director** David M. Tompkins; **manager** Marcus Spiegler; **specialist** Jessie Mudjitaba

Art director Kelly Buckheit Krause; **associate art director** Aaron Morales; **illustrators** Chris Bickel, Katharine Sutliff; **senior art associates** Holly Bishop, Laura Creveling, Preston Huey; **associates** Nayomi Kevitiyagala, Jessica Newfield; **photo editor** Leslie Blizard

***Science* International**

Europe (science@science-int.co.uk) **editorial: international managing editor** Andrew M. Sugden; **senior editor/perspectives** Julia Fahrenkamp-Uppenbrink; **senior editors** Caroline Ash (Geneva: +41 (0) 222 346 3106), Stella M. Hurtley, Ian S. Osborne, Stephen J. Simpson, Peter Stern; **associate editor** Joanne Baker **editorial support** Alice Whaley; Deborah Dennison **administrative support** Janet Clements, Jill White; **news: europe news editor** John Travis; **deputy news editor** Daniel Clery; **correspondent** Gretchen Vogel (Berlin: +49 (0) 30 2809 3902, FAX +49 (0) 30 2809 8365); **contributing correspondents** Michael Balter (Paris), Martin Enserink (Amsterdam and Paris), John Bohannon (Vienna); **intern** Krista Zala

Asia Japan Office: Asca Corporation, Eiko Ishioka, Fusako Tamura, 1-8-13, Hirano-cho, Chuo-ku, Osaka-shi, Osaka, 541-0046 Japan; +81 (0) 6 6202 6272, FAX +81 (0) 6 6202 6271; asca@os.gulf.or.jp; **asia news editor** Richard Stone +66 2 662 5818 (rstone@aaas.org); **japan news bureau** Dennis Normile (contributing correspondent, +81 (0) 3 3391 0630, FAX 81 (0) 3 5936 3531; dnormile@gol.com); **china representative** Hao Xin, + 86 (0) 10 6307 4439 or 6307 3676, FAX +86 (0) 10 6307 4358; cindyhao@gmail.com; **south asia** Pallava Bagla (contributing correspondent +91 (0) 11 2271 2896; pbagla@vsnl.com)

Africa Robert Koenig (contributing correspondent, rob.koenig@gmail.com)

EXECUTIVE PUBLISHER **Alan I. Leshner**
PUBLISHER **Beth Rosner**

Fulfillment & Membership Services (membership@aaas.org) **director** Marlene Zendell; **manager** Waylon Butler; **systems specialist** Andrew Vargo; **customer service supervisor** Pat Butler; **specialists** Laurie Baker, Tamara Alfson, Karena Smith, Vicki Linton, Latoya Casteel; **circulation associate** Christopher Refice; **data entry supervisor** Cynthia Johnson; **specialists** Tomeka Diggs, Tarrika Hill, Erin Layne

Business Operations and Administration director Deborah Rivera-Wienhold; **business manager** Randy Yi; **senior business analyst** Lisa Donovan; **business analyst** Jessica Tierney; **financial analysts** Michael LoBue, Farida Yeasmin; **rights and permissions: administrator** Emilie David; **associate** Elizabeth Sandler; **marketing: director** John Meyers; **marketing managers** Darryl Walter, Allison Pritchard; **marketing associates** Julianne Wielga, Mary Ellen Crowley, Catherine Featherston, Alison Chandler, Lauren Lamoureux; **international marketing manager** Wendy Sturley; **marketing executive** Jennifer Reeves; **marketing/member services executive** Linda Rusk; **japan sales** Jason Hannaford; **site license sales: director** Tom Ryan; **sales and customer service** Mehan Dossani, Kiki Forsythe, Catherine Holland, Wendy Wise; **electronic media: manager** Lizabeth Harman; **project manager** Trista Snyder; **assistant manager** Lisa Stanford **production associates** Nichele Johnston, Kimberly Oster

Advertising director worldwide ad sales Bill Moran

Product (science_advertising@aaas.org): **midwest** Rick Bongiovanni: 330-405-7080, FAX 330-405-7081 • **west coast/w. canada** Teola Young: 650-964-2266 **east coast/e. canada** Christopher Breslin: 443-512-0330, FAX 443-512-0331 • **uk/europe/asia** Julie Skeet: +44 (0) 1223-326-524, FAX +44 (0) 1223-325-532 **japan** Mashy Yoshikawa: +81 (0) 33235 5961, FAX +81 (0) 33235 5852 **traffic manager** Carol Maddox; **sales coordinator** Deiandra Simms

Commercial Editor Sean Sanders: 202-326-6430

Classified (advertise@sciencecareers.org): **u.s.: recruitment sales manager** Ian King: 202-326-6528, FAX 202-289-6742; **u.s./industry:** Darrell Bryant: 202-326-6533; **midwest/canada:** Daryl Anderson: 202-326-6543; **northeast:** Allison Millar: 202-326-6572; **southeast:** Fernando Junco: 202-326-6740; **west:** Katie Putney: 202-326-6577; **sales coordinators** Erika Bryant, Rohan Edmonson, Shirley Young; **international: sales manager** Tracy Holmes: +44 (0) 1223 326525, FAX +44 (0) 1223 326532; **sales** Christina Harrison, Svitlana Barnes; **sales assistant** Louise Moore; **japan:** Jason Hannaford: +81 (0) 52 757 5360, FAX +81 (0) 52 757 5361; **advertising production operations manager** Deborah Tompkins; **associates** Christine Hall, Amy Hardcastle; **publications assistants** Robert Buck, Mary Lagnaoui

AAAS Board of Directors **retiring president, chair** John P. Holdren; **president** David Baltimore; **president-elect** James J. McCarthy; **treasurer** David E. Shaw; **chief executive officer** Alan I. Leshner; **board** John E. Dowling, Lynn W. Enquist, Susan M. Fitzpatrick, Alice Gast, Linda P. B. Katehi, Cherry A. Murray, Thomas D. Pollard, Kathryn D. Sullivan

AAAS
ADVANCING SCIENCE, SERVING SOCIETY

You Stand in Front of Our Instruments All Day... We Stand Behind Them...24x7

High-Value, Substantially Expanded Services from Applied Biosystems

With over 25 years of experience in the development, manufacture, and service of innovative instruments, and with over 1000 highly trained, dedicated service professionals, AB Global Services is uniquely qualified to deliver a full suite of real-world lab services. From Remote Services to On-Site Application Consulting to Qualification and Professional Services and everything in between, AB Global Services is your value-added partner to help boost your productivity and maximize the return on your technology investment.

- Instrument Repair and Maintenance
- Smart Services
- Qualification Services
- Professional Services
- On-Site Application Consulting
- Training

To learn more go to http://info.appliedbiosystems.com/service or contact your local Applied Biosystems sales representative.

Applied Biosystems

Are you sure your monochromator microplate reader doesn't use filters?

With Tecan's exclusive quad4 monochromator™ technology, as featured in the Safire²™ and the Infinite™ M200, you can be sure there are no filters used for stray light reduction – there's nothing to compromise the performance or flexibility of a monochromator plate reader.

With quad4 technology you'll soon see the difference.

quad4 monochromators™

With Tecan's exclusive quad4 monochromator™ technology, as featured in the Safire²™ and the Infinite™ M200, you can be sure there are no filters used for stray light reduction – there's nothing to compromise the performance or flexibility of a monochromator plate reader.

With quad4 technology you'll soon see the difference.

quad4 monochromators™

Talk to Tecan

www.tecan.com/quad4

TECAN.

Liquid Handling & Robotics | **Detection** | Sample Management | Components | Services & Consumables

Austria +43 62 46 89 33 **Belgium** +32 15 42 13 19 **China** +86 10 586 95 936 **Denmark** +45 70 23 44 50 **France** +33 4 72 76 04 80 **Germany** +49 79 51 94 170
Italy +39 02 215 21 28 **Japan** +81 44 556 73 11 **Netherlands** +31 18 34 48 17 4 **Portugal** +351 21 000 82 16 **Singapore** +65 644 41 886 **Spain** +34 93 490 01 74
Sweden +46 31 75 44 000 **Switzerland** +41 44 922 89 22 **UK** +44 118 9300 300 **USA** +1 919 361 5200 **Other** +43 62 46 89 33

Mysterious Bee-havior

Beekeepers in 26 states have lost up to 50% of their colonies this winter to a mysterious ailment scientists are struggling to understand.

Dubbed Colony Collapse Disorder (CCD), the malady began late last fall, but the extent of the problem became clear only in January. Afflicted bees stop tending their broods and eventually abandon their colonies. Unlike previous die-offs due to pesticides, bee corpses aren't turning up around hive entrances. "They just disappear," says Sacramento beekeeper Franklin Carrier.

To tackle the problem, scientists around the country have set up a CCD working group that is scanning for novel pathogens with gene chips and using neural networks to analyze the buzz at infected hives—which the U.S. Army has found to provide an early indication of airborne toxins. Researchers are also looking at bee genes to see whether Cape honeybees from Africa may have infiltrated U.S. populations. Cape females produce their own young rather than tending to the queen's brood, causing the social structure to collapse.

So far, no prime suspect has emerged. Entomologist Diana Cox-Foster of Pennsylvania State University in State College thinks a toxin may be implicated, because waxworms and neighboring bees are not invading deserted hives.

CCD is only the latest in a string of misfortunes to hit commercial honeybees weakened by varroa mites and infections. The working group hopes to have an explanation by June. Time is of the essence: Bees provide 80% of the country's pollination services, and the almond trees are already in bloom.

One World, OneGeology

Countries that have spent decades mapping their surfaces can now add their pieces to the global puzzle. OneGeology, a new international project to consolidate data from geologic maps around the world, made its debut in London last week. "Geology has no respect for national boundaries," notes project leader Ian Jackson of the British Geological Survey. So national geological agencies "need to start thinking more in groups."

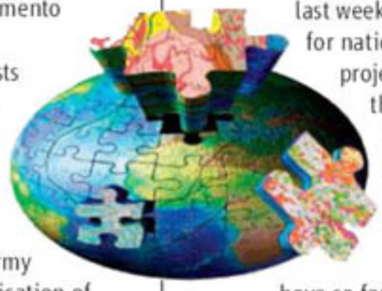

Some 55 nations have so far joined the effort, with each planning to contribute geologic maps of its territory at a scale of 1:1 million. The International Union of Geological Sciences will figure out how to standardize national databases. The project (at onegeology.com) will also transfer mapping know-how to less developed countries. The team hopes to have an online database available in 2008.

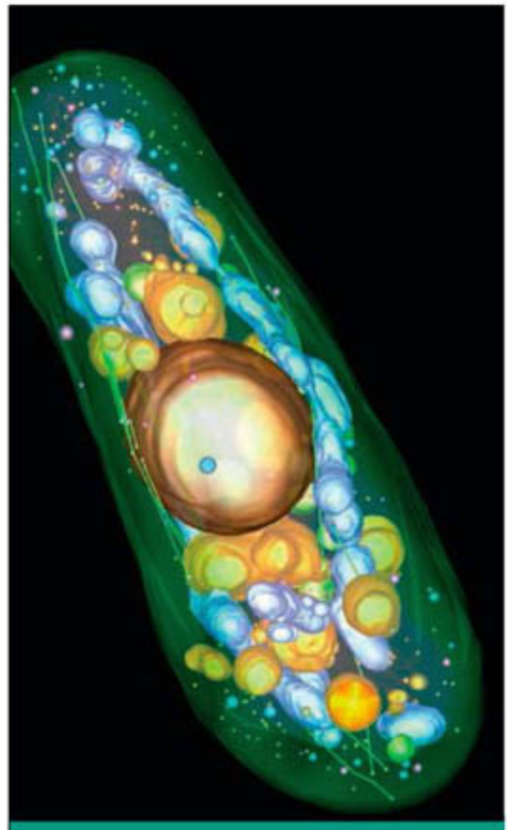

ULTRASTRUCTURE GOES 3D

Using the microscopic equivalent of computed tomography, scientists have created a 3D map showing the precise locations of the innards of a cell, including nucleus, mitochondria, and the microtubules that hold it all together.

A group led by Claude Antony at the European Molecular Biology Laboratory in Heidelberg, Germany, with Richard McIntosh's laboratory at the University of Colorado, Boulder, used the new technique, called electron tomography, to visualize the structure of fission yeast at a magnification of 14,500×. The work was published in the March issue of *Developmental Cell*. "This high-quality analysis … allows us for the first time to have a detailed description of the microtubular arrays," says Nobel laureate Paul Nurse of Rockefeller University in New York City. Biologist Jeremy Hyams of Massey University in Palmerston North, New Zealand, says it "opens a new chapter in our understanding of cell structure."

A Toothsome Resource

NET WATCH

With these shapely molars (below), an arctic fox (*Alopex lagopus*) can munch on lemmings, berries, or the remains of a seal carcass left behind by a polar bear. Researchers keen to analyze the fox's teeth or those of other mammals will find a wealth of data at MorphoBrowser from the University of Helsinki in Finland.

The database holds 3D scans of molars and premolars captured using confocal microscopy, computerized tomography, and other techniques. Paleontologists, developmental biologists, and anthropologists can check out the choppers of more than 100 extinct and living species and of several transgenic and mutant mouse strains.

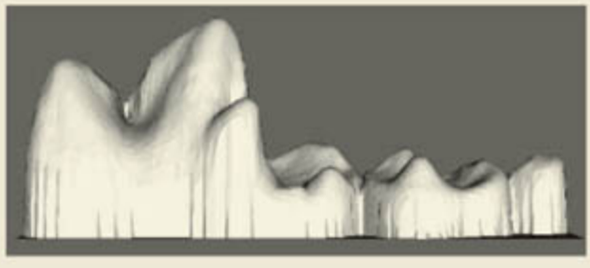

To simplify comparisons, tools sort out similar teeth based on variables such as shape and crown type. Students might also find the database handy because it allows them to examine tiny teeth that are difficult to study in laboratory specimens. >> pantodon.science.helsinki.fi/morphobrowser

CREDITS (TOP TO BOTTOM): PHOTOS.COM; JOHANNA HOOG/EMBL; CNERC 2007; UNIVERSITY OF HELSINKI

The power of small x8

1µl analysis — increased throughput

The NanoDrop® ND-8000 8-Sample Spectrophotometer

1µl samples. No cuvettes. No dilutions.

Revolutionary technology. **8 readings in under 30 seconds.** The NEW NanoDrop® ND-8000 8-Sample Spectrophotometer is powerful — eight 1µl samples at once.

Full spectrum UV/Vis analysis of 1µl samples for quantitation, purity assessments and more: nucleic acids, microarrays, proteins and general spectrophotometry.

Measurement is quick and easy — pipette up to eight samples and measure. Each sample is read using two path lengths to achieve an extensive dynamic range (e.g., 2-3700 ng/µl dsDNA), virtually eliminating the need for dilutions. Then just a quick wipe clean and you're ready for your next samples. What could be easier — or more powerful?

And for the power of small in single-sample absorbance or fluorescent measurements, check out the NanoDrop® ND-1000 Spectrophotometer or the NanoDrop® ND-3300 Fluorospectrometer (ultra low fluorescent detection limit of sample mass — e.g., 2 pg dsDNA).

Ready to experience the power of small x8? **Test a NanoDrop® ND-8000 8-Sample Spectrophotometer in your own lab.**

FREE one-week evaluation **www.nanodrop.com**
302.479.7707

NanoDrop

EDITED BY YUDHIJIT BHATTACHARJEE

Movers

GLOBAL THINKER. Douglas Lin, a theoretical astrophysicist at the University of California, Santa Cruz (UCSC), has been named founding director of the Kavli Institute for Astronomy and Astrophysics (KIAA) at Beijing University. KIAA is one of two Chinese institutes established last June with support from the Kavli Foundation.

The new institute, which plans to recruit up to 15 faculty members from all over the world, will focus on particle cosmology, star and planet formation, and gravitational physics and high-energy phenomena. Beijing University President Xu Zhihong says he expects the institute's autonomy to be a model for strengthening research on campus.

Lin, who says he "feels equally at home on the shores of the Pacific and Atlantic," was born in New York City, grew up in Beijing, attended McGill University in Montreal, Canada, and received his Ph.D. from Cambridge University in the United Kingdom. For the next 2 years, he plans to split his time between KIAA and UCSC, where he has been a professor since 1979. From then on, he expects to spend at least 3 months every year at KIAA.

ON CAMPUS

TAKING A LONG VIEW. Over the years, astronomer Richard Kron has used the 1-meter refracting telescope at Yerkes Observatory in Williams Bay, Wisconsin, to get students interested in science. He's now hoping to save the long-obsolete observatory, built in 1897, by turning it into a science education center.

In a cost-saving move, the University of Chicago announced in 2005 that it was going to sell Yerkes and 18 hectares of surrounding woods. A New York real estate company offered $10 million. After local residents objected to its plans to build 72 houses and a hotel, the university tapped Kron—who directed Yerkes from 1989 to 2001 and is a professor at the university—to lead a committee to study alternative uses for the site. Kron thinks that an education center would be ideal if it can pay its own way. The panel began meeting last month, and Kron hopes to submit a plan by the summer.

HONORS

HOME ON THE MOON. A desolate spot on the methane-soaked surface of Saturn's largest moon Titan has been named in honor of Hubert Curien, a former French science minister and advocate of European space science.

Curien, a soft-spoken crystallography professor who died in February 2005 at the age of 80, headed France's giant research agency, CNRS, and its space agency, CNES, before serving as minister under four governments. He also chaired the European Space Agency (ESA) council and played a key role in setting up its long-term science program and the Ariane launcher project.

A ceremony to name the site where the European Huygens probe landed a month before Curien died took place this week at ESA headquarters in Paris. "It is … a true honor for us to pay tribute to his memory by linking his name forever to this very significant place on the surface of an alien world that, also thanks to him, we were able to reach," said ESA Director General Jean-Jacques Dordain.

Misconduct >>

MEA CULPA. Indian science policy heavyweight Raghunath Mashelkar has acknowledged that a 2004 book he co-authored on intellectual property contains plagiarized text. It's the second such incident in the past month for Mashelkar, a chemical engineer who earlier this year retired as head of India's main research agency (*Science*, 2 March, p. 1205).

The book, *Intellectual Property and Competitive Strategies in the 21st Century*, contains a page-and-a-half-long section copied line by line from a 1996 paper by Darrell Posey and Graham Dutfield in the *Bulletin of the Working Group of Traditional Resource Rights*. Dutfield, a patent law researcher at the University of London, discovered the plagiarism 3 years ago and complained to the publisher, but the story became public after *The Times of India* reported it last month. In the 2006 Indian edition, the copied text appears within quotation marks, with a footnote referencing the source.

Mashelkar says he's very sorry. "I was working on so many things at the time that I took the help of researchers to add new information to what I had written," he told *Science* in a phone interview during which he broke down. "Unfortunately, they copied verbatim from somebody else's writings. I know it is a sin. But I was so pressed for time that this skipped my attention."

CREDITS (TOP TO BOTTOM): LI SHULIN; YERKES OBSERVATORY; GAUTAM SINGH/AP PHOTO

Got a tip for this page? E-mail people@aaas.org

How not to deter looting 1479

Putting CO_2 in its place 1481

SPACE SCIENCE

NASA Declares No Room for Antimatter Experiment

The Alpha Magnetic Spectrometer (AMS) is a model of international cooperation, led by a dynamic Nobel Prize winner, and promises to do impressive science in space. But it may never get a chance to do its thing.

The problem is that NASA has no room on its space shuttle to launch the $1.5 billion AMS mission, which is designed to search for antimatter from its perch on the international space station. "Every shuttle flight that I have has got to be used to finish the station," NASA Administrator Michael Griffin told a Senate panel on 28 February.

Griffin's categorical statement could spell doom for the innovative experiment, which received a glowing review in December from an independent scientific review panel appointed by the mission's sponsor, the U.S. Department of Energy (DOE). The decision is sure to send ripples around the world, considering that 16 countries have contributed large sums of money to the effort. And it is one of the only significant scientific facilities planned for the space station.

AMS is the brainchild of Samuel Ting, a physicist at the Massachusetts Institute of Technology in Cambridge and Nobel laureate. One of its major goals is to understand the uneven distribution of matter and antimatter in the universe by searching for antimatter. The experiment, nearing completion in Geneva, Switzerland, could also help search for dark matter and a new form of quark matter called strangelets.

NASA and Ting announced the experiment with much fanfare in 1995, and the shuttle flew a small prototype in 1998. Although the loss of the Columbia orbiter put launch of the AMS on indefinite hold, Ting has continued work on the spacecraft, which should be ready to be shipped to Kennedy Space Center in Florida by 2008 after testing at Geneva's CERN and the European Space Agency's facility in Noordwijk, the Netherlands.

NASA has spent $55 million to build the skeleton, which will hold the device in the shuttle hold—the 6800-kg AMS would take up nearly half a shuttle bay—and be attached to the long truss on the space station. Although DOE has contributed about $30 million, the vast bulk of AMS funding has come from international partners such as Italy and France, as well as the unlikely combination of Taiwan and China. "The AMS project is sure to be viewed as a model for international collaboration in science," noted one reviewer in the DOE study chaired by Barry Barish, a physicist at the California Institute of Technology in Pasadena. That study "had only praise and some wonder" at Ting's ability to create such a far-reaching coalition.

Barish last week called the NASA news "disappointing" and said it would be "a big blow for international collaborators." He added that Ting has already been looking for other routes into space. One alternative is to launch the AMS on an expendable rocket with a robot that could guide it to the space station. The only realistic candidate, NASA officials say, is the Japanese H-2 transfer vehicle now under development. To alter both that vehicle and the AMS for such a mission, however, would cost between $254 million and $564 million, says Mark Sistilli, NASA AMS program manager.

Another alternative would be to place it in orbit aboard a rocket, which could leave the AMS in orbit until the shuttle could pick it up. That option could cost $380 million to $400 million and would entail a complex docking maneuver. A final option, according to Sistilli, would be to turn the AMS into a free-flying spacecraft with its own radiators and solar panels. Such a conversion, however, could top $1 billion.

DOE officials declined comment, and Ting was traveling in Asia and could not be reached. But Sistilli, who agrees that "the science is terrific and the international commitment is huge," says that NASA will continue to fund its portion of the project and hope for a positive outcome. "We didn't want to outright kill it," he says. "We don't really know how to handle the situation."

–ANDREW LAWLER

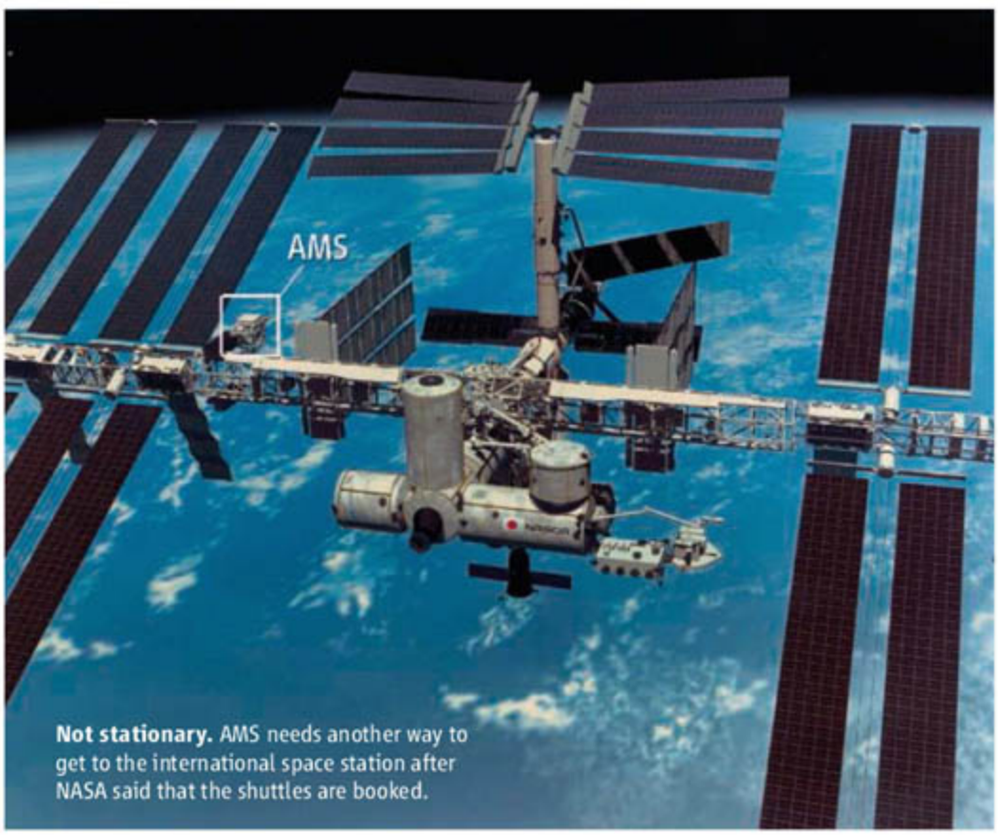

Not stationary. AMS needs another way to get to the international space station after NASA said that the shuttles are booked.

CREDIT: NASA

CANCER RESEARCH

Budget Pressure Puts High-Profile Study in Doubt

A budget crunch has delayed and could scuttle a major U.S. cancer-prevention trial set to begin in April. The $100 million experiment aims to compare a new drug, letrozole, to older pills for preventing breast cancer in women after menopause. Just 1 day after the trial won a high-level approval, John Niederhuber, director of the National Cancer Institute (NCI), flagged it for an intense review, to take place on 23 March. This private session will also look broadly at improving prevention trials.

The reversal has upset the center that designed the trial, the National Surgical Adjuvant Breast and Bowel Project (NSABP) in Pittsburgh, Pennsylvania. NSABP may be best known for pioneering tamoxifen therapy and new methods of breast surgery. Oncologist D. Lawrence Wickerham, NSABP's associate chair, says, "We were ecstatic on 22 January" when NCI's executive committee endorsed the project, known as the STELLAR trial, after 18 months of reviews. Then on 23 January, "we were informed that Niederhuber had apparently unilaterally" placed it on hold, rejecting an 8–2 approval by his executive committee. Wickerham says it suggests that cancer prevention is being pushed into "second class."

Niederhuber told *The Cancer Letter*, which first reported this decision, that NCI programs were under "a great deal of stress" and that some NCI grantees had "strong feelings" that the STELLAR proposal "was not good science" and not a good use of funds. Niederhuber declined *Science*'s request for an interview on grounds that it might affect the 23 March review. In a statement, NCI said the fresh look at STELLAR was "part of ongoing deliberations about difficult decisions regarding the best use of scarce resources that have resulted from 5 years of below-inflation appropriations." NCI notes that the trial "would cost approximately $100 million, would involve about 13,000 women, and require at least 10 years before results would be available."

STELLAR asks a specific question: Does letrozole, a drug in the new aromatase inhibitor (AI) class, work better as a preventative for postmenopausal women at high risk for breast cancer than an older drug, raloxifene? (Other data already indicate that raloxifene is better than an earlier preventative, tamoxifen.) Based on cancer treatment results, many think that letrozole will have milder side effects and provide better protection. All these drugs are designed to blunt the effects of estrogen; tamoxifen and raloxifene block estrogen from stimulating tumor growth, whereas AI drugs stop the synthesis of estrogen.

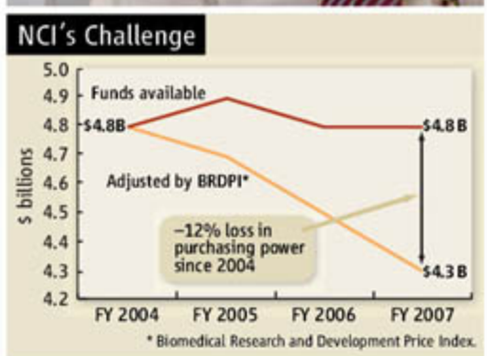

Tough choices. NCI Director John Niederhuber is grappling with a shrinking real budget.

Paul Goss, director of breast cancer research at Harvard's Massachusetts General Hospital in Boston, says that AI drugs have had great success in treating cancer, which has raised hopes for prevention. Data consistently show that AI drugs reduce estrogen in postmenopausal women to a very low level, he says, and women who took AI drugs after cancer in one breast were far less likely to develop a new tumor in the other breast. (Rates were reduced by about 60% to 75%, compared to 40% for tamoxifen.)

At the same time, Goss says, people are raising questions about the trial's value. He notes, for example, that two other big trials of AI drugs—one led by the National Cancer Institute of Canada's clinical trial group, which he chairs, and another funded by the charity Cancer Research UK—are already under way. Each uses an AI from a different company: Letrozole is made by Novartis, the Canadian trial is testing a Pfizer drug, and the U.K. trial is testing an AstraZeneca drug. The Canadian and U.K. trials compare women given the test drug to those in control groups given a dummy pill. These placebo-controlled trials can get by with relatively small enrollments (4000 to 6000). In contrast, STELLAR will need to enroll 13,000 to find subtle differences between two active drugs. This means STELLAR will cost more and deliver results long after the others. Goss says that STELLAR's head-to-head comparison would give a more definitive reading on each drug, but he questions whether the results will come soon enough to affect clinical practice.

Niederhuber and others have mentioned another concern: Women may not be interested in STELLAR's results. For example, only a small fraction of those at risk for breast cancer have embraced tamoxifen as a preventative, despite its proven value. (The drug has serious side effects, including a risk of endometrial cancer and blood clots.) Whether AI drugs would be more popular is a guess. Cynthia Pearson, director of a cancer activist group, the National Women's Health Network in Washington, D.C., says she "would not be so sorry" if the STELLAR trial were set aside, because "I don't agree with the whole line … that breast cancer treatment drugs should be used in healthy women."

For these and other reasons, Niederhuber has put STELLAR on a list of projects that need to be reconsidered in light of NCI's tight 2007 budget. Many could be trimmed, he told NCI's Board of Scientific Advisors on 5 March. NCI is looking at reductions in tobacco-control research and seven intramural research projects, as well as potential 10% cuts in NCI's flagship comprehensive cancer centers, clinical trials, and the NCI director's budget.

–ELIOT MARSHALL

CREDITS (TOP TO BOTTOM): MARTY KATZ; SOURCE: OB/NIH

two phase filter

- Maximum protection against aerosols

- Binds biomolecules

- **ep Dualfilter T.I.P.S.** available in ten sizes

NEW! ep Dualfilter T.I.P.S.®

Stop aerosols!

Unique two-phase filter protection with ep Dualfilter T.I.P.S.®

The new Eppendorf ep Dualfilter T.I.P.S., with their unique two-phase filter, provide the perfect shield against contamination.

The filter consists of two visible phases, each with a different pore size. This two-phase filter protection ensures ultimate absorption of aerosols ❶ and biomolecules ❷, outmatching all conventional filters. Rely on it.

For more information go to
www.eppendorf.com/dualfilter

Features of the ep Dualfilter T.I.P.S.
Double protection provided by the two phase filter

- Provides maximum protection for both pipette and sample
- Ultimate absorption of aerosols and biomolecules
- Free from PCR inhibitor additives
- Patent pending two phase filter technology
- Supplied sterile, Eppendorf PCR clean and pyrogen-free
- IvD conformity
- Batch-related certificates available

eppendorf

In touch with life

Your local distributor: www.eppendorf.com/worldwide · Application Support: +49 180-3 66 67 89
Eppendorf AG · Germany · +49 40 538 01-0 • Eppendorf North America, Inc. 800-645-3050

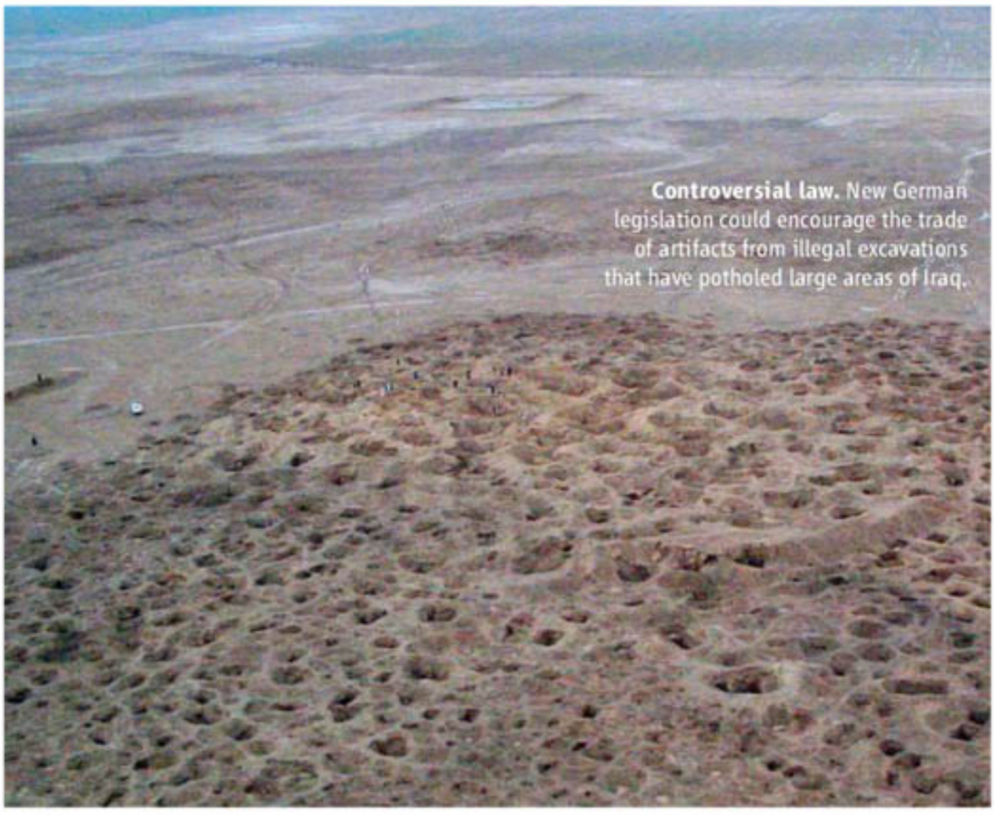

Controversial law. New German legislation could encourage the trade of artifacts from illegal excavations that have potholed large areas of Iraq.

CREDIT: DEUTSCHES ARCHÄOLOGISCHES INSTITUT, BERLIN

ARCHAEOLOGY

German Law Stirs Concern Illegal Artifacts Will Be Easier to Sell

Last week, the German Senate ratified the 1970 UNESCO Convention on Cultural Property, but archaeologists around the world fear that the long-delayed approval will do more harm than good. Many worry that Germany's interpretation of the convention will make the country a haven for illegally excavated antiquities from Iraq and elsewhere.

The UNESCO convention has been a defining document in the global battle to protect artistic and especially archaeological heritage from theft, looting, and destruction. Yet governments can make their own decisions on how to implement it. Whereas the United States and many of the other 112 signatories to the convention restrict or prohibit trade in broad categories of artifacts, the German law passed last Friday requires countries to publish lists of specific items they consider valuable to their cultural heritage. Only those items will be protected under German law, which means trade in undocumented artifacts, such as those looted from archaeological sites, will be difficult to restrict. "This is a bad signal," says Michael Mueller-Karpe, an archaeologist at the Roman-German Central Museum in Mainz. "It tells the world that whatever isn't published isn't worth protecting."

The idea of restricting specifically listed objects may make sense for museum collections but not for looted artifacts, say archaeologists. By the time they reach the market, such artifacts—Egyptian sculpture, Akkadian cuneiform tablets from Iraq, and Cambodian stone carvings, for instance—are typically stripped of the painstaking archaeological documentation and context that makes them scientifically valuable.

Still, Germany's implementation of the convention is well within the treaty's original requirements. "According to UNESCO, stolen objects have to be from documented collections," says Neil Brodie, research director of Cambridge University's Illicit Antiquities Research Centre. "There's no legal obligation for countries to treat illegally excavated objects as stolen." Mueller-Karpe calls the convention the "Grave-robbing Law" because he feels it encourages such theft.

Many countries have gone further than Germany in restricting the trade in illegally excavated artifacts. In the United States, for instance, dealers trading in certain categories of items are required to have export licenses from the country of origin or prove that the object has been out of the country of origin ▶

Sow Not Cool

A federal judge has ordered farmers to halt planting transgenic alfalfa seed, the first time that a court has withdrawn a genetically engineered crop from the market. The temporary injunction follows an earlier decision by the same judge that the U.S. Department of Agriculture (USDA) should have carried out a more rigorous assessment of the environmental risks of Roundup Ready alfalfa before the agency approved it in 2005 (*Science*, 23 February, p. 1069). USDA asked the court to allow continued sale of the seed during the required environmental impact study, but Judge Charles Breyer of the U.S. District Court in San Francisco, California, sided instead with environmental groups calling for a halt on planting. Farmers must stop plantings by 30 March, and Breyer will issue a final ruling after a 27 April hearing.

Daniel Putnam, an alfalfa specialist at the University of California, Davis, says that Breyer's decisions strike him as uninformed. The judge argued that the transgenic alfalfa could spread to nearby fields, but alfalfa is harvested before it produces seeds. The ruling "will cause very much consternation in agriculture," he says. **–DAN CHARLES**

Minds Closed to Open Access

Although fans of the concept, scientists remain reluctant to publish in open-access outlets, a new study suggests. The survey, led by information scientists at Munich University in Germany and the University of Arkansas, Little Rock, found that although two-thirds of 688 respondents—mainly information systems, German literature, and medical scientists from around the world—read open-access literature, only a third chose to publish their work that way. The majority viewed open access as faster (79%) and reaching a larger readership (75%) than traditional publishing. Yet many also believed that colleagues don't publish in open access (73%), that open access has deficient impact factors (58%), and that publishing via open access would damage their chances of tenure and promotion (60%).

Information scientist Ángel Borrego of Barcelona University in Spain says the survey, published last week, reiterates what others have called a "Jekyll-and-Hyde syndrome" in which scientists behave differently as readers than as authors. Matthew Cockerill, publisher of the open-access *BioMed Central*, says the study shows the need "to more clearly communicate the benefits of open access" and gain a "critical mass" of researchers publishing in open-access titles. **–ELISABETH PAIN**

since before the agreement went into effect. "The important part is the difference between designated categories and a list of specific objects," says Patty Gerstenblith, a professor at DePaul University College of Law in Chicago, Illinois. "A list simply doesn't work, because artifacts that are taken out of the ground are unknown."

Indeed, as more countries crack down on the trade of artifacts—the United Kingdom and Switzerland, long notorious as transit countries for illegal antiquities, ratified the UNESCO treaty in 2002 and 2003, respectively—German archaeologists fear that the country's loopholes could make it a destination where dealers turn stolen property into legal merchandise that can then be traded worldwide. Until now, objects with no proof of origin have been assumed stolen. But under the new law, if they're not listed, they can be presumed legal and potentially sold with Germany as their country of origin—making it easier to move them to the United States or elsewhere. "It's like an antiquities laundry," says Mueller-Karpe.

> "The new law won't make any improvement, and **the situation can't get much worse than it is right now.**"
>
> —Eckhard Laufer, German Task Force on Illegal Excavation

Eckhard Laufer, a police official and part of the German Task Force on Illegal Excavation, says the new law is a missed opportunity. "We'll have to wait and see, but I'm afraid it's totally inadequate," Laufer says. "The new law won't make any improvement, and the situation can't get much worse than it is right now."

German coin collectors and art and antiquities dealers counter that the new law is too strong. "Germany always does things 150%. The more strict the laws are, the more objects are going to go to a gray market," says Christoph von Mosch, a Munich art dealer with a degree in classical archaeology. Countries can now make claims on artifacts worth more than €1000 for up to a year after they are posted for sale, creating complications and paperwork that some dealers say puts them at a competitive disadvantage.

That it has taken Germany 36 years to ratify the original UNESCO convention doesn't bode well for prompt action on the 1995 UNIDROIT Convention, a much more stringent agreement that characterizes illegal excavation as theft and requires the return of stolen objects and cultural property. So far, only a few dozen countries have signed. Along with Germany, Brodie says, "none of the major market or transit countries"—including the United States, the U.K., Switzerland, France, and Belgium—"have ratified it."

–ANDREW CURRY

Andrew Curry is a freelance writer in Berlin.

CLIMATE CHANGE

Is a Thinning Haze Unveiling the Real Global Warming?

The sunlight-reflecting haze that cools much of the planet seems to have thinned over the past decade or so, remote-sensing specialists report on page 1543. If real, the thinning would not explain away a century of global warming, experts say, but it might explain the unexpectedly strong global warming of late, the accelerating loss of glacial ice, and much of rising sea levels. However, many other researchers are highly suspicious of the data and frustrated by the lack of any quantitative measures of their reliability.

The observations come from Advanced Very High Resolution Radiometer (AVHRR) instruments flown aboard weather satellites. Designed to measure cloud cover for weather forecasters, they can also measure the much weaker sunlight reflected from the aerosol particles of haze. And unlike newer, more precise instruments, they have been measuring aerosols since 1981.

Michael Mishchenko and his colleagues at NASA Goddard Institute for Space Studies (GISS) in New York City took advantage of AVHRR longevity to search for long-term trends in aerosols. Since the early 1990s, they say, the global aerosol layer has been thinning rather dramatically. "We can't claim it's 100% real," says Mishchenko. AVHRR is "not a very good instrument. It's just a weather satellite." But the data check out when compared with some ground-based observations and are broadly consistent with certain other satellite data, the authors write.

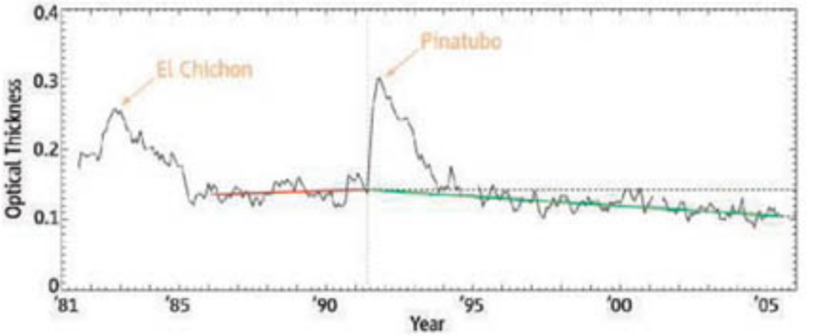

Down for real? Satellite data show a thinning of global hazes (declining green line), but calibration questions cloud the issue.

CREDIT: M. MISHCHENKO *ET AL.*, SCIENCE

If aerosols are really thinning that much, substantially more sunlight has been escaping reflection back into space and warming the planet. That extra energy, rather than an unrecognized quirk in the climate system, would explain the greater-than-forecasted warming of the 1990s and early 2000s that another team noted last month (www.sciencemag.org/cgi/content/abstract/1136843). The extra warming might in turn explain the accelerated loss of sea ice from the Arctic Ocean and from the great ice sheets, which feed rising seas.

First things first, however, say critics. "What [Mishchenko and colleagues] are trying to do is admirable," says Sarah Doherty of the University of Washington, Seattle, who has studied the calibration of AVHRR instruments. But "there's just too much uncertainty."

The problem, Doherty says, lies in part in stringing together records from five different instruments flown on five different satellites over the years. At times, the next instrument was not launched before its predecessor failed, preventing a precise calibration. Mishchenko and colleagues "need to say how well they know the uncertainties," she says. Without quantitative estimates of uncertainty, she can't tell whether the trend is real.

–RICHARD A. KERR

CARBON EMISSIONS

Report Backs More Projects to Sequester CO_2 From Coal

A new academic study of capturing and storing carbon emissions from coal burning—the 800-pound gorilla in the climate policy debate—says that billions of dollars in demonstration projects are needed to help put the ape in a cage.

Worldwide, the 5.4 billion tons of coal burned each year generate roughly a third of the world's carbon dioxide emissions. But coal's low cost compared to other energy sources makes it irresistible to nations with plentiful deposits. China, for example, weekly puts online two new coal-fired generating plants. This week, scientists at the Massachusetts Institute of Technology (MIT) in Cambridge, led by physicist Ernest Moniz and chemist John Deutch, propose policy and research to help governments achieve big cuts by capturing and burying the CO_2 (web.mit.edu/coal). The study describes a number of daunting technical hurdles and warns against a "rushed attempt" to deploy the two leading technological fixes before the science is mature.

That cautionary note has sparked criticism from more bullish experts. "We know enough technologically to do it today," says mechanical engineer George Peridas of the Natural Resources Defense Council in Washington, D.C., which wants new plants to be forced to include technology to capture carbon emissions. "From a climate perspective, the risk [of waiting] is huge."

Using a computer model, MIT researchers examined how charging utilities a global price for emitted carbon dioxide (either $7 or $25 per ton) might impact coal consumption by 2050. The scenarios suggest that the policies "will limit" the expected growth in the use of coal but not bring it below current levels. Improvements in the process of capturing emitted carbon and sequestering it underground will therefore be "critical," the report's authors say. The study calls for the U.S. Department of Energy (DOE) to continue funding technologies for capturing carbon from the two main ways of burning it: pulverized coal (PC) and integrated gasification combined cycle (IGCC). PC plants grab CO_2 just before emissions travel to the smokestack; IGCC plants remove the gas after the coal is gasified but before it is burned.

The report calls on the U.S. government to spend up to half a billion dollars a year to subsidize demonstration projects run by partnerships with the private sector. It says that FutureGen, the current DOE effort to demonstrate a carbon-capturing IGCC facility by 2012, lacks "clarity of purpose." It also faults DOE's assessment of U.S. geologic sequestration sites as "not uniform"—an atlas due out in May omits detail on coal-rich regions in Wyoming, for example—preferring a national map prepared by the U.S. Geological Survey.

Drill squad. A new report recommends scaling up work on carbon sequestration, such as this study of saline formations by DOE geochemists.

Experts praise the report's support for demonstration projects but criticize its technology-neutral stance on the competing technologies. Joseph Chaisson of the Clean Air Task Force in Boston says the report uses "out-of-date" data that blunt the comparative advantage for IGCC, adding that utilities are actively exploring new industrial gasifiers. Geologist Susan Havorka of the University of Texas, Austin, questions the report's emphasis on giant injection sites as test beds, saying that ongoing "small tests" can give important clues in tracking CO_2 behavior.

Moniz says the group accounted for recent industry progress, but that there are too many unknowns to favor one technology. A plant built now with one capture technology would be hard to retrofit for a different one. "It's not as simple as just dropping in" a sequestration module, he says. Meanwhile, some companies are moving forward. Last week, a group of investors and Dallas-based TXU announced plans to build two IGCC demonstration plants.

–ELI KINTISCH

CREDIT: LAWRENCE LIVERMORE NATIONAL LABORATORY

SCIENCESCOPE

Like a Rock

NASA told U.S. lawmakers last week it doesn't have the money to track the vast majority of asteroids that might threaten Earth, a goal set by Congress. Even so, the space agency is quietly examining how to send two or three humans to an asteroid as a trial run for a return to the moon.

The 90-day mission would allow NASA to test its new Constellation rocket, provide physiological and psychological data on deep-space flights, and study asteroids "to refine impact physics models," according to a 5 February report by the office in charge of building a new human launcher. The study argues that the trip, possibly by 2017, could put humans "on the way to Mars while producing exciting new science." Carl Walz, a NASA exploration manager, says NASA has no plans to push for such a mission.

–ANDREW LAWLER

NOAA Pushes Fish Farms

Hoping to help expand fish farming into offshore waters, the National Oceanic and Atmospheric Administration (NOAA) this week proposed setting up a permitting system and environmental regulations, as well as requiring studies on how to make the farms more ecologically sustainable. A 2005 bill that contained similar provisions faced tough opposition on environmental issues in Congress. We "heard the concerns," says NOAA Fisheries Service Director William Hogarth. So the new proposal includes calls for monitoring of disease and fish escape and requires an assessment of economic impacts on fishing communities. It would also require research to devise new feed that doesn't require as much wild fish. Hogarth hopes the legislation will be introduced by a lawmaker quickly, although Gerald Leape of the National Environmental Trust in Washington, D.C., calls the effort a "tough lift" due to powerful lawmakers wary of new competition for fishing industries in their states.

–ERIK STOKSTAD

X-rays in Chinese Sights

As part of its quest spaceward, China has set 2010 as the launch year for its first satellite observatory, an x-ray telescope. The instrument will keep a close eye on black holes and other phenomena by detecting photons with energies above 20 KeV. Chief project scientist Li Tipei of Qinghua University in Beijing told Chinese reporters last year that the imaging telescope would have world-class sensitivity and spatial resolution among x-ray instruments.

–HAO XIN

Asking for the Moon

Thanks to several upcoming robotic missions, lunar science is poised for its biggest boost in a generation. But NASA managers have made it clear that research will be the tail on the exploration dog

TEMPE, ARIZONA—Fashion isn't restricted to Paris runways. A decade ago, space scientists became enamored with the possibility of past life on Mars. More recently, moons such as Europa, Titan, and Enceladus captured the imagination of researchers. Soon, Earth's only satellite will get a chance to strut her stuff again, after being out of style for more than 3 decades. Four countries—Japan, India, China, and the United States—are preparing to launch robotic lunar probes in the next 18 months. China is planning a human mission, and NASA is pushing ahead with plans for a human outpost by the end of the next decade based on a 2004 vision laid down by President George W. Bush.

With the moon back in the footlights, the question for U.S. scientists is whether lunar science can sustain funding for a long-term research program. Science has always played second fiddle to engineering human flight at NASA, and the new exploration program is no exception. As NASA Administrator Michael Griffin bluntly told the 250 scientists who gathered here last week at the request of NASA's Advisory Council, a return to the moon "is not all about you." If scientists want a dedicated human research sortie, he added, they'll need to find the $2 billion or so it would cost.

That message, along with NASA's recent decision to shelve a series of lunar robotic missions, stunned some participants. "The rather pessimistic view of lunar science outlined by Mike Griffin," says Brown University geologist Carle Pieters, left her "depressed and discouraged." Yet she and other scientists say they want to be involved in lunar planning. A weeklong session generated a long list of intriguing projects to pursue, along with advance word from a National Research Council (NRC) panel now studying lunar science that its report would urge NASA to ramp up funding for such research. "We don't want to preclude what could be a fascinating scientific opportunity," says Neil Tyson, an astronomer at the American Museum of Natural History in New York City. "The ship is leaving the dock, and the question is whether we'll be on it."

Back to the future

The gathering in Tempe hearkened back to a 1965 meeting on Massachusetts's Cape Cod that gave researchers an opportunity to inject scientific research into the Apollo program. Harrison Schmitt, a geologist who went on to become the first and only scientist to visit the moon and now chairs the agency's advisory council, was so impressed by the meeting that he asked NASA to repeat it. Schmitt says he overcame NASA's initial resistance by arguing that it needed a clear set of scientific priorities.

The early days of lunar science benefited greatly from the Cold War race to the moon. The United States and the Soviet Union sent more than 60 robotic missions—crash landers, soft landers, orbiters, sample returns—between 1958 and 1976. And that 18-year tally doesn't count the nine piloted Apollo flights that circled or landed on the lunar surface. By contrast, only four missions have visited the moon in the last 31 years.

Scientists still know remarkably little about Earth's satellite. Pressing scientific questions include why the moon's magnetic field appears to have shut off, how dust and plasma interact near the surface, and the nature of hydrogen deposits at the poles. The Apollo soil samples are insufficiently diverse to answer fundamental geological questions because they were drawn largely from the maria in the mid-latitudes of the moon's near side. The solar system's largest hole—the Aitken Basin near the south pole—has yet to be explored, and Mars has been mapped more accurately than the moon's pockmarked surface, which contains clues to the extent and timing of the heavy bombardment that shaped the early solar system. Like Greenland's ice cap, the moon's undisturbed layers preserve a long history—for example, a concise record of the sun's radiance over billions of years.

Scientists soon will have a shot at answering these and other questions. This year, Japan will launch a 3-ton, 14-sensor probe called Selene. China is completing work on Chang'e 1, which will examine the lunar crust and temperature and the space environment between Earth and the moon. Next year, India plans to send Chandrayaan-1,

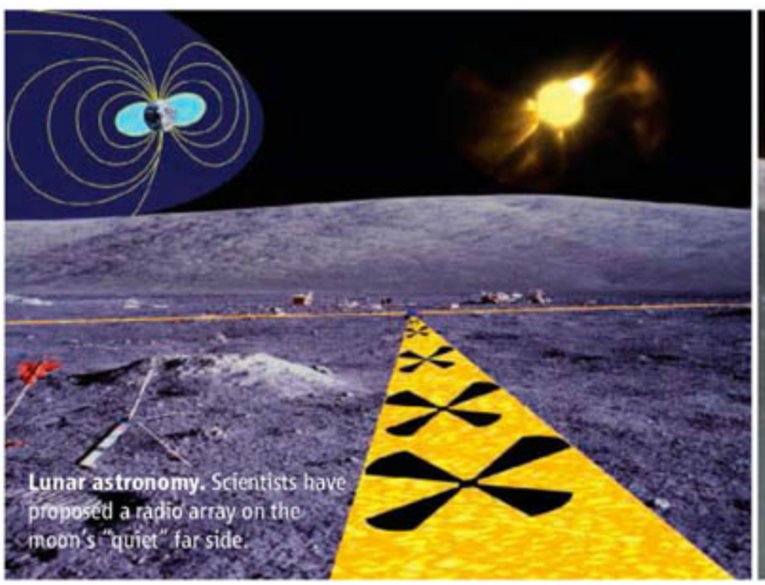

Lunar astronomy. Scientists have proposed a radio array on the moon's "quiet" far side.

Old digs. Geologist Harrison Schmitt on the lunar surface during the last Apollo mission in December 1972.

CREDITS (LEFT TO RIGHT): NAVAL RESEARCH LABORATORY; AP

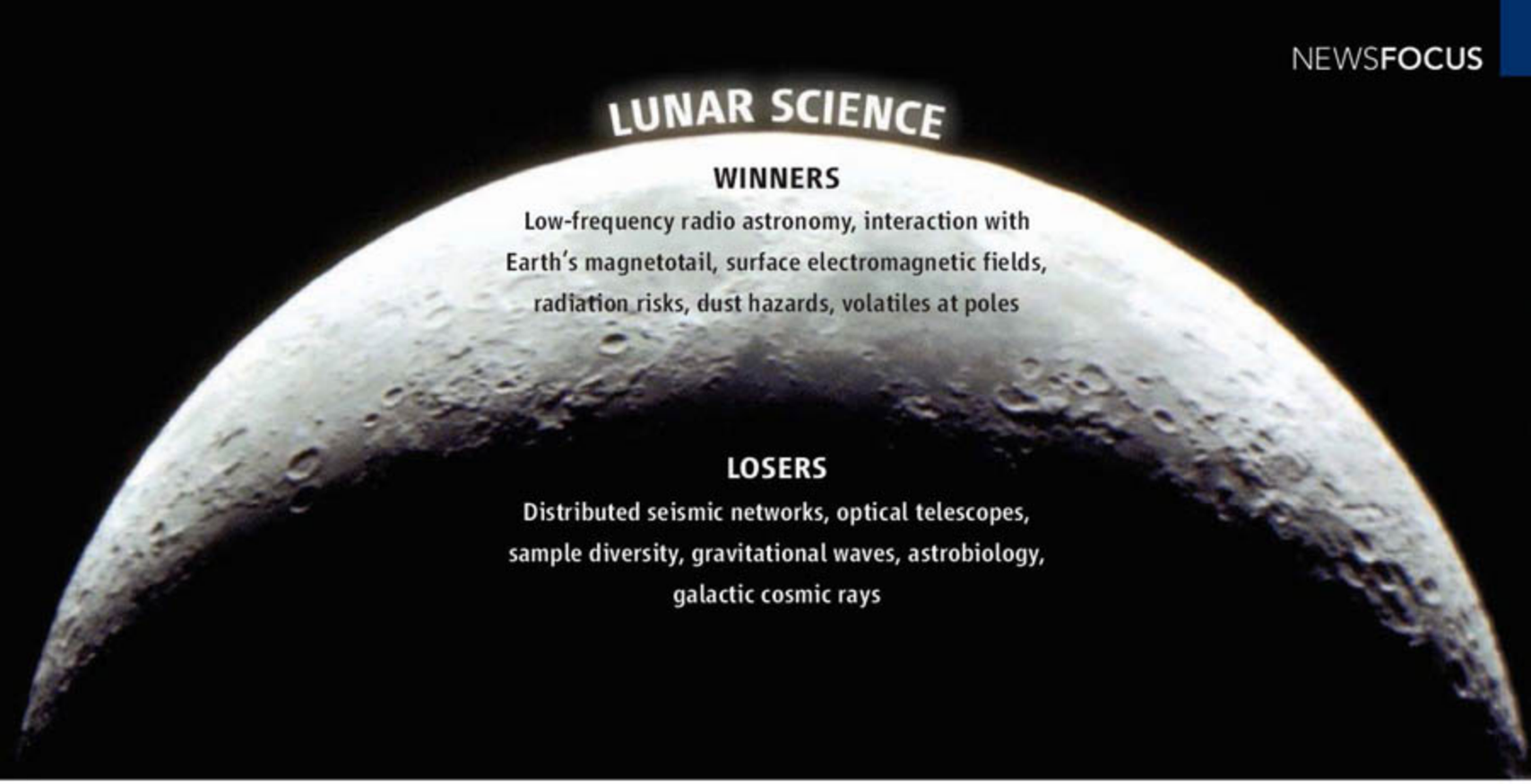

CREDIT: JUPITER IMAGES

with a NASA-funded instrument on board, around the moon, followed by a more ambitious sample-return mission in 2010. "Chandrayaan-2 will have a lander that will touch down on the lunar surface and pick up samples," says G. Madhavan Nair, chair of the Indian Space Research Organization. And German officials recently said they are considering building a lunar probe outside the umbrella of the European Space Agency, which launched a 2003 moon orbiter but has no plans for further flights.

Meanwhile, NASA is readying the Lunar Reconnaissance Orbiter (LRO) for a late 2008 launch. It's designed to provide detailed maps of the moon to assist in planning for human missions. That mission will last a year, after which NASA scientists will take over its operation.

NASA plans to boost its lunar funding from $27 million in 2008 to $97 million in 2011. That pot will help cover the cost of operating LRO as well as paying for small instruments to go aboard foreign probes such as Chandrayaan-2. In addition, NASA officials promise to make more money available for scientists to analyze data from both U.S. and foreign spacecraft. "There is a real richness of data" headed to Earth, says Pieters, who is co-chair of the NRC panel. She says the panel's report will urge greater international cooperation on lunar robotic efforts.

Visioning science

LRO's central mission, however, is not science. The spacecraft is the first step in NASA's march to send humans back to the moon by 2020. The agency's exploration agenda begins with finishing the space station and retiring the space shuttle in 2010, followed by a 2015 launching of a large new rocket. Aside from LRO, there's no room for research during the first decade of the exploration effort; NASA just put on hold a series of orbiters and landers after LRO that could provide exploration—and science—data prior to the arrival of humans.

Scott Horowitz, NASA's exploration chief, says that those robotic missions would be nice to do—if the agency had the money. All he really needs, he told the scientists, is "a damn good map," which LRO will provide. He made it clear his interest is not in blue-sky research. "We don't have to get rocks back."

And the role of science even once humans arrive remains tenuous. In December, NASA decided to build an outpost rather than send a series of missions to several locations. That disappointed scientists hoping to collect a variety of lunar samples—an important goal highlighted in the NRC interim report—and build a distributed seismic network. Griffin, however, says the base gives potential foreign partners the chance to contribute in a manner similar to their involvement with the space station. It also creates opportunities for space tourism and the possibility of exploiting potential resources such as water, ice, and minerals. "We're not going back to the moon and on to Mars solely for science," Griffin reminded the Tempe audience.

The base, tentatively planned for the rim of the south pole's Shackleton Crater, would initially be home to a crew of four staying for 1 to 2 weeks, says Laurie Leshin, science and exploration chief at NASA's Goddard Space Flight Center in Greenbelt, Maryland. Astronauts could travel a few kilometers around the landing site and collect up to 100 kilograms of lunar samples. Griffin envisions the base as analogous to the U.S. National Science Foundation's McMurdo Station in Antarctica, which serves as a logistics and transportation hub for research across the continent.

But Leshin acknowledged that "science might be deferred" in the early stages of exploration. And in Tempe, Griffin stopped short of saying that there will be a permanent human presence at the outpost. "Our return to the moon is as a training ground, a step along the path to Mars," he said.

Although Griffin and Horowitz downplayed the role of research, scientists used the meeting to generate a host of ideas for projects that could be conducted from the lunar outpost, including the study of nearby regolith, volatiles, impact craters, the solar wind, and a low-frequency radio observatory on the far side, in the quiet zone protected from noisy Earth. "This is the most exciting experiment which could be done from the surface of the moon," says Mario Livio, an astrophysicist at the Space Telescope Science Institute in Baltimore, Maryland.

But the researchers also concluded that the highest-priority lunar science missions

Taking a Stern Look at NASA Science

Finding room for lunar research in NASA's $5.4 billion science budget is one of many challenges facing Alan Stern, who next month takes over the troubled program. He's a planetary scientist from the Southwest Research Institute in Boulder, Colorado, and a one-time astronaut candidate. Last week, during a meeting with the National Academies' Space Studies Board, Stern pledged to wring more science out of a flat budget and find ways to ease controversial cuts to university grants.

Stern's portfolio includes nearly 100 projects in space or being readied for launch. But several are mired in cost overruns. Two years ago, the price tag for the biggest item, the James Webb Space Telescope, shot up more than $1 billion to $4.5 billion, although its costs now seem under control. More recently, NASA was forced to budget 10% more for the $250 million Orbiting Carbon Observatory, slated for launch next year to collect precise measurements of carbon dioxide in Earth's atmosphere, and the $1.69 billion Mars Science Laboratory rover, which will leave Earth in 2009.

Not surprisingly, those larger mortgages are squeezing everything else. Some disciplines, such as astrobiology, face dramatic cuts (*Science*, 19 January, p. 318), and NASA has no plans for major earth science missions in the next decade. To make matters worse, last year, NASA chief Michael Griffin froze the science budget after ordering $3.1 billion in cuts to the 5-year plan for science to cover shortfalls in the space shuttle and space station programs.

Stern hopes to ease the crisis through "innovative thinking" rather than any additional funding. "We're living in a zero-sum game," he told the academy panel. He plans to save some money by cutting back on what he deems the agency's excessive oversight of small satellite projects. "We've shot ourselves in the foot," he says about well-meaning attempts to avoid failure that have substantially added to costs.

Sober forecast. Alan Stern warns scientists they're playing a zero-sum game.

A recent academy report calling for a new flotilla of earth science platforms is out of step with the available resources, he says. He's even willing to consider killing a space mission if it's the only way to preserve a robust budget for research and analysis, which is mostly conducted by academic scientists.

Stern warns that long-running missions may need to be turned off to make room for new projects. "There are going to be things that I do that cause pain," he says. He's also decided to recuse himself from a mission competition to examine Mars's atmosphere, in which he had hoped to play a lead role. At the same time, he plans to remain principal investigator of the Pluto mission that just passed Jupiter.

–A.L.

could be done better, faster, and more cheaply using robots. And they agreed that, with the exception of the radio observatory, the moon is a poor place to conduct astronomy or Earth sciences.

Even so, the results of NASA's multibillion-dollar vision could trickle down to science. The new heavy-lift launcher could orbit space telescopes with mirrors 10 meters across when it isn't ferrying humans to the moon. And new spacecraft systems could lay the groundwork for a new generation of sophisticated planetary probes. "Science is not a priority in the vision, but unless scientists voice what their needs are, nothing is going to happen," says Livio. "We'd like to ensure they include the capabilities which could be used for space science."

And there is still the possibility that robotic missions could prove critical for exploration after LRO. Some NASA officials predict that the agency will need to study the effects of moon dust and radiation on equipment and astronauts, as well as to follow up LRO observations on potential water at the lunar poles. And NASA's Ames Research Center in Mountain View, California, is proposing a set of $100 million missions that could deliver 50 kg of payload to orbit or 10 kg to the surface. Paying for them is another matter, however, as the budgets of both the exploration and science offices are being squeezed.

Dual mission. The 2008 Lunar Reconnaissance Orbiter will be turned over to scientists after scoping out possible landing sites.

NASA's science office is already considering some lunar projects as part of its regular mission competitions. Geophysicist Maria Zuber of the Massachusetts Institute of Technology in Cambridge has proposed examining the lunar gravitational field and the moon's interior structure using an orbiter. And planetary scientists agreed in a 2003 NRC decadal survey of their discipline that a robotic mission to the Aitken Basin is a high priority; NASA may consider such a mission in the near future.

Some researchers worry that lunar science is a passing fad that may not last into the next administration. "A lot of scientists I know are staying away from this" because they expect the vision to collapse once Bush leaves office in 2009, says Lucy Fortson, an astronomer at the University of Chicago in Illinois.

However, those who have been waiting patiently for more than 3 decades welcome the resurgence of interest in lunar research and don't mind that science isn't in the driver's seat. "The moon is now front and center, and the lunar community is quite comfortable with the fact that science is not the preeminent activity," says astronomer Wendell Mendell of NASA's Johnson Space Center in Houston. "We've been waiting for so long, it's good to have anything."

–ANDREW LAWLER

With reporting by Pallava Bagla.

CREDITS (TOP TO BOTTOM): JUD MCCREHIN; NASA GODDARD SPACE FLIGHT CENTER

EDUCATION RESEARCH

U.S. Math Tests Don't Line Up

The latest national assessment of high school achievement can't be compared with previous ones, the government says. Does no trend mean no progress?

For more than 3 decades, the National Assessment of Educational Progress (NAEP) has monitored how much U.S. students know in a variety of subjects. The recent trends for 12th-grade mathematics are disturbing: Scores haven't improved, and U.S. students rank near the bottom on international comparisons. So math experts around the country eagerly awaited the latest trend data, based on a test taken by 9000 high school seniors in 2005. The government's answer last month turned out to be a surprising "we don't know."

Officials at the Department of Education's National Center for Education Statistics (NCES), which runs the program, say that the 2005 scores cannot be compared to the 1996 and 2000 assessments. The 2005 test contained more algebra and less numeracy, it used a different format, and students were allowed to bring their own calculators rather than use ones provided at the test site. "We wanted to offer some sort of comparison," says Peggy Carr, NCES's associate director. "After all, NAEP is about educational progress, and for that you need trends. But we decided in the end that there were too many changes."

Race to the bottom. The last three NAEP tests show that a shrinking share of high school seniors have even basic math skills—and the racial gap persists.

IMAGE: GETTY IMAGES; SOURCE: NATIONAL CENTER FOR EDUCATION STATISTICS

The new test was intended to be more rigorous than previous versions, explains Mary Crovo of the National Assessment Governing Board (NAGB), which sets policies for NAEP. But after the board approved the changes in content, she says, testing experts advised that it had also lost the ability to draw any comparisons with the 2000 test. Psychometricians say that the gold standard would have been a bridging study: having one set of students take the 2000 test and a matched sample take the 2005 test, both under the 2000 rules. Any scoring difference could then reliably be attributed to a student's knowledge of mathematics. No bridging study was done, although Carr and Crovo disagree on the reasons. "It was a funding decision by NCES," says Crovo. Carr says, however, "we initially thought that we should do one, but NAGB said it wouldn't be appropriate because [the 2005 test] used a new framework."

An outside study funded by the department did, however, find some basis for comparison. After analyzing answers to the 60% to 65% of the questions on the two tests that were identical, researchers at the Human Resources Research Organization (HumRRO) in Alexandria, Virginia, found evidence that there were "probable gains in 12th-grade mathematics between 2000 and 2005." Although the report (posted at humrro.org) is studded with caveats, it finds that the calculator policy had "minimal affect, if any," and that the new format may actually disguise a larger real gain.

Whether the 2005 NAEP scores can be compared with those of earlier tests is more than a simple disagreement among psychometricians. Although the NAEP is not part of the state-by-state assessment of student achievement mandated under the federal No Child Left Behind Act, the test matters. Proponents of national standards see NAEP as a promising way to achieve their goal in the face of the famously decentralized U.S. educational system (*Science*, 2 February, p. 595). Even the Bush Administration, which cherishes the principle of local control, has dubbed NAEP "the nation's report card" to emphasize its importance.

The comparability of the two tests also has bearing on efforts to erase the sizable achievement gap between white and Asian students, on the one hand, and their African-American and Hispanic peers on the other. Using a three-point scale—basic, proficient, and advanced—to measure achievement, the 2005 NAEP test found that a staggering 39% of U.S. high school seniors lack even a basic understanding of high school mathematics. That's up from 35% in the 2000 test and 31% in 1996. Using that same scale, the large achievement gap by race and ethnicity has persisted. The 2005 test reports that some 70% of blacks and 60% of Hispanics fell below that minimal cutoff, compared with 30% for whites and 27% for Asian-Americans. In a depressing spiral to the bottom, the percentage of students from each racial and ethnic group falling below "basic" has increased from 1996 to 2005.

For many math educators, what's most depressing is that changes in NAEP results, if any, are minimal. The HumRRO analysis estimates an increase of three to five points on a scale of 300, a bump-up consistent with the recent pattern in math scores for elementary and middle school students. "A three-point gain seems about right to me," agrees Tom Loveless, director of the Brown Center for Education Policy at the Brookings Institution in Washington, D.C., and co-author of a 2006 study comparing student achievement on NAEP and state assessments.

"Even if you could compare the two tests, there are clearly no major improvements" in the mathematical abilities of U.S. high schoolers, says William Schmidt, U.S. coordinator for the 1995 Third International Mathematics and Science Study, which revealed a growing achievement gap between U.S. students and the rest of the world as they move through the educational system. "I'm not surprised," says Schmidt, a math educator at Michigan State University in East Lansing. "The country hasn't made a commitment to the sort of rigorous and demanding curriculum that is needed to raise achievement." Until that happens, he says, nothing will really change. And once it does, the results should be obvious to everyone.

–JEFFREY MERVIS

Floating laboratory. *Sorcerer II*, a private yacht outfitted to collect and freeze microbial samples, netted a huge bounty of DNA sequence.

METAGENOMICS

Ocean Study Yields a Tidal Wave of Microbial DNA

Data glut or unprecedented science? A global hunt for marine microbial diversity turns up a vast, underexplored world of genes, proteins, and "species"

After relishing the role of David to the Human Genome Project's Goliath, J. Craig Venter is now positioning himself as a Charles Darwin of the 21st century. Darwin's voyage aboard the H.M.S. *Beagle* 170 years ago to the Galápagos Islands netted a plethora of observations—the bedrock for his theory of evolution. Four years ago, Venter set sail for the same islands and returned 9 months later with his own cache of data—billions of bases of DNA sequence from the ocean's microbial communities. But whether that trip will prove anything more than a fishing expedition remains to be seen.

On 13 March, Venter, head of the J. Craig Venter Institute in Rockville, Maryland, and a bevy of co-authors rolled out 7.7 million snippets of sequence, dubbed the Global Ocean Sampling, in a trio of online papers in *PLoS Biology*. As a first stab at mining these data, which have just become publicly available to other scientists, Venter's team has found evidence of so many new microbial species that the researchers want to redraw the tree of microbial life. They have also translated the sequences into hypothetical proteins and made some educated guesses about their possible functions.

Some scientists are wowed by the effort. Others worry that researchers will not be able to make sense of all this information. The diversity of microbes uncovered is "overwhelming, … tantamount to trying to understand the plot of a full-length motion picture after looking at a single frame of the movie," says Mitch Sogin, a molecular evolutionary biologist at the Marine Biological Laboratory in Woods Hole, Massachusetts. And Venter doesn't necessarily disagree. In 2004, as the data were first rolling in, Venter confidently predicted that his salty DNA survey would "provide a different view of evolution." To make that happen, however, he now says, "we need even more data."

Microbial explorers. J. Craig Venter (*left*) and Anthony Knap of the Bermuda Biological Station for Research aboard Venter's yacht.

The big trawl

This is the second time that the American millionaire genome sequencer has returned to port laden with DNA. Venter's 2004 study of microbes living in the Sargasso Sea was easily the largest DNA sequencing of environmental samples ever accomplished (*Science*, 2 April 2004, p. 66). This time around, he sailed from Halifax, Canada, through the Panama Canal and finished up 6500 kilometers southwest of the Galápagos. The funding for the $10 million project came from the Gordon and Betty Moore Foundation, the U.S. Department of Energy, and Venter's nonprofit foundation. The research vessel, the *Sorcerer II*, is Venter's private yacht tricked out as a floating laboratory.

The researchers sampled at 41 locations, isolating and subsequently freezing bacterium-sized cells. They also recorded the temperature, salinity, pH, oxygen concentration, and depth.

Back at Venter's institute, technicians extracted and sequenced the DNA. Using a whole-genome shotgun approach, they shattered all the DNA in a sample into fragments of specific sizes, sequenced each one, and then assembled these sequences together by matching the ends of the DNA with a powerful overlap-hunting computer program. In principle, this approach allows the reconstruction of entire genomes of the different organisms in a sample.

Three years and 6.3 billion bases of DNA sequence later, at least one thing is clear: The DNA in a typical community of marine microbes is so diverse that nothing close to a whole genome can be assembled, even with all the sequencing that Venter has mustered. Half of his 7.7 million DNA sequence fragments are so different that they could not be linked at all.

Nonetheless, the researchers could estimate the number of species in the samples based on slowly evolving marker genes. Judging by these glimpses of genomes, Venter's team identified more than 400 microbial species new to science, and more than 100 of those are sufficiently different to define new taxonomic families, they report. "This is a great milestone event" for environmental microbiology, says Dawn Field, a molecular evolutionary biologist at the Centre for Ecology and Hydrology in Oxford, U.K., who predicts that "these papers will become among the most highly cited of all time in biology."

Diversity deep end

The fact that Venter's brute-force sequencing approach fell short of capturing whole genomes shows that scientists are far from a full accounting of the species packed in a drop of seawater, says David Scanlan, a

CREDITS (TOP TO BOTTOM): J. CRAIG VENTER INSTITUTE

marine microbiologist at the University of Warwick, U.K. And this "astounding" genetic diversity points to what Scanlan and others call the "paradox of the plankton."

Traditional ecological theory predicts that when multiple species compete for the same resources—in the case of ocean microbes, light and dissolved nutrients—then one, or a few, species should eventually outcompete the rest. If that were the case, then many of the sequences plucked from the waters by Venter's crew should map down onto a few dominant genomes.

But rather than a sharp portrait of a few different microbes, the data create a pointillist painting of a countless mob. The vast majority of the microbes that found themselves snared in Venter's filters were genetically unique, says Scanlan: "It's a clear message that there's a tremendous gene pool in the ocean."

The diversity itself could be the solution to the paradox, according to Douglas Rusch, a computational biologist at the Venter Institute, and his colleagues. The staggering variety of genes may endow each species with sufficiently different metabolic tool kits to take advantage of slightly different combinations of resources, including the waste products of others, such that they can all coexist.

The newly detailed diversity also suggests that microbial taxonomy needs a major overhaul, says Ian Joint, a marine microbiologist at the Plymouth Marine Laboratory in the U.K. The current taxonomy carves up microbes into different "ribotypes" by comparing the sequence of the highly conserved genes of the protein-synthesizing ribosome. Because there is so much diversity within the DNA even after dividing them into ribotypes, Venter's team proposes to throw out ribotyping altogether. Instead, they are defining groups of microbes based on the environment in which they were collected and how well their DNA matches a reference set of fully sequenced marine microbial genomes. Doing so has allowed Venter's team to group sequence fragments into different "subtypes." Venter's team says that each of these subtypes represents a "distinct, closely related population" of microbes that fill a particular niche in their local environment. However, many more marine microbial genomes must be sequenced to make this scheme work, says Joint.

SOURCE: J. CRAIG VENTER INSTITUTE

Marine data-mining

The samples brought to port by *Sorcerer II* do more than shake up microbial taxonomy. Based on their best guess as to the beginning and end of each gene teased out from the DNA sequences, Venter Institute computational biologist Shibu Yooseph and his colleagues have concluded that the DNA encodes 6.12 million hypothetical proteins. That finding almost doubles the number of known proteins in a single stroke. It also shows that the end of protein diversity is not in sight, says David O'Connor, a molecular biologist at the University of Southampton, U.K. Most of the predicted proteins are of unknown function, and a quarter of them have no similarity to any known proteins. Venter expects that some of these can be exploited to develop new synthetic materials, clean up pollution, or bioengineer fuel production.

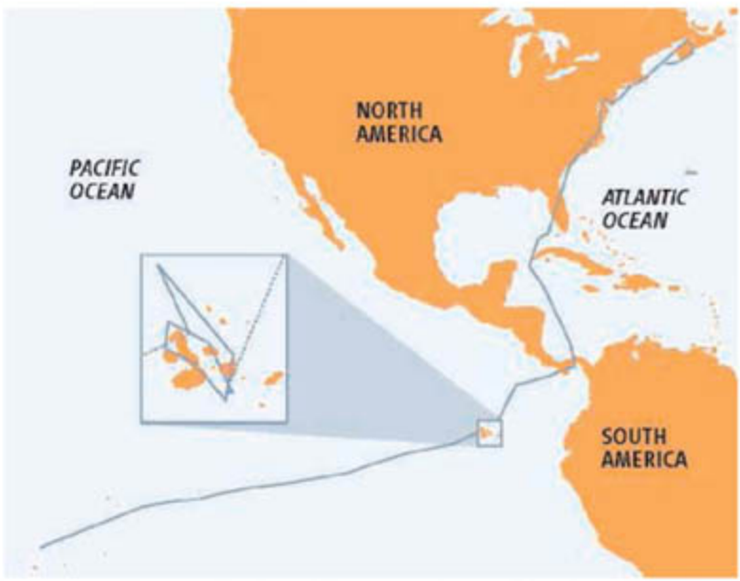

Taking stock. *Sorcerer II* collected bacteria at dozens of sites in the Atlantic and Pacific, particularly around the Galápagos Islands (*inset*).

But the hypothetical proteins are already offering a new view of basic microbial biology. A team led by Venter and Gerard Manning, a computational biologist at the Salk Institute for Biological Studies in San Diego, California, says that the current picture of the proteins responsible for coordinating marine microbes' gene expression and metabolism is off the mark. By comparing predicted amino acid sequences with those of known proteins, they found a surprising abundance of signaling proteins thought to be used only by multicellular organisms. Among the hypothetical proteins from their marine samples, the researchers found 28,000 of the so-called eukaryotic protein kinases, as well as another 19,000 of a group that are highly similar to these kinases—triple the number previously known.

These analyses of Venter's metagenomic data hint at the work that lies ahead for protein researchers. "Claims by some biologists that complete catalogs of the protein universe would be attainable within a decade now look naïve," O'Connor points out.

Thus to some, the data produced by Venter's voyage are an exciting starting point for protein, gene, and microbe discovery. It's something "people will be working on for quite some time," says Howard Ochman, a molecular evolutionary biologist at the University of Arizona in Tucson. But for others, the value of this tidal wave of data is uncertain. James Prosser, a molecular biologist at the University of Aberdeen, U.K., worries that adding all of this sequence to the existing gene and protein databases could "swamp" the system, cluttering the results of searches for well-characterized genes.

To help researchers deal with not just Venter's 100 gigabytes of sequence data but also other relevant information about a microbe's environment and location, Venter's team and Larry Smarr, a computer scientist at the California Institute for Telecommunications and Information Technology in San Diego, have built a metagenomics version of GenBank, the online genetic database curated by the National Center for Biotechnology Information in Bethesda, Maryland. In addition to doing the typical gene searches and genome comparisons, the new system, known as the Community Cyberinfrastructure for Advanced Marine Microbial Ecology Research and Analysis (CAMERA), can hunt for correlations between DNA sequence and environment for clues about co-occurring microbes. So far, however, CAMERA has only a few active users.

A more serious drawback of Venter's study, says Prosser, is that the samplings do not appear to have been carried out with any specific scientific hypotheses or aims in mind. The cynical view is that these are little more than "fishing trips," he says. "There would be greater potential for scientific advances if more focused, better designed studies were carried out."

Will the voyage of the *Sorcerer II* live up to Venter's hopes? It took Darwin 25 years after returning from his expedition to publish his theory of evolution. With the three papers online this week, Venter, at least, has hopped on the fast track. But in terms of synthesizing the big picture of marine microbiology, he and his colleagues are still out to sea. **–JOHN BOHANNON**

Tall order. Starches and sugars in corn kernels readily ferment into alcohol; corn stalks are more challenging.

CELLULOSIC ETHANOL

Biofuel Researchers Prepare To Reap a New Harvest

After decades in the background, technology for converting agricultural wastes into liquid fuels is now poised to enter the market

When U.S. President George W. Bush announced an initiative in January to reduce U. S. gasoline use by 20% in 10 years, critics could be forgiven for thinking it sounded familiar. Presidents since Jimmy Carter have called for reducing U.S. dependence on foreign oil. But so far there's been little to show for it. Shale oil, electric cars, and hydrogen fuel cells have all at one time or another had their 15 minutes of fame. But all have failed to make a dent in U.S. gasoline use.

Today, biofuels are the alternatives du jour, with ethanol chief among them. And in the United States, that currently means corn ethanol. But the big hope for the field is a technology called "cellulosic ethanol," which aims to turn all kinds of plant material—from corn stalks and wheat straw to forest trimmings—into fuel. According to a 2005 study by the U.S. departments of Energy and Agriculture, the U.S. could convert 1.3 billion dry tons a year of biomass to 227 billion liters (60 billion gallons) a year of ethanol with little impact on food or timber harvests and in the process displace 30% of the nation's transportation fuel. Not bad for what amounts to a lot of unwanted yard waste.

No commercial cellulosic-ethanol plants exist today. But despite the failures of previous alternative fuels, decades of research in biotechnology, chemistry, and chemical engineering are merging to bring cellulosic-ethanol technology to the verge of a payoff. A host of small and large chemical companies have jumped into the area, propelled by recent high gas prices and nearly $2 billion in private and venture-capital funding for biofuels last year alone, according to London-based research firm New Energy Finance. A handful of cellulosic-ethanol demonstration plants have popped up as a result. And last month, the U.S. Department of Energy (DOE) announced awards of $385 million for six commercial-scale cellulosic-ethanol refineries (see table, p. 1489) that are expected to produce more than 130 million gallons of ethanol per year.

That's still just a small fraction of the some 5 billion gallons of corn-based ethanol produced in the U.S. annually. But confidence in the new technology is riding high. Experts believe that scientific successes are now coming in a steady stream, which should progressively improve the technology and chip away at ethanol prices. "I think we will be there with cellulosic ethanol much more quickly than anybody realizes," says Bruce Dale, a chemical engineer at Michigan State University (MSU) in East Lansing who has worked on ethanol conversion technology for 30 years.

Fuel versus food?

Ethanol hasn't always been an alternative fuel. Henry Ford originally planned to use it to power his Model T's. But it was quickly supplanted by cheap and plentiful gasoline, which packs 30% more energy per gallon than ethanol does.

Ethanol began making its comeback after the oil shocks of the 1970s. Brazil launched a national effort to convert sugar cane into ethanol in 1975 in hopes of reducing its vulnerability to high oil prices. As part of that effort, the country's federal government required gas stations to blend 25% ethanol into gasoline and encouraged carmakers to sell engines capable of running on pure ethanol. As a result, ethanol production in Brazil has climbed steadily, from 0.9 billion gallons in 1980 to 4.2 billion gallons last year. And the price of the fuel has dropped steadily to $0.81 cents a gallon, according to a recent article by José Goldemberg, the State of São Paulo's Secretary for the Environment (*Science*, 9 February, p. 808).

U.S. ethanol producers have seen a similar surge in output. In 2005, they turned out roughly 4 billion gallons of ethanol, or about 3% of the 140 billion gallons of gasoline used in the U.S. each year. Today, most of that ethanol is blended with gasoline at a 10:90 ethanol-to-gasoline ratio to boost the fuel's octane rating, which allows it to burn more cleanly, reducing urban smog. Two years ago, Congress mandated a production increase to 7.5 billion gallons a year by 2012. And the president's recent initiative aims to produce as much as 35 billion gallons of alternative fuels by 2017. The European Commission too has called for 10% of its transportation fuel to come from biofuels such as ethanol and biodiesel by 2020.

But crops such as corn and sugar cane won't be enough to produce all this fuel. According to one recent DOE study, U.S. corn grain ethanol production is likely to top out somewhere around 12 billion gallons a year. "Even if you took all the starch and converted it to fuel, it only gets you to about 10% of our gasoline," says Jim McMillan, a biochemical engineer with the

CREDITS (TOP TO BOTTOM): JUPITER IMAGES

National Renewable Energy Laboratory (NREL) in Golden, Colorado. Long before that point, diverting too much of the corn crop would cause dramatic rises in the cost of the food. And even at today's modest levels of ethanol production, a price pressure is already being felt. Corn prices in the United States hit a 10-year high of $4.47 a bushel ($176 per metric ton) last month, nearly double the price a year ago, fueled in part by the increased demand for ethanol.

To get past the food-versus-fuel debate, "you've got to get into cellulose," says McMillan. Doing so would both increase the volume of ethanol that can be made and lower emissions of greenhouse gases. That's where cellulosic ethanol really shines, says Alexander Farrell, an energy resource expert at the University of California, Berkeley. In a paper published last year in *Science* (27 January 2006, p. 506) and in follow-on work, Farrell and colleagues found that because of its high energy inputs, using corn-based ethanol instead of gasoline reduces greenhouse gas emissions only about 18%. With its modest energy inputs, cellulosic ethanol fares much better, reducing greenhouse gas emissions by 88%.

Sweet science

But converting cellulose to fuel is far more difficult than starting with simple sugar, as in Brazil, or corn starch, as in the United States. Starch is a straightforward polymer of glucose that is easily broken down by enzymes. Agricultural and forest wastes, by contrast, are far more complex. This biomass is made up of three ingredients: cellulose, a polymer of the six-carbon sugar glucose that's the main component of plant cell walls; hemicellulose, a branched polymer composed of xylose and other five-carbon sugars; and lignin, which crosslinks the other polymers into a robust structure.

To convert any source of sugars to ethanol, those sugars must first be made accessible. That's simple in the case of sugar cane, where the sugar is harvested and made into a syrup. It's a bit harder with corn grain. But there, engineers simply add enzymes called amylases to clip apart the starch polymer into separate glucose molecules. But with other agricultural products, such as leaves, stalks, grasses, and trees, the material must be broken down so that crystalline fibers made up of hemicellulose and cellulose can be digested into simple sugars before being turned over to microbes that convert them to ethanol, a process known as fermentation.

So far, it's on this fermentation stage that most of the attention in the cellulosic-ethanol field has focused. That's because although yeast naturally converts glucose to ethanol, there are no naturally occurring organisms that convert xylose and other five-carbon sugars to ethanol. *Escherichia coli* and other organisms do metabolize five-carbon sugars. But instead of making ethanol, they naturally produce a variety of acetic and lactic acids as fermentation products. To take advantage of the sugars that make up some 25% of plants, researchers needed to reengineer the workings of microbes.

The first to do so, in 1985, was microbiologist Lonnie Ingram of the University of Florida, Gainesville, who reported that he and his colleagues had inserted a pair of key sugar-fermenting genes into the bacterium *E. coli*. The genes redirected *E. coli*'s metabolism to convert 90% to 95% of the sugars in biomass to ethanol. Ingram's early *E. coli* strains weren't perfect. They could tolerate only about 4% ethanol in the final fermenting solution. Because the fuel must be distilled out of the surrounding water, a highly energy intensive process, ethanol makers strive to minimize the amount of distillation by using organisms that can tolerate the most ethanol possible. Since their early work, Ingram says he and his colleagues have managed to increase *E. coli*'s tolerance to about 6.4% ethanol. Ingram's strains have since been licensed to Celunol, which is building a 1.4-million-gallons-per-year cellulosic-ethanol plant in Jennings, Louisiana.

Other groups, meanwhile, have pushed to impart new talents to other organisms. In 1995, for example, researchers at NREL engineered a bacterium called *Zymomonas mobilis* to ferment xylose and other five-carbon sugars in addition to the six-carbon sugars it favors naturally. The work has since been taken up by researchers at DuPont in Wilmington, Delaware. And last year, DuPont's biofuels technology manager William Provine reported at the annual American Institute of Chemical Engineers meeting in San Francisco, California, that his group has recently come up with a *Zymomonas* strain capable of tolerating up to 10% ethanol. That process too is on the road to commercialization. Last month, officials at DuPont, Broin (a major corn-ethanol producer), and Novozymes announced that, as part of the DOE award, they will expand an existing corn-grain ethanol plant in Emmetsburg, Iowa, to produce approximately 30 million gallons of ethanol a year from corncobs and other cellulosic feedstock.

Company	Location	Size (Millions of gallons per year)	Feedstock	Completion date
Broin	Emmetsburg, Iowa	31	Corn stover (cobs and stalks)	2009
BlueFire Ethanol	Southern California	19	Waste wood	2009
Alico	La Belle, Florida	20	Wood, ag waste	2010
Abengoa Bioenergy	Colwich, Kansas	11.4	Corn stover, wheat straw, etc.	2011
Iogen Biorefinery	Shelley, Idaho	18	Ag waste	2010
Range Fuels	Soperton, Georgia	50	Waste wood, energy crops	2011

The winners. The U.S. Department of Energy recently backed six cellulosic-ethanol refineries.

Yeast researchers have also gotten in on the act. Yeast is today's ethanol heavyweight, given its natural proclivity for turning glucose into ethanol. But because the microbe doesn't naturally process five-carbon sugars, researchers have expanded its abilities to it make better suited for more complex biomass feedstock. In 1993, researchers led by Nancy Ho, a microbiologist at Purdue University in West Lafayette, Indiana, spliced a trio of xylose-fermenting genes into yeast, making it the first yeast strain capable of fermenting xylose to ethanol. Since then, Ho's group has honed yeast's ability to convert a mixture of sugars to ethanol through improvements that include enabling it to use five-carbon

SOURCE: DOE

SBS 13th ANNUAL CONFERENCE & EXHIBITION

Montréal

April 15 –19, 2007

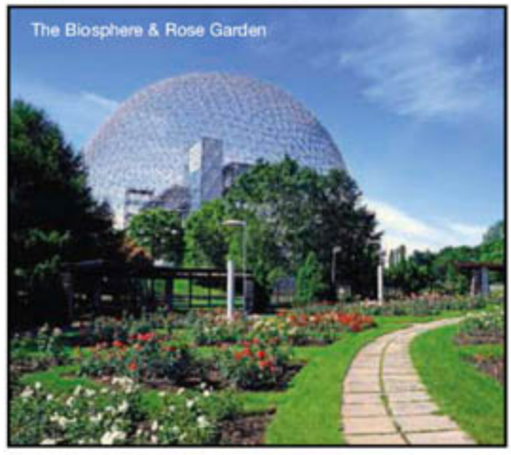

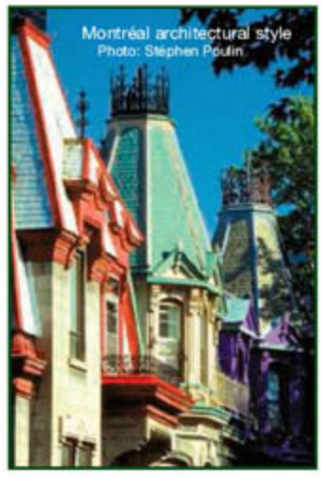

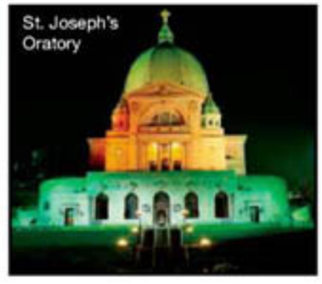

Advancing the Science of Drug Discovery: Bridging Research & Development

- Learn from the experts in Biomarkers, Systems Biology and Target Validation
- Discover what's new in Target Biology and Hit Discovery Strategies
- Get new perspectives on Toxicology and Cell-based Assays from sessions with partnering organizations
- Understand small molecule and immunotherapeutic approaches to disease
- Share ideas, techniques, strategies and innovations for your business
- See the latest innovations and product advancements
- Network with your peers and colleagues

Plan to be here: April 15 –19, 2007

Palais des Congres de Montréal, Montréal, Canada

Society for Biomolecular Sciences SBS

Society for Biomolecular Sciences
36 Tamarack Avenue, #348, Danbury, CT 06811, USA
Phone: +1 (203) 743-1336 • Fax: +1 (203) 748-7557 • Email: email@sbsonline.org • Web Site: www.sbsonline.org

Register at www.sbsonline.org

Growth industry. A new agricultural-waste-to-ethanol plant in Jennings, Louisiana, is among the first of a new crop of cellulosic-ethanol facilities.

CREDIT: CELUNOL CORP.

sugars other than xylose and boosting the speed at which the organism produces ethanol.

Tougher, softer, faster

Despite their successes in coaxing organisms to convert sugars to ethanol, most researchers recognize that much work remains to be done. "We are still climbing the mountain," McMillan says, and are "relatively low" on the slope. For example, yeast can convert a bath of glucose to ethanol in just a few hours, but microbes working on a complex mix of sugars can take 1 to 2 days to do the same thing. In a commercial plant, that means lower fuel output. So researchers around the globe are focusing heavily on increasing the expression of fermenting enzymes to step up the speed.

Another focal point for researchers, Ho and others say, has been toughening up the microbes. "All of these strains, while they are good at making ethanol, their robustness is nowhere near baker's yeast [working] on glucose," says McMillan. In addition to the intolerance many organisms have for ethanol, a wide variety of other compounds from broken-down biomass inhibit enzymes in fermentation.

Researchers are also looking for improvements in other parts of the process. One that has come under scrutiny is the chemical processing used to prepare plants for fermentation. Traditionally, researchers break apart the plant fibers by exposing biomass to dilute acids and steam. The result is a soup that can then be exposed to cellulase and hemicellulase enzymes, which further break fibers down into simple sugars for fermentation. But acid-steam processing has several drawbacks. For one, the acid reacts with sugars, reducing by about 10% the amount of total sugars that can later be fermented, MSU's Dale says. The acid byproducts, he adds, also inhibit celluloses and other key enzymes. Finally, the acids typically cannot be recovered and used again, which adds to the costs.

So Dale and other researchers are now commercializing a process that, instead of acids, uses basic compounds such as ammonia to accomplish the job. In recent years, Dale's group has developed a low-temperature process that readily breaks down leaves, grasses, and straws. It also allows facility operators to recover and reuse the ammonia and creates fewer enzyme inhibitors than do acid treatments. According to a recent analysis by Tim Eggeman, a chemical engineer with Neoterics International in Lakewood, Colorado, the technique could drop the cost of cellulosic ethanol 40 cents per gallon. At least for now, however, the technique doesn't work well with lignin-rich woody feedstock such as trees. So the hunt is still on for improvements in that arena.

A final target for many researchers lies inside plants themselves. Some companies and academic groups are working to reengineer plants such as corn, poplar trees, and switchgrass to boost their yields and make them easier to turn into fuel. In 1999, for example, researchers led by Vincent Chiang, a molecular biologist and organic chemist at North Carolina State University in Raleigh, reported that they had engineered poplar trees with 50% less lignin than conventional varieties and more cellulose instead. Originally, that work aimed at increasing the cellulose content for paper production. But Chiang says the result is equally valuable for improving the carbohydrates in trees for conversion to ethanol. "The idea is to generate as much polysaccharides as possible," Chiang says.

Since their early success, Chiang says, his group has been unable to reduce the lignin content below the initial 50%. More recently, he and his colleagues have turned to tinkering with genes that control the cellulose fibers within trees, aiming to reduce the crystallinity. Although the work is still unpublished, "we have altered several cellulose synthase genes and have pretty much figured out which are the important ones," Chiang says. The hope, he says, is to make it easier for cellulase enzymes to break down the polymer into glucose units during processing. That, in turn, would reduce the amount of enzymes that need to be added prior to fermentation and chip away at the overall cost. Related efforts are also under way to improve other potential energy crops—for example, reducing the lignin content and increasing the yield of grasses such as switchgrass and *Miscanthus*.

These and other advances lead alternative-fuel experts to predict that the cost of cellulosic ethanol will continue to decline, just the cost of as corn- and sugar cane– based ethanol has. "Each step has a newness to it that allows for optimization. Each one of them helps bring the cost down," says John Pierce, who oversees DuPont's bio-based technologies in Wilmington, Delaware. Although there are no commercial cellulosic-ethanol plants today, most estimates put the current cost of producing a gallon of cellulosic ethanol at between $3 and $4. By the time the full-scale production plants come on line beginning in 2009, that cost is expected to be about $2 a gallon. DOE's current goal is to drop the price to $1.07 a gallon, at which point it will be competitive with making ethanol from corn.

Yet even if cellulosic ethanol is destined to compete head-to-head with corn-based ethanol, it is benefiting right now by being in the second rank. "Corn ethanol has certainly paved the way for a lot of alternative fuels," says Ingram. In addition to pioneering the commercialization of enzymes used to digest starch and reducing their price dramatically, corn ethanol producers have created an infrastructure for handling large volumes of biomass and spurred gasoline suppliers to incorporate ethanol into their supply chains. Numerous U.S. automakers have also begun producing E85 vehicles, able to burn a mixture of 85% ethanol and 15% gasoline. Cellulosic-ethanol makers will inherit this established infrastructure, easing their way into the market—and perhaps even helping them create the first real alternative to gasoline. **–ROBERT F. SERVICE**

The cAMP-Glo™ Assay, as close as it gets...

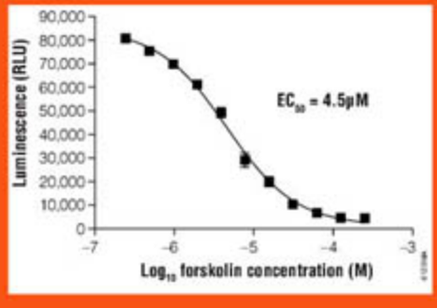

…to the real thing. The inherent complexity of GPCR signaling demands simple, robust technologies for quantifying receptor activation. The new cAMP-Glo Assay provides the simplest method available for measuring G_S or G_i coupled receptor activity. The wide dynamic range and high sensitivity of the bioluminescent cAMP-Glo Assay makes it ideally suited for 1536-well plate applications.

To receive more information and qualify for a FREE SAMPLE visit:
www.promega.com/campglo

PROMEGA CORPORATION • www.promega.com

Promega

LETTERS

edited by Etta Kavanagh

The Uncertain Future of Research Chimpanzees

THE OTHERWISE EXCELLENT NEWS FOCUS ARTICLE BY JON COHEN ON THE FUTURE OF "THE endangered lab chimp" (26 Jan., p. 450) does not emphasize one compelling reason why studies of captive chimpanzees should continue—the significant differences in their disease patterns, incidence, and severity from those of humans (*1*). As human and chimpanzee proteins are >99% identical (*2*), it should be possible to explain some of these surprising disease differences at the molecular level. Thus, more studies are needed not because chimpanzees are good models for human diseases, but rather because they are surprisingly bad models in many instances, for example, HIV infection progressing to AIDS and *P. falciparum* malaria. Such investigations could adopt approaches similar to those currently used for studying human diseases, and the results would benefit the care of both humans and chimpanzees. The NIH spent many dollars to sequence the chimpanzee genome (*2*). If the existing captive chimpanzee population is allowed to die out in sanctuaries without adequate funding or facilities for such research, some of the most biomedically valuable benefits of the chimpanzee genome sequencing will never be realized.

AJIT VARKI

Distinguished Professor of Medicine and Cellular and Molecular Medicine, Co-Director, Glycobiology Research and Training Center, University of California, San Diego, La Jolla, CA 92093, USA.

References

1. A. Varki, T. K. Altheide, *Genome Res.* **15**, 1746 (2005).
2. The Chimpanzee Sequencing and Analysis Consortium, *Nature* **437**, 69 (2005).

E-Letters

Please see our online letters section, E-Letters, for further discussion of chimpanzee research >> www.sciencemag.org/cgi/letters/315/5811/450

MORE THAN 25 YEARS AGO, *SCIENCE* PUBlished a letter from me (*1*) criticizing an NIH report on future U.S. needs for chimpanzees in research, which called for 300 to 350 chimpanzees a year and a major expansion of captive breeding. We now know that those figures were exaggerated. In 1994, NIH reported a chimpanzee surplus and requested advice from the National Research Council; this led to a breeding moratorium that began in 1995.

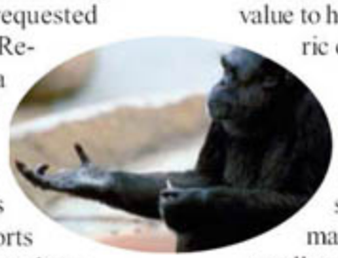

Jon Cohen's article, The endangered lab chimp" (News Focus, 26. Jan., p. 450) reports that scientists are projecting a shortage and calling for renewed breeding. However, when various countries are ending chimpanzee research, it is time for the United States to follow suit.

We base this on ethical, financial, and scientific arguments. Chimpanzees have very complex mental and social needs that simply cannot be met in laboratory housing. Ethically, we should not use them merely as a utilitarian means to an end (collecting data) no matter how useful we think they might be. Chimpanzee research has produced far less value to human health than scientific rhetoric commonly claims.

Each chimpanzee bred will cost up to $500,000 or more for lifetime care. High costs stack the odds against chimpanzee research producing significant human health benefits, partially due to small study group sizes (usually two to four individuals).

Scientist support for invasive chimpanzee research has declined greatly. We challenge those few who advocate renewed chimpanzee breeding to justify their arguments on the basis of appropriately sophisticated ethical and scientific analyses. Vague allusions to the need for chimpanzees to combat some future Ebola-like disease do not meet the standard required.

This is the ideal moment to phase out the use of this endangered species in invasive research and send the remaining laboratory chimpanzees to permanent sanctuary.

ANDREW N. ROWAN

The Humane Society of the United States, 2100 L Street NW, Washington, DC 20037, USA.

Reference

1. A. N. Rowan, *Science* **203**, 1069 (1979).

IN HIS ARTICLE "THE ENDANGERED LAB CHIMP" (News Focus, 26 Jan., p. 450), Jon Cohen describes the unwinnable dilemma presented by the intersection of our need to conduct scientific research on chimpanzees to better understand both them and ourselves with our strong ethical obligation to do chimpanzees no harm. There is a way to recast the problem that will make a resolution possible.

Much of the argument for breeding comes from the realization that if the moratorium is not lifted, the captive research population will become extinct; John Vandeberg calculates that by 2037 only postreproductive individuals will remain. Will that mark the beginning of the end of captive chimpanzee research? Only if there are no other chimpanzees. However, the goal of conservationists is to ensure large, stable wild populations on an indefinite basis, and capture of wild chimpanzees will always be possible (one assumes that by 2030, available methods would not be as brutal and wasteful as those of today).

There is no need to end the moratorium any time soon, and with efficient, humane, and noninvasive use of existing individuals, most of the truly important biological questions about our kin are likely to be answered well before 2030. As for the possible epidemic mentioned in the article's last paragraph: If it happens sooner, we have sufficient numbers, and if it happens later, surely the compelling need generated by a (hypothetical) devastating threat that cannot be addressed in any other way will justify carefully implemented exemptions to bans on captures from the wild. Transfer of maintenance funds from

CREDIT: PHOTOS.COM

dwindling captive populations to in situ conservation would ensure this option.

There are arguments for breeding captive apes; preservation of an "endangered population" is not one of them.

JIM MOORE

Department of Anthropology, University of California, San Diego, La Jolla, CA 92093–0101, USA.

IN HIS THOUGHTFUL ARTICLE ON THE ISSUE of whether chimpanzees should continue to be bred for use in biomedical research ("The endangered lab chimp," News Focus, 26 Jan., p. 450), Jon Cohen raises a critical issue that may have important consequences for human welfare. Chimpanzees have proven to be the only animal model for the study of some important human pathogens, particularly hepatitis B (HBV) and C (HCV) viruses. The use of chimps was vital to the development of HBV vaccines and is currently an important component of efforts to develop an HCV vaccine. As Cohen points out, emergence of future pathogens with similarly reduced host ranges may also provide an important need for chimpanzees in the future.

The future availability of these animals for use in medical research depends on whether the United States continues its current moratorium on the breeding of these animals. If this ban is modified or reversed, it would also be essential that chimpanzees always be housed in social groups with enriched facilities for play, ideally outdoors, and that when research studies are finished, the animals be transferred to outdoor sanctuaries for retirement in large social groups. It is also important that the lives and health of chimpanzees in research not be endangered. Fortunately, chimpanzees do not develop clinical illness when infected with the hepatitis viruses. We have adhered to these goals in our work with chimpanzees in our laboratory, Vilab II, in Liberia. (This laboratory, which I headed for 32 years, is still the responsibility of the New York Blood Center, not the Hepatitis Research Foundation, as stated in Cohen's article.) The Blood Center has decided to close it for future research and transfer the remaining animals to island sanctuaries. The reasons for this decision are partly economic and also reflect the fact that sanctuary organizations, now being sought to take long-term responsibility for this sanctuary, generally do not permit continuation of research. The Hepatitis Research Foundation, which supports research on the development of HCV vaccines and immunotherapies, would like to continue limited but important research in parallel to the development and maintenance of the sanctuary. Such research would not need to involve the sanctuary animals, as chimpanzees that have been held as pets in Liberia or confiscated by the wildlife authorities are available and would have a better future if they passed through Vilab II on the way to retirement in the sanctuary.

Only a very small number of chimpanzees are needed to provide preliminary evidence of the protective efficacy of an HCV vaccine. If such studies cannot be done, large and very costly human clinical trials would be required. Without prior indications of efficacy of a candidate vaccine, funds for such trials would be difficult to obtain, and thus the development of an HCV vaccine may be delayed for decades.

ALFRED M. PRINCE

Chairman, Hepatitis Research Foundation; formerly Head, Vilab II, and Member of the Lindsley F. Kimball Research Institute of the New York Blood Center, 310 East 67th Street, New York, NY 10021, USA. E-mail: amprince00@optonline.net

Ivory-Billed or Pileated Woodpecker?

OUR DETAILED ANALYSIS [D. A. SIBLEY *ET AL.*, "Comment on 'Ivory-billed woodpecker (*Campephilus principalis*) persists in continental North America,'" Technical Comments, 17 Mar. 2006, www.sciencemag.org/cgi/content/full/311/5767/1555a] showed that a bird videotaped in Arkansas (*1*) cannot be an ivory-billed woodpecker and is consistent only with a pileated woodpecker (*Dryocopus pileatus*). The Response [J. W. Fitzpatrick *et al.*, "Response to Comment on 'Ivory-billed woodpecker (*Campephilus principalis*) persists in continental North America,'" Technical Comments, 17 Mar. 2006, www.sciencemag.org/cgi/content/full/311/5767/1555b] failed to refute our primary points—black secondaries evident on the upper wing, brighter white at primary bases, and a black band curving smoothly around the wingtip—and instead disputed secondary parts of our analysis.

A photomontage (fig. 1B in the Response) that superficially matches video field 33.3 combines part of the foreshortened wing of an ivory-billed woodpecker specimen with an image of trees. About 60% of the black forewing (~13% of the wing length) was omitted, as if hidden behind a tree (see figure), contradicting earlier reconstructions (*1*). By this new reconstruction, with foreshortened wing and hidden "wrist," the putative "wrist-to-tail-tip" measurements in (*1*) would have underestimated the true distance; yet, those measurements matched "the upper range for ivory-billed woodpecker" (*1*). Extrapolation suggests that the true measurement would be too large for an ivory-billed woodpecker. This undermines the plausibility of various reconstructions of posture—"perched" (*2*) or "begins to take flight" (*1*)—and consequently the claim that field 33.3 shows white on the bird's dorsal wing surface. We maintain that this white patch represents the underside of a spread wing.

To match video field 33.3, Fitzpatrick *et al.* created a montage (fig. 1B of the Response) from photographs of a mounted woodpecker specimen and tupelo trunks. The specimen was photographed from the side and leaning away, with wings folded, an arrangement unlike that proposed in (*1*) and implausible because it would be difficult for a bird in this position to cling to the trunk. Our sketch shows the entire specimen, including omitted parts of the body and wing "behind" the tree (gray shading). The montage matches neither the position of the bird's tail in video field 33.3 (blue shading) nor the position of the actual tree in the video (orange lines).

Contrary to the Response of Fitzpatrick *et al.*, models of bird flight, in which a flapping bird viewed from behind can show the underside of both wings simultaneously, are supported by photographs shown in our Comment, research (*3*–*5*), and video (*6*, *7*). The underwings of a pileated woodpecker can appear mostly white in video (*6*, *7*).

"Suggestive" audio recordings [Fitzpatrick *et al.*'s Response; (*8*)] remain inconclusive, as

do other lines of evidence (e.g., sightings, wingbeat rates). Thus, no published evidence confirms the claimed rediscovery of an ivory-billed woodpecker.

DAVID A. SIBLEY,[1] LOUIS R. BEVIER,[2] MICHAEL A. PATTEN,[3] CHRIS S. ELPHICK[4]

[1]Post Office Box 1031, Concord, MA 01742, USA. [2]Department of Biology, Colby College, Waterville, ME 04901, USA. [3]Oklahoma Biological Survey and Sutton Avian Research Center, University of Oklahoma, Norman, OK 73019, USA. [4]Department of Ecology and Evolutionary Biology, University of Connecticut, Storrs, CT 06269, USA.

References

1. J. W. Fitzpatrick *et al.*, *Science* **308**, 1460 (2005).
2. (*1*), as originally published online 28 Apr. 2005; see www.sciencemag.org/cgi/reprint/1114103v1.pdf.
3. D. Bilo, in *Instationäre Effekte an schwingenden Tierflügeln*, W. Nachtigall, Ed. (Franz Steiner, Mainz, Germany, 1981), pp. 102–114.
4. S. M. Gatesy, K. P. Dial, *J. Exp. Biol.* **176**, 55 (1993).
5. B. Tobalske, personal communication.
6. J. M. Collinson, *BMC Biol.*, in press.
7. Video by D. Nolin (available at http://birdviewing.com/upload/NolinPileatedVideos.wmv).
8. R. A. Charif *et al.*, *Science* **309**, 1489 (2005).

Response

WE DISAGREE THAT SIBLEY *ET AL.* SHOWED that the bird in the Luneau video "is consistent only with a pileated woodpecker (*Dryocopus pileatus*)." We showed their analysis and assumptions to be flawed or lacking on many counts in our previous Response. We refuted their primary points regarding putative presence of a black trailing edge and rounded black wingtip. Moreover, an impression of brighter white near the primary bases is not diagnostic for pileated, as the primaries are also basally white in most ivory-billed woodpecker specimens.

We presented a photomontage to illustrate that a lateral view of an opening wing of an ivory-billed woodpecker launching off a tree trunk can produce a black-and-white pattern similar to that in field 33.3 of the Luneau video. We did not intend the montage to be a precise match for wing angles and body position of the bird in the video, because (i) these parameters cannot be determined precisely from the video, and (ii) no photographs or mounts are available to illustrate an ivory-billed woodpecker wing as it is opened during launch. Even if field 33.3 does depict the underside of the bird's wing as proposed by Sibley *et al.*, the absence of a broad black border formed by dark primary and secondary feathers on the distal and posterior portions of the wing renders it inconsistent with pileated woodpecker.

We do not dispute that "[t]he underwings of a pileated woodpecker can appear mostly white in video." Rather, we note that (i) all such videos also reveal black trailing edges, contrary to the Luneau video, and (ii) many fields in the Luneau video reveal the dorsal, not ventral, wing surface, and these also show extensive white along the trailing edge.

We continue to regard all aspects of the Luneau video as fully consistent with ivory-billed woodpecker.

JOHN W. FITZPATRICK,[1] M. LAMMERTINK,[1] M. D. LUNEAU,[2] K. V. ROSENBERG,[1] T. W. GALLAGHER,[1] R. W. ROHRBAUGH[1]

[1]Cornell Laboratory of Ornithology, 159 Sapsucker Woods Road, Ithaca, NY 14850, USA. [2]Department of Engineering Technology and Department of Information Technology, University of Arkansas at Little Rock, Little Rock, AR 72204, USA.

Keep Astrobiology Funding Alive

FORTY YEARS AGO, UPON RECEIPT OF MY PH.D. in microbiology, I faced a dilemma as to what to do next. I had a postdoctoral fellowship to

Karolinska Institutet in Stockholm, but also was quite interested in the new NASA "Scientist as Astronaut" Program in Houston. Seeking guidance, I wrote to Joshua Lederberg, and, much to my surprise, he replied immediately. "There will be no manned mission to Mars for at least 40 years," he wrote presciently. So, I followed his advice and went to Sweden, but still regretted not being able to "see that first cell on Mars, under the microscope."

We have learned so much about our immediate extraterrestrial environment in these 40 years, virtually all of it through instrumentation in spacecraft, not via manned flights. Yes, we now suspect that there may have been life on Mars in the distant past. Lakes of methane on Titan and a liquid ocean five times the volume of Earth's on Europa beckon. But these are much more accessible and economically viable via instrument probes rather than sending manned missions into space.

Our splendid and productive Astrobiology Program may succumb to wrongheaded administrative directives that have no scientific merit and put humans onto Mars and beyond ("Astrobiology fights for its life," A. Lawler, News Focus, 19 Jan., p. 318). Such subversion of our wonderful quest for life beyond Earth may bring the United States some military advantage or international bragging rights, but it has no place in legitimate inquiry into perhaps the most challenging question facing mankind.

BRUCE MOLHOLT

Department of Environmental Studies, University of Pennsylvania, Philadelphia, PA 19104, USA.

TECHNICAL COMMENT ABSTRACTS

COMMENT ON "Global Genetic Change Tracks Global Climate Warming in *Drosophila subobscura*"

Francisco Rodríguez-Trelles and Miguel Ángel Rodríguez

Balanyà *et al.* (Reports, 22 September 2006, p. 1773) build on earlier claims that chromosomal inversion polymorphisms of *Drosophila subobscura* are rapidly evolving in response to global warming. However, that conclusion is not adequately buttressed by their data, because they overlooked the lag between calendar and climatological dates created by the progressive lengthening of the growing season in their sampling approach.

Full text at www.sciencemag.org/cgi/content/full/315/5818/1497a

RESPONSE TO COMMENT ON "Global Genetic Change Tracks Global Climate Warming in *Drosophila subobscura*"

Joan Balanyà, Josep M. Oller, Raymond B. Huey, George W. Gilchrist, Luis Serra

Rodríguez-Trelles and Rodríguez advocate standardizing old and new collections by climate rather than by calendar and also propose that some of our samples were biased by inappropriate timing. Their first suggestion applies to few species, and its implementation alters photoperiodic cues. Their second point is valid, but our conclusions are robust: Observed genetic changes reflect global warming, not sampling artifacts.

Full text at www.sciencemag.org/cgi/content/full/315/5818/1497b

Letters to the Editor

Letters (~300 words) discuss material published in *Science* in the previous 3 months or issues of general interest. They can be submitted through the Web (www.submit2science.org) or by regular mail (1200 New York Ave., NW, Washington, DC 20005, USA). Letters are not acknowledged upon receipt, nor are authors generally consulted before publication. Whether published in full or in part, letters are subject to editing for clarity and space.

BIOGRAPHY

From Gombe to the World

Meredith F. Small

Her image is imprinted in our minds—the willowy young British woman with the blonde ponytail. She's standing in the forest with a wild chimpanzee sitting by her side, a hairy hand tentatively reaching out to touch her khaki shorts.

Jane Goodall is, by any standard, an icon. And what makes her life story so interesting is that she achieved her iconic status not by being a movie star or a politician but by working really hard at issues she believes in.

In *Jane Goodall: The Woman Who Redefined Man*, Dale Peterson (a lecturer in Tufts University's English Department) provides an exhaustive chronology of her life to date. She was born in 1934 as Valerie Jane Morris-Goodall. Her father was a race car driver for Aston Martin; he, too, loved to be on the go. Her mother, Vanne, came from a strongly matriarchal family that was a stable foundation during World War II and as the Morris-Goodall marriage fell apart. Vanne and her two daughters, Valerie Jane and Judy, took up permanent residence at her grandmother's house, The Birches, in Bournemouth in 1940 and never left.

We read biographies to find out what makes someone special, but nothing in Goodall's early years stands out. She was educated locally and went to secretarial school rather than university. She had no economic advantages and was neither pushed by her parents nor formed by surmounting some personal disaster. Goodall was just a normal girl who liked nature and boys. Her early adulthood was apparently a social whirl where everyone was "mad," in her words, and that was a compliment. She also attracted a bevy of men and was engaged to several. But she left them all in her dust when she sailed for Africa in 1957.

In that first journey, perhaps, lie the keys to Goodall's unusual life. She had always dreamed of Africa, and she saved diligently for the trip. She also took advantage of an invitation from a school chum to visit Kenya, and her mother encouraged her to go. In other words, Goodall was persistent in her goal, embraced risk, and had the full support of her family.

During her life, Goodall continued to leap into new situations, persisting where others would have run away and usually altering her circumstances as she went. For example, Goodall accepted employment with the notoriously lecherous Louis Leakey at the Kenya National Museums and not only foiled his ardor but managed to turn Leakey into a pillar of support. Later, to gain funding from Stanford University, she accepted the transformation of her small, personal, study site into a major research station, and she accepted that change wholeheartedly.

Through all these changes, Goodall wrote copious letters home, and her mother and sister came regularly to Africa and stayed for months. When she accepted Leakey's offer to watch chimpanzees in the wild, a venture most women would fear, Vanne came along. And no matter the pull of Africa, Goodall stayed decidedly connected to England. She gave birth to her son in London, sent him to school in Bournemouth, and to this day spends time at The Birches.

Her family provided a stability that was often missing in Africa. Goodall and her first husband, wildlife photographer Hugo van Lawick, divorced. Her second husband, Derek Bryceson (the director of Tanzania's National Parks), died after a long illness. Both of these men were apparently drawn to Goodall's zest for life and her dedication to chimpanzees, and yet they were both jealous of that commitment and tried to control her. Goodall was conflicted about motherhood and career, a situation familiar to any woman who has a life outside the home. And her work life was plagued by financial woes, funding for Gombe, and constant demands on her time, especially once her fame grew to international proportions.

But Goodall is a master at rising to the occasion, especially when she believes in a cause. In the late 1980s, Goodall reinvented herself after seeing chimpanzees in deplorable captive situations. Suddenly, she was on a mission from God not to just watch chimps, but to save them. That mission quickly translated into saving the world by spreading her own brand of conservation and hope.

Jane Goodall
The Woman Who Redefined Man

by Dale Peterson

Houghton Mifflin, Boston, 2006. 768 pp. $35, C$45.95. ISBN 9780395854051.

On a path at Gombe. A frame from the 1965 CBS/National Geographic special "Miss Goodall and the Wild Chimpanzees."

CREDIT: CBS/LANDOV

Goodall now travels around the world, 300 days a year, giving talks and accepting accolades. Whereas her early years as a chimpanzee researcher are easy to follow, this more recent Goodall is harder to understand. Peterson presumably had easy access to his subject—he has coauthored a book with Goodall (*1*) and edited two volumes of her letters (*2*, *3*)—but for these later decades he seems to have access only to her airline mileage summaries. Why, readers might well ask, does a 70-year-old woman choose a life on the run? Peterson only overhears her terse answer to this question: "There's so much to do."

Peterson's account includes few direct quotes from Goodall, but no wonder. Her thoughts and feelings can be found in the two "autobiographies in letters" she has produced with the author as well as several well-written personal accounts of her researches and experiences.

Also missing from this biography is any criticism. Peterson is a fan and apparently reluctant to interview anyone besides other fans. In actuality, colleagues of Goodall have complained that she has been given more credit than is due for her work on chimpanzees and that she quickly abandoned fieldwork for the public limelight. Her activism also seems misguided to some. They wonder why she is using funds to build chimp sanctuaries for a

The reviewer is at the Department of Anthropology, Cornell University, Ithaca, NY 14853, USA. E-mail: ms32@cornell.edu

few animals instead of ensuring the preservation of whole habitats for groups of chimps.

But Goodall has always been an iconoclast who follows her heart. From the start, she forged a path like no one else, and her lasting accomplishments are many. Goodall established and maintained the longest-running chimpanzee field site in the world. She hired Tanzanians as observers before others hired Africans. She welcomed students and colleagues to her study area, thereby producing a copious database on the Gombe chimps. She has contributed much of what we know about chimpanzees and their behavior, including that which may be reflected in human evolution. These days, Goodall's activism for conservation, especially her Roots and Shoots program, is affecting a generation of children.

And in that influence lies Goodall's most important contribution. For over half a century, she has been a mentor to young people, especially young women. Thousands of girls have said to themselves, "I can do what I want with my life because Jane Goodall did it." For that alone, she deserves her status as icon.

References

1. D. Peterson, J. Goodall, *Visions of Caliban: On Chimpanzees and People* (Houghton Mifflin, Boston, 1993).
2. J. Goodall, *Africa In My Blood: An Autobiography in Letters: The Early Years*, D. Peterson, Ed. (Houghton Mifflin, Boston, 2000).
3. J. Goodall, *Beyond Innocence: An Autobiography in Letters: The Later Years*, D. Peterson, Ed. (Houghton Mifflin, Boston, 2001).

10.1126/science.1136574

MUSEUMS: PALEOANTHROPOLOGY

Our Branch in the Tree of Life

R. Scott Winters

At Laetoli, Tanzania, (just south of Africa's Great Rift Valley) in the 1970s, Mary Leakey uncovered one of the most significant insights into our prehistory: two sets of ancient, human footprints. The 3.5-million-year-old volcanic ash captured a snapshot of the morphology and behavior of our distant ancestors. Two individuals, clearly bipedal, had been walking side-by-side across the landscape where humanity's genome took shape. In recent years, our understanding of human origins has been progressively refined due to an increasing number of multidisciplinary advances. Our attention on human identity has shifted from where have we come from to how did we get here.

Hall of Human Origins

Ian Tattersall and Rob DeSalle, curators

American Museum of Natural History, New York. www.amnh.org/exhibitions/permanent/humanorigins/

The Anne and Bernard Spitzer Hall of Human Origins opened last month at the American Museum of Natural History. A sweeping and expansive look at human evolution, the hall braids together the complementary and mutually reinforcing evidence from the fossil record and genomic studies. The permanent exhibit is expertly curated by two of the museum's preeminent researchers, paleoanthropologist Ian Tattersall and genomics researcher Rob DeSalle.

In recent years, our knowledge of humanity's origins has changed dramatically and at an accelerating pace. Remaining current with the breadth and depth of this research is an enormous challenge, and a museum that wants to maintain timely and relevant displays faces substantial difficulties. Impressively, the Hall of Human Origins is designed to evolve along with our understanding of its subject, enfolding new discoveries and interpretations as they become available. Replacing the museum's earlier Hall of Human Biology and Evolution, the new 9000-square-foot exhibit is intended to be dynamic. It includes a multimedia "Science Bulletin" that changes regularly to present current research and a hands-on educational laboratory. These aspects are made possible by an insightful, albeit rare, endowment for continuing renovations to the hall.

CREDIT: DENIS FINNIN/AMERICAN MUSEUM OF NATURAL HISTORY

Visitors entering the exhibit first encounter an iconographic interpretation of humanity's place in the world. A human skeleton stands between our nearest extant and extinct relatives, respectively a chimpanzee and a Neandertal. Behind the skeletons is a large, offset panel that collectively functions as a single screen that displays a high-definition video of fertilization, cellular development, and dividing chromosomes. This arrestingly beautiful entrance elegantly conveys the themes of the exhibit while simultaneously acknowledging and reinterpreting a classic image from the former hall.

The exhibit is divided into three thematic sections. The first, Understanding Our Past, explores in some depth how different types of evidence inform our understanding of human evolution. Visitors staying to the left as they enter the hall explore the world of genomic data, whereas those keeping to the right investigate fossil evidence. One of the highlights in this section is a rare sample of 40,000-year-old Neandertal DNA donated by the Max Planck Institute for Evolutionary Anthropology (Munich, Germany). Each of the two investigative paths reinforces a core theme that contemporary humans are part of an evolutionary continuum, as shown by genetic and morphological similarities. This presentation forces visitors to confront the problem of defining "humanness" when the boundary between species erodes and their similarities and differences become increasingly ambiguous. At the end of this first section, the two lines of evidence converge into an elegant display where Buffon's classic argument for homology (illustrated via morphological similarities of the skeletal forelimb in mammals) is coupled with information about the genetic underpinnings. The display clearly yet subtly illustrates how evolutionary studies are informed by studying characteristics shared among organisms.

Within the exhibit, the middle section is the most expansive and impressive. The History of Human Evolution displays more

The reviewer is in the Division of Oncology, Children's Hospital of Philadelphia, 34th Street and Civic Center Boulevard, Philadelphia, PA 19104, USA. E-mail: winters@genome.chop.edu

than 200 casts of remarkable hominid fossils and artifacts. Centered in the room's entrance is one of the hall's most powerful presentations: an *Australopithecus* couple walking together leaving behind the Laetoli trackway. Museum visitors may remember this pair from the former hall, but the reinterpretation provides a fresh and dynamic perspective. The figures are positioned at floor level to provide a clear but disturbing perspective on the fragility of these waist-high relatives of ours. Another representative of the genus is presented immediately behind the pair, a cast of the remarkably near complete 3.18-million-year-old "Lucy" from Ethiopia's Afar Depression.

Also retained from the former hall are three habitat tableaux, which are augmented by a new, fourth diorama of early hominid life. The juxtaposition of these old and new interpretations illuminates the extent of changes in our understanding of human origins and, more importantly, our sensibility about humans' place within the tapestry of life. The three original vignettes (Neandertal, *Homo ergaster*, and Cro-Magnon) presented our ancestors as conquerors of the wilds: using tools to prepare a hide, butchering a carcass, and building a shelter made of bone and tusk. The new vision of our ancestral world depicts a hyena poised to attack a crouching "Peking Man" (*Homo erectus*). It is a clear and accurate reminder that for most of the history of our lineage we have been prey rather than predator.

Other highlights of the exhibit include a complete interpretation of a Neandertal skeleton, derived from the combination of six different individuals across four continents. Also presented are casts of very contemporary—and sometimes controversial—specimens such as the reconstructed skull of *Homo floresiensis*, the "Hobbit" from Indonesia.

After they survey the evidence for the course of our lineage's evolution, visitors are confronted with the titular question of the exhibit's final section, What Makes Us Human? Throughout the hall's earlier sections, they encountered examples of the apparent disparity between our intraspecies differences and interspecies similarities. As a result, it appears that what differentiates humans are our behaviors, such as creativity. The discourse in the section focuses on the novelty of language, music, art, and tools in humans. It presents the defining achievements that we frequently attribute as unique to *Homo sapiens*. However, any distinctiveness anchored on such achievements is undermined as examples found in other organisms show that these, too, are part of an evolutionary series. This final section reveals just how little we know about the cognitive nature of our species and the void waiting to be filled with future research.

With the display of some 200 casts, dioramas, and artifacts, it would be easy for the exhibit to overwhelm visitors and confuse their interpretation of the course of human evolution. However, the hall's presentation and exceptional curation continuously reinforce a central, albeit complex, theme: evolution is an experimenting process of variation coupled with selection. As a result, modern humans are a mosaic of traits that arose, and are exhibited, across various ancestral groups, which themselves are chimeras of characteristics. The Hall of Human Origins offers another excellent example of the American Museum of Natural History's ability to interpret difficult and complex subjects in ways that the general public will find both approachable and enjoyable.

10.1126/science.1140474

CREDIT: BOSHU NAGASE/COURTESY JOHNS HOPKINS UNIV. PRESS

BROWSINGS

Antarctic Fishes.

Illustrated in the Gyotaku Method by Boshu Nagase. Mitsuo Fukuchi and Harvey J. Marchant. Johns Hopkins University Press, Baltimore, MD, 2007. 136 pp. $45. ISBN 9780801886102. Rosenberg, Kenthurst, NSW, Australia, 2006. £23.99, A$59.95. ISBN 9781877058462.

Most fish from Antarctica and the surrounding Southern Ocean are familiar to only a few researchers and commercial fishers. Rather than a comprehensive survey of these often endemic species, this book focuses on 54 examples that are readily available, taken commercially, or important for their ecologic or scientific roles—e.g., as prey for higher predators or as the subject of studies of adaptations to life in very cold waters. For each, the authors provide a brief description that covers the fish's habits and distribution and usually mentions interesting aspects of its ecology or physiology. Each is depicted in a full-page illustration. Nagase created these delicate, detailed fish rubbings by molding a moistened sheet of paper over a specimen and dabbing colored inks onto the paper using a silk-covered wad of cotton. The widely distributed icefish *Neopagetopsis ionah* (above), which lives at depths of 20 to 900 m in the sea-ice zone encircling Antarctica, received its specific name from the fact that for some time it was known only from specimens obtained from the stomachs of sperm whales.

The Shock of the Old.

Technology and Global History Since 1900. David Edgerton. Oxford University Press, New York, 2007. 288 pp. $26. ISBN 9780195322835. Profile, London, £18.99. ISBN 9781861972965.

Most histories of technology and considerations of the interaction of technology and society stress invention and innovation. Thus accounts of the 20th century typically progress from automobiles, airplanes, and radio through rockets, nuclear power, and computers to today's frontiers of information, biotechnology, and nanotechnology. In opposition to this future-focused approach, Edgerton offers a convincing case that we ought to pay far more attention to what people actually used and still use. He notes the staying power of older technologies—such as spinning wheels, rickshaws, mosquito netting, chemistry, and corrugated iron—that continue to serve crucial functions around the globe. He argues that histories usually fail to recognize the great variety of novel technologies, overestimate the rates at which they achieve their impact, and often misinterpret the nature of that impact. Among the many other thought-provoking conclusions in this fresh and accessible account: the eclipse of individual inventors and mechanical invention by high technologies has been exaggerated; universities have had and still have only a marginal role in innovations; most of the income U.S. universities make from intellectual property stems from federally funded medical research rather than patented innovations.

PUBLIC HEALTH

Return of the Population Growth Factor

The Millenium Development Goals set by the United Nations cannot be achieved unless family planning is made easily available in the lowest-income countries.

Martha Campbell,[1]* John Cleland,[2] Alex Ezeh,[3] Ndola Prata[1]

Academic analysts, the news media, and the international community have frequently engaged in divisive debates over population and international family planning, with periods of attention and funding followed by years of neglect, particularly in the last decade. On 31 January, the All Party Parliamentary Group on Population, Development, and Reproductive Health of the U.K. Parliament (the group) issued a report, *Return of the Population Growth Factor: Its Impact upon the Millennium Development Goals* (MDGs) (*1*). The report, the product of extensive hearings and analysis of written and verbal testimony, cited overwhelming evidence that "the MDGs are difficult or impossible to achieve with current levels of population growth in the least developed countries and regions." It recommends a substantial increase in support for international family planning, particularly for the 2 billion people currently living on less than $2 per day. The report does not argue that population is the only, or even the leading, factor in achievement of the MDGs. Instead, it presents a compelling case that continued neglect of family planning in developing countries will severely undermine crucially important goals.

The Population Pendulum

In the 1960s and '70s, many developing countries adopted national population policies and family planning services. Although some Asian policy initiatives incorporated coercive elements, most family planning efforts were entirely voluntary and proved remarkably successful. Initiatives relied on both public and private sectors to provide modern methods from voluntary sterilization to condoms, with appropriate information. Between 1960 and 2000, the percentage of married women in developing countries using contraceptives jumped from <10% to 60%, and total fertility rates fell from six to about three (*2*).

Despite these successes, surveys continued to indicate that many women in developing countries wanted to space their children or limit childbearing altogether, but still did not have access to the most effective contraceptive methods. When the world's scientific academies, including the American Academy of Sciences and the Royal Society of London, gathered in New Delhi in 1993, they concluded that "humanity is approaching a crisis point with respect to the interlocking issues of population, environment, and development." The academies agreed, "the goal should be to reach zero population growth within the lifetime of our children." (*3*).

The United Nations 1994 International Conference on Population and Development (ICPD), held in Cairo, noted the need to slow population growth in developing countries, but the political emphasis of their Programme of Action (PoA) was on holistic approaches to reproductive health. Many women's advocates at the ICPD criticized promotion of family planning to reduce population growth as inherently coercive. The PoA estimated that by 2005 the cost of meeting the broad agenda set out at Cairo would be $25 billion annually (adjusted for inflation), with one-third to be provided by international donors. It was a bold agenda, but it lacked sufficient political traction. Many of its goals proved unattainable in resource-poor settings, whereas attention to family planning was largely ignored. By 2004, the investment by developed countries in international family planning had fallen to 13% of the target set by the ICPD (*4*).

CREDIT: MICHAEL KAMBER/THE NEW YORK TIMES/REDUX

The crisis in Niger. "Niger's population is set to increase from 14 million to 80 million in 2050 if current fertility remains the same—an unimaginable scenario in a country already unable to feed itself, facing widespread destruction of local ecosystems through over-grazing, continued mass poverty, underemployment and massive dependence on international aid....so, without massive investment in family planning programmes, the outlook is bleak." (*6*).

Population Growth and MDG Goals

The evidence provided and analyzed in (*1*) included the following points.

MDG 1: Eradicate extreme poverty and hunger. It will be almost impossible to reach the target of halving the number of people living on less than $1 a day by 2015 without a large-scale recommitment to family planning. In sub-Saharan Africa, partly as a result of rapid population growth, the number of people living in extreme poverty rose from 231 million in 1990 to 318 million in 2001. The U.N. Population Fund (UNFPA) pointed out that almost 1.5 billion young men and women will enter the 20-to-24-years age cohort between 2000 and 2015, and if they don't find jobs "they will fuel political instability." (*5*).

MDG 2: Achieve universal primary education. Voluntary limitation of family size is also essential for developing countries striving to meet the MDG of eliminating gender disparities in primary and secondary education by 2015. Children in large families, especially girls, are less likely to enter school, more likely to drop out, and are sick and hungry more often than children from small families in the same community. In the poorest coun-

[1]School of Public Health, University of California, Berkeley, CA 94720–7360, USA. [2]London School of Hygiene and Tropical Medicine, WC1 3DP, UK. [3]African Population and Health Research Centre, Nairobi, Kenya. M.C. was an advisor to the member of Parliament who initiated the hearings; J.C., A.E., and N.P. were among the expert witnesses.

*Author for correspondence. E-mail: campbell@berkeley.edu

tries as a whole, two million additional schoolteachers are required each year to keep up with population growth and to maintain the current, inadequate levels of primary education. Uneducated girls marry earlier and tend to have more unintended pregnancies, setting up a pernicious cycle of sexual inequality and high fertility (*6*).

MDG 3: Promote gender equality and empower women. The ability to choose if and when to have a child is central to the autonomy of women. Sir David King, the Science Adviser to the U.K. government, told the group that with respect to fertility decline, "There is little doubt in my mind that female empowerment to control fertility is a key part of that equation." (*7*).

MDG 4: Reduce child mortality. Given the same level of health care, a child born less than 18 months after an older sibling has a death rate two to four times that of a baby born after a 36-month interval (*8*). An estimated one million infant deaths a year could be prevented if all births were spaced a minimum of 2 years apart.

MDG 5: Improve maternal health. The expansion of the health infrastructure to meet the needs of women in childbirth cannot keep up with the growth of the population as long as fertility is high. Family planning saves women's lives by reducing unintended pregnancies and unsafe abortions, and it is estimated that improved access to family planning could prevent 150,000 maternal deaths each year (*9*). The proportion of potentially fertile women who want no more children or wish to postpone the next birth for at least 2 years, but are not using contraception, exceeds 20% in 24 sub-Saharan nations and 30% in nine of these countries (*10*).

MDG 6: Combat HIV/AIDS, malaria, and other diseases. Family planning, by preventing unintended pregnancies in the first place, is the most cost-effective way of reducing mother-to-child transmission of AIDS. In 1 year, even the low use of contraception in sub-Saharan Africa prevents over twice as many cases of maternal-to-child transmission of HIV than the cumulative total of cases prevented by antiretroviral therapies (170,000 cases versus 65,100) (*11*). Condoms are now the most popular method of contraception among sexually active single women in Africa and Latin America (*2*). However, the difference between the number of condoms needed in Africa and the supply is roughly 1.9 billion a year (*12*).

MDG 7: Ensure environmental sustainability. The roots of environmental degradation are found in consumption patterns among the world's economic powerhouses and rising demands of growing local populations. For example, burgeoning demand for goods in North America, Europe, and China leads to deforestation in Brazil and Africa, but so do the needs of subsistence farmers to feed their large families. In oral evidence, Sir David King noted that, "the massive growth in the human population through the 20th century has had more impact on biodiversity than any other single factor." (*7*).

Population Momentum

The loss of attention to population has created formidable problems for the future. Some countries are undergoing explosive and possibly unsustainable population growth: Niger with 15 million today could hit 80 million in 2050, and Afghanistan could grow from 30 million to 82 million. In 1950, Sri Lanka had the same population as Afghanistan, but it implemented a realistic set of fertility regulation choices, and as a result, it will have one-quarter the population of Afghanistan a century later (*13*). In 1970, there were 5 million more people in Bangladesh than Pakistan, but Bangladesh focused on making family planning available in culturally acceptable ways, while Pakistan did not. As a result, by 2050 Pakistan will have 62 million more people than Bangladesh (*13*).

Next Steps

Much is known about ways to support government, nongovernmental organization, and private sector initiatives to make family planning widely accessible at low cost (*14, 15*). Perhaps the most urgent need is to remove the barriers to access that are not based on any evidence and that so often prevent the adoption of modern methods of family planning (*16*). In Ethiopia, only physicians and nurses are allowed to provide injectable contraceptives, making them inaccessible to the very large number of women who prefer this method above all others. Injectables are the second most commonly used contraceptive method in Africa, after the pill. They are not as cost-effective as IUDs, but IUDs are unpopular. Of course, strict control of needle contamination is needed. In some parts of Africa, women who do manage to get to a family planning clinic are turned back unless they are menstruating that day (*16*). Family planning clinics in northern Pakistan refuse Afghan refugees contraception unless their husband gives permission, even though women with economic means can buy the same products in the local bazaar without any intrusive questions asked (*16*).

The most-needed contraceptives are off-patent and low-cost, but even so, supplies often dry up. In Ghana, 10% of service delivery points were out of contraceptive pills or condoms at least once each year in the late 1990s, and in Tanzania it was 27% (*17*). More than $1 billion per year is needed in support of contraceptive supplies for low-income countries, but actual support from donors is in the $200 million per year range (*4*). One possibility that was brought up in the hearings is that China, with its high-volume manufacturing capacity, might supply an increasing proportion of the pills, condoms, and injectable contraceptives for the developing world.

Between 2005 and 2050, the world population is projected to grow by 2.6 billion—a number roughly equal to the total global population in 1950 (2.5 billion) (*13*). Decisions made now can influence the growth rate. If the rates are not altered, hundreds of millions of families will suffer from poverty, hunger, inadequate education, and lack of employment opportunities, all of which might otherwise have been avoided.

References and Notes

1. All Party Parliamentary Group on Population Development and Reproductive Health, "Return of the Population Growth Factor: Its Impact on the Millennium Development Goals" (HMSO, London, 2007); for the report and oral and written evidence, see www.appg-popdevrh.org.uk/
2. J. Cleland *et al.*, *Lancet* **368**, 1810 (2006).
3. F. Graham-Smith, Ed., *Population—the Complex Reality: A Report of the Population Summit of the World's Scientific Academies* (The Royal Society, London, 1994).
4. J. J. Speidel, "Population Donor Landscape Analysis for Review of Packard Foundation International Grantmaking in Population, Sexual and Reproductive Health and Rights" (Packard Foundation, Los Altos, CA, 2005).
5. U.N. Population Fund (UNFPA), written evidence (*1*) (March 2006), p. 9.
6. J. Cleland, J. Blacker, S. Mayhew, O. Campbell, London School of Hygiene and Tropical Medicine, written evidence (*1*), pp. 12 and 17.
7. D. King, oral evidence (*1*) (3 July 2006), pp. 14 and15.
8. S. O. Rutstein, *Int. J. Gynaecol. Obstet.* **89** (suppl. 1), S7 (2005).
9. M. Collumbien, M. Gerressu, J. Cleland, in *Comparative Quantification of Health Risks: Global and Regional Burden of Disease Attributable to Selected Major Risk Factors*, M. Ezzati, A. Lopez, A. Rodgers, C. Murray, Eds. (World Health Organization, Geneva, 2004) p. 1255–1319.
10. C. F. Westoff, "New estimates of unmet need and demand for family planning" (Demographic and Health Surveys, ORC Macro, Calverton, MD, in press).
11. H. W. Reynolds, M. J. Steiner, W. Cates Jr., *Sex. Transm. Infect.* **81**, 184 (2005).
12. J. D. Shelton, B. Johnson, *BMJ* **323**, 139 (2001).
13. United Nations, Economic and Social Affairs, *World Population Prospects: The 2004 Revision, Highlights* (United Nations, New York, 2005), Table VIII.2, p. 34.
14. M. Potts, A. Rosenfield, *Lancet* **336**, 1293 (1990).
15. M. Potts, A. Rosenfield, *Lancet* **336**, 1227 (1990).
16. M. Campbell, N. N. Sahin-Hodoglugil, M. Potts, *Stud. Fam. Plann.* **37**, 87 (2006).
17. J. Bates, Y. Chandani, K. Crowley, J. Duravich, S. Raw, *Implications of Health Sector Reform for Contraceptive Logistics: A Preliminary Assessment for sub-Saharan Africa* (John Snow, Inc., Family Planning Logistics Management, for the U.S. Agency for International Development, Arlington, VA, 2000).

10.1126/science.1140057

CLIMATE CHANGE

Why Is It Hard to Predict the Future of Ice Sheets?

Ice sheet behavior is strongly influenced by processes at its margin and base. Observations of rapid changes at these boundaries are helping modelers to improve predictions of future changes.

David G. Vaughan and Robert Arthern

The recent report from the Intergovernmental Panel on Climate Change (IPCC) (*1*) highlights the improved accuracy of measurements of current sea-level rise, as well as greater certainty in the projected impacts of global warming on non-polar glaciers and thermal expansion of the oceans. These advances heighten confidence in projections of the most predictable components of sea-level rise, but the IPCC's projections specifically exclude the contribution that could arise from rapidly changing flow in ice sheets, especially in Greenland and West Antarctica. Why does so much uncertainty surround the future of ice sheets and their impact on sea-level rise?

Compared with the coupled ocean-atmosphere climate system, an ice sheet might seem a rather simple system to model numerically. Ice sheets are composed of a single, largely homogeneous material. Their viscous flow is governed by the Navier-Stokes equation formulated in the mid-19th century. They move so slowly that turbulence, Coriolis, and other inertial effects can be ignored. Stresses within the ice are handled well in the latest generation of ice sheet models (*2*). It is in specifying the stress boundary conditions on two of the ice sheet interfaces—its base and its seaward margin—that the difficulty arises.

At the base of the ice sheet, the stress resisting ice flow can vary by orders of magnitude, depending on the pressure of subglacial meltwater and the slipperiness of sediments. The transience and complexity of water flow beneath ice streams is only now becoming apparent (*3*). At the basal boundary, interactions among water flow, friction, sediment deformation, and heat flow become so intertwined that calculating the resistive stress from first principles tests the ingenuity of glaciologists. Nor is it certain that the basal boundary condition will remain constant on the decadal to centennial time scales that are of interest to the IPCC, especially in Greenland, where meltwater can flood through crevasses to lubricate the base of the ice sheet (*4*).

The authors are with the British Antarctic Survey, Natural Environment Research Council, Madingley Road, Cambridge CB3 0ET, UK. E-mail: dgv@bas.ac.uk

CREDIT: P. HUEY/SCIENCE

At the margin of the ice sheet, the ice begins to float, interacts with the ocean, and eventually calves into icebergs. This boundary controls whether the ice sheet is stable to perturbations, induced perhaps by warmer oceans or atmosphere. Early theories suggested that the location of the margin might be unstable enough that a small perturbation could trigger runaway retreat inland (see the figure) (*5*). Since then, glaciologists have debated whether such extreme behavior could really occur. A new boundary-layer theory for coastal ice shows the way forward (*6*). This theory still needs to be incorporated into large-scale ice sheet models, but early indications are that the instability highlighted by earlier theories should be taken seriously.

Recent observations of widespread acceleration of glaciers draining the Greenland Ice Sheet have brought our uncertainty in specifying these boundary conditions to prominence. Greenland appears capable of responding to changing atmospheric and ocean conditions around its margins much faster than expected (*7*–*9*). The immediate challenge for modelers is to improve the description of the basal and terminal processes such that these changes can be reproduced in model simulations. This is a substantial task, but it is made more feasible by the observations of change that reveal the time scales of response [see also the accompanying Perspective by Truffer and Fahnestock (*10*)], and it provides a superb opportunity to test whether the processes we expect to be important are correctly represented in the models.

In recent years, many changes have also been observed in West Antarctica: thinning and loss of buttressing ice shelves, accelerating glacier flow, thinning of the seaward portion of many glaciers in the region, and inland retreat of the point at which the ice begins to float. The latest theoretical advances have done nothing to allay fears concerning the potential instability of marine ice sheets (*6*) (see the figure). Determining whether small changes could really trigger substantial deglaciation is complicated enough. To compound this, there are no clear-cut records of marine ice sheet deglaciation for comparison, either on Earth today or in the geological record.

There have probably been many marine ice sheet deglaciations during the glacial cycles of the past 2 million years, but the geological record was bulldozed away as the ice sheets subsequently readvanced. Only the record of the last deglaciation, since about 18,000 years ago, remains intact. This deglaciation caused two periods of global sea-level rise at rates far higher than those projected by the IPCC (*2*). However, most of that rise resulted from non-marine ice sheets, and the sea-level curve on its own does not tell us to what extent marine ice sheets are unstable. Indeed, there is still major uncertainty as to how much of the West Antarctic Ice Sheet survived in recent interglacial periods that were globally warmer than today and that are the best analog for future greenhouse warming. In the absence of a sufficiently well-documented example of marine ice sheet retreat, hypotheses of instability could be missing important processes that limit the rate or extent of retreat, or conversely,

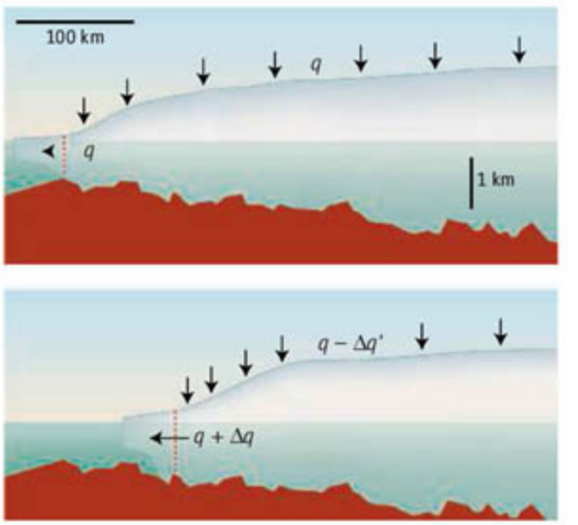

Concerns about stability. The ice sheet covering West Antarctica is the last great marine ice sheet. Its bed lies below sea level and slopes down inland from the coast. The profile shown is based on Thwaites Glacier, West Antarctica (*11*). In the top panel, the ice sheet is in equilibrium; influx from snowfall (q) is balanced by outflow. A small retreat (lower panel) will provoke changes in both the influx and the outflow. If these changes act to promote further retreat, the ice margin is unstable.

promote sudden episodes of retreat.

The accuracy (or "skill") that can be achieved by predictive models rests as much on the quality of data available for testing as it does on the insightful representation of the physical processes. Weather prediction models exhibit a good deal of skill, not because the atmosphere is simpler or better understood than ice flow, but because those models are run and tested with different starting conditions every day and are modified when proved inadequate. Ice sheet models cannot rely so heavily on this cycle of model validation and improvement because of fewer data and much longer time scales.

The uncertainty over the future of the world's ice sheets may persist as the major uncertainty in projections of sea-level rise, perhaps even into the next round of IPCC assessment. Nonetheless, important advances are being made. Ongoing changes in the West Antarctic Ice Sheet and in Greenland are being observed in great detail from satellites (*3*, *9*, *11*); field work is beginning to be directed toward the key areas of the West Antarctic Ice Sheet (*12*); and the history of West Antarctic deglaciation is being constrained on the basis of marine sediment records and dating of rock exposures (*13*). New theories of ice flow appropriate to the coastal boundary are available (*6*). New tools for combining data and models to predict ice flow are also being developed (*14*). New data are coming in and new models are there to be tested—perhaps this is not so different from weather forecasting after all.

The IPCC report has appropriately highlighted the urgent need to reduce uncertainty over the future of ice sheets in Greenland and Antarctica. Accurately predicting how stresses will evolve at the base and the margin has become the priority for ice sheet modelers. Observations are vital for testing these predictions. Recent observations of changes in Greenland and West Antarctica provide the best opportunity for ice sheet modelers to make progress, because they are key to what will happen in the future.

References and Notes

1. The IPCC Working Group I Fourth Assessment Report Summary for Policymakers was released on 2 February 2007 (www.ipcc.ch); the full Working Group I report will be released in May 2007.
2. R. B. Alley, P. U. Clark, P. Huybrechts, I. Joughin, *Science* **310**, 456 (2005).
3. H. A. Fricker, T. Scambos, R. Bindschadler, L. Padman, *Science* **315**, 1544 (2007); published online 15 February 2007 (10.1126/science.1136897).
4. H. J. Zwally *et al.*, *Science* **297**, 218 (2002); published online 6 June 2002 (10.1126/science.1072708).
5. J. Weertman, *J. Glaciol.* **13**, 3 (1974).
6. C. Schoof, *J. Fluid Mech.* **573**, 27 (2007).
7. A. Luckman, T. Murray, R. de Lange, E. Hanna, *Geophys. Res. Lett.* **33**, L03503 (2006).
8. E. Rignot, P. Kanagaratnam, *Science* **311**, 986 (2006).
9. I. M. Howat. I. Joughin, T. A. Scambos, *Science* **315**, 1559 (2007); published online 8 February 2007 (10.1126/science.1138478).
10. M. Truffer, M. Fahnestock, *Science* **315**, 1508 (2007).
11. A. Payne, P. Sammonds, Eds., Special issue on Evolution of the Antarctic Ice Sheet: New Understanding and Challenges, *Philos. Trans. R. Soc. London Ser. A* **364**(1844) (2006).
12. J. W. Holt *et al.*, *Geophys. Res. Lett.* **33**, L09502 (2006).
13. J. O. Stone *et al.*, *Science* **299**, 99 (2003).
14. R. J. Arthern, R. C. A. Hindmarsh, *Philos. Trans. R. Soc. London Ser. A* **364**, 1841 (2006).

10.1126/science.1141111

PHYSICS

Critical Insights

Ultracold atomic gases provide a new experimental tool that promises to advance our understanding of both classical and quantum phase transitions.

Ehud Altman

Phase transitions, which mark the appearance of a new ordered state, display some of the most fascinating phenomena in nature. Some of these transitions are discontinuous, that is, there is an abrupt change as a parameter such as temperature is varied. An example is the freezing of water into ice. In this case the properties of water are unaffected by the coming change. Continuous transitions, such as formation of magnetic order in a ferromagnet, are markedly different. As the material approaches the critical point, fluctuations of the new order grow in size and eventually govern the macroscopic properties of the system, making them universal.

On page 1556 of this issue, Donner *et al.* report an experiment with ultracold atomic gases in which they observe these fluctuations directly (*1*), watching how they grow from microscopic to macroscopic dimensions as the transition to a Bose-Einstein condensate is approached. What is even more exciting, the fluctuations are monitored as they evolve in time, potentially offering a glimpse at the dynamics of phase transitions. Such experiments could also be applied to systems of ultracold atoms undergoing quantum phase transitions at zero temperature, promising to advance our rather rudimentary understanding of the dynamics associated with these phenomena.

Studies of these dilute gases of weakly interacting ultracold atoms were at the focus of the field in the 1990s after the pioneering observations of Bose-Einstein condensation (*2*, *3*). Much of the excitement back then resulted from observations of the macroscopic quantum coherence exhibited by the condensates (*4*). Just as a laser is a coherent source of light, Bose-Einstein condensates behave as coherent sources of matter. Thus, streams of atoms coming out of two condensates display a macroscopic interference pattern similar to that formed by two coherent sources of light.

On the fundamental level, experiments with weakly interacting Bose gases did not lead to big surprises. By and large, they confirmed the theoretical understanding developed in the 1950s and 1960s. However, the simplicity of the system led to new experimental tools that enabled precise control over microscopic parameters. The current trend in the field is to use these tools to alter the strength of interactions between atoms. This can be done, for example, by loading atoms into lattices generated by standing waves of laser light or by trapping atoms in one- or two-dimensional arrangements. If the interactions are strong enough, simple macroscopic coherence may give way to interesting and not yet fully understood many-body states.

The experiment carried out by Donner *et al.* takes a step back to revisit the weakly interacting gas, but now concentrating on the properties just above the transition temperature T_c, where the coherence is not yet truly macroscopic. At this critical stage, bubbles of the coherent condensate exist in the gas as temporary fluctuations that herald the coming of the ordered phase. The size and lifetime of these fluctuations grow without limit at the critical point. In a sense, focusing on the critical regime is another way to amplify the strength of interactions. The modern theory of critical phenomena implies that even weak interactions between individual pairs of particles generate effective interactions between the critical fluctuations that grow in magnitude concomitantly with the size of the fluctuations. Therefore, dynamics at these scales is

The author is in the Department of Condensed Matter Physics, Weizmann Institute of Science, Rehovot, 76100, Israel. E-mail: altman@wisemail.weizmann.ac.il

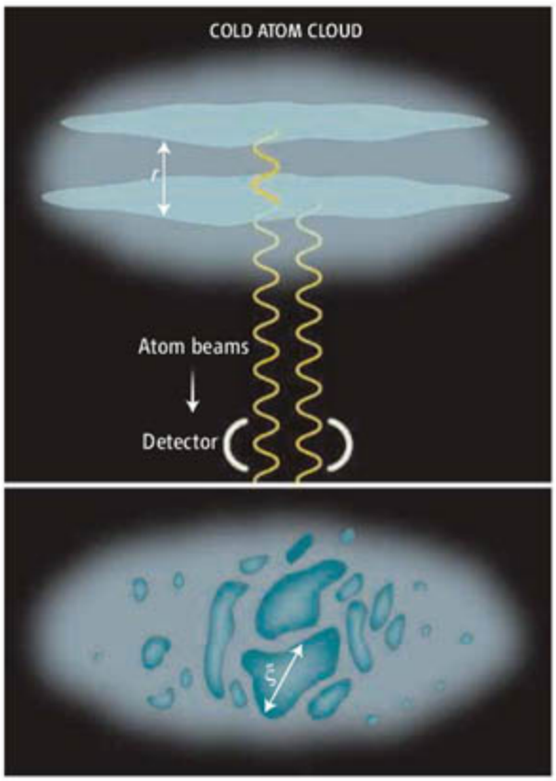

Mapping a phase transition. (**Top**) Streams of atoms are extracted from two slices of an ultracold atom cloud. If the gas is coherent over the distance r, the two beams form an interference pattern. (**Bottom**) The decay of the interference with distance is used to measure the size of critical fluctuations, temporary puddles of Bose-Einstein condensate that form in the uncondensed state as the phase transition is approached.

highly correlated and cannot be described by a theory of weakly interacting particles.

Early studies of ultracold gases observed only the fully condensed gas and thus could not access the physics of the critical regime near the transition to a Bose-Einstein condensate. As a consequence of the nonuniform density in the atom trap, the transition first occurs in the middle of the gas and only gradually creeps outward with decreasing temperature. For all the global properties that experiments could probe, this inherent inhomogeneity completely overwhelmed the effect of the critical fluctuations.

To overcome this problem, Donner *et al.* developed an ingenious scheme for measuring correlations between well-defined regions (see the figure). By irradiating the cold gas with a properly formed microwave field, they were able to extract atoms from just two predetermined slices separated by an adjustable distance r. The streams of outgoing atoms fell through an optical cavity, where they were counted and a temporal interference signal was obtained. The amplitude of the interference fringes, averaged over a sufficiently long time, is a measure of the coherence maintained over the distance r. Below T_c the entire condensate behaves as a single macroscopic wave function, and thus the amplitude of interference does not decay with distance. On the other hand, above T_c the amplitude is expected to decay over a length scale ξ, which reflects the spatial extent of typical fluctuations. This length scale is expected to diverge at the critical point as $(T - T_c)^{-\nu}$, where n is a critical exponent.

As evidence that they are truly looking at the critical fluctuations, Donner *et al.* measured this critical exponent. According to the theory of critical phenomena, ν is a universal number determined only by the dimensionality of the problem and the symmetry change occurring at the transition, not by the microscopic details (such as the specific atom in the gas). Indeed, the measured exponent agreed with data on a phase transition in liquid helium (*5*), which belongs to the same universality class as the Bose-Einstein condensation transition of weakly interacting bosons.

Admittedly, measurement of a critical exponent, especially with the rather low accuracy achieved in this experiment, is not of much topical interest. However, the importance of the new approach lies in what is yet to come. The ability to continuously monitor the correlations over time opens intriguing possibilities in the study of dynamics of phase transitions. For example, a question recently touched upon by the same research group (*6*) is how phase coherence is established in time when the temperature is lowered through the transition at a finite rate.

This new approach is by no means limited to the study of the classical condensation transition. A similar setup can be envisioned for a system of interacting bosons on an optical lattice, which undergoes a quantum phase transition from a superfluid to an insulating state (*7*). In such quantum phase transitions, critical fluctuations are driven by quantum uncertainty rather than thermal noise. The nonequilibrium dynamics around such critical points is currently a subject of intense research. Systems of ultracold atoms are already advancing our understanding of quantum phases of matter. Now they promise to shed new light on the mysteries of phase transitions and quantum critical points.

References

1. T. Donner *et al.*, *Science* **315**, 1556 (2007).
2. M. H. Anderson *et al.*, *Science* **269**, 198 (1995).
3. K. B. Davis *et al.*, *Phys. Rev. Lett.* **75**, 3969 (1995).
4. M. R. Andrews *et al.*, *Science* **275**, 637 (1997).
5. L. S. Goldner *et al.*, *J. Low Temp. Phys.* **93**, 131 (1993).
6. S. Ritter *et al.*, *Phys. Rev. Lett.* **98**, 090402 (2007).
7. M. Greiner *et al.*, *Nature* **415**, 39 (2002).

10.1126/science.1140809

AIDS/HIV

Finding Footprints Among the Trees

Paul Klenerman and Andrew McMichael

High-quality statistical analyses allow tracking of HIV evasion of the host immune response through epitope mutations and suggest refined strategies for vaccine development.

To establish a long-term persistent infection, HIV has evolved many strategies. One of these is to mutate at the sites in virus proteins that stimulate immune responses. This gives rise to variant viruses that evade recognition by host immune cells (T cells) and antibodies. An earlier analysis of virus sequences in HIV-infected populations indicated that such "immune escape" plays a major role in the evolution of the virus (*1*). But on page 1583 in this issue, Bhattacharya *et al.* (*2*) take another look at HIV sequence data in infected populations and find that viral lineage (or genetic relatedness) is a confounding factor in the analysis of HIV sequence evolution. This means that the effect of immune escape may not be as strong as suspected. Virus variability may not be as predictable as first thought, making it harder to cover the variation of HIV by vaccines.

The targets of T cell immune responses are very diverse and are determined by the host human leukocyte antigen (HLA) or tissue type. HLA class I molecules are expressed on most cells and, when the cell is infected, HLA molecules "present" peptides derived from virus proteins to T cells of the $CD8^+$ subtype.

P. Klenerman is in the Nuffield Department of Clinical Medicine, Peter Medawar Building, University of Oxford, Oxford OX1 3SY, UK. A. McMichael is at the Weatherall Institute of Molecular Medicine, John Radcliffe Hospital, University of Oxford, Oxford OX3 9DS, UK. E-mail: andrew.mcmichael@ndm.ox.ac.uk

HLA proteins are highly polymorphic so that in different individuals, $CD8^+$ T cells respond to different viral peptides, depending on the individual's HLA type. A virus can escape a host's T cell response by mutating one or more of these presented viral peptides such that they no longer bind to HLA molecules, fail to interact with the T cell's receptors, or are not processed correctly within the cell. The T cell response then becomes ineffective.

It has been known since 1991 that HIV can mutate and escape from T cell immune responses (*3*), but in 2002, Moore *et al.* proposed that T cell escape mutants were much more frequent and predictable than previously thought (*1*). The authors sequenced the virus gene encoding the HIV Pol protein in a large cohort of HIV-infected patients in Perth, Western Australia. In many cases, they were able to correlate variation at specific sites in the *pol* gene with the HLA type of the host. In other words, the HLA type of the patient imposed a characteristic change (through T cell selection), or "footprint," on the virus sequence in that patient. This indicated that analysis of viral sequences in the context of HLA type could help identify viral sequences that stimulate T cell responses (*4*) (see the figure).

Bhattacharya *et al.* have now applied a more rigorous statistical approach to this kind of viral sequence analysis. In particular, they have taken into account the historical relatedness of HIV sequences within the patient cohort, using phylogenetic trees to estimate how the sequences have diverged over time. Although original data from the study by Moore *et al.* were not reexamined, studies of a similar cohort revealed that many apparent associations between viral sequences and HLA alleles could be attributed to the presence of patients who came from different ethnic groups who were infected with different subtypes of the virus. In other words, apparent viral mutations are actually representative of subtypes (clades) of viruses that are historically and geographically connected. A clear example is an association between certain polymorphisms in the *Gag/Pol* sequence of HIV and HLA C*1701. The polymorphisms are actually common in subtype C HIV-1, a southern African subtype. HLA C*1701 is common in Africans but rare in Caucasians. Thus, the association between these HIV variants and this HLA type is due to a "founder effect."

Although many apparent HIV-HLA sequence associations identified through methods applied by Moore *et al.* were lost by applying these robust statistical techniques and incorporating phylogenetic trees, some HLA-determined T cell "footprints" remained. Bhattacharya *et al.* found seven such examples from 80 original candidates. In four of these, the mutations were within the sequences of viral epitopes known to be presented by the patients' HLA types. In the other three cases, the authors made peptides corresponding to the epitope predicted from their statistical analysis. By testing patient T cells in vitro, the predicted epitope was indeed correct. Thus, the refined method does identify viral mutations that escape T cell recognition, but the extent of this escape process is not as abundant as proposed by Moore *et al.*

How common, then, is escape from T cells? It is clear from Bhattacharya *et al.* that when phylogeny is considered, a significant minority of mutations in the HIV genomic sequence represent escape mutations. These findings do add to the burgeoning data on individual escape mutations in HIV seen in patients as they progress from acute to chronic infection and AIDS (*3*, *5*–*11*). Also, a study of macaques infected with simian immunodeficiency virus (*12*) charted the evolution of virus escape from T cells in acute infection. The macaque study implies more escape than is seen using the new population-based approach of Bhattacharya *et al.* However, escape will show up in HIV-HLA sequence association analyses only if the HLA type occurs repeatedly in the cohort and if a viral escape mutation is exactly the same in most of the patients with a given HLA type; the latter is demonstrably not always the case.

The generation of viral mutations that afford escape from T cells is often used as an argument that T cells control HIV infection (and therefore, that T cells should be stimulated with vaccines). Indeed, selection of an escape mutant must imply that a suppressive force is exerted by the T cell. On the other hand, the selection of escape mutants shows that T cells do not control overall infection—a battle is won but the war is lost. This situation is very similar to escape of the virus envelope from antibody-mediated neutralization—when escape occurs, there is no overall control by the immune system. What may be more important is when T cells select viral mutants that are less fit (because the mutation affects a function or structure that is important to the virus); in this case, immune escape could be beneficial for the host (*11*, *13*, *14*).

The findings of Bhattacharya *et al.* have implications for the study of other viruses, notably hepatitis C virus (HCV). Several groups who have taken phylogeny into account have identified "footprints" of T cells on HCV, including a large single-source outbreak among Irish women (*15*, *16*). A clear footprint on HCV was also observed in an epitope restricted by HLA-B27, an allele that is protective in both HCV and HIV (*17*). Because the sequence diversity of HCV is even greater than that of HIV, taking into account the viral phylogeny when studying HCV-related immunology will likely be of

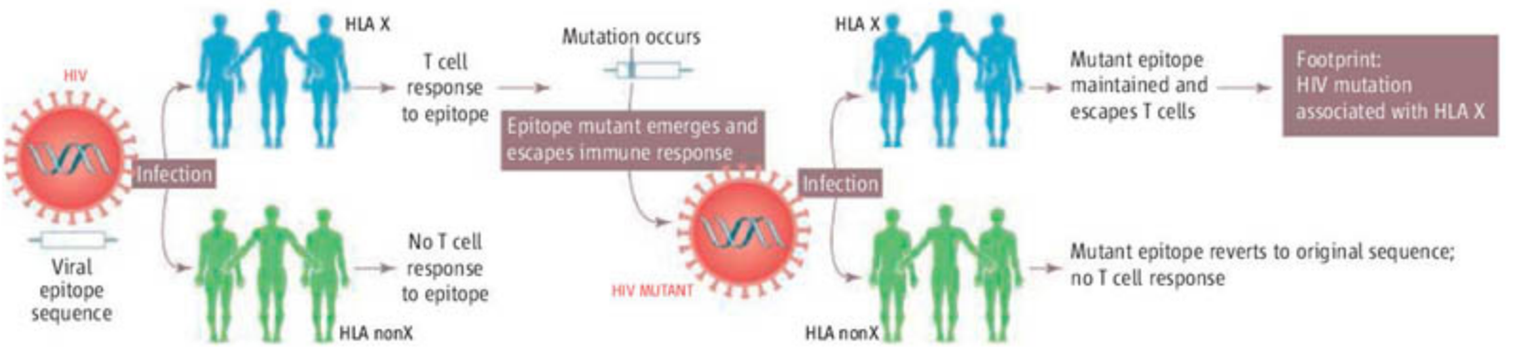

HLA footprints in HIV populations. If a virus infects individuals with a particular HLA type (HLA X), mutations in a viral epitope may emerge that allow it to "escape" from host (T cell) detection. If the virus infects individuals who lack this HLA, (HLA nonX), immune escape will not occur and the viral epitope will remain unmutated. If virus bearing the escape mutation is then transmitted to a HLA nonX individual, the virus may revert (perhaps due to a fitness advantage of the unmutated sequence). The mutation remains strongly associated with the HLA X group, and is evident as an HLA "footprint." However, if viruses circulate separately between the HLA X and nonX populations over a long time period, other mutations in the HIV genome may occur that do not result from immune escape. These may appear to be HLA associated, but are not true HLA footprints and may be distinguished through phylogenetic analysis of the viruses, as shown by Bhattacharya *et al.* (*2*).

CREDIT: P. HUEY/SCIENCE

even greater consequence than for HIV.

What does this mean for HIV or HCV vaccine design? It might be possible to design vaccines that anticipate the frequently selected escape mutations by using more than one viral amino acid sequence in the vaccine (*18*), though this would require very complex vaccines. An alternative would be to use vaccines to redirect the immune response to the most conserved regions of the virus, which may be invariant because of functional or structural constraints. However, the extraordinary power of viruses like HIV and HCV to escape almost any means of host attack remains a daunting hurdle to overcome. The phylogenetic trees may have eliminated some T cell footprints, but they reveal the enormous complexity of the viral epidemic both within individuals and within populations.

References

1. C. B. Moore *et al.*, *Science* **296**, 1439 (2002).
2. T. Bhattacharya *et al.*, *Science* **315**, 1583 (2007).
3. R. E. Phillips *et al.*, *Nature* **354**, 453 (1991).
4. A. McMichael, P. Klenerman, *Science* **296**, 1410 (2002).
5. D. A. Price *et al.*, *Proc. Natl. Acad. Sci. U.S.A.* **94**, 1890 (1997).
6. P. J. Goulder *et al.*, *Nat. Med.* **3**, 212 (1997).
7. P. Borrow *et al.*, *Nat. Med.* **3**, 205 (1997).
8. A. D. Kelleher *et al.*, *J. Exp. Med.* **193**, 375 (2001).
9. N. A. Jones *et al.*, *J. Exp. Med.* **200**, 1243 (2004).
10. A. Leslie *et al.*, *J. Exp. Med.* **201**, 891 (2005).
11. A. J. Leslie *et al.*, *Nat. Med.* **10**, 282 (2004).
12. D. T. Evans *et al.*, *Nat. Med.* **5**, 1270 (1999).
13. A. K. Iversen *et al.*, *Nat. Immunol.* **7**, 179 (2006).
14. W. W. Yeh *et al.*, *J. Virol.* **80**, 8168 (2006).
15. S. Gaudieri *et al.*, *J. Virol.* **80**, 11094 (2006).
16. S. C. Ray *et al.*, *J. Exp. Med.* **201**, 1753 (2005).
17. C. Neumann-Haefelin *et al.*, *Hepatology* **43**, 563 (2006).
18. W. Fischer *et al.*, *Nat. Med.* **13**, 100 (2007).

10.1126/science.1140768

STRUCTURAL BIOLOGY

A Glimpse of Biology's First Enzyme

The structure of an RNA enzyme that catalyzes the joining of RNA has been solved, providing insight into what may have been the most ancient enzyme of biology.

Gerald F. Joyce

Biology uses DNA genomes and protein enzymes to carry out the operations of the cell. RNA plays many important roles, but it is subservient to DNA and proteins. In the distant evolutionary past, though, things may have been very different. Almost 40 years ago, it was first suggested that both genomic information and enzymatic function once resided exclusively in RNA (*1*–*3*). Crick speculated that the first enzyme may have been an RNA molecule that catalyzed the replication of other RNA molecules (*2*). After catalytic RNA was discovered, Gilbert coined the term "RNA world", which he similarly envisioned as being based on RNA molecules that catalyze the synthesis of copies of themselves (*4*).

We now have the first glimpse of what such an RNA replicase might have looked like. On page 1549 of this issue, Robertson and Scott report the crystal structure of an RNA enzyme obtained by test-tube evolution that catalyzes the joining of two RNA molecules that are bound at adjacent positions along an RNA template (*5*).

Protein enzymes that catalyze the copying of RNA use as building blocks the four nucleoside 5′-triphosphates (NTPs). These are bound to an RNA template and joined through the reaction between the 3′-hydroxyl group of one NTP and the 5′-triphosphate of the next, forming a 3′,5′-phosphodiester linkage (see the figure, top panel). It is not clear whether the hypothetical replicase enzyme of the RNA world operated by the same mechanism, but it is a reasonable bet. The template provides a favorable orientation for the reaction, and the 5′-triphosphate offers a desirable combination of being very stable in water yet thermodynamically highly activated for the reaction. All that is needed is the right catalyst to facilitate the reaction.

No known RNA enzyme in biology catalyzes the polymerase-like joining of RNA. However, the powerful methods of in vitro evolution have made it possible to generate such enzymes from scratch, starting from a large population of RNAs with random sequences (*6*). The usual approach is first to evolve an RNA enzyme that is an RNA ligase, which can join two oligonucleotides in a

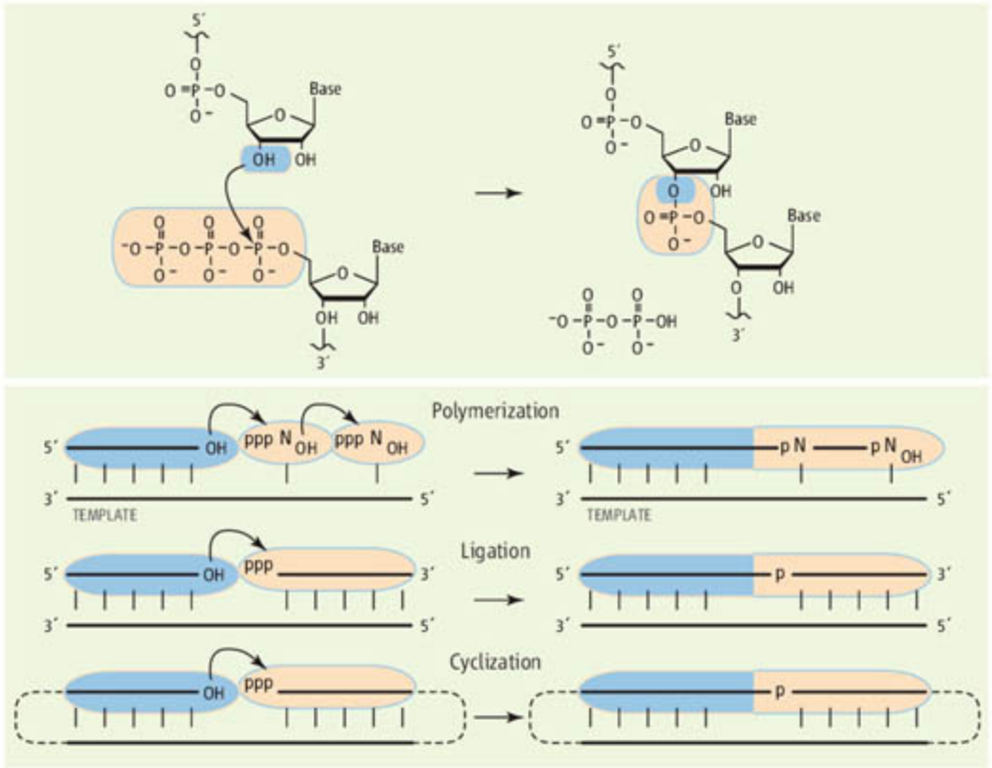

RNA-templated joining of RNA. (**Top**) The 3′-hydroxyl of one nucleotide (blue) attacks the 5′-triphosphate of another (orange) to form a 3′,5′-phosphodiester. This reaction is the basis for RNA polymerase proteins and for in vitro evolved RNA enzymes with RNA ligase or RNA polymerase activity. (**Bottom**) Somewhat different reaction formats are used for the polymerization of NTPs, the joining of RNAs by a ligase, and the formation of a circular RNA as carried out by Robertson and Scott (*5*). $pppN_{OH}$ indicates an NTP, OH the attacking 3′-hydroxyl, ppp the reactive 5′-triphosphate, and pN the site of the newly-formed phosphodiester.

The author is in the Departments of Chemistry and of Molecular Biology, The Scripps Research Institute, La Jolla, CA 92037, USA. E-mail: gjoyce@scripps.edu

template-directed manner. Then, through further evolution, the researcher attempts to coax the ligase to accept NTPs as substrates and to add multiple NTPs in succession.

Bartel and colleagues (*7*) have used one such in vitro evolved ligase, the class I ligase, and evolved it further to polymerize as many as 14 successive NTPs with high fidelity. Despite valiant efforts, however, it appears unlikely that this particular polymerase enzyme will ever be evolved to the point that it can copy RNA molecules as long as itself (~200 nucleotides). Nonetheless, it is likely that scientists will eventually apply a similar approach to a different set of RNA molecules to achieve more extensive polymerization and ultimately complete replication.

The class I ligase is the Ferrari of in vitro evolved ligase enzymes. Under optimal reaction conditions, it has a catalytic rate of up to 360 per minute. Like a Ferrari, however, it has very narrow tolerances and has been tweaked in imaginative ways to extract maximum performance. Three other RNA enzymes, the L1 ligase (*8*), R3C ligase (*9*), and DSL ligase (*10*), have substantial structural and biochemical similarity and may be regarded as three different versions of the family sedan. All catalyze the template-directed joining of an oligonucleotide 3′-hydroxyl and oligonucleotide 5′-triphosphate, but at a rate of only about 0.3 per minute. All have a simple three-helix junction architecture, in which the nucleotides that are essential for catalysis surround the junction and the site of ligation is offset from the junction by several base pairs. It is the L1 ligase that has been crystallized by Robertson and Scott, who solved its structure at a resolution of 2.6 Å (*5*).

Robertson and Scott crystallized the product of an autoligation reaction, in which the L1 ligase was configured to join its own 3′-hydroxyl to its own 5′-triphosphate (see the figure). Two different forms of the circular product were present in the asymmetric unit of the crystal: one in an "undocked" conformation, with the three-helix junction splayed out and no contact between the catalytically essential nucleotides and the ligation site, and the other in a "docked" conformation, with many of these essential nucleotides held near the ligation site. The docked conformation (which can reasonably be interpreted as the active form of the enzyme) is stabilized by tertiary contacts involving a guanine-adenine-uracil base triple and by ionic interactions between a single Mg^{2+} ion and three phosphate groups.

The crystal structure reflects the product of ligation rather than the reactants. One must therefore be cautious in drawing conclusions about the reaction mechanism. Rather than a free 3′-hydroxyl and a reactive 5′-triphosphate bearing four negative charges, the 3′,5′-phosphodiester is already in place. Nonetheless, some inferences regarding the reaction mechanism may be drawn from the structure, which reveals a network of hydrogen bonding and ionic interactions centered about the ribose sugar that bears the attacking 3′-hydroxyl. The adjacent 2′-hydroxyl appears to be kept out of the fray by its interaction with a tightly bound water molecule. If this were not the case, the reaction might instead result in formation of an unnatural 2′,5′-phosphodiester, rather than the 3′,5′-phosphodiester of RNA.

The L1 ligase is not a polymerase, let alone a replicase, but it performs the same chemistry that would be expected for an RNA molecule with RNA replicase properties. Its crystal structure gives us a view toward what may have been the first enzyme of biology, or at least the central enzyme of the RNA world. In the years ahead, we can expect to see the structure of other ligases, and eventually of polymerase and replicase RNA enzymes. These laboratory mimics of our deepest evolutionary ancestors will not appear to be alien objects. Like the L1 ligase, they will have comfortingly familiar structural features and an active site built of the usual stuff of biochemistry: hydrogen bonding, ionic, and hydrophobic interactions that have been crafted by processes of Darwinian evolution. Unlike the ancient RNA replicase enzymes that likely became extinct more than 3.5 billion years ago, these modern recreations will be available for detailed investigation.

References

1. C. Woese, *The Genetic Code: The Molecular Basis for Genetic Expression* (Harper & Row, New York, 1967), pp. 179–195.
2. F. H. C. Crick, *J. Mol. Biol.* **38**, 367 (1968).
3. L. E. Orgel, *J. Mol. Biol.* **38**, 381 (1968).
4. W. Gilbert, *Nature* **319**, 618 (1986).
5. M. P. Robertson, W. G. Scott, *Science* **315**, 1549 (2007).
6. D. P. Bartel, J. W. Szostak, *Science* **261**, 1411 (1993).
7. W. K. Johnston, P. J. Unrau, M. S. Lawrence, M. E. Glasner, D. P. Bartel, *Science* **292**, 1319 (2001).
8. M. P. Robertson, A. D. Ellington, *Nature Biotechnol.* **17**, 62 (1999).
9. J. Rogers, G. F. Joyce, *RNA* **7**, 395 (2001).
10. Y. Ikawa, K. Tsuda, S. Matsumura, T. Inoue, *Proc. Natl. Acad. Sci. U.S.A.* **101**, 13750 (2004).

10.1126/science.1140736

CLIMATE CHANGE

Rethinking Ice Sheet Time Scales

Satellite data show that ice sheets can change much faster than commonly appreciated, with potentially worrying implications for their stability.

Martin Truffer and Mark Fahnestock

According to glaciology textbooks, glaciers respond to climate change on time scales that vary from a decade or more for nonpolar glaciers to millennia for polar ice sheets. These numbers have lured the scientific community into thinking that while small glaciers undergo rapid changes, the big ice sheets adjust at a leisurely pace.

Lately, the ice sheets have been teaching us differently. Recent reports documented rapidly increasing discharge of Greenland's outlet glaciers (*1*–*3*). These glaciers are responsible for most of the ice sheet's mass loss, acting as "bathtub drains" to the vast interior ice mass (see the figure). On page 1559 of this issue, Howat *et al.* (*4*) report that ice discharge can also decrease at a high rate: Two of the major outlet glaciers in southeastern Greenland—Helheim and Kangerdlugssuaq—doubled their discharge of ice into the ocean within 1 year in 2004. Two years later, the discharge quickly dropped back close to its former rate.

Near the other pole, Fricker *et al.* [page 1544 (*5*)] report changes in ice surface elevation from data recorded by NASA's Ice, Cloud, and land Elevation Satellite (ICESat). These observations are interpreted as a sign of moving subglacial water under a large ice stream. At one ice stream location, the surface drop can be explained by the drainage of 2 km^3 of subglacial water. Elsewhere, the ice surface rose sufficiently to account for the storage of this water. Earlier studies had shown the existence of such elevation changes (*6*, *7*), but Fricker *et al.*'s analysis reveals a surprisingly active system of subglacial hydrology in a part of the world where little or no surface melting occurs.

Today, we can monitor ice sheets with unprecedented spatial and temporal resolu-

M. Truffer is at the Geophysical Institute, University of Alaska, Fairbanks, AK 99775, USA. E-mail: truffer@gi.alaska.edu M. Fahnestock is at the Institute for the Study of Earth, Oceans and Space, University of New Hampshire, Durham, NH 03824, USA.

tion, thanks to an array of Earth-observing satellites and many ground-based studies. The resulting news has consistently had an element of surprise with regard to time scales. Invariably, processes are happening more rapidly than previously thought possible (*2–4*, *8*, *9*). The discovery of moving water pockets underneath the West Antarctic ice streams by Fricker *et al.* and the rapidly oscillating fluxes at two of Greenland's outlet glaciers reported by Howat *et al.* further illustrate how rapidly ice sheets can change.

These observations of rapid change (*1–9*) highlight shortcomings in our understanding of relevant physical processes, such as the connection of ice to surrounding sediment, rock, and water. These boundary conditions help to regulate outlet glacier and ice shelf systems. In outlet glaciers, the ice/bed interaction is subject to a substantial flux of water. As recently highlighted by the Intergovernmental Panel on Climate Change (*10*), the largest uncertainty in sea-level projections lies in the ability to capture changes in such outlet systems in numerical models [see also the accompanying Perspective by Vaughan and Arthern (*11*)]. The modeling challenge is one of time scales: Water that moves rapidly under Antarctic ice streams and outlet glaciers that fluctuate on an annual basis do not mesh easily with the millennial-scale variations in ice mass, snow fall, and internal temperature required for modeling the thick interiors of large ice sheets.

It remains uncertain how important these rapid changes are for the future stability of the ice sheets. However, the closer we look, the more ice sheet outlet systems appear to behave like much smaller glacier systems in nonpolar regions.

The comparison is not reassuring. The closest analogs of Greenland's outlet glaciers are large tidewater glaciers, which also end in the ocean but are not fed by large ice sheets. Perhaps the best studied of these is Columbia Glacier, which has retreated ~15 km in the past 20 years and thinned by ~400 m near the current terminus (*12*). Columbia's retreat rates and ice discharge have been highly variable, with ice discharge at times reduced to pre-retreat rates, only to pick up again later. In that context, last year's reduction of ice flux at Helheim and Kangerdlugssuaq Glaciers (*1*) does not mean that they have stabilized. The question remains whether changes in the past 5 years have left the system as a whole more vulnerable.

CREDIT: MARTIN TRUFFER

A drain for Greenland's ice sheet. This photo of the calving front of Jakobshavns Isbrae, the major outlet glacier in West Greenland, was taken on 29 August 2006. At the lower right, broken-off pieces of ice are floating in the ocean. The ice cliff is >100 m high. The helicopter is a Sikorski S61, which can carry 12 passengers. Jakobshavns Isbrae currently dumps an estimated 46 km^3 of ice into the ocean every year (*4*).

One difference between outlet and tidewater glaciers is the size of the ice reservoir that feeds them. It is an open question how much fluctuating ice discharge at outlets affects the interior ice. On the smaller scale, however, tidewater glacier retreat can draw down an entire ice field. In Glacier Bay, Alaska, an entire ice field disappeared within ~200 years. Some of this ice was more than 1500 m thick, and a total volume of more than 3000 km^3 was lost (*13*). Initial accelerated discharge depleted the ice reservoir, thinning it substantially. A positive feedback was established, because the ice surface was at lower elevation and thus exposed to higher temperatures and increased melting. The volume of the vanished ice at Glacier Bay is almost three orders of magnitude smaller than that of the Greenland Ice Sheet; nevertheless, it does demonstrate that relatively rapid collapse helped by outlet glacier dynamics is possible on the scale of an ice field.

Fricker *et al.* show that even the Antarctic Ice Sheet—where, in contrast to Greenland, only negligible surface melting occurs today—experiences rapid changes in basal conditions through transfer of subglacial water. The amount of subglacial water, its pressure, and its connectivity all influence basal slipperiness and hence ice discharge. The mapping of subglacial plumbing from space reported by Fricker *et al.* is a major breakthrough that should help to improve our ability to model these systems.

Many questions remain. In Greenland, as well as in Antarctica, large changes are always initiated at the ice-ocean interface. Furthermore, recent changes in Greenland have occurred while the climate has warmed. Are these changes caused by a warming ocean or by increased water runoff from the ice? How do quick changes in ice sheet boundary conditions affect its long-term behavior?

Substantial progress in understanding can only come from interdisciplinary studies exploring the effects of a changing ocean on outlet glaciers, of increased runoff of glacial freshwater on ocean and fjord circulation, and of meltwater on ice flow. Greenland differs from Antarctica in that it has a substantial zone where ice melts, and meltwater runs off and presumably reaches the base. Understanding the relative roles of the processes leading to flow acceleration will help to constrain potential differences between the two ice sheet's reactions to future climate change. As sci-

entists grapple with the spectrum of time scales that drive outlet glaciers in a changing climate, observations such as those documented in this issue will help to lead the way.

References and Notes

1. I. R. Joughin, W. Abdalati, M. Fahnestock, *Nature* **432**, 608 (2004).
2. A. Luckman, T. Murray, *Geophys. Res. Lett.* **32**, L08501 (2005).
3. E. Rignot, P. Kanagaratnam, *Science* **311**, 986 (2006).
4. I. M. Howat. I. Joughin, T. A. Scambos, *Science* **315**, 1559 (2007); published online 8 February 2007 (10.1126/science.1138478).
5. H. A. Fricker, T. Scambos, R. Bindschadler, L. Padman, *Science* **315**, 1544 (2007); published online 15 February 2007 (10.1126/science.1136897).
6. L. Gray *et al.*, *Geophys. Res. Lett.* **32**, L03501 (2005).
7. D. J. Wingham, M. J. Siegert, A. Shepherd, A. S. Muir, *Nature* **440**, 1033 (2006).
8. R. A. Bindschadler *et al.*, *Science* **301**, 1087 (2003).
9. A. M. Smith *et al.*, *Geology* **35**, 127 (2007).
10. The IPCC Working Group I Fourth Assessment Report Summary for Policymakers was released on 2 February 2007 (www.ipcc.ch); the full Working Group I report will be released in May 2007.
11. D. G. Vaughan, R. Arthern, *Science* **315**, 1503 (2007).
12. S. O'Neel, T. W. Pfeffer, R. Krimmel, M. Meier, *J. Geophys. Res.* **110**, F03012 (2005).
13. C. F. Larsen *et al.*, *Earth Planet. Sci. Lett.* **237**, 548 (2005).

14. We acknowledge NSF grant ARC 0531075.

10.1126/science.1140469

DEVELOPMENT

Built to Run, Not Fail

Networks of genes that control organism development are organized in a basic architecture that is conserved across processes and species.

Paola Oliveri and Eric H. Davidson

On first encounter, gene regulatory networks for development often seem so complicated as to defy intuitive understanding. But the overall maze of gene interactions that they represent is actually composed of subcircuits that perform separate functions. The subcircuits are often of elegant and sometimes counterintuitive design, even more so, the ways they are combined in the overall network. As the underlying subcircuit structure is clarified, we see that gene regulatory networks in fact provide a direct and simply organized bridge from the phenomena of development to the detailed genomic programs that encode it. Among the most fascinating aspects of gene regulatory networks are their design principles, for these are often interestingly different from what would seem the "simplest" solution. Gene regulatory networks for development are the direct product of evolution, and the character of their design both illuminates evolution and is illuminated by it.

Each of the specific biological functions which together make up a developmental process is programmed by a specific subcircuit of the network. In other words, large gene regulatory networks have a modular structure: They are composed of different subcircuits that work together to accomplish whole "pieces" of development, such as specification of dorsoventral pattern in the fly embryo or of the endomesoderm territories of the sea urchin embryo. Overall, such gene regulatory networks involve scores of genes [>50 in these cases (*1*)] organized into many subcircuits, where a single subcircuit controls a specific developmental task. These tasks include specifying regulatory states of a group of cells (i.e., determining which regulatory genes they will express); mounting molecular signals that induce new regulatory states in recipient cells; coordinating the expression of genes that control cell differentiation; stabilizing newly established regulatory states; defining tissues and setting their boundaries; and interpreting prior regulatory instructions. There is a plethora of regulatory jobs different from one another—such as the development of embryos, or of stem cells, or of adult body parts—that all require different kinds of subcircuits. The subcircuit components of gene regulatory networks have evolved independently of one another, and at different rates (*2*), and are assembled in different contexts in related organisms. Both in their functional organization and in the separate evolutionary histories of their subcircuits, gene regulatory networks are modular in construction.

The individual subcircuits each consist of a few regulatory genes, including their genomic cis-regulatory information processors, which respond in a combinatorial and conditional manner to the transcription factors encoded by other genes of the same module. In considering structure-function causality in gene regulatory network subcircuits, the architecture of the module tells it all. The architecture is the design of the causal linkages between genes of the subcircuit. This is a hard-wired feature because it is constructed by the inherited cis-regulatory control sequences of these genes. The biological function depends on the architecture. For example, positive cross-regulatory interactions among a set of genes that encode transcription factors can stabilize the particular regulatory state generated by these genes. As another example, it is the particular set of genes regulated by a given gene that is turned on in response to an inductive signal that determines what the developmental effect of the signal will be.

There are two essential consequences of this concept of a modular network architecture and subcircuit design. First, subcircuit architectures are as varied as the biological jobs they do. Thus, although subcircuits are indeed the modular functional components of developmental gene regulatory networks, they are to be distinguished from simpler "building blocks" or "motifs" that are used for many diverse developmental functions (e.g., feedforward or feedback elements, per se). For instance, feedforward motifs are to be found in every conceivable context in diverse gene regulatory networks (*3*), whereas the individually designed subcircuits here considered are specific to the type of biological job they do. Second, subcircuit architectures are built from diverse classes of transcription factor, and by and large, a given type of factor is not dedicated to any given type of subcircuit. In terms of logic outputs, circuits that transduce signals and distribute their outputs may operate very similarly, whatever the nature of the signaling system or the identity of the immediate early response factor. The same is true of cross-regulatory subcircuits. It is the genomic architecture of the subcircuit, and not the nature of the factors the genes encode or the families they belong to, that uniquely indicates subcircuit function [multiple examples of subcircuits from diverse developmental systems can be found in (*3*)].

As we have come to understand developmental gene regulatory networks, there arises an impression of "overlayered" circuit design—or more precisely, deployment of multiple subcircuits—that in different ways support the same end result. In development, the major regulatory task is to specify spatial domains of gene expression. Typically, multi-

The authors are in the Division of Biology, California Institute of Technology, Pasadena, CA 91125, USA. E-mail: davidson@caltech.edu; poliveri@caltech.edu

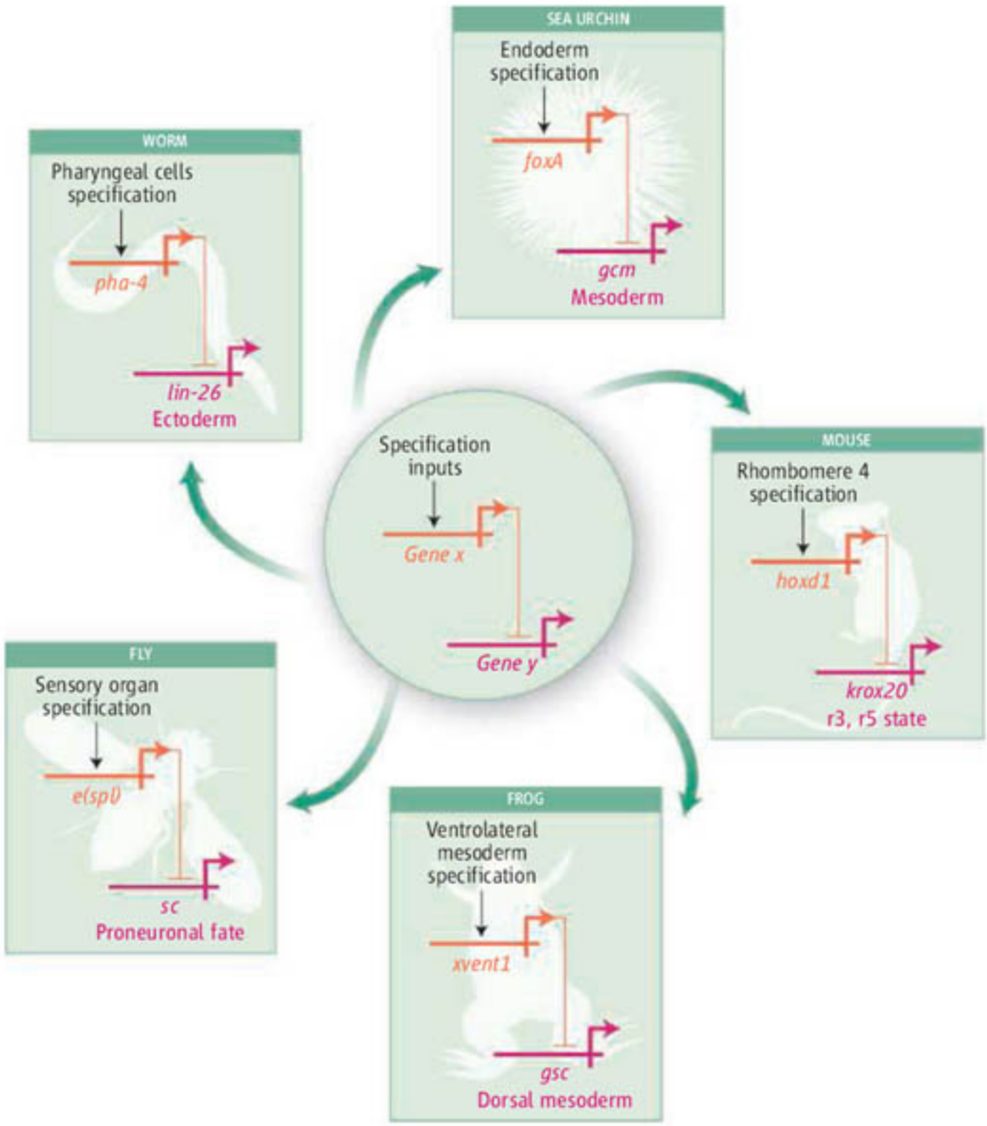

Same design, different actors. Common subcircuit architecture (center) in diverse instances of the exclusion effect. Specific organisms,and cell types or domains are shown, each specified by unique set of specification inputs. Horizontal lines represent cis-regulatory apparatus of the indicated gene. Genes shown in orange are transcriptional repressors, which are directly activated in the specification process (black arrow). Genes shown in magenta are major drivers of indicated alternative (excluded) cell fates.

ple, distinct kinds of subcircuits are brought to bear in a given spatial specification process, all of which function to ensure the outcome once a unique set of regulatory genes is activated in a given spatial domain of an embryo.

First, the new regulatory state is locked down, by deployment of positive feedback or other cross-regulatory relationships among the regulatory genes. The lockdown is dynamic because it requires continuous transcription of the cross-regulated genes, but it acts to stabilize the regulatory state.

Second, the cells within the newly defined spatial domain are linked together by intercellular signaling, by use of subcircuits that make continuation of the regulatory state dependent on reception of the signal. These subcircuits use another kind of intercellular feedback in that the gene encoding the signal responds to its own signal transduction system. Thus, all cells of the domain both receive and emit that same signal—a "community effect."

In addition to this, the same signal transduction system that promotes the regulatory state within the domain acts as an obligate repressor of genes that respond to it outside the domain. Signal transduction systems often have the Janus-like quality that they act positively in cells receiving the signal but otherwise behave as repressors (*4*, *5*).

Finally, the specification apparatus very frequently also includes transcriptional repressors, which, within the specified spatial domain, target key regulatory genes whose expression is required for alternative regulatory states that could have been available to these cells. This is a so-called "exclusion effect," and numerous examples can be found across species (see the figure). In each developmental case, the identity of the specific transcription factor that executes the repression is distinct, as are the specifically excluded target transcription factors. The design is the same, the biochemical actors diverse.

So it is not enough in an embryo just to arrange to turn on the right regulatory genes in the right place. These genes must also be dynamically locked on; the regulatory state of cells in a given spatial domain must further be made dependent on signaling among them all; the expression of these same regulatory genes must be specifically forbidden anywhere else; and then, on top of all that, specific alternative states must be excluded. These components are of course interlinked, and experimental tests of whether this is a "necessary" design are not simple. In the sea urchin embryo, where all of the above are to be found, disarming any one of these subcircuits produces some abnormality in expression.

We may interpret this as we like—as overengineering; or as design deluxe, replete with bells and whistles; or as the expected result of an evolutionary process in which individual regulatory modules have been added in and overlain at different times, so that some are more ancient and others more new (*1*). However, once integrated into the regulatory system, they are there to stay, barring evolutionary redirection. But the generality of this quality of developmental gene regulatory networks is emerging as a fact of life—it is what we see in modern animals. The consequences of evolutionary history determine the shape of the control apparatus that determines life processes. Perhaps in current system design we are seeing something of the grim pressures that modern lineages survived in past evolutionary bottlenecks—of the absolute necessity for lineage survival of genomic regulatory systems built to run and not to fail.

References and Notes

1. M. Levine, E. H. Davidson, *Proc. Natl. Acad. Sci. U.S.A.* **102**, 4936 (2005).
2. E. H. Davidson, D. H. Erwin, *Science* **311**, 796 (2006).
3. E. H. Davidson, *The Regulatory Genome: Gene Regulatory Networks in Development and Evolution* (Academic Press, San Diego, CA, 2006).
4. S. Barolo, J. W. Posakony, *Genes Dev.* **16**, 1167 (2002).
5. T. Minokawa, J. P. Rast, C. Arenas-Mena, C. B. Franco, E. H. Davidson, *Gene Expr. Patterns* **4**, 449 (2004).
6. P. Oliveri, K. D. Walton, E. H. Davidson, D. R. McClay, *Development* **133**, 4173 (2006).
7. J. C. Kiefer, P. A. Smith, S. E. Mango, *Dev. Biol.* **303**, 611 (2007).
8. E. H. Davidson, *Genomic Regulatory Systems: Development and Evolution* (Academic Press, San Diego, CA, 2001).

9. Supported by NIH grant HD-37105.

10.1126/science.1140979

INTRODUCTION

Momentous Changes at the Poles

EARTH'S POLAR REGIONS ARE PRICELESS REPOSITORIES OF INFORMATION ABOUT past climates, as well as harbingers of our planet's future. To get a better picture of where the Arctic and Antarctica have been and where they are going, and how changes at the poles might affect humanity's temperate perches, scientists from dozens of nations earlier this month launched a 2-year research initiative called the International Polar Year (IPY). This special issue helps raise the curtain on the IPY with an exploration of some of the more vibrant research under way at the ends of the Earth.

Polar processes exert a tremendous influence on many of our planet's ecological and biogeochemical cycles. Sea ice helps control ocean circulation, thereby influencing heat transport from low to high latitudes, rainfall patterns, ocean biology, and the composition of the atmosphere. Serreze *et al.* (p. 1533) examine the causes of the decrease in Arctic sea-ice coverage in recent decades and offer forecasts for the next century. Reduced sea ice could spark an Arctic version of the California Gold Rush. Krajick (p. 1525) discusses how nations are staking claims in the Arctic in the hopes of exploiting minerals and hydrocarbons locked beneath the sea floor.

How fast sea levels rise over the coming century—potentially one of the most serious consequences of global warming—will depend on how fast the polar ice sheets melt. Shepherd and Wingham (p. 1529) synthesize studies of the world's ice sheets to present a global picture, with emphasis on recent changes in the mass of the Greenland and Antarctic ice sheets. The polar seas are rich sources of marine productivity, and millions of people depend on their bounty. Warming is expected to have huge consequences for high-latitude denizens, as Bohannon (p. 1520) and Stokstad (p. 1522) show. Change is also in the air (literally) at the poles. Law and Stohl (p. 1537) examine the progress made in understanding the Arctic's atmospheric chemistry and discuss how anthropogenic and natural factors have affected, and may affect, the Arctic's role in mediating regional and global climate.

The Arctic and Antarctica offer some of the most extreme environments on the planet. For scientists, this poses logistical challenges, especially with the stepped-up research activities taking place at the poles during the IPY, as Mervis explains (p. 1514). Clery (p. 1523) discusses how astronomers are overcoming hostile conditions to install ever-bigger telescopes high on the Antarctic Plateau. At the other end of the globe, scientists are teaming up with indigenous people in the Arctic to fill gaps in their knowledge, writes Couzin (p. 1518).

The burst of scientific activity during the IPY should yield vital insights into the state of our planet for many years to come. If present trends continue, the message from our polar regions could be quite alarming indeed.

– ELIZABETH PENNISI, JESSE SMITH, RICHARD STONE

Polar Science

CONTENTS

See also related Editorial p. 1465; Podcast; Science Careers material on p. 1459 or at www.sciencemag.org/sciext/polarscience/

Science

NEWS

IPY Means Doing What It Takes To Get to the Ends of the Earth

The International Polar Year poses unprecedented logistical challenges—and scientific opportunities—for governments around the world

POWERED BY FOUR MASSIVE engines, the *Polarstern* can crunch through 1.5 meters of sea ice at 5 knots as it takes scientists where they want to go in the polar regions. But there is one obstacle that even this 25-year workhorse of Germany's polar research program can't overcome: high Russian tariffs.

For the past several years, prohibitively expensive fees to pass through Russia's Exclusive Economic Zone (EEZ), which extends 320 km from its coast, have forced Arctic researchers from many nations to rearrange their plans. In 2005, for example, scientists at the Alfred Wegener Institute for Polar and Marine Research (AWI) in Bremerhaven, Germany, rerouted a research cruise after learning that taking the shortest route home from the East Siberian Sea would cost them nearly half a million dollars. "Our program has some money, but we were not willing to pay such a high amount," says AWI senior scientist Ursula Schauer.

This year, Schauer, a physical oceanographer, is once again hoping to take the ship through the Russian EEZ. And although she hasn't won the lottery, she's counting on something even more valuable to make it happen: the International Polar Year (IPY). Last October, Russia decided to slash its tariff by half for foreign vessels taking part in IPY, a 2-year research extravaganza that kicked off this month and continues until March 2009 (ipy.org). Cheered on by Artur Chilingarov, a vice speaker of the Duma, Russia's legislature, and head of its IPY committee, the Russian government has agreed to give a green light to any IPY-approved project. "Artur is the pole on which we hoist our IPY flag," says Sergey Priamikov, a physical oceanographer at the Arctic and Antarctic Research Institute in St. Petersburg who also heads the Eurasian branch of the IPY program office.

IPY is the fourth in a series of polar lollapaloozas going back to 1882. The previous effort, the 1957–58 International Geophysical Year (IGY), laid the groundwork for the international regimen that governs Antarctic research. Although it has no money to give out, IPY serves as both administrative umbrella and cheerleader for a mélange of research collaborations that individual countries and organizations have pledged to support. Its volunteer leadership has vetted more than 1200 proposals and created a honeycomb chart of some 200 approved projects that incorporate IPY's six research themes—most prominently, to understand the changing polar environment and the impact of those changes. "We hope IPY will create a greater community of cooperation," says Australia's Ian Allison, co-chair of IPY's joint committee.

Such global teamwork can be just as important as money, says glaciologist Olav Orheim, head of IPY activities at the Norwegian

Research Council. The council is pouring all of a 50% increase in its annual research budget—some $50 million—into 26 IPY projects extending to 2010, including a joint Antarctic traverse with U.S. scientists that will mark the Scandinavian country's first overland visit to the South Pole since legendary explorer Roald Amundsen was the first to arrive in 1911. "We hope that IPY will create a legacy of cooperation that will remove the unpredictability and logistical challenges that have plagued polar research," says Orheim.

On the move. Scientists from several nations will carry out extensive ice coring and other research activities throughout eastern Antarctica during IPY.

CREDITS (TOP TO BOTTOM): PETER REJCEK/NATIONAL SCIENCE FOUNDATION; A. MORALES/SCIENCE (SOURCE: IPY)

The right stuff

The logistical challenges are indeed formidable. A surge in activity at the poles during IPY will strain the world's existing capacity—from ships and planes to labs and communications equipment—to do science in these unforgiving conditions.

Canada's Arctic program, for instance, is scrambling to secure enough boats. "Last year, we realized we were facing a potential shortage because of the demand from oil and mineral companies and from ecotourism," says David Hik, an Alpine ecologist at the University of Alberta, Edmonton. Hik heads Canada's IPY office, which oversees the government's new $128 million investment in polar research, 80% of which will be spent during IPY. "We also expect a crunch on helicopters and fixed-wing craft because of the limited number of pilots with experience landing on ice or in remote camps," he says.

Much of the stampede is to address a major IPY theme, understanding climate change in the Arctic. An alphabet soup of projects includes SEARCH (Study of Environmental Arctic Change), DAMOCLES (Developing Arctic Modeling and Observing Capabilities for Long-Term Environmental Studies), and IASOA (International Arctic Systems for Observing the Atmosphere). Orheim also has high hopes for an ongoing meteorological project linked up with IPY, called THORPEX, that aims to quantify the impact of polar warming on the stability of the Gulf Stream and global climate by tracking water inflow into the Arctic in unprecedented detail. "There is a lot of speculation about what is happening but very few facts," he says. Adds Schauer, a member of the scientific steering committee for DAMOCLES: "This is the first time so many international partners have focused on the physical aspects of climate change. We know the ice shrinks every year, but we don't really know why."

At sea

Ship time for polar research is a precious commodity. Funding agencies around the world must match scientists' needs with a suitable vessel in the right place at the right time. Schauer, whose request for the *Polarstern* to pass through the Russian EEZ this fall is wending its way through a thicket of government ministries, has even created a Web site (asci-ipy.de) to make the horse-trading more transparent and to foster collaboration. But that's not enough to level the playing field.

Take the *Oden*, Sweden's heavy-duty research icebreaker, which fills the same niche as Germany's *Polarstern* and the U.S. Coast Guard's *Healy*. Whereas German and U.S. officials have decided to dedicate the next 2 years of ship time to IPY-related cruises, the *Oden* is available to any group with the money—$25,000 a day, plus fuel costs—to charter it. That leaves Swedish researchers, whose government has not allocated any new funding for IPY, at a disadvantage. "Our polar research secretariat has scheduled one Arctic expedition every other year on the *Oden*," says Michael Tjernstrom, a meteorologist at Stockholm University who has put together the IPY-endorsed Arctic Summer Cloud-Ocean Study that hopes to win the coveted cruise slot in the summer of 2008. But with funding tight, he says, "it's really very difficult for us to find the money."

Sweden's loss is a gain for other countries. This summer, a U.S.–led team will charter the *Oden* to explore the seldom-visited Gakkel Ridge in the central Arctic basin. The AGAVE project will deploy a new generation of autonomous vehicles deep under the Arctic ice pack to hunt for undiscovered life forms nurtured by hydrothermal vents that dot the slow-spreading ridge.

AGAVE didn't even start out as an IPY project. It was initially funded by the U.S. National Science Foundation (NSF) and NASA before IPY took shape, says principal investigator Robert Reves-Sohn, a marine geophysicist at Woods Hole Oceanographic Institution in Massachusetts. After delays in finding a ship pushed the project into the IPY time frame, Reves-Sohn broadened the mission's scientific agenda and invited non–U.S. scientists. Those changes—including adding Japanese sensors to the underwater robots and German seismometers to ice floes at the surface—earned AGAVE an IPY stamp of approval. "We expanded the scientific scope at no cost to the U.S.," says Reves-Sohn.

Finding common ground

At the other end of the world, IPY is accelerating a revival of a hallowed Antarctic tradition—the research traverse. These forbidding land treks are akin to research cruises because of the wealth of data collected on the move. Popular during IGY and into the 1970s as a means of gathering geophysical information about the largely unexplored interior of the frozen continent, traverses gradually fell out of fashion as scientists opted to mine a confined area, often season after season.

Several traverses are in the works for IPY (see map). Although their emphases vary from glaciology to geophysics to climate science, each team has agreed to pool data whenever possible to help fill in what remains a very sketchy picture of the continent. Many will build on the International Trans-Antarctic Scientific Expedition (ITASE), an ongoing series of expeditions to gather continent-wide environmental parameters. They feature drilling ice cores for climate information

Long (and Perilous) March Heralds China's Rise as Polar Research Power

SHANGHAI—Bo Sun remembers the first time he and his fellow Chinese adventurers struck out from Zhongshan Station on the East Antarctic coast, trekking inland across uncharted terrain in 1996. "It was terrible," says Bo. "We did not know how to handle it." Their lumbering vehicles frequently got stuck in drifts. Death traps lurked, unseen, beneath wispy ice bridges. "Sometimes when we looked back, a big crevasse appeared. Our hearts jumped," says Bo, a glaciologist at the Polar Research Institute of China (PRIC) in Shanghai.

But they lived, and they learned—how to avoid getting stranded by forging ahead during a storm, for example, and what to eat on the energy-sapping traverses. Along the way, they've mapped major crevasse fields. "Now we are experts at recognizing where the dangers are," says Bo. After several short trips to build up their capacity, Bo and his colleagues in January 2005 reached their objective—the highest point on Antarctica's ice sheets, Dome Argus (Dome A)—and returned home, completing the 2500-kilometer roundtrip in 10 weeks.

The conquest marked a coming of age of China's polar program. Radar echo soundings during the traverse suggested that the ice at the bottom of Dome A could be the oldest on the continent, going back as much as 1.2 million years, says PRIC Director Zhang Zhanhai.

The rising power got a late start in Antarctica. Its researchers first visited the continent in 1980, and Zhongshan was opened in 1989. (China's Great Wall Station debuted on King George Island in the South Shetlands in 1985.) During the International Polar Year (IPY) and beyond, China is set to really take off. In 2006, the government approved $70 million for major polar projects, including $4 million for IPY research in 2007; $19 million for new PRIC headquarters in Shanghai; $22 million to overhaul the Zhongshan and Great Wall stations; and $25 million to renovate the Snow Dragon (*Xuelong*), a Ukrainian-built research vessel that will cap IPY with a globe-girdling expedition to plumb the effects of rapid Arctic change on the mid-latitudes.

But it's Dome A that could well turn Chinese scientists into the new darlings of Antarctic research. Their 2005 radar soundings from Argus, 4093 meters above sea level, revealed that the ice there astride the Gamburtsev Mountain Range is 3070 meters thick—twice what modeling had suggested, says Bo. In the next few years, China hopes to start drilling at Dome A to retrieve what could be an unparalleled window on past Antarctic climate. Finding ice that "captures our planet's climate in a different phase … is the Holy Grail of the ice-core community," says Robin Bell, an Antarctic expert at Columbia University's Lamont-Doherty Earth Observatory in Palisades, New York, who concurs with PRIC's estimated age of the Dome A ice.

In the meantime, the centerpiece of China's 3-year IPY program is PANDA, a geophysics initiative at Prydz Bay near Zhongshan Station, and Dome A. In collaboration with researchers from five countries, China 3 years ago drilled a 310-meter ice core on the Amery Ice Shelf in Prydz Bay. Drilling will continue in 2007–08, and during a traverse to Dome A in late 2007, scientists will install a series of magnetometers to probe how the solar wind energizes electrons in the magnetosphere to form auroras.

Seeing them off. Zhongshan Station in East Antarctica is the staging ground for China's traverses inland to Dome A.

The traverse will cast its gaze downward, too. Following up on the 2005 traverse findings, China is planning airborne radar mapping of the enigmatic Gamburtsevs and the overlying ice sheet with help from Australian, German, U.K., and U.S. researchers. "We know little about the boundary of ice and rock," says Bo.

Also during IPY, China will lay the groundwork for a major-league astronomy observatory at Dome A. Like the South Pole and Dome C (p. 1523), Argus provides the thin, clear skies ideal for serious stargazing. The Purple Mountain Observatory in Nanjing is teaming up with Australian and U.S. astronomers on a Dome A survey in 2007–08 to determine the best spot for a major telescope facility, and an array of four 15-centimeter telescopes will be installed to hunt for planets orbiting nearby stars. Later in 2008, PRIC will ship three 50-centimeter telescopes to Dome A that will provide the first picture of a large portion of the sky in polarized light, says Wang Lifan, director of the Chinese Center for Antarctic Astronomy.

In the short term, Zhang says, "nobody will winter over at Dome A." Construction of a year-round station is set to begin in 2011, but for the next decade, the annual work window at Dome A will be narrow as the monthlong traverse leaves roughly 2 weeks on site. "There's only a short time that the weather is suitable for people," Bo says. "But the place is so fantastic"—fantastic enough to endure the hardships Bo and his team faced to get there.

–RICHARD STONE

Bus to Argus. The 2005 traverse.

CREDITS (TOP TO BOTTOM): COURTESY OF PRIC

going back as far as 1000 years, operating surface and subsurface radar that help to provide ground truth for satellites, and gathering hard-to-get Antarctic weather data.

When ITASE began in the 1990s, "we thought that Antarctic climate might be a simple picture," says one of the project's initiators, glaciologist Paul Mayewski of the University of Maine, Orono. "But it's a vast place. And after 15 years, we know enough now to realize where the sensitive spots are." In January, his team completed the first, 500-km leg of a planned 6000-km traverse over three seasons that will take them from McMurdo Bay past the South Pole to Dome A, the highest point on the continent, and then back to the pole.

The latest ITASE expedition also complements routes taken by other traverses flying the IPY banner. "Once we can get to Dome A," Mayewski says, "we can match our data with what is being collected by the Chinese arriving from the opposite side and also with TASTE-IDEA," a 3-year, European-led traverse beginning in the fall of 2007 that will cross the less-familiar East Antarctic ice divide. More information will come from a U.S.–Norwegian traverse beginning this fall that will travel to the South Pole from Norway's Troll Station near the African coast of Antarctica and then return to Troll in the 2008–09 season (traverse.npolar.no).

"We'll be going through no man's land," says Jan Gunnar Winther, director of the Norwegian Polar Institute and leader of the joint project, which will cost an estimated $15 million. In addition to drilling ice cores, the 11-member team will launch drones for airborne photography and operate a scanning electron microscope to analyze the transitions from fresh snow to compacted old snow to ice. "It will fill a huge hole in the data," says Winther. "It's also by far the biggest traverse that we've ever done."

IPY's integrative nature provides a rationale for traverses that might be hard to justify on their own, says Ian Goodwin, ITASE co-chair and a glaciologist at the University of Newcastle, Australia. For example, he says, "IPY is likely the only way" to get the necessary support to carry out exploratory geophysics.

IPY also represents a golden opportunity for nations relatively new to polar research to build up their scientific infrastructure. In addition to China's big spurt (see p. 1516), South Korea, for example, last year committed $183 million to two polar projects: a $107 million research vessel with icebreaking capabilities, to be ready in 2010, and a $76 million research station, its first on the Antarctic mainland, to be completed in 2011. That money comes on top of the $38 million a year that it spends through the Korean Polar Research Institute (KOPRI), which this winter funded a six-member team that searched for meteorites near Patriot Hills in western Antarctica, the first-ever Korean expedition on the continent.

The new ship will service existing Korean stations in the Arctic and on King George's Island off the Antarctic Peninsula. It will allow Korean scientists to do research at both poles now performed on leased Russian and European icebreakers. KOPRI is eyeing two sites for the station, one in West Antarctica, off the Amundsen Sea, and the other farther east, near Queen Maud Land off the Weddell Sea.

Becalmed. The French polar yacht *Vagabond* is used as a base camp for DAMOCLES environmental research in the Arctic.

CREDIT: ERIC BROSSIER/VAGABOND/DAMOCLES

Power to the people

Arguably the biggest logistical challenge facing polar science isn't an IPY-inspired project. It's the simultaneous construction of the 10-meter South Pole Telescope (SPT) and installation of the 1-km^2 Ice Cube neutrino array (see p. 1523) at the U.S. Amundsen-Scott station, now in the final stages of a major upgrade. The way NSF has managed those three projects offers a blueprint for supporting science in inhospitable surroundings.

"The scope of Antarctic science has changed over the past 20 years," says Erick Chiang, head of NSF's Antarctic logistical support, a $66-million-a-year program to enable NSF's $322 million a year in polar research. "The projects are more complex, and they address larger problems. But probably the biggest change for researchers has been a move away from designing a proposal around what's there and toward an approach that says, 'Here's what we want to do. Let's see what NSF can support.' "

That can-do spirit has taken the South Pole station close to its operational limits. "Last March, it became clear that there was a looming power crunch," recalls John Carlstrom, director of the Kavli Institute for Cosmological Physics at the University of Chicago in Illinois and SPT project leader. "The station was already running at capacity without any telescope activity and with nothing new for Ice Cube. Our first reaction was to wonder if there had been a mistake or poor planning," he says. "But NSF put together a tiger team—the first time we'd ever done that for power issues. Now we have a plan that should get us through this year and give us more time to think."

The interim solution was improved fuel efficiency and energy conservation, says Chiang. But the larger lesson, he believes, is the inherent difficulty of anticipating where science might be headed. The final design of the new station was completed in 1997: "Nobody then could have anticipated SPT and Ice Cube," Chiang notes.

Nor can scientists anticipate the new lines of inquiry that might come out of IPY. But it's clear that the scientific onslaught taking place at the ends of the Earth will bolster polar research for decades to come.

–JEFFREY MERVIS

With reporting by Ahn Mi-Young in Seoul and Richard Stone in Bangkok.

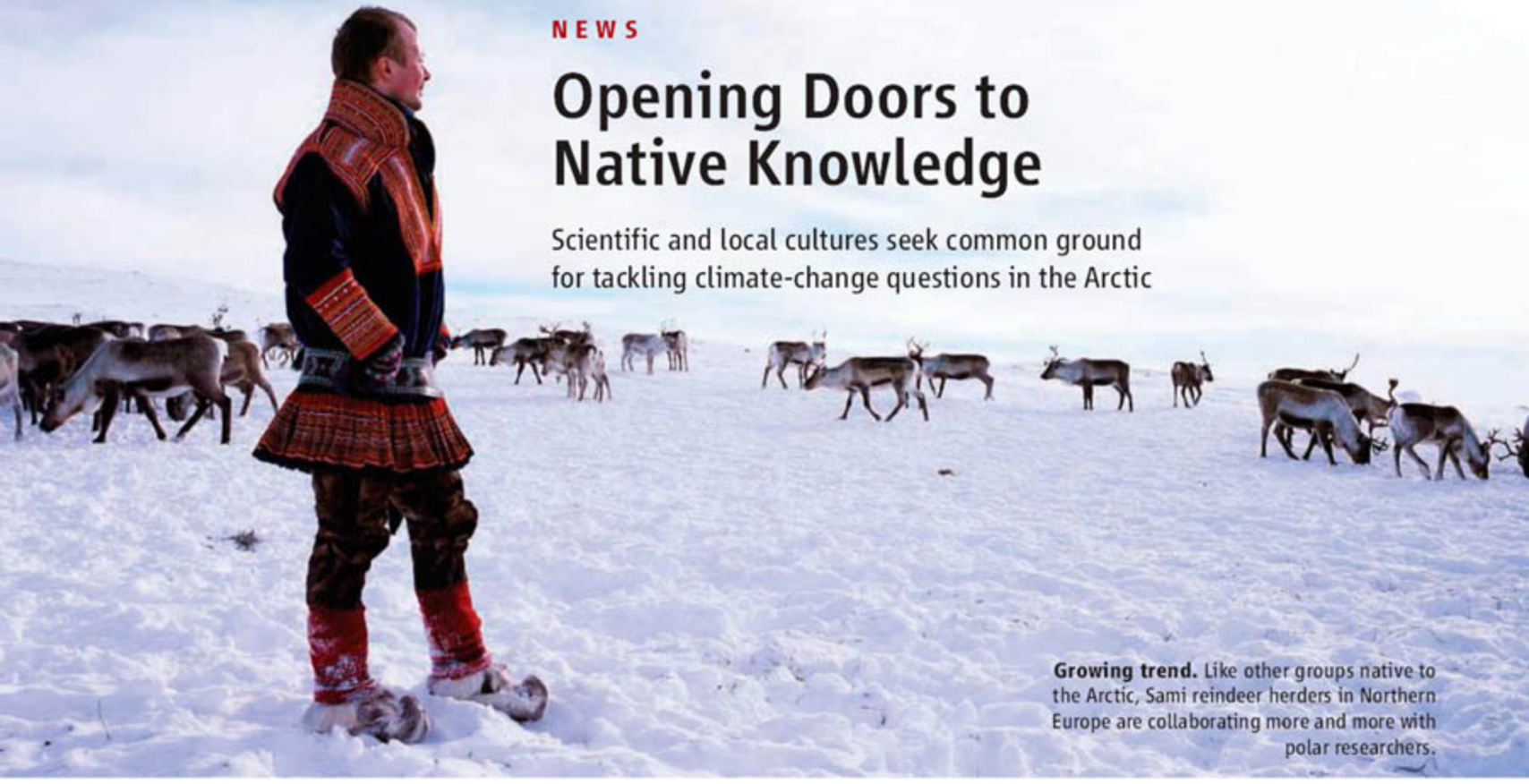

NEWS

Opening Doors to Native Knowledge

Scientific and local cultures seek common ground for tackling climate-change questions in the Arctic

Growing trend. Like other groups native to the Arctic, Sami reindeer herders in Northern Europe are collaborating more and more with polar researchers.

CREDIT: ANDY WHALE/CORBIS

"I say that there are three sure signs of spring," says Caleb Pungowiyi, a 65-year-old Siberian Yu'pik who lives in Kotzebue, Alaska. "The ducks and the geese coming back, tourists coming back, and scientists who come back to check their instruments." Some Inuit in Alaska call these researchers *Siksik*, the Inuit word for the ground squirrel, which pokes its head up only in the summer. For their part, these "squirrels" have traditionally gone about their business, rarely tapping the natives for their expertise.

But as climate change sweeps through the Arctic, decades-old divisions between the indigenous people who live there and the scientists who parachute in and out are slowly dissolving. Projects that draw on traditional knowledge of animal migrations, ice patterns, shrubbery, and weather are popping up from Baffin Island, Canada, to Rovaniemi, Finland. The goal is to use local information—say, about the health of individual caribou or about whales killed by hunters—to supplement and enrich scientific data, such as sea-ice or vegetation changes. "We're living in a period of extreme uncertainty, and these perspectives add insight," says Gary Kofinas, who studies resource management at the University of Alaska, Fairbanks. "I think it's fair to say that we need all the help we can get."

Collaborations between scientists and indigenous people are also driven by external pressures. The influential 2005 Arctic Climate Impact Assessment ranked indigenous knowledge high on the list of topics that scientists should pay attention to. And the International Polar Year, which began this month, lists the sustainability and perspectives of societies living in the Arctic as one of six themes shaping its research agenda.

But although many researchers are enthusiastic about these nascent collaborations, and some projects have already yielded interesting new directions or confirmed scientific findings, drawing on traditional knowledge to supplement hard science is still largely uncharted territory. There is no way yet to quantify uncertainty in the information supplied by indigenous people. And even as native collaborators begin to take on ever-larger roles in scientific projects, there is no systematic strategy for reconciling conflicts between scientific data and traditional knowledge.

"The partnership is in its infancy," says Igor Krupnik, a cultural anthropologist at the Smithsonian National Museum of Natural History in Washington, D.C., who has worked extensively with Arctic indigenous people. Their insight "is great stuff, but you have to be careful."

Breaking the ice

Many scientists point to the Arctic Climate Impact Assessment, an international project coordinated by members of eight Arctic countries, as a turning point in efforts to draw on indigenous knowledge. Initially, "indigenous people were listed as chapter number 10, 11, or 12, back at the very end" of the report, recalls Krupnik, one of the authors. But gradually, as the document was assembled, the chapter on indigenous knowledge climbed the ladder, ending up as number three. It's a subtle distinction, but Krupnik considers it highly symbolic. The report "was very instrumental," he says, in awakening people to the value of traditional knowledge as "very solid science."

Those who work with indigenous communities agree that locals possess information that scientists have difficulty accessing independently. "I'm looking at computer screens or satellite images, but I don't have the time to wander around the landscape like the Sami do," says Terry Callaghan, who runs the Abisko Scientific Research Station in Sweden, referring to the native population that herds reindeer in three Nordic countries and Arctic Russia. Furthermore, although some scientists such as Callaghan spend time in the Arctic year-round, their presence through the winter is rare. That makes locals such as the Sami unique observers of how

changing winter weather patterns are altering the landscape.

Scientists and native people say traditional knowledge can be especially helpful in providing an in-depth, up-close view of the Arctic. Whereas scientists might be well-versed in, say, sea-ice extent, the Inuit know the ice much more intimately—hole by hole, crack by crack—says Shari Gearheard, a geographer at the University of Colorado, Boulder, who lives in Clyde River on Baffin Island. Over the next 3 years, she and local partners will be traveling across sea-ice hunting grounds in Baffin Island, Alaska, and Greenland, recording what they see. Already she's learned more about sea-ice dynamics than she would have had she struck out alone. "There are certain cracks that are in the same place every year, but some are moving now, and there are new ones that are not expected," Gearheard says.

Such attention to detail has impressed Krupnik and walrus biologist G. Carleton Ray of the University of Virginia, Charlottesville. Yu'pik Eskimos on Alaska's St. Lawrence Island, in the Northern Bering Sea, not only examine hunted walruses for everything from gut parasites to the texture of their blubber, they also have a far more descriptive language than biologists. *Ayviquma*, for example, means mother, yearling, and young calf in one group. *Amiinaqut nunavaget* defines a group of walruses isolated on an ice floe. Such precision, Krupnik says, makes the historical record passed through generations especially valuable.

So far, some of these recollections match up well with scientific data. As part of a project with the Sami reindeer herders around Abisko and Sami academics from northern Norway, Callaghan has found that Sami observations of how snow depth has changed over 50 years generally jibe with long-term data collected by scientists. The Sami also informed him that during the middle 1980s, the wind had switched directions. Combing through climate records, Callaghan found an abrupt climate change at that time. The mean annual temperature had jumped by about 1.5°C.

Culture clash

But for every observation like this one, which underscores the remarkable intergenerational memory of many indigenous people, there are other recollections that might be difficult to interpret or even trust. "One Sami said, 'The sky isn't as blue as it used to be.' He was talking about changing atmospheric conditions, but it was an observation I could not accept," says Callaghan. "You can't remember color; you can't pass it down through generations."

Furthermore, how to use indigenous knowledge is something that dogs Arctic researchers. "Human knowledge is not scientific knowledge," says Tero Mustonen, a subsistence fisher in the Finnish Arctic who also studies human ecology. "It's not universal, it's not systematic, it's not free of biases." And layering that knowledge onto scientific data can be especially troublesome when they conflict, Krupnik adds.

Some scientists are trying to gain a better sense of how indigenous people gather information about their natural environment by literally working side by side with them, as Gearheard does in her travels onto sea ice. The hope is that such collaborations might ease the translation of indigenous knowledge into scientific data, where that's appropriate, and make science more useful to the locals. For example, at the University of Lapland in Rovaniemi, Finland, biogeographer and vegetation scientist Bruce Forbes is 3 years into a 4-year project examining how the terrestrial ecosystem in parts of Siberia and the Eastern European Arctic are changing. He and his colleagues migrate with the Nenets reindeer herders, living and working alongside them in teepeelike structures.

During one such migration last November, a major "icing event" occurred in which the air temperature warmed enough for rain, then plunged again. The water froze atop the snow, making it difficult for the reindeer to access food. By documenting how the Nenets reacted to this situation, which until recently was very rare, the scientists are developing a keener sense of how resilient and adaptable their hosts may be in the face of climate change.

Thanks to these efforts, an indigenous slant on Arctic science is on the rise, bringing to the fore issues about the control, acquisition, and dissemination of information. There is no good standard for deciding when indigenous knowledge is intellectual property, for example. To strike a balance, Kofinas, Krupnik, and others are increasingly including indigenous collaborators as co-authors on papers. Yet, for a local to say, " 'You can't publish it without my approval' … would never go over well in my university," says Kofinas.

In it together. Baffin Island locals Teema Qillaq, Lasalie Joanasie, and Andy Murray help install a monitoring station to assess changes in sea ice.

CREDIT: SHARI GEARHEARD

For their part, indigenous people and their governments are becoming ever more proactive. In Canada, they actively screen projects that fall into their geographic region. For a caribou-monitoring network called the Arctic Borderlands Ecological Knowledge Co-op, Inuit in Canada and Alaska conduct interviews with other residents about caribou populations. "It's local folks running the show," Kofinas says.

Pungowiyi, the Alaskan native, also thinks it's time to get more involved with the "ground squirrels." He recently submitted his first proposal to the U.S. National Science Foundation with Henry Huntington, a social scientist in Eagle River, Alaska, to examine climate change effects that indigenous people are observing on land and in the ocean. Understanding the Arctic requires more than numbers and satellite photos, he insists. There's a need to "put a human face to the effects," he points out. "That's what we're trying to get to."

–JENNIFER COUZIN

On ice. The icebreaker RV *Nathaniel B. Palmer* crunched through winter pack ice to reach open water in Antarctica's frozen Ross Sea for algae studies.

NEWS

Sailing the Southern Sea

An international project sorts out the dynamics of climate and nutrient fluxes in this polar ocean community

The spirit of John Martin still seems to haunt oceanography 14 years after his death from cancer. When he was a researcher at Moss Landing Marine Laboratories in California, Martin proposed that massive blooms of photosynthetic plankton in the frigid Southern Ocean around Antarctica and other nutrient-rich but iron-starved waters could be an antidote to global warming. By pulling carbon dioxide out of the atmosphere to build their tiny bodies and then sequestering that carbon as they die and drift to the bottom of the ocean, these microscopic algae could reduce greenhouse gases and cool Earth. The only thing holding them back, Martin argued, was a dearth of iron, a necessary part of their photosynthetic machinery. To drive the point home, he once stood up at a conference in Woods Hole, Massachusetts, and said half-jokingly, "Give me a half tanker of iron, and I will give you an ice age."

It was an idea that launched 1000 ships, "or certainly hundreds," says Giacomo (Jack) DiTullio, an oceanographer at Hollings Marine Laboratory in Charleston, South Carolina. Although Martin did not live to see it, his colleagues at Moss Landing and others confirmed that lack of iron does limit growth: In a 1995 experiment, spreading dissolved iron over a 64-km^2 patch of ocean near the Galápagos Islands caused a temporary, 30-fold boost in phytoplankton biomass.

DiTullio has also followed in Martin's wake. As head of the Controls on Ross Sea Algal Community Structure (CORSACS) project, he and his colleagues are sorting out what—in addition to iron—makes plankton communities tick in the Ross Sea, the southernmost part of the Southern Ocean. It is one of the biggest potential hot spots for the phytoplankton blooms Martin envisioned.

The CORSACS researchers have looked at half a dozen environmental parameters—iron, light, carbon dioxide, temperature, and several trace nutrients—not only individually but also in combination. Doing so is "both novel and necessary" for understanding how this community can contribute to climate change, says Philip Boyd, an oceanographer at the University of Otago in Dunedin, New Zealand.

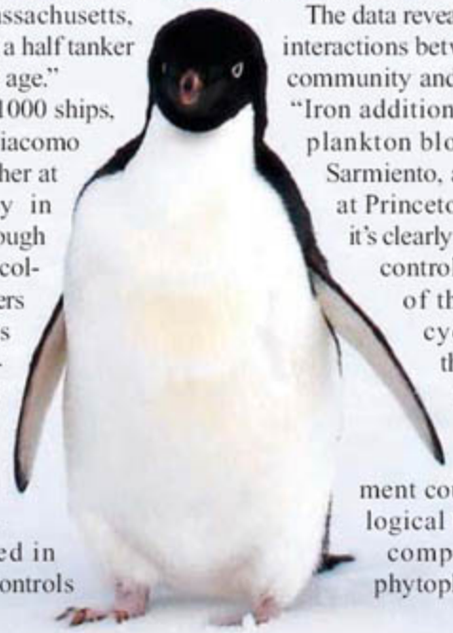

The data reveal a tangled web of interactions between the plankton community and its environment. "Iron addition works" to spark plankton blooms, says Jorge Sarmiento, a climate modeler at Princeton University, but it's clearly not the only factor controlling this key part of the global carbon cycle. In addition, the study indicates that changes in the Southern Ocean environment could shift the ecological balance between competing species of phytoplankton and, consequently, alter the contribution of phytoplankton to the carbon cycle. Such shifts could in turn exert "a very large impact on the air-sea balance of carbon dioxide," says Sarmiento. CORSACS's challenge is to nail down these complexities so they can be built into climate models.

Probing a complex soup

The Ross Sea is a tough place to work. Its thick blanket of ice covers all but a France-sized pool, or polynya, where sunlight allows phytoplankton to flourish. For two cruises (December 2005 to January 2006 and then again November to December 2006), the researchers worked there around the clock, often with wet and freezing hands, while their shipboard laboratory pitched wildly beneath their feet. Although satellite data, easily collected from the comfort of one's office chair, can provide information about plankton densities and environmental conditions, "there's just no other way to answer the kind of questions we're after," says DiTullio. To predict how the phytoplankton community will react to a changing environment, the researchers had to survey conditions in real time and test samples onboard to avoid confounding factors introduced by shipping them to labs on land.

The team dangled sampling devices that tracked iron and other nutrient concentrations, as well as light, temperature, and pH at various depths throughout the cruises. At the same time, they studied the species composition, biomass, and photosynthetic activity. As Martin predicted, the survey data "consistently demonstrated iron limita-

CREDIT: WOODS HOLE OCEANOGRAPHIC INSTITUTION

tion of growth," says DiTullio. Wherever iron was available—blown in as dust or transported in water upwelling from the deep—the plankton multiplied, but only as long as the iron lasted. Several experiments onboard the ship showed the same phenomenon: Adding iron boosts growth until the metal is gone.

But there is more to life than iron. Mak Saito, an oceanographer at the Woods Hole Oceanographic Institution in Massachusetts, wondered how vitamin B-12, another necessary nutrient, might affect algal growth. Only prokaryotic organisms such as bacteria are capable of making the molecule from scratch. In most ecosystems, there are more than enough bacteria to go around. "But the polar environments are unique," says Saito, because these bacteria can be so rare there that B-12 might limit community growth. To test that idea, he took samples of plankton from three locations—ranging from low to high bacterial concentrations—and incubated them for a week in bottles with or without a supplement of the vitamin.

Sure enough, adding B-12 boosted the algae's growth in bottles with sparse bacteria, whereas it had no effect when plenty of bacteria were present. An input of iron may be necessary for the phytoplankton to grow, says Saito, but so is access to vitamin B-12.

CORSACS researcher Phillipe Tortell, an oceanographer at the University of British Columbia in Vancouver, Canada, wanted to know what increased carbon dioxide concentrations might do to the productivity of the Ross Sea. Tortell incubated samples of algae in bottles with a range of carbon dioxide concentrations, from preindustrial levels up to more than twice current levels. As one would expect for photosynthesizers, higher carbon dioxide led to higher metabolic rates and faster reproduction. But a surprise was that increased carbon dioxide changed the species mix, causing one group of diatoms, known as *Chaetoceros*, to dominate the rest. This result sounds like good news for climate-change buffering, as these particular diatoms form long chains of cells that sink efficiently, making them adept carbon sequesterers.

But the story is not that simple, says Tortell.

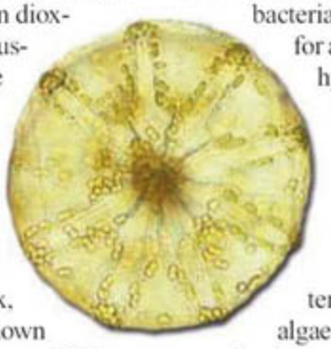

CREDIT: G. DITULLIO

Algal politics

Tortell's carbon dioxide experiments highlight the dynamic nature of the Ross Sea ecosystem. The Southern Ocean is home to a diversity of species that compete for resources using different life strategies. In the Ross Sea, the diatoms and *Phaeocystis*, a green-brown, single-celled photosynthesizer that forms mucus-covered colonies, compete to be the top-dog alga. And the dominant species can vastly change the community's impact on the carbon cycle. Thus, understanding what gives one group of plankton an edge over another is key to predicting how the Ross Sea community will evolve in response to climate change, says Tortell.

Saito has made a start. His group has discovered dense clusters of bacteria thriving within the mucus of *Phaeocystis* colonies. The bacteria may provide B-12 in exchange for a free ride in the mucus's carbohydrate-rich environment. And the mucus may benefit both species by acting as a sponge for iron. Because of this symbiosis, "*Phaeocystis* may outcompete diatoms," says Saito.

This interplay between bacteria and algae and between the algae themselves is occurring against a backdrop of the many environmental changes associated with global warming. For instance, the atmosphere is likely to become dustier due to increased droughts and soil degradation—potentially delivering more iron to the Southern Ocean. Warmer surface waters could also shift the ocean's ecological balance. And increased precipitation and ice melt will decrease the salinity of surface waters, which in turn will slow down mixing with saltier, lower levels. Less mixing means more time spent near the surface, says DiTullio, which is effectively "an increase in the average light level experienced by phytoplankton."

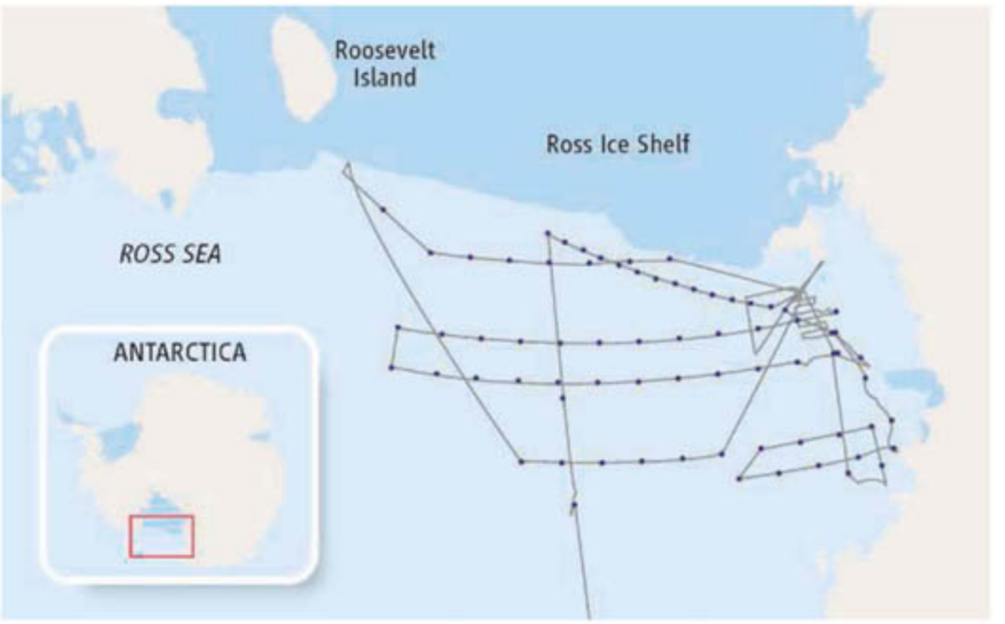

A broad sampling. The CORSACS team crisscrossed the Ross Sea (*above*) to understand what gives some plankton species, like this diatom (*below*), an edge over others.

To test how these changes may act in concert on algal growth, a team led by David Hutchins, an oceanographer at the University of Southern California in Los Angeles, grew cultures of plankton during both cruises while tweaking temperature, light, and carbon dioxide and iron concentration simultaneously. Models of the Ross Sea based on field observations have "typically assumed that high light and high iron would favor diatom communities," says Hutchins. But under high light and high iron concentrations in his experiments, *Phaeocystis* thrived whereas diatoms lagged.

These dynamics make the Southern Sea a devilishly complex environment for climate researchers to model. Whatever ecological shifts wait over the horizon, says Hutchins, they will alter "the efficiency of the biological pump" for pulling carbon dioxide out of the atmosphere. And what sign will be attached to that change—positive or negative—is still anyone's guess.

At this point, the CORSACS cruises have generated more questions than answers. In April, the researchers will gather in South Carolina to analyze the data. But one thing is already clear, says Boyd: "They indicate that climate change will simultaneously impact a wide range of ocean properties in Antarctica." The big question is what those changes will mean for global climate in the coming decades—an unplanned experiment on a far grander scale than anything Martin ever imagined.

–JOHN BOHANNON

NEWS

Boom and Bust in a Polar Hot Zone

Changes in penguin and other populations on the Antarctic peninsula reflect the turmoil caused by climate change

When William Fraser first arrived in Antarctica in 1976 to study Adélie penguins, their nesting sites were surrounded by sturdy sea ice. "We could ski for miles," recalls Fraser, an ecologist with Polar Oceans Research Group, a small nonprofit organization in Sheridan, Montana.

No longer. In the past 30 years, Fraser and his colleagues have witnessed a stunning change in the climate, one that is altering the mix of species in the West Antarctic Peninsula, an icy mountain range that reaches toward South America. Air and ocean temperatures have risen, causing less ice to form and more snow to fall. "This ecosystem is on fire," says Hugh Ducklow of the College of William and Mary Virginia Institute of Marine Science in Gloucester Point.

Slippery slope. Some Adélie penguins in Antarctica suffer from a loss of sea ice and prey, such as the silverfish (*inset*).

The change has taken a dramatic toll on some species, especially Adélie penguins, as their habitat and a key prey are disappearing. Also, new experiments suggest that increased snowfall is adversely affecting nesting. "The story for Adélies is absolutely dismal," Fraser says.

But the tale is not one of universal suffering. On the peninsula, the populations of other species of marine birds and mammals are booming. As sea ice diminishes, living conditions seem to be improving for them. Across Antarctica, even Adélies are benefiting in some places. They are expanding into areas where sea ice was once too extensive.

No one knows how long such favorable conditions will last. But as the hottest of polar hot spots, the West Antarctic Peninsula provides a sneak preview for the rest of the continent. "This is one of the best examples we have of an ecosystem where we can see the responses of rapid climate change," says Ducklow. As such, "it may be harbinger of what will happen elsewhere as the system breaks down," adds Gerald Kooyman, a penguin biologist at the Scripps Institution of Oceanography in San Diego, California.

In hot water

The West Antarctic Peninsula has proven especially vulnerable to climate change. The peninsula's mean winter temperature has risen 6°C since 1950—the fastest rate on the planet. The ocean has warmed by nearly 0.7°C.

Those trends have made Palmer Station, located at the northern end of the peninsula, a focal point for research on the impact of climate change on polar ecosystems. For the past 17 years, Fraser and about two dozen researchers have fanned out from this base camp to sample a swath of 120,000 km^2. They're studying the ecosystems' physical and biological components, including penguins, seals, fish, and krill, which anchor the food web.

The clearest trend is in the penguins. Adélies on the peninsula have suffered a 70% decline from the 1970s, yet nearby populations of gentoo and chinstrap penguins have gone through the roof. One difference is that Adélies prefer fairly wide expanses of ice, whereas the chinstraps, for example, like open water. Sea ice is forming later and retreating sooner each winter, resulting in 85 fewer days of ice cover than 25 years ago, Ducklow and his colleagues reported in January in the *Philosophical Transactions of the Royal Society of London*.

Adélie penguins may also be affected by a decline in silverfish, which were once half this penguin's diet. Now the penguins eat mostly krill, which are just as nutritious but not as reliable as a food source because their populations periodically bottom out. When krill decline, the penguins have a harder time feeding their chicks, says Fraser.

There's trouble for Adélies on land as well. Adélies nest on rocky ground, near the shore. Fraser and his colleagues have studied seven major colonies in the 50 square kilometers around Palmer Station. About a dozen years ago, they noticed that some of the colonies were shrinking much more severely than others, even though the birds were feeding in the same area.

He wondered whether snowfall was a factor. By comparing snow accumulation at various colonies, Fraser discovered that chicks tended to weigh less in colonies with deeper snow. The colony with the most snow, on Litchfield Island, has fared the worst, declining from roughly 1000 breeding pairs in 1975 to zero last year.

To confirm his suspicion, Fraser and his colleagues erected a fence near a northeast-facing colony where winds normally blow snow away, causing snow to accumulate on half the nests. According to unpublished results, chicks behind the snow fence weighed up to 15% less than chicks from nests a few meters away with no snow. The explanation, Fraser says, is that Adélies only lay eggs on dry ground. Penguins in areas with more snow wait longer to breed, and their later-hatching chicks miss the 2 weeks when krill are most abundant. The chicks gain

CREDITS (TOP TO BOTTOM): DLILLC/CORBIS; JOEL L. BELLUCCI

less weight and are much less likely to survive the next winter.

He points out that although Adélie populations have fluctuated over millennia, the current decline is unprecedented. Within a decade, there may be no more Adélies within 200 kilometers of Palmer Station.

This doomsday prediction doesn't tell the whole story, however. As Adélie penguins lose ground, other species are thriving. Species that prefer open ocean used to be limited to the north and east parts of the peninsula, where the ocean didn't freeze during the winter. Now, with ever more open water, these species are expanding their ranges.

In the past decade, Palmer Station has seen a huge proliferation of southern fur seals and southern elephant seals—species that were present only as small colonies in the 1990s. In one case, a population of six seals now numbers 5000. The presence of these species suggests that a sub-Antarctic ecosystem is replacing the polar ecosystem of Adélies and silverfish.

But as this ecosystem moves southward, so too is the "polar" world, and that's good news for the overall survival of Adélie penguins. Some 400 kilometers south of Palmer Station, the populations of Adélies in Marguerite Bay have tripled since the 1950s. Just as Adélies don't like a lack of ice, they also dislike a surfeit—the greater expanse makes it strenuous to reach open water for foraging. The warming climate and reduced sea ice are apparently making Marguerite Bay a nicer place for Adélies to live. That's true farther south too, says David Ainley of H. T. Harvey & Associates in San Jose, California, who studies Adélies in the southern Ross Sea. "As ice shelf breaks up, there should be more habitat, and we should be seeing more penguins."

Still, Ainley and others caution that it's dicey to predict exactly what will happen as ecosystems continue to respond to climate change. But looking back on the fate of the Adélies he has watched for 3 decades, Fraser offers a warning: "If Antarctica is a model for how ecosystems might change in other parts of the world, the changes will be severe."

–ERIK STOKSTAD

NEWS

For Extreme Astronomy, Head Due South

Over the past decade, small telescopes in Antarctica have revealed key features of the early universe. Now astronomers are rolling out the big guns

Some astronomers choose to build telescopes in idyllic locations—atop Mauna Kea in Hawaii, for instance, or in the Canary Islands. Not John Carlstrom. During the just-finished austral summer, his team shipped 270 metric tons of equipment to the South Pole and raced to assemble a new radio telescope with a 10-meter dish before winter shuts down flights and maroons Amundsen-Scott South Pole Station for 9 months. "Everything has to be ready to go," says Carlstrom, of the University of Chicago in Illinois. "There's only so much you can do in 3 months."

To extreme astronomers, Antarctica's unrivaled view of the stars makes the prodigious and risky work to build a scope there worthwhile. Water vapor, the enemy of radio astronomers who tune in to microwave signals, is virtually absent at the bone-dry pole. And microwaves are not the only game in town. Alongside Carlstrom's South Pole Telescope (SPT), a giant neutrino observatory, IceCube, is taking shape.

They are the vanguard. Surveys on the Antarctic plateau have pinpointed perches with little atmospheric turbulence, ideal for astronomy at infrared wavelengths. "These are the best sites in the world by a big factor," argues astronomer Edward Kibblewhite of the University of Chicago. As a result, optical astronomers are hatching plans for front-rank observatories across the frozen continent.

Some astronomers are hedging their bets on whether the risk is worth taking. "Almost every common system that we use at our very large telescopes now would fail in the extreme conditions in Antarctica," says Daniel Fabricant of the Harvard-Smithsonian Center for Astrophysics in Cambridge, Massachusetts. Today's pioneers have yet to prove that big optical or infrared scopes in Antarctica are feasible, he says. Kibblewhite, for one, is taking up the gauntlet: "The pain of building there is offset by the fantastic capabilities."

Cold, high, and dry

Since the early 1990s, astrophysicists have eagerly pitched camp in Antarctica to study the cosmic microwave background (CMB) radiation, a relic of the early universe when the plasma of electrons and protons coalesced into atoms and the universe became transparent. Over the eons, photons from that primordial fog have cooled to microwave wavelengths. Since the CMB's discovery in 1965, researchers have interrogated it for clues to what the universe was like in those early days and to test various models of the big bang.

Because water vapor absorbs microwaves, CMB astrophysicists must put their telescopes in space or some other ultradry place. Some flocked to mountaintops or deserts. Others chose Antarctica, where moisture freezes out of the air. Early scopes on the ice looked for wrinkles in the CMB—variations in the radiation's temperature across the sky. The field really took off after the Cosmic Background Explorer satellite charted wrinkles over the whole sky in the early 1990s. The satellite's map revealed an early universe of uneven density, in which denser regions led to galaxy clusters seen today.

Continuing the work, the Degree Angular Scale Interferometer, based at the South Pole, discovered in 2002 that CMB radiation is slightly polarized, giving a picture of how regions of different densities were moving early on. And BOOMERANG, a CMB telescope flown over Antarctica by balloon in 1998 and 2003, allowed cosmologists to estimate the universe's overall density, leading to the conclusion that spacetime has no overall curvature: The universe is flat.

The latest CMB scope at the pole is QUaD. It is scrutinizing polarization in an attempt to put limits on certain properties of the early universe, such as how much normal matter there was. But in QUaD's first season in 2005, the experiment almost ground to a halt when it nearly exhausted South Pole station's liquid nitrogen and helium, used to chill the scope's detectors to 0.3 kelvin. "The biggest challenge is having no access [during the winter]," making maintenance difficult, says QUaD astronomer Walter Gear of the University of Cardiff, United Kingdom.

Crystal-clear vision. The new South Pole Telescope, with its heated 10-meter dish, will study the properties of enigmatic dark energy.

Another recent arrival at the pole is the Background Imaging of Cosmic Extragalactic Polarization (BICEP) telescope. BICEP aims to answer one of the burning questions of cosmology. Big bang theory predicts that the infant universe underwent a rapid expansion known as inflation. It's impossible to peer into the opaque young universe to verify that inflation occurred. But if it did, it would have created a cosmic perfusion of gravitational waves—something absent from other theories. The technology does not exist to detect a gravitational-wave background, but the waves should have left a faint fingerprint in the form of a slight swirl in the CMB's polarization. BICEP is the first scope designed to detect this, says project leader Andrew Lange of the California Institute of Technology in Pasadena.

To perceive gravity's subtle signature in the early universe, a telescope must peer at one patch of sky for days on end. "At the South Pole, you can stare relentlessly at the target," Lange says, because the same stars circle the pole at the same elevation. After BICEP's first season last year, the team is honing its detectors and expects to reach the required sensitivity in the next year or two. "We could see something soon," says Lange.

Big science arrives

With the installation of the 10-meter SPT, a behemoth has taken its place beside the much smaller scopes. Although the CMB is also the target of this newcomer, its principal goal is not to study the early universe but rather to probe the nature of dark energy, a mysterious, unseen force that is speeding up the universe's expansion. SPT will study the evolution of galaxy clusters over the universe's history. Because dark energy seems to push everything apart, it inhibits the growth of galaxy clusters, so studying how clusters have developed should reveal something about dark energy. Rather than observe clusters directly, SPT will look for the imprint they have left on the CMB as it has wafted through space.

Building the delicate instrument at the pole was no mean feat. All moving parts must be sheltered for warmth, while the exposed dish's aluminum panels are kept ice-free with electric heaters. It took three field seasons to assemble the scope; after finishing its construction in January, most SPT crew members flew home and will control the scope from the relative comfort of Chicago. Three colleagues will winter at the pole to ensure SPT runs smoothly. The scope saw first light on 16 February, and Carlstrom expects initial science results this austral winter.

SPT's completion was a sprint compared to IceCube, one of two major rivals in observing neutrinos from deep space. These particles are born in the hearts of stars and cosmic calamities such as supernovae and gamma ray bursts. They are chargeless, nearly massless, and race by at close to light speed. Space is teeming with them. But they rarely interact with normal matter. Billions pass right through your body every second without ever interacting.

Researchers detect the ghostly particles by putting a large volume of water under surveillance. After a neutrino strikes a nucleus, the streaking subatomic shards produce a flash of light that spreads in a cone shape. The cone's orientation reveals the direction the neutrino came from, making it possible to retrace the neutrino's path—perhaps all the way back to the cosmic event that spawned it.

Researchers estimate that roughly a cubic kilometer of water is necessary to get a fix on neutrino sources. A European team plans to use the Mediterranean as an instrument by floating strings of detectors anchored to the sea floor. Their U.S. counterparts are using ice rather than water, boring into the Antarctic plateau with a hot water drill and then lowering strings of detectors into the holes, which will fill with water and freeze. It's a mammoth undertaking. Each borehole is 2.5 kilometers deep, takes 48 hours to drill, and creates 750,000 liters of water. IceCube's crew members have been honing their techniques: Two years ago, they dug a single hole; in 2005–06, they managed eight; and this season, the team sank 13. The target is now 14 holes per season; with at least 70 planned, installation has a few years to go.

Other astronomers, inspired by the groundbreaking polar work, are hoping to get in on the action. Three years ago, Michael Burton and his colleagues at the University of New South Wales in Sydney, Australia, used an automated test scope to survey Dome C, a bulge on the plateau that's home to the French-Italian Concordia station. There they found "uniquely stable conditions," Burton says, "two times better than any temperate latitude site." The key is scant turbulence above about 30 meters that can be corrected using adaptive optics, Kibblewhite says.

As part of the International Polar Year, the Australian team in 2007–08 will set up another test scope at Dome A, where China has ambitious plans for astronomy (see p. 1516). The Australians' long-term goal is to erect a 2-meter telescope called PILOT at Concordia. "Big enough to do interesting science, but not too expensive," Burton says. PILOT's images, he predicts, will be similar in quality to those of the Hubble Space Telescope. Kibblewhite and U.S. collaborators have grander plans: a 15-meter telescope at one of the domes, with a mirror made of many small segments to reduce weight and cost. Planning is in the early stages.

Kibblewhite believes that with astronomy's history of international collaboration, it won't be long until nations work together to build large observatories in Antarctica. If so, they will owe a debt to Carlstrom and other polar astronomy pioneers. **–DANIEL CLERY**

CREDIT: COURTESY SPT TEAM/JEFF MCMAHON

NEWS

Race to Plumb the Frigid Depths

In the Arctic Ocean, research fueled by national claims could reveal past climates, unknown life forms—and vast natural resources

By all appearances, Trine Dahl-Jensen and Ruth Jackson have transcended national boundaries in the name of science. Working for the geological surveys of Denmark and Canada, respectively, the geophysicists are mapping the structure of undersea rocks hundreds of kilometers north of Greenland and Canada's Ellesmere Island. In this forbidding region, habitual convergences of winds and currents force ice floes into solid jumbles 100 meters thick. Polar bears, whales, and even icebreakers are frozen out. Most knowledge of the depths comes from a few sounding tracks made by Cold War subs. To gather data, Dahl-Jensen and Jackson land by helicopter, set off explosives, collect echoes from the bottom, and then scramble back to the Canadian military base of Alert, humanity's northernmost toehold on land.

Actually, national interests are their reason for being here. The five nations bordering the Arctic Ocean are in an underwater land rush to legally divvy up much of the sea bottom, based on its geology. In this particular region, Canada and Denmark have teamed up to cut costs. Other scientists are hunting for oil and minerals or seeking sea-floor records that might suggest how fast global warming could peel back Arctic ice. Denmark and Canada have budgeted $80 million for mapping over several years. Jackson compares it to the Americans' 1867 purchase of Alaska from Russia. "It might not have seemed too useful at the time," she says, "but give it another 30 or 100 years."

Similar nationally funded projects have already sparked some nasty disputes, but the money is sloshing over into the International Polar Year (IPY), where it might foster cooperation. Researchers say that once the politics are sorted out, the same data can clarify murky geological, ecological, and climate questions, to the benefit of all. Territorial claims "are giving us an opportunity to work in unknown areas of the world that we would never get to otherwise," says Dahl-Jensen. "There are all kinds of scientific spinoffs."

Undersea land grab

Studying the Arctic sea floor, never mind laying claim to it, once seemed impossible. The heavy ice cover on the 14-million-square-kilometer northern ocean has long kept even basic bathymetry vague. In the 1990s, the U.S. Navy declassified a smattering of sub soundings and invited civilian scientists on cruises. The Russians have prowled Arctic waters secretly for decades and still keep much of their data off-limits. Only during the last decade have cruises by Canadian, German, and Swedish breakers opened a window to sea-floor geology, and it was not until 2001 that the U.S. Coast Guard commissioned its first Arctic science icebreaker, the *Healy*. Its inaugural cruise to the Gakkel Ridge, in the deep central Arctic, revealed rumbling volcanoes and apparent hydrothermal vents where conventional tectonic theory predicted there would be none (see sidebar, p. 1527).

Boom with a view. A drilling rig in the Beaufort Sea. Warming temperatures should make it easier to extract oil and gas from the High Arctic.

CREDIT: DORAN CLARK/GETTY IMAGES

Such discoveries herald resources that might soon become accessible. Undersea vents commonly precipitate metals, including copper, gold, and silver. With undersea mining in its infancy, these deposits might not be tapped soon, but other resources could become available, says James Hein, a senior researcher at the U.S. Geological Survey (USGS), who tracks Arctic minerals. These might include placer deposits of diamonds or gold washed by rivers onto shallow continental shelves from Canada or Siberia. Dramatic summer melting in the last decade has opened shipping channels, and companies have begun prospecting. "No one is going to know what they've found until they're ready to move," says Hein.

The big prize, almost certainly, is hydrocarbons. In 2000, USGS estimated that maybe a quarter of the world's undiscovered hydrocarbons—an estimated 3.1 trillion to 11 trillion barrels of oil—lies in the Arctic. USGS research geologist Donald Gautier is co-heading a new circumpolar hydrocarbon survey. When it comes out in 2008, "it is logical to think" the estimate will go up, he says. Along with known oil and gas reserves already mapped in near-shore zones, such as Alaska's Prudhoe Bay, deposits may be locked up in gas hydrates farther out. One speculative map from the Geological Survey of Canada forecasts hydrate fields extending to the pole. Although all wells currently hug the shore, many companies are developing hardware to expand deep into ice-covered waters, says Graham Thomas, chief of cold-regions technology for the oil company BP.

Geologic information is central to the territorial claims themselves. Under the U.N. Convention on the Law of the Sea, the United States, Russia, Norway, Canada, and Denmark (which administers Greenland) may claim underwater rights beyond their 200-nautical-mile economic zones via any submerged "natural prolongation" of their landmasses. The U.N. rules are based on formulas that take into account the contour line where water depth reaches 2500 meters, along with details of seabed geology, including measurements of sediments that may have eroded off continental shelves. Most of the Arctic Ocean is ringed with expansive shallow continental shelves and possibly related topographic features, so nearly the whole ocean may someday be claimed, except for a couple of small doughnut holes way out in the middle. The United States, which has yet to ratify the convention, has been mapping the seabed since 2003; it could

gain some 600,000 square kilometers of Alaskan shelf, worth $650 billion if present oil estimates hold up.

The really dicey part is mapping the deep, central Arctic, which is crisscrossed by a half-dozen huge underwater mountain ranges that may or may not be connected to certain landmasses, depending on whose scientists you listen to. One major feature is the 1800-kilometer-long Lomonosov Ridge, which runs from above the central Siberian continental shelf through the North Pole, to above Greenland and Ellesmere. Most scientists agree that it peeled off from the shelf of what is now Russia and Scandinavia some 60 million years ago. One end stuck near Siberia while the rest pivoted outward, like a splinter being pried off a log. Based on this history and proximity, the Russians say it is theirs, up to the pole. On the other side of the pole, Jackson and Dahl-Jensen are building the case for Canada and Greenland. If they succeed, Denmark stands to gain up to 180,000 square kilometers—four times the size of Denmark itself.

By measuring seismic waves passing through the sea floor, the scientists hope to establish that the rocks under the Lomonosov are deep-seated and of low density, and thus probably of continental origin. They are also mapping sediments and bathymetry in an effort to show that their lands and the Lomonosov may be linked. Never mind where the ridge came from, says Jackson. "The question is what it's attached to now." Under a 2005 agreement, their findings are secret, but the scientists make no bones about their governments' aim: With the ridge neatly straddling a midline above Greenland and Ellesmere, although not actually connecting to either, the nations aim to divide it up.

Some experts don't buy this argument. Lawrence Lawver, a marine geophysicist at the University of Texas, Austin, says such claims "are based more on desire than geology." It's hard to argue that the Lomonosov is part of either Greenland or Canada, he says: "It's just moving past as they wave hello."

Lawver and other Western researchers reserve harsher words for their Russian colleagues. Along with half the Lomonosov, Russia claims much of the vast, deep Alpha-Mendeleyev ridge system and parts of the adjoining Amerasian basin, which span eastern Siberia to central North America. Added to everything else they want, this would give Russia half the ocean bed. Their arguments include Siberia's proximity to one end of the Mendeleyev, dredged-up continental rocks eroded from the ridges, and magnetic signatures and other geophysical measurements that they claim show that Eurasian-type continental crust underlies both the ridge and parts of the adjoining basin. Viktor Poselov, deputy director of the Gramberg Research Institute for Geology and Mineral Resources of the World Ocean in St. Petersburg, invokes a theory of "vertical tectonics." In this scenario, much of what is now the Arctic sea floor is continental crust that sank as a block and became "oceanized," Russian documents assert.

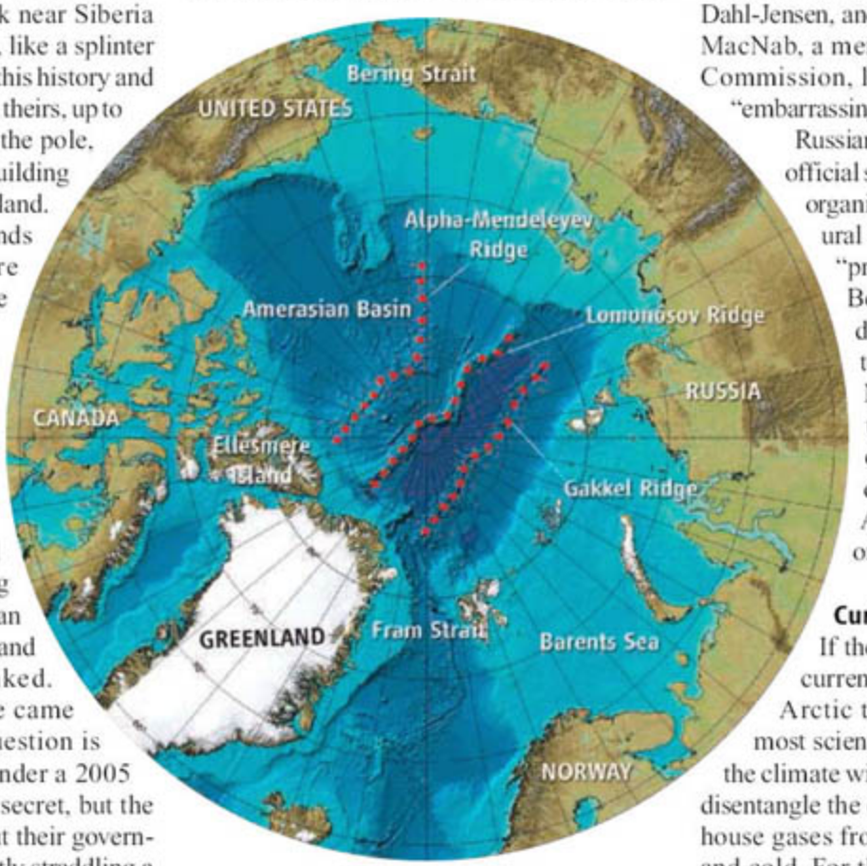

Cold rush. The five nations bordering the Arctic Ocean are using geology to lay claim to large chunks of sea bottom—and the virgin mineral and hydrocarbon assets buried beneath.

It is hard to find a non-Russian who agrees. In 2001, Russia submitted its proposed claim to the U.N.'s scientific Commission on the Limits of the Continental Shelf—still the only formal proposal by any country—and it was quickly sent back for more work. North American and European scientists assert that the geophysics is at best ambiguous. Most say that any continental rocks from the bottom are migrants swept out by ice from present-day continents—probably North America. They variously propose the Alpha-Mendeleyev system to be a product of hot-spot activity, mid-ocean spreading, or subduction—all purely oceanic processes not tied to Eurasia.

Arthur Grantz, a retired USGS polar expert, calls the idea that buoyant crust could somehow sink into the abyss "kind of nutty." He and others contend it is a notion peculiar to Russia—and old-fashioned even there—and long discredited by plate tectonics. "I understand where they're coming from, though," Grantz says. "They're under great pressure. Their government gave them a lot of money, and it expects them to come up with a certain result." Lawver, Dahl-Jensen, and others agree. Geologist Ron MacNab, a member of the Canadian Polar Commission, labels Russia's conclusions "embarrassing" and "Stalinist."

Russian scientists have shot back. An official summary of a 2003 conference organized by their Ministry of Natural Resources calls the criticisms "presumptuous" and "strange." Because there is so little credible data, the Arctic sea floor's history is largely a mystery, admits MacNab—and scientists are unlikely to figure it out if they don't stop bickering. "We're developing a train wreck in the Arctic unless we get together on this," he says.

Curious cores

If the sea ice keeps melting at its current rate, the confrontation over Arctic territory will intensify; yet most scientists are loath to predict what the climate will do, because it is difficult to disentangle the effects of humanmade greenhouse gases from natural cycles of warmth and cold. For this, bottom cores recording past sea-ice cover, water temperatures, and movements of glacial sediments may provide the most telling evidence.

The first deep-sea Arctic sediment cores of great age—still the only such samples—were brought up by the Integrated Ocean Drilling Program (IODP) in 2004, 320 kilometers from the North Pole. Detailed analyses published in *Nature* and *Geophysical Research Letters* last year portray the Arctic of 45 million to 55 million years ago as a landlocked, scummy pond. Sea temperatures were warm enough to support thick layers of ferns and algae. Younger layers show long-term cooling, with more cold-water plankton and superthick glaciations or sea ice scouring the bottom. Subsequent warm

CREDIT: INTERNATIONAL BATHYMETRIC CHART OF THE ARCTIC OCEAN

Deep impact. Experts debate how well Arctic benthic communities will weather warming.

Thriving Arctic Bottom Dwellers Could Get Strangled by Warming

Ten years ago, biologists skirting Canada's mainland Arctic coast on an icebreaker lowered a video camera to the bottom and got a surprise. Instead of the desolation they expected below ice-covered waters, there was a crowd. Slender brittle stars elbowed each other; fish glided by; anemones writhed under the camera's bright light. This wonderland could be jeopardized by climate change. "We don't know until it happens, but if you have no ice, you probably have no typical Arctic fauna," says Julian Gutt, a marine ecologist at the Alfred Wegener Institute for Polar and Marine Research in Bremerhaven, Germany.

The Arctic bottom fauna, or benthos, is surprisingly rich in species, abundance, and ecological significance. Of the northern ocean's 5000 known marine invertebrates, 90% live on the bottom. In shallow waters, they form the basic diet of many topside creatures including seabirds, walruses, bearded seals, and bowhead whales. Although many of the tiny creatures are migrants from North Atlantic waters, up to 20% are Arctic endemics.

The bounty exists because of the cold, not in spite of it. During the brief summer warmth, ice algae and cold-water plankton explode into life. In warmer waters, such simple organisms are devoured by zooplankton, which are devoured by predators, and so on up the food chain; thus nutrients stay in the water column. But in icy Arctic water, zooplankton do not grow fast enough to consume the sudden rushes of plant life. As a result, much of the plant life sinks to the bottom, where creatures there get it. For this reason, the benthos "can have production that is actually greater than in the tropics," says Bodil Bluhm, a benthic ecologist at the University of Alaska, Fairbanks (UAF).

Many biologists hypothesize that climate change could hurt the Arctic benthos and the large creatures that live off it by wiping out ice (and hence ice algae), lengthening growing seasons for zooplankton, and giving warm-water species a foothold. "The way the system works now is very much in favor of the benthos," says UAF polar ecologist Rolf Gradinger. "If the system changes, things could go downhill fast."

A preview might come from the Bering Sea, between Russia and Alaska. There, higher water temperatures and pullbacks in seasonal ice have progressed fast in recent decades. Oxygen uptake in sediments (an indicator of carbon supply to living things) has dropped by two-thirds, and populations of benthic creatures such as mussels have declined by half. Diving ducks, walruses, and gray whales are moving away, while pollock and other southern pelagic fish are streaming in (*Science*, 10 March 2006, p. 1461).

Preliminary evidence suggests that higher temperatures may be starting to have similar effects in the more northerly Barents and Laptev seas, off Scandinavia and Siberia, says Dieter Piepenburg, a marine biologist at the University of Kiel in Germany. Piepenburg, who wrote a 2005 review on Arctic benthos in *Polar Biology*, says it remains to be seen whether this would spell the end. He says that Arctic benthic organisms have probably already weathered not only warm cycles but also cold ones so extreme that deep ice sheets repeatedly scoured bottoms clean of life far out to sea. Piepenburg thinks the organisms may have migrated to deep waters and then recolonized when the coast was clear.

Those deep waters may also contain more life than previously believed. In 2001, U.S. researchers over the remote Gakkel spreading ridge detected chemical plumes indicating hydrothermal vents—which feed biological hot spots in other parts of the world—but were unable to locate a source. Indeed, no vents have yet been found anywhere in the Arctic, but as part of the International Polar Year (IPY), U.S. researchers in July will return to the Gakkel and deploy new under-ice autonomous vehicles to hunt down and sample the chemical plumes. If they find vents and vent creatures, the organisms may well be unique, because the narrow straits connecting the Arctic to other oceans are too shallow to allow movement of deep-sea creatures and thus mingling of genes.

Researchers are bound to discover many polar organisms, especially in deep places like this, says Gradinger, who is leading the Arctic Ocean inventory for the worldwide Census of Marine Life. The deep basins are mostly unexplored, he says, and many small creatures that live buried in sediments even in shallow areas have yet to be glimpsed. IPY may help change this; within its framework, Gradinger counts 20 biological collecting projects slated so far.

–K.K.

CREDITS (TOP TO BOTTOM): COURTESY OF V. JUTERZENKA, PIEPENBURG, SCHMID; DLILLC/CORBIS

periods occurred, but the timing, amplitudes, causes, and possible interactions of warm-cold cycles are perplexing. Most other cores gathered so far go back only a few hundred thousand years. Even IODP's cores are missing a giant chunk of time—sediments from 43 million to 18 million years before present—because they were apparently uplifted and eroded away in some as-yet-unidentified event.

Efforts are under way to beef up the records. Last year, the *Healy* and the Swedish icebreaker *Oden* teamed up in the central Arctic Ocean to pull sea-floor cores that researchers hope will cover the last million years. Leonid Polyak, a marine geologist at Ohio State University in Columbus who participated, says some cores exhibit up to 80 cycles of apparent glacial melting, indicated by alternating bands of different-colored grains. Polyak says it appears that the bands come at intervals of 20,000 years, suggesting that they represent fluctuations in Earth's orbit; however, he is unsure, because the cores have not yet been well dated. His colleague Dennis Darby, a paleoclimatologist at Old Dominion University in Norfolk, Virginia, says one core from 1300 kilometers north of

Alaska shows a separate 240-year freeze-thaw cycle, written in sediments scraped from continental shelves by sea ice. Darby believes this periodicity must be connected to some ocean-circulatory pattern that presumably still exists but has not yet been noted in modern times. He, Polyak, and others presented preliminary findings at the American Geophysical Union (AGU) meeting in San Francisco, California, last December.

Next August, during IPY, a European consortium hopes to recover cores from the Fram Strait, which runs between Greenland and Norway, connecting the Arctic Ocean to the North Atlantic. Here they hope to find records tracing sea ice and currents decade by decade during historical time. This would fill an important gap. Although researchers have good decadal climate records from glacial ice cores, they lack comparable data from the sea because sediment accumulates too slowly in most of the Arctic.

Researchers identified the Fram site last October as a place where currents concentrate sediments faster. They hope to cover the Medieval Warm Period, when melting may have rivaled today's. "The extent of short-term ocean variability during the past, especially in warm periods, is practically unknown," says paleoceanographer Robert Spielhagen of the Leibniz Institute of Marine Sciences in Kiel, Germany, who is involved in the coring. "If scientists or policymakers want to understand our present situation, we have to have those records."

Another open question is the extent to which long-term tectonic rearrangement of the landmasses around the heavily landlocked Arctic Ocean has influenced climate. Before the drift of landmasses opened the Fram Strait, the region was more closed in. Slower circulation, or no circulation, could be one reason it was once so warm, says geologist Martin Jakobsson of Stockholm University. Estimates of when the strait formed vary; recent research says 15 million years ago. In any case, the circulation may have helped vent heat to the Atlantic, pushing the Arctic into the deep freeze we see today, Jakobsson says. Understanding the Fram's history would help us predict what will happen if the circulation begins to change again, he says.

Other events, including sea-level fluctuations and periodic blockages or openings of the shallow Bering Strait between the Arctic and the Pacific, may also have influenced climate. And entirely unexpected events may have been critical. At the December AGU meeting, a group of top Arctic researchers including Bernard Coakley, a geophysicist at the University of Alaska, Fairbanks, proposed that a previously undetected 200-by-600-kilometer meteorite crater lies at the bottom of the central Arctic Ocean. Such a massive event, which they say may have taken place more than 800,000 years ago, surely would have disrupted climate signals. But so far the group has only a hypothesis, based on overturned bottom sediments found in cores and unusual nickel spherules found on some of Canada's northernmost islands. "Climate change is a very alarming issue, but anyone who says we really understand it—what are they basing this on?" says Jakobsson.

Transcending borders

It's hoped that IPY will soften rhetoric and get nations working together. At least a half-dozen Arctic cruises are planned for the Polar Year, all of which will include scientists from several nations. Russia has submitted three proposals to resurvey major ridges and basins using seismic reflection, bottom sampling, gravity measurements, and other methods. In an abstract, Poselov acknowledges that existing data on areas Russia is claiming are "subject to controversial interpretations" and proposes that Russia, Sweden, Germany, and the United States pool their icebreakers, possibly in 2008, to study the Alpha-Mendeleyev ridges and other remote areas. "It's quite possible something will work out," says Coakley, who is helping pull together various efforts.

> "Anyone who says we really understand [climate change]—**what are they basing this on?"**
>
> —Martin Jakobsson, Stockholm University

Germany already plans to send its icebreaker, the *Polarstern*, to the Alpha in 2008. Studies would include identifying sites for future deep drilling—not attempted in the Arctic since the initial IODP foray in 2004. Scientists at the Alfred Wegener Institute for Polar and Marine Research in Bremerhaven are already talking about the drilling itself—again, via a multiship expedition—although this would come after IPY.

Large-scale cooperation is needed both for science and safety. Pressure from constantly shifting pack ice makes it nearly impossible for an icebreaker to remain stationary long enough to drill; the 2004 deep cores came up only with triple teamwork: One vessel drilled while two others broke up approaching floes. And an icebreaker has never penetrated the region north of Greenland and Ellesmere, where Jackson and Dahl-Jensen are working. This summer, as part of IPY, a European group chaired by Jakobsson hopes to get there in the *Oden* to do geophysical, geological, and paleoclimate work; the Swedish government is negotiating to rent a nuclear Russian breaker to make sure the diesel-powered *Oden* does not get trapped. Even so, says Jakobsson, there is no guarantee they will make it in.

The treachery of the ice became clear last August, when the *Healy* stopped 800 kilometers northwest of Barrow and two U.S. Coast Guard officers descended through a crack in the ice on a practice dive. After they failed to surface, comrades hauled them up on a line from an estimated depth of 60 meters. They were dead. The Coast Guard is investigating what went wrong—still a mystery. Pending reviews of safety protocols, the *Healy*'s remaining 2006 cruises were canceled.

Some say simpler is better. Since 2003, groups from Columbia University, the University of Hawaii, and other institutions have been developing seismic-sounding buoys to be set adrift in the ice, where they can take advantage of vigorous, predictable currents to sweep large areas without a need for icebreakers. Plans to deploy a large number for IPY have slipped, but a few should be put in next year, and perhaps 100 by 2009, says Yngve Kristoffersen, a marine geoscientist at the University of Bergen in Norway. For setting them out, he is pushing for a new mode of transport: hovercraft.

The cause has been taken up by John K. Hall, an American marine geophysicist who recently retired from the Geological Survey of Israel. Hall became a convert after a 2005 trip through the central Arctic on the *Healy*, during which, he says, ice-topography measurements showed that 85% of the voyage could have been made by hovercraft, at a tiny fraction of the cost. He has committed money inherited from his grandparents—the makers of Chiclets gum—to buy a small, well-heated vessel that will float up to 73 centimeters off the ice. Hall plans to test the vehicle around the Norwegian island of Svalbard next year. He does not wish to fly the flag of any nation. He jokes: "Well, maybe just a black one, with skull and crossbones."

–KEVIN KRAJICK

Kevin Krajick is a writer in New York City.

REVIEW

Recent Sea-Level Contributions of the Antarctic and Greenland Ice Sheets

Andrew Shepherd[1] and Duncan Wingham[2]*

After a century of polar exploration, the past decade of satellite measurements has painted an altogether new picture of how Earth's ice sheets are changing. As global temperatures have risen, so have rates of snowfall, ice melting, and glacier flow. Although the balance between these opposing processes has varied considerably on a regional scale, data show that Antarctica and Greenland are each losing mass overall. Our best estimate of their combined imbalance is about 125 gigatons per year of ice, enough to raise sea level by 0.35 millimeters per year. This is only a modest contribution to the present rate of sea-level rise of 3.0 millimeters per year. However, much of the loss from Antarctica and Greenland is the result of the flow of ice to the ocean from ice streams and glaciers, which has accelerated over the past decade. In both continents, there are suspected triggers for the accelerated ice discharge—surface and ocean warming, respectively—and, over the course of the 21st century, these processes could rapidly counteract the snowfall gains predicted by present coupled climate models.

Antarctica and Greenland hold enough ice to raise global sea levels by some 70 m (*1*) and, according to the geological record (*2*), collapses of Earth's former ice sheets have caused increases of up to 20 m in less than 500 years. Such a rise, were it to occur today, would have tremendous societal implications (*3*). Even a much more gradual rise would have great impact. Accordingly, one goal of glaciological survey [e.g., (*4*, *5*)] is to determine the contemporary sea-level contribution due to Antarctica and Greenland. For much of the 20th century, however, the size of these ice sheets hindered attempts to constrain their mass trends, because estimating whole–ice sheet mass change could be done only by combining sparse local surveys, with consequent uncertainty. For example, a 1992 review (*6*) concluded that the available glaciological measurements allowed Antarctica to be anything from a 600 Gt year^{-1} sink to a 500 Gt year^{-1} source of ocean mass [500 Gt of ice equals 1.4 mm equivalent sea level (ESL)], accounting for nearly all of the 20th-century sea-level trend of 1.8 mm year^{-1} (*1*) or, in the other direction, leaving a mass shortfall of some 1000 Gt year^{-1}. Even the 2001 Intergovernmental Panel on Climate Change (IPCC) report (*1*) preferred models to observations in estimating Antarctic and Greenland sea-level contributions.

However, in the past decade, our knowledge of the contemporary mass imbalances of Antarctica and Greenland has been transformed by the launch of a series of satellite-based sensors. Since 1998, there have been at least 14 satellite-based estimates (*7*–*20*) of the mass imbalance of Earth's ice sheets (Table 1). At face value, their range of some –366 to 53 Gt year^{-1}, or 1.0 to –0.15 mm year^{-1} sea-level rise equivalent, explains much of the eustatic component of 20th-century sea-level rise [1.5 mm year^{-1} in (*21*)], but we argue that the contribution is smaller and the problem of closing the 20th-century sea-level budget remains. Equally, the new observations provide a picture of considerable regional variability and, in particular, the long-predicted [e.g., (*1*)] snowfall-driven growth [e.g., (*10*, *22*)] is being offset by large mass losses from particular ice stream and glacier flows [e.g., (*12*, *23*)]. There is, moreover, evidence in Greenland and Antarctica of recent accelerations in these flows (*12*, *24*, *25*). It is apparent that the late 20th- and early 21st-century ice sheets at least are dominated by regional behaviors that are not captured in the models on which IPCC predictions have depended, and there is renewed speculation (*26*, *27*) of accelerated sea-level rise from the ice sheets under a constant rate of climate warming.

Although the observations in Table 1 have narrowed the uncertainty in estimates of the eustatic contribution to sea level, the range of values is notably wider than their stated uncertainties. Accordingly, we give consideration to the limitations of the three methods—accounting the mass budget [e.g., (*9*)], altimetry measurement of ice-sheet volume change [e.g., (*7*)], and observing the ice sheets' changing gravitational attraction [e.g., (*11*)]—used to calculate the estimates in Table 1. In light of these limitations, we discuss the recent changes in the Antarctic and Greenland ice sheets (AIS and GIS), and we conclude with some remarks on the future evolution of the ice sheets.

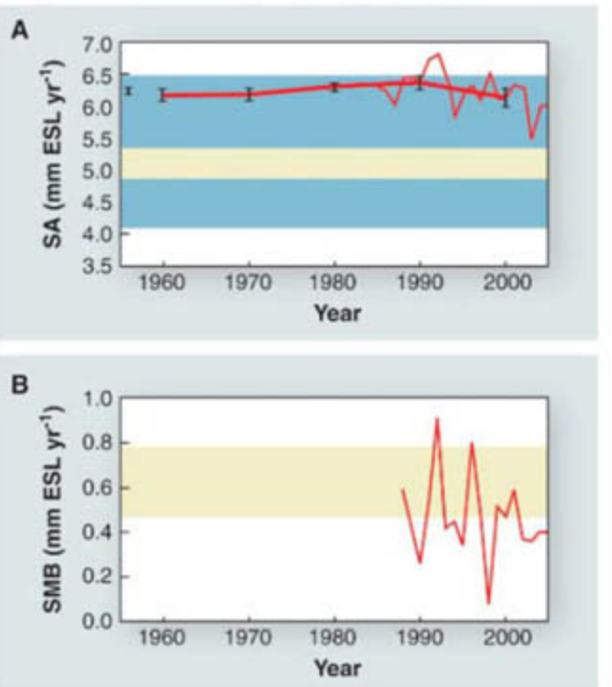

Fig. 1. Fluctuations in (**A**) the rate of snow accumulation (SA) of Antarctica [redrawn from (*38*)] and (**B**) the net surface mass balance (SMB) of Greenland [drawn from the data of (*32*)], determined from model reanalyses of meteorological observations expressed as ESL rise. Also shown are the ranges of published mean accumulation rates determined from glaciological observations (yellow) and climate models (blue).

Methods and Their Sensitivity to Accumulation Rate

The mass-budget method [e.g., (*9*, *12*)] compares the mass gain due to snowfall to mass losses due to sublimation, meltwater runoff, and ice that flows into the ocean. It has been given new impetus by the capability of interferometric synthetic aperture radar (InSAR) to determine ice surface velocity. This has improved earlier estimates of the ice flux to the ocean (*5*) and provides a capability to identify accelerations of ice flow. The method is hampered by a lack of accurate accumulation and ice thickness data. For Antarctica, where surface melting is negligible, accumulation may be determined by spatially averaging the history of accumulation recorded in ice cores, or from meteorological forecast models. Estimates of the temporally averaged accumulation or "mean" accumulation range, respectively, from 1752 to 1924 Gt year^{-1} (*1*) and from 1475 to 2331 Gt year^{-1} (*28*). The meteorological data are acknowledged to be of inferior accuracy (*28*), and their wide range can perhaps be discounted. The range of the core-based estimates, which use substantially the same core records, arises from differences in their spatial interpolation. Recent compilations have used the satellite-observed microwave temperature, which is correlated with accumulation, to guide the interpolation, and a careful study (*29*) placed the

[1]Centre for Polar Observation and Modelling, School of Geosciences, University of Edinburgh, EH8 9XP, UK. [2]Centre for Polar Observation and Modelling, Department of Earth Sciences, University College London, WC1E 6BT, UK.

*To whom correspondence should be addressed. E-mail: Andrew.Shepherd@edu.ac.uk (A.S.); djw@cpom.ucl.ac.uk (D.W.)

error of individual drainage-basin accumulation at 5%. The extent to which this error may average out over the entire sheet is not known: The microwave interpolation field [see (*29*)] depends on factors other than accumulation (e.g., temperature) that may bias the outcome. There is also the difficulty that, although accumulation is averaged over decades or centuries, the ice-flux measurements are limited to those of the satellite measurements [1995 to 2000 in (*9*)]. This complicates comparison of the estimated mass imbalance with altimetry estimates whose interval [e.g., 1992 to 2003 in (*14*)] is precisely defined. To date, 58% of Antarctica has been surveyed, although the method may in principle be extended to the remainder. Some 70% of Greenland has also been surveyed, but the impact of the satellite observations in determining the time-averaged imbalance is lessened because runoff from land-terminated ice, which in Greenland accounts for some 60% of the mass loss, remains largely unmeasured. The range of estimates of net accumulation and runoff [169 to 283 Gt year^{-1} in (*1*), about 20% of the total accumulation] has complicated mass imbalance estimates for some time [e.g., (*30*, *31*)] and will continue to do so.

Satellite and aircraft, radar, and laser altimetry provide a detailed pattern of change in the ice sheets' interior (*7*, *10*, *14*, *17*, *18*) and have played a key role in distinguishing changes related to accumulation and ice dynamics. The longest records to date span 1992 to 2003 (*10*, *14*), and imbalances estimated from them differ from longer averages estimated by other methods as a result of fluctuations in accumulation and ablation. Ice cores [see (*7*)] and model reanalyses (*28*, *32*) show fluctuations in accumulation, relative to their temporal means, on the order of 15% in individual years, and a similar variability in rates of ablation (*32*, *33*) (Fig. 1). The problem is exacerbated because the density of snow differs from that of ice by a factor of three, and decadal fluctuations in snowfall mass are exaggerated in the observed volume fluctuations over those due to ice dynamics in the same ratio. A correction is possible if the snowfall fluctuation is independently known, but the only estimates available today are from meteorological forecast models, and a recent study (*14*) of Antarctica concluded that there was too little correspondence between the altimeter and meteorological data sets for this method to be reliable. Differences between estimates of mass change made from the same observations of volume change (*10*, *14*, *18*) arise largely through different approaches to the conversion of volume to mass. To give an idea of the uncertainty, Wingham *et al.* (*14*) showed that, in the absence of other data, an altimeter estimate covering 73% of the Antarctic interior could vary by 90 Gt year^{-1} without contradicting the observed volume change. ERS-1 and -2 radar altimetry (for which the longest records are available) has been limited to latitudes between 81.5°N and 81.5°S and to terrain of low slope. Because these regions lie in the ice sheet's interior, which is characterized by growth in Greenland in general and in Antarctica in some places, there is a tendency for these estimates to be more positive (Table 1). These difficulties may be overcome with the satellite laser altimeter records initiated by ICESat (Ice, Cloud, and land Elevation Satellite) in 2003 or, in the future, with the high-resolution radar altimeter of CryoSat-2.

Although differences in the time-averaged imbalances from the interferometric and altimetry methods are to be expected, the methods are highly complementary. For example, the retreat of the West Antarctic Pine Island Glacier grounding line observed by InSAR (*34*) is in close agreement with the drawdown of the inland ice observed with satellite altimetry (*23*). More recently, a combination of the two methods has provided considerable insight into the unstable hydraulic connection between subglacial lakes in East Antarctica (*35*).

The GRACE (Gravity Recovery and Climate Experiment) satellites have permitted the changing gravitational attraction of the ice sheets to be estimated (*11*, *13*, *15*, *16*, *19*, *20*). These estimates (Table 1) are more negative than those provided by mass budget or altimetry, but care is needed in making comparisons. The method is new, and a consensus about the measurement errors has yet to emerge [e.g., (*36*)], the correction for postglacial rebound is uncertain [e.g., (*37*)], contamination from ocean and atmosphere mass changes is possible [e.g., (*16*)], and the results depend on the method used to reduce the data [compare, e.g., (*20*) and (*16*)]. The GRACE record is also short (3 years) and, as was the case with early altimeter time series [e.g., (*7*)], is particularly sensitive to the fluctuations in accumulation described above. For example, whereas (*13*) puts the total 2002 to 2005 Antarctic Ice Sheet mass loss at 417 ± 219 Gt, a subsequent meteorological study (*38*) has put the 2002 to 2003 snowfall deficit at 309 Gt, a value that explains most of the observed change.

East Antarctica

Although the East Antarctic Ice Sheet (EAIS) is the largest reservoir of ice on Earth, it exhibits the smallest range of variability among recent mass balance estimates (Table 1). Since 1992, altimetric (*7*, *10*, *14*, *17*, *18*), interferometric (*9*), and gravimetric (*13*, *19*) surveys have put the EAIS annual mass trend in the range −1 to 67 Gt year^{-1}. Growth of the EAIS mitigates the current sea-level rise. Gains are limited to Dronning Maud Land and

Table 1. Mass balance (MB) of the East Antarctic (EAIS), West Antarctic (WAIS), Antarctic (AIS), and Greenland (GIS) ice sheets as determined by a range of techniques and studies. Not all studies surveyed all of the ice sheets, and the surveys were conducted over different periods within the time frame 1992 to 2006. For comparison, 360 Gt of ice is equivalent to 1 mm of eustatic sea-level rise.

Study	Survey period	Survey area 10^6 km^2 (%)	EAIS MB Gt year^{-1}	WAIS MB Gt year^{-1}	AIS MB Gt year^{-1}	GIS MB Gt year^{-1}
Wingham *et al.* (*7*)*	1992–1996	7.6 (54)	−1 ± 53	−59 ± 50	−60 ± 76	
Krabill *et al.* (*8*)*	1993–1999	1.7 (12)				−47
Rignot and Thomas (*9*)†	1995–2000	7.2 (51)	22 ± 23	−48 ± 14	−26 ± 37	
Davis and Li (*17*)*	1992–2002	8.5 (60)			42 ± 23	
Davis *et al.* (*10*)*	1992–2003	7.1 (50)	45 ± 7			
Velicogna and Wahr (*11*)‡	2002–2004	1.7 (12)				−75 ± 21
Zwally *et al.* (*18*)*	1992–2002	11.1 (77)	16 ± 11	−47 ± 4	−31 ± 12	11 ± 3
	1996					−83 ± 28
Rignot and Kanagaratnam (*12*)†	2000	1.2 (9)				−127 ± 28
	2005					−205 ± 38
Velicogna and Wahr (*20*)‡	2002–2005	12.4 (88)	0 ± 51	−136 ± 19	−139 ± 73	
Ramillien *et al.* (*19*)‡	2002–2005	14.1 (100)	67 ± 28	−107 ± 23	−129 ± 15	−169 ± 66
Wingham *et al.* (*14*)*	1992–2003	8.5 (60)			27 ± 29	
Velicogna and Wahr (*13*)‡	2002–2006	1.7 (12)				−227 ± 33
Chen *et al.* (*15*)‡	2002–2005	1.7 (12)				−219 ± 21
Luthcke *et al.* (*16*)‡	2003–2005	1.7 (12)				−101 ± 16
Range			−1 to 67	−136 to −47	−139 to 42	−227 to 11

*Altimetry. †InSAR mass budget. ‡Gravimetry.

Wilkes Land, and their spatial distribution (Fig. 2A) is strongly suggestive of snowfall-driven growth. Two glaciers in East Antarctica are losing mass (Fig. 2B). From 1992 to 2003, the fast-flowing trunks of the Totten and Cook glaciers deflated by 5.0 ± 0.5 and 2.4 ± 0.2 km^3 year^{-1}. Although these figures are only in rough coincidence with those determined from interferometry [0 ± 2 and -8 ± 5 km^3 year^{-1}, respectively, in (*9*)], the signals are clear and the trends definitely established.

West Antarctica and the Antarctic Peninsula

The West Antarctic Ice Sheet (WAIS) contains enough ice to raise global sea levels by more than 5 m and, according to altimetry and interferometry, one key sector is in a state of rapid retreat (*23*, *34*). Glaciers draining into the Amundsen Sea (Fig. 2A) are losing mass because of an ice-dynamic perturbation. During the 1990s, for example, the Pine Island Glacier retreated by up to 1.2 km year^{-1} (*34*), thinned by up to 1.6 m year^{-1} (*23*), and accelerated by around 10% (*39*); the ice loss has been implicated in the freshening of the Ross Sea some 1000 km away (*40*). Throughout the 1990s, independent altimeter (*7*, *14*, *17*, *18*) and interferometer (*9*) surveys of the WAIS as a whole were in notable, possibly fortuitous, agreement (Table 1), placing its annual losses in the range 47 to 59 Gt year^{-1}. The mass balance of the WAIS has been dominated by the losses from glaciers of the Amundsen sector, canceled to a degree by some snowfall-driven coastal growth and growth arising from the well-established shutdown of the Kamb Ice Stream (*41*).

There has been a report of an accelerated recent sea-level contribution (*42*) based on satellite and aircraft altimetry, and the gravimetric surveys have also estimated a rate of mass loss since 2002 of between 107 and 136 Gt year^{-1} (Table 1). Such an acceleration (an increase in sea-level trend of 0.2 mm year^{-1}, or about 10%) would be a cause for considerable concern. However, the altimeter data from which accelerated mass losses were derived in (*42*) span less than 5% of the WAIS area and use three altimeters with markedly different measurement errors. Furthermore, both data sets span a short time interval in which forecast models indicate that a 309-Gt accumulation deficit occurred (*38*). Taking these factors into account, it is unlikely that the WAIS mass loss has altered substantially since the 1990s.

During the past decade, there have been notable glaciological changes at the Antarctic Peninsula (AP): The Larsen Ice Shelf thinned (*43*) and sections collapsed (*44*), accelerating ice discharge into the oceans by some 0.07 mm year^{-1} ESL rise (*45*). However, the majority of AP ice forms the continental ice cap of Dyer Plateau. This exhibits snowfall-driven growth (Fig. 2A) that is sufficient to cancel the accelerated flow from the Larsen-A and -B catchments. The AP contribution to sea level is negligible.

Greenland

Since the most recent IPCC report, there have been seven estimates of Greenland mass imbalance based on satellite altimetry (*18*), interferometry (*12*), and gravimetry (*11*, *15*, *16*, *19*, *20*). There is consensus that during the 1990s the interior underwent modest snowfall-driven growth, which appears to be associated with a precipitation trend present in the meteorological record (*32*), offset by losses from lower altitude regions (Fig. 3, A and B). The decadal imbalance is not accurately determined. The more positive satellite altimeter estimate (*18*) is affected by signal loss in the steeper coastal margins; the aircraft laser measurements (*8*) are relatively sparse, although more sensitive to losses from marginal glaciers; and the mass-budget estimate (*12*) is undermined by the uncertainty of some 50 Gt year^{-1} in the accumulation. Nonetheless, the consensus of these measurements suggests a net loss in the 1990s of some 50 Gt year^{-1}.

Satellite interferometry (*12*, *24*) has also established that from 1996 to 2005, mass losses through flow increased by 102 Gt year^{-1}, and meteorological estimates (*32*) (Fig. 1B) of the surface-mass imbalance decreased some 20 Gt year^{-1} in the same period because of increased melting. Gravimetric surveys too support an increased mass loss (*11*, *15*, *16*, *19*, *20*). However, the interferometric and gravimetric records are short and reflect the considerable variability in the mass flux of tidewater glaciers and the surface mass balance. For example, the ice fluxes of two glaciers that by 2005 were responsible for 43 Gt year^{-1} of the increased discharge had by late 2006 declined to within 10 Gt year^{-1} of their level in 2000 (*46*), whereas in the past 14 years, the 3-year variability in surface mass imbalance has ranged from -130 to 120 Gt year^{-1} (Fig. 1B). In addition, not all gravimetric estimates capture the known spatial distribution of change; one that does (*16*) (Fig. 3B) is some 120 Gt year^{-1} more positive than other estimates, and some understanding of the cause of these discrepancies is needed. Increased mass loss from Greenland has occurred, but the decadal change is probably modest.

Implications for the Future

It is reasonable to conclude that, today, the EAIS is gaining some 25 Gt year^{-1}, the WAIS is losing about 50 Gt year^{-1}, and the GIS is losing about 100 Gt year^{-1}. These trends provide a sea-level contribution of about 0.35 mm year^{-1}, a modest component of the present rate of sea-level rise of 3.0 mm year^{-1}. Because 50 Gt year^{-1} is a very recent contribution, the ice sheets made little contribution to 20th-century sea-level rise. However, what has also emerged is that the losses are dominated by ice dynamics. Whereas past assessments (*47*) considered the balance between accumulation and ablation, the satellite observations reveal that glacier accelerations of 20 to 100% have occurred over the past decade. The key question today is whether these accelerations may be sustained, or even increase, in the future.

The question is difficult because the causes of the instabilities have yet to be established. The geo-

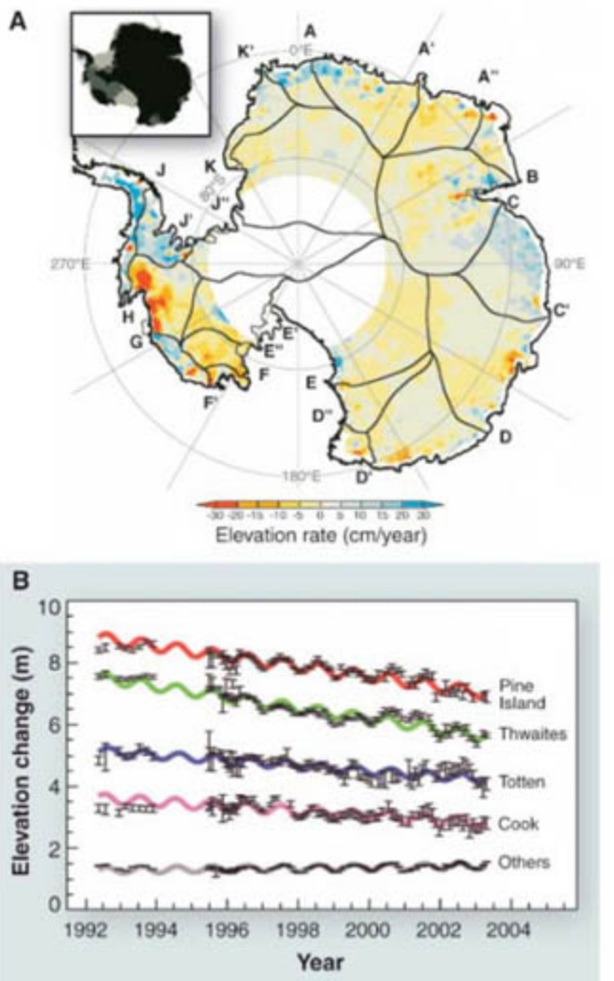

Fig. 2. (**A**) Rate of elevation change of the Antarctic Ice Sheet, 1992 to 2003, from ERS satellite radar altimetry [redrawn from (*14*)]. Also shown (inset) is the bedrock geometry, highlighting floating (light gray), marine-based (mid-gray) and continental-based (black) sectors. (**B**) Elevation change of the trunks (flow in excess of 50 m year^{-1}) of the Pine Island [Basin GH in (A)], Thwaites (Basin GH), Totten (Basin C′D), and Cook (Basin DD′) glaciers. All the deflating glaciers coincide with marine-based sectors of the ice sheet. An ice-dynamic origin of the thinning of the East Antarctic glaciers has yet to be confirmed by interferometry. However, the correlation of the thinning with flow velocity and the fact that the thinning rate is secular make ice dynamics the likely cause of all Antarctic mass losses.

logical record (*48*) suggests that some 10,000 years ago, the Amundsen sector of the WAIS extended only 100 km farther than today, confining the present rate of retreat to more recent times, and the drawdown of the Amundsen sector ice streams has been linked (*49*) to a recent trigger in the ocean. A comparable argument may be extended to the thinning glaciers in East Antarctica and Greenland, which are also marine terminated. Equally, there is no direct evidence of a warming of the Amundsen Sea, and it has long been held possible that the marine-terminated WAIS, and the Amundsen sector in particular, may be geometrically unstable (*50*), and the retreating East Antarctica streams have a similar geometry (Fig. 2A). In Greenland, where summer melting is widespread and increasing, Global Positioning System measurements have shown the melting to affect flow velocity in the ice sheet interior (*26*), introducing the possibility that increased surface meltwater is reaching the bed and accelerating the ice flow to the ocean.

The discovery that particular ice streams and glaciers are dominating ice sheet mass losses means that today our ability to predict future changes is limited. Present numerical models capture neither the details of actual ice streams nor, in Greenland, those of hydraulic connections between the surface and the bed. In addition, the detailed mechanics at the grounding line still remain to be fully worked out. In consequence, the view that the changing sea-level contribution of the Antarctic and Greenland ice sheets in the 21st century will be both small and negative as a result of accumulating snow in Antarctica [e.g., –0.05 mm year^{-1} in (*1*)] is now uncertain.

Because our predictive ability is limited, continued observation is essential. The satellite record clearly identifies the particular ice streams and glaciers whose evolution is of greatest concern. The causes of their instability need to be identified. Their detailed basal topography, their basal hydrology, and the details of the interaction with their surrounding shelf seas need to be established. Numerical models that capture the detailed dynamics of these glaciers and their hydrology are required. Of equal importance are meteorological and ice core measurements that will increase confidence in forecast models of accumulation and ablation fluctuations, because to a considerable extent these limit interpretations of the short satellite records. There is a great deal that the International Polar Year may achieve.

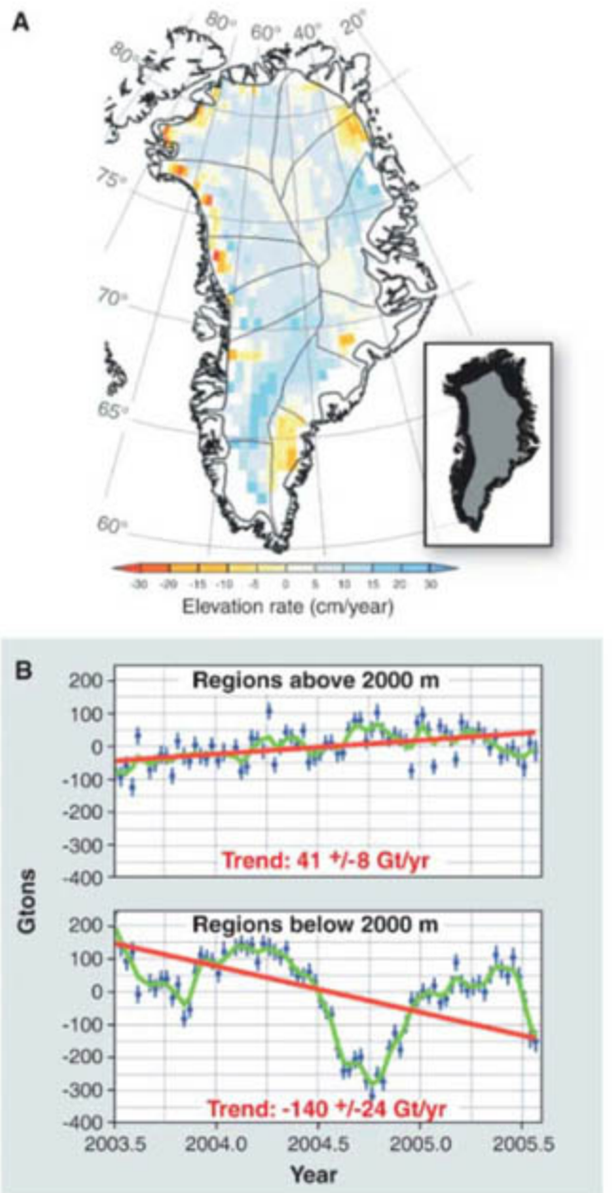

Fig. 3. (**A**) Rate of elevation change of the Greenland Ice Sheet, 1992 to 2003, determined from satellite radar altimetry [from (*22*)], and (**B**) time series of elevation change of individual sectors, 2003 to 2005, determined from satellite gravimetry [from (*16*)]. Also shown (inset) is the ice surface geometry, highlighting areas above (gray) and below (black) 2000 m elevation. Both instruments concur that high elevation areas are growing and low elevation areas are losing mass. According to gravimetry (*16*) and repeat InSAR measurements of ice discharge (*12*), the rate of mass loss at low elevations has increased over the past decade (see Table 1).

References and Notes

1. J. A. Church, J. M. Gregory, in *Climate Change 2001: The Scientific Basis*, J. T. Houghton *et al.*, Eds. (Cambridge Univ. Press, Cambridge, 2001), chap. 11, pp. 641–693.
2. R. G. Fairbanks, *Nature* **342**, 637 (1989).
3. N. Stern, *The Economics of Climate Change: The Stern Review* (Cambridge Univ. Press, Cambridge, 2006).
4. C. S. Benson, "Stratigraphic studies in the snow and firn of Greenland ice sheet" Research Report 70 (Cold Regions Research and Engineering Lab, Hanover, NH, 1962).
5. C. R. Bentley, M. B. Giovinetto, Proceedings of the International Conference on the Role of Polar Regions in Global Change (Geophysical Institute, University of Alaska, Fairbanks, AK, 1991), pp. 481–486.
6. S. S. Jacobs, *Nature* **360**, 29 (1992).
7. D. J. Wingham, A. Ridout, R. Scharroo, R. Arthern, C. K. Shum, *Science* **282**, 456 (1998).
8. W. Krabill *et al.*, *Science* **289**, 428 (2000).
9. E. Rignot, R. H. Thomas, *Science* **297**, 1502 (2002).
10. C. H. Davis, Y. Li, J. R. McConnell, M. M. Frey, E. Hanna, *Science* **308**, 1898 (2005).
11. I. Velicogna, J. Wahr, *Geophys. Res. Lett.* **32**, art-L18505 (2005).
12. E. Rignot, P. Kanagaratnam, *Science* **311**, 986 (2006).
13. I. Velicogna, J. Wahr, *Science* **311**, 1754 (2006).
14. D. J. Wingham, A. Shepherd, A. Muir, G. J. Marshall, *Philos. Trans. R. Soc. A Math. Phys. Eng. Sci.* **364**, 1627 (2006).
15. J. L. Chen, C. R. Wilson, B. D. Tapley, *Science* **313**, 1958 (2006).
16. S. B. Luthcke *et al.*, *Science* **314**, 1286 (2006).
17. C. H. Davis, Y. H. Li, paper presented at Science for Society: Exploring and Managing a Changing Planet (IEEE, Anchorage, Alaska, 20–24 Sep 2004), pp. 1152–1155.
18. H. J. Zwally *et al.*, *J. Glaciol.* **51**, 509 (2005).
19. G. Ramillien *et al.*, *Global Planet. Change* **53**, 198 (2006).
20. I. Velicogna, J. Wahr, *Nature* **443**, 329 (2006).
21. W. Munk, *Science* **300**, 2041 (2003).
22. O. M. Johannessen, K. Khvorostovsky, L. P. Bobylev, *Science* **310**, 1013 (2005).
23. A. Shepherd, D. J. Wingham, J. A. D. Mansley, H. F. J. Corr, *Science* **291**, 862 (2001).
24. I. Joughin, W. Abdalati, M. Fahnestock, *Nature* **432**, 608 (2004).
25. A. Luckman, T. Murray, R. de Lange, E. Hanna, *Geophys. Res. Lett.* **33**, art-L03503 (2006).
26. H. J. Zwally *et al.*, *Science* **297**, 218 (2002).
27. R. Bindschadler, *Science* **311**, 1720 (2006).
28. A. J. Monaghan, D. H. Bromwich, S. H. Wang, *Philos. Trans. R. Soc. A Math. Phys. Eng. Sci.* **364**, 1683 (2006).
29. R. J. Arthern, D. P. Winebrenner, D. G. Vaughan, *J. Geophys. Res. Atmos.* **111**, D06107 (2006).
30. E. J. Rignot, S. P. Gogineni, W. B. Krabill, S. Ekholm, *Science* **276**, 934 (1997).
31. N. Reeh, H. H. Thomsen, O. B. Olesen, W. Starzer, *Science* **278**, 205 (1997).
32. J. E. Box *et al.*, *J. Clim.* **19**, 2783 (2006).
33. N. P. M. van Lipzig, E. van Meijgaard, J. Oerlemans, *Int. J. Climatol.* **22**, 1197 (2002).
34. E. J. Rignot, *Science* **281**, 549 (1998).
35. D. J. Wingham, M. J. Siegert, A. Shepherd, A. S. Muir, *Nature* **440**, 1033 (2006).
36. M. Horwath, R. Dietrich, *Geophys. Res. Lett.* **33**, art-L07502 (2005).
37. M. Nakada *et al.*, *Mar. Geol.* **167**, 85 (2000).
38. A. J. Monaghan *et al.*, *Science* **313**, 827 (2006).
39. I. Joughin, E. Rignot, C. E. Rosanova, B. K. Lucchitta, J. Bohlander, *Geophys. Res. Lett.* **30**, 1706 (2003).
40. S. S. Jacobs, C. F. Giulivi, P. A. Mele, *Science* **297**, 386 (2002).
41. S. Anandakrishnan, R. B. Alley, *Geophys. Res. Lett.* **24**, 265 (1997).
42. R. Thomas *et al.*, *Science* **306**, 255 (2004).
43. A. Shepherd, D. Wingham, T. Payne, P. Skvarca, *Science* **302**, 856 (2003).
44. H. Rott, P. Skvarca, T. Nagler, *Science* **271**, 788 (1996).
45. E. Rignot *et al.*, *Geophys. Res. Lett.* **31**, art-L18401 (2004).
46. I. M. Howat, I. Joughin, T. A. Scambos, *Science* **315**, 1559 (2007).
47. R. B. Alley, P. U. Clark, P. Huybrechts, I. Joughin, *Science* **310**, 456 (2005).
48. A. L. Lowe, J. B. Anderson, *Quat. Sci. Rev.* **21**, 1879 (2002).
49. A. J. Payne, A. Vieli, A. P. Shepherd, D. J. Wingham, E. Rignot, *Geophys. Res. Lett.* **31**, art-L23401 (2004).
50. J. Weertman, *J. Glaciol.* **13**, 3 (1974).

10.1126/science.1136776

REVIEW

Perspectives on the Arctic's Shrinking Sea-Ice Cover

Mark C. Serreze,[1]* Marika M. Holland,[2] Julienne Stroeve[1]

Linear trends in arctic sea-ice extent over the period 1979 to 2006 are negative in every month. This ice loss is best viewed as a combination of strong natural variability in the coupled ice-ocean-atmosphere system and a growing radiative forcing associated with rising concentrations of atmospheric greenhouse gases, the latter supported by evidence of qualitative consistency between observed trends and those simulated by climate models over the same period. Although the large scatter between individual model simulations leads to much uncertainty as to when a seasonally ice-free Arctic Ocean might be realized, this transition to a new arctic state may be rapid once the ice thins to a more vulnerable state. Loss of the ice cover is expected to affect the Arctic's freshwater system and surface energy budget and could be manifested in middle latitudes as altered patterns of atmospheric circulation and precipitation.

The most defining feature of the Arctic Ocean is its floating sea-ice cover, which has traditionally ranged from a maximum extent of about 16×10^6 km^2 in March to a minimum extent of 7×10^6 km^2 at the end of the summer melt season in September (Fig. 1). Consistent satellite-derived monthly time series of sea-ice extent are provided by the Nimbus-7 Scanning Multichannel Microwave Radiometer (October 1978 to August 1987) and the Defense Meteorological Satellite Program Special Sensor Microwave/Imager (1987 to present). Based on regression analysis of the combined record over the period 1979 to 2006, ice extent has declined for every month (Fig. 2), most rapidly for September, for which the trend is $-8.6 \pm 2.9\%$ per decade or about 100,000 km^2 per year. Ice extent is defined as the area of the ocean with a fractional ice cover (i.e., an ice concentration) of at least 15% (*1*–*3*).

Every year since 2001 has yielded pronounced September minima, the most extreme of which was in 2005 (5.56×10^6 km^2). When compared to the mean ice extent over the period 1979 to 2000, this represents a spatial reduction of 21% (1.6×10^6 km^2), an area roughly the size of Alaska (Fig. 1). Comparisons with earlier records, which combine visible-band satellite imagery and aircraft and ship reports, suggest that the September 2005 ice extent was the lowest in at least the past 50 years. Data for the past few years suggest an accelerating decline in winter sea-ice extent (*4*).

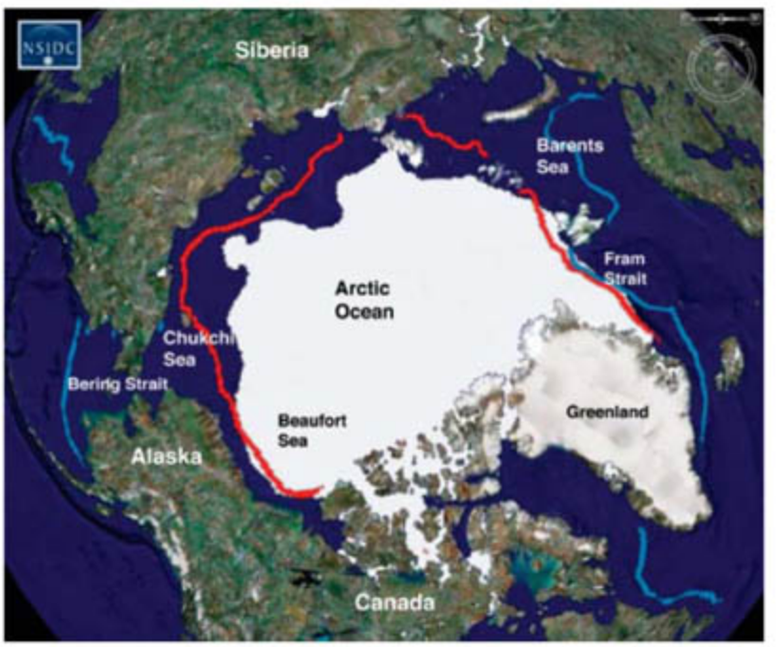

Fig. 1. Sea-ice extent (bright white area) for September 2005. Median ice extents based on the period 1979 to 2000 for September (red line) and March (blue line) illustrate the typical seasonal range. Geographic features referred to in the text are labeled. Credit: NSIDC image in Google Earth.

Evidence for accompanying reductions in ice thickness (*5*) is inconclusive. Upward-looking sonar aboard submarines provides information on ice draft—the component of the total thickness (about 90%) that projects below the water surface. Comparisons between early sonar records (1958 to 1976) and those for 1993 to 1997 indicate reductions of 1.3 m in mean late summer ice draft over much of the central Arctic Ocean (*6*), but sparse sampling complicates interpretation. Further analysis of the submarine-acquired data in conjunction with model simulations points to thinning through 1996 but modest recovery thereafter (*7*). Results from an ice-tracking algorithm applied to satellite data from 1978 to 2003 document decreasing coverage of old, thick ice (*8*).

Understanding the Observed Ice Loss

The observed decline in ice extent reflects a conflation of thermodynamic and dynamic processes. Thermodynamic processes involve changes in surface air temperature (SAT), radiative fluxes, and ocean conditions. Dynamic processes involve changes in ice circulation in response to winds and ocean currents. These include changes in the strength and location of the Beaufort Gyre (a mean annual clockwise motion in the western Arctic Ocean) and characteristics of the Transpolar Drift Stream (a motion of ice that progresses from the coast of Siberia, across the pole, and into the North Atlantic via the Fram Strait). Nearly all of the ice export from the Arctic to the Atlantic occurs through this narrow strait between northern Greenland and Svalbard (Fig. 1).

Estimated rates of SAT change over the Arctic Ocean for the past several decades vary depending on the time period and season, as well as the data source being considered. Although natural variability plays a large role in SAT variations, the overall pattern is one of recent warming, which is in turn part of a global signal (*9*). Using a record that combined coastal station observations with data from drifting buoys (from 1979 onward) and Russian "North Pole" stations (1950 to 1991), Rigor *et al.* (*10*) found positive SAT trends from 1979 to 1997 that were most pronounced and widespread during spring. Although there are biases in the buoy data relative to the North Pole data, especially for October through April (*11*), independent evidence for warming during spring, summer, and autumn since 1981 is documented in clear-sky surface temperatures retrieved from advanced very-high-resolution radiometer satellite imagery (*12*). Further support for warming comes from analysis of satellite-derived passive microwave brightness temperatures that indicate earlier onset of spring melt and lengthening of the melt season (*13*), as well as from data from the Television Infrared Observation Satellites Operational Vertical Sounder that point to increased downwelling radiation to the surface in spring over the past decade, which is linked to increased cloud cover and water vapor (*14*). Our assessments of autumn and winter data fields from the National Centers for

[1]Cooperative Institute for Research in Environmental Sciences, National Snow and Ice Data Center, Campus Box 449, University of Colorado, Boulder, CO 80309–0449, USA. [2]National Center for Atmospheric Research, Post Office Box 3000, Boulder, CO 80307, USA.

*To whom correspondence should be addressed. E-mail: serreze@kryos.colorado.edu

Environmental Prediction and National Center for Atmospheric Research (NCEP-NCAR) reanalysis (*15*) point to strong surface and low-level warming for the period 2000 to 2006 relative to 1979 to 1999. Weaker warming is evident for summer.

All of these results are consistent with a declining ice cover. However, at least part of the recent cold-season warming seen in the NCEP-NCAR data is itself driven by the loss of ice, because this loss allows for stronger heat fluxes from the ocean to the atmosphere. The warmer atmosphere will then promote a stronger longwave flux to the surface.

Links have also been established between ice loss and changes in ice circulation associated with the behavior of the North Atlantic Oscillation (NAO), Northern Annular Mode (NAM), and other atmospheric patterns. The NAO refers to covariability between the strength of the Icelandic Low and that of the Azores High, which are the two centers of action in the North Atlantic atmospheric circulation. When both are strong (or weak), the NAO is in its positive (or negative) phase. The NAM refers to an oscillation of atmospheric mass between the Arctic and middle latitudes and is positive when arctic pressures are low and midlatitude pressures are high. The NAO and NAM are closely related and can be largely viewed as expressions of the same phenomenon.

From about 1970 through the mid-1990s, winter indices of the NAO-NAM shifted from negative to strongly positive. Rigor *et al.* (*16*) showed that altered surface winds resulted in a more cyclonic motion of ice and an enhanced transport of ice away from the Siberian and Alaskan coasts (i.e., a more pronounced Transpolar Drift Stream). This change in circulation fostered openings in the ice cover. Although these openings quickly refroze in response to low winter SATs, coastal areas in spring were nevertheless left with an anomalous coverage of young, thin ice. This thin ice then melted out in summer, which was expressed as large reductions in ice extent. Summer ice loss was further enhanced as the thinner ice promoted stronger heat fluxes to the atmosphere, fostering higher spring air temperatures and earlier melt onset.

Given that the NAO-NAM has regressed back to a more neutral state since the late 1990s (*17*), these processes cannot readily explain the extreme September sea-ice minima of recent years. Rigor and Wallace (*18*) argued that recent extremes represent delayed impacts of the very strongly positive winter NAO-NAM state from about 1989 to 1995. As the NAO-NAM rose to this positive state, shifts in the wind field not only promoted the production of thinner spring ice in coastal areas but flushed much of the Arctic's store of thick ice into the North Atlantic through Fram Strait.

Rothrock and Zhang (*19*) modified this view. Using a coupled ice-ocean model, they argued that although wind forcing was the dominant driver of declining ice thickness and volume from the late 1980s through mid-1990s, the ice response to generally rising air temperatures was more steadily downward over the study period (1948 to 1999). In other words, without the NAO-NAM forcing, there would still have been a downward trend in ice extent, albeit smaller than that observed. Lindsay and Zhang (*20*) came to similar conclusions in their modeling study. Rising air temperature has reduced ice thickness, but changes in circulation also flushed some of the thicker ice out of the Arctic, leading to more open water in summer and stronger absorption of solar radiation in the upper (shallower depths of the) ocean. With more heat in the ocean, thinner ice grows in autumn and winter.

Recent years have experienced patterns of atmospheric circulation in spring and summer fa-

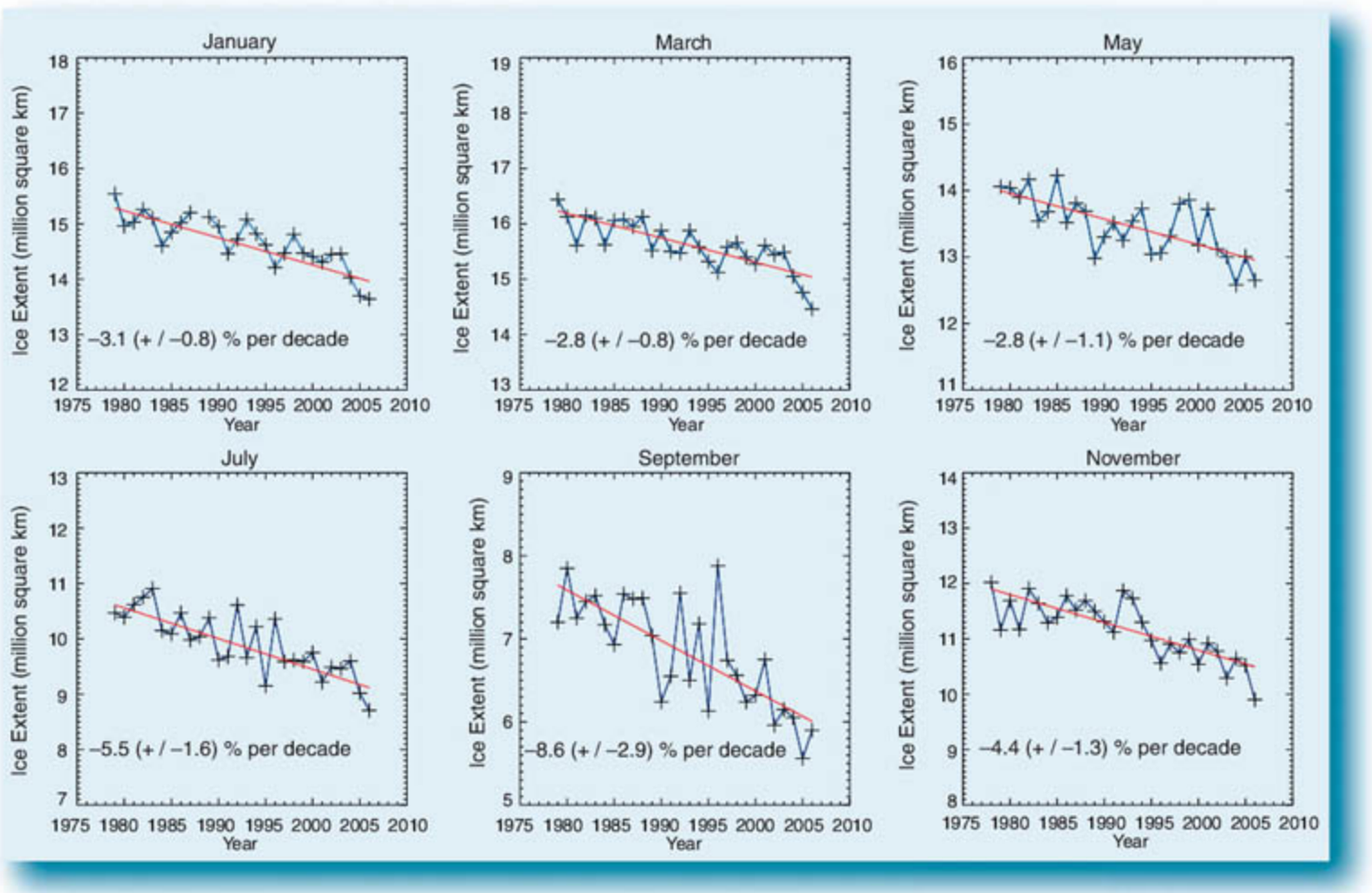

Fig. 2. Time series of arctic sea-ice extent for alternate months and least-squares linear fit based on satellite-derived passive microwave data from November 1979 through November 2006. Listed trends include (in parentheses) the 95% confidence interval of the slope. Ice extent is also declining for the six months that are not shown, ranging from −2.8 ± 0.8% per decade in February to −7.2 ± 2.3% per decade in August.

voring ice loss. By altering both the Beaufort Gyre and Transpolar Drift Stream, these patterns have reduced how long ice is sequestered and aged in the Arctic Ocean (*21*). The strength of a cyclonic atmospheric regime that sets up over the central Arctic Ocean in summer is important. Along with promoting offshore ice motion, the pronounced cyclonic summer circulations of 2002 and 2003 favored ice divergence, as is evident from the low ice concentrations in satellite imagery. Ice divergence in summer spreads the existing ice over a larger area, but enhanced absorption of solar energy in the areas of open water promotes stronger melt. There was also very little September ice in the Greenland Sea (off the east coast of Greenland) for these summers, which may also be linked to winds associated with this summer atmospheric pattern (*22*).

To further complicate the picture, it appears that changes in ocean heat transport have played a role. Warm Atlantic waters enter the Arctic Ocean through eastern Fram Strait and the Barents Sea and form an intermediate layer as they subduct below colder, fresher (less dense) arctic surface waters. Hydrographic data show increased import of Atlantic-derived waters in the early to mid-1990s and warming of this inflow (*23*). This trend has continued, characterized by pronounced pulses of warm inflow. Strong ocean warming in the Eurasian basin in 2004 can be traced to a pulse entering the Barents Sea in 1997 and 1998. The most recent data show another warm anomaly poised to enter the Arctic Ocean (*24*, *25*). These inflows may promote ice melt and discourage ice growth along the Atlantic ice margin. Once Atlantic water enters the Arctic Ocean, the cold halocline layer (CHL) separating the Atlantic and surface waters largely insulates the ice from the heat of the Atlantic layer. Observations suggest a retreat of the CHL in the Eurasian basin in the 1990s (*26*). This likely increased Atlantic layer heat loss and ice-ocean heat exchange. Partial recovery of the CHL has been observed since 1998 (*27*).

Maslowski *et al.* (*28*) proposed a connection between ice loss and oceanic heat flux through the Bering Strait. However, hydrographic data collected between 1990 and 2004 document strong variability in this inflow as opposed to a longer-term trend. An observed increase in the flux between 2001 and 2004 is estimated to be capable of melting 640,000 km^2 of 1-m-thick ice, but fluxes in 2001 are the lowest of the record (*29*). Subsequent analysis (*30*) nevertheless reveals a link between ice loss and increases in Pacific Surface Water (PSW) temperature in the Arctic Ocean beginning in the late 1990s, concurrent with the onset of sharp sea-ice reductions in the Chukchi and Beaufort seas. The hypothesis that has emerged from those observations is that delayed winter ice formation allows for more efficient coupling between the ocean and wind forcing. This redirects PSW from the shelf slope along Alaska into the Arctic Ocean, where it is more efficient in retarding winter ice growth. An imbalance between winter ice growth and summer melt results, accelerating ice loss over a large area.

To summarize, the observed sea-ice loss can in part be connected to arctic warming over the past several decades. Although this warming is part of a global signal suggesting a link with greenhouse gas (GHG) loading, attribution is complicated by a suite of contributing atmospheric and oceanic forcings. Below we review the evidence for an impact of GHG loading on the observed trends and projections for the future, based on climate model simulations.

Simulations from Climate Models

Zhang and Walsh (*31*) showed that most of the models used in the Intergovernmental Panel on Climate Change Fourth Assessment Report (IPCC AR4) have climatological sea-ice extent within 20% of the observed climatology over their adopted base period of 1979 to 1999, with good simulation of the seasonal cycle. The multimodel ensemble mean realistically estimates observed ice extent changes over this base period, and most individual models also show a downward trend. Our analysis of an IPCC AR4 multimodel ensemble mean hindcast for the longer base period 1979 to 2006 also reveals consistency with observations regarding larger trends in September versus those in winter. These results provide strong evidence that, despite prominent contributions of natural variability in the observed record, GHG loading has played a role.

Rates of ice loss both for the past few decades and those projected through the 21st century nevertheless vary widely between individual models. Our analyses show that in the IPCC AR4 models driven with the Special Report on Emissions Scenarios (SRES) A1B emissions scenario (in which atmospheric CO_2 reaches 720 parts per million by 2100), a near-complete or complete loss (to less than 1×10^6 km^2) of September ice will occur anywhere from 2040 to well beyond the year 2100, depending on the model and the particular run for that model. Overall, about half the models reach September ice-free conditions by 2100 (*32*). Figure 3 shows the spatial pattern of the percent of models that predict at least 15% fractional ice cover for March and September, averaging output over the period 2075–2084. Even by the late 21st century, most models project a thin ice cover in March. By contrast, about 40% of the models project no ice in September over the central Arctic Ocean.

The scatter among models reflects many factors, including the initial (late-20th century) simulated ice state, aspects of the modeled ocean circulation, simulated cloud conditions, and natural variability in the modeled system (e.g., NAO-NAM–like behavior). These tie in strongly to the strength and characteristics of the positive ice-albedo feedback mechanism. In general, GHG loading results in a stronger and longer summer melt season, thinning the ice and exposing more of the dark (low albedo) ocean surface that readily absorbs solar radiation. Autumn ice growth is delayed, resulting in thinner spring ice. This thin ice is more apt to melt out during the next summer, exposing more open water, which results in even thinner ice during the following spring. Negative feedbacks, such as the fact that thinner ice grows more rapidly than thicker ice when exposed to the same forcing, can counteract these changes but are generally weaker.

Although there is ample uncertainty regarding when a seasonally ice-free Arctic Ocean will be realized, the more interesting question is how it arrives at that state. Simulations based on the Community Climate System Model version 3 (CCSM3) (*33*) indicate that end-of-summer ice extent is sensitive to ice thickness in spring. If the ice thins to a more vulnerable state, a "kick" associated with natural climate variability can result in rapid summer ice loss because of the ice-albedo feedback. In

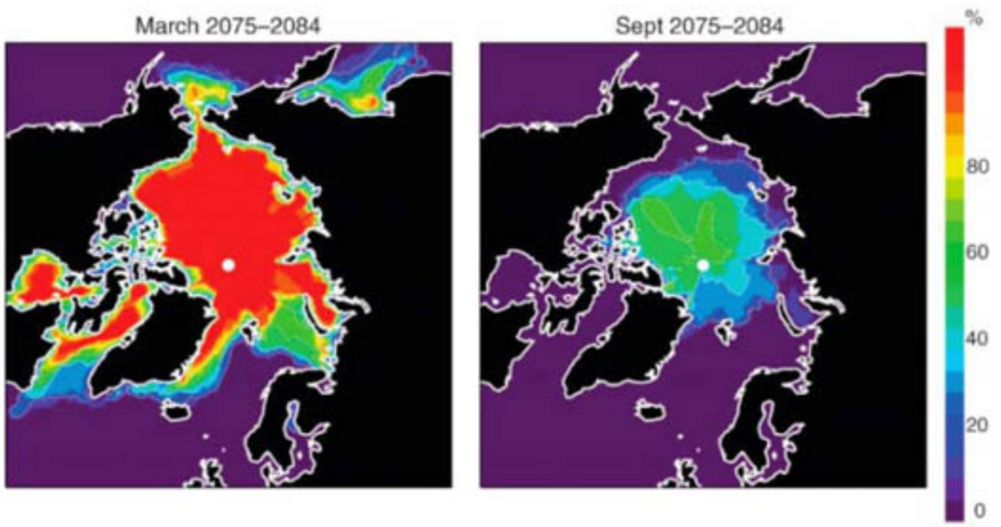

Fig. 3. Spatial pattern of the percent of IPCC AR4 model simulations (SRES A1B scenario) with at least 15% ice concentration for March (**left**) and September (**right**), averaged over the decade 2075 to 2084. For example, a value of 60% at a given location means that 60% of simulations predicted sea ice. Results are based on 11 models with realistic 20th-century September sea-ice extent.

the events simulated by CCSM3, anomalous ocean heat transport acts as this trigger. Such abrupt transitions are typically four times as fast as the observed trends over the satellite record. In one ensemble member, September ice extent decreases from about 6×10^6 to 2×10^6 km^2 in 10 years, resulting in near ice-free September conditions by 2040. A number of other climate models show similar rapid ice loss events.

Impacts

Loss of the sea-ice cover will have numerous impacts. A sharply warmer Arctic in autumn and winter is expected as a result of larger heat fluxes from the ocean to the atmosphere. This is the primary fingerprint of arctic amplification of greenhouse warming (*34*). As ice retreats from the shore, winds have a longer fetch over open water, resulting in more wave action. This effect is already resulting in coastal erosion in Alaska and Siberia. Ice loss is also affecting traditional hunting practices by members of indigenous cultures and contributing to regional declines in polar bear health and abundance (*35*).

In their modeling study, Magnusdottir *et al.* (*36*) found that declining ice in the Atlantic sector promotes a negative NAO-NAM atmospheric circulation response, with a weaker, southward-shifted storm track. Singarayer *et al.* (*37*) forced the Hadley Centre Atmospheric Model with observed sea ice from 1980 to 2000 and projected sea-ice reductions until 2100. In one simulation, mid-latitude storm tracks were intensified, increasing precipitation over western and southern Europe in winter. Experiments by Sewall and Sloan (*38*) revealed impacts on extrapolar precipitation patterns leading to reduced rainfall in the American West. Although results from different experiments with different designs vary, the common thread is that sea ice matters.

Climate models also indicate that by increasing upper-ocean stability and suppressing deepwater formation, North Atlantic freshening may disrupt the global thermohaline circulation, possibly with far-reaching consequences. Increased freshwater export from the Arctic is a potential source of such freshening. Observations implicate an arctic source for freshening in the North Atlantic since the 1960s (*39*). Total freshwater output to the North Atlantic is projected to increase through the 21st century, with decreases in ice export more than compensated by the liquid freshwater export. However, reductions in ice melt and associated freshening in the Greenland-Iceland-Norwegian (GIN) seas resulting from a smaller ice transport through Fram Strait may more directly affect the deepwater formation regions and counteract increased ocean stability due to the warming climate (i.e., a warmer upper ocean is more stable). This outcome could help maintain deepwater formation in the GIN seas (*40*).

Conclusions

Natural variability, such as that associated with the NAO-NAM and other circulation patterns, has and will continue to have strong impacts on the arctic sea-ice cover. However, the observed ice loss for the Arctic Ocean as a whole, including the larger trend for September as compared to that of winter, is qualitatively reproduced in ensemble mean climate model hindcasts forced with the observed rise in GHG concentrations. This strongly suggests a human influence (*31*). However, there is a large amount of scatter between individual simulations, which contributes to uncertainty regarding rates of ice loss through the 21st century. An emerging issue is how a seasonally ice-free Arctic Ocean may be realized: Will it result from a gradual decline with strong imprints of natural variability, or could the transition be rapid once the ice thins to a more vulnerable state? Links between altered ocean heat transport and observed ice loss remain to be resolved, as does the attribution of these transport changes, but pulses such as those currently poised to enter the Arctic Ocean from the Atlantic could provide a trigger for a rapid transition.

In this regard, future behavior of the CHL, which insulates the sea ice from the warm Atlantic layer, is a key wild card. Another uncertainty is the behavior of the NAO-NAM. Despite its return to a more neutral phase, there is evidence, albeit controversial, that external forcing may favor the positive state that promotes ice loss. The mechanisms are varied but in part revolve around the idea that stratospheric cooling in response to increasing GHG concentrations, or through ozone destruction, may "spin up" the polar stratospheric vortex, resulting in lower arctic surface pressures. Another view is that the NAO-NAM could be bumped to a preferred positive state via warming of the tropical oceans (*41*). However, as noted earlier, declining sea ice in the Atlantic sector may invoke a negative NAO-NAM response (*36*).

Given the agreement between models and observations, a transition to a seasonally ice-free Arctic Ocean as the system warms seems increasingly certain. The unresolved questions regard when this new arctic state will be realized, how rapid the transition will be, and what will be the impacts of this new state on the Arctic and the rest of the globe.

References and Notes

1. Ice extent time series are available from the National Snow and Ice Data Center (NSIDC) based on the application of the NASA team algorithm (used here) and a bootstrap algorithm to the passive microwave brightness temperatures (http:/nsidc.org/data/seaice/). Trends computed from both are negative in all months, but those from the bootstrap series are slightly smaller (which yielded a September trend of –7.9% per decade). Trends are computed from anomalies referenced to means over the period 1979 to 2000. Surface melt in summer contaminates the passive microwave signal, resulting in the underestimation of ice concentration. Use of ice extent (a binary ice–no ice classification) largely circumvents this problem.
2. Trends for all months are significant at the 99% confidence level, based on an F test with the null hypothesis of a zero trend. Trends are also significant (exceeding the 95% level) based on the approach of Weatherhead *et al.* (*3*), which computes the trend significance from the variance and autocorrelation of the residuals.
3. E. C. Weatherhead *et al.*, *J. Geophys. Res.* **103**, 10.1029/98JD00995 (1998).
4. J. C. Comiso, *Geophys. Res. Lett.* **33**, L18504 (2006).
5. Ice thickness can be described from a probability distribution, which has a peak at about 3 m. Although ice at the peak of the distribution is predominantly multiyear ice that has survived one or more melt seasons and thicker than younger first-year ice (representing a single year's growth), ridging can result in very thick first-year ice (up to 20 to 30 m).
6. D. A. Rothrock, Y. Yu, G. A. Maykut, *Geophys. Res. Lett.* **26**, 3469 (1999).
7. D. A. Rothrock, J. Zhang, Y. Yu, *J. Geophys. Res.* **108**, 3083 (2003).
8. C. Fowler, W. J. Emery, J. A. Maslanik, *IEEE Geosci. Remote Sens. Lett.* **1**, 71 (2004).
9. M. C. Serreze, J. A. Francis, *Clim. Change* **76**, 241 (2006).
10. I. G. Rigor, R. L. Colony, S. Martin, *J. Clim.* **13**, 896 (2000).
11. I. V. Polyakov *et al.*, *J. Clim.* **16**, 2067 (2003).
12. J. C. Comiso, *J. Clim.* **16**, 3498 (2003).
13. J. C. Stroeve, T. Markus, W. N. Meier, *Ann. Glaciol.* **25**, 382 (2006).
14. J. A. Francis, E. Hunter, *EOS Trans. Am. Geophys. Union* **87**, 509 (2006).
15. E. Kalnay *et al.*, *Bull. Am. Meteorol. Soc.* **77**, 437 (1996).
16. I. G. Rigor, J. M. Wallace, R. L. Colony, *J. Clim.* **15**, 2648 (2002).
17. J. E. Overland, M. Wang, *Geophys. Res. Lett.* **32**, L06701 (2005).
18. I. G. Rigor, J. M. Wallace, *Geophys. Res. Lett.* **31**, L09401 (2004).
19. D. A. Rothrock, J. Zhang, *J. Geophys. Res.* **110**, C01002 (2005).
20. R. W. Lindsay, J. Zhang, *J. Clim.* **18**, 4879 (2005).
21. J. A. Maslanik, S. Drobot, C. Fowler, W. Emery, R. Barry, *Geophys. Res. Lett.* **34**, 10.1029/2006GL028269 (2007).
22. J. C. Stroeve *et al.*, *Geophys. Res. Lett.* **32**, L04501 (2005).
23. R. R. Dickson *et al.*, *J. Clim.* **13**, 2671 (2000).
24. I. V. Polyakov *et al.*, *Geophys. Res. Lett.* **32**, L17605 (2005).
25. W. Walczowski, J. Piechura, *Geophys. Res. Lett.* **33**, L12601 (2006).
26. M. Steele, T. J. Boyd, *J. Geophys. Res.* **103**, 10419 (1998).
27. T. J. Boyd, M. Steele, R. D. Muench, J. T. Gunn, *Geophys. Res. Lett.* **29**, 1657 (2002).
28. W. Maslowski, D. C. Marble, W. Walczowski, A. J. Semtner, *Ann. Glaciol.* **33**, 545 (2001).
29. R. A. Woodgate, K. Aagaard, T. L. Weingartner, *Geophys. Res. Lett.* **33**, L15609 (2006).
30. K. Shimada *et al.*, *Geophys. Res. Lett.* **33**, L08605 (2006).
31. X. Zhang, J. E. Walsh, *J. Clim.* **19**, 1730 (2006).
32. O. Arzel, T. Fichefet, H. Goosse, *Ocean Model.* **12**, 401 (2006).
33. M. M. Holland, C. M. Bitz, B. Tremblay, *Geophys. Res. Lett.* **33**, L23503 (2006).
34. S. Manabe, R. J. Stouffer, *J. Geophys. Res.* **85**, 5529 (1980).
35. I. Stirling, C. L. Parkinson, *Arctic* **59**, 261 (2006).
36. G. Magnusdottir, C. Deser, R. Saravanan, *J. Clim.* **17**, 857 (2004).
37. J. S. Singarayer, J. Bamber, P. J. Valdes, *J. Clim.* **19**, 1109 (2006).
38. J. O. Sewall, L. C. Sloan, *Geophys. Res. Lett.* **31**, L06209 (2004).
39. B. J. Peterson *et al.*, *Science* **313**, 1061 (2006).
40. M. M. Holland, J. Finnis, M. C. Serreze, *J. Clim.* **19**, 6221 (2006).
41. N. P. Gillett, M. P. Baldwin, M. R. Allen, in *The North Atlantic Oscillation: Climate Significance and Environmental Impact*, J. W. Hurrell, Y. Kushnir, G. Ottersen, M. Visbeck, Eds. (American Geophysical Union, Washington, DC, 2003), Geophysical Monograph Series 134, chap. 9.

42. This study was supported by NSF, NASA, and NOAA. M. Savoie, L. Ballagh, W. Meier, and T. Scambos are thanked for their assistance.

10.1126/science.1139426

REVIEW

Arctic Air Pollution: Origins and Impacts

Kathy S. Law[1] and Andreas Stohl[2]

Notable warming trends have been observed in the Arctic. Although increased human-induced emissions of long-lived greenhouse gases are certainly the main driving factor, air pollutants, such as aerosols and ozone, are also important. Air pollutants are transported to the Arctic, primarily from Eurasia, leading to high concentrations in winter and spring (Arctic haze). Local ship emissions and summertime boreal forest fires may also be important pollution sources. Aerosols and ozone could be perturbing the radiative budget of the Arctic through processes specific to the region: Absorption of solar radiation by aerosols is enhanced by highly reflective snow and ice surfaces; deposition of light-absorbing aerosols on snow or ice can decrease surface albedo; and tropospheric ozone forcing may also be contributing to warming in this region. Future increases in pollutant emissions locally or in mid-latitudes could further accelerate global warming in the Arctic.

Even though early Arctic explorers had noticed atmospheric haze and dirty deposits on the snow (*1*), the remote Arctic atmosphere was long believed to be extremely clean. However, pilots flying over the North American Arctic in the 1950s observed widespread haze (*2*) that could be seen every winter and early spring. It took until the 1970s for scientists to realize that the haze was air pollution transported from the middle latitudes (*3*). Arctic haze continues to be an air quality problem, and the acidic compounds (mainly sulfate) associated with it can be washed out with precipitation or deposited at the surface, leading to increased acidity in natural ecosystems (*4*). Long-range transport of pollution to the Arctic also carries toxic substances, such as mercury or persistent organic pollutants, that can have adverse effects on ecosystems and human health.

Over the past 20 years there has been much research on the climatic consequences of this pollution, which is also present in summer, albeit at lower concentrations. Climate change is proceeding fastest at the high latitudes of the Arctic. Surface air temperatures have increased more than the global average over the past few decades and are predicted to warm by about 5°C over a large part of the Arctic by the end of the 21st century, the most rapid of any region on Earth (*5*). Models also predict that summer sea ice may completely disappear by 2040 (*6*). These changes are caused by global increases in long-lived greenhouse gases (GHGs), whose effects are enhanced in the Arctic through feedback mechanisms such as the sea-ice albedo feedback. However, air pollution also affects Arctic climate, particularly through changes in surface radiative forcing.

[1]Service d' Aéronomie, CNRS, IPSL/Université Pierre et Marie Curie, Boitê 102, 4 Place Jussieu, Paris Cedex 05, 75252 France. E-mail: kathy.law@aero.jussieu.fr. [2]Norwegian Institute for Air Research (NILU), Instituttveien 18, 2027 Kjeller, Norway. E-mail: ast@nilu.no

Arctic Haze

Arctic haze is a mixture of sulfate and particulate organic matter and, to a lesser extent, ammonium, nitrate, black carbon (BC) (*7*), and dust aerosols (*8*). It also contains relatively high levels of ozone precursors such as nitrogen oxides (NO_x) and volatile organic compounds (VOCs) (*9*). Aerosol haze particles are well aged, very efficient at scattering solar radiation, and also weakly absorbing. The haze has a distinct seasonal cycle with a maximum in late winter and early spring (*3*) when the removal processes in the dry and stable Arctic atmosphere are very slow. For example, Fig. 1 shows the seasonal cycle in BC measured at Alert [62.3°W, 82.5°N, 210 m above sea level (ASL)] (*10*). Near the surface, the haze starts disappearing in April, but layers at higher altitudes may persist into May. Trends in trace constituents and aerosols are complex in the Arctic region. Although sulfate, aerosol light scattering, and absorption exhibit significant downward trends at most Arctic stations (*8*) because of emission reductions in the haze's source regions, nitrate concentrations have been increasing over the past two decades (*4*).

Air Pollution Transport into the Arctic

Practically all pollution in the high Arctic originates from more southerly latitudes. Local pollution sources are currently small and limited to near the Arctic Circle. These include volcanic emissions in Alaska and Kamchatka; anthropogenic emissions from conurbations like Murmansk; industrial emissions, most notably in the northern parts of Russia; and emissions from the oil industry and shipping (*4*). Surfaces of constant potential temperature (*11*) form a dome above the cold Arctic lower troposphere, forcing air parcels traveling northward to ascend (*12*, *13*). This isolates the Arctic lower troposphere from the rest of the atmosphere by a transport barrier, the Arctic front. On time scales of a few days to weeks, the Arctic lower troposphere is accessible only to pollution originating from very cold source regions (*14*, *15*). The polar dome is not zonally symmetric and can extend to about 40°N over Eurasia in January, thus making northern Eurasia the major source region for the Arctic haze. Air masses leaving densely populated areas on the east coasts of Asia and North America are too warm and moist to directly penetrate the polar dome, but they can ascend to the Arctic middle or upper troposphere. However, Greenland, because of its high topography, is exposed to pollution from southeast Asia and North America more strongly than is the rest of the Arctic (*16*).

The polar dome also makes it difficult for stratospheric air masses to reach the Arctic lower troposphere. A recent model study suggested a strong vertical gradient in the influence of stratospheric air masses (*16*). For a transport time scale

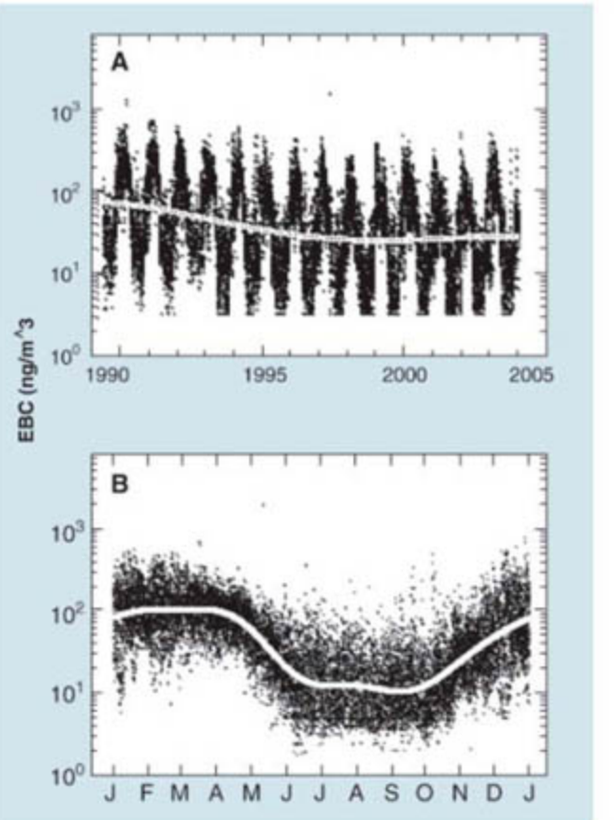

Fig. 1. Long-term trends (**A**) and seasonal variation (**B**) of 6-hourly equivalent BC concentrations at Alert. [Reproduced/modified from (*10*) by permission of the American Geophysical Union. Copyright 2006 American Geophysical Union.]

of 10 days, a 10% contribution from stratospheric air masses was found between 3 and 5 km, but near sea level these contributions had decreased to only 1% and 0.3% in winter and summer, respectively, much less than in the mid-latitudes.

The mean circulation in winter is characterized by low-level transport from northern Eurasia across the Arctic toward North America. In January, boundary layer air in the North American part of the Arctic has, on average, experienced about 2 weeks of complete darkness en route (*16*). In summer, the overall pathway is directed from the North Atlantic Ocean across the high Arctic toward the North Pacific Ocean, and the transport is only half as fast as in winter. Because of the slower transport and more-efficient removal processes in summer, pollution concentrations are lower and high-latitude sources of air pollution become even more important, relative to more southerly sources, than in winter.

Tropospheric Ozone

Observed ozone trends in the Arctic are complex, with Canadian sites showing increases in the 1990s, particularly in the winter and spring, whereas decreases were observed in the 1980s (*17*). Although changes in anthropogenic emissions at mid-latitudes are likely to have played a role, changes in natural emissions or transport patterns also could have been important. Recent climate model simulations suggest that increases in tropospheric ozone, caused by increases in anthropogenic emissions, could have contributed 0.4° to 0.5°C during winter and spring to 20th-century surface temperature trends (roughly 30% of observed trends) in the Arctic (*18*). This is likely due to longer ozone lifetimes and enhanced atmospheric infrared absorption in the dry Arctic winter and subsequent feedbacks on snow-ice albedo. Note that these calculations did not include boreal forest fire emissions or possible changes in the stratospheric ozone flux. The latter has been put forward to explain ozone trends in the Canadian Arctic upper troposphere (*19*).

To date, the main focus has been on understanding the annual springtime increase in ozone. Ozone lidar data collected from February to May 2000 between Colorado (United States) and northern Canada and Greenland as part of the Tropospheric Ozone Production about the Spring Equinox (TOPSE) airborne campaign clearly show this transition throughout the free troposphere (Fig. 2) (*20*). Analysis of odd nitrogen (NO_y) and its constituents confirmed previous ground-based studies showing that, as temperatures warm, thermal decomposition of peroxy acetyl nitrate (PAN) (produced from oxidation of VOCs) is the primary driving factor, leading to enhanced photochemical ozone production from released NO_x (*21*, *22*). This springtime breakdown of the Arctic haze's pollution reservoir and its subsequent southward transport may also contribute to spring ozone maxima observed at remote mountain sites in Northern mid-latitudes (*17*, *23*). However, inconsistencies were found between observations and model calculations of oxygenated organic and nitrogen-containing species {e.g., nitrous acid (HONO), pernitric acid (HNO_4), and PAN [e.g., (*21*)]}, and also, more recently in hydroxyl radical (OH) data collected at the high-altitude Summit site in Greenland (38.4°W, 72.6°N, 3208 m ASL) (*24*), suggesting that our knowledge of Arctic photochemistry and processes, such as wet scavenging, is incomplete. New measurements of other important nitrogen species such as the nitrate radical (NO_3) and dinitrogen pentoxide (N_2O_5), which play a key role in nighttime chemistry, may also reveal new insights, as has recently been shown at mid-latitudes (*25*).

An analysis of TOPSE ozone lidar data also suggested a rather low contribution from the stratospheric flux of ozone during the winter-spring (less than 15%) (*20*), confirmed by more recent transport analyses (*16*). Few global model estimates exist and include more southerly latitudes, where net exchange is stronger, leading to higher estimates for the fraction of ozone originating from the stratosphere [e.g., 30 to 50% in spring, 30° to 90°N (*22*)] than what would have been obtained for the Arctic alone. Stratospheric air masses could also be a source of NO_y in the troposphere and therefore nitrate in snow.

The springtime ozone budget is also complicated by the occurrence of dramatic ozone depletion events in the Arctic boundary layer, first observed in the 1980s (*26*) and evident in surface ozone records (*17*) (see also Fig. 2). These events are strongly correlated to deposition of gaseous mercury onto snow surfaces [e.g., (*27*)]. They are related to the rapid release of bromine radicals (so-called bromine explosions), seen by satellite as clouds of bromine oxide (BrO) over regions of sea ice, which then destroy ozone through a series of autocatalytic reactions. The bromine originates from seawater, but the exact mechanism by which it is transformed to reactive bromine in the atmosphere is unclear. Mechanisms involving formation of sea-salt aerosols from frost flowers on sea ice (*28*), or sea-salt–contaminated snow on newly formed sea ice (*29*), have been proposed. The wider impact of these halogens on the Arctic ozone budget (and indeed the oxidizing capacity of the troposphere) is also uncertain. Recent calculations constrained by BrO satellite measurements suggest that ozone levels in the Arctic boundary layer could be reduced by more than 50% because of halogen chemistry over the high northern latitudes in spring (*30*).

The summertime ozone budget has yet to be quantified in the Arctic. In particular, the impact of boreal forest fire emissions, which have already been shown at mid-latitudes to produce large amounts of ozone because of their large loading of

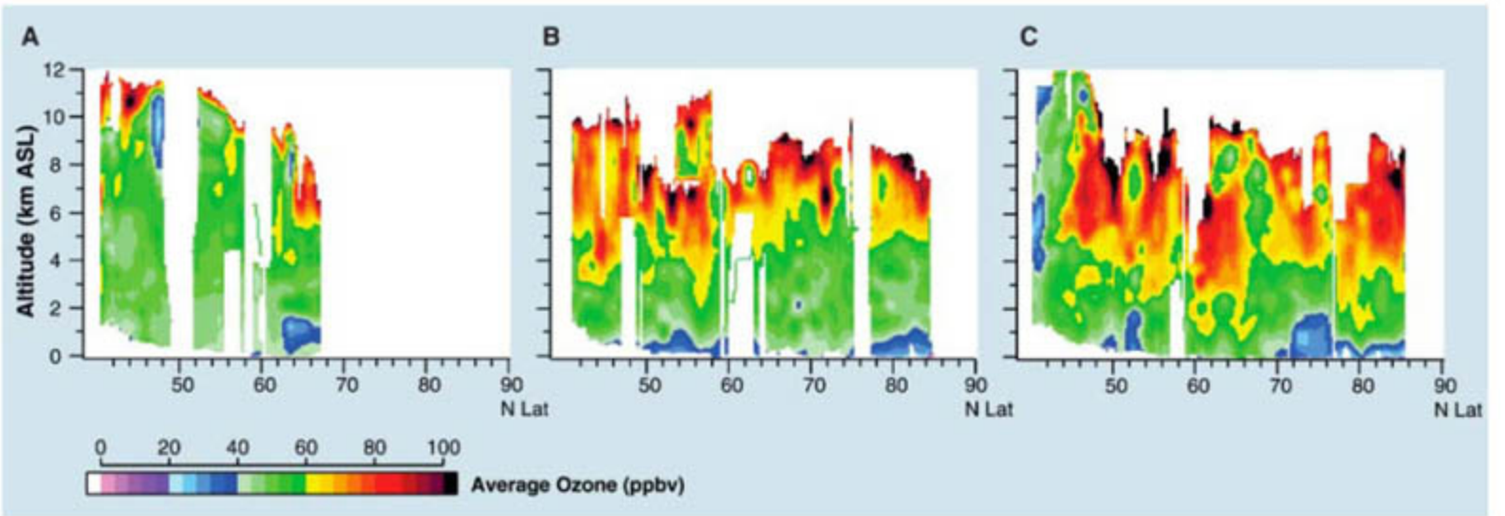

Fig. 2. Average latitudinal distribution of vertical ozone concentrations in parts per billion (ppb), measured by airborne lidar, during deployments (**A**) 4–9 February 2000, (**B**) 19–26 March 2000, and (**C**) 15–23 May 2000. Data was collected during each deployment on flights between Broomfield, Colorado (United States) (40°N, 105°W), and northern Canada and northern Greenland as part of the TOPSE experiment. [Reproduced/modified from (*20*) by permission of the American Geophysical Union. Copyright 2003 American Geophysical Union]

nitrogen-containing constituents, most notably PAN (*31*), is poorly known. Another process, identified relatively recently, is the production of NO_x (and HONO) from photolysis of nitrate in the snowpack in the presence of sunlight (*32*). Although very high levels of NO_x [>600 parts per trillion] have been observed at South Pole (elevation of 2840 m) because of the existence of prolonged periods with a very stable shallow boundary layer (*33*), much lower enhancements have so far been reported in the Arctic (*34*), making it unlikely that these emissions are important on regional scales at northern high latitudes.

Climatic Effects of Light-Absorbing Aerosols

Measurements at Barrow (156.6°W, 71.3°N, 11 m ASL) have shown that the single scattering albedo of haze aerosols in the Arctic can be as low as 0.9 in winter (*35*), indicating that these aerosols contain large amounts of light-absorbing material. In the Arctic, the efficiency of sunlight absorption in aerosol layers is greater than the efficiency at lower latitudes because of the high albedo of snow and ice and multiple reflection and scattering of light between the surface and the aerosol layers. BC, which is responsible for most of the aerosol light absorption, is a minor but important component of the Arctic haze (*10*) and causes heating in the haze layers (*8*). In addition, deposition of BC onto snow and ice results in a reduction of the surface albedo (*36*, *37*). It has been suggested that the climate forcing due to this albedo effect is relevant when compared with the effect of GHGs (*38*). Its efficacy, measured as the effectivity in increasing the surface air temperature per unit of forcing, is twice as large as that of carbon dioxide, and it may be even more effective in melting snow and ice.

BC concentrations are highest during the Arctic haze season and lowest in summer (*10*). As a result of emission reductions, BC concentrations have declined by 54% at Alert and 27% at Barrow from 1989 to 2003, but with some indication of a recent trend reversal (Fig. 1). In winter, BC originates mostly from anthropogenic activities, but the regional distribution of sources is debated. In a climate model study, it was argued that, after recent strong emission increases in southeast Asia and decreases elsewhere, southeast Asia is now the largest BC source for the Arctic (*39*). However, this result also has been questioned (*16*), because the large temperature difference between southeast Asia and the Arctic lower troposphere does not allow for direct transport between the two regions. Observations linked with trajectory calculations suggested Russian sources have the strongest influence on BC levels at Alert and Barrow (*10*). More BC measurements in the Arctic, especially at higher altitudes, are required to clarify the relative importance of different BC sources.

During summer, atmospheric BC concentrations are much lower than in late winter and early spring (*10*) but still are important for the Arctic radiation budget because of the abundance of solar radiation. A recent model study suggests that, in summer, boreal forest fires are the dominant source for BC in the Arctic because many of the fires burn at high latitudes (*16*). Chemical signatures of biomass burning emissions have been preserved in Arctic snow and ice records (*40*), and biomass burning plumes have been observed in the Arctic (*41*, *42*). For example, large pan-Arctic enhancements of atmospheric BC concentrations occurred as a result of strong burning in the boreal forests of North America in summer 2004 (Fig. 3A), which also lead to a decrease in the snow albedo at Summit (Greenland) during one episode (*43*). In spring 2006, smoke from agricultural fires in eastern Europe was transported into the European Arctic and led to the highest concentrations of many pollutants ever measured at the Zeppelin station (11.9°E, 78.9°N, 478 m ASL) on Svalbard, Norway, as well as a dramatic reduction in visibility (Fig. 3, B and C) (*44*). Atmospheric BC concentrations reached record levels and also led to a visible discoloration of drifting snow on a glacier. All this points toward a strong influence of biomass burning on Arctic BC levels, snow-ice albedo, and radiation transmission in the Arctic atmosphere.

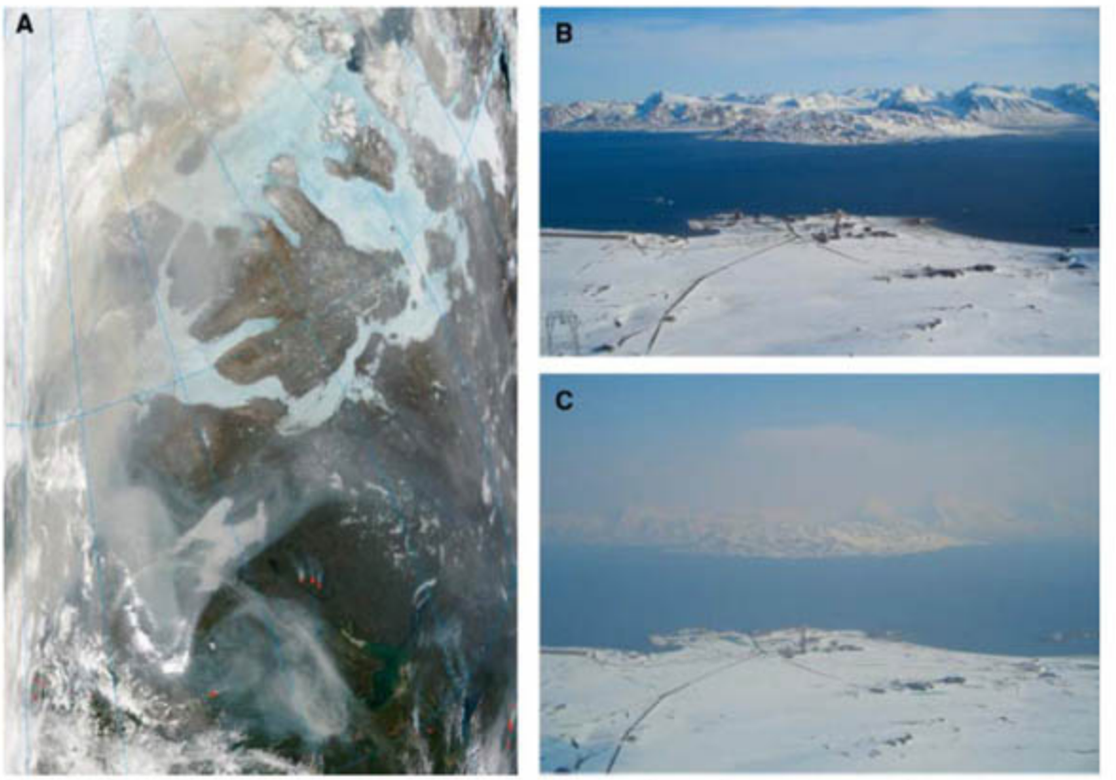

Fig. 3. (**A**) Moderate Resolution Imaging Spectroradiometer (MODIS) satellite image from 5 July 2004, showing the intrusion of thick smoke from boreal forest fires (red dots) into the Canadian Maritime Arctic. Image courtesy of MODIS Rapid Response Project at NASA Goddard Space Flight Center. View from the Zeppelin station near Ny Ålesund on Svalbard, Norway, under clear conditions (**B**) on 26 April 2006 and (**C**) on 2 May 2006, when smoke from agricultural fires burning in Eastern Europe was transported to the station (*43*). [Image courtesy of A.-C. Engvall, Stockholm University]

Pyro-Convection

It has been known for some time that forest fires can inject emissions into the upper troposphere, but it was discovered only recently that injections deep into the stratosphere also occur and are in fact quite common (*45*–*47*). The highest altitude where smoke from boreal forest fires was observed in situ is 17 km, several kilometers above the tropopause, and at potential temperatures greater than 380 K (*46*). Remote sensing observations indicate that even deeper injections into the stratospheric overworld are possible (*47*). The lifetime of aerosols (and also many trace gases) at these altitudes can be months, thus prolonging their possible radiative effects. It has been suggested that a cold bias in the high-latitude lower stratosphere that exists in many climate models could be removed by including high-altitude BC injections from boreal fires (*48*). However, nothing is known about the impact of pyro-convection on stratospheric chemistry.

Indirect Aerosol Effects

Aerosols also influence irradiances in the Arctic indirectly via changes in the

microphysical properties of clouds. Enhanced particle concentrations increase the number concentration and decrease the size of cloud droplets (*49*), which increases the cloud albedo. They can also reduce rain formation and increase cloud lifetime. The Arctic is particularly susceptible to aerosol indirect effects, because the low aerosol number concentrations result in a large fraction of particles being activated during cloud formation (*8*). It has also been suggested that aerosols can increase the longwave emissivity of Arctic liquid-phase clouds (*50*). Most liquid-phase clouds contain enough water to be considered blackbodies with unit emissivity at thermal wavelengths; in which case, aerosol effects can be ignored. However, Arctic clouds are often so thin that their emissivity increases with increasing cloud droplet number concentrations. This enhances the downwelling thermal radiation fluxes, an effect opposed to the indirect effects on the solar radiation. The effect is most important in winter and early spring, when Arctic haze aerosols are abundant, thin clouds exist, and the radiation balance is tied toward thermal fluxes because of the absence or small magnitude of solar radiation. It may trigger more rapid warming of the Arctic in spring and, thus, an earlier snowmelt. However, a quantitative understanding of aerosol indirect effects, including those involving mixed-phase and ice clouds, remains elusive.

Future Changes

The disappearance of summertime sea ice could have a huge impact on trace gas and aerosol distributions in the Arctic. For example, increased areas of open ocean could lead to increases in natural dimethyl sulfide emissions and production of sulfate aerosols (*51*), whereas emissions of halogens and NO_x from the ice and snow could be reduced. There is evidence that ship traffic is already affecting the summertime Arctic atmosphere, with strong signatures seen in marine aerosols (*52*). Increased deposition of soot from increased shipping after the reduction of summertime sea ice could further accelerate sea-ice melting. Increases in surface ozone by a factor of 2 to 3, to levels currently observed at Northern Hemisphere mid-latitudes as a result of increasing ship NO_x emissions, have been predicted (*53*). Similar effects might also be expected from an increase in Arctic oil drilling.

As northern high latitudes warm because of climate change, boreal forest fires are becoming more frequent (*54*), thus increasing pollution transport into the Arctic. This may also trigger a feedback cycle, where forest fire emissions lead to earlier melting of Arctic snow and ice and thus further warming. Furthermore, the polar dome, which currently presents a barrier to pollution transport into the Arctic, may weaken in the future as the Arctic continues to warm relatively faster than the lower latitudes, thus allowing more efficient pollution import into the Arctic. This could be facilitated by, for instance, an upward trend in the North Atlantic Oscillation, which correlates with the transport of pollutants into the Arctic (*55*, *56*).

Future Directions

Clearly many uncertainties still exist in our knowledge of processes governing the buildup of air pollution in the Arctic and its role in climate change. Within the framework of the International Polar Year (IPY), the scientific community is mobilizing to tackle these issues through a series of coordinated field measurement programs and analysis using climate models that also include trace gases and aerosols.

Most of the ongoing and predicted rapid changes in the Arctic climate are a direct consequence of the increasing levels of long-lived greenhouse gases and positive feedbacks specific to the Arctic (*5*). In order to combat these changes, reductions in the emissions of long-lived greenhouse gases, particularly carbon dioxide, are urgently needed. However, the Arctic may also benefit more than other regions from reductions in the emissions of short-lived climate agents. In particular, reducing BC emissions could slow atmospheric warming and the melting of snow and ice, and reducing tropospheric ozone concentrations could slow the increase in Arctic surface air temperatures. Increases in emissions of BC and ozone precursors in the Arctic itself should be strictly avoided.

References and Notes

1. A. E. Nordenskiöld, *Science* ns-**2**, 732 (1883).
2. J. M. Mitchell, *J. Atmos. Terr. Phys.* (special suppl.), 195 (1957).
3. L. A. Barrie, *Atmos. Environ.* **20**, 643 (1986).
4. "Acidifying pollutants, Arctic haze, and acidification in the Arctic," Arctic Monitoring and Assessment Programme (AMAP), Oslo, Norway (2006).
5. Intergovernmental Panel on Climate Change (IPCC), *Climate Change 2001: The Scientific Basis*, J. T. Houghton, Ed. (Cambridge Univ. Press, New York, 2001).
6. M. M. Holland, C. M. Blitz, B. Trembley, *Geophys. Res. Lett.* **33**, 10.1029/2006GL028024 (2006).
7. We use the term black carbon (BC) here, although it is poorly defined. Often, light absorption is measured and converted to "equivalent" BC.
8. P. K. Quinn *et al.*, *Tellus* **59B**, 99 (2007).
9. S. Solberg, C. Dye, N. Schmidbauer, *J. Atmos. Chem.* **25**, 33 (1996).
10. S. Sharma, E. Andrews, L. A. Barrie, J. A. Ogren, D. Lavoué, *J. Geophys. Res.* **111**, 10.1029/2005JD006581 (2006).
11. Potential temperature (Θ) is almost a conserved quantity in the atmosphere. Radiational cooling decreases Θ by about 1 K/day in the free troposphere, whereas condensation of water vapor increases Θ.
12. A. Klonecki *et al.*, *J. Geophys. Res.* **108**, 10.1029/2002JD002199 (2003).
13. The ascent of moist air parcels is even stronger because of the extra heat released by the condensation of water vapor.
14. T. N. Carlson, *Atmos. Environ.* **15**, 1473 (1981).
15. T. Iversen, *Geophys. Res. Lett.* **11**, 457 (1984).
16. A. Stohl, *J. Geophys. Res.* **111**, 10.1029/2005JD006888 (2006).
17. S. J. Oltmans *et al.*, *Atmos. Environ.* **40**, 10.1016/j.atmosenv.2006.01.029 (2006).
18. D. Shindell *et al.*, *J. Geophys. Res.* **111**, 10.1029/2005JD006348 (2006).
19. D. W. Tarasick, V. E. Fioletov, D. I. Wardle, J. B. Kerr, J. Davies, *J. Geophys. Res.* **110**, 10.1029/2004JD004643 (2005).
20. E. V. Browell *et al.*, *J. Geophys. Res.* **108**, 10.1029/2001JD001390 (2003).
21. C. Stroud *et al.*, *Atmos. Environ.* **37**, 10.1016/S1352-2310(03)00353-4 (2003).
22. L. K. Emmons *et al.*, *J. Geophys. Res.* **108**, 10.1029/2002JD002665 (2003).
23. S. A. Penkett, K. A. Brice, *Nature* **319**, 655 (1986).
24. S. J. Sjostedt *et al.*, *Atmos. Environ.* **41**, 10.1016/j.atmosenv.2006.08.058 (2007).
25. S. S. Brown *et al.*, *Science* **311**, 67 (2006).
26. L. A. Barrie, J. W. Bottenheim, J. W. Schnell, P. J. Crutzen, R. A. Rasmussen, *Nature* **334**, 138 (1988).
27. P. A. Ariya *et al.*, *Tellus* **B56**, 397 (2004).
28. A. M. Rankin, E. W. Wolff, S. Martin, *J. Geophys. Res.* **107**, 4683 (2002).
29. W. R. Simpson *et al.*, *Atmos. Chem. Phys. Discuss.* **6**, 11051 (2006).
30. T. Zeng *et al.*, *J. Geophys. Res.* **111**, 10.1029/2005JD006706 (2006).
31. E. Real *et al.*, *J. Geophys. Res.*, 10.1029/2006JD007576, in press (2007).
32. F. Dominé, F. P. B. Shepson, *Science* **297**, 1506 (2002).
33. D. Davis *et al.*, *Atmos. Environ.* **38**, 5375 (2004).
34. R. E. Honrath *et al.*, *Atmos. Environ.* **36**, 2629 (2002).
35. P. K. Quinn *et al.*, *J. Geophys. Res.* **107**, 10.1029/2001JD001248 (2002).
36. S. G. Warren, W. J. Wiscombe, *J. Atmos. Sci.* **37**, 2734 (1980).
37. A. D. Clarke, K. J. Noone, *Atmos. Environ.* **19**, 2045 (1985).
38. J. Hansen, L. Nazarenko, *Proc. Natl. Acad. Sci. U.S.A.* **101**, 423 (2004).
39. D. Koch, J. Hansen, *J. Geophys. Res.* **110**, 10.1029/2004JD005296 (2005).
40. S. Whitlow, P. Mayewski, J. Dibb, G. Holdsworth, M. Twickler, *Tellus* **46B**, 234 (1994).
41. N. C. Hsu *et al.*, *Geophys. Res. Lett.* **26**, 1165 (1999).
42. M. G. Iziomon, U. Lohmann, P. K. Quinn, *J. Geophys. Res.* **111**, 10.1029/2005JD006223 (2006).
43. A. Stohl *et al.*, *J. Geophys. Res.* **111**, 10.1029/2006JD007216 (2006).
44. A. Stohl *et al.*, *Atmos. Chem. Phys.* **7**, 511 (2007).
45. M. Fromm *et al.*, *Geophys. Res. Lett.* **27**, 1407 (2000).
46. H.-J. Jost *et al.*, *Geophys. Res. Lett.* **31**, 10.1029/2003GL019253 (2004).
47. M. Fromm *et al.*, *J. Geophys. Res.* **110**, 10.1029/2004JD005350 (2005).
48. P. J. Rasch *et al.*, *Eos* **86** (suppl.), abstr. A22B–01 (2005).
49. S. Twomey, *J. Atmos. Sci.* **34**, 1149 (1977).
50. T. J. Garrett, C. F. Zhao, *Nature* **440**, 787 (2006).
51. A. J. Gabric, B. Qu, P. Matrai, A. C. Hirst, *Tellus* **57B**, 391 (2005).
52. Z. Xie, L. Sun, J. D. Blum, Y. Huang, W. He, *J. Geophys. Res.* **111**, 10.1029/2005JD006253 (2006).
53. C. Granier *et al.*, *Geophys. Res. Lett.* **33**, 10.1029/2006GL026180 (2006).
54. B. J. Stocks *et al.*, *Clim. Change* **38**, 1 (1998).
55. S. Eckhardt *et al.*, *Atmos. Chem. Phys* **3**, 1769 (2003).
56. J. F. Burkhart, R. C. Bales, J. R. McConnell, M. A. Hutterli, A. Manuel, *J. Geophys. Res.* **111**, 10.1029/2005JD006771 (2006).

57. This work was supported by the Norwegian Research Council and the French Agence Nationale de la Recherche (ANR) and Centre National de la Recherche Scientifique (CNRS) in the framework of the Polar Study Using Aircraft, Remote Sensing, Surface Measurements and Modeling of Climate, Chemistry, Aerosols, and Transport (POLARCAT) project. We thank the POLARCAT community for the exchange of ideas. We also appreciate the discussions with colleagues during and after a workshop organized by J. Hansen on Arctic climate and air pollution held in New York in January 2007.

10.1126/science.1137695

SCIENCE & ENGINEERING
VISUALIZATION CHALLENGE

CALL FOR ENTRIES

ENTRY DEADLINE: MAY 31, 2007

SCIENCE AND ENGINEERING'S MOST POWERFUL STATEMENTS
ARE NOT MADE FROM WORDS ALONE

When the left brain collaborates with the right brain, science emerges with art to enhance communication and understanding of research results—illustrating concepts, depicting phenomena and drawing conclusions.

The National Science Foundation (NSF) and the journal *Science*, published by the American Association for the Advancement of Science, invite you to participate in the fifth annual Science and Engineering Visualization Challenge. The competition recognizes scientists, engineers, visualization specialists and artists for producing or commissioning innovative work in visual communication.

Winners in each category will be published in the September 28, 2007 issue of *Science* and *Science* Online, and will be displayed on the NSF Web site.

Award Categories

- Illustration
- Informational Graphics
- Interactive Media
- Non-Interactive Media
- Photographs

COMPLETE ENTRY INFORMATION:
WWW.NSF.GOV/NEWS/SPECIAL_REPORTS/SCIVIS

NSF

Science
AAAS

Long-Term Satellite Record Reveals Likely Recent Aerosol Trend

Michael I. Mishchenko,* Igor V. Geogdzhayev, William B. Rossow, Brian Cairns, Barbara E. Carlson, Andrew A. Lacis, Li Liu, Larry D. Travis

Recent observations of downward solar radiation fluxes at Earth's surface have shown a recovery from the previous decline known as global "dimming" (*1*), with the "brightening" beginning around 1990 (*2*). The increasing amount of sunlight at the surface profoundly affects climate and may represent certain diminished counterbalances to greenhouse gas warming, thereby making the warming trend more evident during the past decade.

It has been suggested that tropospheric aerosols have contributed notably to the switch from solar dimming to brightening via both direct and indirect aerosol effects (*1*, *2*). It has further been argued (*3*) that the solar radiation trend mirrors the estimated recent trend in primary anthropogenic emissions of SO_2 and black carbon, which contribute substantially to the global aerosol optical thickness (AOT). A similar increase of net solar flux at the top of the atmosphere (TOA) over the same period appears to be explained by corresponding changes in lower-latitude cloudiness (*4*), which confounds the interpretation of the surface radiation record. Therefore, it is important to provide a direct and independent assessment of the actual global long-term behavior of the AOT. We accomplish this by using the longest uninterrupted record of global satellite estimates of the column AOT over the oceans, the Global Aerosol Climatology Project (GACP) record (*5*). The record is derived from the International Satellite Cloud Climatology Project (ISCCP) DX radiance data set composed of calibrated and sampled Advanced Very High Resolution Radiometer (AVHRR) radiances. A detailed discussion of the sampling resolution, calibration history, and changes in the corresponding satellite sensors can be found in (*6*).

The global monthly average of the column AOT is depicted for the period August 1981 to June 2005 (Fig. 1, solid black curve). The two major maxima are caused by the stratospheric aerosols generated by the El Chichon (March 1982) and the Mount Pinatubo (June 1991) eruptions, also captured in the Stratospheric Aerosol and Gas Experiment (SAGE) stratospheric AOT record (*7*). The quasi-periodic oscillations in the black curve are the result of short-term aerosol variability.

The overall behavior of the column AOT during the eruption-free period from January 1986 to June 1991 (Fig. 1, red line) shows only a hint of a statistically significant tendency and indicates that the average column AOT value just before the Mount Pinatubo eruption was close to 0.142. After the eruption, the GACP curve is a superposition of the complex volcanic and tropospheric AOT temporal variations. However, the green line reveals a long-term decreasing tendency in the tropospheric AOT. Indeed, even if we assume that the stratospheric AOT just before the eruption was as large as 0.007 and that by June 2005 the stratospheric AOT became essentially zero (compare with the blue curve), still the resulting decrease in the tropospheric AOT during the 14-year period comes out to be 0.03. This trend is significant at the 99% confidence level.

Admittedly, AVHRR is not an instrument designed for accurate aerosol retrievals from space. Among the remaining uncertainties is radiance calibration, which, if inaccurate, can result in spurious aerosol tendencies. Similarly, substantial systematic changes in the aerosol single-scattering albedo or the ocean reflectance can be misinterpreted in terms of AOT variations. However, the successful validation of GACP retrievals using precise sun photometer data taken from 1983 through 2004 (*8*, *9*) indicates that the ISCCP radiance calibration is likely to be reliable. This conclusion is reinforced by the close correspondence of calculated and observed TOA solar fluxes (*4*). Furthermore, the GACP AOT record appears to be self-consistent, with no drastic intrasatellite variations, and is consistent with the SAGE record.

The advantage of the AVHRR data set over the data sets collected with more advanced recent satellite instruments is its duration, which makes possible reliable detection of statistically significant tendencies like the substantial decrease of the tropospheric AOT between 1991 and 2005. With all the uncertainties, the tropospheric AOT decrease over the 14-year period is estimated to be at least 0.02. This change is consistent with long-term atmospheric transmission records collected in the former Soviet Union (*5*).

Our results suggest that the recent downward trend in the tropospheric AOT may have contributed to the concurrent upward trend in surface solar fluxes. Neither AVHRR nor other existing satellite instruments can be used to determine unequivocally whether the recent AOT trend is due to long-term global changes in natural or anthropogenic aerosols. This discrimination would be facilitated by an instrument like the Aerosol Polarimetry Sensor (APS), scheduled for launch in December 2008 as part of the NASA Glory mission (*10*). It is thus imperative to provide uninterrupted multidecadal monitoring of aerosols from space with dedicated instruments like APS in order to detect long-term anthropogenic trends potentially having a strong impact on climate.

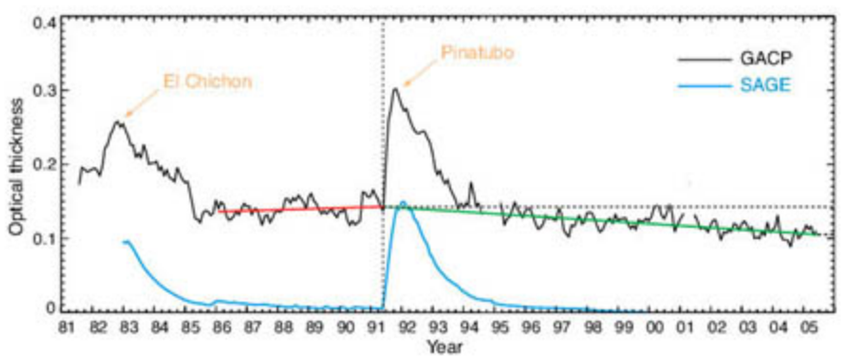

Fig. 1. GACP record of the globally averaged column AOT over the oceans and SAGE record of the globally averaged stratospheric AOT.

References and Notes

1. M. Wild *et al.*, *Science* **308**, 847 (2005).
2. R. T. Pinker, B. Zhang, E. G. Dutton, *Science* **308**, 850 (2005).
3. D. G. Streets, Y. Wu, M. Chin, *Geophys. Res. Lett.* **33**, L15806 (2006).
4. Y. Zhang, W. B. Rossow, A. A. Lacis, V. Oinas, M. I. Mishchenko, *J. Geophys. Res.* **109**, D19105 (2004).
5. I. V. Geogdzhayev, M. I. Mishchenko, E. I. Terez, G. A. Terez, G. K. Gushchin, *J. Geophys. Res.* **110**, D23205 (2005); and references therein.
6. W. B. Rossow, R. A. Schiffer, *Bull. Am. Meteorol. Soc.* **80**, 2261 (1999); and references therein.
7. J. Hansen *et al.*, *J. Geophys. Res.* **107**, 4347 (2002).
8. L. Liu *et al.*, *J. Quant. Spectrosc. Radiat. Transfer* **88**, 97 (2004).
9. A. Smirnov *et al.*, *Geophys. Res. Lett.* **33**, L14817 (2006).
10. M. I. Mishchenko *et al.*, *J. Quant. Spectrosc. Radiat. Transfer* **88**, 149 (2004).
11. This research is part of NASA/Global Energy and Water Cycle Experiment GACP and was funded by the NASA Radiation Sciences Program, managed by H. Maring and D. Anderson.

24 October 2006; accepted 20 December 2006
10.1126/science.1136709

NASA Goddard Institute for Space Studies, 2880 Broadway, New York, NY 10025, USA.

*To whom correspondence should be addressed. E-mail: mmishchenko@giss.nasa.gov

An Active Subglacial Water System in West Antarctica Mapped from Space

Helen Amanda Fricker,[1]* Ted Scambos,[2] Robert Bindschadler,[3] Laurie Padman[4]

Satellite laser altimeter elevation profiles from 2003 to 2006 collected over the lower parts of Whillans and Mercer ice streams, West Antarctica, reveal 14 regions of temporally varying elevation, which we interpret as the surface expression of subglacial water movement. Vertical motion and spatial extent of two of the largest regions are confirmed by satellite image differencing. A major, previously unknown subglacial lake near the grounding line of Whillans Ice Stream is observed to drain 2.0 cubic kilometers of water into the ocean over ~3 years, while elsewhere a similar volume of water is being stored subglacially. These observations reveal a widespread, dynamic subglacial water system that may exert an important control on ice flow and mass balance.

At least 145 subglacial lakes have been mapped beneath the Antarctic Ice Sheet (*1*). Recent pivotal studies based on satellite data have demonstrated that Antarctic subglacial water can move in large volumes between lakes, on short time scales and over long distances (*2*, *3*). Large outbursts of subglacial water have been observed in coastal regions (*4*), but it is not known how frequently these occur, nor the total amount of water involved continent-wide. Water beneath an ice stream, acting as a lubricant either between the ice and subglacial bed or between grains of a subglacial till, affects ice flow rates (*5*). Subglacial lakes have recently been linked to the broad onset of faster flow of the Recovery Ice Stream (*6*) and are located at the heads of other Antarctic ice stream tributaries (*7*). The drastic deceleration (a "shutdown") ~150 years ago of Kamb Ice Stream has been attributed to a decrease in subglacial water supply (*8*). Thus, knowledge of subglacial water movement is fundamental to understanding Antarctic ice stream dynamics and to predicting future Antarctic ice sheet behavior and sea-level contribution.

Subglacial water systems are pressurized to near the weight of the overlying ice (*9*), so movement of water can cause an elevation change of the ice surface that can be detected by satellites. Past observations interpreted to be Antarctic sub-

[1]Institute of Geophysics and Planetary Physics, Scripps Institution of Oceanography, University of California, San Diego, La Jolla, CA 92093, USA. [2]National Snow and Ice Data Center, University of Colorado, Boulder, CO 80302, USA. [3]NASA Goddard Space Flight Center, Greenbelt, MD 20771, USA. [4]Earth & Space Research, Corvallis, OR 97333, USA.

*To whom correspondence should be addressed. E-mail: hafricker@ucsd.edu

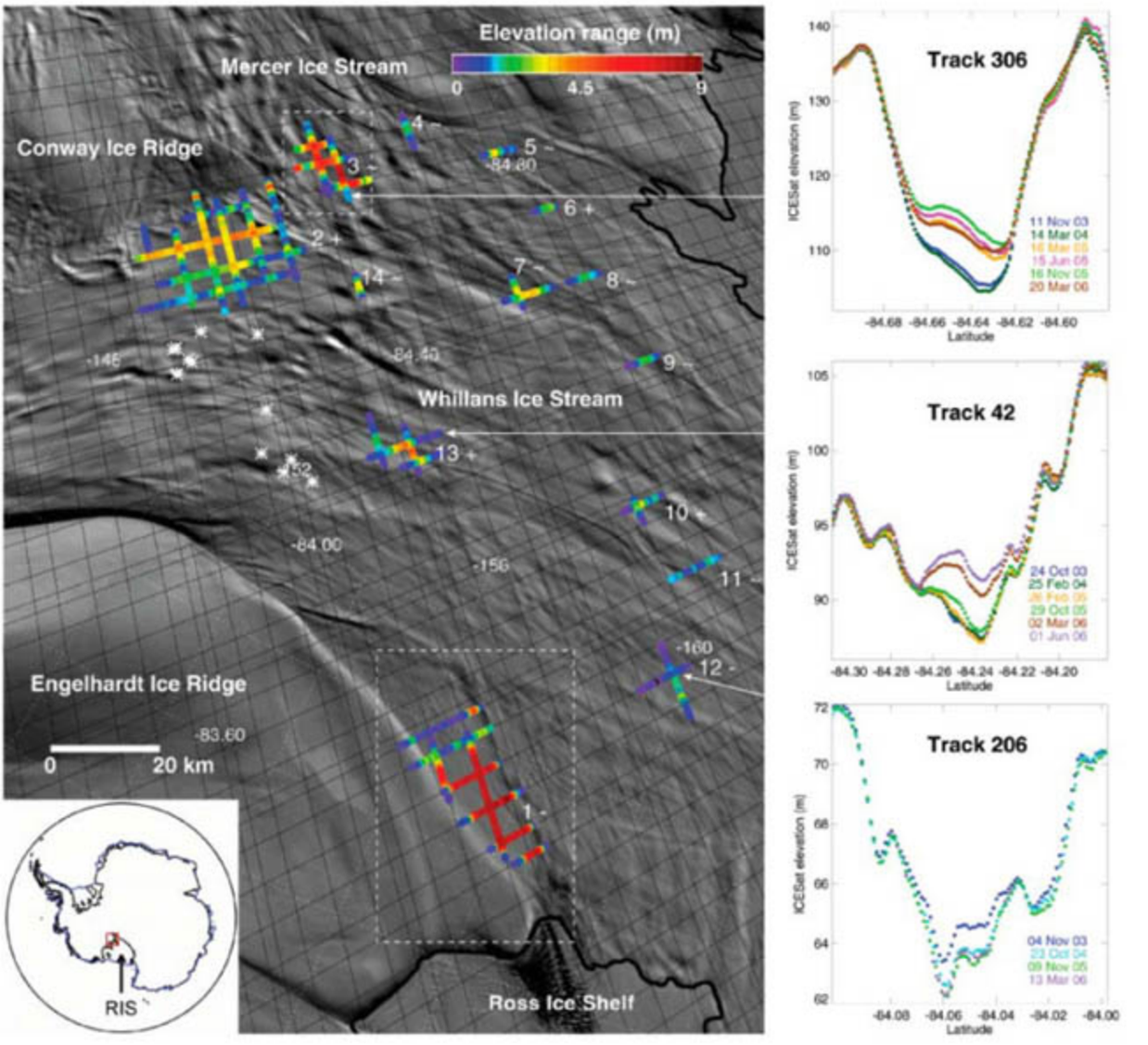

Fig. 1. (**Left**) Locations of elevation-change events identified through ICESat repeat-track analysis on lower WIS and MIS (2003 to 2006). Straight black lines show the ICESat reference ground tracks. Colored track segments represent range in elevation amplitude for each elevation-change event. Events cluster into 14 elevation-change regions, which are either rising (+), falling (–), or oscillating (~). Ice flow is from top left to lower right. Background image is MODIS Mosaic of Antarctica (MOA) (*30*), and inset map shows its location in Antarctica. Bold black line indicates the break-in-slope associated with the grounding zone of the Ross Ice Shelf (RIS). White dashed boxes show regions covered in Fig. 2. White asterisks indicate locations of small surface-collapse features observed on WIS in 1987–1988 (fig. S4). (**Right**) Repeat ICESat elevation profiles along track segments that cross each type of region (~, +, –). Arrows point to the location of each track segment on the image.

glacial water movement have been made with interferometric synthetic aperture radar (InSAR) (*2*) and satellite radar altimetry (*3*). However, InSAR data for high southern latitudes (>80°S) are presently limited to a brief period during late 1997 (*10*, *11*). Radar altimetry has a relatively long record and many repeat observations, but has limited coverage and spatial resolution (*12*).

ICESat Laser Altimetry

Our approach combines accurate, repeated elevation profiling from satellite laser altimetry with satellite image differencing to map and monitor elevation changes. NASA's Ice, Cloud, and land Elevation Satellite (ICESat), which carries the Geoscience Laser Altimeter System (GLAS), provides elevation data with a small (~65 m) spatial footprint, high vertical accuracy [±20 cm (*13*)], and high along-track resolution (~170 m). We analyzed all available ICESat data across the Whillans and Mercer ice streams (WIS and MIS) (Fig. 1) from a series of 10 data-acquisition periods spanning February 2003 through June 2006 (Table 1) for apparent elevation changes using repeat-track analysis (*14*, *15*). This indicated 101 candidate elevation-change "events." Horizontal offsets of repeated tracks (up to ~500 m) cause apparent elevation changes in the presence of nonzero cross-track slopes. To focus on temporal variability, we conservatively discarded events where the elevation trend was correlated with track offset. Most of the 46 remaining events showed a change in elevation confined to a trough or basin bounded by steeper sections of the ice stream surface (Fig. 1). Plotting these events on an image map showed that they clustered in 14 distinct elevation-change regions in the vicinity of the WIS/MIS confluence and grounding line (Fig. 1). Events within each region had consistent patterns of timing and displacement magnitude. The large (~350 km^2) region, near the grounding line of Ross Ice Shelf (RIS) next to Engelhardt Ice Ridge (near the bottom of Fig. 1), has the largest-amplitude signal and is a special case that will be discussed later. The other two large regions are located on either side of Conway Ridge; one on WIS (~500 km^2) and the other on MIS (~120 km^2). The remaining elevation-change regions in the lower glacier trunk are smaller, being sampled by just one to four tracks, and sum to an estimated area of 250 km^2. None are identified over the central trunk of WIS between 148°W and 140°W, but there are five additional smaller-amplitude regions farther upstream (fig. S1). Some events may be undetectable with our technique and conservative criteria, especially in the central ice stream where topography is rougher. Overall, ~10% of the lower WIS/MIS area shown in Fig. 1 is occupied by elevation-change regions. The smallest along-track extent of the 46 events was 3.5 km and the mean extent was 9.1 km, suggesting that ICESat track spacing in this area (3 to 5 km) (Fig. 1) is adequate to capture most changing regions.

Table 1. ICESat operations periods, orbit repeat periods, dates of data acquisition, and release numbers (*46*) for the data used in this work. ICESat has operated in two repeat orbits: 8 and 91 days, the latter with a 33-day subcycle. The last 33 days of the Laser 2a 91-day operations period (since 10/25/2003) have been repeated in all subsequent operations periods (Laser 2b onward) ~4 months apart.

Operations period	Repeat (days)	Dates	Release
Laser 1	8	02/20/03–03/29/03	118
Laser 2a	8	09/25/03–10/04/03	426
Laser 2a	91	10/04/03–11/19/03	426
Laser 2b	91	02/17/04–03/21/04	428
Laser 2c	91	05/18/04–06/21/04	117
Laser 3a	91	10/03/04–11/08/04	428
Laser 3b	91	02/17/05–03/24/05	428
Laser 3c	91	05/20/05–06/23/05	122
Laser 3d	91	10/21/05–11/24/05	428
Laser 3e	91	02/22/06–03/28/06	428
Laser 3f	91	05/24/06–06/26/06	126

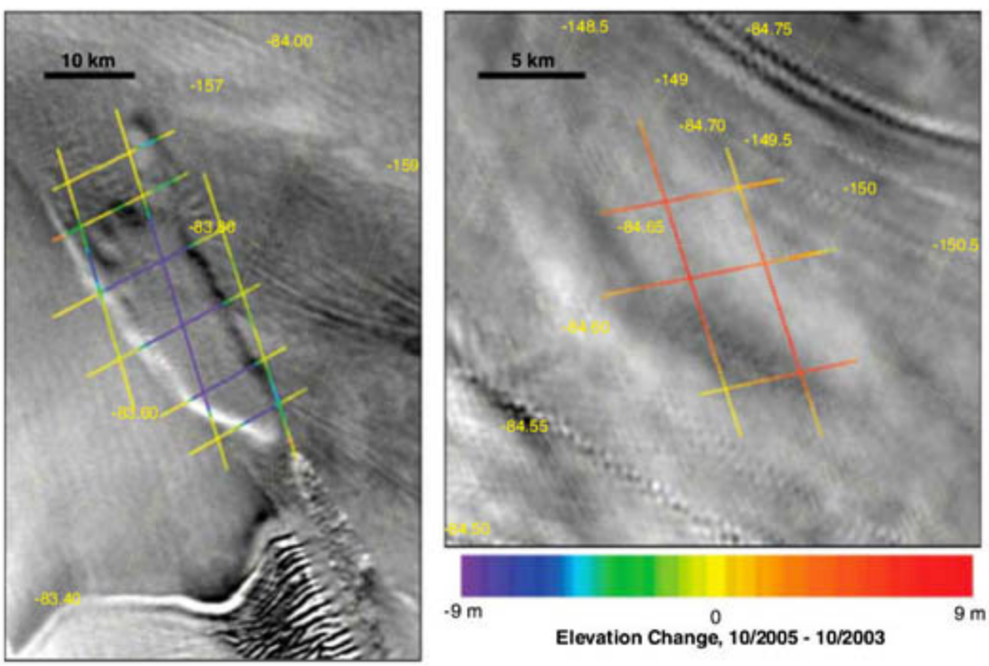

Fig. 2. MODIS difference images (December 2005 minus December 2003) over regions 1 (left) and 3 (right). ICESat tracks across both regions are color-coded by the elevation change from October/November 2003 to October/November 2005, close in time to when the images that were differenced were acquired. Illumination of all images used to make the difference images was from the upper right. Images for region 1 are shown as an animated sequence in movie S2.

Satellite Image Differencing

To map the spatial extent of the elevation-change regions and to confirm the ICESat-detected changes, we used a technique involving subtraction of similarly illuminated groups of satellite images. High-precision radiometric images of a uniform snow/ice surface are sensitive to surface slope (*16*, *17*). We used images from the Moderate-resolution Imaging Spectroradiometer (MODIS) sensor, flying on NASA's Terra and Aqua satellites. We constructed a multiyear series of calibrated surface reflectance images from multiple cloud-masked, destriped, visible-band scenes acquired over brief intervals (a few weeks) each year (fig. S2). This "image stacking" process yields scenes with improved radiometric and spatial detail (*18*). By subtracting these images, the resultant image emphasizes areas where surface slope changed [see "Satellite Image Differencing" in (*19*)]. Figure 2 illustrates how image differencing complements the ICESat analysis by defining the spatial extent of the two regions with the largest elevation changes. For these regions, image differencing confirmed the sign of surface elevation change and the relative magnitude of the surface slope changes. No additional regions of change were identified.

Interpretation

The detected elevation-change regions display a variety of temporal signatures. The three largest regions show nearly constant activity between

each ICESat operation period, whereas other regions were frequently quiescent. The track segments undergoing change between ICESat operation periods were nearly constant. Transects of elevation differences (not shown) for small regions were approximately Gaussian in shape, whereas tracks across the larger regions (1 and 2 in Fig. 1) had flat central portions with the differences decreasing toward each end. The constancy of the spatial extent during growth or decay, the short time scale of the changes, the shape of the flexural boundaries (*14*), and the locations of the changes (in basins) are all consistent with water-driven elevation change, and not consistent with the sudden formation or erosion of subglacial landforms as recently reported beneath another Antarctic ice stream (*20*). We interpret these elevation-change regions as surface expressions of ponded subglacial water, and the observed surface movement to be due to water gain or loss through a system of conduits beneath the ice streams. This concept is visualized in movie S1. We have detected similar signals on MacAyeal Ice Stream (fig. S3). We refer to regions 1, 2, 3, and 13 as subglacial lakes Engelhardt, Conway, Mercer, and Whillans, respectively, based on nearby named ice features.

Using ice-thickness data (*21*) and a smoothed digital elevation model from ICESat data (*22*), we mapped the hydraulic potential [or subglacial pressure field; see "Calculation of hydraulic potential pressure" in (*19*)] and compared it with the distribution of inferred active subglacial water locations (Fig. 3). Resolution of our pressure map is 7.5 km. Errors in the estimated potential are ±10 kPa of the mean at this averaging scale, but larger (~100 kPa) localized variations may be associated with smaller-scale surface or bed topography. Relative minima in the subglacial pressure field identify areas that would tend to collect and retain water; steep pressure gradients promote rapid water movement; and the direction of subglacial water flow is toward lower pressure and normal to equipotential contours. Several of the identified elevation changes, including subglacial lakes Whillans, Mercer, and Engelhardt, coincide with lows in the regional subglacial pressure, while Subglacial Lake Conway is in an area of low potential gradient.

Although existence of a subglacial water system long has been suspected beneath active West Antarctic ice streams (*5*, *8*), the present observation of rapid movement between several reservoirs is unprecedented. The only direct evidence of pooled subglacial water comes from drilling in the upstream portion of Kamb Ice Stream (*23*). Indirect evidence comes from InSAR (*2*), seismic data (*24*), and airborne observations of small collapse features on WIS in 1987–1988 (Fig. 1 and fig. S4). Although they are close by, these locations do not coincide with features identified here. WIS and MIS are fast-flowing ice streams and have a soft till layer at their beds (*25*). Given the recent observation that large volumes of sediment can be transported rapidly beneath ice streams (*20*), it is possible that on longer time scales (decades to centuries), the features we have identified may migrate. A large bottom crevasse, at least 12 km long, detected at the base of WIS (*26*) by radio-echo sounding may have been the expression of a conduit that formed part of the subglacial system at that time.

Subglacial Lake Engelhardt Drainage Event

ICESat observations. The observed drainage of Subglacial Lake Engelhardt is particularly noteworthy. Figure 4 shows sequential elevation profiles for two ICESat tracks across the lake and the elevation evolution at three crossovers (*27*). The first ICESat profile across the lake was acquired in February 2003 (Laser 1), along a track of an 8-day repeat-orbit configuration that was almost coincident with Track 206 from the 91-day repeat-orbit configuration used for all observations from October 2003 onward (Fig. 1). Between October 2003 and November 2005, elevations decreased by ~9 m at a gradually decreasing rate over most of the basin, while maintaining the flat surface shape in the region's center. Drainage ceased after November 2005. The ICESat data have sufficient along-track resolution to reveal the expected ice flexure at the lake margins during drainage (*28*). ICESat data acquired during 2006 suggest that some uplift has occurred, indicative of slow refilling of the lake (*29*).

Image differencing. Annual difference images spanning the period 2000 to 2005 are consistent with drainage starting in 2003 and continuing through 2005 (Fig. 2 and fig. S2). The images also confirm the flat surface shape in the center during deflation and the flexure at the edges, and reveal several elongated areas

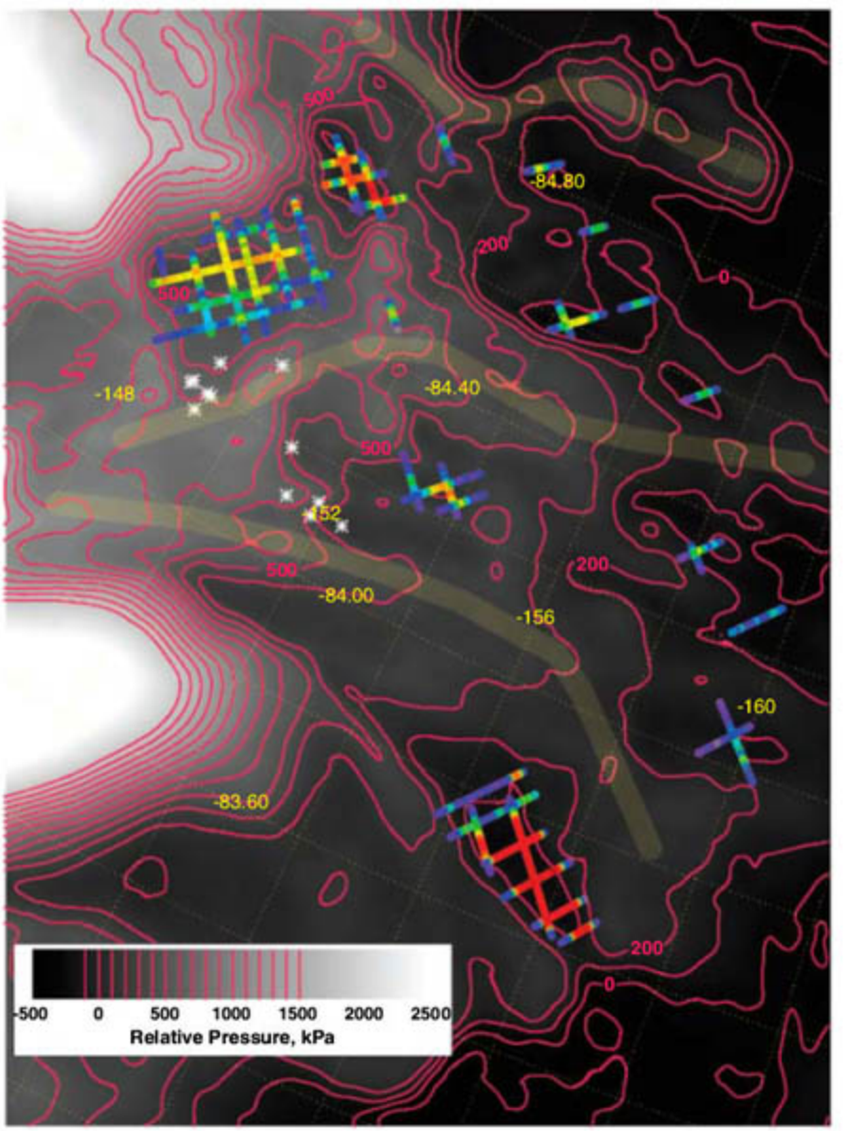

Fig. 3. Inferred subglacial water (hydrostatic) pressure at the base of the ice, in kilopascals (kPa), relative to the value at the grounding line near Subglacial Lake Engelhardt. The pressure-field resolution is ~7.5 km [see "Calculation of hydraulic potential pressure" in (*19*)]. Contours (interval 100 kPa) and gray-scale both represent hydrostatic pressure (dark indicates lower pressure). The broad yellow bars highlight "ridges" in the pressure field that may separate subglacial drainages. Figure covers the same area as Fig. 1, and colored track values represent range in elevation amplitude as in Fig. 1. White asterisks indicate locations of small surface-collapse features observed on WIS in 1987–1988 (fig. S4).

near the region's upstream end. They also show that the downstream end of the feature is ~7 km from the grounding line of the Ross Ice Shelf as mapped by both surface slope change in MODIS imagery (*30*) and ICESat repeat-track analysis (*14*). The outline of the basin is marked by the increasing slope at its edges (Fig. 4 profiles), and ICESat profile locations of greatest change fit precisely within the boundary of the basin as defined by the imagery.

Hydraulic path, discharge rate, and total volume lost. The hydraulic path for the Subglacial Lake Engelhardt water was across the grounding line into the ocean. The subglacial pressure field (Fig. 3) shows that lake pressure was likely 100 to 200 kPa higher than the pressure of the ocean at the grounding line before drainage (*31*). The downstream end of the lake is closed off from the ocean by a weak pressure barrier of ~50 kPa. This was presumably breached during drainage by a conduit too small to be resolved in the potential map. Based on the subsidence area and the elevation decrease, the lake lost ~2.0 km^3 of water to the ocean cavity beneath RIS. The initial maximum rate of 1.25 km^3 $year^{-1}$ (~40 m^3 s^{-1}) was sustained for 18 months. For comparison, jökulhlaups (outbursts of subglacially stored water) typically reach discharge rates one to two orders of magnitude larger but only last for days (*32*). The relatively low pressure differential (*33*) may explain the absence of an exponential growth in the discharge typical of jökulhlaups, leading to the observed more gradual drainage at a nearly constant rate. We cannot determine from the data the dimensions of the outlet conduit (*34*), nor whether it consisted of a single channel either in the ice or the subglacial till (*35*), a flowing water sheet (*36*), or a network of linked channels. Previous authors (*3*) inferred a steady flow rate for a subglacial lake in East Antarctica (*37*), which they attributed to a modification of the overburden pressure as the ice roof deformed to accommodate the changing water volumes. For Lake Engelhardt drainage, flexure is limited to a narrow (~1 km) zone at the margin, and little energy was expended to deform the roof (*38*); therefore, the roof subsidence must have kept pace with the drainage. Termination of discharge may have occurred because the declining pressure head could no longer overcome closure of the outlet path, or the lake had achieved hydraulic equilibrium with the adjacent sub-ice-shelf cavity. We see no evidence of a tidal response of the lake since discharge ceased.

Lake history and possible trigger mechanism. We examined historic data sets (both field and satellite) to assess prior states of Subglacial Lake Engelhardt and found no evidence of prior drainage (supporting online text). The 2003–2006 drainage event may have been triggered by a longer-term ice thinning and local upstream migration of the grounding line (*39*), causing the lake seal (ice dam) to break. This thinning and migration of the grounding zone can be seen in fig. S2 and movie S2. We calculated migration rates of 443 ± 60 m $year^{-1}$ and 330 ± 100 m $year^{-1}$ from ICESat (2003 to 2006) and MODIS (2000 to 2005), respectively.

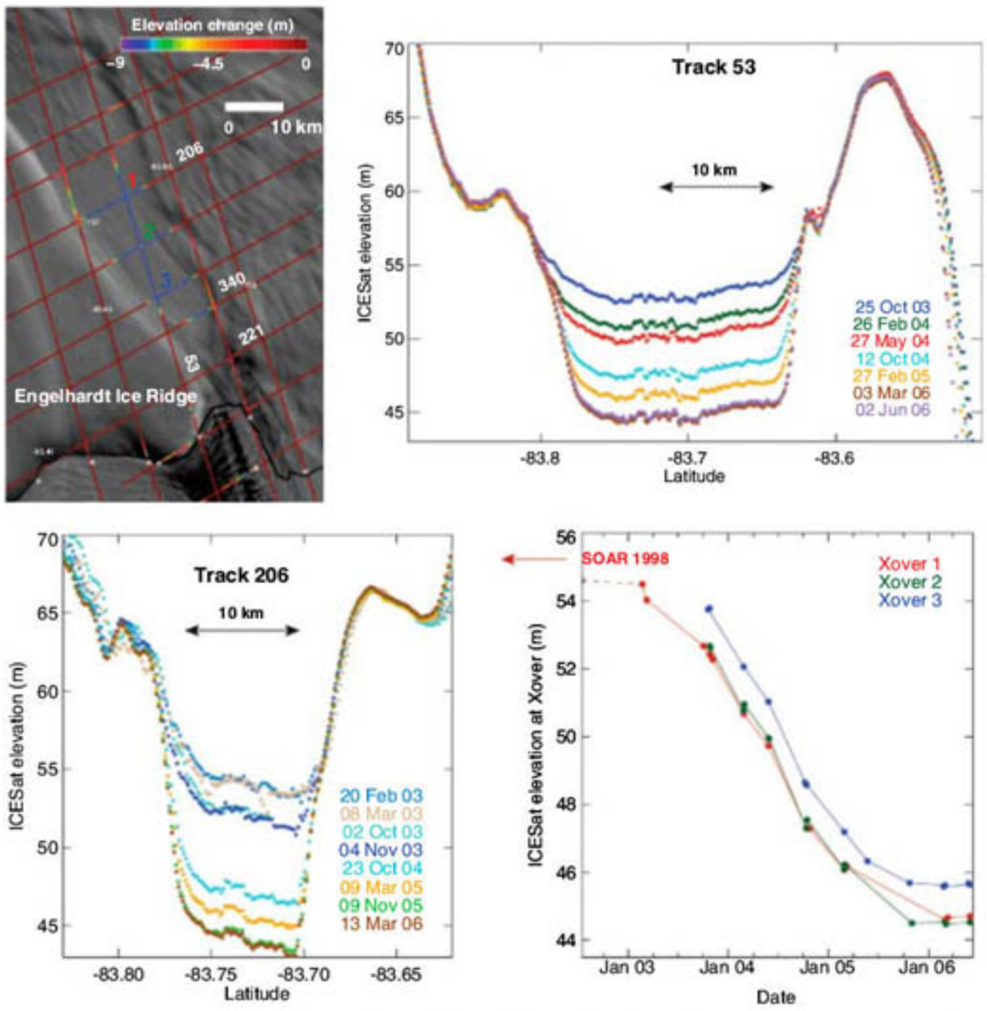

Fig. 4. (Top left) ICESat 91-day tracks across newly discovered Subglacial Lake Engelhardt on northwestern WIS. Background image is MOA (*30*). Tracks are color-coded by elevation change between October 2003 and November 2005. White asterisks locate tide-induced ice-flexure limits for the grounding line derived from ICESat repeat-track analysis (*14*). (Top right and bottom left) Repeat ICESat profiles along two tracks across the lake (see top left panel for locations). Track 206 was an almost exact repeat of an 8-day track, and the first three profiles were acquired in this orbit (Laser 1 and Laser 2a; Table 1). (Bottom right) ICESat elevations against time at three orbit crossovers in the center of the lake (see top left panel for locations), including the 8-day data at crossover 1 in February/March 2003. SOAR data from 1998 (indicated by an arrow) are discussed in the supporting online material.

Hydraulic Linkage and Volume Estimate for Water Within the WIS/MIS System

The subglacial hydraulic pressure field beneath the ice streams (Fig. 3) includes three major divides that control water flow direction and separate regions of subglacial water activity (*40*). More than half of the subglacial area of WIS is hydraulically directed toward Subglacial Lake Conway. Drainage from this subglacial reservoir appears to be directed southward into Subglacial Lake Mercer and, from there, westward to spread more broadly across the ice plain. ICESat's temporal records of elevation change in this catchment support our interpretation; Subglacial Lake Mercer and regions 4 and 5 (Fig. 1) all indicate water loss between late 2005 and mid-2006, whereas the four regions downstream (6, 7, 8, and 9) grow by an amount equal to half of their combined drained volume. Subglacial Lake Whillans lies in a more restricted catchment that narrows upstream. It was relatively quiescent until a sudden surface inflation began in late 2005 at a rate of ~8 m $year^{-1}$. Regions 10, 11, and 12 downstream are active throughout the ICESat measurement period, with a small net gain in volume. The third catchment feeds Subglacial Lake Engelhardt and is confined to the northern margin of WIS by the northernmost divide in the pressure field.

We have shown that Subglacial Lake Engelhardt drained during the first 2.7 years of the ICESat mission, with a total volume loss of −2.0 km^3. In the same period, Subglacial Lake Conway steadily filled, with a total volume increase of 1.2 km^3. The surface of Subglacial Lake Mercer oscillated, rising between 2003 and late 2005 (see Track 306 on Fig. 1, and Fig. 2) and sinking from late 2005 to mid-2006, for a net volume gain of 0.12 km^3. The remaining

elevation-change areas summed to a total volume increase of 0.27 km^3, but we found little temporal coherence between them. Ignoring the few regions far upstream on WIS and the isolated Subglacial Lake Engelhardt, the incremental water stored during each interval between ICESat observations (~4 months) varied from +0.05 to +0.4 km^3. The total volume increase was 1.6 km^3 summed over 33 months (or ~0.6 km^3 $year^{-1}$), which is approximately equal to the volume of water lost from Subglacial Lake Engelhardt (2.0 km^3). The average annual rate of water storage is similar to the estimated area-integrated production rate for basal water (0.53 km^3 $year^{-1}$) over the entire 168,000-km^3 catchment of WIS (*41*). Thus, a substantial fraction of the subglacial water produced beneath these ice streams transits through the observed subglacial water system. The volume of fresh water injected into the ocean cavity under the RIS is small relative to the net production from basal melt under the RIS, but may influence the thermohaline circulation in the sub-ice-shelf cavity close to the source.

Net storage of water in the system, sustained from one ICESat observation interval to the next, is not an equilibrium situation: Eventually the water must either freeze onto the base of the ice stream or be discharged, perhaps in the manner we observed for Subglacial Lake Engelhardt. Because that lake lost as much volume as was gained elsewhere, the net change in water volume in the whole system for 2003 to 2006 was close to zero. However, the subglacial catchment map shows that it is not the same water; Subglacial Lake Engelhardt is not hydraulically linked to any of the other observed lakes in the system. Present basal conditions of WIS and MIS promote basal freezing (*41*), probably inhibiting water discharge and possibly explaining the current tendency to store subglacial water. Additionally, tidally modulated stick-slip motion [which results in twice-daily transitions between rapid ice flow and nearly no ice flow (*42*)], observed over most of the lower part of WIS, may interfere with the movement of subglacial water on a daily basis. Water will flow toward isolated low-pressure regions, which are preferentially located in the types of local surface depressions we identify as collecting subglacial water. As water accumulates, as it is presently doing in Subglacial Lake Conway, the hydrostatic pressure will eventually overcome the glaciostatic pressure leading to lake discharge (*32*), and the water will drain either to another basin or across the grounding line into the ocean. This cycle of draining and filling may influence the ice stream velocity, on short time scales of weeks to months. Variability of subglacial water production and storage may explain the recent slowdown of WIS (*43*, *44*).

Summary

Repeat-track ICESat laser altimetry, with complementary image differencing, provides a new, effective technique for monitoring water movement under glacial ice. Using this approach, we have discovered a widespread, active water system underneath the Whillans and Mercer ice streams, two of the largest streams draining the West Antarctic Ice Sheet. The detected motions are large, extensive, and temporally variable. They suggest that there is a net gain in water over the observation interval (2003 to 2006), which is likely both reflecting and influencing the motion of these major Antarctic ice streams. These observations provide clues to understanding the stability of ice streams through their sensitivity to basal lubrication. The time scale for subglacial water transport (months to years) is short compared with that of other known drivers of glacial flow variability, suggesting a mechanism for more rapid changes in ice stream behavior than have previously been assumed.

References and Notes

1. M. Siegert, S. Carter, I. Tabacco, S. Popov, D. Blankenship, *Antarct. Sci.* **17**, 453 (2005).
2. L. Gray *et al.*, *Geophys. Res. Lett.* **32**, L03501 (2005).
3. D. J. Wingham, M. L. Siegert, A. Shepherd, A. S. Muir, *Nature* **440**, 1033 (2006).
4. I. Goodwin, *J. Glaciol.* **34**, 95 (1988).
5. B. Kamb, *Antarct. Res. Ser.* **77**, 157 (2001).
6. R. E. Bell, M. Studinger, C. A. Shuman, M. A. Fahnestock, I. Joughin, *Nature* **445**, 904 (2007).
7. M. Siegert, J. Bamber, *J. Glaciol.* **46**, 703 (2000).
8. R. B. Alley, S. Anandakrishnan, C. R. Bentley, N. Lord, *Ann. Glaciol.* **20**, 187 (1994).
9. A. Iken, R. A. Bindschadler, *J. Glaciol.* **32**, 101 (1986).
10. The three-dimensional InSAR technique requires ascending and descending passes, which only exist in a few areas of Antarctica. InSAR data for Antarctica are mainly derived from the tandem mission of European Remote-sensing Satellite–1 (ERS-1) and ERS-2 (18 months in 1995–1996). RADARSAT provided InSAR data as far as the South Pole, but only for 3 months in 1997 (*9*).
11. K. C. Jezek, *Ann. Glaciol.* **29**, 286 (1999).
12. U.S. Navy's GEOSAT operated to 72°S during 1985 to 1989 in a 17-day orbit; the European Space Agency has flown three radar altimeters (RAs) in a 35-day orbit to 81.5°S: ERS-1 (1991 to 2000); ERS-2 (1995 to 2003); and Envisat (2002 to present). All four of these satellites miss much of the dynamic West Antarctic ice streams. The RA has a large footprint (~2 to 3 km over flat ice for ERS). Steep slopes on the ice streams cause tracking problems for the RA, limiting its vertical accuracy.
13. C. A. Shuman *et al.*, *Geophys. Res. Lett.* **33**, L07501 (2006).
14. H. A. Fricker, L. Padman, *Geophys. Res. Lett.* **33**, L15502 (2006).
15. ICESat data were filtered for clouds by use of the gain and energy parameters. Elevation anomalies for each segment were calculated by resampling the remaining repeat-track data onto common latitude values and calculating the difference between each elevation profile and the mean. At each point, the elevation range was also calculated.
16. T. A. Scambos, G. Kvaran, M. Fahnestock, *Remote Sens. Environ.* **69**, 56 (1999).
17. R. A. Bindschadler, P. L. Vornberger, *Ann. Glaciol.* **20**, 327 (1994).
18. T. A. Scambos, M. A. Fahnestock, *J. Glaciol.* **44**, 97 (1998).
19. Materials and methods are available as supporting material on *Science* Online.
20. A. M. Smith *et al.*, *Geology* **35**, 127 (2007).
21. S. Shabtaie, C. R. Bentley, *Ann. Glaciol.* **11**, 126 (1988).
22. J. DiMarzio, J. Zwally, A. Brenner, B. Schutz, Boulder, Colorado, USA: National Snow and Ice Data Center. Digital media (2007).
23. S. W. Vogel *et al.*, *Geophys. Res. Lett.* **32**, L14502 (2005).
24. S. R. Atre, C. R. Bentley, *Ann. Glaciol.* **20**, 177 (1994).
25. D. D. Blankenship, C. R. Bentley, S. T. Rooney, R. B. Alley, *J. Geophys. Res.* **92**, 8903 (1987).
26. C. R. Bentley, R. Retzlaff, N. Lord, A. N. Novick, *Antarct. J. U.S.* **26**, 62 (1991).
27. In satellite altimetry data, crossover analysis is a powerful means to validate elevation along any single track (*45*) and is the method previously used to detect subglacial water movement in ERS RA data (*3*).
28. G. W. Evatt, A. C. Fowler, C. D. Clark, N. R. J. Hulton, *Philos. Trans. R. Soc. A* **364**, 1769 (2006).
29. The latest ICESat data shown in Fig. 4 (Laser 3f data; May to June 2006) suggest that minor uplift occurred, but at levels close to the ICESat detection limit. Initial examination of data from the most recent operations period (Laser 3g, November to December 2006) suggests that this filling has continued, but since those data are still uncalibrated for precise pointing, we cannot yet confidently assert that the signal is real.
30. T. A. Scambos, T. Haran, M. A. Fahnestock, T. Painter, J. Bohlander, *Remote Sens. Environ.*, in press.
31. This estimate is in part affected by some surface lowering that had already taken place at the epoch of ICESat's Laser 2a data, which were used to create the digital elevation model.
32. M. J. Roberts, *Rev. Geophys.* **43**, RG1002 (2005).
33. A pressure of 100 kPa corresponds to a 10-m vertical difference in water-column height.
34. From the MODIS imagery (Figs. 2 and 4), we observe that the shortest length for a channel connecting the lake to the ocean is ~7 km long. ICESat data along Track 221 show a depression ~2 km wide, which gives an upper bound to the width of the outlet channel.
35. H. Rothlisberger, *J. Glaciol.* **11**, 177 (1972).
36. G. E. Flowers, H. Bjornsson, F. Palsson, G. K. C. Clarke, *Geophys. Res. Lett.* **31**, L05401 (2004).
37. The discharge curve we observe is similar to that for Lake L1 in (*3*). The drop in elevation is ~9 m for Lake Engelhardt compared to ~3.5 m for Lake L1, and the time scale is 26 months for Lake Engelhardt compared to 16 months for Lake L1.
38. The dimensions of Subglacial Lake Engelhardt are ~30 km by ~10 km, i.e., 14 to 40 times the ice thickness (~700 m), so the central ice cannot be supported at the lake margins. The flat surface profiles in the center of the lake confirm this.
39. R. Bindschadler, P. Vornberger, *Science* **279**, 689 (1998).
40. Errors in the surface-elevation and ice-thickness fields used for subglacial pressure mapping could modify the subglacial water catchments and allow some exchange of water between them. These issues were examined by adding ±5-m and ±50-m random errors to the surface and bed elevations, respectively. The major features discussed here did not change.
41. I. Joughin, S. Tulaczyk, D. R. MacAyeal, H. Englehardt, *J. Glaciol.* **50**, 96 (2004).
42. R. A. Bindschadler, M. King, R. A. Alley, S. Anandakrishnan, L. Padman, *Science* **301**, 1087 (2003).
43. R. Bindschadler, P. Vornberger, L. Gray, *J. Glaciol.* **51**, 620 (2005).
44. I. Joughin *et al.*, *Geophys. Res. Lett.* **32**, L22501 (2005).
45. H. J. Zwally, R. A. Bindschadler, A. C. Brenner, T. V. Martin, R. H. Thomas, *J. Geophys. Res.* **88**, 1589 (1983).
46. ICESat data release numbers are of the form YXX. Y refers to the amount of orbit and attitude calibration applied (a good indicator of quality), where 1 is the lowest and 4 is the highest. XX refers to the software version used to process the data.

47. We thank K. Yanagimachi, C. Bentley, D. Blankenship, J. Bohlander, G. Clarke, N. Lord, B. Smith, and D. Young for their contributions to this work. Thanks to J. Zwally, B. Schutz, and NASA's ICESat project. Thanks also to two anonymous referees for helpful comments on this manuscript. This work was supported by NASA. This is ESR contribution number 86.

Supporting Online Material

www.sciencemag.org/cgi/content/full/1136897/DC1
Materials and Methods
SOM Text
Figs. S1 to S4
References
Movies S1 and S2

30 October 2006; accepted 8 February 2007
Published online 15 February 2007;
10.1126/science.1136897
Include this information when citing this paper.

The Structural Basis of Ribozyme-Catalyzed RNA Assembly

Michael P. Robertson and William G. Scott*

Life originated, according to the RNA World hypothesis, from self-replicating ribozymes that catalyzed ligation of RNA fragments. We have solved the 2.6 angstrom crystal structure of a ligase ribozyme that catalyzes regiospecific formation of a 5′ to 3′ phosphodiester bond between the 5′-triphosphate and the 3′-hydroxyl termini of two RNA fragments. Invariant residues form tertiary contacts that stabilize a flexible stem of the ribozyme at the ligation site, where an essential magnesium ion coordinates three phosphates. The structure of the active site permits us to suggest how transition-state stabilization and a general base may catalyze the ligation reaction required for prebiotic RNA assembly.

The discovery of RNA enzymes (or ribozymes) in the 1980s (*1*–*3*) reignited interest in the chemical basis of the origin of life and resulted in formulation of the RNA World hypothesis (*4*). If RNA, in principle, can be both a genome and a catalyst, prebiotic self-replicating RNA molecules are likely an immediate evolutionary precursor and possibly a constituent of the first living organisms. All extant protein-based RNA polymerases synthesize RNA by catalyzing the templated ligation of a nucleotide triphosphate to form a 5′ to 3′ phosphodiester bond (Fig. 1A). Although natural ribozymes catalyze various phosphodiester bond isomerizations, hydrolysis, and even peptide bond formation (*5*), no naturally occurring nucleotide triphosphate ligase ribozyme that catalyzes the reaction required of an RNA polymerase has been discovered.

Ribozymes that specifically and regioselectively catalyze the template-dependent 5′ to 3′ phosphodiester bond ligation reaction that would have been required for a prebiotic self-replicating ribozyme (*6*) have, however, been created in the laboratory with artificial evolution and selection techniques (*7*–*13*), thus providing a proof of principle that RNA can catalyze the chemical step required for self-replication. The absence of natural polymerase or replicase ribozymes may be simply a consequence of a selection process that favored protein-based enzymes over less efficient ribozymes, rather than evidence that disfavors their existence in a prebiotic RNA World. In addition, chimeric RNA molecules consisting of a ligase ribozyme joined to an exogenous template-binding domain have been created by using a combination of in vitro evolution and rational design (*14*, *15*). These ligase-based ribozymes are capable of polymerizing an entire turn of an RNA helix and are therefore true RNA-dependent RNA polymerases (*16*).

To better understand the stereochemistry and mechanism of this reaction in the context of ribozyme catalysis, we have obtained the crystal structure of an L1 RNA ligase reaction product in two conformational states, one of which appears to be close to the likely transition-state geometry of the active ribozyme, and the other appears to be in a relaxed or undocked state.

The L1 ligase ribozyme. The L1 RNA ligase ribozyme was isolated from a population of synthetic random-sequence RNAs by in vitro selection (*9*). This ribozyme catalyzes nucleophilic attack by a 3′-hydroxyl group on the α-phosphorus of the ribozyme's 5′-triphosphate, creating a new phosphodiester linkage and releasing pyrophosphate (Fig. 1A). Although many in vitro selected ribozyme ligases produce unnatural 5′ to 2′ phosphodiester linkages, the L1 ligase is one of five ligase ribozymes known to catalyze the regiospecific formation of the natural 5′ to 3′ phosphodiester bond (*8*, *9*, *11*–*13*). The L1 ribozyme is highly flexible and, thus, responsive to structural perturbations that influence interconversion between active and inactive conformations. This has been exploited to engineer the L1 ligase into a molecular sensor for oligonucleotides (*9*), small molecules such as ATP (*9*) and FMN (*17*), proteins (*18*), and peptides (*19*). These allosteric molecular switch constructs have activation ratios as high as 50,000-fold over basal ligase activity.

Previous mutation and footprinting data (*9*, *20*) revealed that the L1 ligase folds into a

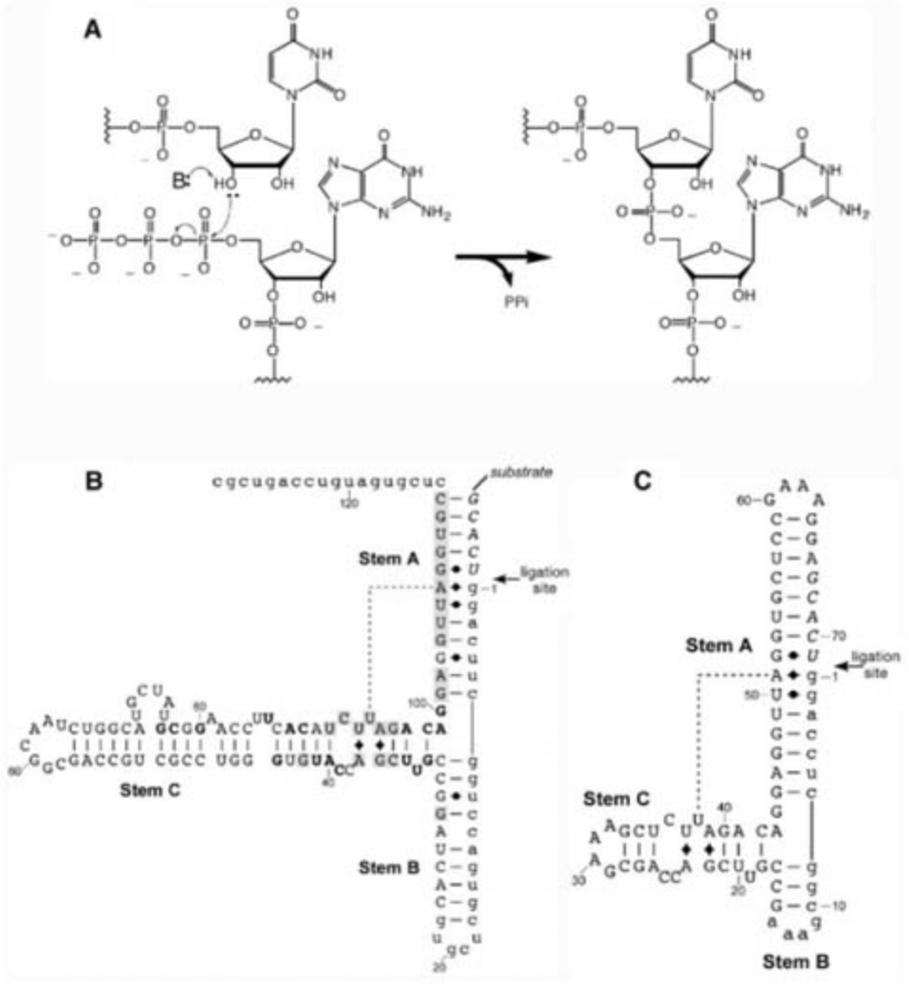

Fig. 1. Ligation reaction and L1 ligase secondary structures. (**A**) Ligation reaction catalyzed by the L1 ligase in which the 3′-hydroxyl of the 3′-terminal residue of the substrate oligonucleotide attacks the α-phosphorus of the ribozyme's 5′-terminal guanosine triphosphate, which creates a new phosphodiester bond. (**B**) The proposed secondary structure of the full-length L1 ribozyme. Nucleotides in lowercase are derived from the constant-sequence regions of the original N90 library; uppercase residues are derived from the randomized region of the pool. The substrate oligonucleotide is italicized. Positions within shaded boxes were invariant among clones isolated from a mutagenized reselection of the L1 ligase; positions in boldface were conserved in >85% of isolated clones. The dotted line indicates a base triple. [Figure adapted from (*9*).] (**C**) The secondary structure of the minimized crystallization construct, L1X6c.

The Center for the Molecular Biology of RNA and Department of Chemistry and Biochemistry, Robert L. Sinsheimer Laboratories, University of California, Santa Cruz, Santa Cruz, CA 95064, USA.

*To whom correspondence should be addressed. E-mail: wgscott@chemistry.ucsc.edu

triple-stemmed secondary structure, with the majority of conserved residues located either in positions predicted to base pair with experimentally unvaried sequences or within a "catalytic core" region of ~17 nucleotides adjacent to the three-helix junction (Fig. 1B). Stem A includes the highly conserved, complementary template that pairs with the substrate oligonucleotide and aligns the 3′ end of the substrate with the 5′ end of the ribozyme at the ligation junction. Stem A forms a simple helix with mostly Watson-Crick pairing except for three nonstandard pairings that occur directly at the ligation junction, namely, two G:U pairs on either side of a G:A pair. Although various types of unpaired nucleotides or nonstandard pairing at the ligation junction are seen in other ligase ribozymes (*8*, *10*–*12*) and presumably function to contort the helical geometry in a way that facilitates catalysis, template-mediated proximity effects are not sufficient to account for the observed catalytic rate enhancement. An additional highly conserved region of the ribozyme consists of ~17 mostly invariant or covariant nucleotides in stem C that reside immediately adjacent to the three-helix junction. This region, previously referred to as the ribozyme "core" (*20*), contains four predicted Watson-Crick base pairs, an absolutely conserved G:A pair, and several highly conserved but presumed unpaired nucleotides, whose function is unclear from the secondary structure. The remainder of stem C beyond the conserved core region, as well as the majority of stem B, can be replaced with stable tetraloops without reducing ribozyme activity.

To optimize crystallization, we created a 71-nucleotide construct, L1X6c (Fig. 1C), whose autocatalyzed ligation product is a covalently closed circular adduct, in which stems A, B, and C are each capped with GAAA tetraloops (*21*). The ligation rate of a bimolecular version of L1X6c having covalently distinct enzyme and substrate strands (instead of the tetraloop capping stem A) is 1.8/hour at pH 7.6 in the presence of 1.3 μM substrate and 60 mM $MgCl_2$ [supporting online material (SOM)]; the more difficult to measure unimolecular reaction will likely be faster because of the lack of an unfavorable entropy contribution inherent in a bimolecular reaction.

The L1 ribozyme crystal structures. The 71-nucleotide L1X6c ribozyme, when transcribed, folds into an active structure that autoligates to form a closed circular adduct (Fig. 1C). The 2.6 Å resolution crystal structure was solved (*22*) by piecewise molecular replacement using ideal A-form RNA model helices (Fig. 2, A to D). Two ligase molecules form an asymmetric unit within the crystal. Each is a roughly γ-shaped molecule in which stems A and B coaxially stack, and the shorter stem C forms an almost perpendicular branch from the three-strand junction. The secondary structure closely conforms to that previously predicted on the basis of biochemical mapping and footprinting, except A23 forms a reverse-Hoogsteen pair with U37 instead of pairing with U38.

The two ligase molecules in the asymmetric unit, despite their identical secondary structures, are not superimposable; stem C branches in opposite directions when stems A and B of the two conformers are overlaid (Fig. 2C). The two molecules of the asymmetric unit, designated P and Q, are in distinctly different conformations. Stem C of the ligase molecule P is angled away from

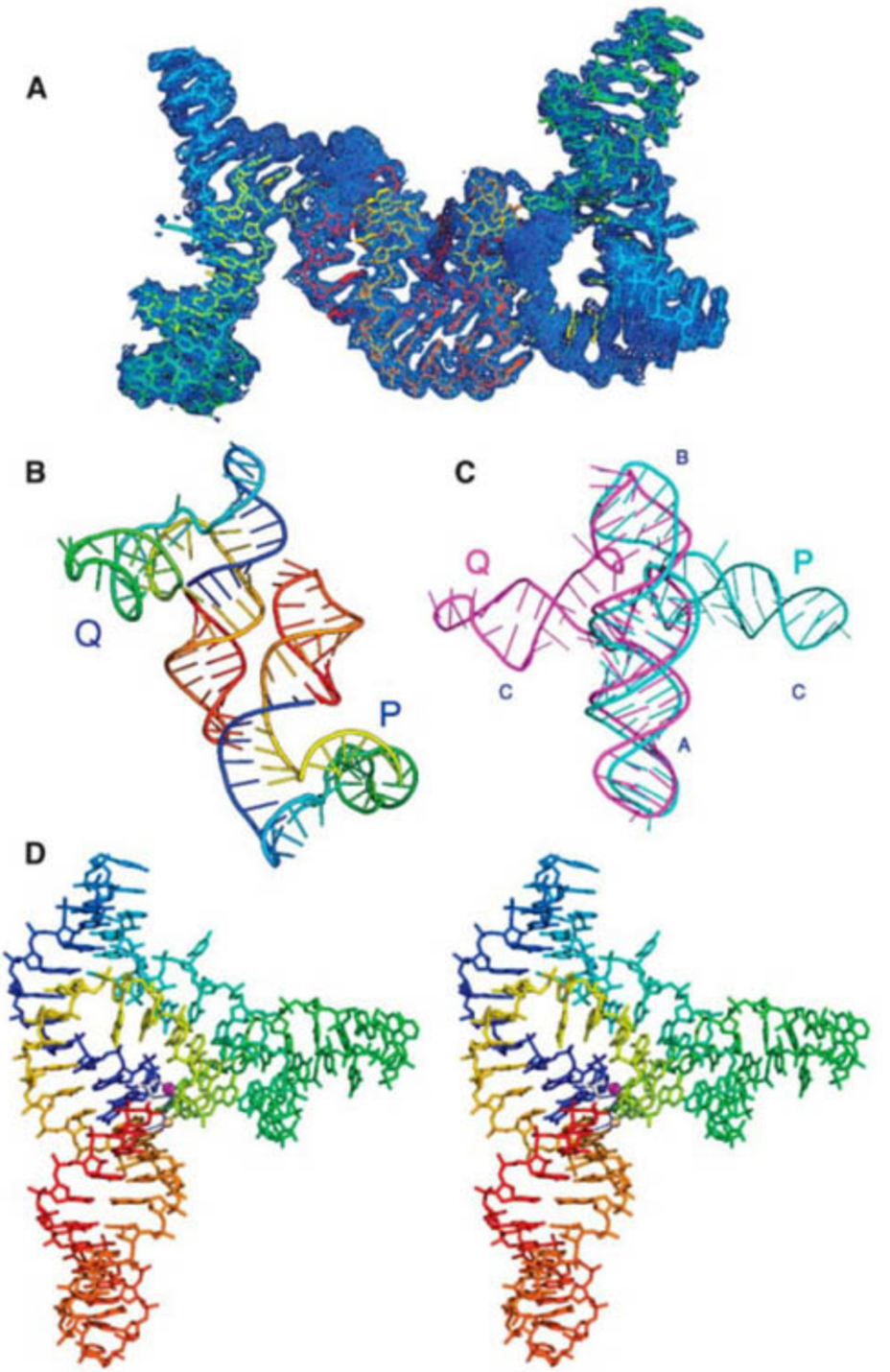

Fig. 2. The crystal structure of the L1 ligase ribozyme. (**A**) The refined all-atom structure of the crystallographic asymmetric unit of the L1 ribozyme, superimposed on a simulated annealing composite-omit sigma-A–weighted $2F_{obs} - F_{calc}$ map contoured at 1.2 RMSD (root mean square deviation). The two RNA chains are each rainbow color-coded such that the 5′ terminus is blue and the 3′ terminus is red. (**B**) A complementary cartoon representation of the crystallographic dimer with the same color scheme, but with the electron density omitted for clarity. The phosphodiester backbone is shown as a ribbon, and the side chains are depicted schematically as sticks. (**C**) A least-squares superposition of molecules P and Q, with molecule P depicted in cyan and Q in magenta. Stems A, B, and C are labeled. (**D**) An all-atom stereograph of the docked conformation of the ligase ribozyme (Q) color-coded as in (A and B). In addition, the phosphate at the ligation site is shown in gray, the Mg^{2+} ion believed to be involved directly in ligation catalysis is represented as a magenta sphere, and a water molecule at the active site is shown in beige. Contacts between the metal ion and three nonbridging phosphate oxygens and between the RNA and the water molecule are depicted as blue-gray dotted lines.

the ligation site, and this molecule is in a relaxed, presumably inactive, conformation. In contrast, stem C of ligase molecule Q forms tertiary contacts with the ligation site, in which an invariant uridine (residue 38 in stem C) makes a reverse–Watson-Crick base-pair with the invariant A51 at the ligation junction in stem A. We therefore conclude that molecule Q is crystallographically trapped in a docked, putatively active conformation that fulfills interactions inferred to be required from sequence invariance. This situation is somewhat similar to that observed for the hammerhead ribozyme. The truncated form of the hammerhead ribozyme (*23*, *24*) lacks the distant tertiary contacts that stabilize the cleavage site in an active conformation. When these tertiary contacts are included, the structure of the three-stranded junction changes to reposition invariant active-site nucleotides to facilitate acid-base catalysis (*25*). Fortunately, in the present case, both a relaxed and a potentially active conformer were found to be present as two crystallographically independent molecules within a single crystal.

The superposition of coaxial stems A and B of molecules P and Q indicates that most of stem A is unchanged in the two conformers apart from the three-helix junction and the transition to stem B. As the phosphate backbone approaches and traverses the three-helix junction, the undocked conformer, P, begins to become slightly underwound relative to the docked conformer, Q, which more closely resembles an ideal A-form helix. Overlaying the stem A tetraloops of molecules P and Q allows comparison of the relative dispositions of the stem B tetraloops in the two conformers, revealing that conformer P has become unwound by ~79° and is displaced by 8 Å relative to conformer Q.

The conserved catalytic core. The positions previously identified as the ribozyme "core" residues can now be subdivided into two functional clusters. The first functional cluster is made up of the unpaired nucleotides U19, A43, and G44 and the G18:C42 pair defining the helical junction. This region appears to function as a hinge, which allows stem C to pivot relative to stems A and B. Distortion of this hinge region accompanies helical unwinding of stems A and B in the undocked molecule. This prevents stem C from making the tertiary contacts with the catalytic site required to form the docked conformer. A43 and G44 stack on each other but do not pair or interact with other nucleotides in either conformer. Although these two positions are highly conserved among L1 ligase variants, they always occur in the context of a five-nucleotide CG···CAG motif encompassing positions C17, G18, C42, A43, and G44, with all but A43 and G44 involved in base pairing. A pentuple substitution of these positions observed in various selection experiments reveals a distinct UA···UGU motif that retains the same pairing layout as the CG···CAG motif but confers a 13-fold increase in the ribozyme's catalytic activity. In general, the L1 ligase variants contained either one motif or the other, but did not tolerate mutations of fewer than all five positions simultaneously (*20*). In light of the current crystal structure, it seems likely that these five positions have a significant effect on the hinging characteristics and positioning of stem C, and the UA···UGU motif either favors access to the active orientation of stem C or disfavors access to one or more inactive conformations. Also associated with this hinge region is the unpaired, yet highly conserved U19 that flips its base out of the helical stack of stem C. Despite being one of the most highly conserved positions in the molecule (invariant in at least 25 out of 26 sequences), this nucleotide, nonetheless, makes no apparent secondary or tertiary contacts. Although it is possible that an unobserved interaction has been disrupted by the crystallization process, given the context of the position and the global fold of the ligase, this residue may serve simply to add flexibility to the hinge domain.

Two Watson-Crick base pairs join the hinge to the other functional cluster within the core, composed of nucleotides G22 to A23 and U37 to A39. G22 forms a sheared G:A pair with A39, and A23 forms a reverse-Hoogsteen pair with U37. The contortion created by these adjacent, non–Watson-Crick pairs induces the invariant U38 to flip out of the helical stack (Fig. 3A). In the docked conformer, the U at position 38 is the single nucleotide base in stem C that interacts with the ligation junction of stem A as a specific tertiary base-pairing contact in a G:A:U base triple with G1 and A51, the ligation-site nucleotide and its pairing partner, respectively (Fig. 3B). G1 forms a sheared G:A pair with A51, and U38 pairs with A51 in a reverse–Watson-Crick orientation with G1 rotated by 12.8° relative to the U38:A51 plane. In the undocked structure, the orientation of stem C prevents U38 from participating in this base triple or any other interaction, and the resulting disorder of this residue is evident in the electron density map. The consequence of this interaction on the detailed conformation of the ligation site can be observed by overlaying the ligation junctions of the docked and undocked conformers (Fig. 4A). The active site phosphorus is shifted 1.86 Å between conformers P and Q. Although the construct crystallized for these experiments was the ligation product of the reaction, and specific conclusions regarding the preligation complex cannot be extrapolated, it is clear that the interaction with U38 to form the G:A:U base triple has a discernible effect on the positions of the active site atoms.

Mg^{2+} binding and the ribozyme's chemical mechanism. The L1 ligase is an obligate metalloenzyme that is highly specific for Mg^{2+}. It was selected in the presence of 60 mM $MgCl_2$ and functions optimally in Mg^{2+} concentrations as high as 100 mM. None of the other common divalent metal ions, including manganese, are able to substitute for Mg^{2+}, which suggests a role for Mg^{2+} in the chemical mechanism of catalysis. Inspection of $2F_{obs} - F_{calc}$ and $F_{obs} - F_{calc}$ difference Fourier maps allowed identification of several potential high-occupancy Mg^{2+} sites above 5σ. The most

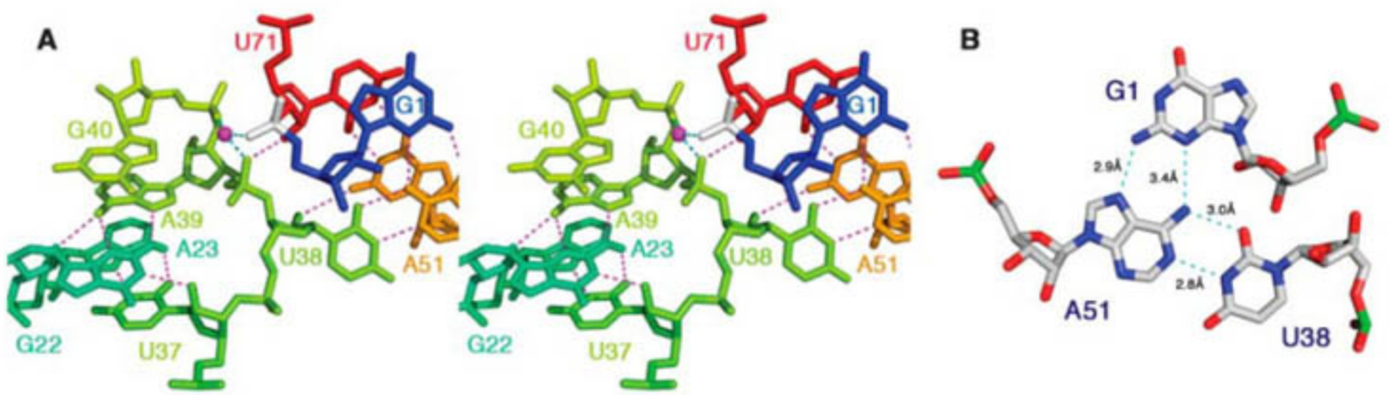

Fig. 3. Architecture of the ribozyme core and interhelical base triple interaction. (**A**) Stereograph of the spatial disposition of the invariant nucleotides in the active site of the ribozyme Q, using the color-coding of Fig. 2A. The sheared G22:A39 and reverse-Hoogsteen A23:U37 exclude U38 from the helical stack, permitting it to make a tertiary interaction with the stem A ligation site in the form of a base triple. The ligation-site phosphate is shown in white; hydrogen bonds are indicated as magenta dotted lines, a Mg^{2+} ion that bridges the helices of stems A and C is shown as a magenta sphere, and its three direct coordinations to the A39, G40 (light green) and G1 (white) phosphates are shown as light blue dotted lines. U71 (shown in red) forms a wobble pair with G52 (shown in orange). (**B**) Close-up of the interhelical G1:A51:U38 base triple. The G:A interaction is a sheared base pair, and the A:U interaction is a reverse–Watson-Crick base pair.

prominent of these peaks (Fig. 4B) is located proximal to the ligation site of the docked structure Q and is centered 2.2 Å from the nonbridging phosphate oxygens of A39 and G40 of stem C, making an angle of 91° between them. This site is also 4.5 Å from the N7 of G40, a distance and orientation consistent with a water-mediated coordination (*26*). On the basis of the nearly perfect resemblance to the ideal geometry for an octahedrally coordinated Mg^{2+} ion, and its incompatibility with water hydrogen-bonding distances, we have assigned this as a Mg^{2+} site. In addition to coordinating the two adjacent phosphates in stem C, the Mg^{2+} ion also makes a 2.2 Å contact to the ligation-site phosphate of G1 (Fig. 4B), thus bridging the stem C and stem A helices. This bridge and the U38:G1:A51 base triple form the main tertiary contacts that stabilize the docking of stems C and A in the ligase ribozyme and lock the molecule into what appears to be an active conformation.

The bond distances (2.2 Å) and angle (91°) between the nonbridging phosphate oxygens of A39 and G40 and the ligation-site Mg^{2+} are both (within experimental error) ideal for an octahedrally coordinated complex. The geometry of the complex with respect to the ligation-site phosphate is less ideal, with a Mg-O distance of 2.2 Å and angles of 86° and 153° between the phosphate oxygen of G1 and the phosphate oxygens of A39 and G40, respectively. Based upon the location of the Mg^{2+} ion bound to the ligation-site phosphate, the previously observed strict requirement for Mg^{2+} ions in the ligase reaction, as well as the details of this ion's coordination geometry, we propose that the ligation-site Mg^{2+} ion binds tightly to three phosphates that make up a specific Mg^{2+} binding pocket that is formed when stem C makes specific tertiary contacts with the invariant ligation site nucleotides. In addition, we hypothesize that the catalytic role of this Mg^{2+} ion may include screening the excess negative charge that accumulates in the transition state.

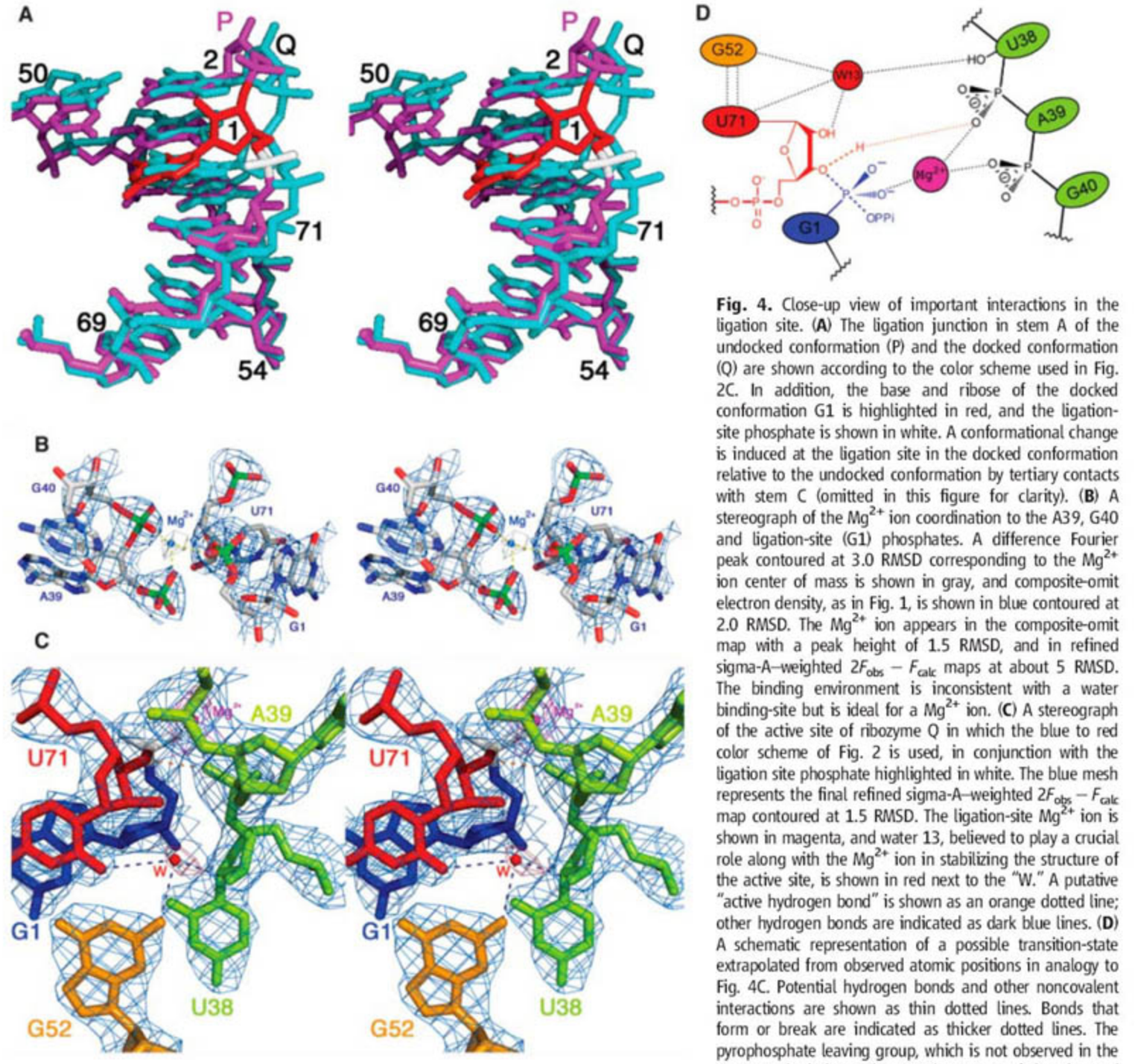

Fig. 4. Close-up view of important interactions in the ligation site. (**A**) The ligation junction in stem A of the undocked conformation (P) and the docked conformation (Q) are shown according to the color scheme used in Fig. 2C. In addition, the base and ribose of the docked conformation G1 is highlighted in red, and the ligation-site phosphate is shown in white. A conformational change is induced at the ligation site in the docked conformation relative to the undocked conformation by tertiary contacts with stem C (omitted in this figure for clarity). (**B**) A stereograph of the Mg^{2+} ion coordination to the A39, G40 and ligation-site (G1) phosphates. A difference Fourier peak contoured at 3.0 RMSD corresponding to the Mg^{2+} ion center of mass is shown in gray, and composite-omit electron density, as in Fig. 1, is shown in blue contoured at 2.0 RMSD. The Mg^{2+} ion appears in the composite-omit map with a peak height of 1.5 RMSD, and in refined sigma-A–weighted $2F_{obs} - F_{calc}$ maps at about 5 RMSD. The binding environment is inconsistent with a water binding-site but is ideal for a Mg^{2+} ion. (**C**) A stereograph of the active site of ribozyme Q in which the blue to red color scheme of Fig. 2 is used, in conjunction with the ligation site phosphate highlighted in white. The blue mesh represents the final refined sigma-A–weighted $2F_{obs} - F_{calc}$ map contoured at 1.5 RMSD. The ligation-site Mg^{2+} ion is shown in magenta, and water 13, believed to play a crucial role along with the Mg^{2+} ion in stabilizing the structure of the active site, is shown in red next to the "W." A putative "active hydrogen bond" is shown as an orange dotted line; other hydrogen bonds are indicated as dark blue lines. (**D**) A schematic representation of a possible transition-state extrapolated from observed atomic positions in analogy to Fig. 4C. Potential hydrogen bonds and other noncovalent interactions are shown as thin dotted lines. Bonds that form or break are indicated as thicker dotted lines. The pyrophosphate leaving group, which is not observed in the structure, is designated as OPPi. Because of the observed 2.9 Å separation of 3′-O and the O1P of A39, which is also coordinated by the Mg^{2+} ion, the potential for an active hydrogen bond involved in nucleophile generation is indicated. As the bond between the 3′-O and the phosphorus of G1 forms, the (unobserved) pyrophosphate group departs.

L1 ribozyme catalysis and regioselectivity. The ribose of U71 that contains the 3′-hydroxyl nucleophile of the ligation reaction participates in an extensive hydrogen-bonding network within the catalytic pocket including the A39 phosphate of stem C, and the 2′-hydroxyl of U38 via water W13 (Fig. 4C). This network suggests why the L1 ligase is regioselective for formation of the biologically relevant 5′ to 3′ phosphodiester bond rather than a 5′ to 2′ bond. The 3′-oxygen of U71 in the ligation product is only 2.9 Å from the nonbridging phosphate oxygen that is coordinated with the ligation-site Mg^{2+} ion. Although clearly within hydrogen-bonding distance, the 3′-oxygen cannot donate a hydrogen bond to the phosphate oxygen because it has already formed an ester linkage to the G1 phosphate. If the positions of these atoms are retained in the preligation complex, the O1P phosphate of A39 would be ideally positioned to abstract a proton from the 3′-oxygen, thus generating the attacking nucleophile. Although the 2′-hydroxyl of U71 also resides within potential hydrogen-bonding distance to this phosphate oxygen, it, unlike the 3′-oxygen, has a tightly bound water molecule as a hydrogen-bonding partner. This water molecule, W13, interacts specifically not only with the 2′-hydroxyl of U71, but also with the 2′-hydroxyl of U38, the exocyclic amine of G52, and possibly, the exocyclic oxygen of U71 (Fig. 4C). This hydrogen-bonding network may sequester the 2′-hydroxyl of U71 away from the ligation-site phosphate, and in the event of deprotonation, the 2′-alkoxide might be resupplied with a proton from water W13, which would effectively quench the side reaction (Fig. 4D).

The in vitro–evolved L1 RNA ligase ribozyme, therefore, appears to fold into a compact structure in which a set of invariant nucleotides interact to create a catalytic pocket capable of juxtaposing the ligation ends with a bound Mg^{2+} ion cofactor. The network of specific structural interactions that promote catalysis of phosphodiester bond formation, including transition-state stabilization interactions and functional group positioning for general base catalysis, as well as the propensity to fold into a preformed active site capable of binding a substrate and a metal ion cofactor, are each reminiscent of what has been observed in several natural ribozymes. The L1 ligase ribozyme thus demonstrates, in principle, that RNA indeed has the ability to evolve into a structure capable of catalyzing regiospecific phosphodiester bond ligation and appears to use strategies of transition-state stabilization and acid-base catalysis similar to those that exist for natural ribozymes and protein enzymes.

References and Notes

1. K. Kruger *et al.*, *Cell* **31**, 147 (1982).
2. C. Guerrier-Takada, K. Gardiner, T. Marsh, N. Pace, S. Altman, *Cell* **35**, 849 (1983).
3. A. J. Zaug, T. R. Cech, *Science* **231**, 470 (1986).
4. R. F. Gesteland, J. F. Atkins, Eds., *The RNA World* (Cold Spring Harbor Laboratory Press, Plainview, New York, 1993).
5. J. A. Doudna, T. R. Cech, *Nature* **418**, 222 (2002).
6. K. E. McGinness, G. F. Joyce, *Chem. Biol.* **10**, 5 (2003).
7. D. P. Bartel, J. W. Szostak, *Science* **261**, 1411 (1993).
8. E. H. Ekland, J. W. Szostak, D. P. Bartel, *Science* **269**, 364 (1995).
9. M. P. Robertson, A. D. Ellington, *Nat. Biotechnol.* **17**, 62 (1999).
10. L. F. Landweber, I. D. Pokrovskaya, *Proc. Natl. Acad. Sci. U.S.A.* **96**, 173 (1999).
11. J. Rogers, G. F. Joyce, *Nature* **402**, 323 (1999).
12. L. Jaeger, M. C. Wright, G. F. Joyce, *Proc. Natl. Acad. Sci. U.S.A.* **96**, 14712 (1999).
13. Y. Ikawa, K. Tsuda, S. Matsumura, T. Inoue, *Proc. Natl. Acad. Sci. U.S.A.* **101**, 13750 (2004).
14. W. K. Johnston, P. J. Unrau, M. S. Lawrence, M. E. Glasner, D. P. Bartel, *Science* **292**, 1319 (2001).
15. M. S. Lawrence, D. P. Bartel, *Biochemistry* **42**, 8748 (2003).
16. M. S. Lawrence, D. P. Bartel, *RNA* **11**, 1173 (2005).
17. M. P. Robertson, A. D. Ellington, *Nucleic Acids Res.* **28**, 1751 (2000).
18. M. P. Robertson, A. D. Ellington, *Nat. Biotechnol.* **19**, 650 (2001).
19. M. P. Robertson, S. M. Knudsen, A. D. Ellington, *RNA* **10**, 114 (2004).
20. M. P. Robertson, J. R. Hesselberth, A. D. Ellington, *RNA* **7**, 513 (2001).
21. See RNA preparation in materials and methods, available as supporting material on *Science* Online.
22. See crystallization and structural solution in materials and methods, available as supporting material on *Science* Online.
23. H. W. Pley, K. M. Flaherty, D. B. McKay, *Nature* **372**, 68 (1994).
24. W. G. Scott, J. T. Finch, A. Klug, *Cell* **81**, 991 (1995).
25. M. Martick, W. G. Scott, *Cell* **126**, 309 (2006).
26. D. Bandyopadhyay, D. Bhattacharyya, *J. Biomol. Struct. Dyn.* **21**, 447 (2003).

27. We thank A. Ellington, H. Noller, members of the Scott laboratory and of the RNA Center at UCSC for helpful discussions and support, and the NIH and W. M. Keck Foundation for funding. We dedicate this paper to Professor Stanley L. Miller. Coordinates and data: F_{obs} and coordinates have been deposited with Protein Data Bank accession code 2OIU. These data, as well as the composite-omit $2F_{obs} - F_{calc}$ and other electron density maps described in the paper, are available from http://xanana.ucsc.edu/L1.

Supporting Online Material

www.sciencemag.org/cgi/content/full/315/5818/1549/DC1
Materials and Methods
Figs. S1 and S2
Table S1
References

12 October 2006; accepted 25 January 2007
10.1126/science.1136231

REPORTS

Resonant Amplification of Magnetic Domain-Wall Motion by a Train of Current Pulses

Luc Thomas,* Masamitsu Hayashi, Xin Jiang, Rai Moriya, Charles Rettner, Stuart Parkin*

The current-induced motion of magnetic domain walls confined to nanostructures is of interest for applications in magnetoelectronic devices in which the domain wall serves as the logic gate or memory element. The injection of spin-polarized current below a threshold value through a domain wall confined to a pinning potential results in its precessional motion within the potential well. We show that by using a short train of current pulses, whose length and spacing are tuned to this precession frequency, the domain wall's oscillations can be resonantly amplified. This makes possible the motion of domain walls with much reduced currents, more than five times smaller than in the absence of resonant amplification.

Recent theoretical (*1*–*5*) and experimental (*6*–*14*) work has focused on the manipulation of magnetic domain walls (DWs) in nanoscaled magnetoelectronic devices by means of spin-polarized current passing directly through the DW. Current-induced motion of DWs has distinctly different characteristics from their motion brought about by magnetic fields, making it particularly useful for memory storage applications (*15*). For metallic nanowires (typically permalloy, $Ni_{81}Fe_{19}$), current-driven DW motion occurs only at zero or low magnetic fields if the current density exceeds a threshold value on the order of 10^8 A/cm^2. It is not yet clear whether this threshold has a fundamental origin or is related to pinning sites in the nanowires. Nevertheless, such high current densities are impractical for device applications, and it is crucial to find ways to reduce this threshold value.

Spin-polarized current injected across a DW confined to a pinning potential results in damped oscillations of the DW within the potential well, in which the DW position along the nanowire oscillates out of phase with its momentum (*14*). Here we show that oscillations in the DW position and momentum can be resonantly

IBM Almaden Research Center, 650 Harry Road, San Jose, CA 95120, USA.

*To whom correspondence should be addressed. E-mail: lucthom@us.ibm.com (L.T.); parkin@almaden.ibm.com (S.P.)

amplified by using a short sequence of current pulses, whose lengths and separations are tuned to its oscillation frequency.

We first introduce a one-dimensional (1D) analytical model to describe the resonant depinning of a DW from a parabolic potential well. Such a well mimics an intrinsic or artificially created defect, such as a notch, in the nanowire. The 1D model was first introduced to describe the field-induced dynamics of DWs (*16*) and has recently been extended to include interactions with spin-polarized current (*1*–*5*). In this model, the DW dynamics can be described by just two variables: the DW position q and the angle Ψ by which the DW's magnetization is tilted out of the plane of the nanowire. The deviation of Ψ from its equilibrium value is akin to the DW's momentum (*17*).

The temporal evolution of q and Ψ for a DW excited by dc current and by single and several current pulses, each of the same amplitude as the dc current, are compared in Fig. 1A. The current density is expressed in terms of the spin torque amplitude, which has the dimension of a velocity. For dc current (Fig. 1A, a panels), both q and Ψ oscillate, out of phase with each other, but with the same characteristic frequency. The latter is related to the DW's mass and the slope of the pinning potential (*13*, *14*). The oscillation amplitude decreases with time because of Gilbert damping. Figure 1A (b panels) shows clearly that using short current pulses as compared to the damping time can lead to amplification of the DW's oscillations. Amplification occurs when the current is cut off at times close to odd multiples of half the precession period when q is close to zero (the DW is near the center of the well) and Ψ is large. When the DW is only weakly pinned, the amplification of the DW's motion induced by a single current pulse may be sufficient to depin the DW (*14*). However, for stronger pinning potentials, additional properly timed current pulses can further amplify the DW's motion within the well. This occurs, for example, when two half-period long pulses of the same current polarity are injected into the DW separated by a half-period spacing (Fig. 1A, c panels). Amplification is even larger when successive current pulses of opposite polarities are used (Fig. 1A, d panels).

The mechanism responsible for the resonant amplification of the DW's trajectory can be understood by considering its trajectory in position/momentum phase space (Fig. 1B). In the absence of current, the DW is at $q = 0$, $\Psi = 0$ (black dot in Fig. 1B). With sufficiently long pulses, the DW spirals toward a new equilibrium state at $q = 0$ and a nonzero value of Ψ (negative for positive current), as shown by the red dot in Fig. 1B (see also a panels in Fig. 1A). At any given point in time, the DW's trajectory is a spiral toward an equilibrium point along the $q = 0$ axis but with different Ψ values, depending on the current amplitude and polarity. For example, when the current is suddenly turned off, the DW circles toward the point $q = 0$, $\Psi = 0$. If this happens when the DW has high momentum (large $|\Psi|$), then the initial radius of its new trajectory is increased so that the DW undergoes a larger excursion than it would otherwise have done with a longer current pulse. An even larger increase in the amplitude of the DW's orbit results if the current direction is

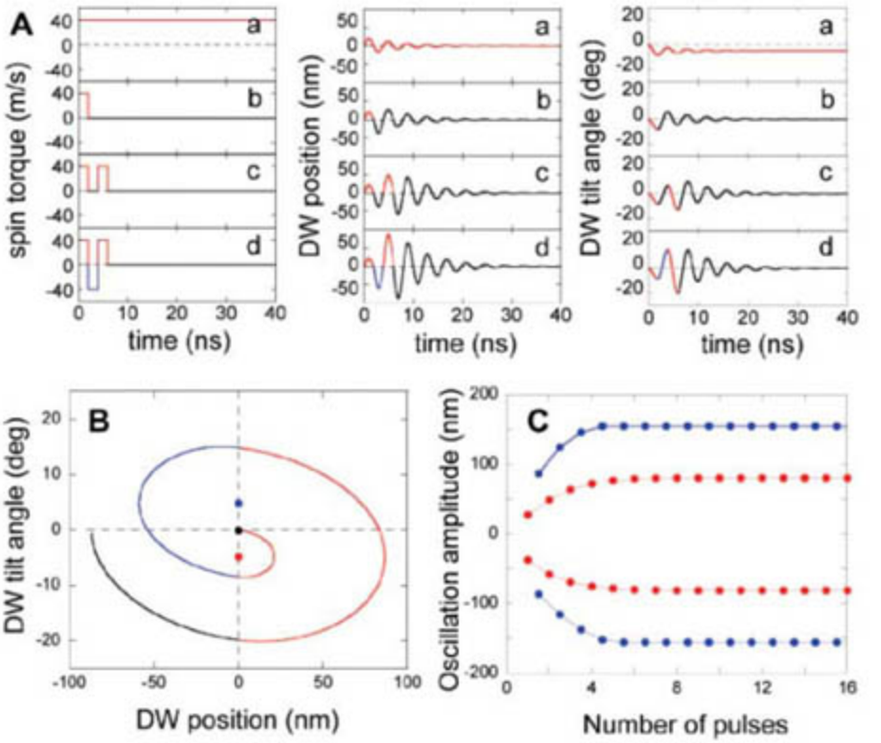

Fig. 1. (**A**) Pulse patterns, DW position, and DW tilt angle as a function of time, calculated using the 1D model (*17*). The deviation of the DW's tilt angle from its equilibrium value is proportional to the DW's momentum. (**B**) Trajectory of the DW in position/momentum phase space for 1.5 bipolar pulses. Dots show the equilibrium positions for zero (black), positive (red), and negative (blue) current. (**C**) Maximal values of the DW displacement along positive and negative directions for unipolar (red) and bipolar (blue) patterns of pulses at resonance.

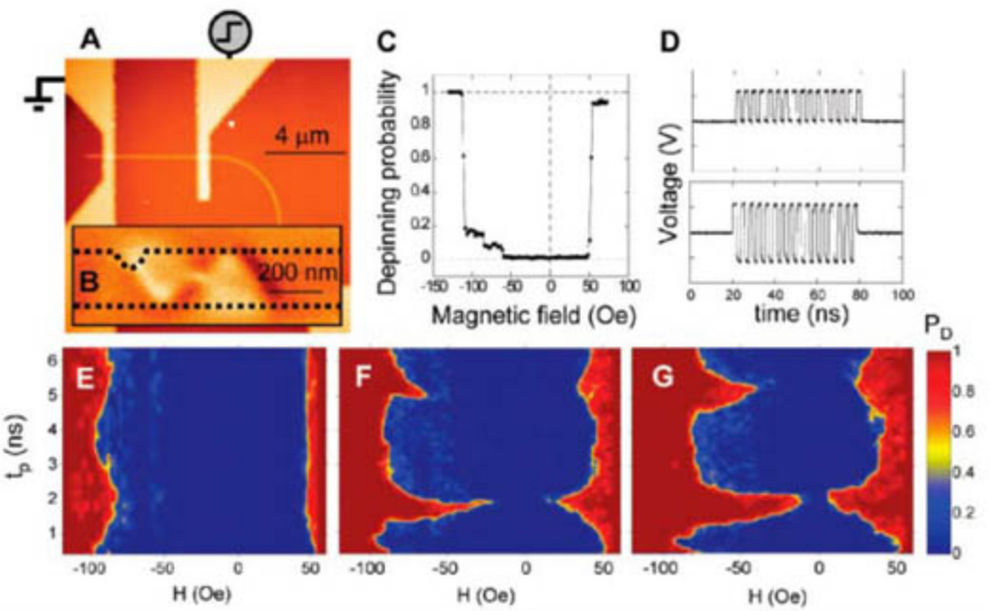

Fig. 2. (**A**) Atomic force microscopy (AFM) image of the permalloy nanowire and its electrical contacts. (**B**) Magnetic force microscopy image of a vortex DW pinned at the notch. Dashed lines show the edges of the wires as determined from the corresponding AFM image. (**C**) Probability of depinning a DW from the notch versus applied magnetic field. (**D**) Examples of pulse patterns: 16 unipolar pulses (top panel) and 15.5 bipolar pulses (bottom panel). (**E** to **G**) DW P_D at a constant pulse voltage of 1 V versus magnetic field H and pulse length t_p, for a single pulse (E), 16 unipolar pulses (F), and 15.5 bipolar pulses (G).

reversed rather than switched off, because the new equilibrium point is further away at a positive value of Ψ (blue dot in Fig. 1B). The amplitude of the DW's circling trajectory can be further increased by using a succession of properly timed unipolar or bipolar current pulses. However, because of Gilbert damping, this effect saturates after a few pulses, for reasonable values of the damping constant α (for example, $\alpha = 0.01$ in Fig. 1C). If the resonantly amplified DW motion exceeds the extent of the pinning potential, it follows that the DW will be depinned. The depinning current can thereby be reduced by an order of magnitude (*17*).

The predictions of the model were tested in a 200-nm-wide, 40-nm-thick permalloy nanowire (Fig. 2A). Experimental details can be found in (*14*, *17*). A triangular notch 120 nm wide and 70 nm deep, fabricated on one side of the wire, acted as a pinning site for the DW. A DW was positioned at the notch and was detected by its dc resistance. Magnetic force microscopy showed that the DW had a vortex structure (Fig. 2B). The strength of the pinning potential can be estimated from the fields required to depin the DW in the absence of current. Positive and negative fields drive the DW away from and across the notch, respectively. DWs were depinnned with a probability higher than 0.5 when the field magnitude H exceeded $H_D^+ = +53$ Oe and $H_D^- = -111$ Oe (D, depinning), respectively, for positive (+) and negative (–) fields (Fig. 2C). The current-induced depinning of the DW from the notch was probed by applying a series of current pulses between two contacts to the nanowire (Fig. 2A). A static magnetic field was also used to assist DW motion in either direction along the nanowire. The device resistance was measured before and after the injection of the current pulses to probe whether the DW had been depinned. This sequence was repeated 10 times under each set of conditions to determine the probability of depinning the DW, P_D. Two types of current pulse patterns were used, hereafter referred to as unipolar or bipolar (Fig. 2D, top and bottom panels, respectively). Positive voltage corresponds to current flowing from right to left in Fig. 2A (*17*).

Maps of P_D are shown in Fig. 2, E to G, for a constant pulse amplitude $V_p = 1.0$ V (corresponding to ~10^8 A/cm^2) as a function of the pulse length t_p and magnetic field H applied during the pulse. When a single pulse was applied (Fig. 2E), the DW only depinned when aided by large magnetic fields, and $H_D^+ \sim 48$ Oe was essentially independent of the pulse length t_p. In contrast, H_D^- exhibited slight oscillations between –84 Oe and –98 Oe as a function of t_p. This behavior can be explained by the precessional motion of the DW excited by current (*14*). When the current pulse length matches an odd multiple of half the precession period, the DW is depinned in slightly smaller fields. However, because the pinning from the notch is quite strong, this effect is observed only when the field is close to the zero-current depinning field. A much larger effect was observed for a train of 16 unipolar (Fig. 2F) or bipolar (Fig. 2G) pulses. In these cases, the depinning fields became extremely sensitive to the pulse length. Both H_D^+ and H_D^- were strongly reduced for $t_p \sim 1.9$ ns and also, to a lesser extent, for $t_p \sim 5.7$ ns (*18*).

Figure 3, A to C, shows maps of P_D for series of 16 pulses of a fixed length of 1.9 ns, corresponding to the first resonance peak of Fig. 2, F and G, as a function of the pulse amplitude and magnetic field. In the first case (Fig. 3A), there was no spacing between the pulses (the sequence was a single pulse of length 30.4 ns), and the critical current increased rapidly when the field was reduced. The data are asymmetric for positive and negative fields because of the asymmetry of the pinning potential profile (*12*). By contrast, the polarity of the current plays very little role in this regime of field-assisted current-driven depinning. For a sequence of 16 unipolar pulses (Fig. 3B), the critical current was strongly reduced. The depinning fields were reduced to ~ ±15 Oe for 1.0-V pulses. These depinning fields were essentially unchanged for higher pulse amplitudes, although they increased slightly at the highest amplitudes. For a sequence of 16 bipolar pulses (Fig. 3C), the critical current reduction was even more pronounced. Depinning fields were reduced to ±10 Oe for 0.5-V pulses. This represents a reduction of the critical current by a factor of more than 5 as compared to the single-pulse case. No zero-field depinning was observed, even for pulse amplitudes much larger than 0.5 V. We suggest that this is related to the tails of the pinning potential well from the notch, which may extend over long distances, most likely due to the elasticity of the DW profile, which is not included in the 1D model discussed above. Thus, in the absence of field, the DW probably remains trapped at the end of the sequence of current pulses, even though the DW may have moved a long distance. Such a behavior is well reproduced with the 1D model when, for example, a Lorentzian-shaped potential well is used. Tailoring the pinning potential profile by changing the notch shape and depth or by stiffening the magnetic material may allow for resonant DW depinning in zero field.

Finally, we explored the coherence time of the current-induced DW resonant motion by using a sequence of two unipolar or bipolar pulses. The pulse length was varied from 0.4 to 3.4 ns, corresponding to the first resonance peak in Fig. 2, F and G, and the interval between the center of the two pulses t_I was increased from 0 to 45 ns (i.e., $t_I = 0$ when the two pulses overlap one another). In this pump-probe experiment, the first pulse excites the precessional motion of the DW. Depending on the phase and amplitude of the DW precession at the time of the second probe pulse, the DW may or may not be depinned. Results are shown in Fig. 4 for a constant pulse amplitude $V_p = 1.3$ V and a constant field $H = -69$ Oe. Oscillations in P_D are clearly observed as a function of the time interval between the two pulses, which persist for times as long as

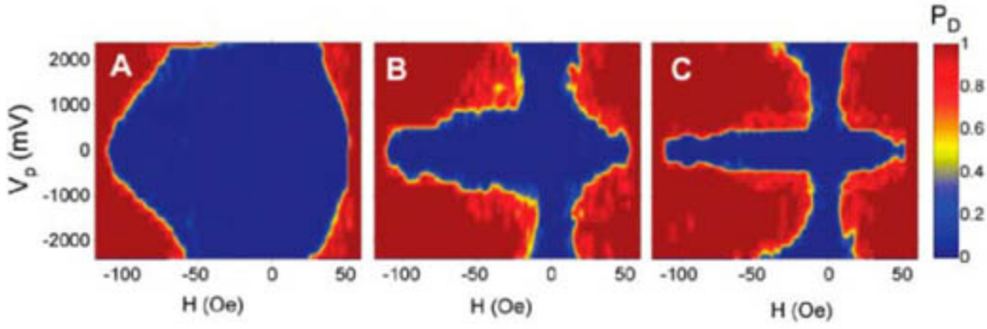

Fig. 3. DW P_D at constant pulse length versus magnetic field H and pulse amplitude V_p for different pulse patterns: (**A**) a single pulse 30.4 ns long; (**B**) 16 unipolar pulses, each 1.9 ns long (Fig. 2F); and (**C**) 15.5 bipolar pulses, each 1.9 ns long (Fig. 2G).

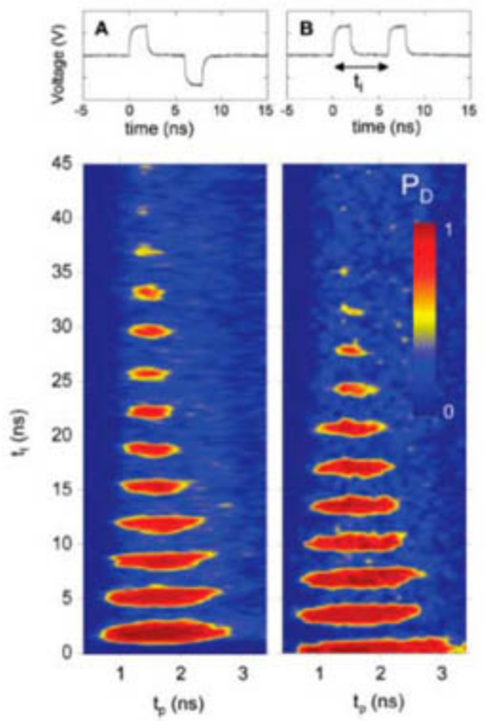

Fig. 4. DW P_D at constant magnetic field $H = -69$ Oe and pulse amplitude $V_p = 1.3$ V for a sequence of two pulses versus pulse length t_p and interval between the two pulses t_I for (**A**) bipolar pulses and (**B**) unipolar pulses. Pulse profiles are shown in the top two panels.

40 ns. As t_1 is progressively increased, Gilbert damping causes the amplitude of the oscillations to decrease, so that depinning is observed only in an increasingly narrower range of t_1 and t_p.

In good agreement with the 1D model, the probability of DW depinning on t_1 occurs out of phase for unipolar and bipolar pulses. For unipolar pulses, the second pulse leads to DW depinning when the interval is a multiple of the precession period, whereas for bipolar pulses, depinning is observed for odd multiples of half the precession period.

By using the concept of resonant amplification, DWs can be excited and moved with much reduced power, and, moreover, by tailoring pinning potentials, individual DWs in neighboring sites can be addressed. These results thus facilitate magnetoelectronic memory and logic devices with functionalities that are not possible with charge-based devices.

References and Notes

1. Z. Li, S. Zhang, *Phys. Rev. B* **70**, 024417 (2004).
2. G. Tatara, H. Kohno, *Phys. Rev. Lett.* **92**, 086601 (2004).
3. S. E. Barnes, S. Maekawa, *Phys. Rev. Lett.* **95**, 107204 (2005).
4. S. Zhang, Z. Li, *Phys. Rev. Lett.* **93**, 127204 (2004).
5. A. Thiaville, Y. Nakatani, J. Miltat, Y. Suzuki, *Europhys. Lett.* **69**, 990 (2005).
6. N. Vernier, D. A. Allwood, D. Atkinson, M. D. Cooke, R. P. Cowburn, *Europhys. Lett.* **65**, 526 (2004).
7. A. Yamaguchi *et al.*, *Phys. Rev. Lett.* **92**, 077205 (2004).
8. M. Klaui *et al.*, *Phys. Rev. Lett.* **95**, 026601 (2005).
9. M. Klaui *et al.*, *Phys. Rev. Lett.* **94**, 106601 (2005).
10. M. Yamanouchi, D. Chiba, F. Matsukura, H. Ohno, *Nature* **428**, 539 (2004).
11. D. Ravelosona, D. Lacour, J. A. Katine, B. D. Terris, C. Chappert, *Phys. Rev. Lett.* **95**, 117203 (2005).
12. M. Hayashi *et al.*, *Phys. Rev. Lett.* **97**, 207205 (2006).
13. E. Saitoh, H. Miyajima, T. Yamaoka, G. Tatara, *Nature* **432**, 203 (2004).
14. L. Thomas *et al.*, *Nature* **443**, 197 (2006).
15. S. S. P. Parkin, U.S. Patent 6,834,005 (2004).
16. A. P. Malozemoff, J. C. Slonczewski, *Magnetic Domain Walls in Bubble Material* (Academic Press, New York, 1979).
17. More details are available as supporting material on *Science* Online.
18. The second resonance occurs for pulse lengths of 3/2 oscillation periods, which is three times longer than that of the first resonance (1/2 oscillation period).

19. We acknowledge financial support from Defense Microelectronics Activity.

Supporting Online Material

www.sciencemag.org/cgi/content/full/315/5818/1553/DC1
Materials and Methods
Fig. S1
Reference

16 November 2006; accepted 16 January 2007
10.1126/science.1137662

Critical Behavior of a Trapped Interacting Bose Gas

T. Donner,[1] S. Ritter,[1] T. Bourdel,[1] A. Öttl,[1] M. Köhl,[1,2]* T. Esslinger[1]

The phase transition of Bose-Einstein condensation was studied in the critical regime, where fluctuations extend far beyond the length scale of thermal de Broglie waves. We used matter-wave interference to measure the correlation length of these critical fluctuations as a function of temperature. Observations of the diverging behavior of the correlation length above the critical temperature enabled us to determine the critical exponent of the correlation length for a trapped, weakly interacting Bose gas to be $\nu = 0.67 \pm 0.13$. This measurement has direct implications for the understanding of second-order phase transitions.

Phase transitions are among the most striking phenomena in nature. At a phase transition, minute variations in the conditions controlling a system can trigger a fundamental change of its properties. For example, lowering the temperature below a critical value creates a finite magnetization of ferromagnetic materials or, similarly, allows for the generation of superfluid currents. Generally, a transition takes place between a disordered phase and a phase exhibiting off-diagonal long-range order, which is the magnetization or the superfluid density in the above cases. Near a second-order phase transition point, the fluctuations of the order parameter are so dominant that they completely govern the behavior of the system on all length scales (*1*). In fact, the large-scale fluctuations in the vicinity of a transition already indicate the onset of the phase on the other side of the transition.

Near a second-order phase transition, macroscopic quantities show a universal scaling behavior that is characterized by critical exponents (*1*) that depend only on general properties of the system, such as its dimensionality, symmetry of the order parameter, or range of interaction. Accordingly, phase transitions are classified in terms of universality classes. Bose-Einstein condensation in three dimensions, for example, is in the same universality class as a three-dimensional XY model for magnets. Moreover, the physics of quantum phase transitions occurring at zero temperature can often be mapped onto thermally driven phase transitions in higher spatial dimensions.

The phase transition scenario of Bose-Einstein condensation in a weakly interacting atomic gas is unique, as it is free of impurities and the two-body interactions are precisely known. As the gas condenses, trapped bosonic atoms of a macroscopic number accumulate in a single quantum state and can be described by the condensate wave function, the order parameter of the transition. However, it has proven to be experimentally difficult to access the physics of the phase transition itself. In particular, the critical regime has escaped observation because it requires an extremely close and controlled approach to the critical temperature. Meanwhile, advanced theoretical methods have increased our understanding of the critical regime in a gas of weakly interacting bosons (*2*–*5*). Yet a theoretical

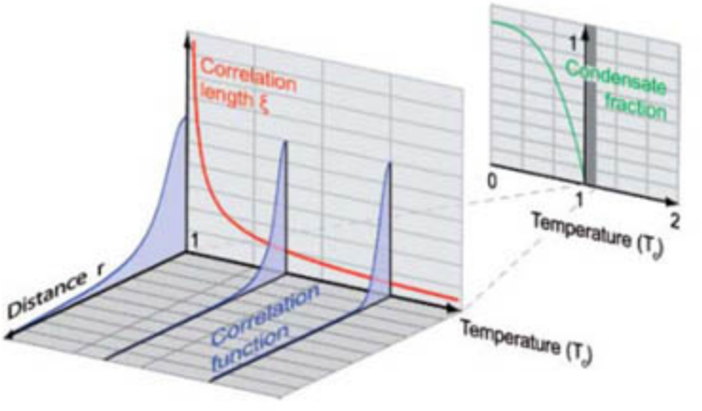

Fig. 1. Schematics of the correlation function and the correlation length close to the phase transition temperature of Bose-Einstein condensation. Above the critical temperature T_c the condensate fraction is zero, and for $T >> T_c$ the correlation function decays approximately as a Gaussian on a length scale set by the thermal de Broglie wavelength λ_{dB}. As the temperature approaches the critical temperature, long-range fluctuations start to govern the system and the correlation length ξ increases markedly. Exactly at the critical temperature, ξ diverges and the correlation function decays algebraically for $r > \lambda_{dB}$ (Eq. 1).

[1]Institute of Quantum Electronics, Eidgenössische Technische Hochschule (ETH) Zürich, CH-8093 Zürich, Switzerland. [2]Cavendish Laboratory, University of Cambridge, Cambridge CB3 0HE, UK.

*To whom correspondence should be addressed. E-mail: koehl@phys.ethz.ch

description of the experimental situation, a Bose gas in a harmonic trap, has remained elusive.

We report on a measurement of the correlation length of a trapped Bose gas within the critical regime just above the transition temperature. The visibility of a matter-wave interference pattern gave us direct access to the first-order correlation function. Exploiting our experimental temperature resolution of 0.3 nK (0.002 times the critical temperature), we observed the divergence of the correlation length and determined its critical exponent ν. This direct measurement of ν through the single-particle density matrix complements the measurements of other critical exponents in liquid He (*6*–*8*), which is believed to be in the same universality class as the weakly interacting Bose gas.

In a Bose gas, the physics of fluctuations of the order parameter is governed by different length scales. Far above the phase transition temperature, classical thermal fluctuations dominate. Their characteristic length scale is determined by the thermal de Broglie wavelength λ_{dB}, and the correlation function can be approximated by $\langle\Psi^{\dagger}(r)\Psi(0)\rangle \propto \exp(-\pi r^2/\lambda_{dB}^2)$, where r is the separation of the two probed locations (*9*) (Fig. 1). Nontrivial fluctuations of the order parameter Ψ close to the critical temperature become visible when their length scale becomes larger than the thermal de Broglie wavelength. The density matrix of a homogeneous Bose gas for $r > \lambda_{dB}$ can be expressed by the correlation function

$$\langle\Psi^{\dagger}(r)\Psi(0)\rangle \propto \frac{1}{r}\exp(-r/\xi) \qquad (1)$$

(*10*, *11*), where ξ denotes the correlation length of the order parameter. The correlation length ξ is a function of absolute temperature T and diverges as the system approaches the phase transition (Fig. 1). This results in the algebraic decay of the correlation function with distance $\langle\Psi^{\dagger}(r)\Psi(0)\rangle \propto 1/r$ at the phase transition. The theory of critical phenomena predicts a divergence of ξ according to a power law,

$$\xi \propto |(T - T_c)/T_c|^{-\nu} \qquad (2)$$

where ν is the critical exponent of the correlation length and T_c is the critical temperature. The value of the critical exponent depends only on the universality class of the system.

Although for noninteracting systems the critical exponents can be calculated exactly (*1*, *12*), the presence of interactions adds richness to the physics of the system. Determining the value of the critical exponent through Landau's theory of phase transitions results in a value of $\nu = \frac{1}{2}$ for the homogeneous system. This value is the result of both a classical theory and a mean-field approximation to quantum systems. However, calculations by Onsager (*13*) and the more recent techniques of the renormalization group method (*1*) showed that mean-field theory fails to describe the physics at a phase transition. Very close to the critical temperature—in the critical regime—the fluctuations become strongly correlated and a perturbative or mean-field treatment becomes impossible, making this regime very challenging.

Consider a weakly interacting Bose gas with density n and the interaction strength parameterized by the s-wave scattering length $a = 5.3$ nm in the dilute limit $n^{1/3}a \ll 1$. In the critical regime, mean-field theory fails because the fluctuations of Ψ become more dominant than its mean value. This can be determined by the Ginzburg criterion $\xi > \lambda_{dB}^2/(\sqrt{128}\pi^2 a) \approx 0.4$ μm (*14*, *15*). Similarly, these enhanced fluctuations are responsible for a nontrivial shift of the critical temperature of Bose-Einstein condensation (*2*–*4*, *16*). The critical regime of a weakly interacting Bose gas offers an intriguing possibility to study physics beyond the usual mean-field approximation (*17*), which until now has been observed in cold atomic gases only in reduced dimensionality (*18*–*21*).

In our experiment, we let two atomic beams, which originate from two different locations spaced by a distance r inside the trapped atom cloud, interfere. From the visibility of the interference pattern, the first-order correlation function (*22*) of the Bose gas above the critical temperature and the correlation length ξ can be determined.

We prepared a sample of 4×10^6 ^{87}Rb atoms in the $|F = 1, m_F = -1\rangle$ hyperfine ground state in a magnetic trap (*23*). The trapping frequencies were $(\omega_x, \omega_y, \omega_z) = 2\pi \times (39, 7, 29)$ Hz, where z denotes the vertical axis. Evaporatively cooled to just below the critical temperature, the sample reached a density of $n = 2.3 \times 10^{13}$ cm^{-3}, giving an elastic collision rate of 90 s^{-1}. The temperature was controlled by holding the atoms in the trap for a defined period of time, during which energy was transferred to the atoms as a result of resonant stray light, fluctuations of the trap potential, or background

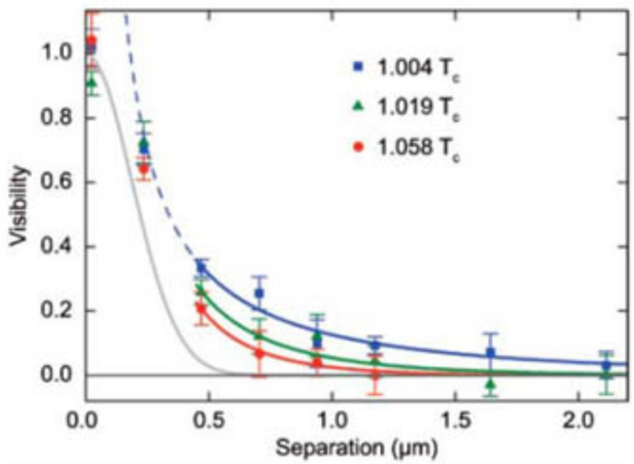

Fig. 2. Spatial correlation function of a trapped Bose gas close to the critical temperature. Shown is the visibility of a matter-wave interference pattern originating from two regions separated by r in an atomic cloud just above the transition temperature. The gray line is a Gaussian with a width given by λ_{dB}, which changes only marginally for the temperature range considered here. The experimental data show phase correlations extending far beyond the scale set by λ_{dB}. The solid line is a fit proportional to $(1/r)\exp(-r/\xi)$ for $r > \lambda_{dB}$. Each data point is the mean of 12 measurements on average; error bars are ±SD.

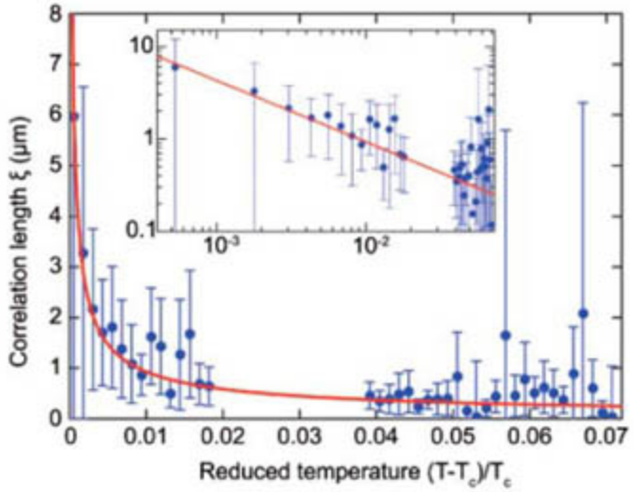

Fig. 3. Divergence of the correlation length ξ as a function of temperature. The red line is a fit of Eq. 2 to the data, with ν and T_c as free parameters. Plotted is one data set for a specific temporal offset t_0. The error bars are ±SD, according to fits to Eq. 1. They also reflect the scattering between different data sets. Inset: Double logarithmic plot of the same data.

gas collisions. From absorption images, we determined the heating rate to be 4.4 ± 0.8 nK s^{-1}. Using this technique, we covered a range of temperatures from $0.001 < (T - T_c)/T_c < 0.07$ over a time scale of seconds.

For output coupling of the atoms, we used microwave frequency fields to spin-flip the atoms into the magnetically untrapped state $|F = 2, m_F = 0\rangle$. The resonance condition for this transition is given by the local magnetic field, and the released atoms propagate downward because of gravity. The regions of output coupling are chosen symmetrically with respect to the center of the trapped cloud and can be approximated by horizontal planes spaced by a distance r (*22*); the two released atomic beams interfere with each other. For the measurement, we typically extracted 4×10^4 atoms over a time scale of 0.5 s, which is about 1% of the trapped sample. We detected the interference pattern in time at single-atom resolution with the use of a high-finesse optical cavity placed 36 mm below the center of the magnetic trap. An atom entering the cavity mode decreases the transmission of a probe beam resonant with the cavity. The geometry of our apparatus is such that only atoms with a transverse momentum $(p_x, p_y) \approx 0$ are detected, resulting in an overall detection efficiency of 1% for every atom output coupled from the cloud. From the arrival times of the atoms, we determined the visibility $V(r)$ of the interference pattern (*24*). From repeated measurements with different pairs of microwave frequencies, we measured $V(r)$ with r ranging from 0 to 4 λ_{dB} (where $\lambda_{dB} \approx 0.5$ μm).

With the given heat rate, a segmentation of the acquired visibility data into time bins of $\Delta t = 72$ ms allowed for a temperature resolution of 0.3 nK, which corresponds to $0.002\ T_c$. The time bin length was chosen to optimize between shot noise–limited determination of the visibility from the finite number of atom arrivals and sufficiently good temperature resolution. For the analysis, we chose time bins overlapping by 50%.

Figure 2 shows the measured visibility as a function of slit separation r very close to the critical temperature T_c. The visibility decays on a much longer length scale than predicted by the thermal de Broglie wavelength λ_{dB}. We fit the long distance tail $r > \lambda_{dB}$ with Eq. 1 (solid line) and determined the correlation length ξ. The strong temperature dependence of the correlation function is directly visible. As T approaches T_c, the visibility curves become more long-ranged, and similarly the correlation length ξ increases. The observation of long-range correlations shows how the size of the correlated regions strongly increases as the temperature is varied only minimally in the vicinity of the phase transition.

Figure 3 shows how the measured correlation length ξ diverges as the system approaches the critical temperature. Generally, an algebraic divergence of the correlation length is predicted. We fit our data with the power law according to Eq. 2, leaving the value of T_c as a free fit parameter, which has a typical relative error of 5×10^{-4}. Therefore, our analysis is independent of an exact calibration of both temperature and heating rate, provided that the heating rate is constant. The resulting value for the critical exponent is $\nu = 0.67 \pm 0.13$. The value of the critical exponent is averaged over 30 temporal offsets $0 < t_0 < \Delta t$ of the analyzing time bin window, and the error is the reduced χ^2 error. Systematic errors on the value of ν could be introduced by the detector response function. We found the visibility for a pure Bose-Einstein condensate to be 100% with a statistical error of 2% over the range of r investigated. This uncertainty of the visibility would amount to a systematic error of the critical exponent of 0.01 and is neglected as compared to the statistical error. The weak singularity of the heat capacity near the λ-transition (*1*) results in an error of ν of less than 0.01.

Finite size effects are expected when the correlation length is large (*25*, *26*), and they may lead to a slight underestimation of ν for our conditions. Moreover, the harmonic confining potential introduces a spatially varying density. The phase transition takes place at the center of the trap, and nonperturbative fluctuations are thus expected within a finite radius R (*5*). Using the Ginzburg criterion as given in (*14*), we find $R \approx 10$ μm, whereas the root-mean-square size of the thermal cloud is 58 μm. The longest distance we probed in our experiment is 2 μm, which is well below this radius R.

To date, in interacting systems the critical exponent ν has been determined for the homogeneous system. The λ-transition in liquid He is among the most accurately investigated systems at criticality. One expects to observe the same critical exponents even though the density differs by 10 orders of magnitude. In the measurements with liquid He, the critical exponent of the specific heat α has been measured in a spaceborne experiment (*8*). Through the scaling relation $\alpha = 2 - 3\nu$, the value of the critical exponent $\nu \approx 0.67$ is inferred, in agreement with theoretical predictions (*27*, *28*). Alternatively, the exponent $\zeta \approx 0.67$ (which is related to the superfluid density $\rho_s = |\Psi|^2$ instead of the order parameter Ψ) can be measured directly in second-sound experiments in liquid He (*6*, *7*). Although it is believed that $\nu = \zeta$ (*29*), a measurement of ν directly through the density matrix has so far been impossible with He. Further, this unique access to spatial correlations opens up new possibilities to study phase transitions using quantum gases of variable dimensionality or with tunable interactions.

References and Notes

1. J. Zinn Justin, *Quantum Field Theory and Critical Phenomena* (Oxford Univ. Press, Oxford, 1996).
2. G. Baym, J.-P. Blaizot, M. Holzmann, F. Laloë, D. Vautherin, *Phys. Rev. Lett.* **83**, 1703 (1999).
3. P. Arnold, G. Moore, *Phys. Rev. Lett.* **87**, 120401 (2001).
4. V. A. Kashurnikov, N. V. Prokof'ev, B. V. Svistunov, *Phys. Rev. Lett.* **87**, 120402 (2001).
5. P. Arnold, B. Tomasik, *Phys. Rev. A* **64**, 053609 (2001).
6. L. S. Goldner, N. Mulders, G. Ahlers, *J. Low Temp. Phys.* **93**, 131 (1993).
7. M. J. Adriaans, D. R. Swanson, J. A. Lipa, *Physica B* **194**, 733 (1993).
8. J. A. Lipa, J. A. Nissen, D. A. Stricker, D. R. Swanson, T. C. P. Chui, *Phys. Rev. B* **68**, 174518 (2003).
9. M. Naraschewski, R. J. Glauber, *Phys. Rev. A* **59**, 4595 (1999).
10. K. Huang, *Statistical Mechanics* (Wiley, New York, 1987).
11. In the general d-dimensional case, $\langle \Psi^\dagger(r)\Psi(0)\rangle \propto r^{-(d-2+\eta)} \exp(-r/\xi)$, where η is a critical exponent. The calculated and measured values of η are on the order of 10^{-2}, and therefore we neglect η in our analysis.
12. For a noninteracting gas, the critical exponent can be calculated as $\nu = 1$ for homogeneous systems and $\nu = ½$ for harmonically trapped systems.
13. L. Onsager, *Phys. Rev.* **65**, 117 (1944).
14. S. Giorgini, L. P. Pitaevskii, S. Stringari, *Phys. Rev. A* **54**, R4633 (1996).
15. The numerical coefficient may be different for a trapped gas and has been omitted in (*25*).
16. N. Prokof'ev, O. Ruebenacker, B. Svistunov, *Phys. Rev. A* **69**, 053625 (2004).
17. Q. Niu, I. Carusotto, A. B. Kuklov, *Phys. Rev. A* **73**, 053604 (2006).
18. T. Stöferle, H. Moritz, C. Schori, M. Köhl, T. Esslinger, *Phys. Rev. Lett.* **92**, 130403 (2004).
19. B. Paredes *et al.*, *Nature* **429**, 277 (2004).
20. T. Kinoshita, T. Wenger, D. S. Weiss, *Science* **305**, 1125 (2004); published online 29 July 2004 (10.1126/science.1100700).
21. Z. Hadzibabic, P. Krüger, M. Cheneau, B. Battelier, J. Dalibard, *Nature* **441**, 1118 (2006).
22. I. Bloch, T. W. Hänsch, T. Esslinger, *Nature* **403**, 166 (2000).
23. A. Öttl, S. Ritter, M. Köhl, T. Esslinger, *Rev. Sci. Instrum.* **77**, 063118 (2006).
24. T. Bourdel *et al.*, *Phys. Rev. A* **73**, 043602 (2006).
25. K. Damle, T. Senthil, S. N. Majumdar, S. Sachdev, *Europhys. Lett.* **36**, 7 (1996).
26. J. A. Lipa *et al.*, *Phys. Rev. Lett.* **84**, 4894 (2000).
27. M. Campostrini, M. Hasenbusch, A. Pelissetto, P. Rossi, E. Vicari, *Phys. Rev. B* **63**, 214503 (2001).
28. E. Burovski, J. Machta, N. Prokof'ev, B. Svistunov, *Phys. Rev. B* **74**, 132502 (2006).
29. B. D. Josephson, *Phys. Lett.* **21**, 608 (1966).

30. We thank G. Blatter, F. Brennecke, A. Kuklov, G. Shlyapnikov, M. Troyer, and W. Zwerger for insightful discussions. Supported by a European Union Marie Curie fellowship under contract MEIF-CT-2005-023612 (T.B.), SEP Information Sciences, the Optical Lattices and Quantum Information (OLAQUI) project of the European Union, and the Quantum Systems for Information Technology (QSIT) project of ETH Zürich.

13 December 2006; accepted 2 February 2007
10.1126/science.1138807

Rapid Changes in Ice Discharge from Greenland Outlet Glaciers

Ian M. Howat,[1,2]* Ian Joughin,[1] Ted A. Scambos[2]

Using satellite-derived surface elevation and velocity data, we found major short-term variations in recent ice discharge and mass loss at two of Greenland's largest outlet glaciers. Their combined rate of mass loss doubled in less than a year in 2004 and then decreased in 2006 to near the previous rates, likely as a result of fast re-equilibration of calving-front geometry after retreat. Total mass loss is a fraction of concurrent gravity-derived estimates, pointing to an alternative source of loss and the need for high-resolution observations of outlet dynamics and glacier geometry for sea-level rise predictions.

The recent, marked increase in ice discharge from many of Greenland's large outlet glaciers has upended the conventional view that variations in ice-sheet mass balance are dominated on short time scales by variations in surface balance, rather than ice dynamics. Beginning in the late 1990s and continuing through the past several years, the ice-flow speed of many tidewater outlet glaciers south of 72° North increased by up to 100%, increasing the ice sheet's contribution to sea-level rise by more than 0.25 mm/year (*1*). The synchronous and multiregional scale of this change and the recent increase in Arctic air and ocean temperatures suggest that these changes are linked to climate warming. The possibility that ice dynamics are so highly sensitive to climate change is of concern, because the physical processes that would drive such a relationship are poorly understood and are not realistically included in ice-sheet models used to predict rates of sea-level rise.

Current estimates of change in Greenland's ice discharge are based on velocity measurements taken 4 to 5 years apart (*1*). However, 50 to 100% increases in ice speed and thinning of tens of meters over a single year have been documented in Greenland and elsewhere (*2*–*6*). Therefore, discharge should be highly variable as well, even at subannual time scales. Large increases in tidewater glacier speed have been attributed to decreased flow resistance and increased along-flow stresses during retreat of the ice front (*2*, *3*, *7*). This suggests that changes in velocity and discharge are coupled to changes in tidewater glacier geometry and that the observed rapid changes may be a transient response to disequilibrium at the front. Therefore, accurate estimates of current rates of discharge and the potential for near-future change require observations of outlet glacier geometry and speed at high temporal resolution.

To assess short-term variability in outlet glacier dynamics, we examined speed, geometry, and discharge at two of Greenland's three largest outlet glaciers between 2000 and 2006. Located on the central east coast, Kangerdlugssuaq (KL) and Helheim (HH) represent 35% of east Greenland's total discharge (*1*). The calving fronts of both glaciers appeared relatively stable from the mid-20th century (*8*, *9*) until 2002, when HH retreated more than 7 km in 3 years (*2*). This was followed by a 5-km retreat of KL during the winter of 2004 to 2005 (*4*). These retreats are much greater than the 1- to 2-km seasonal fluctuations previously observed (*4*, *5*) and followed a sustained period of low-elevation ice thinning (*8*, *10*). Retreats were concurrent with accelerated ice flow (*1*, *2*). This acceleration increased rates of mass loss by 28 and 15 Gt/year at KL and HH, respectively, between 2000 and 2005, representing >40% of the ice sheet's increase in mass loss (*1*).

We measured summer surface speed and elevation for these glaciers using imagery acquired by the Advanced Spaceborne Thermal Emission and Reflection radiometer (ASTER) sensor aboard the Terra satellite, launched in 1999. We constructed Photogrammetric Digital Elevation Models (DEMs) from ASTER stereobands (3N and 3B) and validated them (Figs. 1D and 2D) using laser altimetry data sets collected by NASA's Airborne Topographic Mapper (ATM) in 2001, 2003, and 2005 (*10*). The root-mean-squared differences between DEM and ATM elevations are 10 m, which is similar to the uncertainty quoted in ASTER DEM validation studies (*11*) (Figs. 1D and 2D). Summer surface velocity was obtained from automated feature tracking between repeat, orthorectified principal component images of bands 1 to 3 (*2*, *12*). Uncertainty in these measurements is ~5 m per image pair, or 0.1 to 0.8 m/day for the data presented here. We determined winter velocities (±3% uncertainty) using radar speckle tracking between Canadian Space Agency Radar Satellite

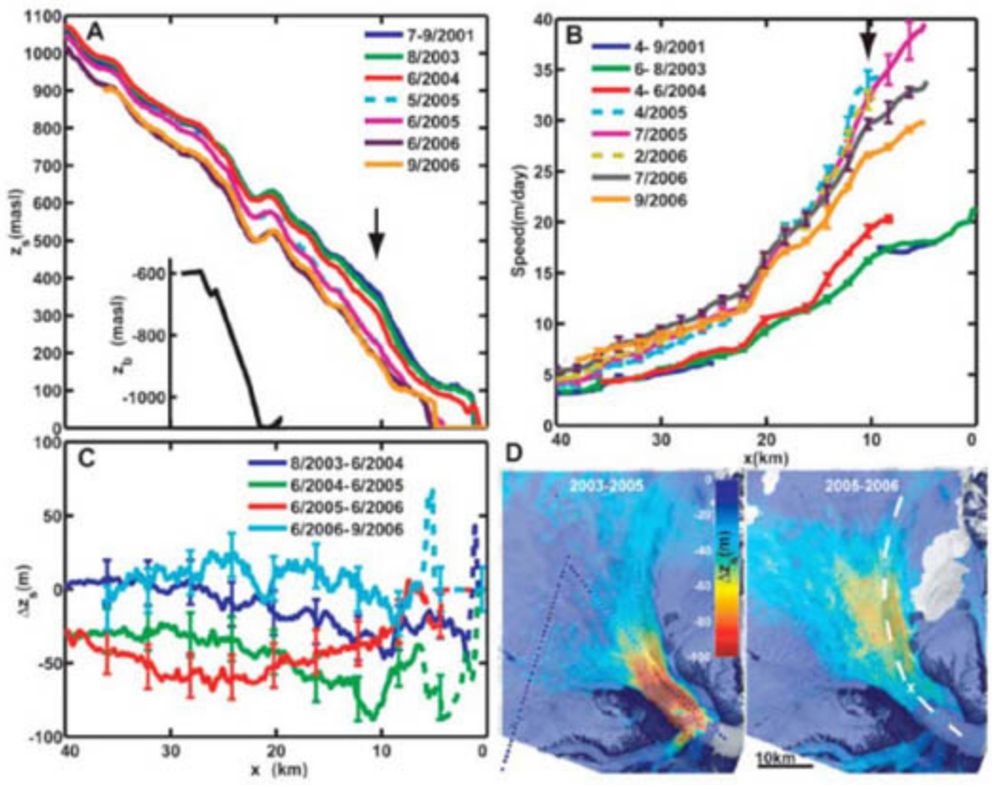

Fig. 1. KL glacier. (**A**) Surface elevation (z_s) from (solid) ASTER DEMs and (dashed) Airborne ATM laser altimetry and bed elevation (z_b) from CoRDS. (**B**) Surface velocity obtained from (solid) optical feature tracking and (dashed) radar speckle tracking along the main flow line, denoted by white dashes in (D). Arrows point to location of flux gate used for discharge calculation. (**C**) Elevation change along the same profile. Dashed segments are changes due to movement of the ice front. (**D**) Maps of elevation change from differenced ASTER DEMs overlaid on the 21 June 2005 image. Circles show repeat ATM altimetry measurements for the same time period and x marks flux-gate location. Error bars in (B) and (C) show means ± SD.

[1]Polar Science Center, Applied Physics Lab, University of Washington, 1013 Northeast 40th Street, Seattle, WA 98105–6698, USA. [2]National Snow and Ice Data Center, University of Colorado, 1540 30th Street, Boulder, CO, 80309–0449, USA.

*To whom correspondence should be addressed. E-mail: ihowat@apl.washington.edu

(RADARSAT) image pairs (24-day separation) (*13*). In some cases, combinations of multiple elevation and speed data sets from the same season improved spatial coverage and reduced errors. The University of Kansas Coherent Radar Depth Sounder (CoRDS) surveyed ice thickness and bed elevation at both glaciers in 2001 (*14*).

From summer 2004 to spring 2005, KL retreated by 5 km (*4*), and its speed increased by 80% near the front and by ~20% at 30 km inland (Fig. 1). Between April and July 2005, the increase in speed migrated rapidly inland with a ~5% decrease in speed close to the front and a ~7% increase in speed in areas farther inland (up-glacier). This upstream propagation continued from July 2005 through July 2006, with the near-front deceleration of ~15% and up-glacier acceleration of ~25%, with the transition between speedup and slowdown at ~15 km. The glacier thinned rapidly during acceleration, with 80 m of thinning near the front and thinning of at least 40 m extending 40 km inland by summer 2005. Thinning moved inland between 2005 and 2006, with a peak thinning of 68 m at about 26 km, but with virtually no thinning at the front. Average thinning over the glacier during the summer of 2006 declined to near zero, with some apparent thickening in areas on the main trunk.

Images from June 2003 are the first to indicate substantial retreat (2.1 km) at HH. During additional retreat over that summer, speedup of 20 to 40% extended at least 20 km up-glacier (Fig. 2). The ice front and speed changed little in 2004, but 4 km of new retreat yielded another major speedup (25%) in the summer of 2005. Many of the earlier data do not extend far inland, but echoing the pattern on KL, speeds from 2006 show a progressive inland acceleration accompanied by deceleration (25%) extending from about 15 km toward the ice front. As with KL, rapid thinning accompanied the large speed increases. By late summer 2006, strain rates indicate a region of compression at about 12 to 15 km. The initial HH acceleration in 2003 produced 40 m of thinning within about 15 km of the ice front. This thinning slowed to 10 m/year when there was little retreat from 2003 to 2004. The 4-km retreat from 2004 to 2005 moved the ice front over a 200-m bathymetric depression, bringing it to or near flotation. Between the summers of 2005 and 2006, the rate of thinning decreased within 20 km of the front, reaching zero at the front and increasing to 50 m/year 25 km from the front. During this period, the glacier advanced 4 km as a floating or near-floating tongue to near the 2003–2004 front position. It appears that the front of this floating tongue may have regrounded in summer 2006, contributing to the deceleration and the region of compression.

On both KL and HH, the data show a markedly similar progression of increasing down-glacier speed and thinning synchronous with retreat, followed by an inland migration of the speed increase. As the front restabilized, speed and thinning increased up-glacier and decreased down-glacier. This progression of dynamic response strongly suggests that the notable increases in acceleration and thinning are related to changes in calving-front position through variations in longitudinal stresses (*2*). Consistent with standard theories of tidewater glacier dynamics (*15*), rapid retreat at HH occurred as the front moved into deeper water and stopped where the bed slope reversed (Fig. 2). At both glaciers, the initial acceleration and thinning after retreat were concentrated within 10 to 20 km of the ice front, which would be the expected range of stress coupling (*16*). Relative thinning down-glacier increases the surface slope and driving stress up-glacier. By this means, thinning and acceleration are advected up-glacier (*17*). This can be seen at KL, where the maximum thinning rates moved ~10 km up-glacier between 2005 and 2006 (Fig. 1). This propagation rate is equal to about five times the distance-integrated 2005 ice speed, which is the approximate rate of advection of a kinematic wave traveling through ice (*18*).

We estimated discharge anomalies relative to the year 2000, when the glaciers were near balance, taking into account the changes in both speed and thickness (Fig. 3). At each glacier, our discharge estimates from 2000 to 2005 agree closely with mass-budget estimates (*1*). At KL, roughly 80% of the total increase in discharge occurred in less than 1 year in 2005, followed by a 25% drop the next year (Fig. 3). At HH, discharge increased 5 Gt/year between 2000 and

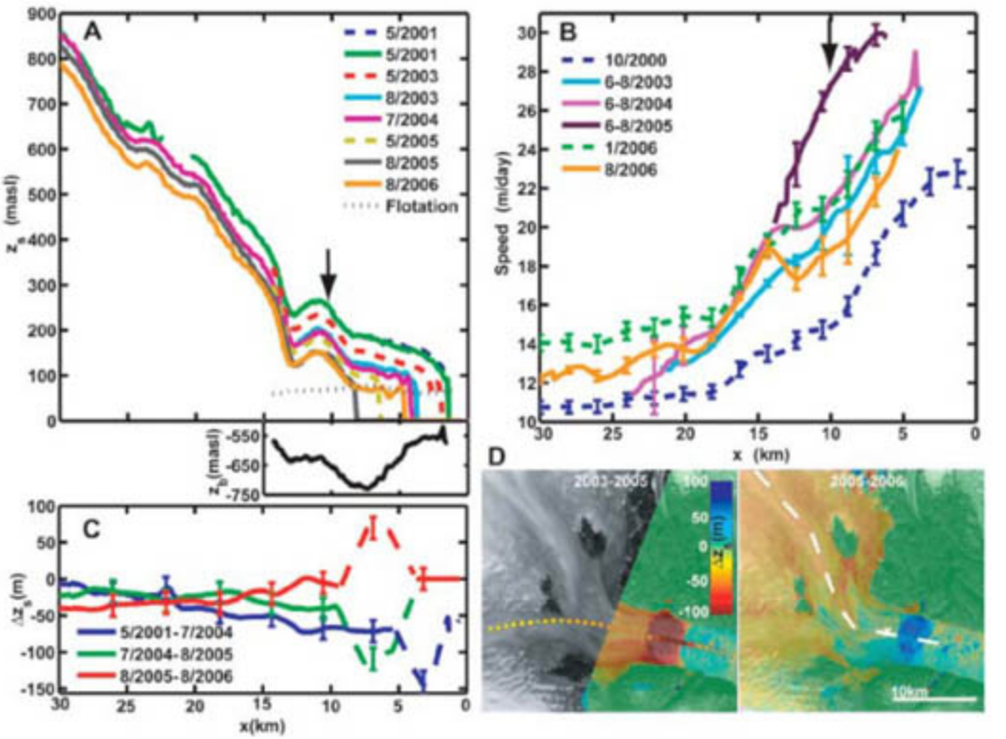

Fig. 2. (**A** to **D**) Same as Fig. 1 for HH, except (D) uses a 29 August 2005 image background.

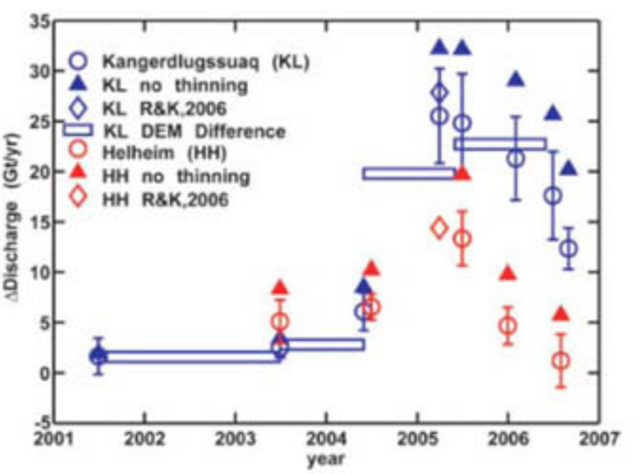

Fig. 3. Discharge anomaly from year 2000. Circles with error bars are calculated from speed and thickness change across flux gates shown in Figs. 1 and 2 with initial ice thickness obtained by dividing the year 2000 flux by the product of glacier width and 2000 speed (*1*). Uncertainties are the combinations of errors in ice elevation and speed. Triangles are the discharge anomaly with ice thickness held constant. Diamonds are the 2000 to 2005 discharge-change values from mass budget (*1*). Rectangles are KL mass-loss estimates from differencing repeat on-ice ASTER DEMs over the area shown in Fig. 1D. Spatial DEM coverage for HH is incomplete, preventing mass-loss calculations. The horizontal ranges in these estimates are the image acquisition dates, and the vertical range is the uncertainty.

2003 and by another 7 Gt/year between 2004 and 2005. It then dropped by more than 13 Gt/year in 2006, returning to near its 2000 value.

Integrating the time series of discharge anomaly from 2000 to 2006 gives totals of 52 Gt at KL and 30 Gt of excess discharge at HH (Fig. 3). Extensive DEM coverage of KL allows for a direct estimate of volume change over the lower basin (47 Gt), excluding any additional thinning at higher elevation. This loss estimate (47 Gt) agrees well with the KL discharge anomaly. When the existing imbalances from 2000 are factored in, the combined net loss of ice from 2000 to 2006 is 90 Gt, with 63 Gt of this loss in the interval from summer 2004 to summer 2006. The sharp increase in mass loss through these glaciers between 2004 and 2005 (32 Gt) can explain about 30% of the mass loss indicated by Gravity Recovery and Climate Experiment (GRACE) gravity observations for southeast Greenland (*19*).

Other GRACE observations suggest a 450 Gt ice loss from south Greenland between May 2004 and April 2006 that the authors mostly attribute to increased discharge from HH and KL (*20*). Although the timing of the increased loss agrees well with the KL and HH acceleration, our results suggest that the combined loss from these glaciers over this period can only account for 13% of this loss. Absent an extensive but unobserved acceleration elsewhere, measurements for other south Greenland glaciers suggest a loss increase from 2000 to 2005 of roughly 23 Gt/year (*1*). This suggests that despite large dynamic changes, much of the loss between 2004 and 2006 estimated from GRACE may be related to surface balance anomalies or other causes.

Our results indicate that large variations in outlet glacier discharge can produce large discharge anomalies in a span of a few years. Although the initial triggering for the recent changes is unclear, it is well known that very small perturbations to thickness can induce retreat in calving glaciers (*15*). In the cases we examined, large imbalances appear to have caused rapid adjustments in the glacier geometry, leading to a quick (~2-year) return to near balance, though some degree of moderate thinning may persist. The surface drawdown of 100 m or more at low elevations within the outlets may have substantial effects on summertime surface melt rates, potentially predisposing them to further ice thinning and retreat. However, prediction of near-future change will require detailed data on bed elevation and ice thickness. This is not yet available for most of the outlet glaciers.

Dynamic re-equilibration after a perturbation in geometry may not always be as rapid as observed here. For example, Jakobshavn Isbrae has maintained high speeds for several years after retreat and acceleration (fig. S1) (*3*). In this case, retreat from the fjord increased inflow from the sides, potentially resulting in lower thinning rates (~15 m/year) (*5*, *10*). Likewise, many glaciers along Greenland's northwest coast have retreated into the ice sheet with sustained thinning at rates of a few meters per year but show no apparent change in speed (*1*). This suggests that geometry and other characteristics unique to each glacier may determine the time scale over which discharge anomalies occur.

The highly variable dynamics of outlet glaciers suggest that special care must be taken in how mass-balance estimates are evaluated, particularly when extrapolating into the future, because short-term spikes could yield erroneous long-term trends. Rather than yielding a well-defined trend, our results are notable in that they show that Greenland mass balance can fluctuate rapidly. If these changes are the result of recent warm summers (*21*), continued warming may cause a long-term drawdown of the ice sheet through a series of such discharge anomalies, perhaps with a similar degree of variability. Therefore, accurate estimates of ice-sheet mass balance will require subannual observations of outlet glacier dynamics to avoid aliasing this rapidly varying signal.

References and Notes

1. E. Rignot, P. Kanagaratnam, *Science* **311**, 986 (2006).
2. I. M. Howat, I. Joughin, S. Tulaczyk, P. Gogineni, *Geophys. Res. Lett.* **32**, L22502 (2005).
3. I. Joughin, W. Abdalati, M. Fahnestock, *Nature* **432**, 608 (2004).
4. A. Luckman, A. Murray, R. De Lange, E. Hanna, *Geophys. Res. Lett.* **33**, L03503 (2006).
5. R. H. Thomas *et al.*, *J. Glaciol.* **49**, 231 (2003).
6. T. A. Scambos, J. A. Bohlander, C. A. Shuman, P. Skvarca, *Geophys. Res. Lett.* **31**, L18402 (2004).
7. R. H. Thomas, *J. Glaciol.* **50**, 57 (2004).
8. R. H. Thomas *et al.*, *Geophys. Res. Lett.* **27**, 1291 (2000).
9. A. Weidick, *U.S. Geol. Surv. Prof. Pap. 386-C* (1995), pp. C85–C87.
10. W. Krabill *et al.*, *Geophys. Res. Lett.* **31**, L24402 (2004).
11. B. T. San, M. L. Suzen, *Int. J. Remote Sens.* **26**, 5013 (2005).
12. T. A. Scambos, M. J. Dutkiewicz, J. C. Wilson, R. A. Bindschadler, *Remote Sens. Environ.* **42**, 177 (1992).
13. I. Joughin, *Ann. Glaciol.* **34**, 195 (2002).
14. S. Gogineni *et al.*, *J. Geophys. Res.* **106**, 33761 (2001).
15. M. F. Meier, A. Post, *J. Geophys. Res.* **92**, 9051 (1987).
16. B. Kamb, K. A. Echelmeyer, *J. Glaciol.* **32**, 267 (1986).
17. A. J. Payne, A. Vieli, A. P. Shepherd, D. J. Wingham, E. Rignot, *Geophys. Res. Lett.* **31**, L23401 (2004).
18. C. J. Van der Veen, in *Fundamentals of Glacier Dynamics* (A. A. Balkema, Rotterdam, Netherlands, 1999), p. 313.
19. S. B. Luthcke *et al.*, *Science* **314**, 1286 (2006).
20. I. Velicogna, J. Wahr, *Nature* **443**, 329 (2006).
21. I. Joughin, *Science* **311**, 1719 (2006).

22. NASA grants NNG06GE55G and NNG06GE50G supported the contribution of I.M.H. and T.A.S. NSF grant ARC-0531270 supported I.R.J.'s contribution.

Supporting Online Material

www.sciencemag.org/cgi/content/full/1138478/DC1
Fig. S1
Reference

6 December 2006; accepted 24 January 2007
Published online 8 February 2007;
10.1126/science.1138478
Include this information when citing this paper.

Conformationally Controlled Chemistry: Excited-State Dynamics Dictate Ground-State Reaction

Myung Hwa Kim,[1,2] Lei Shen,[1] Hongli Tao,[3] Todd J. Martinez,[3]* Arthur G. Suits[1,2]*

Ion imaging reveals distinct photodissociation dynamics for propanal cations initially prepared in either the cis or gauche conformation, even though these isomers differ only slightly in energy and face a small interconversion barrier. The product kinetic energy distributions for the hydrogen atom elimination channels are bimodal, and the two peaks are readily assigned to propanoyl cation or hydroxyallyl cation coproducts. Ab initio multiple spawning dynamical calculations suggest that distinct ultrafast dynamics in the excited state deposit each conformer in isolated regions of the ground-state potential energy surface, and, from these distinct regions, conformer interconversion does not effectively compete with dissociation.

From stereoselective synthesis to protein folding, conformational dynamics lie at the heart of chemistry (*1*). Molecular conformers typically interconvert via hindered rotations about single bonds, and the low energy barriers to these processes lead to equilibration even at low temperatures. Recent efforts to explore the detailed conformational energy landscapes of molecules have relied on stimulated emission pumping in jet-cooled beams, exciting then re-trapping molecules in different local minima to probe the interconversion barriers (*2*, *3*). Single-molecule methods have also been used to investigate conformational heterogeneity: Otherwise identical molecules exhibit vastly different rates in key steps of enzymatic processes (*4*, *5*). Conformational selectivity has been suggested as a means of achieving laser control of chemical outcomes (*6*). However, the low barriers for intercon-

[1]Department of Chemistry, Wayne State University, Detroit, MI 48202, USA. [2]Department of Chemistry, Stony Brook University, Stony Brook, NY 11794, USA. [3]Department of Chemistry, University of Illinois, Champaign, IL 61801, USA.

*To whom correspondence should be addressed. E-mail: asuits@chem.wayne.edu (A.G.S.); tjm@spawn.scs.uiuc.edu (T.J.M.)

version relative to the energy of photoexcitation or chemical transformation make this a daunting challenge.

Despite these considerations, limited evidence of conformation-selective dynamics has been seen. Park and co-workers reported distinct time-of-flight profiles in dissociation of specific iodopropane ion conformers prepared by mass-analyzed threshold ionization (*7*). They ascribed this result to the formation of distinct product isomers via direct dissociation from repulsive excited states. In another study, the product distribution observed upon photodissociation of *cis*- or *trans*-formic acid in an argon matrix depended markedly on the initial conformation (*8*). Theoretical calculations were unable to reproduce this effect in the ground state, so excited-state processes or matrix interactions were suggested as the likely source of the conformational specificity (*9*). A recent theoretical study has predicted distinct photoionization dynamics for different glycine conformers, but no experiments have yet been reported to confirm this prediction (*10*).

Here, we show strongly conformation-specific product distributions in photodissociation of propanal cation, and these experimental results are interpreted with the aid of ab initio multiple spawning (AIMS) calculations of the excited-state dynamics. The calculations reveal characteristics of the excited-state potential energy surface (PES) responsible for this behavior.

Propanal exists in two different conformations: a cis form with a planar CCCO backbone and a gauche form with the carbonyl rotated out of the plane. For the neutral molecule, the gauche form lies 270 to 400 cm^{-1} higher in energy than the cis form, and the cis-to-gauche interconversion barrier is ~800 cm^{-1} (*11*). The molecular structures of the cation conformers are quite similar to those of the neutral molecules, but the gauche form is slightly lower in energy and the barrier separating it from the cis form is ~344 cm^{-1} (*12*). In the experiments reported here, we spectroscopically selected one of the two conformers in a molecular beam, ionized it, and then subjected the resulting ions to photodissociation. Ion images (*13*, *14*) revealed the full product velocity distributions for the photodissociation event for a particular conformer.

The experiments were performed in a reflectron multimass imaging apparatus operated in the linear mode, with the use of dc slice imaging (*15*, *16*). A molecular beam of propanal seeded in helium was crossed by an ultraviolet (~370 nm) laser beam tuned to a two-photon resonance of *cis*- or *gauche*-propanal via the 3s Rydberg state (*17*). Ionization by a third photon produced the cation in the same conformation (>98%) and the same vibrational level (>80%) as the initially prepared Rydberg state (*12*). The conformationally and vibrationally selected ions then absorbed a fourth photon, which resulted in dissociation. Although several distinct product channels exist, we focus on the reaction $C_3H_6O^+ \rightarrow C_3H_5O^+ + H$, the H atom elimination process. The $C_3H_5O^+$ product ions were accelerated under dc slice imaging conditions onto a 120-mm microchannel plate detector coupled to a phosphor screen, which is viewed by a video camera. Product images were integrated over ~200,000 laser shots. The product translational energy distributions were obtained from the images by means of a finite slice image reconstruction program (*18*).

Product images of $C_3H_5O^+$ (Fig. 1), obtained by dissociation of propanal cation, are shown in order of increasing excitation energy. Images were acquired for dissociation of the *cis*-propanal cation in the vibrationless level (Fig. 1A), with one quantum of the ν_{15}^+ vibrational mode excitation (CCCO backbone deformation) (Fig. 1B), for the vibrationless level of the gauche form of the cation (Fig. 1C), and for the cis form with two quanta of ν_{15}^+ mode excitation (Fig. 1D). The total excitation energy varied ~0.05 eV across these one-color experiments. All images

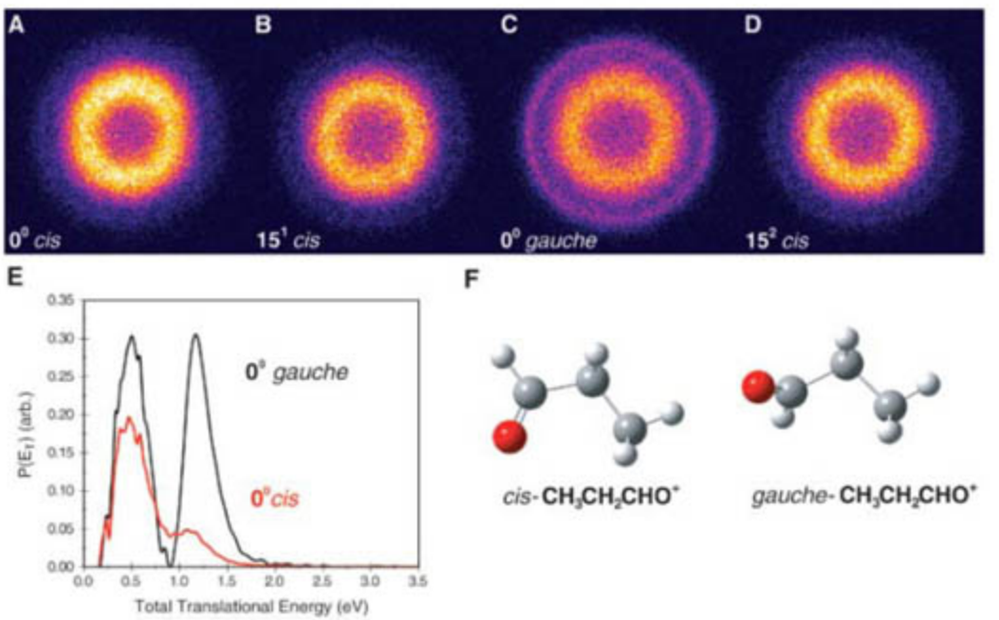

Fig. 1. (**A** to **D**) Sliced ion images of the $C_3H_5O^+$ product of propanal cation photodissociation, starting from the indicated conformer and vibrational level. (**E**) Total translational energy distributions from the images in (A) to (D) for the cis origin (red line) and gauche origin (black line). $P(E_T)$ is the probability of a given translational energy (E_T) (arbitrary units). (**F**) Equilibrium structures for the propanal cation conformers.

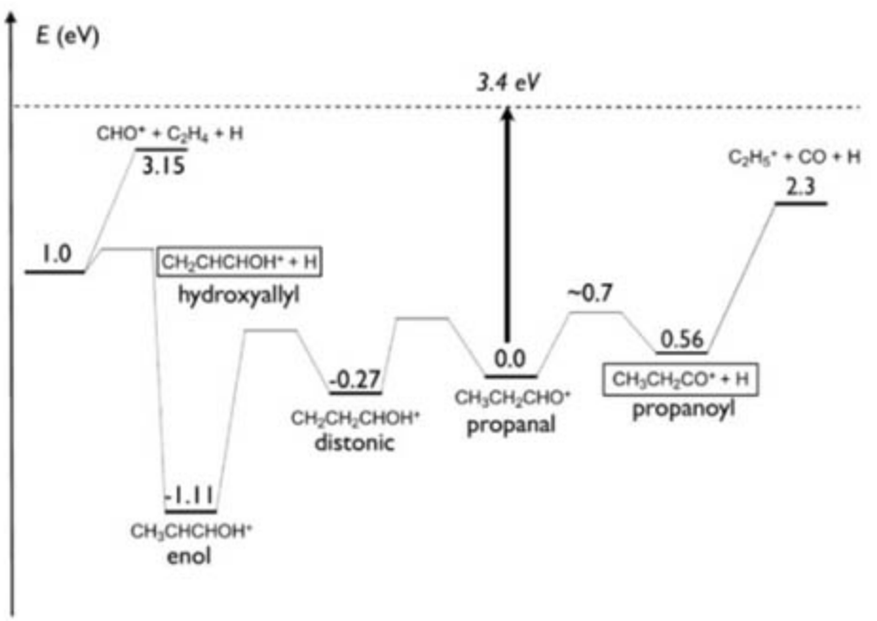

Fig. 2. Energy-level diagram for key isomers and products of propanal cation dissociation relative to the cation ground state (*20*, *21*). The excitation energy is shown as a dashed line. The difference in energy between the two conformers is too small to show on this diagram. *E*, energy.

show two rings; however, the outer ring is very weak for dissociation of the cis conformers and relatively intense for the gauche conformer. The translational energy distributions are shown in Fig. 1E for the vibrationless case for both the cis and the gauche conformers, obtained from the images in Fig. 1, A and C, respectively. Two product peaks are seen for each conformer but with different relative intensities. The faster component accounts for ~18% of the cis dissociation yield and ~48% of the gauche dissociation yield (*19*).

A further notable feature of the images is revealed in the translational energy distributions: The two rings show an abrupt truncation on the low-energy side that suggests the onset of secondary decomposition of vibrationally excited products. This feature allows unambiguous assignment of each peak to distinct product isomers (Fig. 2). For production of propanoyl cation ($CH_3CH_2CO^+$) + H, our excitation frequency leaves 2.87-eV excess energy available after dissociation, based on the recent threshold determination of 0.56 eV for this channel (*20*, *21*). The onset of secondary decomposition of propanoyl (to ethyl cation + CO) is expected at ~1.75 eV above this threshold, based on established thermochemistry (Fig. 2). Therefore, any propanoyl cation product formed with less than 1.13 eV of translational energy will undergo additional fragmentation and will not appear at the $C_3H_5O^+$ mass in our images. This fragmentation accounts for the abrupt cutoff of the fast peak at translational energies lower than ~1.0 eV and allows definitive assignment of the fast peak to the $CH_3CH_2CO^+$ + H channel.

Production of hydroxyallyl cation ($CH_2CHCHOH^+$) + H has a higher energy threshold, and hence less available energy for product recoil, than that of propanoyl cation. We therefore expect the former cation to show a lower translational energy release (*22*). Furthermore, this product has a secondary fragmentation threshold (to $HCO^+ + C_2H_4$) ~3.20 eV above the propanal cation origin. Thus, hydroxyallyl cations formed with less than ~0.2-eV translational energy will undergo fragmentation and will not appear at a mass/charge ratio = 57. This behavior is observed for the slow peak; we therefore confidently assign the slow peak to the hydroxyallyl channel.

Although the overall energetics allow these unambiguous peak assignments, they provide little insight into the origin of the dramatically different branching ratios exhibited by the two conformers, nor do they clarify whether the key dynamical events that are responsible occur in the electronically excited states or in the ground state (after internal conversion). The absence of angular anisotropy in the images suggests a long dissociation lifetime; moreover, the relatively low translational energy release implies high internal excitation in the products, which is also consistent with a long intermediate lifetime and dissociation from the ground state. However, it is difficult to imagine ground-state processes, with ~3.0-eV excess energy, that are sensitive to conformational differences on the order of 0.03 eV. To gain insight into these issues, we turned to AIMS calculations of the excited-state dynamics.

The AIMS method solves the electronic and nuclear Schrodinger equations simultaneously, allowing for a consistent and flexible description of electronic excitation and bond rearrangement. The breakdown of the Born-Oppenheimer approximation through nonadiabatic effects and electronic population dynamics is treated with the use of an adaptive basis set for the nuclear wave function (*23*, *24*). We used a state-averaged complete active space self-consistent field (SA-CASSCF) method (*25*) to solve the electronic Schrodinger equation, with an active space of five electrons in five orbitals (*26*). In both the cis and gauche forms of the cation, the singly occupied molecular orbital (SOMO) in the ground electronic state is a nonbonding (n) orbital localized primarily on the carbonyl group. In the first excited electronic state (D_1), the SOMO is of π character, again localized on the carbonyl. As expected for a carbonyl-localized $\pi \rightarrow n$ transition, D_1 is optically dark in both conformers. The second excited state (D_2) is accessed via a $\sigma \rightarrow n$ transition and is optically bright. Note that, for this open shell system, the lowest electronic excitations involve electron promotion from lower, doubly occupied orbitals to the highest, singly occupied orbital. The experiment thus excites both conformers to D_2. However, the AIMS simulations predict that decay from D_2 to D_1 is extremely fast and involves very little nuclear motion. As shown in Fig. 3, more than half of the population internally converts to D_1 within 10 fs. This rapidity stems from a conical intersection that connects D_2 and D_1 very close to the Franck-Condon point. The geometry of this intersection is very similar to the Franck-Condon geometry (figs. S1 and S2), and its local topography is strongly peaked (fig. S3), which promotes

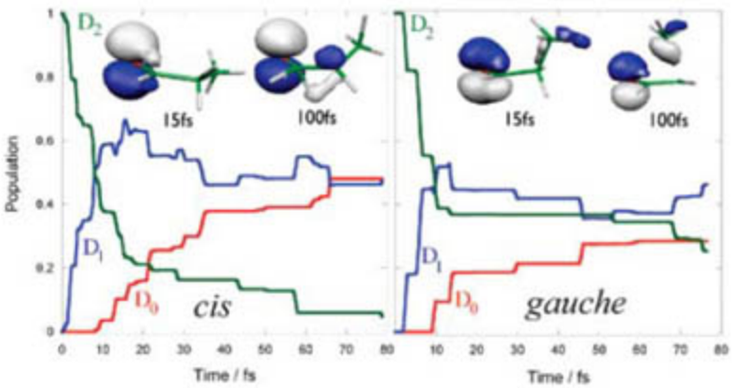

Fig. 3. Electronic population for cis (**left**) and gauche (**right**) conformers of propanal cation after photoexcitation to D_2. In both cases, more than half of the population has quenched to D_1 within 10 fs. The inset for each conformer shows the molecular structure and SOMO for a representative trajectory on D_1 shortly after internal conversion from D_2 and at a later time in the dynamics.

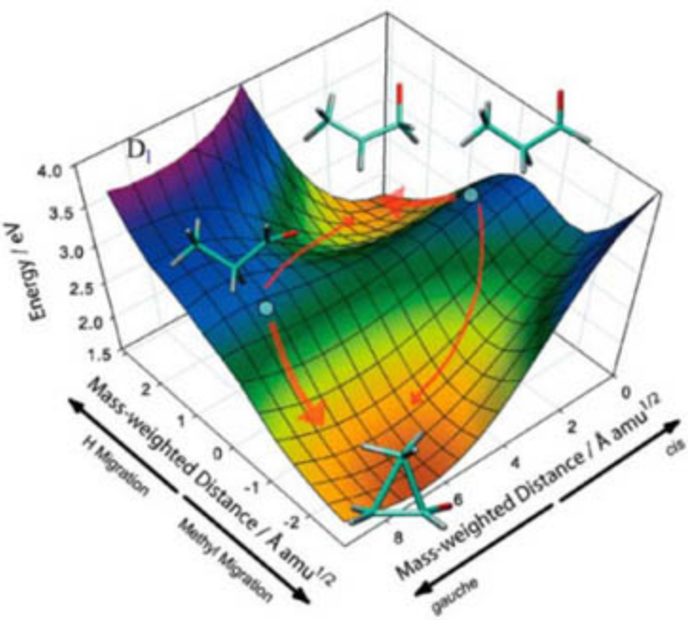

Fig. 4. Two-dimensional cut of the D_1 PES for propanal cation showing reaction pathways from the Franck-Condon point (shown as a solid circle for each of the cis and gauche conformers) to the hydrogen-migration and methyl-migration minima for cis and gauche conformers. The slope of the D_1 PES in the Franck-Condon region strongly favors formation of different products for cis and gauche conformers. The thick red arrows highlight the dominant pathways from each of the conformers, and the thin red arrows indicate minor pathways. The cis conformer is directed toward the hydrogen-migration excited-state minimum. In contrast, the gauche conformer is directed toward the methyl-migration excited-state minimum. Both of these minima are in the close vicinity of D_1/D_0 conical intersections, and surface crossing to D_0 is rapid. amu, atomic mass unit.

ultrafast and efficient population transfer. The effects of local topography around conical intersections have been discussed previously (*27*–*29*), and Yarkony has introduced quantitative measures of this topography (*29*). Explicit calculation of these measures (table S1) corroborates the strongly peaked character of the D_2/D_1 intersections for both the cis and gauche forms of propanal cation.

On the D_1 surface, the dynamics of the cis and gauche conformers become very different. The cis conformer has a high probability of undergoing hydrogen migration to yield $CH_3CHCH_2O^+$, which rapidly converts to D_0, through an D_1/D_0 conical intersection (see trajectory animation in movie S1). Further migration of an H atom from the methyl group to the O atom, accompanied by a loss of H from C1, would lead to hydroxyallyl cation. In contrast, the gauche conformer is more likely to undergo methyl migration, because the methyl group carries much of the positive charge (see trajectory animation in movie S2). When this structure converts to D_0, the methyl group migrates back to its original site, yielding energetic propanal cation in the starting geometry. Thus, excitation of the cis and gauche conformers leads ultimately to very different intermediate structures in the ground state, which in turn fragment through chemically distinct pathways to give the observed experimental signals (*30*).

The short D_2 lifetime suggests that the observed dynamics do not depend on the starting state and the same behavior would be observed with initial excitation to D_1. Further AIMS simulations, modeling excitation to D_1, confirmed this hypothesis. The origin of the different behavior for the two conformers is made clear from examination of the PESs for D_1. We located two distinct minima on D_1 arising in the AIMS dynamical studies: a hydrogen-migration geometry for the cis conformer and a methyl-migration geometry for the gauche conformer. In Fig. 4, we show a two-dimensional cut (*31*) of the D_1 PES containing the cis and gauche Franck-Condon points and the two D_1 minima. The difference in slope for each of the two pathways in each conformer is marked (see also fig. S4) and shows that the preference for different products can be directly related to the gradient of the D_1 PES at the Franck-Condon point for these two molecules.

The origin of the two distinct minima on D_1 comes from charge localization for the different conformers. The ground state has the positive charge localized largely on the carbonyl group, because the SOMO is an *n* orbital on the O atom. By virtue of orthogonality, the excited state will likely localize the positive charge differently. One possibility is to place the charge on the central C atom, which then prefers to have only a single H atom. This favors migration of the H atom, as observed for the cis conformer. A second possibility is to localize the positive charge on the terminal methyl group. This leads to migration of the methyl group such that it is placed above the electron-rich C=C π bond that is formed in the ensuing vinoxy ($OCH{=}CH_2$) species [i.e., an example of an attractive π-cation interaction (*32*)]. There are energetically favorable pathways to both of these D_1 minima from the Franck-Condon region of both conformers. However, geometric considerations at the Franck-Condon point on D_1 explain why the hydrogen-migration pathway is more strongly preferred starting from the cis conformer and the methyl-migration pathway is more strongly preferred starting from the gauche conformer. For the cis conformer, migration of the methyl group is blocked by the O atom, favoring the hydrogen-migration product. For the gauche conformer, there is no such obstacle to methyl migration; moreover, in this conformation, the aldehydic H blocks the hydrogen-migration pathway. Therefore, the behavior of the D_1 surface is opposite for the two conformers, with a steeper gradient toward the hydrogen-migration or methyl-migration minimum for the cis and gauche forms, respectively. We have explored the D_1 PES with more accurate electronic structure methods (which are too computationally demanding for use in AIMS studies), and the same qualitative features were observed (fig. S4).

The calculations reveal essential differences in the dynamics of the two conformers on the excited-state surface, but the dissociation ultimately takes place on the ground-state surface. This picture resolves the apparent paradox mentioned above: The conformational specificity appears consistent only with excited-state dynamics, in which the available excess energy is small, whereas the actual dissociation event must take place from the ground electronic state to give products with substantial vibrational excitation and an isotropic angular distribution. The distinct dynamics for the two conformers in the excited state place them in isolated regions of configuration space upon internal conversion to the ground state. Interconversion between the two conformers cannot then effectively compete with H elimination to the two distinct product channels. Although the products show characteristics of a statistical distribution (high internal excitation and isotropic angular distribution), the results show that there is little or no communication between these regions of the ground-state surface at these energies. We should note that decomposition on the ground state does not lead exclusively to propanoyl for gauche nor hydroxyallyl for cis. Rather, the gauche form returns near the starting geometry and dissociates to both products, which is consistent with the behavior seen in previous mass spectrometry studies (*20*) that ascribed formation of hydroxyallyl to isomerization via the distonic ion (Fig. 2) and the enol. The cis form, in contrast, strongly favors formation of hydroxyallyl, owing to the dynamics in D_1 and the location of the D_1/D_0 intersection.

These observations suggest a few features that are likely to be common to systems exhibiting this class of conformationally mediated dynamics. Either dissociation must occur directly in the excited state to give distinct product channels, as suggested for $C_3H_7I^+$, or else internal conversion to lower dissociative states must access regions sufficiently remote that the rates for decomposition via distinct pathways greatly exceed the rates for conformational interconversion. There is no reason to suppose this behavior is limited to propanal cation.

References and Notes

1. C. A. Royer, *Chem. Rev.* **106**, 1769 (2006).
2. B. C. Dian, A. Longarte, T. S. Zwier, *Science* **296**, 2369 (2002).
3. B. C. Dian, J. R. Clarkson, T. S. Zwier, *Science* **303**, 1169 (2004).
4. X. Michalet, S. Weiss, M. Jaeger, *Chem. Rev.* **106**, 1785 (2006).
5. W. Min *et al.*, *Acc. Chem. Res.* **38**, 923 (2005).
6. F. F. Crim, *J. Phys. Chem.* **100**, 12725 (1996).
7. S. T. Park, S. K. Kim, M. S. Kim, *Nature* **415**, 306 (2002).
8. L. Khriachtchev, E. Macoas, M. Pettersson, M. Rasanen, *J. Am. Chem. Soc.* **124**, 10994 (2002).
9. E. Martinez-Nunez *et al.*, *J. Phys. Chem. A* **109**, 2836 (2005).
10. D. Shemesh, R. B. Gerber, *J. Chem. Phys.* **122**, 241104 (2005).
11. G. F. Metha, M. A. Buntine, D. C. McGilvery, R. J. S. Morrison, *J. Mol. Spectrosc.* **165**, 32 (1994).
12. M. H. Kim, L. Shen, A. G. Suits, *Phys. Chem. Chem. Phys.* **8**, 2933 (2006).
13. D. W. Chandler, P. L. Houston, *J. Chem. Phys.* **87**, 1445 (1987).
14. A. T. J. B. Eppink, D. H. Parker, *Rev. Sci. Instrum.* **68**, 3477 (1997).
15. M. H. Kim, B. D. Leskiw, A. G. Suits, *J. Phys. Chem. A* **109**, 7839 (2005).
16. D. Townsend *et al.*, *Science* **306**, 1158 (2004).
17. N. C. Shand, C.-L. Ning, M. R. F. Siggel, I. C. Walker, J. Pfab, *J. Chem. Soc. Faraday Trans.* **93**, 2883 (1997).
18. A. V. Komissarov, M. P. Minitti, A. G. Suits, G. E. Hall, *J. Chem. Phys.* **124**, 014303 (2006).
19. These values are given for the detected products only and do not account for the fraction that have undergone secondary decomposition.
20. J. Dannacher, J. P. Stadelmann, *Int. J. Mass Spectrom.* **208**, 147 (2001).
21. Uncertainties in quoted thermochemical values are on the order of 0.15 eV.
22. C. E. Hudson, D. J. McAdoo, L. L. Griffin, J. C. Traeger, *J. Am. Soc. Mass Spectrom.* **14**, 136 (2003).
23. M. Ben-Nun, T. J. Martinez, *Adv. Chem. Phys.* **121**, 439 (2002).
24. T. J. Martinez, *Acc. Chem. Res.* **39**, 119 (2006).
25. B. O. Roos, *Adv. Chem. Phys.* **69**, 399 (1987).
26. We use 10 trajectory basis functions for each of the cis and gauche conformers. The initial position and momenta of these basis functions are randomly chosen from a Wigner distribution representing the vibrational ground state of the given conformer in the harmonic approximation. The 6-31G** basis set is used to represent the electronic wave function, along with the SA-CASSCF method equally weighting the lowest three doublet states.
27. G. J. Atchity, S. S. Xantheas, K. Ruedenberg, *J. Chem. Phys.* **95**, 1862 (1991).
28. M. Ben-Nun, F. Molnar, K. Schulten, T. J. Martínez, *Proc. Natl. Acad. Sci. U.S.A.* **99**, 1769 (2002).
29. D. R. Yarkony, *J. Chem. Phys.* **114**, 2601 (2001).
30. After 100 fs of simulation time for the cis conformer, 30% of the final population has undergone hydrogen migration. For the gauche conformer, 0% undergoes hydrogen migration. We have examined 10 initial conditions for each conformer (leading to more than 50 trajectory basis functions per conformer after adaptive

expansion of the basis set through the spawning procedure). Many more simulations should be performed to get accurate branching ratios, but these results demonstrate the differing propensities in the two conformers.
31. These pathways are determined by linear interpolation in internal coordinates between the structures representing the Franck-Condon point and each of the excited-state minima. The *x* axis is mass-weighted distance, in order to allow comparison of the two possible paths for each conformer.
32. J. P. Gallivan, D. A. Dougherty, *Proc. Natl. Acad. Sci. U.S.A.* **96**, 9459 (1999).
33. This work was supported by the NSF under award numbers CHE-04-15393 (A.G.S.) and CHE-05-35640 and CHE-02-11876 (T.J.M.).

Supporting Online Material
www.sciencemag.org/cgi/content/full/315/5818/1561/DC1
Figs. S1 to S4
Table S1
Movies S1 and S2

18 October 2006; accepted 25 January 2007
10.1126/science.1136453

A Cytochrome c Oxidase Model Catalyzes Oxygen to Water Reduction Under Rate-Limiting Electron Flux

James P. Collman,* Neal K. Devaraj, Richard A. Decréau, Ying Yang, Yi-Long Yan, Wataru Ebina, Todd A. Eberspacher, Christopher E. D. Chidsey*

We studied the selectivity of a functional model of cytochrome c oxidase's active site that mimics the coordination environment and relative locations of Fe_{a3}, Cu_B, and Tyr^{244}. To control electron flux, we covalently attached this model and analogs lacking copper and phenol onto self-assembled monolayer–coated gold electrodes. When the electron transfer rate was made rate limiting, both copper and phenol were required to enhance selective reduction of oxygen to water. This finding supports the hypothesis that, during steady-state turnover, the primary role of these redox centers is to rapidly provide all the electrons needed to reduce oxygen by four electrons, thus preventing the release of toxic partially reduced oxygen species.

During the final stage of respiration, cytochrome c oxidase (CcO) catalyzes the reduction of O_2 to H_2O to power its proton pump activity. This four-electron reduction must take place without releasing toxic partially reduced oxygen species (PROS).

Although CcO has been extensively studied in single-turnover experiments, the mechanism by which the enzyme reduces O_2 under steady-state conditions, where the electron flux is rate limiting, is poorly understood (*1*, *2*). Specifically, the role of Cu_B and a posttranslationally modified tyrosine residue (Tyr^{244}) have been frequent subjects of discussion. It has been assumed that, during turnover, Cu_B and Tyr^{244} each deliver an electron to bound oxygen in the active site, in addition to the two electrons from the Fe in $heme_{a3}$. This rapid intramolecular reduction in a hydrophobic site should reduce the lifetimes of potential PROS-releasing intermediates (*3*). The oxidized active site is then thought to be slowly recharged by ferrous cytochrome c (cyt c) (*4*, *5*) such that O_2 only binds when both Cu_B and Fe_{a3} have been reduced.

This scenario has proved challenging to test in the native enzyme, because of its inherent complexity, and in site-specific mutants, because they have been found to be inactive (*6*–*8*). We previously developed functional models of the CcO active site (*9*–*12*) and showed that a model that contains two redox sites, an iron heme, and a distal copper, but lacking a phenol to mimic Tyr^{244} can manifest the selective four-electron catalytic reduction of oxygen at physiological pH and potential. However, our catalysts were adsorbed on graphite electrodes such that electron transfer was very rapid; in contrast to the enzyme, in which electrons arrive slowly from cyt c. We describe the steady-state catalytic reduction of O_2 by using synthetic CcO models that also mimic the Tyr^{244} site and are attached to self-assembled monolayer (SAM) films on gold electrodes in order to control electron flux. This strategy enabled us to examine the influence of each redox center (copper and phenol), while varying the rates of electron delivery and simultaneously measuring the formation of PROS electrochemically. We find that, under conditions where electron delivery limits the turnover rate, the presence of copper and a redox-active phenol to mimic tyrosine sharply reduces the formation of PROS. These model studies support the belief that both Cu_B and Tyr^{244} are required to selectively reduce oxygen by four electrons under the physiological condition of rate-limiting electron transfer from cyt c.

Our new structural and functional analog of the CcO active site (catalyst **1a**) possesses groups that mimic Fe_{a3}, Cu_B, and Tyr^{244} (Fig. 1) (*13*). A myoglobin-like heme was fitted with a proximal imidazole, a distal copper was bound to a tris-imidazole ligand about 5 Å above the heme, and a phenol group was covalently attached to one of the copper-ligating imidazoles and directed toward the oxygen binding site on the heme (*14*). In single-turnover experiments, this fully reduced synthetic model, containing both copper and phenol, activated and reduced oxygen by

Department of Chemistry, Stanford University, Stanford, CA 94305–5080, USA.

*To whom correspondence should be addressed. E-mail: jpc@stanford.edu (J.P.C.); chidsey@stanford.edu (C.E.D.C.)

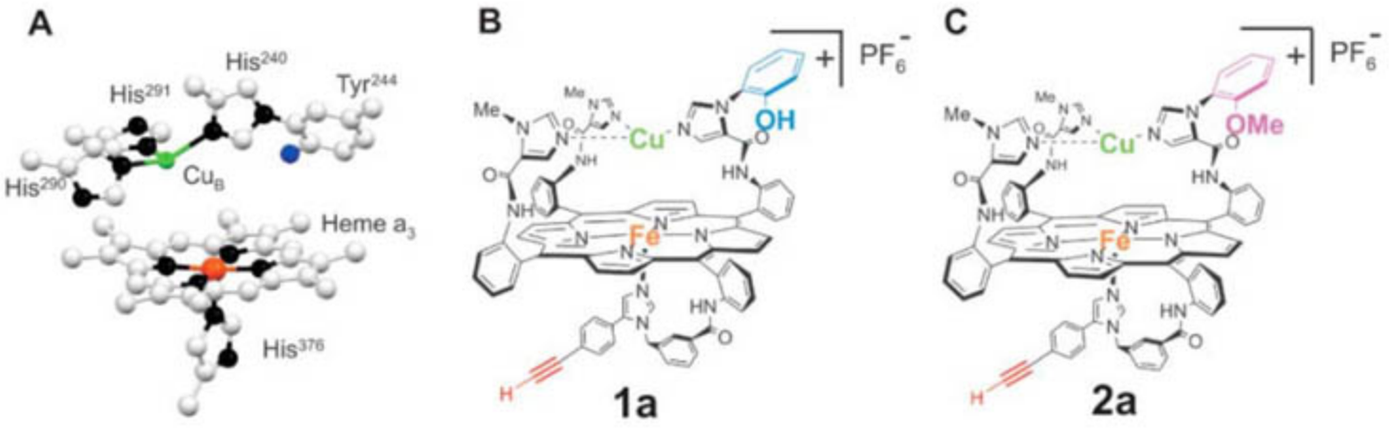

Fig. 1. (**A**) Crystal structure of the active site of CcO from the bovine heart (*13*). (**B**) Model **1a** reproduces the key elements of the active site of CcO. (**C**) Model **2a**, in which the phenol is masked as a methyl ether. Model **2a** can be treated with dilute acid to yield the iron-only model (**2b**), which is not shown.

four electrons in a manner similar to that of the mixed-valence form of the native enzyme. The oxidized product of this reaction contains a ferryl and a phenol radical. Its electron spin resonance (ESR) spectrum is shown in Fig. 2.

In order to control electron flux to these model compounds, we attached this model and analogs lacking copper and phenol onto mixed SAM–coated gold electrodes (*15*–*19*). Electron-transfer rates to redox groups covalently coupled to SAMs can be predictably tuned by varying the length and the degree of conjugation of the SAM (*20*–*22*). Although most functional monolayers are made by simply tethering a thiol to the redox molecule of interest, the complexity of our synthetic CcO models and the reactivity of the heme center with free thiols required an alternative method. Recently we demonstrated that azide-terminated mixed SAMs can be modified with acetylene-bearing molecules (*23*–*25*) through a Cu(I)-catalyzed azide-alkyne cycloaddition (*26*, *27*). This very efficient technique yields mixed SAMs that deliver electrons at reproducible rates to covalently attached redox molecules, such as porphyrins (*28*).

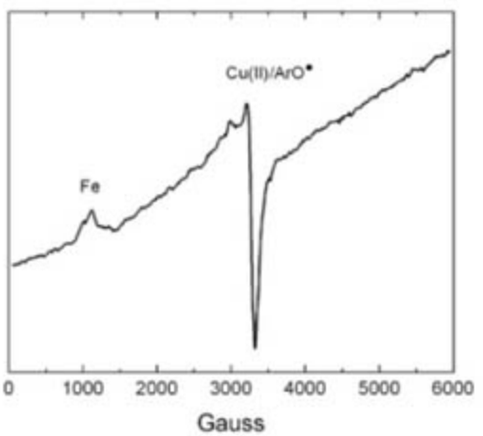

Fig. 2. ESR spectrum of the product formed by O_2 reacting with the fully reduced catalyst **1a**.

The synthetic CcO models were fitted with a terminal acetylene and then covalently attached to azide-terminated mixed SAMs on electrode surfaces (Fig. 3) (*29*). The electron delivery pathway is analogous to that in CcO, in which an outer-sphere electron donor (Fe_a in native CcO and the electrode in our model system) is covalently coupled to the proximal imidazole of an oxygen-binding heme (*13*).

In order to mimic a situation where electron transfer to the heme is the rate-limiting step during catalysis, we covalently attached these CcO models onto mixed SAMs composed of 1-azidohexadecanethiol and hexadecanethiol ("slow" SAM **S1**). Such SAMs strongly retard the rate of electron transfer to immobilized redox molecules (*28*). For comparison, we also attached CcO models to a highly conjugated azide-terminated SAM composed of azidophenyleneethynylenebenzyl thiol and octanethiol ("fast" SAM **S2**). SAM **S2** is known to facilitate rapid electron transfer from the electrode to immobilized redox molecules (*28*).

SAMs functionalized with CcO models were characterized by using conventional electrochemical techniques (*29*). The standard electron-transfer rate constant, k^0, between the gold electrode and the iron center of our models was $6 \pm 0.1\ s^{-1}$ on SAM **S1**. In contrast, k^0 on SAM **S2** was too fast to measure with conventional electrochemical methods (*28*) but is at least $1 \times 10^4\ s^{-1}$. This large variation in k^0, controlled by changing the nature of the intervening SAM, allowed us to drastically vary the rate of electron transfer to our CcO models. Catalyst coverage was limited by the azide-terminated thiol to less than 4×10^{-11} moles cm^{-2}, about 5% of the coverage of thiols in the SAMs. At these low coverages, the catalysts do not interact with one another.

In the absence of O_2 at pH = 7, the redox potentials of both the heme iron and the distal copper are nearly identical, consistent with the similar potentials of Fe_{a3} and Cu_B observed in CcO and in our earlier synthetic models (*30*). In air-saturated aqueous solutions buffered at pH = 7, the reversible couple disappears and is replaced by a large irreversible current caused by O_2 reduction (fig. S2). The potential at which catalysis begins is the same on both slow and th fast SAM [0.3 V versus normal hydrogen electrode (NHE)] and is identical to the onset potential observed for O_2 reduction by native cyt c/CcO complexes absorbed on gold (*31*).

Although the SAM does not affect the potential of reduction, it strongly affects the kinetics of catalysis. On SAM **S1**, the electrochemical process is limited by electron transfer. In contrast, electron delivery to the catalysts immobilized on SAM **S2** is sufficiently rapid that the supply of O_2 limits the turnover frequency.

In order to measure the selectivity of catalysis under these two rate-limiting regimes (SAM **S1** and SAM **S2**), we used rotating ring-disk voltammetry. There are very few examples reported on the use of rotating ring-disk voltammetry with SAMs (*32*–*34*) because of the difficulty of forming reproducible SAMs on such electrodes (*18*). We have developed a procedure to form gold disk electrodes with the required surface properties to promote high-quality SAM formation (*29*). A catalyst-modified SAM-coated gold disk electrode is encircled by a PROS-detecting Pt ring electrode. The two-electrode assembly is rotated, and the gold disk is set to a potential at which oxygen reduction takes place. PROS produced during O_2 reduction are swept

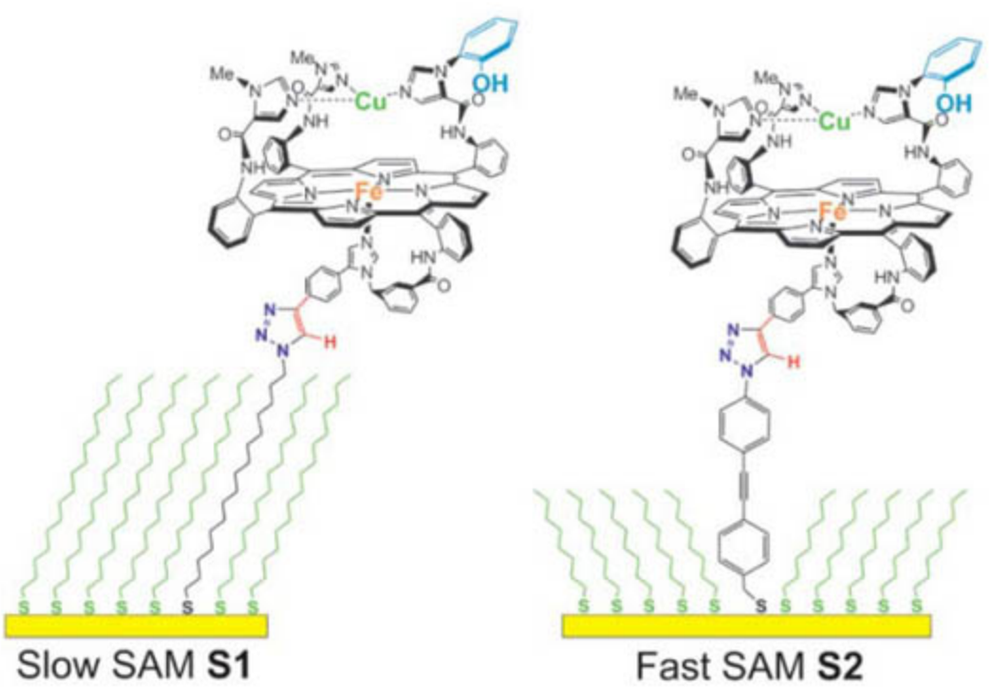

Fig. 3. Slow SAM **S1** functionalized with model **1a** (**left**) and fast SAM **S2** functionalized with model **1a** (**right**).

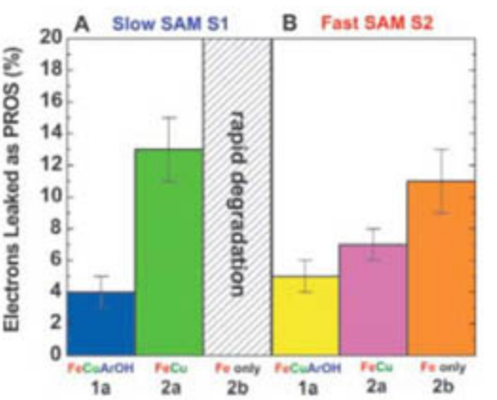

Fig. 4. Percentage of electrons released as PROS for catalysts **1a**, **2a**, and **2b** on either (**A**) SAM **S1** or (**B**) SAM **S2**. Data taken at 0.1 V versus NHE in air-saturated electrolyte buffered at pH = 7. The catalyst coverage on either SAM was 4×10^{-11} moles cm^{-2}. Ring-disk assembly was rotated at 300 revolutions per minute. Error bars indicate standard deviation from the mean.

from the disk to the ring, where they are electrochemically detected. For an ideal four-electron electrocatalyst, no PROS would be detected. We measured the percentage of electrons released as PROS for catalysts **1a**, **2a**, and **2b** immobilized on SAM **S1** and SAM **S2** (Fig. 4).

When attached to SAM **S2**, the incomplete CcO model **2b**, which lacks both copper and a redox-active phenol, is moderately selective at reducing O_2 to H_2O; 89 ± 2% of the electrons are used to form H_2O. Addition of copper (catalyst **2a**) decreases the amount of peroxide detected at the ring by over 30%. Copper is known to increase the oxygen-binding affinity of both synthetic CcO models and CcO itself and to improve the selectivity of CcO models absorbed on edge-plane graphite (*6*, *30*, *35*). Interestingly, the copper- and phenol-containing catalyst **1a** on SAM **S2** shows only a slightly improved selectivity over catalyst **2a**, in which the phenol is masked. We believe this limited influence of the redox-active phenol results from the ability of the electrode to deliver an additional electron rapidly through SAM **S2**. This behavior is reminiscent of fully reduced CcO during single turnover experiments; Fe_a can rapidly (~30 μs) provide an electron to a partially reduced oxygen intermediate, and a tyrosine radical is not observed (*2*). This result demonstrates that during turnover Tyr^{244} is not required when a fourth electron can be rapidly delivered from outside the active site.

During in vivo operation, CcO is never in the fully reduced state because electron delivery by cyt c is far slower than the rate at which internal electrons are delivered to oxygen bound at the active site (*36*). Thus, studies of CcO models immobilized on SAM **S1**, where electron transfer limits turnover, have greater physiological relevance. Compared with SAM **S2**, on SAM **S1** models lacking either copper or phenol show a marked decrease in selectivity. For example, the iron-only model **2b** on SAM **S1** rapidly degrades and is likely consumed by substantial PROS formation. This is unlike the case with similar iron-only porphyrins directly absorbed on edge-plane graphite (*30*) but is similar to our previous work using lipid films to force slow diffusional delivery of electrons (*37*). When immobilized on SAM **S1**, model **2a**, which contains both iron and copper but not a redox-active phenol, is more stable than the iron-only model but still shows a marked degree of PROS leakage. This catalyst can store no more than three electrons at the active site before oxygen binding (two from iron and one from copper); therefore, one additional electron would be required from the electrode in order for oxygen to be reduced by four electrons. If the electron transfer rate between electrode and catalyst is slow, partially reduced intermediates must persist before additional electrons are delivered, and in the interim PROS can leak and degrade the catalyst (Fig. 5A).

In contrast, catalyst **1a**, equipped with both copper and phenol, is highly selective at reducing oxygen to water on SAM **S1** (Fig. 5B). Compared with the catalyst without a redox-active phenol **2a**, the complete catalyst **1a** releases over threefold less PROS. Remarkably, the selectivity of catalyst **1a** is nearly identical whether immobilized on SAM **S1** or SAM **S2**. Thus, **1a** mimics one of the most important and fascinating features of CcO: its ability to selectively reduce oxygen by four electrons when the electron-transfer flux is rate limiting.

CcO is believed to reduce oxygen by four electrons with >99% selectivity (*36*). Catalyst **1a** on SAM **S1** is only about 96% selective for four-electron reduction (*38*). We suggest two plausible reasons for PROS formation. First, our Fe-Cu models do not require complete reduction of the metal centers in order to bind O_2, whereas in CcO an apparent cooperativity between Fe_{a3} and Cu_B redox centers ensures that only the fully reduced active site binds O_2 (*1*, *36*). In the present model, it is possible to form a partially reduced active site (Fe^{+2}/Cu^{+2}) that would bind O_2. This process could lead to occasional production of PROS when electron transfer is rate limiting.

A second disparity is that these active-site models are in direct contact with water, whereas CcO is buried in a membrane. Exposure to a water interface should favor hydrolytic autoxidation, thereby increasing PROS formation (*39*). To test this hypothesis, we treated the SAM films with a hydrophobic surfactant (*29*). It has been demonstrated that such surfactant films can act as hydrophobic blocking layers and influence the physical properties of redox molecules within the SAM (*40*, *41*). In preliminary studies, we have found that this treatment reduces the percent of electrons contributing to PROS by almost a factor of 3 (*29*).

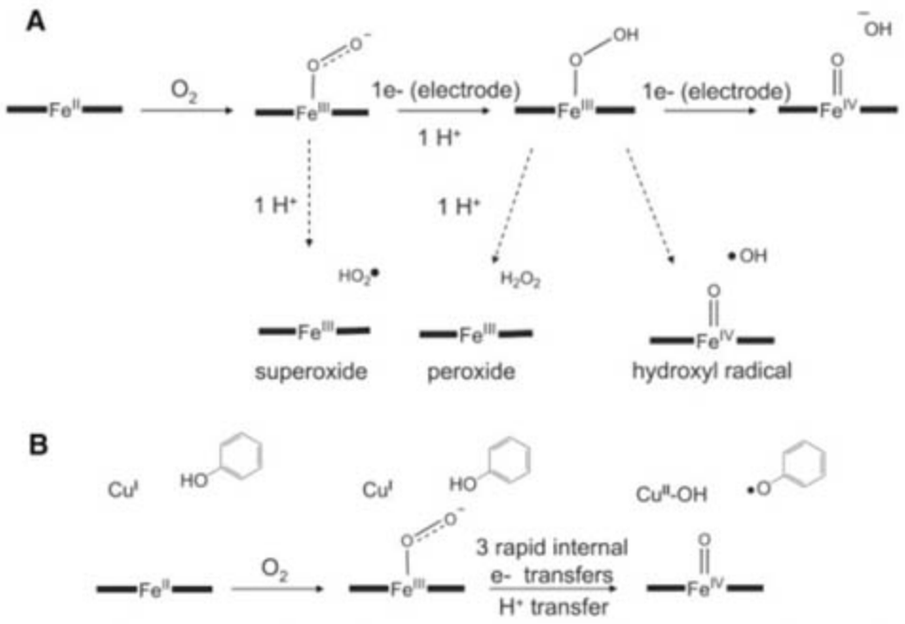

Fig. 5. Possible intermediates during the reduction of oxygen to the redox level of water. (**A**) A monometallic heme, such as catalyst **2b**, requires electrons to be delivered externally in order to reduce oxygen by four electrons. If those electrons are delivered slowly, the lifetimes of PROS-releasing intermediates increase. (**B**) Catalyst **1a** equipped with both copper and phenol can bind oxygen and rapidly reduce it to the redox level of water without requiring external electrons. PROS release is minimized.

References and Notes

1. M. Brunori, A. Giuffre, P. Sarti, *J. Inorg. Biochem.* **99**, 324 (2005).
2. J. E. Morgan, M. I. Verkhovsky, G. Palmer, M. Wikstrom, *Biochemistry* **40**, 6882 (2001).
3. D. A. Proshlyakov *et al.*, *Science* **290**, 1588 (2000).
4. B. Chazotte, C. R. Hackenbrock, *J. Biol. Chem.* **264**, 4978 (1989).
5. S. S. Gupte, C. R. Hackenbrock, *J. Biol. Chem.* **263**, 5248 (1988).
6. T. Mogi, T. Hirano, H. Nakamura, Y. Anraku, Y. Orii, *FEBS Lett.* **370**, 259 (1995).
7. T. K. Das, C. Pecoraro, F. L. Tomson, R. B. Gennis, D. L. Rousseau, *Biochemistry* **37**, 14471 (1998).
8. U. Pfitzner *et al.*, *J. Bioenerg. Biomembr.* **30**, 89 (1998).
9. J. P. Collman, L. Fu, P. C. Herrmann, X. Zhang, *Science* **275**, 949 (1997).
10. J. P. Collman *et al.*, *J. Am. Chem. Soc.* **116**, 9783 (1994).
11. J. P. Collman *et al.*, *J. Am. Chem. Soc.* **121**, 1387 (1999).
12. J. P. Collman, C. J. Sunderland, R. Boulatov, *Inorg. Chem.* **41**, 2282 (2002).
13. T. Tsukihara *et al.*, *Science* **269**, 1069 (1995).
14. J. P. Collman, R. A. Decréau, C. Zhang, *J. Org. Chem.* **69**, 3546 (2004).
15. K. S. Alleman, K. Weber, S. E. Creager, *J. Phys. Chem.* **100**, 17050 (1996).
16. S. Z. Zou, R. S. Clegg, F. C. Anson, *Langmuir* **18**, 3241 (2002).
17. D. A. Offord *et al.*, *J. Am. Chem. Soc.* **120**, 4478 (1998).
18. J. E. Hutchison, T. A. Postlethwaite, R. W. Murray, *Langmuir* **9**, 3277 (1993).
19. J. Zak, H. P. Yuan, M. Ho, L. K. Woo, M. D. Porter, *Langmuir* **9**, 2772 (1993).
20. C. E. D. Chidsey, *Science* **251**, 919 (1991).
21. S. Creager *et al.*, *J. Am. Chem. Soc.* **121**, 1059 (1999).

22. H. O. Finklea, D. D. Hanshew, *J. Am. Chem. Soc.* **114**, 3173 (1992).
23. J. P. Collman, N. K. Devaraj, T. P. A. Eberspacher, C. E. D. Chidsey, *Langmuir* **22**, 2457 (2006).
24. J. P. Collman, N. K. Devaraj, C. E. D. Chidsey, *Langmuir* **20**, 1051 (2004).
25. J. K. Lee, Y. S. Chi, I. S. Choi, *Langmuir* **20**, 3844 (2004).
26. V. V. Rostovtsev, L. G. Green, V. V. Fokin, K. B. Sharpless, *Angew. Chem. Int. Ed.* **41**, 2596 (2002).
27. C. W. Tornoe, C. Christensen, M. Meldal, *J. Org. Chem.* **67**, 3057 (2002).
28. N. K. Devaraj, R. A. Decreau, W. Ebina, J. P. Collman, C. E. D. Chidsey, *J. Phys. Chem. B* **110**, 15955 (2006).
29. Materials and methods are available as supporting material on *Science* Online.
30. R. Boulatov, J. P. Collman, I. M. Shiryaeva, C. J. Sunderland, *J. Am. Chem. Soc.* **124**, 11923 (2002).
31. A. S. Haas *et al.*, *J. Phys. Chem. B* **105**, 11351 (2001).
32. S. K. Cha, *Bull. Korean Chem. Soc.* **25**, 786 (2004).
33. T. H. Degefa, P. Schon, D. Bongard, L. Walder, *J. Electroanal. Chem.* **574**, 49 (2004).
34. E. Katz, H. L. Schmidt, *J. Electroanal. Chem.* **368**, 87 (1994).
35. J. A. Sigman, B. C. Kwok, Y. Lu, *J. Am. Chem. Soc.* **122**, 8192 (2000).
36. G. T. Babcock, M. Wikstrom, *Nature* **356**, 301 (1992).
37. J. P. Collman, R. Boulatov, *Angew. Chem. Int. Ed.* **41**, 3487 (2002).
38. The peroxide detected at the ring electrode could arise either from direct release of peroxide during the catalytic cycle or from release and rapid disproportionation of superoxide (*42*). The hydrolytic autoxidation of heme oxygen complexes in aqueous solution is a well-documented phenomenon (*39*, *43*). This process is known to be catalyzed by protons, and preliminary results indicate that the selectivity of all of our catalysts can be markedly improved by raising the pH (to the range of 8 to 12). Furthermore, our prior work with CcO models on edge-plane graphite provided evidence that superoxide is a substantial source of PROS (*30*).
39. K. Shikama, *Chem. Rev.* **98**, 1357 (1998).
40. S. E. Creager, G. K. Rowe, *Langmuir* **9**, 2330 (1993).
41. G. B. Sigal, M. Mrksich, G. M. Whitesides, *Langmuir* **13**, 2749 (1997).
42. D. T. Sawyer, J. S. Valentine, *Acc. Chem. Res.* **14**, 393 (1981).
43. J. P. Collman, Y. L. Yan, T. Eberspacher, X. J. Xie, E. I. Solomon, *Inorg. Chem.* **44**, 9628 (2005).

44. We dedicate this scientific contribution to the memory of the late H. Taube. We thank J. I. Brauman, T. D. P. Stack, C. C. Cummins, R. Boulatov, and P. H. Dinolfo for helpful discussions. N.K.D., R.A.D., and W.E. acknowledge a Stanford graduate fellowship, a Lavoisier fellowship, and a Dreyfus undergraduate fellowship, respectively. This material has its basis in work supported by the NIH under grant GM-17880-35.

Supporting Online Material

www.sciencemag.org/cgi/content/full/315/5818/1565/DC1
Materials and Methods
Figs. S1 to S4
References

3 October 2006; accepted 23 January 2007
10.1126/science.1135844

Thermoelectricity in Molecular Junctions

Pramod Reddy,[1]* Sung-Yeon Jang,[2,3]*† Rachel A. Segalman,[1,2,3]‡ Arun Majumdar[1,3,4]‡

By trapping molecules between two gold electrodes with a temperature difference across them, the junction Seebeck coefficients of 1,4-benzenedithiol (BDT), 4,4′-dibenzenedithiol, and 4,4″-tribenzenedithiol in contact with gold were measured at room temperature to be +8.7 ± 2.1 microvolts per kelvin (μV/K), +12.9 ± 2.2 μV/K, and +14.2 ± 3.2 μV/K, respectively (where the error is the full width half maximum of the statistical distributions). The positive sign unambiguously indicates p-type (hole) conduction in these heterojunctions, whereas the Au Fermi level position for Au-BDT-Au junctions was identified to be 1.2 eV above the highest occupied molecular orbital level of BDT. The ability to study thermoelectricity in molecular junctions provides the opportunity to address these fundamental unanswered questions about their electronic structure and to begin exploring molecular thermoelectric energy conversion.

Study of charge transport in molecules is of fundamental interest, with potential applications in molecular electronics (*1*) and energy-conversion devices (*2*, *3*). Current-voltage (I-V) characteristics of single molecules have been extensively investigated by trapping a single molecule in break junctions formed by mechanical strain (*4*), electromigration (*5*), and scanning tunneling microscopes (*6*). Although such measurements have provided substantial insight into charge transport through molecular junctions, critical aspects about the electronic structure cannot be uniquely obtained by I-V characteristics alone. For example, whether molecular junctions are p-type or n-type—i.e., whether the position of the Fermi level, E_F, of the metal contacts is closer to the highest occupied molecular orbital (HOMO) or to the lowest unoccupied molecular orbital (LUMO)—generally remains unknown because of uncertainties in the microscopic details of the contacts (*7*–*10*). A specific example of this is benzenedithiol (BDT); in this case, although the electrical conductance has been studied extensively both experimentally (*4*, *11*) and theoretically (*7*, *12*–*15*), some groups suggest that the E_F of the electrodes lies close to the HOMO level (*7*, *13*, *15*) and other groups contend that E_F lies near the LUMO level (*12*, *14*). Although sweeping the gate bias in single-molecule transistors could potentially yield this information, Coulombic interactions caused by charge accumulation on the molecule could perturb the electronic structure (*16*, *17*).

It has been suggested that the sign of the Seebeck coefficient, S, of molecular junctions can indicate the sign of the charge carrier and the relative position of E_F with respect to the HOMO or LUMO levels (*8*). Indeed, thermopower measurements that use a scanning probe microscope have yielded nanoscale spatial distributions of electron and hole concentrations in inorganic semiconductors (*18*) and have led to chemical potential microscopy at the atomic scale (*19*, *20*). Here, we report an alternative approach: We measured S for molecular junctions formed by trapping molecules between gold electrodes, and then we measured the voltage generated across them when a temperature bias was imposed across the junction.

In general, S is associated with bulk materials and is obtained by measuring the voltage difference created across a material in response to an applied temperature differential. In such bulk materials, charge transport is diffusive in nature. The concept of an effective S is also valid for junctions where the transport may be ballistic. For such junctions, however, a more general form of the Seebeck coefficient is needed and is given as

$$S = \frac{1}{eT}\frac{\int_0^\infty \sigma(E)(E - E_F)dE}{\int_0^\infty \sigma(E)dE} \qquad (1)$$

where $\sigma(E)$ is the energy-dependent differential electrical conductivity, E_F is the Fermi level (or more accurately, the chemical potential), e is the charge of an electron, and T is the absolute temperature; the denominator in Eq. 1 is the electrical conductivity, σ. As Eq. 1 suggests, S reflects the asymmetry in $\sigma(E)$ with respect to E_F. In bulk materials, this asymmetry results from energy-dependent carrier scattering or the asymmetry in the density of states. For ballistic transport, the asymmetry can be created by a potential barrier at a junction, such as that created between E_F of a metal and the HOMO or LUMO level of a molecule. Here, S is not an intrinsic property of a material, but that of the heterojunction. Hence, we call it a junction Seebeck coefficient, $S_{junction}$. Because $S_{junction}$

[1]Applied Science and Technology Program, University of California, Berkeley, CA 94720, USA. [2]Department of Chemical Engineering, University of California, Berkeley, CA 94720, USA. [3]Materials Science Division, Lawrence Berkeley Laboratory, Berkeley, CA 94720, USA. [4]Departments of Mechanical Engineering and Materials Science and Engineering, University of California, Berkeley, CA 94720, USA.

*These authors contributed equally to this paper.
†Present address: Optoelectronic Materials Research Center, Korea Institute of Science and Technology, Seoul 136-791, Korea.
‡To whom correspondence should be addressed. E-mail: majumdar@me.berkeley.edu (A.M.); segalman@berkeley.edu (R.A.S.)

measures the size of an energy barrier, it is not expected to depend on the number of molecules trapped between the electrodes and is, therefore, an intrinsic property of the junction. This is in contrast to the junction's electrical conductance, which depends on the number of molecules.

A modified scanning tunneling microscope (STM) setup is shown schematically in Fig. 1A: A customized control circuit drives a Au STM tip at a constant speed toward a Au substrate in air under ambient conditions. The Au tip is kept in contact with a large thermal reservoir at room temperature, which maintains the tip temperature very close to ambient (*21*–*23*). The Au substrate can be heated with an electric heater to a desired temperature above ambient to create a tip-substrate temperature difference, ΔT. When the Au STM tip approaches the hot substrate, a tip-substrate voltage bias is applied and the current is continuously monitored. When the conductance reaches a sufficiently high threshold of $0.1G_o$, where $G_o = 2e^2/h$ is the quantum of charge conductance [see (*23*) for a discussion on the choice of $0.1G_o$], our previous experiments on electrical conductance have shown that the tip-substrate distance is sufficient to trap molecules between the electrodes (*24*). Once this threshold is reached, the voltage bias and the current amplifier are disconnected, and the voltage amplifier is connected instead (Fig. 1A) to measure the tip-substrate thermoelectric voltage induced by ΔT. The tip is then slowly withdrawn to a sufficiently large distance (~15 nm) and the output voltage ΔV is continuously monitored with the tip grounded.

When the Au substrate is covered by thiol-terminated molecules, we have shown that molecular bridges are formed between the Au tip and the substrate, and the electrical conductance of single molecules can be monitored in air (*24*). In our experiment, we covered the Au substrate with BDT, dibezenedithiol (DBDT), or tribenzenedithiol (TBDT) (*25*) molecules. If molecules of BDT, DBDT, or TBDT are trapped between the tip and substrate with a superimposed ΔT, we should expect to see a thermoelectric voltage generated between the electrodes (*8*), which should last as long as one or more molecules are trapped and vanish once all of the molecules break away.

A typical thermoelectric voltage curve obtained in the experiment that was performed with a ΔT of 20 K and with the substrate covered with BDT molecules is shown in Fig. 1B. We observed a constant thermoelectric voltage of about $\Delta V = -200$ μV (Fig. 1B, blue curve), which lasted until all of the molecules trapped in the junction broke away. Notably, the distance the tip travels (~ 1 to 2 nm) before all of the molecules break away is much longer than the molecular length. Because the thiol group on the molecule binds sufficiently strongly to Au, and because Au atoms are sufficiently mobile at room temperature, it has been proposed that Au chains are formed both on the tip and the substrate when the STM tip is pulled away (*6*). In contrast to electrical conductance measurements (*24*), which decrease in steps as molecules break away one at a time, no steps were observed in the ΔV, suggesting that $S_{junction}$ is independent of the number of molecules. As the ΔT increases from 0 to 30 K, the thermoelectric voltage signal increases (Fig. 1C). Control experiments performed on clean gold surfaces without any molecules (red, Fig. 1B) demonstrate that no measurable ΔV is generated in the absence of molecules.

To obtain a statistically significant value of ΔV of a Au-BDT-Au junction, we performed roughly 1000 consecutive experiments at each value of ΔT. These data were used to construct histograms for each temperature differential without any data preselection. The histograms thus obtained (Fig. 2, A to C) were used to estimate the average and the variation in $S_{junction}$. The relation between $S_{junction}$ of the Au-molecule-Au junction and the measured voltage is (*23*)

$$S_{junction} = S_{Au} - \frac{\Delta V}{\Delta T} \qquad (2)$$

where S_{Au} is the Seebeck coefficient of bulk Au, which is ~1.94 μV/K at 300 K (*26*). In Fig. 2D, ΔV_{peak} is plotted as a function of ΔT, where ΔV_{peak} corresponds to the ΔV at the peak of the distribution. The error bars in Fig. 2D correspond to the full-width half-maximum (FWHM) of the distributions. From the slope $\Delta V_{peak}/\Delta T$ and Eq. 2, one obtains $S_{Au\text{-}BDT\text{-}Au} = +8.7 \pm 2.1$ μV/K, where the error is FWHM. Similar experiments were also performed with DBDT and TBDT, and statistical analysis revealed that $S_{Au\text{-}DBDT\text{-}Au} = +12.9 \pm 2.2$ μV/K and $S_{Au\text{-}TBDT\text{-}Au} = +14.2 \pm 3.2$ μV/K (*23*) (Fig. 2E). There seems to be a linear dependence of thermopower with molecular length, which is in contrast to the exponential dependence of electrical resistance that is generally attributed to tunneling across the molecule. The histograms of ΔV for Au-TBDT-Au junctions at 20 and 30 K (fig. S4, A to C) exhibit deviations from a Gaussian curve. Furthermore, the FWHMs for the histograms at 20 and 30 K increased considerably compared with those of Au-BDT-Au junctions, which may arise from the effect of the conformational changes in the molecules trapped in the junctions. The plot of the peak values of the histograms versus the temperature differential for DBDT and TBDT (figs. S3D and S4D) show deviations from linearity. This deviation may arise because the applied temperature differentials of 20 and 30 K across molecules are so high that linear transport theory may not adequately describe the temperature dependence of the thermoelectric voltage.

The relative position of the HOMO and LUMO levels with respect to the E_F of the metal

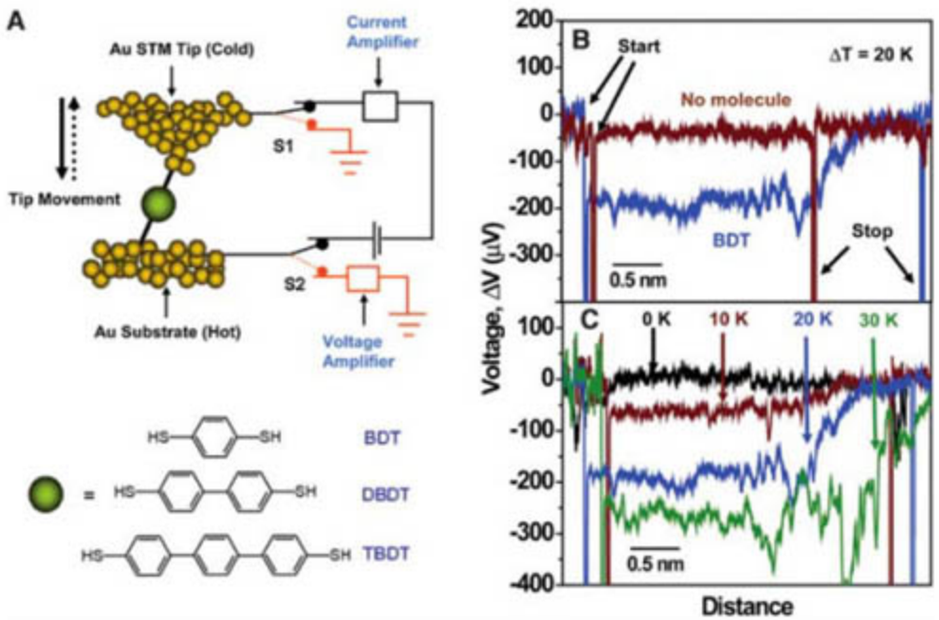

Fig. 1. Experimental setup and measurements. (**A**) Schematic description of the experimental set up based on an STM break junction. Molecules of BDT, DBDT, or TBDT are trapped between the Au STM tip kept at ambient temperature and a heated Au substrate kept at temperature ΔT above the ambient. When the tip approaches the substrate, a voltage bias is applied and the current is monitored to estimate the conductance. When the conductance reaches a threshold of $0.1G_o$, the voltage bias and the current amplifier are disconnected. A voltage amplifier is then used to measure the induced thermoelectric voltage, ΔV, and the tip is gradually pulled away from the substrate. (**B**) A plot of the thermoelectric voltage measured as a function of the tip-sample distance when a temperature differential $\Delta T = 20$ K is applied (Au tip at ambient and substrate at ambient + 20 K). The blue curve is obtained when a Au-BDT-Au junction is broken. The red curve shows a control experiment performed on a clean gold substrate. (**C**) Typical thermoelectric voltage traces for tip-substrate temperature differentials of 0, 10, 20, and 30 K for Au-BDT-Au junctions.

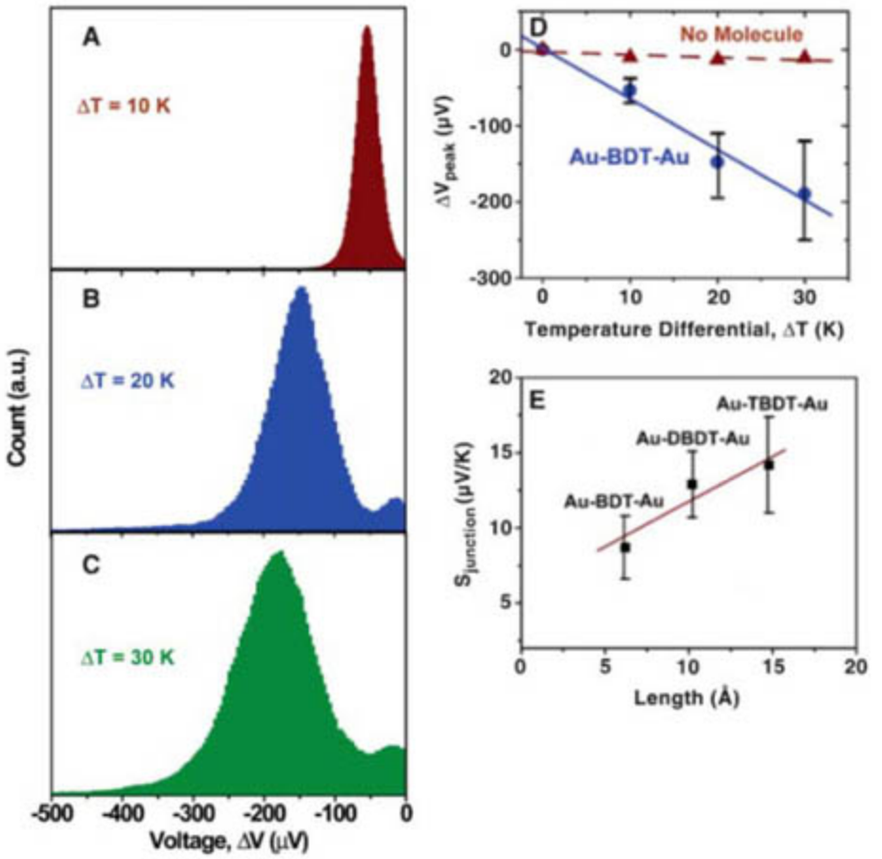

Fig. 2. Histograms obtained by analyzing approximately 1000 consecutive thermoelectric voltage curves obtained in measurements of Au-BDT-Au junctions with tip-substrate temperature differential (**A**) ΔT = 10 K, (**B**) ΔT = 20 K, and (**C**) ΔT = 30 K. a.u., arbitrary units. (**D**) Plot of the peak values of the thermoelectric voltage in histograms as a function of the temperature differential. The error bars represent FWHM of the corresponding histograms. It can be seen that the measured voltage varies linearly with the temperature differential, as expected. (**E**) Plot of measured junction Seebeck coefficient as a function of molecular length for BDT, DBDT, and TBDT.

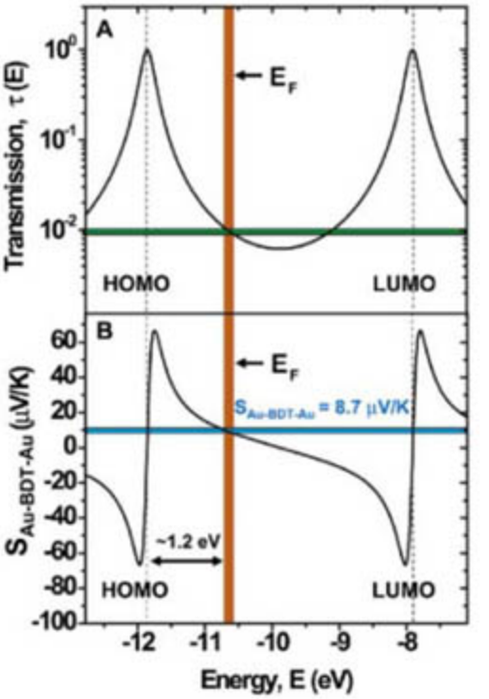

Fig. 3. Relating the measured Seebeck coefficient of Au-BDT-Au junction to the position of Fermi level. (**A**) Theoretical prediction (*8*) of the transmission function of a Au-BDT-Au junction plotted as a function of the relative position of the Fermi level of the Au electrodes with respect to the HOMO and LUMO levels. (**B**) The predicted (*8*) Seebeck coefficient of a Au-BDT-Au junction as a function of the relative position of the Fermi level with respect to the HOMO and LUMO levels. When the measured value of $S_{Au\text{-}BDT\text{-}Au} = +8.7 \pm 2.1$ μV/K (blue band) is shown, it is clear that the Fermi level is ~1.2 eV above the HOMO level. At this energy level, the transmission function is $\tau(E) \sim 0.01$.

electrodes can be related to the measured value of $S_{junction}$ (*8*). The Landauer formula (*27*) is used to relate $S_{junction}$ to the transmission function, $\tau(E)$. It is shown that $S_{junction}$ can be obtained as

$$S_{junction} = -\frac{\pi^2 k_B^2 T}{3e} \frac{\partial \ln(\tau(E))}{\partial E}\bigg|_{E=E_F} \quad (3)$$

where k_B is the Boltzmann constant.

The transmission function for the case of Au-BDT-Au junction, which was derived with the use of the nonequilibrium Green's function formalism in conjunction with extended Huckel theory (*8*), is shown in Fig. 3A. It is clear that $\tau(E) \sim 1$ when the E_F aligns with either the HOMO or the LUMO levels and decreases rapidly to below 0.01 in between. Using this transmission function in Eq. 3, we calculated $S_{Au\text{-}BDT\text{-}Au}$ (Fig. 3B) and found that $S_{Au\text{-}BDT\text{-}Au}$ is positive (p-type) if E_F is closer to the HOMO level and negative (n-type) if it is closer to the LUMO level. Using the measured value of $S_{Au\text{-}BDT\text{-}Au} = +8.7 \pm 2.1$ μV/K, we see from Fig. 3B that E_F is ~1.2 eV from the HOMO level. The value of the transmission function at this relative position of the Fermi level was $\tau(E) \sim 0.01$ (Fig. 3A). In the Landauer formalism, we know that the conductance $G_{molecule}$ can be related to the transmission function at E_F as

$$G_{molecule} \approx \frac{2e^2}{h}\tau(E)|_{E=E_F} = \tau(E)|_{E=E_F} G_o \quad (4)$$

Equation 4 implies that the conductance of BDT should be $\sim 0.01 G_o$. This estimated value of the electrical conductance is in excellent agreement with the measured electrical conductance of Au-BDT-Au junction (*11*, *28*).

Junction Seebeck coefficient measurements can provide insight into the electronic structure of the heterojunction, but the results also bear on an as-yet unexplored field of thermoelectric energy conversion based on molecules. The best efficiency in thermoelectric energy conversion can be achieved if charge transport occurs through a single energy level (*29*, *30*). Single-level transport is, however, difficult to realize in inorganic materials. Metal-molecule-metal heterojunctions are ideal in this regard because they (i) provide transport either through the HOMO or LUMO levels and (ii) have very low vibrational heat conductance because of large mismatch of vibrational spectra between the bulk metal and discrete molecules (*31*). Hence, such a hybrid material offers the promise of efficient thermoelectric energy conversion. We show for the first time values for molecular junction Seebeck coefficients, but the tunability of this effect and electrical conductance remains unknown. The length dependence of molecular junction Seebeck coefficients is shown in Fig. 2E for the molecules we studied, but there may be other ways of tuning thermopower, such as by introducing various chemical moieties in the molecule or by controlling the metal-molecule chemical bond.

References and Notes

1. A. Aviram, M. A. Ratner, *Chem. Phys. Lett.* **29**, 277 (1974).
2. W. U. Huynh, J. J. Dittmer, A. P. Alivisatos, *Science* **295**, 2425 (2002).
3. G. Yu, J. Gao, J. C. Hummlen, F. Wudl, A. J. Heeger, *Science* **270**, 1789 (1995).
4. M. A. Reed, C. Zhou, C. J. Muller, T. P. Burgin, J. M. Tour, *Science* **278**, 252 (1997).
5. H. Park *et al.*, *Nature* **407**, 57 (2000).
6. B. Xu, N. J. J. Tao, *Science* **301**, 1221 (2003).
7. P. Damle, A. W. Ghosh, S. Datta, *Chem. Phys.* **281**, 171 (2002).
8. M. Paulsson, S. Datta, *Phys. Rev. B* **67**, 241403 (2003).

9. F. Zahid, A. W. Ghosh, M. Paulsson, E. Polizzi, S. Datta, *Phys. Rev. B* **70**, 245317 (2004).
10. Consider a molecule strongly bound to one electrode and very weakly bound to the other. An example of this is scanning tunneling spectroscopy; the tip is weakly interacting with the molecule, which is strongly bound to a substrate. Under bias, such a configuration produces asymmetric I-V curves because the chemical potential of the tip crosses the HOMO and LUMO levels of the molecule, whereas that of the substrate is pinned to the molecular levels. Hence, by applying a tip bias, one can determine the chemical potential position with respect to the HOMO and LUMO levels. However, to make realistic molecular devices, the molecule cannot be weakly bound to one electrode, given that otherwise the device would be mechanically unstable and electrically irreproducible because of uncertainties of the contact. But in the case of a molecule strongly bound to both the electrodes, the chemical potential of both of electrodes is pinned and hence, symmetric I-V curves are produced under bias (*9*). This symmetry in the I-V characteristics makes it impossible to determine whether transport is through HOMO or LUMO levels (*9*).
11. X. Y. Xiao, B. Q. Xu, N. J. Tao, *Nano Lett.* **4**, 267 (2004).
12. M. Di Ventra, S. T. Pantelides, N. D. Lang, *Phys. Rev. Lett.* **84**, 979 (2000).
13. E. G. Emberly, G. Kirczenow, *Phys. Rev. B* **58**, 10911 (1998).
14. J. G. Kushmerick *et al.*, *Phys. Rev. Lett.* **89**, 086802 (2002).
15. J. Taylor, M. Brandbyge, K. Stokbro, *Phys. Rev. Lett.* **89**, 138301 (2002).
16. W. Liang, M. P. Shores, M. Bockrath, J. R. Long, H. Park, *Nature* **417**, 725 (2002).
17. J. Park *et al.*, *Nature* **417**, 722 (2002).
18. H. K. Lyeo *et al.*, *Science* **303**, 816 (2004).
19. C. C. Williams, H. K. Wickramasinghe, *Nature* **344**, 317 (1990).
20. J. C. Poler, R. M. Zimmerman, E. C. Cox, *Langmuir* **11**, 2689 (1995).
21. One might suspect that the heat flow from the substrate to the tip would cause the tip temperature to increase. However, tip-substrate heat transport is mostly due to conduction through air (thermal conductance through the molecules trapped in between the tip and the substrate or through a liquid meniscus, if present, is very small in comparison) (*22*). Because the tip-sample thermal resistance is sufficiently larger than that between the Au tip and the thermal reservoir, the Au tip will be at the reservoir temperature. Our group has previously shown this to be true (*22*). Further analysis that supports the idea that the tip is at ambient temperature is provided in (*23*). Hence, the temperature difference applied across the substrate and the reservoir is the same as that across the tip-substrate junction.
22. L. Shi, A. Majumdar, *J. Heat. Trans.* **124**, 329 (2002).
23. Materials and methods are available as supporting material on *Science* Online.
24. S. Y. Jang, P. Reddy, A. Majumdar, R. A. Segalman, *Nano Lett.* **6**, 2362 (2006).
25. B. de Boer *et al.*, *Langmuir* **19**, 4272 (2003).
26. F. J. Blatt, *Thermoelectric Power of Metals* (Plenum Press, New York, 1976), pp. xv, 264.
27. M. Buttiker, Y. Imry, R. Landauer, S. Pinhas, *Phys. Rev. B* **31**, 6207 (1985).
28. Paulsson and Datta (*8*) used the measurements of Poler *et al.* (*20*) for an asymmetric junction to predict the position of E_F with respect to HOMO and LUMO levels of a monolayer.
29. G. D. Mahan, J. O. Sofo, *Proc. Natl. Acad. Sci. U.S.A.* **93**, 7436 (1996).
30. T. E. Humphrey, H. Linke, *Phys. Rev. Lett.* **94**, 096601 (2005).
31. R. Y. Wang, R. A. Segalman, A. Majumdar, *Appl. Phys. Lett.* **89**, 173113 (2006).

32. We acknowledge support from NSF under grant no. EEC-0425914, the NSF–Nanoscale Science and Engineering Center (NSEC) Center of Integrated Nanomechanical Systems, the Berkeley–Industrial Technology Research Institute (ITRI, Taiwan) Research Center, and the Department of Energy Basic Energy Sciences (DOE-BES) Thermoelectrics Program and DOE-BES Plastic Electronics Program at the Lawrence Berkeley National Laboratory.

Supporting Online Material

www.sciencemag.org/cgi/content/full/1137149/DC1
Materials and Methods
Figs. S1 to S6
References

3 November 2006; accepted 29 January 2007
Published online 15 February 2007;
10.1126/science.1137149
Include this information when citing this paper.

The Evolutionary Demography of Ecological Change: Linking Trait Variation and Population Growth

Fanie Pelletier,[1] Tim Clutton-Brock,[2] Josephine Pemberton,[3] Shripad Tuljapurkar,[4] Tim Coulson[1]*

Population dynamics and evolutionary change are linked by the fundamental biological processes of birth and death. This means that population growth may correlate with the strength of selection, whereas evolutionary change can leave an ecological signature. We decompose population growth in an age-structured population into contributions from variation in a quantitative trait. We report that the distribution of body sizes within a population of Soay sheep can markedly influence population dynamics, accounting for up to one-fifth of observed population growth. Our results suggest that there is substantial opportunity for evolutionary dynamics to leave an ecological signature and visa versa.

Ecological and evolutionary processes have traditionally been considered to operate at such different time scales that ecologists could ignore evolutionary dynamics, while evolutionary biologists could overlook ecological processes (*1*). Recently, however, there has been growing interest in the effects that ecological and evolutionary processes have on each other (*2*–*4*). For example, genetic variation at one allozyme locus influences population dynamics in a butterfly metapopulation (*5*), and evolutionary change in body and beak size has contributed more than ecological processes to population growth in a Darwin's finch (*4*). In parallel, evolutionary biologists have shown that selection can fluctuate with ecological processes and that this can generate evolutionary change. In the same population of Darwin's finch that was the focus of (*4*), varying ecological conditions in different decades impacted on the strength, direction, and outcome of selection (*6*). Given that ecological and evolutionary processes are intertwined, it is necessary to develop methods to capture their relation. A first step in doing this is to characterize the association between the phenotypic variation on which selection operates and population growth (*7*). Here we ask how quantitative trait variation impacts population growth in a population of Soay sheep (*8*) and how selection varies with population growth.

The population of Soay sheep on Hirta, St. Kilda, has been studied in detail since 1985 (*8*). The structure and size of the population is known for each year (fig. S1). Birth weight (kg) is collected each spring, and adult body weight (kg) and hind leg length (mm)—a measure of skeletal size—are collected annually from individuals caught in the summer catch (on average ~50% of the population) (*9*). The sheep year runs from 1 August to 31 July, and recruitment is calculated as the number of lambs an individual produced in April that are still alive in August. Paternity is assigned using genetic markers to ~60% of lambs with >80% confidence (*10*). Significant age- or environment-specific additive genetic variance exists for birth weight, August body weight, and hind leg length (*8*, *11*, *12*). We estimate heritabilities, h^2 (*13*), using these values and the phenotypic variance estimated from our data set [supporting online material (SOM)].

To link variation in a quantitative trait to population growth requires an understanding of how variation in the trait influences survival and recruitment and how survival and recruitment influence population growth (*14*). One way of doing this is to calculate the proportion of variation in individual contributions to population growth, $p_{t(i)}$, accounted for by a quantitative trait. $p_{t(i)}$ is calculated as the difference between observed population growth and population growth calculated with the contribution of a focal individual removed (*15*). This quantity describes

[1]Division of Biology and the Natural Environment Research Council (NERC) Centre for Population Biology, Imperial College London, Silwood Park, Ascot, Berkshire, SL5 7PY, UK. [2]Department of Zoology, University of Cambridge, Downing Street, Cambridge, CB2 3EJ, UK. [3]Institute of Evolutionary Biology, University of Edinburgh, West Mains Road, Edinburgh, EH9 3JT, UK. [4]Department of Biological Sciences, Stanford University, Stanford, CA 94305–5020, USA.

*To whom correspondence should be addressed. E-mail: t.coulson@imperial.ac.uk

how each individual contributed directly to observed population growth over a time step and is calculated as $p_{t(i)} = \frac{s_{t(i)} - \bar{s}_t}{N_t - 1} + \frac{f_{t(i)} - \bar{f}_t}{N_t - 1}$ where $s_{t(i)}$ and $f_{t(i)}$ represent survival and recruitment of individual i at time t, $\bar{s}_t$ and $\bar{f}_t$ represent population means, and N_t represents population size. The quantity $p_{t(i)}$ can be decomposed into contribution via survival, $S_{t(i)}$, and recruitment, $F_{t(i)}$ where $S_{t(i)} = \frac{s_{t(i)} - \bar{s}_t}{N_t - 1}$ and $F_{t(i)} = \frac{f_{t(i)} - \bar{f}_t}{N_t - 1}$. In diploid systems, $f_{t(i)}$ and $\bar{f}_t$ are calculated as the number of offspring multiplied by ½. The proportion of variation (σ_p) in $p_{t(i)}$ accounted for by a quantitative trait is the contribution of variation in the trait to population growth. For quantitative traits, it is straightforward to calculate the contribution of additive genetic variation in a trait to population growth by multiplying σ_p by the h^2 of the trait.

$S_{t(i)}$, $F_{t(i)}$, and $p_{t(i)}$ and body weight and hind leg length vary with ontogeny and sex in Soay sheep. Failing to correct for this variation would inflate estimates of the contribution of variation in these traits to population growth. To assess the contribution of quantitative traits to population growth, we conducted separate analyses within each age and sex class before combining results across classes. We considered males and females separately and divided each sex into four age-classes—lambs, yearlings, prime-aged adults (2 to 6 years), and senescent individuals (>6 years) (*16*). We examined the statistical relation between each trait and $p_{t(i)}$, $S_{t(i)}$, and $F_{t(i)}$ using generalized additive models (GAMs) (*17*) in R (*18*). We estimated σ_p as the proportion of deviance explained by these GAMs. To calculate the contribution of variation in each trait to population growth across classes, we multiplied the σ_p value for each class by the proportion of the population in each class before summing these products across classes.

In Fig. 1, we show associations between body weight and individual contributions to population growth for data pooled across years. Body weight accounted for 4.7% of population growth, hind leg length 3.19%, and birth weight 1.69%. About two-thirds of the contribution of hind leg and body weight was via lambs and yearlings, while three-fourths of the contribution of birth weight was via lambs and yearlings (Fig. 2, A, B, and C). The relatively small contribution of variation in trait values to population growth occurs because none of the morphological traits account for much variation in $p_{t(i)}$ in two of the more numerous demographic classes—prime aged and senescent females. In contrast, the small contribution of variation in trait values to population growth via adult males occurs because adult males constitute a small proportion of the population rather than because of a lack of an association between body weight and $p_{t(i)}$ (Fig. 1).

Additive genetic variation for body weight contributed 0.88% of population growth, with values of 1.43% and 0.19% for hind leg length and birth weight, respectively. Because population growth is mean fitness (*19*), our results can also be interpreted as the heritability of fitness via the focal traits.

On average, trait variation contributed relatively little to population growth. However, trait variation interacts with environmental variation to influence survival and fecundity in the Soay sheep (*20*) and other ungulates (*21*). Consequently, we next looked for temporal variation in the contribution of variation in quantitative traits to

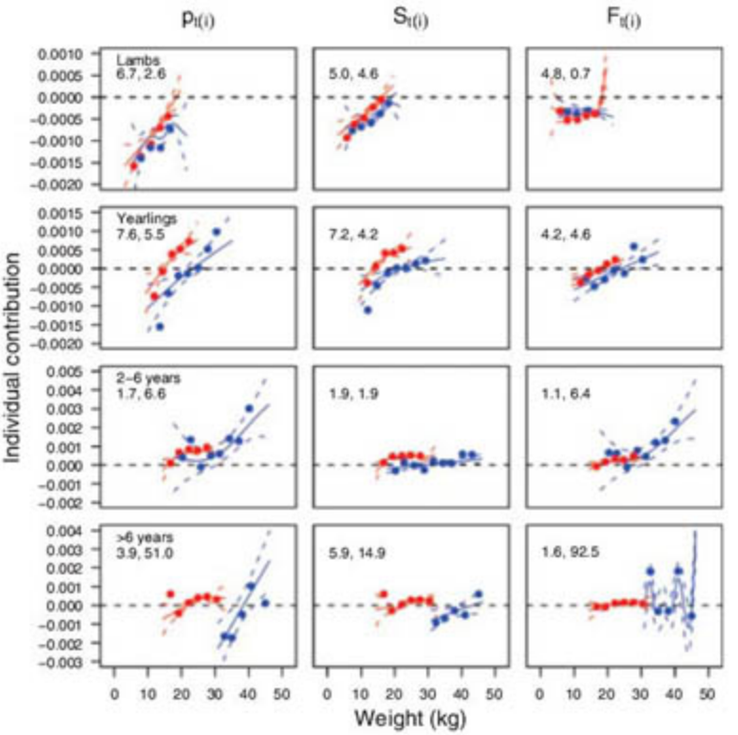

Fig. 1. Associations between body weight and $p_{t(i)}$, $S_{t(i)}$, and $F_{t(i)}$ by age for males (blue) and females (red) with 95% confidence intervals; points show mean values within weight categories. There are few males aged >6 years, so results from this class should be treated cautiously. Numbers (females, males) represent the proportion of deviance accounted for (fig. S3 for birth weight and hind leg length).

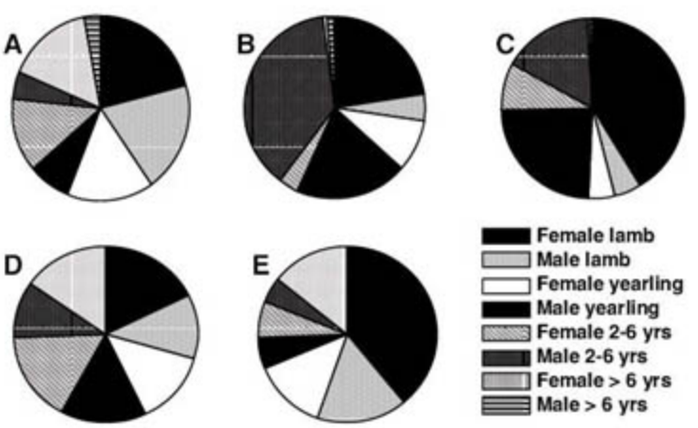

Fig. 2. The relative contribution of (**A**, **D**, and **E**) body weight, (**B**) hind leg length and (**C**) birth weight to population growth via different demographic classes for data pooled across years (A, B, and C) and for years with high (D) and low (E) survival.

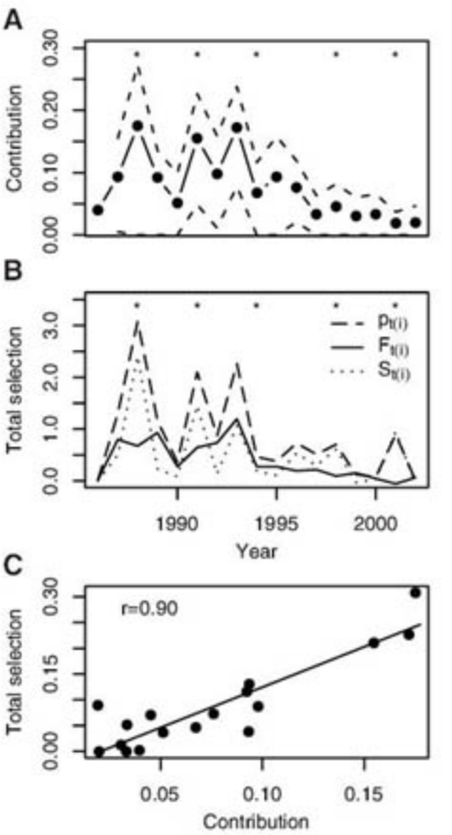

Fig. 3. (**A**) Contributions of body weight to population growth with 95% confidence intervals. (See fig. S4 for birth weight and hind leg length.) Asterisks identify years with low survival. (**B**) Estimates of the strength of selection on body weight. (**C**) Association between selection and contributions to population growth over time for body weight.

population growth. There were insufficient data in some years to fit GAMs, so we first looked to see whether contributions varied between years when mean survival was low and when it was high (SOM). We now focus on body weight, as results for hind leg length are similar (fig. S2), given the high correlation between it and body weight ($r = 0.84$). In low-survival years, variation in body weight accounted for 9.23% of variation in population growth rate, with approximately equal contributions from all demographic classes (Fig. 2D). In contrast, body weight was much less influential in high-survival years, accounting for only 3.87%, with the contribution being primarily from lambs (Fig. 2E). These results suggest an interaction between the distribution of trait values and the environment in influencing population growth.

Although we were unable to fit GAMs through data for each year, we did examine how variation in traits influenced population growth in each year using linear regressions (Fig. 3). We used the r^2 of the associations between trait values and $p_{t(i)}$, $S_{t(i)}$, and $F_{t(i)}$ in each class to assess the proportion of variation accounted for. The contribution of body weight to variation in population growth varied substantially between years, contributing up to nearly one-fifth (18%) of observed population growth (Fig. 3A). Since 1995, the contribution of variation in body size to population growth was less pronounced than in earlier years. In the latter period, winter weather on St. Kilda was relatively good for sheep as the mean of the North Atlantic Oscillation (NAO) was lower than in the earlier period (0.039 versus 2.348). The NAO was significantly correlated with the contribution of variation in body weight to population growth ($r^2 = 0.23$, $t = 2.13$, $P = 0.049$, $n = 16$ years). This provides further support that environmental variation influences how much variation a quantitative trait contributes to population growth, which raises the possibility that the opportunity for evolution is greatest in harsh environments.

The associations we present (Fig. 1) also represent the strength of selection (*22*). Most evolutionary theory assumes that selection is linear (*13*), although nonlinear disruptive or stabilizing selection does dramatically alter evolutionary outcomes (*23*, *24*). We found evidence of nonlinear selection in each age and sex class and that selection operates via different demographic rates in males and females. For example, in prime aged adult females, the strength of selection on body size decreased with increasing weight (Fig. 4); with only individuals less than ~20 kg experiencing significant selection; selection also operated almost entirely via survival in this demographic class (Fig. 1). In contrast, in prime aged males, selection operated primarily via recruitment and increased exponentially with weight (Figs. 1 and 4). The form of the selection functions and the normal distributions of individuals in each class (Fig. 4) suggest that nonlinear selection will not maintain additive genetic variation within this population.

The shape and form of selection varied with time in a pattern similar to the temporal fluctuations observed in the contribution of trait variation to population growth (Fig. 4C). Selection was stronger, and most nonlinear, in years when survival rates were low (SOM). For example, the selection on 2- to 6-year-old adult females seen at low weights (Figs. 1 and 4) was only apparent in crash years. Because selection did not vary in sign with environmental fluctuations, fluctuating selection cannot be the mechanism maintaining the genetic diversity observed in body weight. Because 20 years is a relatively short period, we suspect that the maintenance of additive genetic variance is due to patterns of selection not yet observed and antagonistic effects not yet detected, perhaps linked to traits not yet studied.

In this paper, we have done two things. First, we have shown how to calculate the contribution of variation in a quantitative trait to population growth. We found that trait variation can make a substantial contribution—up to nearly 20% in some years. Contributions via different demographic classes and rates varied with time; they were generally largest in years when many individuals died. A decreasing temporal trend in the contribution of variation in body weight may be due to environmental variation. Additive genetic variation made comparatively small contributions to population growth, but selection on these traits can generate nontrivial ecological effects. Second, our findings describe the modus operandi of selection: In each demographic class, there is evidence of nonlinear selection; selection operates predominantly via survival in adult females and via recruitment in adult males; selection on large adult females is weak but increases with body size in adult males; and the strength and pathways by which selection operates varies with time.

To extend these results to predict evolutionary change in size-related traits, we need to track both heritabilities and individual trajectories through trait space. However, given the nonlinearities we observed, making accurate predictions will be challenging. It would also be informative to examine how nonadditive genetic variance and genetic by environment interactions underpinning quantitative traits contribute to population growth. We found that, as the strength of selection increases, so too does the contribution of trait variation to population growth. This

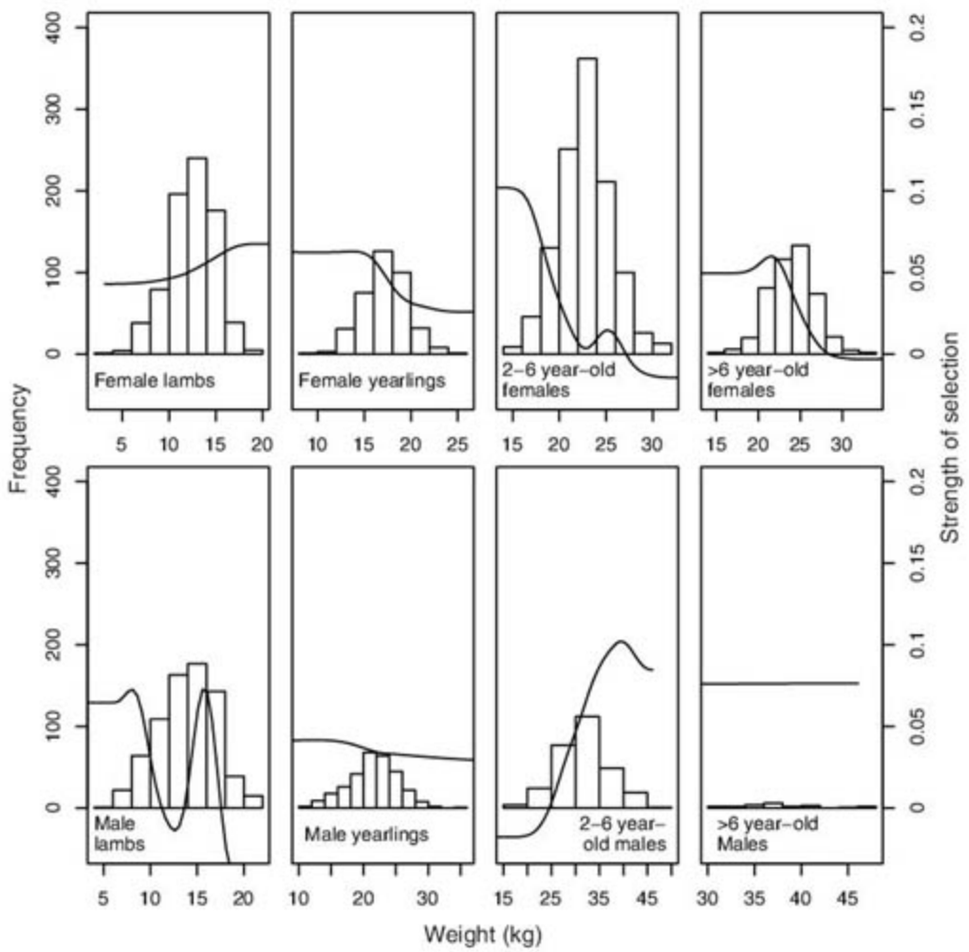

Fig. 4. The strength of selection (the local slope of the nonparametric functions in Fig. 1) on body weight that different components of the population experience. These curves illustrate nonlinearity in selection and show that many individuals in the most numerous demographic classes (e.g., adult females) do not experience significant selection on body size. The frequency distributions show the number of individuals within each class.

link between selection and the ecological consequences of evolutionary change has been apparent since Lande's pioneering work (*14*). Our results are a useful step toward extending stochastic evolutionary demography toward a theoretical framework that describes population dynamics in terms of the quantitative traits on which selection operates. Such a theory would describe the feedback between ecological and evolutionary processes in a stochastic environment and would illuminate the mechanisms shaping additive genetic variation and phenotypic variation.

References and Notes

1. L. B. Slobodkin, *Growth and Regulation of Animal Populations* (Holt, Rinehart and Winston, New York, 1961).
2. I. Saccheri, I. Hanski, *Trends Ecol. Evol.* **21**, 341 (2006).
3. J. M. Thompson, *Trends Ecol. Evol.* **13**, 329 (1998).
4. N. G. Hairston Jr., S. P. Ellner, M. Geber, T. Yoshida, J. E. Fox, *Ecol. Lett.* **8**, 1114 (2005).
5. I. Hanski, I. Saccheri, *PLoS Biol.* **4**, e129 (2006).
6. P. R. Grant, B. R. Grant, *Science* **296**, 707 (2002).
7. T. Coulson, L. E. B. Kruuk, G. Tavecchia, J. M. Pemberton, T. H. Clutton-Brock, *Evolution Int. J. Org. Evolution* **57**, 2879 (2003).
8. T. H. Clutton-Brock, J. M. Pemberton, Eds., *Soay Sheep: Dynamics and Selection in an Island Population* (Cambridge Univ. Press, Cambridge, 2004).
9. Phenotypic data come from 3533 individuals between one and 16 years of age. Sample sizes for morphological measures vary with the variables of interest. Paternity data for males are available from 1986 to 2003 (SOM).
10. A. D. J. Overall, A. E. Byrne, J. Pilkington, J. M. Pemberton, *Mol. Ecol.* **14**, 3383 (2005).
11. A. J. Wilson *et al.*, *PLoS Biol.* **4**, e216 (2006).
12. A. J. Wilson *et al.*, *J. Evol. Biol.* 10.1007/s10682-006-9106-z (2007).
13. D. S. Falconer, T. F. C. Mackay, *Introduction to Quantitative Genetics* (Pearson Prentice Hall, Harlow, ed. 4, 1996).
14. R. Lande, *Ecology* **63**, 607 (1982).
15. T. Coulson *et al.*, *Proc. R. Soc. London B Biol. Sci.* **273**, 547 (2006).
16. E. A. Catchpole, B. J. T. Morgan, T. N. Coulson, S. N. Freeman, S. D. Albon, *J. R. Stat. Soc. Ser. C Appl. Stat.* **49**, 453 (2000).
17. GAMs were fitted using the library mgcv 1.3. Results for the oldest two age classes do not qualitatively change when individual identity is corrected for as a random effect.
18. R Development Core Team, *R: A Language and Environment for Statistical Computing* (R Foundation for Statistical Computing, Vienna, Austria, 2006); www.R-project.org.
19. R. A. Fisher, *The Genetical Theory of Natural Selection* (Dover, New York, 1930).
20. M. C. Forchhammer, T. Clutton-Brock, J. Lindström, S. Albon, *J. Anim. Ecol.* **70**, 721 (2001).
21. J. T. Jorgenson, M. Festa-Bianchet, M. Lucherini, W. D. Wishart, *Can. J. Zool.* **71**, 2509 (1993).
22. S. Arnold, M. J. Wade, *Evolution Int. J. Org. Evolution* **38**, 709 (1984).
23. D. Schluter, *Evolution Int. J. Org. Evolution* **42**, 849 (1988).
24. E. D. Brodie, A. J. Moore, F. J. Janzen, *Trends Ecol. Evol.* **10**, 313 (1995).

25. Thanks to the National Trust for Scotland and the Scottish Natural Heritage for permission to work on St. Kilda and the Royal Artillery for logistical support. J. Pilkington and many volunteers have collected data. A. Mysterud, N. Yoccoz, D. Garant, D. Réale. M. Festa-Bianchet, J.-M. Gaillard, and three anonymous reviewers provided helpful comments on an earlier version. S.T. was supported by National Institute on Aging, NIH, grant P01 AG 22500; F.P. by a Natural Sciences and Engineering Research Council of Canada, NSERC, fellowship.

Supporting Online Material

www.sciencemag.org/cgi/content/full/315/5818/1571/DC1
Materials and Methods
Figs. S1 to S4
Tables S1 and S2
References

19 December 2006; accepted 9 February 2007
10.1126/science.1139024

The Latitudinal Gradient in Recent Speciation and Extinction Rates of Birds and Mammals

Jason T. Weir* and Dolph Schluter

Although the tropics harbor greater numbers of species than do temperate zones, it is not known whether the rates of speciation and extinction also follow a latitudinal gradient. By sampling birds and mammals, we found that the distribution of the evolutionary ages of sister species—pairs of species in which each is the other's closest relative—adheres to a latitudinal gradient. The time to divergence for sister species is shorter at high latitudes and longer in the tropics. Birth-death models fitting these data estimate that the highest recent speciation and extinction rates occur at high latitudes and decline toward the tropics. These results conflict with the prevailing view that links high tropical diversity to elevated tropical speciation rates. Instead, our findings suggest that faster turnover at high latitudes contributes to the latitudinal diversity gradient.

The tropics possess many more species than temperate regions, yet the underlying causes of this latitudinal gradient in species diversity are poorly understood (*1*–*3*). A number of authors have estimated net diversification rates (speciation minus extinction) across a latitudinal gradient and concluded that more species accumulate per unit time at tropical latitudes [including birds (*4*–*7*), primates (*8*), marine bivalves (*9*), foraminifera (*10*), and butterflies (*4*)]. By examining the age distributions of the youngest species of birds and mammals, and how they change with latitude, we examined the contributions of recent speciation and extinction to the latitudinal gradient in net diversification.

We studied a large data set comprising the ages and midpoint latitudes of breeding range for 309 sister species pairs of New World birds and mammals. We defined sister species as the most closely related pair of extant species descended from an immediate common ancestor. Their ages were estimated from genetic distances of mitochondrial DNA from the cytochrome b gene. The rate of evolution in this gene is approximately constant with time within birds and mammals (*11*–*13*) and has been used widely to date phylogenetic events in these groups. The average of the absolute value of midpoint breeding latitude for a sister-species pair was used to approximate the latitude at which speciation occurred. This approach is reasonable for sister-species pairs that have narrow latitudinal ranges, but greater uncertainty exists when latitudinal ranges are broad. Excluding all species pairs with a combined latitudinal range (defined by the northern and southern limits for the pair) of greater than 40° did not affect the relationship between age and midpoint latitude. Latitudinal ranges of species at high latitudes have shifted in response to glacial cycles. However, using the presumed latitudes of species ranges during past glacial maxima, when many temperate species were forced southward, would only steepen the gradients estimated here.

Near the equator, the ages of sister-species pairs spanned the past 10 million years, with a mean age of 3.4 million years ago (Ma) (Fig. 1A). As distance from the equator increased, the upper limit and mean ages of sister species declined significantly [slope = −0.043 ± 0.007 Ma/degree latitude (± SEM), student's t test = −6.5, $P < 0.0001$, intercept = 3.37, degrees of freedom (df) = 307]. At the highest latitudes, all of the sister species diverged less than 1.0 Ma. This pattern of declining age with latitude is opposite to the pattern that would occur if faster rates of speciation had driven the buildup of Neotropical diversity, because the ages of sister species should be youngest where speciation rates are highest.

The differences in species ages between low and high latitudes is partly the result of a longer lag time in tropical faunas between population splitting, as measured by genetic markers, and species designation (Fig. 1, B and C). The evidence for this lies in the coincident latitudinal gradient in the ages of the oldest haplotype splits within 154 currently defined species of birds and mammals (Fig. 1B) and in the oldest phylogroup splits within 130 species (Fig. 1C). Avise (*14*, *15*) defined a phylogroup as a reciprocally monophyletic geographic subdivision

Biodiversity Research Center and Department of Zoology, University of British Columbia, Vancouver, BC V6T 1Z4, Canada.

*To whom correspondence should be addressed. E-mail: weir@zoology.ubc.ca

within a species. By examining sets of closely linked alleles (haplotypes), we were able to use maximum haplotype divergence as well as the age of the deepest phylogroup splits to compare the lag time to species formation, because species at high latitudes are so young that most lack phylogroups. Both haplotype and phylogroup splits are older in the tropics than in temperate zones, on average, implying that the process of speciation takes longer at low latitudes. This may be in part an artifact of the greater taxonomic uncertainty at lower latitudes, because a higher proportion of tropical species are currently undescribed and thus considered together in our analysis. Nevertheless, taxonomic uncertainty is unlikely to be the sole cause of the gradient. This is because the latitudinal gradient in the ages of sister species is present even within the Nearctic fauna of North America, which is well defined taxonomically north of approximately 30°N (slope = −0.041 ± 0.017, $t = -2.44$, $P = 0.017$, intercept = 3.3, df = 99). Reproductive isolation, marking the completion of the speciation process, usually takes time to evolve after population splitting, and our data suggest that this process might take a longer period of time at lower latitudes, although we are not sure why this is the case.

There are differences in the age distributions of sister species across the latitudinal gradient apart from the lag-time difference. Therefore, it may be possible to extract information about speciation (rate of cladogenesis) and extinction rates from the distribution of sister-species ages after correcting for the lag-time, because speciation and extinction can be inferred by the shape of the age distributions of sister species. In phylogenetic simulations using a pure birth model, in which speciation rates are constant through time and no extinction occurs (*16*), ages of sister species approximate an exponential distribution for which the mean is proportional to the speciation rate; adding a lag time shifts the mode in the distribution toward the mean lag time. Extinction changes the shape of these distributions by increasing the breadth of the tails (*17*).

We used maximum likelihood to fit a birth-death (*18*) model in which speciation (λ) and extinction (μ) rates changed linearly across the latitudinal gradient:

$$\lambda = b_\lambda L + c_\lambda \quad (1)$$

$$\mu = b_\mu L + c_\mu \quad (2)$$

where L is the absolute value of latitude, b is the slope, and c is the rate at 0° latitude. The model estimated the slopes (b_λ, b_μ) and intercepts (c_λ, c_μ) for the linear relationships between λ, μ, and L (Fig. 2) by fitting data points at each latitude to simulated probability distributions of sister species ages corresponding to different values of speciation and extinction in a reconstructed birth-death process (*17*). We generated probability distributions of sister-species ages by simulating a large number of phylogenetic trees under a birth-death process and recording the resulting distribution of sister-species ages for a range of parameter values. Simulated trees were corrected for the lag time to species recognition assuming that lag times had an exponential distribution with mean equal either to the average age of the oldest known haplotype splits, or to the average age of phylogroup splits within species at that latitude (*17*).

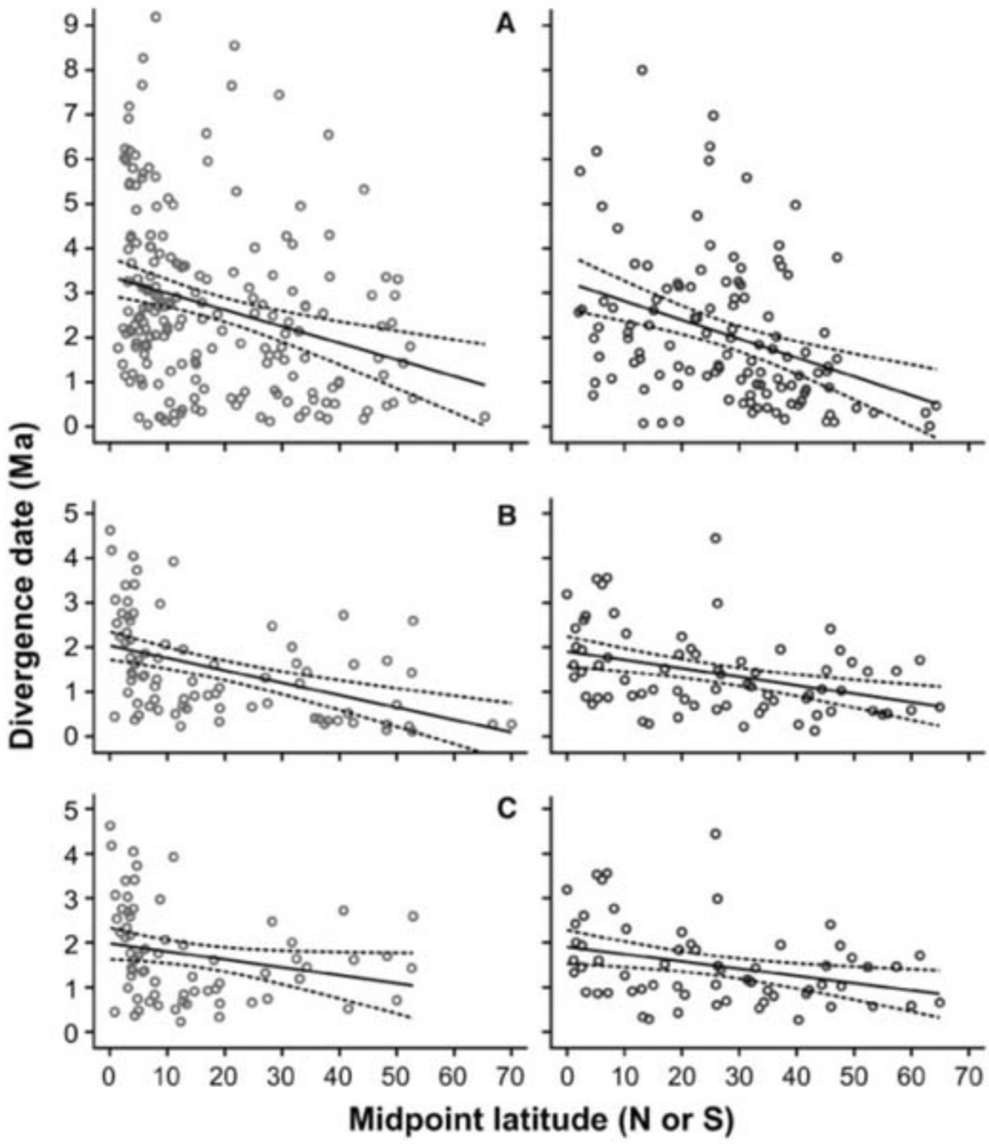

Fig. 1. Relationship between time since splitting and average absolute midpoint latitude for sister taxa of New World birds and mammals. (**A**) Ages of 309 sister-species pairs of New World birds (left; n = 191) and mammals (right; n = 118). Linear regression lines are shown for birds (slope = −0.040, $t = -4.368$, $P < 0.0001$, intercept = 3.38 Ma) and mammals (slope = −0.042, $t = -4.258$, $P < 0.0001$, intercept = 3.26 Ma). (**B**) Ages of 154 maximum coalescent dates for intraspecific haplotype variation within bird (n = 81) and mammal (n = 73) species. Linear regression lines are shown for birds (slope = −0.028, $t = -4.58$, $P < 0.0001$, intercept = 2.03 Ma) and mammals (slope = −0.019, $t = -3.62$, $P < 0.0006$, intercept = 1.91 Ma). (**C**) 130 phylogroup splits for birds (n = 68) and mammals (n = 62). Linear regression lines are shown for birds (slope = −0.018, $t = -2.00$, $P = 0.049$, intercept = 1.98 Ma) and mammals (slope = −0.016, $t = -2.67$, $P < 0.01$, intercept = 1.91 Ma).

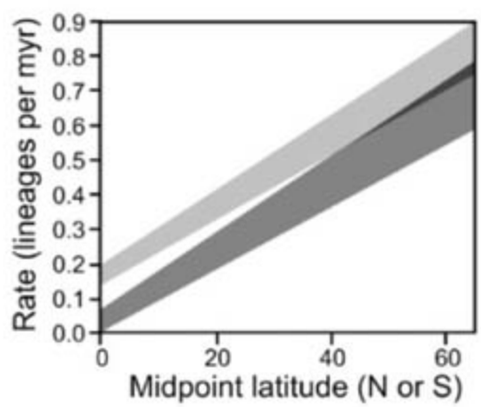

Fig. 2. Estimates of speciation (light gray) and extinction (medium gray) rates in millions of years (myr) across latitude (L) for New World birds and mammals. All rate estimates within 1 log likelihood unit of the maximum likelihood estimate are shown. Region of overlap shown in dark gray.

The maximum likelihood model estimated significantly positive slopes for the relationship between λ (support interval, 0.0076 to 0.0117), μ (support interval, 0.0046 to 0.0135), and latitude for the combined data set of bird and mammal sister species (Fig. 2). Results were similar when maximum haplotype or oldest phylogroup splits were used to correct for lag times, and only the correction with haplotypes is reported here. Estimated speciation and extinction rates were lowest at the equator and increased significantly toward the poles (Fig. 2). The same trends were obtained when excluding sister-species pairs with combined latitudinal ranges greater than 40° and when bird and mammal data sets were fit separately, but results were not significant in the mammal data set. These results hold true even when correcting for the latitudinal gradient in lag time to speciation. We expect that better knowledge of species-level taxonomy in the tropics will revise the lag time and sister-species age gradients. This revision should have minimal influence on the estimates of speciation and extinction, given that they are adjusted for lag time.

These results are surprising because the latitudinal gradient in estimated speciation rate is opposite to the gradient in net rate of diversification estimated by many studies to be highest in tropical taxa (*4*–*10*). For our data on sister species, the gradient in net diversification is not significantly different from zero ($b_\lambda = b_\mu$). Still, the range of estimates for the net diversification gradient supported by this study is consistent with estimates obtained elsewhere for birds (*5*). If the gradient is real, as other studies encompassing longer time periods indicate (*4*–*10*), our findings would support the classic views of Wallace (*19*), Fisher (*20*), and others (*12*, *21*, *22*), who reported that reduced extinction risks at tropical latitudes promoted the gradual buildup of high species diversity there.

These quantitative estimates are based on the assumption that speciation and extinction can be approximated by a continuous birth-death process as latitude becomes higher or lower. Yet, we know that there have been fluctuations in the opportunities for speciation and extinction over the past few million years (*12*, *23*). For example, extensive climatic fluctuations that occurred at high latitudes during the late Pliocene and Pleistocene (2.5 Ma to present) may have concentrated speciation and extinction events in time, resulting in episodic species turnover. In contrast, the bursts of diversification in tropical faunas may predate the late Pliocene and Pleistocene, and the patterns observed today may be the result of a subsequent decline in diversification either because the geological processes that promoted diversification (e.g., formation of Isthmus of Panama, marine incursions, orogeny, and river formation) have slowed or because diversification rates declined as the number of tropical species approached a "carrying capacity" (*7*, *12*).

Given such variability, our estimates are best regarded as averages over the periods studied. Despite these uncertainties, our results suggest that elevated speciation and extinction rates in the temperate zone can drive high turnover of species, whereas rates of species turnover at tropical latitudes are reduced. A recent study of fossil marine bivalves also showed higher per capita rates of genus extinction at high latitudes, suggesting higher species extinction rates as well (*24*) (estimates of per capita speciation rates are still lacking). Together, these results suggest that extinction rates are greatest where species diversity is lowest. Whereas most efforts have aimed at identifying the geological, climatic, and ecological factors that might have elevated tropical speciation rates, our results suggest that both speciation and extinction vary with latitude and contributed importantly to the latitudinal diversity gradient.

References and Notes

1. E. R. Pianka, *Am. Nat.* **100**, 33 (1966).
2. K. J. Gaston, *Nature* **405**, 220 (2000).
3. H. Hillebrand, *Am. Nat.* **163**, 192 (2004).
4. M. Cardillo, *Proc. R. Soc. London Ser. B* **266**, 1221 (1999).
5. M. Cardillo, C. D. L. Orme, I. P. F. Owens, *Ecology* **86**, 2278 (2005).
6. R. E. Ricklefs, in *Tropical Rainforests: Past, Present, and Future*, E. Bermingham, C. W. Dick, C. Moritz, Eds. (Univ. of Chicago Press, Chicago, 2005), pp. 16–40.
7. R. E. Ricklefs, *Ecology* **87**, 2468 (2006).
8. M. Böhm, P. J. Mayhew, *Biol. J. Linn. Soc.* **85**, 235 (2005).
9. J. A. Crame, *Paleobiology* **28**, 184 (2002).
10. M. A. Buzas, L. S. Collins, S. J. Culver, *Proc. Natl. Acad. Sci. U.S.A.* **99**, 7841 (2002).
11. R. L. Honeycutt, M. A. Nedbal, R. M. Adkins, L. L. Janecek, *J. Mol. Evol.* **40**, 260 (1995).
12. J. T. Weir, *Evolution Int. J. Org. Evolution* **60**, 842 (2006).
13. S. Y. W. Ho, M. J. Phillips, A. Cooper, A. J. Drummond, *Mol. Biol. Evol.* **22**, 1561 (2005).
14. J. C. Avise, D. Walker, *Proc. R. Soc. London Ser. B* **265**, 457 (1998).
15. J. C. Avise, D. Walker, G. C. Johns, *Proc. R. Soc. London Ser. B* **265**, 1707 (1998).
16. G. U. Yule, *Philos. Trans. R. Soc. London Ser. B* **213**, 21 (1924).
17. Materials and Methods are available as supporting materials on *Science* Online.
18. D. G. Kendall, *Ann. Math. Statist.* **19**, 1 (1948).
19. A. R. Wallace, *Tropical Nature and Other Essays* (MacMillan, London & New York, 1878).
20. A. G. Fischer, *Evolution Int. J. Org. Evolution* **14**, 64 (1960).
21. G. C. Stebbins, *Flowering Plants: Evolution Above the Species Level* (Harvard Univ. Press, Cambridge, MA, 1974).
22. B. A. Hawkins, J. A. F. Diniz, C. A. Jaramillo, S. A. Soeller, *J. Biogr.* **33**, 770 (2006).
23. J. T. Weir, D. Schluter, *Proc. R. Soc. London Ser. B* **271**, 1881 (2004).
24. D. Jablonski, K. Roy, J. W. Valentine, *Science* **314**, 102 (2006).

25. This work was funded by a doctoral Natural Sciences and Engineering Research Council (NSERC) fellowship and a Smithsonian Short-Term Fellowship (to J.T.W.) and NSERC and Canadian Foundation for Innovation grants (to D.S.). G. Mittelbach, T. Price, S. Otto, R. Ricklefs, and three anonymous reviewers provided useful suggestions for improving this manuscript. DNA sequences generated for this project are reported in database S1.

Supporting Online Material

www.sciencemag.org/cgi/content/full/315/5818/1574/DC1
Materials and Methods
Fig. S1
Tables S1 and S2
References
Database S1

26 September 2006; accepted 13 February 2007
10.1126/science.1135590

Disrupting the Pairing Between *let-7* and *Hmga2* Enhances Oncogenic Transformation

Christine Mayr,[1] Michael T. Hemann,[2] David P. Bartel[1]*

MicroRNAs (miRNAs) are ~22-nucleotide RNAs that can pair to sites within messenger RNAs to specify posttranscriptional repression of these messages. Aberrant miRNA expression can contribute to tumorigenesis, but which of the many miRNA-target relationships are relevant to this process has been unclear. Here, we report that chromosomal translocations previously associated with human tumors disrupt repression of *High Mobility Group A2* (*Hmga2*) by *let-7* miRNA. This disrupted repression promotes anchorage-independent growth, a characteristic of oncogenic transformation. Thus, losing miRNA-directed repression of an oncogene provides a mechanism for tumorigenesis, and disrupting a single miRNA-target interaction can produce an observable phenotype in mammalian cells.

Hmga2 codes for a small, nonhistone, chromatin-associated protein that has no intrinsic transcriptional activity but can modulate transcription by altering the chromatin architecture (*1*, *2*). *Hmga2* is primarily expressed in undifferentiated proliferating cells during embryogenesis and in a wide variety of benign and malignant tumors (*3*–*6*). In many of these tumors, a chromosomal translocation at 12q15 truncates the human *HMGA2* open reading frame (ORF), typically retaining the three DNA-binding domains of HMGA2 while replacing the spacer and the acidic domain at the C terminus by any of a wide variety of ectopic

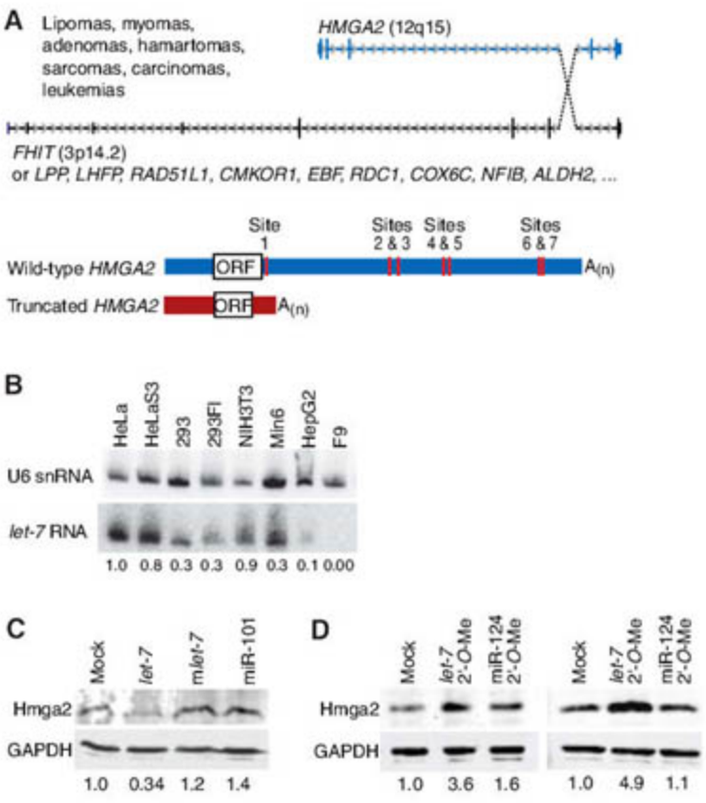

Fig. 1. Chromosomal translocations involving *HMGA2*, and the influence of *let-7* on protein expression. (**A**) Translocations involving *HMGA2* and numerous translocation partners (*3*–*10*) (SOM text). These translocations generate a truncated *HMGA2* mRNA lacking the *let-7* complementary sites of the wild-type mRNA and are associated with the indicated tumors. In its 3′ UTR, human *HMGA2* has seven *let-7* complementary sites, all of which are conserved in the mouse, rat, dog, and chicken (*14*). $A_{(n)}$, polyadenylate tail. (**B**) RNA blot detecting *let-7* RNA in different cell lines. The blot was reprobed for U6 small nuclear RNA (snRNA), and *let-7* signal normalized to that of U6 is indicated. (**C**) Western blot monitoring endogenous Hmga2 48 hours after transfection of F9 cells with the indicated miRNA duplex. The blot was also probed for glyceraldehyde-3-phosphate dehydrogenase (GAPDH), and the normalized Hmga2 signal is indicated. (**D**) Western blot monitoring endogenous Hmga2 at 24 (left) and 48 (right) hours after transfection of NIH3T3 cells with the indicated 2′-*O*-methyl oligonucleotide (2′-*O*-Me). The blot was probed also for GAPDH, and the normalized Hmga2 signal is indicated.

sequences (*3*–*5*, *7*–*10*) (SOM text) (Fig. 1A). The loss of the C-terminal region is nearly always presumed to be the cause of oncogenic transformation. However, the translocations also replace the 3′ untranslated region (3′ UTR), and large fragments of the *Hmga2* 3′ UTR confer repression to luciferase reporters, which has led to the idea that transformation might be caused by the loss of repressive elements in the UTRs (*11*). Indeed, chromosomal rearrangements in some tumors leave the ORF intact but disrupt the 3′ UTR, and this is associated with overexpression of the wild-type Hmga2 protein (*3*, *4*, *10*). Moreover, transgenic mice overexpressing wild-type Hmga2 have similar phenotypes to those expressing the truncated protein; both develop abdominal lipomatosis, then lymphomas, pituitary adenomas, and lung adenomas (*2*, *12*, *13*).

The *Hmga2* 3′ UTR has seven conserved sites complementary to the *let-7* RNA (*14*), a miRNA expressed in later stages of animal development (*15*), leading us to suspect that disrupting *let-7* regulation of *Hmga2* might lead to oncogenic transformation. Consistent with this idea, intro-

[1]Howard Hughes Medical Institute and Department of Biology, Massachusetts Institute of Technology, and Whitehead Institute for Biomedical Research, 9 Cambridge Center, Cambridge, MA 02142, USA. [2]Center for Cancer Research, Massachusetts Institute of Technology, Cambridge, MA 02139, USA.

*To whom correspondence should be addressed. E-mail: dbartel@wi.mit.edu

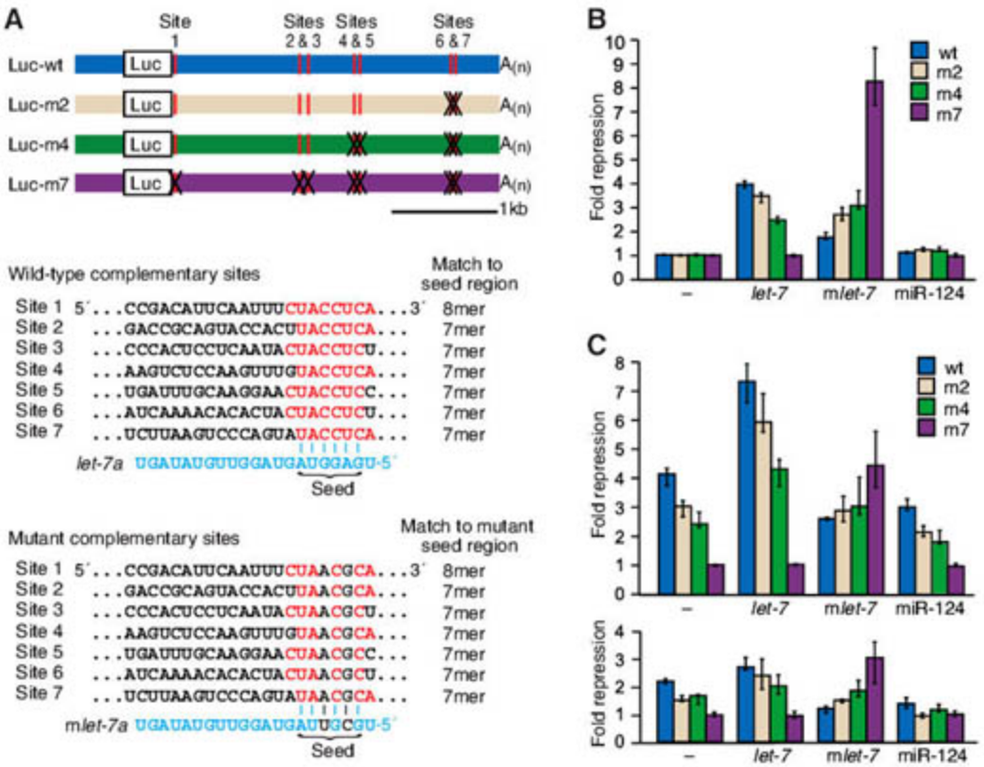

Fig. 2. Luciferase reporter assays showing the influence of miRNA-target pairing. (**A**) Design of Luciferase constructs. The 3′ UTR of murine *Hmga2* was appended to the Luciferase ORF (Luc). *let-7* complementary sites are indicated (vertical red lines), as are mutant sites (black Xs). The Luc-m7, Luc-m4, and Luc-m2 were identical to Luc-wt, except they had seven, four, and two mutant sites, respectively. Each mutant site had two point substitutions that disrupted pairing to *let-7* but created pairing to mutant *let-7* (m*let-7*, bottom, in blue). The seven sites were identified in a search for conserved 7- and 8-nucleotide motifs (7mer and 8mer) matching the seed region of *let-7* (*15*). (**B**) Reporter repression in F9 cells supplemented with the indicated miRNA. Bars are colored to indicate the number of sites mutated in the reporter. Shown are median repression values, with error bars indicating 25th and 75th percentiles; $n = 12$, except experiments with no added miRNA (–), in which $n = 36$. Within each quartet, activity was normalized to that of the Luc-m7 reporter, except for the m*let-7* quartet, for which activity was normalized to that of the Luc-m7 reporter with noncognate miRNA (miR-124). (**C**) Reporter repression in NIH3T3 cells (top) or HeLa cells (bottom) supplemented with the indicated miRNA, performed and displayed as in (B). We also noticed two additional *let-7* complementary sites in the murine *Hmga2* mRNA, but located in the 5′ UTR. When tested in luciferase reporter assays, these sites mediated little or no repression in the different cell lines, and the mutant sites did not respond to m*let-7*, indicating that any effects observed with the 5′ UTR sites were not miRNA specific.

ducing *let-7* RNA repressed Hmga2 in F9 cells (Fig. 1C), an undifferentiated embryonic carcinoma cell line that does not express detectable *let-7* RNA (Fig. 1B). Moreover, introducing a 2′-*O*-methyl oligonucleotide (*16*, *17*) complementary to *let-7* RNA enhanced Hmga2 in NIH3T3 cells (Fig. 1D), a cell line that naturally expresses *let-7* (Fig. 1B). These effects were specific in that they did not occur with noncognate miRNAs (m*let-7* and miR-101, Fig. 1C) or a noncognate inhibitor (miR-124 2′-*O*-Me, Fig. 1D).

To test whether *let-7* directly targets the *Hmga2* 3′ UTR, we constructed reporters with the wild-type 3′ UTR (Luc-wt) and the UTR with point mutations disrupting all seven sites (Luc-m7), the four distal sites (Luc-m4), or the two most distal sites (Luc-m2) (Fig. 2A). In F9 cells, the degree of repression corresponded to the number of intact sites and depended on cotransfection of the *let-7* miRNA, whereas cotransfection of an unrelated miRNA had little effect (miR-124, Fig. 2B). The repression profile inverted when the *let-7* miRNA was replaced with a mutant miRNA, m*let-7* (Fig. 2B), which was designed to recognize the mutant sites instead of the wild-type sites (Fig. 2A). This rescue of repression with compensatory changes in the miRNA confirmed targeting specificity and the importance of direct pairing between the sites and the miRNA.

To examine repression directed by endogenous *let-7*, we repeated the reporter assays using NIH3T3 cells and HeLa cells, which naturally express *let-7* (Fig. 1B). In both cell types, reporter repression depended on the wild-type sites, as would be expected if the endogenous *let-7* miRNA directed repression (Fig. 2C). Adding exogenous *let-7* RNA enhanced repression, suggesting that *let-7* RNA was subsaturating in these cells. Adding mutant *let-7* also caused reporters with mutant sites to be repressed. Adding m*let-7* or miR-124 decreased repression of the reporter with wild-type sites (particularly in HeLa cells), as if the transfected miRNA was competing with endogenous *let-7* RNA for a limiting factor.

Having established that the sites within the *Hmga2* 3′ UTR could mediate *let-7*–directed repression, we tested whether disrupting this repression could promote oncogenic transformation. Assays for anchorage-independent growth were performed with NIH3T3 cells, which form colonies in soft agar when stably transfected with a potent oncogene. Stably transfecting a vector expressing wild-type *Hmga2* did not significantly increase the number of colonies compared with transfecting an empty vector, whereas transfecting a vector expressing a truncated *Hmga2* (Hmga2-tr) (Fig. 3A), shown previously to promote anchorage-independent growth (*18*), produced significantly more colonies (Fig. 3B). As in human tumors, Hmga2-tr lacked the spacer, the acidic domain, and the entire 3′ UTR with its miRNA complementary sites (Fig. 3A). The increase in colonies was attributed to the loss of *let-7* repression rather than the truncation of the protein because stably expressing Hmga2-m7, which had the full ORF but disrupted *let-7* complementary sites (Fig. 3A), produced at least as many colonies as Hmga2-tr, whereas stably expressing Hmga2-ORFtr, which had the truncated ORF but intact miRNA complementary sites (Fig. 3A), produced a number comparable to that of Hmga2-wt (Fig. 3B). Stably expressing Hmga2-m4, which retained the first three *let-7* sites, led to an intermediate number of colonies.

We next tested whether the stably transfected cells used to assay anchorage-dependent growth were also able to form subcutaneous tumors in nude mice. Consistent with our soft-agar results, tumors were observed when injecting cells expressing constructs with mutated *let-7* sites: After 5 weeks, three of four mice injected with Hmga2-m7 cells and two of four mice injected with Hmga2-m4 cells had tumors at the sites of injection. One of four injected with Hmga2-tr cells and one of four injected with Hmga2-ORFtr also had tumors, whereas no tumors were observed 5 weeks after injecting cells stably transfected with either wild-type Hmga2 or empty vector.

Taken together, our results support the proposal that the *let-7* miRNA acts as a tumor-suppressor gene (*19*, *20*) and indicate that a major mechanism of oncogenic *Hmga2* translocations associated with various human tumors is the loss of *let-7* repression. Thus, loss of miRNA-directed repression of an oncogene is another type of oncogene-activating event that should be considered when investigating the effects of mutations associated with cancer. Likewise, mutations that create miRNA-directed repression of tumor-suppressor genes might also impart a selective advantage to the tumor cells. In this regard, we note that *Hmga2* translocations frequently append the *Hmga2* 3′ UTR to the 3′ end of known tumor-suppressor genes, including *FHIT*, *RAD51L1*, and *HEI10* (*5*, *8*, *9*), suggesting that *let-7*–directed repression of these translocation partners might cooperate with disrupting *Hmga2* repression to promote tumorigenesis.

Vertebrate miRNAs can each have hundreds of conserved targets and many additional nonconserved targets (*15*, *21*–*25*), all of which have confounded exploration of the biological impact of particular miRNA-target relationships. In worms, flies, and plants, repression of particular targets is known to be relevant because genetic studies have investigated what happens when that target alone is not repressed by the miRNA (*26*–*28*). Because of the possibility that multiple interactions might need to be perturbed to observe a phenotypic consequence in mammals, it has been unclear whether the importance of a particular mammalian miRNA-target interaction can be demonstrated experimentally. Our results, combined with previous cytogenetic studies that speak to the effect of misregulating the endogenous human *HMGA2* gene, show that disrupting miRNA regulation of *Hmga2* enhances oncogenic trans-

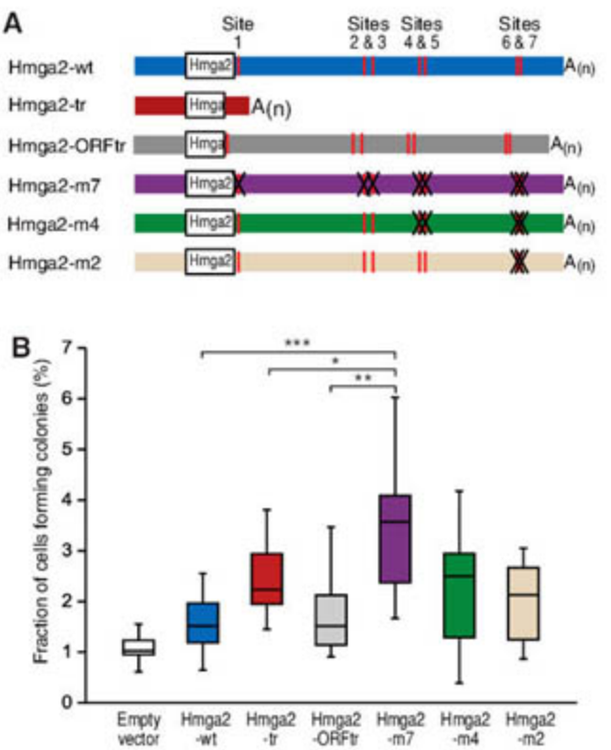

Fig. 3. Soft-agar assay for anchorage-independent growth. (**A**) Hmga2 constructs used for stable transfection, depicted as in Fig. 2A. (**B**) Colony formation. For cells stably transfected with the indicated vector, the percentage that yielded colonies after 28 days is plotted (horizontal line, median; box, 25th through 75th percentile; error bars, range; $n = 12$ from four independent experiments, each in triplicate). All but Hmga2-wt yielded a significantly higher number of colonies than did the empty vector (Mann-Whitney test for each, $P < 0.05$). When compared with Hmga2-wt, a significantly higher number of colonies was observed for Hmga2-tr ($P = 0.003$). Hmga2-m7 showed significantly more colonies than any of the other constructs tested ($P < 0.05$ for each; *, $P = 0.041$; **, $P = 0.002$; ***, $P = 10^{-6}$). No significant difference was observed between Hmga2-wt and the construct with the truncated ORF ($P = 0.61$).

formation, thereby demonstrating that disrupting miRNA regulation of a single mammalian gene can have a cellular phenotype in vitro and a clinical phenotype in vivo.

References and Notes

1. R. Sgarra *et al.*, *FEBS Lett.* **574**, 1 (2004).
2. M. Fedele *et al.*, *Oncogene* **21**, 3190 (2002).
3. E. F. Schoenmakers *et al.*, *Nat. Genet.* **10**, 436 (1995).
4. J. M. Geurts, E. F. Schoenmakers, W. J. Van de Ven, *Cancer Genet. Cytogenet.* **95**, 198 (1997).
5. N. Mine *et al.*, *Jpn. J. Cancer Res.* **92**, 135 (2001).
6. M. Fedele *et al.*, *Carcinogenesis* **22**, 1583 (2001).
7. M. M. Petit, R. Mols, E. F. Schoenmakers, N. Mandahl, W. J. Van de Ven, *Genomics* **36**, 118 (1996).
8. E. F. Schoenmakers, C. Huysmans, W. J. Van de Ven, *Cancer Res.* **59**, 19 (1999).
9. J. M. Geurts, E. F. Schoenmakers, E. Roijer, G. Stenman, W. J. Van de Ven, *Cancer Res.* **57**, 13 (1997).
10. N. Inoue *et al.*, *Blood* **108**, 4232 (2006).
11. L. Borrmann, S. Wilkening, J. Bullerdiek, *Oncogene* **20**, 4537 (2001).
12. S. Battista *et al.*, *Cancer Res.* **59**, 4793 (1999).
13. G. Baldassarre *et al.*, *Proc. Natl. Acad. Sci. U.S.A.* **98**, 7970 (2001).
14. B. P. Lewis, C. B. Burge, D. P. Bartel, *Cell* **120**, 15 (2005).
15. A. E. Pasquinelli *et al.*, *Nature* **408**, 86 (2000).
16. G. Hutvagner, M. J. Simard, C. C. Mello, P. D. Zamore, *PLoS Biol.* **2**, E98 (2004).
17. Materials and methods are available as supporting material on *Science* Online.
18. M. Fedele *et al.*, *Oncogene* **17**, 413 (1998).
19. S. M. Johnson *et al.*, *Cell* **120**, 635 (2005).
20. J. Takamizawa *et al.*, *Cancer Res.* **64**, 3753 (2004).
21. A. Krek *et al.*, *Nat. Genet.* **37**, 495 (2005).
22. L. P. Lim *et al.*, *Nature* **433**, 769 (2005).
23. K. K. Farh *et al.*, *Science* **310**, 1817 (2005).
24. J. Krutzfeldt *et al.*, *Nature* **438**, 685 (2005).
25. A. J. Giraldez *et al.*, *Science* **312**, 75 (2006).
26. B. Wightman, I. Ha, G. Ruvkun, *Cell* **75**, 855 (1993).
27. E. C. Lai, B. Tam, G. M. Rubin, *Genes Dev.* **19**, 1067 (2005).
28. M. W. Jones-Rhoades, D. P. Bartel, B. Bartel, *Annu. Rev. Plant Biol.* **57**, 19 (2006).

29. We thank M. Narita and S. Lowe for providing the Hmga2 antibody, and C. Jan, A. Grimson, and M. Narita for helpful discussions and advice. Supported by grants from the Deutsche Forschungsgemeinschaft (C.M.) and the NIH (D.B.). D.B. is a Howard Hughes Medical Institute Investigator.

Supporting Online Material

www.sciencemag.org/cgi/content/full/1137999/DC1
Materials and Methods
SOM Text
Figs. S1 and S2
References

27 November 2006; accepted 13 February 2007
Published online 22 February 2007;
10.1126/science.1137999
Include this information when citing this paper.

Suppression of MicroRNA-Silencing Pathway by HIV-1 During Virus Replication

Robinson Triboulet,[1] Bernard Mari,[3] Yea-Lih Lin,[2] Christine Chable-Bessia,[1] Yamina Bennasser,[5] Kevin Lebrigand,[3] Bruno Cardinaud,[3] Thomas Maurin,[3] Pascal Barbry,[3] Vincent Baillat,[4] Jacques Reynes,[4] Pierre Corbeau,[2] Kuan-Teh Jeang,[5] Monsef Benkirane[1]*

MicroRNAs (miRNAs) are single-stranded noncoding RNAs of 19 to 25 nucleotides that function as gene regulators and as a host cell defense against both RNA and DNA viruses. We provide evidence for a physiological role of the miRNA-silencing machinery in controlling HIV-1 replication. Type III RNAses Dicer and Drosha, responsible for miRNA processing, inhibited virus replication both in peripheral blood mononuclear cells from HIV-1–infected donors and in latently infected cells. In turn, HIV-1 actively suppressed the expression of the polycistronic miRNA cluster miR-17/92. This suppression was found to be required for efficient viral replication and was dependent on the histone acetyltransferase Tat cofactor PCAF. Our results highlight the involvement of the miRNA-silencing pathway in HIV-1 replication and latency.

RNA silencing is a mechanism for gene regulation involving small noncoding RNA (*1*) as well as an innate host cell defense mechanism against viruses (*2*, *3*). MicroRNA (miRNA) genes are most often transcribed by RNA polymerase II, and the resulting primary (pri) miRNA is processed in the nucleus by the RNAse type III Drosha to produce precursor (pre) miRNA. Pre-miRNAs are then exported to the cytoplasm by exportin 5 and processed into miRNA/miRNA* (guide/passenger) duplexes through the action of the cytoplasmic type III RNAse Dicer. miRNA/miRNA* is incorporated into the RNA-induced silencing complex (RISC) where miRNA* is degraded, with miRNA serving as a guide for its mRNA target. miRNA-armed RISC can enforce either degradation of mRNA (in the case of perfect sequence complementarity) or inhibition of mRNA translation (in the case of imperfect sequence complementarity) (*3*). Accumulating evidence suggests that the miRNA pathway also controls the replication of both RNA and DNA viruses (*4*).

To address whether the miRNA-silencing machinery influences HIV-1 replication, we used specific small interfering RNA (siRNAs) to reduce the expression of endogenous Dicer and Drosha in peripheral blood mononuclear cells (PBMCs) from HIV-1–infected donors who had been either CD8+T cell–depleted to facilitate virus production (*5*) (Fig. 1A) or not (Fig. 1B) (*6*–*8*). On the basis of reverse transcription polymerase chain reaction (RT-PCR) performed on total RNA isolated from cells, we verified that both Dicer and Drosha mRNAs were efficiently reduced (Fig. 1). When siRNA-transfected CD8+ T cell–depleted PBMCs were cocultured with activated PBMCs from healthy donors, HIV-1 from Dicer and Drosha knocked-down cells replicated with faster kinetics compared to virus from cells transfected with nonfunctional Dicer and Drosha siRNA control (Fig. 1A). When total PBMCs from infected donors were used, this effect was more pronounced (Fig. 1B).

The repressive effect of Dicer and Drosha on HIV-1 replication was also observed in latently infected U1 cells, which express a mutant of HIV-1 Tat protein unable to efficiently activate the long terminal repeat (LTR) required for efficient viral transcription (*9*) and consequently produce a low amount of virus (fig. S1A). HIV-1 infection and replication were also more efficient in Dicer or Drosha knocked-down Jurkat cells, compared with control siRNA-transfected cells (fig. S1B). Because knockdown of Dicer and Drosha is transient, the observed effect on virus replication suggests that Dicer- and Drosha-mediated repression of viral gene expression takes place early during virus replication (fig. S1C). To verify this, we evaluated the effect of Dicer and Drosha knockdown in a single-round infection assay in which cells were infected with HIV-1 that harbored a luciferase gene (HIV-1VSV-Luc) pseudotyped with vesicular stomatitis virus (VSV.G) envelope. In a single-round infection assay, we observed by luciferase activity that knockdown of Dicer or Drosha increased virus production when compared with control siRNA-transfected

[1]Laboratoire de Virologie Moléculaire, Institut de Génétique Humaine, Montpellier, France. [2]Laboratoire des Lentivirus et Transfert de Gènes, Institut de Génétique Humaine, Montpellier, France. [3]Institut de Pharmacologie Moléculaire et Cellulaire, UMR6097 CNRS/UNSA, Sophia Antipolis, France. [4]Service des Maladies Infectieuses et Tropicales, Hôpital Gui de Chauliac, Montpellier, France. [5]Laboratory of Molecular Microbiology, National Institute of Allergy and Infectious Diseases, National Institutes of Health, Bethesda, MD, USA.

*To whom correspondence should be addressed. E-mail: bmonsef@igh.cnrs.fr

Jurkat cells (fig. S1B). Thus, both Dicer and Drosha contribute to the suppression of HIV-1 replication.

The findings from knockdown of Dicer and Drosha likely arise from complex effects on non-miRNA and miRNA pathways that influence the processing of cellular and viral miRNAs (*10*). To determine the ability of HIV-1 to modulate the expression level of cellular miRNAs involved in its replication, the expression profile of cellular miRNA in infected and noninfected Jurkat cells were compared with microarray analysis (Fig. 2A and fig. S2). Eleven miRNAs were up-regulated upon infection, including miR-122, miR-370, miR-373* and miR-297, moieties detected only in HIV-1 infected cells. A polycistronic miRNA cluster, miR-17/92—which recently was found to be involved in genomic amplification in malignant lymphoma and lung cancer (*11*–*13*)—was substantially decreased upon HIV-1 infection (Fig. 2B). miR-17/92 encodes miR-17-(5p/3p), miR-18, miR-19a, miR-20a, miR-19b-1, and miR-92-1 (*14*). The microarray results were confirmed for all the indicated miRNAs by Northern blotting (Fig. 2C and fig. S2C). Knockdown of pri-miR-17/92 with specific siRNA enhanced HIV-1 production in Jurkat cells (fig. S4), supporting the interpretation that down-regulation of miR-17/92 affects virus replication.

Sequence analysis indicates that miR-17/92 does not directly target the viral genome (*6*–*8*), which suggests that miR-17/92 might affect HIV-1 replication by targeting cellular protein(s). Indeed, we found that histone acetylase PCAF has four potential target sequences in its 3′UTR for miR-17-5p and miR-20a (fig. S3A). Because PCAF is an important cofactor for Tat in HIV-1 gene expression (*15*, *16*), we asked if miR-17-5p and miR-20a might specifically target PCAF mRNA. HeLa cells were transfected with either nonfunctional siRNA, PCAF-specific siRNAs, or separately with either miR-17-5p or miR-20a. Expression levels of endogenous PCAF protein (Fig. 3A) was reduced in PCAF siRNA- or miR-17-5p- or miR-20a–transfected cells. By contrast, PCAF mRNA (Fig. 3B) was reduced by PCAF siRNA but not by miR-17-5p and 20a. When different siRNAs or miRNA were cotransfected with a PCAF expression vector lacking the 3′UTR region of the gene, only the siRNA specific for PCAF's coding region affected the level of ectopically expressed PCAF (Fig. 3C). We confirmed these results using a reporter

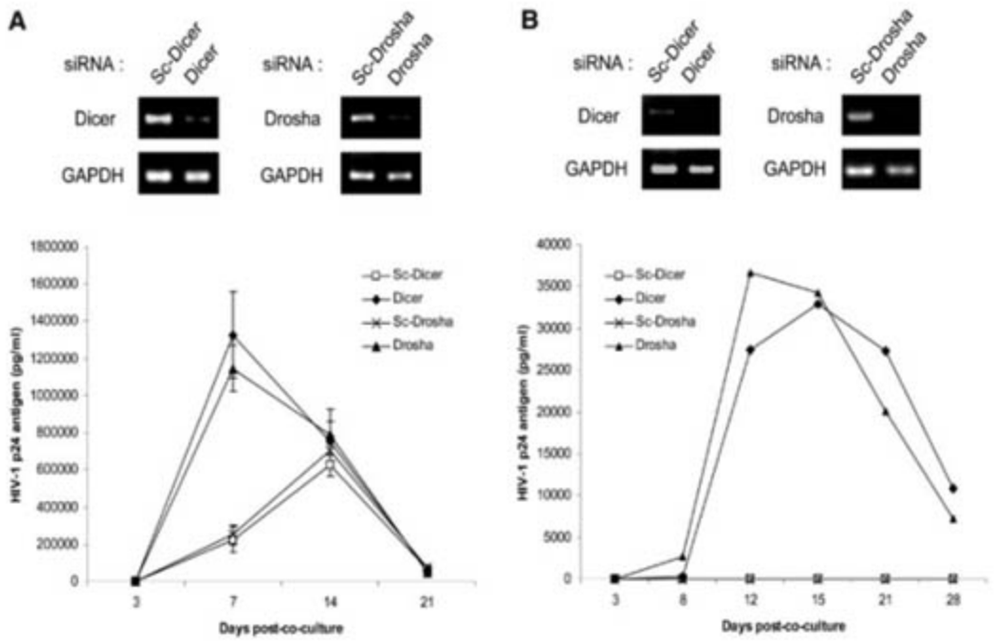

Fig. 1. Dicer and Drosha are required for suppression of HIV-1 replication. Viral production from CD8+ T cell–depleted PBMCs (**A**) and undepleted PBMCs (**B**) transfected with siRNA as indicated. siRNA-transfected cells were either analyzed for expression of Dicer and Drosha mRNA by RT-PCR 48 hours after transfection (top) or cocultured with activated PBMCs from healthy donors (bottom). Virus replication was monitored every 3 or 4 days after coculture by measuring p24 viral antigen in culture supernatant.

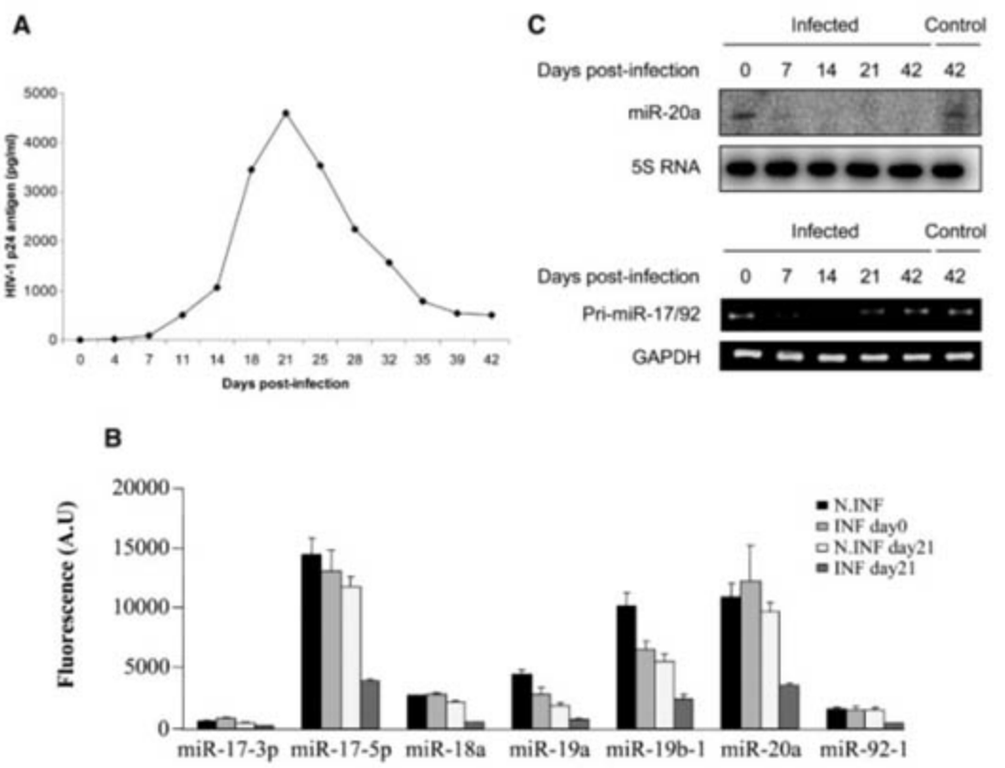

Fig. 2. Expression of the miR-17/92 cluster is down-regulated during HIV-1 infection. (**A**) HIV-1 replication in pNL4-3–infected Jurkat cells was quantified by measuring p24 antigen in culture supernatants every 3 or 4 days. (**B**) Expression of the miR-17/92 cluster members during HIV-1 infection. miRNA from infected (INF) and noninfected (N.INF) Jurkat cells at days 0 and 21 were directly labeled as previously described (*25*) and hybridized on microarrays. Results show normalized fluorescence intensity for all probes corresponding to the miR-17/92 cluster in each condition (n = 4). (**C**) Northern blotting and RT-PCR analyses of pNL4-3–infected cells. Total RNA from infected and noninfected Jurkat cells was extracted and analyzed either by Northern blotting with the indicated probes or by RT-PCR with the indicated primers.

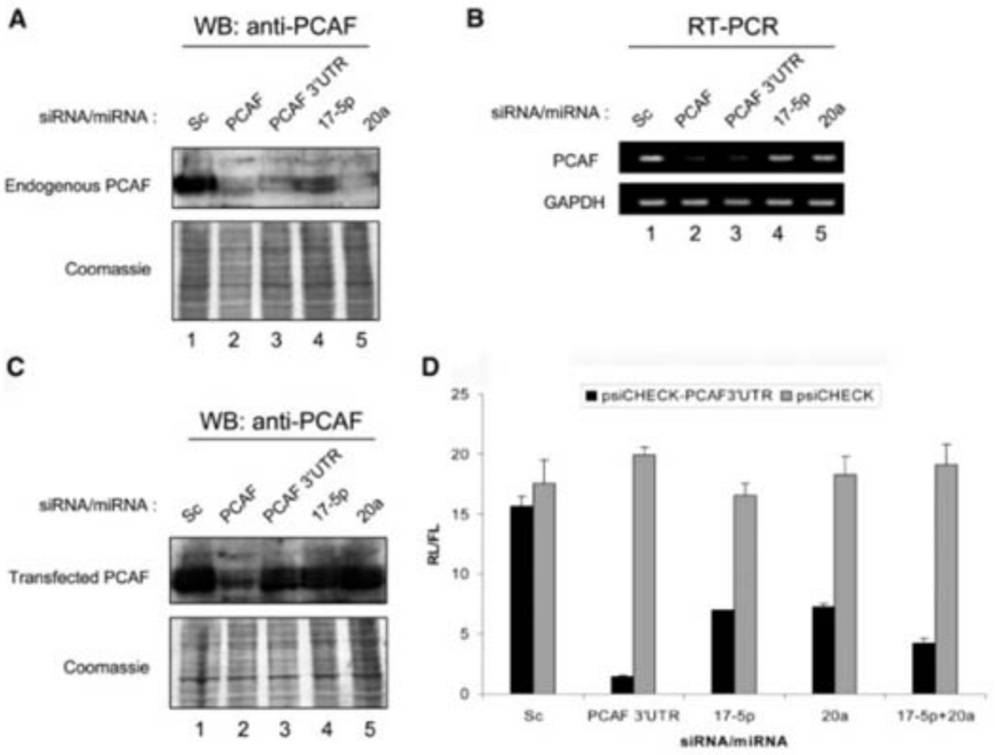

Fig. 3. PCAF mRNA is a target for miR-17-5p and miR-20a. Western blot (**A** and **C**) and RT-PCR (**B**) analysis of PCAF expression in Hela cells transfected with the indicated siRNA or miRNA [(A) and (B)] or cotransfected with siRNA or miRNA and a PCAF expression vector lacking the 3′UTR (C). Proteins were analyzed by Western blot with antibody to PCAF (A and C). Total RNA was analyzed by RT-PCR using PCAF- or GAPDH-specific oligonucleotides (B). (**D**) HeLa cells were cotransfected either with psiCHECK-2PCAF3′UTR or with psiCHECK-2 and siRNA or miRNA, as indicated on the figure. Renilla and firefly luciferase activities were measured 24 hours after transfection. Results are represented as the ratio of renilla luciferase (RL) to firefly luciferase (FL).

construct in which PCAF 3′UTR was inserted downstream of the *renilla* luciferase stop codon (Fig. 3D). Collectively, our results are consistent with miR-17-5p and miR-20a targeting the 3′UTR region of PCAF to inhibit mRNA translation.

To understand the function of miR-17/92 in HIV-1 replication, PBMCs from HIV-1 infected donors were transfected separately with miR-17-5p, miR-20a, or control siRNA, and HIV-1 replication was monitored by measuring HIV-1 p24 antigen in culture supernatant. Transfection of miR-17-5p or miR-20a substantially reduced HIV-1 production (Fig. 4A), with similar results also seen when the same experiments were performed in U1 (fig. S5D) or Jurkat (fig. S6B) cells.

To further analyze the involvement of miR-17-5p and miR-20a in controlling PCAF expression and HIV-1 replication, we used miRNA inhibitors (*6*). Transfection with anti-miR-17-5p or anti-miR-20a, compared with control transfection, enhanced PCAF expression and HIV-1 production (Fig. 4B). Conversely, overexpression of miR-17-5p, miR-20a, or siRNA specific for PCAF 3′UTR reduced PCAF expression and HIV-1 production in transfected Jurkat cells (Fig. 4C). These results support roles played by miR-17-5p and miR-20a in regulating PCAF expression and HIV-1 replication.

If PCAF is a critically relevant factor upregulated by knockdown of Drosha or Dicer, then one prediction would be that coinhibiting PCAF with Dicer/Drosha would partly mitigate the positive effect on HIV-1 replication seen with single knockdown of Dicer/Drosha. To test this reasoning, we compared HIV-1 production in Jurkat cells that had been knocked down for both PCAF and either Drosha or Dicer (Fig. 4D) with cells knocked down only for Drosha or Dicer. Virus enhancement observed with Drosha/Dicer knockdown was indeed attenuated when PCAF also was knocked down (Fig. 4D).

Because PCAF is a cofactor for Tat transactivation of an integrated HIV-1 (*17*), we next wanted to confirm that this effect was Tat-dependent. To do this, knockdown of Drosha decreased Tat-mediated transactivation of an integrated HIV-1 LTR construct (fig. S5). These results verify that PCAF is a factor downstream of Drosha and Dicer knockdown, which mediates enhanced HIV-1 replication. However, knocking down Dicer and Drosha may also reduce the cells' ability to process other RNAs, including autoinhibitory siRNA/miRNA from the HIV-1 genome (*10*, *18*, *19*). The finding that overexpression of PCAF in Jurkat cells knocked down for Drosha or Dicer does not significantly increase HIV production is partly compatible with this result (fig. S6A). The above analysis suggests that disruption of PCAF/Tat by miR-17-5p/miR-20a contributes to the effect of HIV-1 replication by Drosha/Dicer knockdown (Fig. 4E). However, we observed that the inhibition of HIV-1 production by miR-17-5p and miR-20a (fig. S6, B and C) was compensated for by transfection with a PCAF expression vector lacking its 3′UTR sequence (Fig. 4E). These results verify that the anti-HIV effect of miR-17-5p and miR-20a does operate through the PCAF/Tat pathway (*16*).

We provide evidence for an intricate physiological interplay between the cell's miRNA machinery and an invading virus, HIV-1. We report three salient findings: First, that Drosha and Dicer contribute a central role in human cells to a defense against HIV-1. Second, a portion of Drosha and Dicer's effect is explained by a PCAF-miR-17-5p/miR-20 axis, although the entirety of Drosha and Dicer influence on HIV-1 replication likely involves additional cellular and viral miRNAs (*10*, *18*, *20*, *21*). Third, HIV-1 infection suppresses the expression of miR-17-5p/miR-20. These findings may help address the current challenge of how to activate latent viral reservoirs in HIV therapy (*22*–*24*).

References and Notes

1. O. Voinnet, *Curr. Opin. Plant Biol.* **5**, 444 (2002).
2. F. Qu, T. J. Morris, *FEBS Lett.* **579**, 5958 (2005).
3. A. Saumet, C. H. Lecellier, *Retrovirology* **3**, 3 (2006).
4. O. Voinnet, *Nat. Rev. Genet.* **6**, 206 (2005).
5. C. Mackewicz, J. A. Levy, *AIDS Res. Hum. Retroviruses* **8**, 1039 (1992).
6. Materials and methods are available as supporting material on *Science* Online.
7. Institut de Pharmacologie Moléculaire et Cellulaire, Centre National de la Recherche Scientifique, www.microarray.fr/microRNA.
8. Experimental data and associated microarray designs are available in the National Center for Biotechnology Information's Gene Expression Omnibus (GEO) under series GSE4761 and GSE6673 and platforms records GPL3241 and GPL4715.
9. S. Emiliani *et al.*, *J. Virol.* **72**, 1666 (1998).
10. M. L. Yeung, Y. Bennasser, S. Y. Le, K. T. Jeang, *Cell Res.* **15**, 935 (2005).
11. L. He *et al.*, *Nature* **435**, 828 (2005).
12. H. Tagawa, M. Seto, *Leukemia* **19**, 2013 (2005).

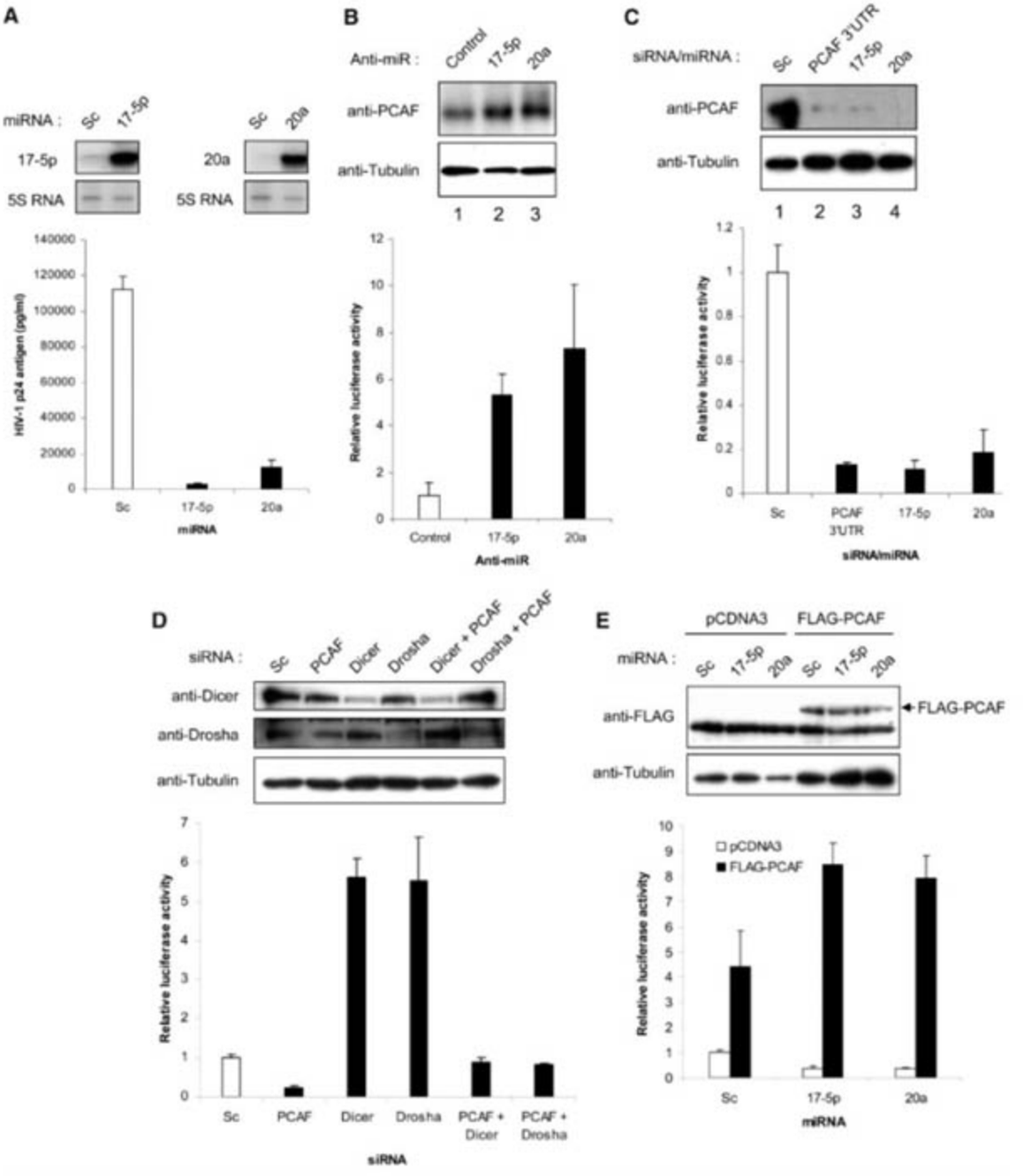

Fig. 4. Antiviral activity of miR-17-5p and miR-20a is mediated through PCAF down-regulation. (**A**) Overexpression of miR-17-5p and miR-20a blocks HIV-1 replication in PBMCs from infected donors. Viral production from CD8+ T cell–depleted PBMCs transfected with miR-17-5p and miR-20a. miRNA-transfected PBMCs from infected donors were either analyzed for expression of miRNA by Northern blot 24 hours after transfection (top) or cocultured with activated PBMCs from healthy donors (bottom). Virus replication was monitored by measuring p24 viral antigen in culture supernatant at day 15 after coculture. (**B**) Inhibition of miR-17-5p and miR-20a using specific LNA enhances PCAF expression and HIV-1 replication in Jurkat cells. Jurkat cells were transfected with anti-miR as indicated. Anti-miR-32 was used as a control. Cells were either analyzed for PCAF and tubulin expression by Western blot (top) or infected with a single-round infectious virus HIV-1-VSV-luc. Luciferase activity was measured 48 hours after infection (bottom). (**C**) Overexpression of miR-17-5p and miR-20a inhibits PCAF expression and HIV-1 replication in Jurkat cells. Jurkat cells were transfected with siRNA or miRNA as indicated. PCAF and tubulin expression was monitored by Western blot (top). Replication of HIV-1-VSV-luc was measured by luciferase activity in cell extracts (bottom). (**D**) PCAF silencing in Jurkat cells partially nullifies the enhancement of HIV-1 replication obtained after Dicer and Drosha knockdown. Jurkat cells were transfected with siRNA as indicated. Cells were either analyzed for Dicer, Drosha, and tubulin expression by Western blot (upper right) or infected with a single-round infectious virus HIV-1-VSV-luc. Luciferase activity in cell extracts was measured 48 hours after infection (bottom). (**E**) PCAF lacking the 3′UTR reverses the repression of HIV-1 replication caused by miR-17-5p and miR-20a. Jurkat cells were transfected with miRNA as indicated, with either pCDNA3 or FLAG-PCAF expression vectors. 48 hours after transfection, FLAG-PCAF and tubulin expressions were monitored by Western blot (top), and replication of HIV-1-VSV-luc was measured by luciferase activity in cell extracts (bottom).

13. Y. Hayashita *et al.*, *Cancer Res.* **65**, 9628 (2005).
14. M. Lagos-Quintana, R. Rauhut, W. Lendeckel, T. Tuschl, *Science* **294**, 853 (2001).
15. R. E. Kiernan *et al.*, *EMBO J.* **18**, 6106 (1999).
16. M. Ott *et al.*, *Novartis Found. Symp.* **259**, 182 (2004).
17. M. Benkirane *et al.*, *J. Biol. Chem.* **273**, 24898 (1998).
18. Y. Bennasser, S. Y. Le, M. Benkirane, K. T. Jeang, *Immunity* **22**, 607 (2005).
19. S. Omoto, Y. R. Fujii, *J. Gen. Virol.* **86**, 751 (2005).
20. Y. Bennasser, S. Y. Le, M. L. Yeung, K. T. Jeang, *Retrovirology* **1**, 43 (2004).
21. M. L. Yeung *et al.*, *Retrovirology* **2**, 81 (2005).
22. K. Lassen, Y. Han, Y. Zhou, J. Siliciano, R. F. Siliciano, *Trends Mol. Med.* **10**, 525 (2004).
23. R. J. Pomerantz, *Curr. Opin. Investig. Drugs* **3**, 1133 (2002).
24. A. Marcello, *Retrovirology* **3**, 7 (2006).
25. T. Babak, W. Zhang, Q. Morris, B. J. Blencowe, T. R. Hughes, *RNA* **10**, 1813 (2004).

26. We wish to thank S. Emiliani, C. Lecellier, E. Bertrand, and A. Saib for critical reading of the manuscript; G. Rios, V. Magnone, and F. Aguila for technical support; and O. Voinnet and C. Lecellier for pGL3b-promoter 17/92 and pGL3b-promoter 23/24 plasmids. Microarray experiments were performed with the Nice-Sophia-Antipolis Transcriptome Platforms of the Genopole (France) facilities. This work was supported by grants from the Human Frontier Science Program, European Union 012182, Sidaction, and Agence Nationale de Recherches sur le Sida to M.B. R.T was supported by the Ministry of Education, Research and Technology, Y.L by Sidaction, and P.B. by the réseau National des génopoles, Provence Alpes Côte d'Azur, and Institut National du Cancer (PL079).

Supporting Online Material

www.sciencemag.org/cgi/content/full/1136319/DC1
Materials and Methods
Figs. S1 to S6
References

16 October 2006; accepted 13 February 2007
Published online 22 February 2007;
10.1126/science.1136319
Include this information when citing this paper.

Founder Effects in the Assessment of HIV Polymorphisms and HLA Allele Associations

Tanmoy Bhattacharya,[1,2] Marcus Daniels,[1] David Heckerman,[3] Brian Foley,[1] Nicole Frahm,[4] Carl Kadie,[3] Jonathan Carlson,[3,5] Karina Yusim,[1] Ben McMahon,[1] Brian Gaschen,[1] Simon Mallal,[6] James I. Mullins,[7] David C. Nickle,[7] Joshua Herbeck,[7] Christine Rousseau,[7] Gerald H. Learn,[7] Toshiyuki Miura,[4] Christian Brander,[4] Bruce Walker,[4,8] Bette Korber[1,2*]

Escape from T cell–mediated immune responses affects the ongoing evolution of rapidly evolving viruses such as HIV. By applying statistical approaches that account for phylogenetic relationships among viral sequences, we show that viral lineage effects rather than immune escape often explain apparent human leukocyte antigen (HLA)–mediated immune-escape mutations defined by older analysis methods. Phylogenetically informed methods identified immune-susceptible locations with greatly improved accuracy, and the associations we identified with these methods were experimentally validated. This approach has practical implications for understanding the impact of host immunity on pathogen evolution and for defining relevant variants for inclusion in vaccine antigens.

HIV escapes the immune system of the human host by mutation, and thus mutational patterns may identify regions important for host immune recognition. Cytotoxic T lymphocytes (CTLs), part of the adaptive immune response, recognize short peptide fragments called epitopes, cleaved from viral proteins and presented on the surface of infected cells by human leukocyte antigens (HLAs). Rapid emergence of sequence variation within some HIV epitopes provides clear evidence for host-driven immune selection during infection (*1*–*4*). HLAs are highly polymorphic and can only present viral epitopes that have the appropriate amino acid composition to enable binding, and so people carrying the same HLA allele have a shared potential to recognize the same epitopes. The viral sequence is, therefore, expected to show patterns of mutations that correlate with the host's HLAs. A population study in Perth, Australia (*5*), indicated that 43% of positions in HIV Pol protein had polymorphisms potentially associated with HLA A and B alleles.

Although the Moore *et al.* study used polymorphisms elsewhere in the HIV protein as well as HLA alleles as explanatory variables in the multiple regression analysis, it did not explicitly control for viral lineage founder effects: Relatively closely related sets of viruses among contemporary viral sequences share some amino acids simply by virtue of common descent and should not be treated as independent. We have now developed a methodology to account for these genetic relationships. Newer sequence data from Perth (*6*), consisting of intermittent fragments spanning different genomic regions of HIV-1 from 234 individuals along with high-resolution HLA genotyping results, were used to explore the importance of lineage effects (*6*, *7*). Because reliable phylogenetic analysis requires long continuous stretches of sequence data, we restricted our analyses to the longest continuous sequence length available from a reasonably large set of subjects, a 1732–base pair (bp) region starting in p17 *gag* and ending in *pol* from 96 sequences (82 subtype B, 2 D, 8 C, and 4 circulating recombinant form CRF01 sequences).

We first analyzed all 234 available sequences over this 1732-bp stretch using methods similar to those of (*5*) and including HLA class II alleles, so that we could compare our methods directly to those previously employed. We found 346 associations between host HLA and HIV mutations, with an uncorrected P-value of <0.05. Correcting for multiple tests, 80 out of 346 associations had a q-value (*8*) of <0.2 (that is, an estimated 80% of these are true positive correlations). Of these 80 associations, 32 were with HLA C*1701, and viral subtyping of the sequences bearing the associated substitutions revealed that all were subtype C virus, in this primarily subtype B cohort. Importantly, subtype C is prevalent in southern Africa, and HLA C*1701 is common only in Africa (*9*). Thus, any substitutions distinguishing the C and B subtypes would appear to be associated with C*1701. Sixty out of 80 associations could similarly be explained by an association of the HLA class I allele with the subtype of the virus (Table 1, Fig. 1A) and, consequently, most likely explained by the demographic and geographical structure of the HIV epidemic rather than immune pressure.

[1]Los Alamos National Laboratory, Los Alamos, NM 87545, USA. [2]Santa Fe Institute, Santa Fe, NM 87501, USA. [3]Machine Learning and Applied Statistics Group, Microsoft Research, Redmond, WA 98052, USA. [4]Partners AIDS Research Center, Massachusetts General Hospital, Harvard Medical School, Boston, MA 02129, USA. [5]Department of Computer Science and Engineering, University of Washington, Seattle, WA 98195, USA. [6]Center for Clinical Immunology and Biomedical Statistics, Royal Perth Hospital, Perth, Australia. [7]Department of Microbiology, University of Washington, Seattle, WA 98195–8070, USA. [8]Howard Hughes Medical Institute, Chevy Chase, MD 20815, USA.

*To whom correspondence should be addressed. E-mail: btk@lanl.gov

Table 1. Summary of the 60 HIV mutation-host HLA associations driven by different subtypes. The number of associated sequence positions for each HLA is given in the "No. of associations" column. Populations with high frequencies of a given HLA are noted (*14*–*16*) and are as expected given the subtypes: CRF01 is common in Asia, C in Africa, and B among Europeans, North Americans, and Australians (www.hiv.lanl.gov/components/hiv-db/new_geography/geography.comp?region=world&form=all). The HIV molecular immunology database was searched (www.hiv.lanl.gov/content/immunology/) for HLA-related epitopes that span the site of interest; the only one found was A2 epitope TLQEQIGW (*17*). Associations embedded in potential epitopes 8 to 12 amino acids long based on HLA anchor motifs (www.hiv.lanl.gov/content/immunology/motif_scan/motif_scan) are also noted. Trees used for reanalysis of all 80 HLA–base pair associations can be found at www.santafe.edu/~tanmoy/Science/Table1/.

HLA	Subtype/CRF	HLA-enriched populations	No. of associations	No. of known epitopes	No. of potential epitopes	Motifs
C*1701	C	African	32	0	4	.A.....L
DRB1*1401	CRF01	Oriental	18	0	-	Unknown
DRB1*0101	B	Caucasoid	2	0	1	YVLFIAMW..LAIVMNQ.AGSTCP..LAIVNFY
C*0102	CRF01	Oriental	1	0	0	..AL.....L
C*0702	B	Caucasoid	1	0	0	.....YFL
A*0201	B	Caucasoid	1	1	1	.LM.....VL
A*0207	CRF01	Oriental	3	0	1	.L.....L
C*0701	B	Caucasoid	2	0	0	.RHK.....Y
Total			60	1	7	

Although confounding effects due to mixed subtypes are relatively easy to detect, viral lineage effects that give rise to within-subtype phylogenetic clusters are also relevant. We therefore devised two strategies to account for the fact that viral sequences related by phylogeny are not statistically independent samples. First, a maximum-likelihood phylogeny was used to infer the mutations that lead to the observed viral sequences, and these inferred mutations were tested for correlation with the HLA of the host carrying the sequence (Fig. 1). We also used a likelihood-ratio test to locate sequence positions where postulating HLA pressure, in addition to the inferred phylogenetic structure, better explains the data. These two statistics yielded similar predictions (Table 2), and both support lineage founder effects, rather than HLA-mediated immune escape, for all 60 associations in Table 1.

Twenty associations remained that were not subtype driven (Table 2). In two cases, the uncorrected signal arises from a few clusters of viral sequences, rather than many independent events (Fig. 1B and Table 2). In both cases, the relevant within-clade clusters were not themselves the consequence of HLA-mediated selection, because they were also found in trees generated from only silent substitutions, which should be independent of immune pressure. Seven of the original 20 associations were strongly supported as HLA-mediated escape or reversion, after consideration of the phylogeny (Table 2 and Fig. 1C), and 13 additional associations, missed by the simple analysis, were also identified (table S1). These associations were also supported by trees that excluded potential intrasubtype recombinants and by a bootstrap analysis (Table 2).

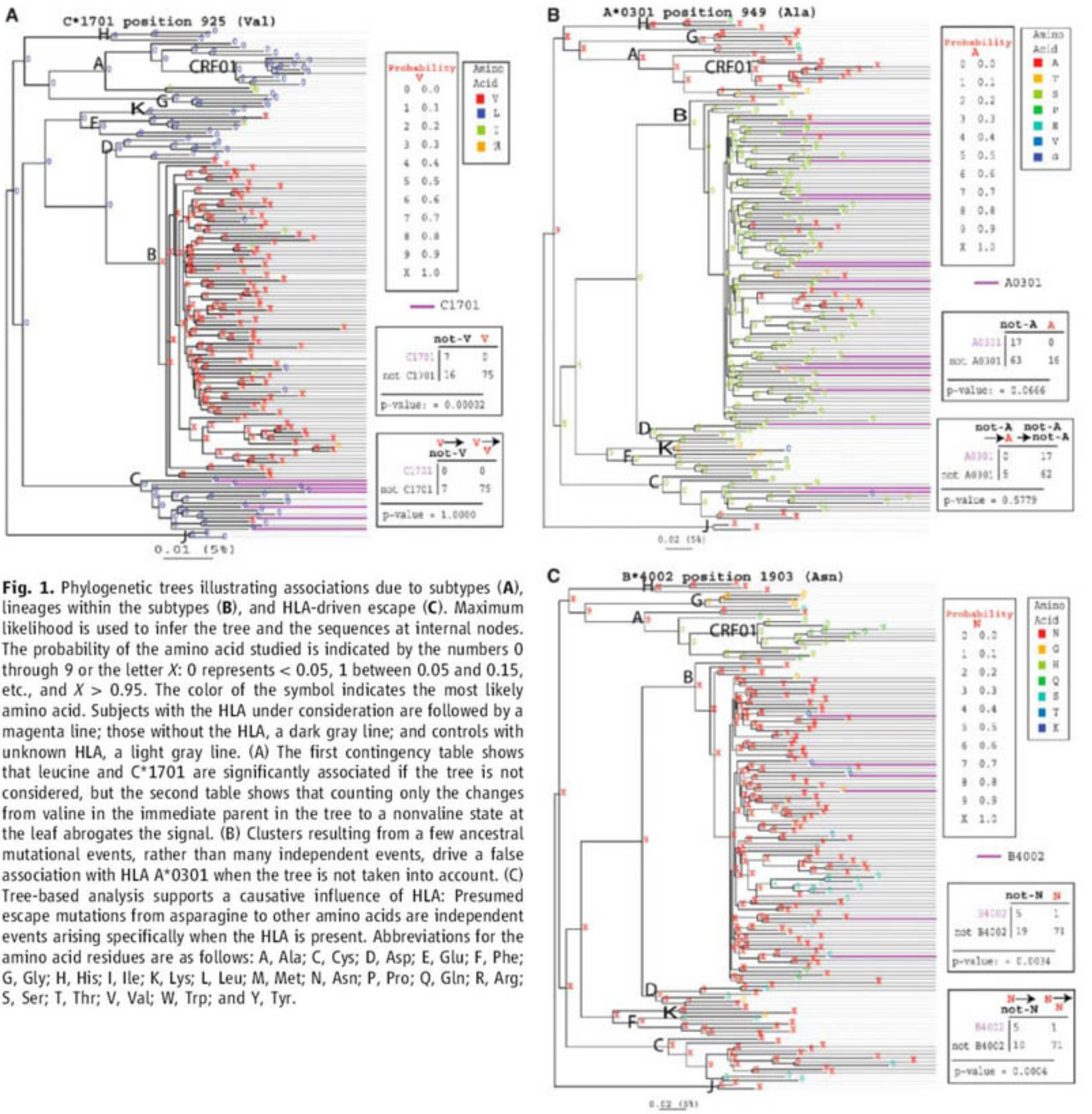

Fig. 1. Phylogenetic trees illustrating associations due to subtypes (**A**), lineages within the subtypes (**B**), and HLA-driven escape (**C**). Maximum likelihood is used to infer the tree and the sequences at internal nodes. The probability of the amino acid studied is indicated by the numbers 0 through 9 or the letter *X*: 0 represents < 0.05, 1 between 0.05 and 0.15, etc., and *X* > 0.95. The color of the symbol indicates the most likely amino acid. Subjects with the HLA under consideration are followed by a magenta line; those without the HLA, a dark gray line; and controls with unknown HLA, a light gray line. (A) The first contingency table shows that leucine and C*1701 are significantly associated if the tree is not considered, but the second table shows that counting only the changes from valine in the immediate parent in the tree to a nonvaline state at the leaf abrogates the signal. (B) Clusters resulting from a few ancestral mutational events, rather than many independent events, drive a false association with HLA A*0301 when the tree is not taken into account. (C) Tree-based analysis supports a causative influence of HLA: Presumed escape mutations from asparagine to other amino acids are independent events arising specifically when the HLA is present. Abbreviations for the amino acid residues are as follows: A, Ala; C, Cys; D, Asp; E, Glu; F, Phe; G, Gly; H, His; I, Ile; K, Lys; L, Leu; M, Met; N, Asn; P, Pro; Q, Gln; R, Arg; S, Ser; T, Thr; V, Val; W, Trp; and Y, Tyr.

To validate our findings, we scanned for associations embedded in known epitopes or in epitopes predicted on the basis of motifs that could act as anchors for HLA binding. Notably, of the 62 cases where the phylogeny is indicated as the underlying cause of the associations (Tables 1 and 2), only one site was embedded in a previously defined HLA epitope. Forty-three of these 62 associations were with HLAs that have described anchor motifs; only 8 out of 43 were embedded in potential epitopes suggested by these motifs. In contrast, 6 out of 7 associations validated by our phylogenetic methods (Table 2) are embedded in HLA-appropriate epitopes, in accord with expectation given a q-value cutoff of 0.2, indicating the strong specificity of the approach. Four out of 7 associations were previously defined experimentally, and the other three were embedded in predicted epitopes (Table 1). Elispot screening of individuals with the appropriate HLA experimentally confirmed that two of the other three associations were embedded in epitopes (fig. S1). Intriguingly, in several cases, the HLA-associated variants were the escape form in some individuals, as predicted, but were the more susceptible form of the epitope in other individuals (fig. S1). These variants differed in positions that affect recognition by T cell receptors.

If founder events are indeed an important confounding influence, methods that do not correct for the phylogeny should also yield associations between silent mutations (that do not alter the amino acid sequence) and host HLA. In the 51 codons in the HIV Gag protein that encoded invariant amino acids, we found 10 variable but silent positions associated with HLAs with $q < 0.20$, a rate statistically indistinguishable from the amino acid–altering mutation–HLA correlations (Fisher's exact $P = 0.64$). The lowest P-values among the silent mutations were with HLA-C*1701 and DRB1*1401 and were subtype-driven, as in the amino acid–altering cases (Table 1). In contrast, we found no spurious correlations between silent substitutions and HLA using our tree-corrected method.

Table 2. Phylogenetic analyses of HIV mutation-host HLA associations not explained by HIV subtype. Levels of tree-based support for HLA immune escape–driven associations are as follows: strongly supported, moderately supported, weakly supported, or not supported. The HLA allele, relevant amino acid (aa), and HXB2 position of the variable nucleotides and amino acids (www.hiv.lanl.gov/content/hiv-db/LOCATE/locate.html) are listed. The first four statistics indicate the level of support in the tree for an amino acid changing in people with the HLA allele and include (i) the P-value in the tree including all 96 sequences, (ii) the P-value in the tree excluding possible intrasubtype recombinant sequences, (iii) support found in 80% or more of bootstrap trees, and (iv) a q-value based on screening all HLAs by all positions for tree-based evidence for associations. The P- and q-values for the likelihood-ratio tree-based statistic are given next, and then the P- and q-values for the uncorrected associations found in the full set of 234 sequences. If an HLA-appropriate epitope spans the position, it is noted; anchor residues are in bold, and the HLA-correlated amino acid is underlined. The epitopes shaded in gray were tested experimentally by interferon-γ ELIspot (fig. S1). The two strongest HLA-nucleotide associations were with B*4001 and were embedded in the same codon; thus, the impact of the E to not-E association with B*4001 is the same for both. There were not enough A*3101-positive subjects in the 96 sequences used for the baseline tree to obtain meaningful results, so we added back HIV sequence fragments from A*3101 individuals and made an additional tree from a shorter alignment 653 nucleotides long.

HLA	aa	HXB2 position	Protein	P-value tree 1	P-value nonrec	80% bootstrap	q-value tree 1	P-value tree 2	q-value tree 2	P-value cohort	q-value cohort	Known epitope (ref), reactivity	HLA motif	Potential epitope
Correlations strongly supported as escape by evidence for selection in the tree ($q < 0.2$)														
B*4001	E	2233	p6	0.00002	0.00001	≤0.0001	0.04	1×10^{-5}	<0.001	0.0001	0.04	KELYPLTSL (*18, 19*)	.E.....L	
B*4001	E	2235	p6	NA	NA	NA	NA	NA	<0.001	0.066	NA	KELYPLTSL (*18, 19*)	.E.....L	
A*3101	K	2113	p1	0.0003	NA	NA	<0.001	NA	<0.001	0.061	NA	KIWPSYKGR	.....R	
A*3101	R	1996	p7	0.0004	NA	NA	<0.001	NA	<0.001	0.055	NA	LARNCRAPRK (*20*)	.....R	
B*4002	N	1903	p2	0.0004	0.0003	≤0.0004	0.19	0.0003	0.37	0.0008	0.13	AEAMSQVTNS* (*19*)	.E.....IAVL	
B*1501	I	2529	Pol	0.0005	0.006	≤0.092	0.19	6×10^{-5}	0.14	4×10^{-6}	0.005	TQIGCTLNF	.AST.....FWY	
A*3101	K	1978	p7	0.0013	NA	NA	0.0008	NA	4×10^{-5}	0.022	NA		.....R	CGKEGHTAR
Correlations moderately supported as escape by evidence for selection in the tree ($q \geq 0.2$, $q < 0.9$)														
B*5701	T	1513	p24	0.0007	NA	NA	0.220	0.0003	1×10^{-7}	0.000		TSTLQEQIGW	.AST.....FWY	
B*1501	V	2481	Pol	0.0057	0.0006	≤0.034	0.524	0.01	0.76	0.0011	0.158		.QL.....YF	VLVGPTPVN
B*0702	G	1858	p24	0.0174	0.03	≤0.059	0.694	0.03	0.88	0.0004	0.089	GPGHKARVL (*17*)	.P.....L	
C*1203	V	1957	p7	0.0246	0.0156	≤0.028	0.742	0.01	0.77	0.0010	0.153		.A.....FWY	NQRKIVKCF
A*0101	V	1216	p24	0.0336	0.0355	≤0.034	0.796	0.02	0.85	0.0002	0.066		.DE.....Y	
DQB10301	P	985	p17	0.0461	0.0204	≤0.046	0.849	0.03	0.89	0.0002	0.061		Unknown	
Correlations weakly supported and not contradicted as escape														
A*2301	N	2361	Pol	0.0942	0.0587	≤0.096	0.927	0.03	0.89	0.0002	0.061		Unknown	
B*4402	N	2361	Pol	0.0963	1.0	≤0.11	0.927	0.009	0.75	0.0016	0.197	EEMNLPGRW (*21*)	.E.....YF	
B*4002	E	1981	p7	0.1042	0.07	≤0.10	0.927	0.14	0.94	0.0007	0.115		E.....IAVL	KEGHTARNCRA
DRB10401	D	1723	p24	0.1101†	0.3351	≤0.25	0.927	0.22	0.97	0.0003	0.081		FLV.....NQST	
C*0602	I	1228	p24	0.1828	0.3684	≤0.37	0.965	0.10	0.95	0.0002	0.061		.....LIVY	HQAISPRTL
Evidence for escape contradicted due to sublineages in the tree														
DQB10502	A	1225	p24	0.2329	0.0669	≥0.11	0.975	0.12	0.95	0.0013	0.171		Unknown	
A*0301	A	949	p17	0.5779†	1.0	≥0.20	0.991	0.72	0.99	0.0002	0.061		LVM.....KYFR	ALETSEGCR

*This is a B*4501 epitope; it is the same supertype as B*4002, so may cross-present. †These P-values are not for escape, as are all others, but for reversion to the susceptible form in the absence of the HLA allele.

We also applied our phylogenetic analyses to a data set provided by the group in Perth that closely approximates the sequence data used in the original Moore study data (*5*) (GenBank accession numbers: DQ409341 to DQ409813) and serologically defined HLA alleles. These 446 sequences consisted of 406 intact subtype B, 23 C, 16 A, and one D sequence, suggesting the potential for subtype-driven associations. Our uncorrected methods yielded 28 correlations between amino acids and HLA types with q-values < 0.2. Nine of these had a $q < 0.2$ based on phylogeny-corrected methods, and 14 were due to lineage effects. We also reexamined the 12 associations reported in (*5*) to have survived correction for multiple tests. The seven among these noted to be embedded in or proximal to known CD8 T cell epitopes in the original study [the red- and blue-boxed associations in the supplemental figure of Moore (*5*)] were validated with our tree-based methods, in contrast to the other five (the black-boxed associations).

Associations between an HLA allele and a subtype consensus amino acid may be the consequence of immune selection in a population with a relatively high frequency of the presenting HLA (*1*, *5*, *8*). Leslie *et al.* (*10*) explored this idea in a detailed characterization of two common variants that confer CTL escape. We reevaluated these data in a phylogenetic context and found that the amino acids associated with CTL escape were likely to have been in the founder virus of the subtype, because the escape amino acid also dominates all phylogenetically related subtypes, regardless of the frequency of the associated HLA allele (Fig. 2). Furthermore, the relative frequency of the escape and nonescape forms has stayed constant over time, suggesting an equilibrium situation rather than selection over time favoring the escape form (fig. S2). Thus, the interpretation of these data is also complicated by the phylogeny—because in this case the associations were within clearly defined CTL epitopes, they may represent immunologically selected stable mutations present in the founder population.

Correlation studies based on previous methods can lead to both false-positives and false-negatives. Many of the signatures of HLA-associated immune escape from previous population-level studies of chronic HIV infection are not supported, and incorporating phylogenetic corrections improves the accuracy of their identification. Furthermore, though immune escape is often observed in individuals (*1*, *2*) and will affect the population frequency of the escape variants, contemporary amino acid frequencies also depend critically on founder effects.

Many confounding factors can obscure identification of HLA-mediated immune escape in population studies: HLA alleles often cross-present the same epitopes, amino acids may be embedded in multiple overlapping epitopes (*11*), an escape variant in one person may be susceptible in another (fig. S1), and compensatory changes to maintain fitness may confound associations (*4*, *12*, *13*). Finally, more data will likely reveal many more associations. Thus, one should not interpret our results as evidence that immune pressure is a weak force in HIV evolution. Rather, we demonstrate that phylogenetic effects need to be accounted for in locating associations resulting from immune selection pressure in population-level studies. If vaccine antigen designs ultimately incorporate immune susceptibility and escape patterns, accuracy in defining these patterns is essential.

The methods developed here are general and can be applied to any search for phenotypic correlations with sequence data. The question of HLA-driven immune escape is of vital importance to the HIV field; by taking genetic lineages into account, a very different interpretation of apparent HLA associations emerges. Contemporary immune selection is merely one contributing factor in a complex array of competing selective forces shaping currently circulating global virus populations.

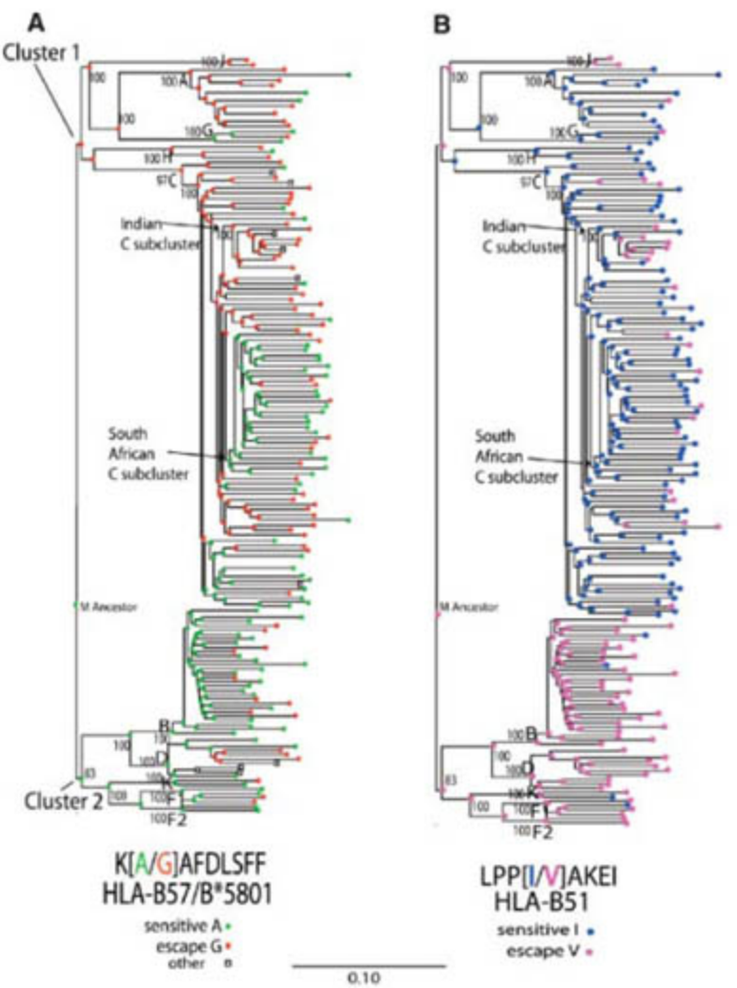

Fig. 2. A full-length genome maximum-likelihood tree superimposing the patterns of escape mutations featured in (*10*) against an evolutionary backdrop of M-group viruses. Maximum-likelihood ancestral reconstructions suggest that the escape forms of these two epitopes have dominated the subtypes in question since their origin. In the Nef epitope (**A**), glycine dominates subtype C and all subtypes found in cluster 1; the probability that the ancestral state of the C clade was glycine is 0.740. In the Integrase epitope (**B**), valine dominates subtype B, and all surrounding subtypes in cluster 2; the probability that the ancestor of subtype B carried the escape mutation is 0.999.

References and Notes

1. J. Martinez-Picado *et al.*, *J. Virol.* **80**, 3617 (2006).
2. P. Ammaranond *et al.*, *AIDS Res. Hum. Retroviruses* **21**, 395 (2005).
3. T. M. Allen *et al.*, *J. Virol.* **79**, 13239 (2005).
4. A. D. Kelleher *et al.*, *J. Exp. Med.* **193**, 375 (2001).
5. C. B. Moore *et al.*, *Science* **296**, 1439 (2002).
6. Supporting materials for details of sequences and analysis are available on *Science* Online.
7. P. Kiepiela *et al.*, *Nature* **432**, 769 (2004).
8. J. D. Storey, R. Tibshirani, *Proc. Natl. Acad. Sci. U.S.A.* **100**, 9440 (2003).
9. R. S. Wells *et al.*, *Immunogenetics* **46**, 173 (1997).
10. A. Leslie *et al.*, *J. Exp. Med.* **201**, 891 (2005).
11. K. Yusim *et al.*, *J. Virol.* **76**, 8757 (2002).
12. F. W. Peyerl *et al.*, *J. Virol.* **78**, 13901 (2004).
13. T. C. Friedrich *et al.*, *J. Virol.* **78**, 2581 (2004).
14. S. Marsh, P. Parham, L. Barber, *HLA FactsBook* (Academic Press, London, 2000), pp. 99–390.
15. S. Corbet *et al.*, *J. Gen. Virol.* **84**, 2409 (2003).
16. N. K. Mehra *et al.*, *Tissue Antigens* **57**, 502 (2001).
17. M. Altfeld *et al.*, *J. Immunol.* **167**, 2743 (2001).
18. X. G. Yu *et al.*, *AIDS* **16**, 321 (2002).
19. N. Frahm, C. Brander, in *HIV Molecular Immunology 2005*, B. Korber *et al.*, Eds. (Los Alamos National Laboratory, Los Alamos, NM, 2005), pp. 3–20; http://hiv.lanl.gov/content/immunology/pdf/2005/brander_article.pdf.
20. A. S. De Groot *et al.*, *Vaccine* **21**, 4486 (2003).
21. W. R. Rodriguez *et al.*, *J. Transl. Med.* **2**, 15 (2004).

22. We thank S. Wolinsky, P. Goulder, and I. James for discussions and A. Chopra, A. Patterson, and S. Guadieri for HIV sequencing and HLA typing. This work was funded by the U.S. Department of Energy at Los Alamos National Laboratory (LANL) (grant DE-AC52-06NA25396), LANL Laboratory Directed Research Development, NIH (grants AI27757 and AI57005), and Microsoft Research.

Supporting Online Material

www.sciencemag.org/cgi/content/full/315/5818/1583/DC1
Materials and Methods
Figs. S1 and S2
Table S1
References
Alignments and Phylogenetic Trees

20 June 2006; accepted 25 January 2007
10.1126/science.1131528

A Slicer-Mediated Mechanism for Repeat-Associated siRNA 5′ End Formation in *Drosophila*

Lalith S. Gunawardane,* Kuniaki Saito,* Kazumichi M. Nishida,* Keita Miyoshi, Yoshinori Kawamura, Tomoko Nagami, Haruhiko Siomi,† Mikiko C. Siomi†

In *Drosophila*, repeat-associated small interfering RNAs (rasiRNAs) are produced in the germ line by a Dicer-independent pathway and function through the PIWI subfamily of Argonautes to ensure silencing of retrotransposons. We sequenced small RNAs associated with the PIWI subfamily member AGO3. Although other members of PIWI, Aubergine (Aub) and Piwi, associated with rasiRNAs derived mainly from the antisense strand of retrotransposons, AGO3-associated rasiRNAs arose mainly from the sense strand. Aub- and Piwi-associated rasiRNAs showed a strong preference for uracil at their 5′ ends, and AGO3-associated rasiRNAs showed a strong preference for adenine at nucleotide 10. Comparisons between AGO3- and Aub-associated rasiRNAs revealed pairs of rasiRNAs showing complementarities in their first 10 nucleotides. Aub and AGO3 exhibited Slicer activity in vitro. These data support a model in which formation of a 5′ terminus within rasiRNA precursors is guided by rasiRNAs originating from transcripts of the other strand in concert with the Slicer activity of PIWI.

Small noncoding RNAs trigger various forms of sequence specific gene silencing, including RNA interference (RNAi), translational repression, and heterochromatin formation in a variety of eukaryotic organisms, commonly referred to as RNA silencing (*1*–*3*). Members of the Argonaute family of proteins are essential components of RNA silencing (*4*, *5*). In *Drosophila*, five genes encode distinct members of the Argonaute family: *AGO1*, *AGO2*, *Aubergine* (*Aub*), *Piwi*, and *AGO3*. *AGO1* and *AGO2* constitute the Argonaute (AGO) subfamily and bind microRNA (miRNA) and small interfering RNA (siRNA), respectively (*6*–*8*). Aub, Piwi, and AGO3 belong to the PIWI subfamily of the Argonaute family (*4*, *5*) and are enriched in germline cells (*9*), and Aub and Piwi have been shown to play important roles in germline cell formation (*10*, *11*). They are involved in silencing retrotransposons and other repetitive elements (*12*–*15*) and exhibit target RNA cleavage (slicing) activity in vitro (*16*). Both Aub and Piwi associate with repeat-associated siRNAs (rasiRNAs) (*15*, *16*). Aub- and Piwi-associated rasiRNAs are derived mainly from the antisense strand of retrotransposons, with little or no phasing, and have a strong preference for uracil (U) at the 5′ end (*15*, *16*). Small RNA processing factors such as Dicer and Drosha are known to cleave preferentially at the 5′ side of U (*17*); however, rasiRNAs are thought to be produced by a Dicer-independent pathway (*15*). The mechanisms governing rasiRNA production remain to be elucidated.

Very little is known about the function of AGO3 (*9*), the third member of the *Drosophila* PIWI subfamily. We isolated a full-length cDNA of AGO3, revealing that the *AGO3* gene is ~83 kb in length (fig. S1). Peptide sequence alignments among *Drosophila* Argonaute proteins revealed that AGO3 is most similar to Piwi (fig. S2A). The Asp-Asp-His motif in the PIWI domain, originally identified as the catalytic center for Slicer activity in human AGO2 (*5*, *18*), is conserved in AGO3 (fig. S2B).

Embryonic RNA expression patterns of *AGO3* are very similar to those of *Piwi* and *Aub*; they are expressed maternally, but their expression disappears by embryonic stages 10 to 12 (*9*). To confirm these results, we produced a monoclonal antibody (mAb) to AGO3 (Fig. 1A), which revealed that AGO3 is strongly expressed in earlier embryonic stages but decreases as development proceeds (Fig. 1B). AGO3 accumulated in the cytoplasm of germline cells including germline stem cells (GSCs), germline cyst cells, nurse cells, and oocytes at earlier stages (Fig. 1C and fig. S3). In testes, AGO3 is expressed in GSC, primary gonial cells, and early spermatocytes (Fig. 1D). Unlike Piwi (*16*), AGO3 expression was undetected in the hub (fig. S3), a tiny cluster of postmitotic somatic cells localized at the apical tip of the testis that functions as a niche for GSC (*19*). Thus, with respect to expression in germline cells, AGO3 is more similar to Aub than to Piwi (*10*, *16*).

All of the other members of the fly Argonautes are specifically associated with a subset of small RNAs: siRNAs, miRNAs, or rasiRNAs (*6*–*8*, *15*, *16*). We therefore investigated whether AGO3 also associates with small RNAs produced in the fly ovary. Immunoprecipitation with AGO3 mAb from ovary lysate revealed small RNAs ~23 to 26 nucleotides (nt) long (Fig. 2A). The size distribution of AGO3-associated small RNAs is similar to that of Aub-associated small RNAs (Fig. 2B); in both cases, the peak is 24 nt and the longest is 27 nt. Small RNAs associated with AGO3 are likely to lack either a 2′ or 3′ hydroxyl group, because they do not migrate faster after β-elimination as opposed to a synthetic siRNA that has 2′ and 3′ hydroxyl groups at the 3′ end, the latter being the hallmarks of Dicer cleavage (Fig. 2C). These results suggest that AGO3-associated small RNAs in the ovary are produced by a pathway similar to those involved in production of rasiRNAs that associate with Aub and Piwi.

We constructed a cDNA library of small RNAs associated with AGO3 in the ovary. Of 420 clones sequenced, 410 matched *Drosophila* genomic sequences in a database search (table S1), and most were rasiRNAs (~86%; 353 of 410), as in the case of Aub and Piwi (table S2). Like rasiRNAs associated with Aub or Piwi (*15*, *16*), rasiRNAs associated with AGO3 included various kinds of transposable elements, both LTR (long terminal repeat) retrotransposons and LINE (long interspersed nuclear element)–like elements (tables S1 and S2). rasiRNAs associated with Aub or Piwi in ovaries are derived mainly from the antisense strand of retrotransposons, and the 5′ end is predominantly U (*15*, *16*). These characteristics were not found for rasiRNAs associated with AGO3. However, AGO3-associated rasiRNAs were derived mainly from the sense strand of retrotransposons (~82%; table S3), and they showed a strong preference for adenine (A) at nucleotide 10, but no preference for U at the 5′ end (Fig. 3A). These results suggest that AGO3-associated rasiRNAs belong to a subset of rasiRNAs that are distinct from Aub- and Piwi-associated rasiRNAs.

Some Argonaute proteins exhibit Slicer activity that directs cleavage of its cognate mRNA target across from nucleotides 10 and 11, measured from the 5′ end of the small RNA guide strand (*20*). Thus, our findings suggest a model for rasiRNA biogenesis, in which the 5′ end of Aub- and Piwi-associated rasiRNAs is determined and cleaved by AGO3-rasiRNA complexes, and the 5′ end of AGO3-associated rasiRNAs is determined by Aub- and Piwi-rasiRNA complexes through a similar rasiRNA-guided cleavage event (Fig. 3B). For instance, AGO3 associated with a rasiRNA with A at nucleotide 10 can target a long RNA molecule by Watson-Crick base pairing and cleave the target RNA, resulting in sliced RNAs with U at the 5′ end. Similarly, when Aub or Piwi associated with

Institute for Genome Research, University of Tokushima, Tokushima 770-8503, Japan.

*These authors contributed equally to this work.
†To whom correspondence should be addressed. E-mail: siomi@genome.tokushima-u.ac.jp (H.S.); siomim@genome.tokushima-u.ac.jp (M.C.S.)

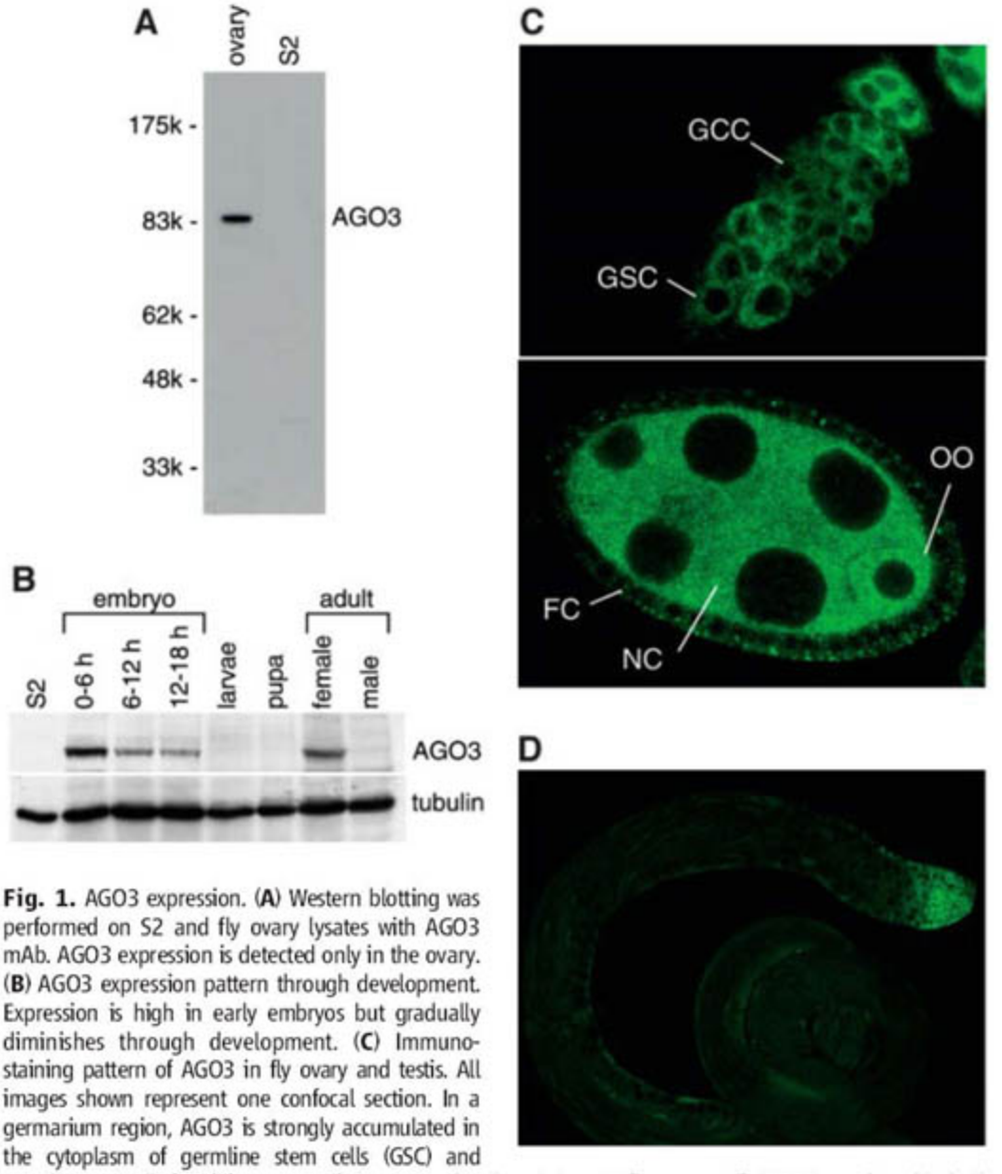

Fig. 1. AGO3 expression. (**A**) Western blotting was performed on S2 and fly ovary lysates with AGO3 mAb. AGO3 expression is detected only in the ovary. (**B**) AGO3 expression pattern through development. Expression is high in early embryos but gradually diminishes through development. (**C**) Immunostaining pattern of AGO3 in fly ovary and testis. All images shown represent one confocal section. In a germarium region, AGO3 is strongly accumulated in the cytoplasm of germline stem cells (GSC) and germline cyst cells (GCC) (upper panel). In an egg chamber at stage 7 (lower panel), AGO3 was found in both oocytes (OO) and nurse cells (NC). A weak signal of AGO3 was also observed in follicle cells (FC). AGO3 is clearly cytoplasmic. (**D**) Fluorescent image of AGO3 in testis. AGO3 expression is detected in germline stem cells, primary gonial cells, and early spermatocytes.

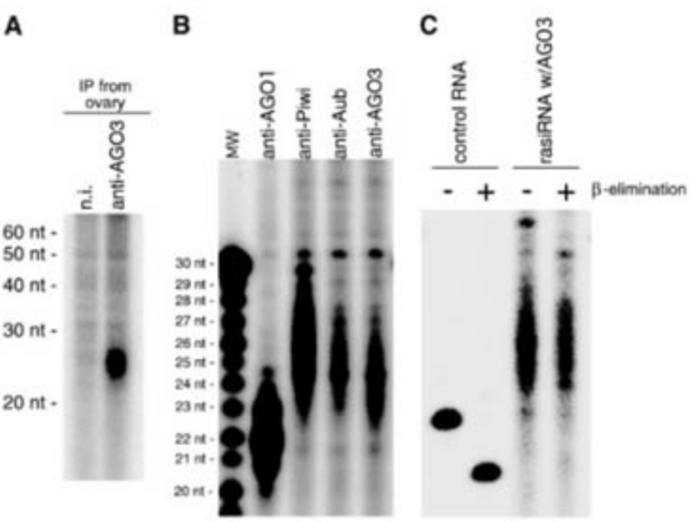

Fig. 2. Small RNAs associated with AGO3 in fly ovary. (**A**) Small RNAs associated with AGO3 immunopurified from ovary are visualized by [^{32}P]adenosine triphosphate labeling. (**B**) Sizes of small RNAs associated with AGO1, Piwi, Aub, and AGO3 are compared. The peak of small RNAs associated with Aub and AGO3 is about 24 nt, whereas that of Piwi is about 26 nt; rasiRNAs with AGO3 contain shorter ones (23 nt) relative to those of Aub. The ~30-nt bands are 2*S* rRNA. (**C**) rasiRNAs associated with AGO3 show resistance to β-elimination treatment, which made 21-nt siRNA (control RNA) without 3′ end modification shorter, indicating that rasiRNAs associated with AGO3 are modified at the 3′ end.

rasiRNAs with U at the 5′ end slices its cognate RNA target, the resulting cleaved RNA will have A at nucleotide 10.

To test this model, we examined AGO3 for Slicer activity by performing in vitro target RNA cleavage assays with glutathione *S*-transferase (GST)–AGO3 fusions (Fig. 4A). The target RNA, *luc* passenger siRNA (21 nt long, 5′ end labeled with ^{32}P) (*8*), was efficiently cleaved by GST-AGO3, as was the case for GST-AGO1 and GST-Aub. The size of the cleaved products (9 nt) indicated that they direct cleavage of target RNA across from nucleotides 10 and 11 as measured from the 5′ end of the small RNA guide strand (Fig. 4A). Both GST-Aub and GST-AGO3 with a longer guide RNA (26 nt) were also able to cleave a long transcript (180 nt) (fig. S4). Long precursors of rasiRNAs both in sense and antisense orientations appear to exist in fly ovaries (fig. S5). These results corroborate the model in which the 5′ end of rasiRNAs within the precursors is determined by rasiRNAs and cleaved by members of PIWI that associate with these rasiRNAs.

Our model predicts that some AGO3-associated rasiRNAs should be complementary to the first 10 nt of Aub- and Piwi-associated rasiRNAs. Sequence comparison between AGO3- and Aub-associated rasiRNAs indeed revealed pairs of rasiRNAs that show complementarities at their first 10 nt (fig. S6). Sixteen of 353 AGO3-associated rasiRNAs had such pairs with 11 of 676 Aub-associated rasiRNAs (fig. S6). However, such pairings were only found between AGO3- and Aub-associated rasiRNAs, and no pairs were observed between AGO3- and Piwi-associated rasiRNAs (353 versus 330). Like Aub-associated rasiRNAs (table S3), Piwi-associated rasiRNAs arise mainly from the antisense strand and their 5′ ends show a strong preference for U (*16*); thus, it is difficult to argue that Piwi is not involved in this type of rasiRNA biogenesis. One possible reason is that Piwi is nuclear, whereas AGO3 and Aub are cytoplasmic (*16*). This type of rasiRNA biogenesis may operate in the cytoplasm. Alternatively, formation of 5′ ends of Piwi-associated rasiRNAs may occur only at an earlier time during germline development.

RasiRNAs are involved in genome surveillance by silencing repetitive elements and controlling their mobilization in the *Drosophila* germ line. It was recently shown that rasiRNAs are produced by a mechanism that requires neither Dicer-1 nor Dicer-2 in flies (*15*). Our data suggest that rasiRNAs in a sense orientation guide formation of the 5′ end of rasiRNAs in an antisense orientation, and vice versa; as well, this cycle of mutual dependency elaborates optimal rasiRNA production (Fig. 4B). In this model, proteins of the PIWI subfamily function as Slicer for formation of the 5′ end during rasiRNA

biogenesis. This model requires that sliced rasiRNA precursors then be cleaved again at the 3′ end by an as yet unidentified endonuclease (or nibbled by exonuclease) to produce mature rasiRNAs before or after loading of the resulting cleavage products onto another member of the PIWI. Once "primary" complexes of rasiRNAs with proteins of PIWI are produced, these complexes will in turn function

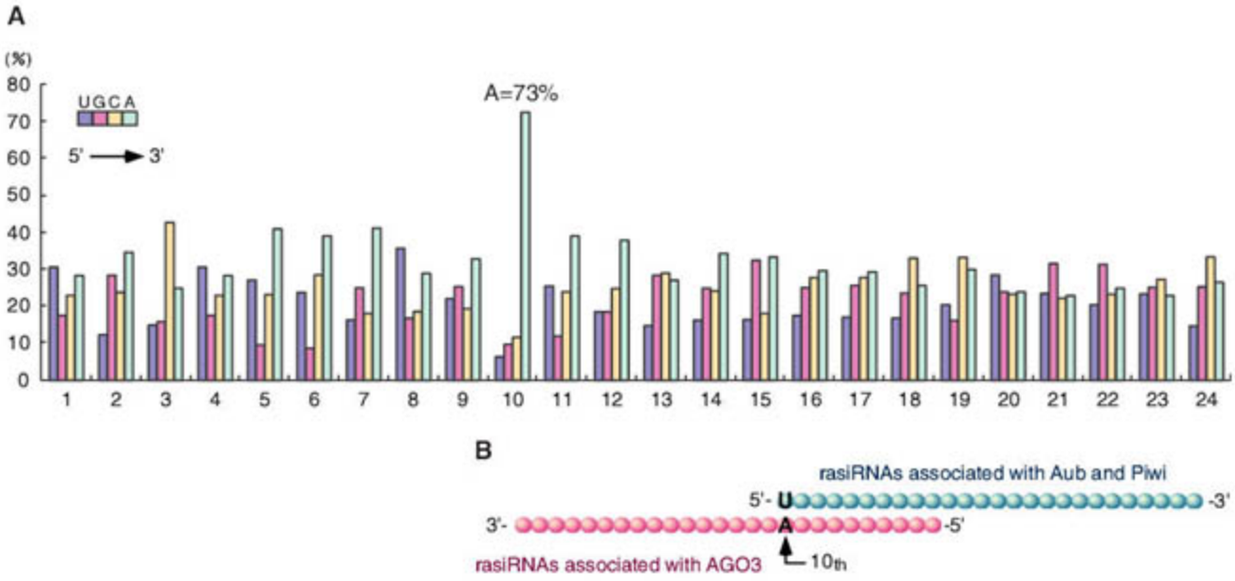

Fig. 3. Characteristics of rasiRNAs associated with AGO3 in the ovary. (**A**) rasiRNAs associated with AGO3 contain A predominantly at nucleotide 10 from the 5′ end. (**B**) A predicted model indicating that the first 10 nt of AGO3-associated rasiRNAs show complementarities to the first 10 nt of Aub- or Piwi-associated rasiRNAs.

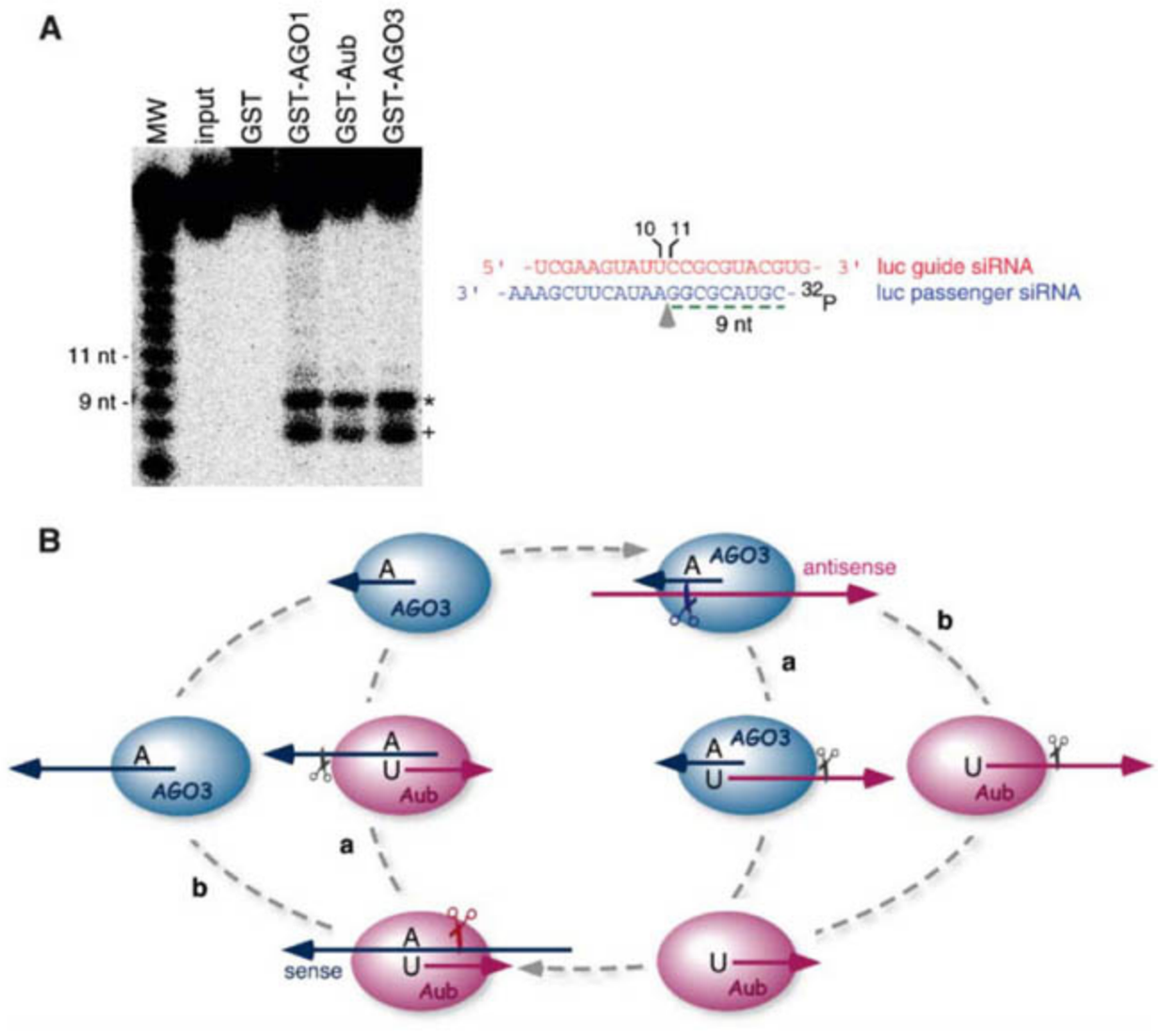

Fig. 4. (**A**) Target RNA cleavage assay using GST-AGO1, GST-AGO3, and GST-Aub produced in *Escherichia coli*. GST-fused proteins were first bound with a single-stranded *luc* guide siRNA; then, target RNA (single-stranded *luc* passenger siRNA labeled with ^{32}P at the 5′ end) was added to the reaction mixture and further incubated. All the proteins, but not GST itself, were able to cleave target RNA across from nucleotides 10 and 11, measured from the 5′ end of the guide RNA. The asterisk indicates cleaved products with the expected size (9 nt); the cross marks by-products of 8 nt in in vitro assays with GST fusions (*8*). (**B**) A model for a rasiRNA biogenesis cycle. AGO3-associated sense rasiRNAs (upper left) guide Slicer-mediated cleavage of primary antisense transcripts, yielding the antisense rasiRNA precursors with U at the 5′ end. Reciprocally, Aub-associated antisense rasiRNAs (lower right) guide Slicer-mediated cleavage of sense transcripts, yielding the sense rasiRNA precursors with A at nucleotide 10. Formation of rasiRNAs at the 3′ end may occur (a) while the precursors still remain in the complexes, or (b) after they are loaded onto the other PIWI by an as-yet-unidentified nuclease.

as the "initiator" of secondary rasiRNA biogenesis, and so nascent rasiRNAs should be continuously supplied in the ovary and testis. Such a process may occur through rasiRNA germline transmission. Of the PIWI members, at least Aub is accumulated to the posterior pole in oocytes and remains in polar granules in early embryos. It is then incorporated in pole cells, the progenitor of the *Drosophila* germ line (*10*).

References and Notes

1. Y. Tomari, P. D. Zamore, *Genes Dev.* **19**, 517 (2005).
2. H. H. Kavi, H. R. Fernandez, W. Xie, J. A. Birchler, *FEBS Lett.* **579**, 5940 (2005).
3. W. P. Kloosterman, R. H. Plasterk, *Dev. Cell* **11**, 441 (2006).
4. M. A. Carmell, Z. Xuan, M. Q. Zhang, G. J. Hannon, *Genes Dev.* **16**, 2733 (2002).
5. J. S. Parker, D. Barford, *Trends Biochem. Sci.* **31**, 622 (2006).
6. K. Okamura, A. Ishizuka, H. Siomi, M. C. Siomi, *Genes Dev.* **18**, 1655 (2004).
7. Y. Tomari, C. Matranga, B. Haley, N. Martinez, P. D. Zamore, *Science* **306**, 1377 (2004).
8. K. Miyoshi, H. Tsukumo, T. Nagami, H. Siomi, M. C. Siomi, *Genes Dev.* **19**, 2837 (2005).
9. R. W. Williams, G. M. Rubin, *Proc. Natl. Acad. Sci. U.S.A.* **99**, 6889 (2002).
10. A. N. Harris, P. M. Macdonald, *Development* **128**, 2823 (2001).
11. D. N. Cox *et al.*, *Genes Dev.* **12**, 3715 (1998).
12. A. I. Kalmykova, M. S. Klenov, V. A. Gvozdev, *Nucleic Acids Res.* **33**, 2052 (2005).
13. A. A. Aravin *et al.*, *Mol. Cell. Biol.* **24**, 6742 (2004).
14. V. V. Vagin *et al.*, *RNA Biol.* **1**, 54 (2004).
15. V. V. Vagin *et al.*, *Science* **313**, 320 (2006); published online 28 June 2006 (10.1126/science.1129333).
16. K. Saito *et al.*, *Genes Dev.* **20**, 2214 (2006).
17. A. A. Aravin *et al.*, *Dev. Cell* **5**, 337 (2003).
18. J. Liu *et al.*, *Science* **305**, 1437 (2004); published online 29 July 2004 (10.1126/science.1102513).
19. Y. M. Yamashita, M. T. Fuller, D. L. Jones, *J. Cell Sci.* **118**, 665 (2005).
20. S. M. Elbashir, W. Lendeckel, T. Tuschl, *Genes Dev.* **15**, 188 (2001).

21. We thank T. Suzuki and V. V. Vagin for technical advice; T. Mori, M. Shinomiya, and A. Kinouchi for assistance with fly husbandry and dissection; and members of the Siomi laboratory for discussions and comments on the manuscript. Supported by the Ministry of Education, Culture, Sports, Science, and Technology of Japan (M.C.S., H.S.) and its 21st Century Centers of Excellence Program (L.S.G., K.S.), the Japan Society for the Promotion of Science (JSPS) (M.C.S. and H.S.), a JSPS research fellowship (K.M.), and the New Energy and Industrial Technology Development Organization (M.C.S).

Supporting Online Material

www.sciencemag.org/cgi/content/full/1140494/DC1
Materials and Methods
Figs. S1 to S6
Tables S1 to S3
References

29 January 2007; accepted 12 February 2007
Published online 22 February 2007;
10.1126/science.1140494
Include this information when citing this paper.

Attention-Like Processes in *Drosophila* Require Short-Term Memory Genes

Bruno van Swinderen

Although there is much behavioral evidence for complex brain functions in insects, it is not known whether insects have selective attention. In humans, selective attention is a dynamic process restricting perception to a succession of salient stimuli, while less relevant competing stimuli are suppressed. Local field potential recordings in the brains of flies responding to visual novelty revealed attention-like processes with stereotypical temporal properties. These processes were modulated by genes involved in short-term memory formation, namely *dunce* and *rutabaga*. Attention defects in these mutants were associated with distinct optomotor effects in behavioral assays.

Studies of visual discrimination in flies have revealed sophisticated perceptual effects that are relevant to selective attention (*1*, *2*), such as associative learning (*3*), context generalization (*4*, *5*), cross-modal binding (*6*), and position invariance (*7*). Visual choice behavior in *Drosophila* is correlated with local field potential (LFP) activity in the brain, centered around 20 to 30 Hz (*8*). This activity is transiently increased in amplitude by classical conditioning (*8*), is suppressed during sleep (*8*) or light anesthesia (*9*), and is modulated by dopamine (*10*). Electrophysiological and behavioral measures of visual attention in flies were developed to test whether these short-term processes depend on the effect of genes involved in memory formation and plasticity (*11*–*13*).

LFP responses to two distinct visual objects (a cross or a box, 180° apart, each moving around the fly once every 3 s) were investigated (Fig. 1A). When the objects were presented individually to wild-type flies, they evoked brain responses that were maximal when the single object swept directly in front of the flies (Fig. 1B). In contrast, *dunce* mutants (dnc^1) (*14*), which are defective in short-term memory (*15*, *16*), displayed attenuated and delayed brain responses to each visual object, as compared to wild-type flies (Fig. 1C).

To test for visual selection between these objects, I presented them together after having increased the salience for one object specifically in a recurrent-novelty paradigm (Fig. 1D) (*17*). To measure visual selection, the 20- to 30-Hz brain response (mapped onto the 3-s sequence) (Fig. 1B) was averaged for 10 s (about three rotations) after each transition to novelty, and this was compared to the response for the 10 s before novelty transitions (red versus blue lines, respectively, in Fig. 1D). When wild-type flies were trained with two identical boxes for 100 s (~33 rotations) before one of the boxes changed to a cross, the response mapped selectively to the sectors of the rotation sequence associated with the (novel) cross (100 s, red line in Fig. 1D), and the response for the competing box was significantly suppressed. Converse experiments attaching novelty salience to the alternate image (the box) after 100 s of cross training mapped 20- to 30-Hz responses to the novel box, showing that novelty selection was plastic (fig. S1). Novelty selection was also found to be position-invariant (*7*) in a subset of trials, suggesting a cognitive effect rather than habituation (fig. S2).

By decreasing the time between transitions in otherwise identical experiments, this paradigm provided a way to estimate the minimum exposure required for selection of recurrent novelty. When the training time was decreased to 50 s (~16 rotations), significant selection of the novel object and corresponding suppression of the competing object were still seen in wild-type flies (fig. S3). However, when the training time was further decreased to 25 s (about eight rotations), these novelty effects were lost (Fig. 1D).

To control for the effect of change alone without novelty, I tested transitions from a cross and a box back to two boxes (Fig. 1E). In this case, an object changed to one that was already present during training. Such changes did not produce any selective 20- to 30-Hz responses for any training time in wild-type flies (100 s and 25 s in Fig. 1E). The response is therefore unlikely to emanate from a startle reflex or an electrical artifact.

Salience is a transient phenomenon. To investigate the extinction of novelty, I analyzed the temporal sequence of selective brain responses for successive rotations of a novel panorama after a transition (Fig. 2A). In wild-type flies, 20- to 30-Hz activity was strongly selective for the novel object (the cross) for 9 s (three successive panorama rotations) on average (red lines in Fig. 2A), and this was matched at a lower level for

The Neurosciences Institute, 10640 John Jay Hopkins Drive, San Diego, CA 92121, USA. E-mail: van@nsi.edu

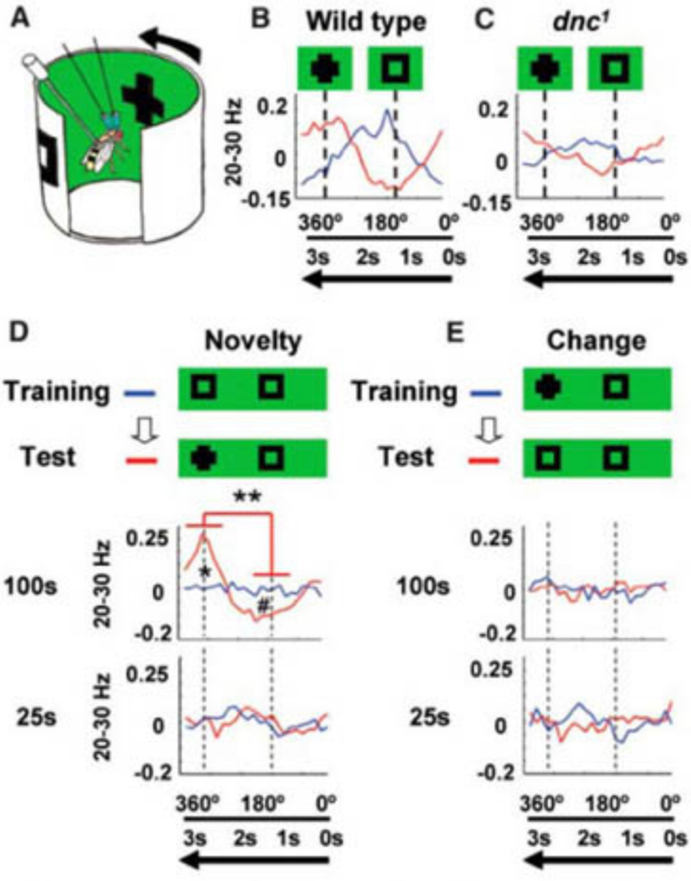

Fig. 1. Fly brain responses. (**A**) The recording arena (*8*, *9*). (**B**) Wild-type flies were presented with a single object, a cross or a box, positioned at opposite portions of a reference 3 s rotation sequence. 20- to 30-Hz LFP responses for either object were mapped onto the rotation sequence (power, superimposed here). Dashed lines show when either object (red, cross; blue, box) swept in front of the fly (n = 6 flies). (**C**) *dnc*^{1} responses to the same objects (n = 6 flies). (**D**) Wild-type flies trained to two identical boxes for 100 or 25 s, after which one of the boxes changed to a cross. The average 20- to 30-Hz response in the first 10 s after a transition is mapped onto the rotation sequence (red line) and contrasted to the last 10 s before introducing novelty (blue line). *, significant selection of novel object; #, significant suppression; **, significant selection of one object versus the other, after novelty ($P < 0.01$ for all comparisons; 100 s, n = 6 flies; 25 s, n = 5 flies). (**E**) Average 20- to 30-Hz responses to change alone without novelty (n = 6 flies).

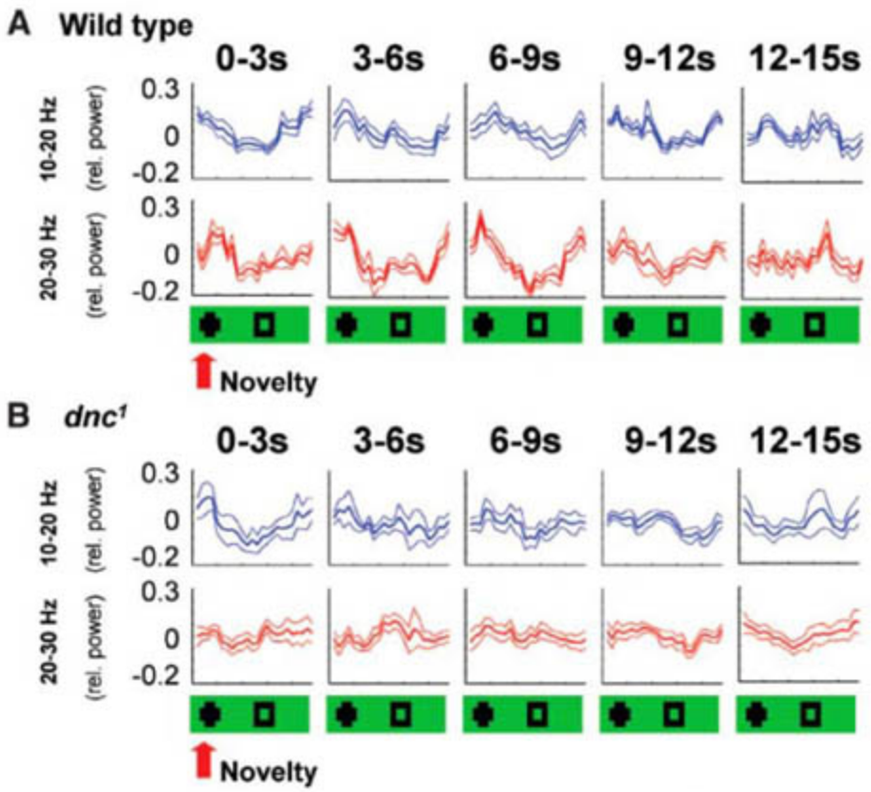

Fig. 2. Temporal analysis of the LFP response to novelty in the wild type and *dnc*^{1}. (**A**) Time course of wild-type LFP responses after a novelty transition (red arrow), for 10 to 20 Hz (blue line, ±SEM, n = 6 flies) and 20 to 30 Hz (red line, ±SEM). (**B**) Time course of *dnc*^{1} LFP responses after a novelty transition, for 10 to 20 Hz (blue line, ±SEM, n = 6 flies) and 20 to 30 Hz (red line, ±SEM).

10- to 20-Hz activity (blue lines in Fig. 2A). Responses to training for the alternate object (making the box novel) revealed similar temporal dynamics: Wild-type flies in the 100-s paradigm stereotypically "attended" to novelty for about 9 s or three sweeps of the panorama (fig. S1).

The robust 100-s training effect was used for subsequent experiments in short-term memory mutants. There, *dnc*^{1} flies failed to show any selective 20- to 30-Hz response to the novel visual stimulus after a transition (red line in Fig. 2B). Instead, they revealed some selective responsiveness in the 10- to 20-Hz range (blue line in Fig. 2B). Further analysis of *dnc*^{1} flies showed that brain responses in this mutant were greatest in the lower-frequency (10 to 20 Hz) bracket, as compared to greater responses at 20 to 30 Hz in the wild type (fig. S4).

Mutations in *rutabaga* (*rut*) affect the same signaling network as mutations in *dnc*^{1} [by producing opposite effects on adenosine 3′,5′-monophosphate (cAMP) levels], and flies display similar behavioral phenotypes in olfactory memory assays (*12*). Electrophysiology uncovered differences between *rut* and *dnc* mutants. Unlike *dnc*^{1}, *rut*^{2080} showed some responsiveness in the 20- to 30-Hz range, but without the sustained 9-s selection characteristic of wild-type flies. Similar to *dnc*^{1}, *rut*^{2080} responded strongly in the 10- to 20-Hz range (fig. S5).

To investigate visual behavior in these strains, I used an optomotor paradigm (*18*) that provides an efficient alternative to flight paradigms (Fig. 3A), because many mutant *Drosophilae* do not fly well [notably, *dnc*^{1} (*16*)]. The defective responsiveness to visual novelty seen in *dnc*^{1} brain recordings (described above) may have predicted poor behavioral responsiveness to visual stimuli, but the opposite was the case: *dnc*^{1} flies displayed the strongest optomotor response of ~100 different strains tested. I evaluated the optomotor performance of seven olfactory learning and memory mutants (*12*, *19*); these spanned a broad range of optomotor phenotypes (Fig. 3B). Like *dnc*^{1}, *rut* mutants also showed unusually strong optomotor responsiveness.

To better describe optomotor performance, individual choices were filmed and quantified as flies progressed through a maze (*17*). Wild-type flies showed a preference for turning into the direction of perceived motion (a positive optomotor response) throughout most successive choice points (Fig. 3C). Another characteristic of wild-type optomotor behavior is some decreased responsiveness at choice points in the middle of the maze (*18*). In contrast, *dnc*^{1} flies proceeded through the first two choice points without displaying any optomotor response but then responded strongly at the remaining six choice points in the maze (Fig. 3C).

The delayed optomotor response in *dnc*^{1} flies reveals a defect in processing a novel visual stimulus (a moving grating) as flies enter the

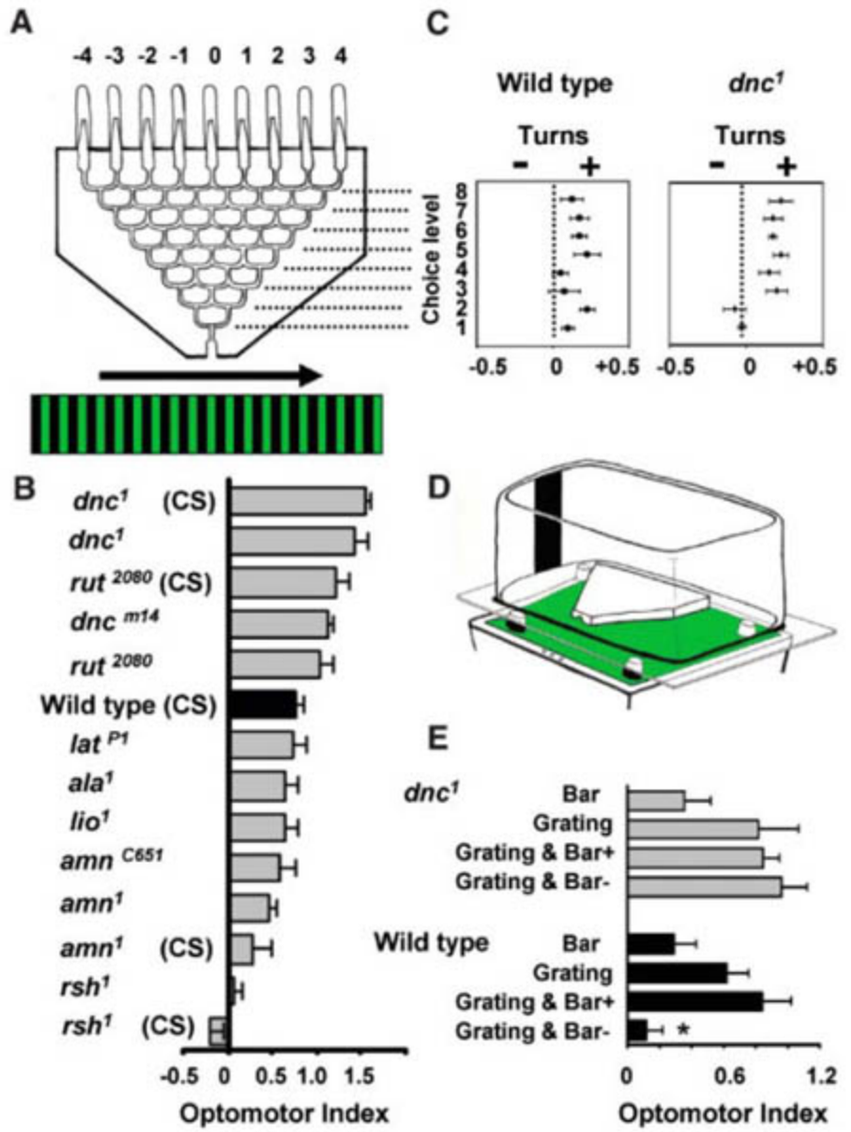

Fig. 3. Optomotor experiments. (**A**) Maze design (*18*). A moving green-and-black grating was displayed on a computer monitor beneath the maze. (**B**) Optomotor responses (±SEM) of mutants to a 3-Hz moving grating ($n = 8$ runs of ~30 female flies per strain). CS, mutant introgressed to wild-type genetic background. (**C**) Turn probabilities (±SEM) at each successive choice level for wild-type and dnc^1 flies ($n = 40$ flies for each). (**D**) A black bar was added to one side of the container surrounding the maze. (**E**) dnc^1 and wild-type responses (±SEM) to the distractor (bar), to a 6-Hz grating (grating), or to both competing visuals combined (grating & bar, + or −). *, significantly different optomotor response ($P < 0.05$) when the distractor was on the − side, as compared to the + side of the maze in combined experiments.

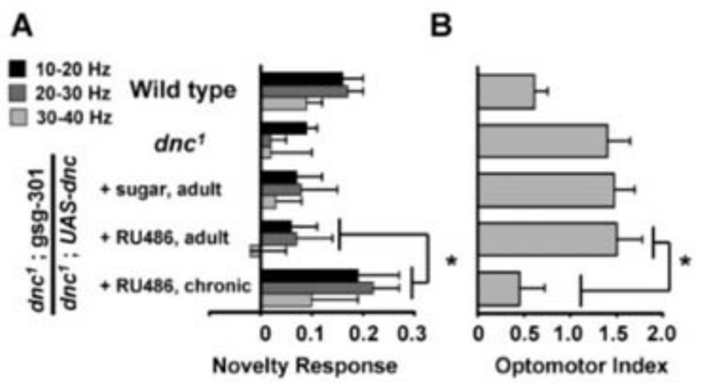

Fig. 4. Wild-type *dnc* is required during development for attention-like processes. (**A**) Magnitude of novelty responses (±SEM) in the brain for three frequency ranges. The pan-neuronal driver ElavGeneSwitch (gsg-301) was used to express a wild-type *dnc* gene (*UAS-dnc*) on a mutant dnc^1 background (dnc^1/dnc^1;gsg-301/*UAS-dnc*) in adults or throughout development. + sugar, adult: controls ($n = 4$ flies); +RU486, adult: the same strain fed 500 μM RU486 for 24 hours as adults before electrophysiology setup and recordings ($n = 4$ flies); +RU486, chronic: the same strain grown on food laced with 25 μM RU486 ($n = 4$ flies). *, $P < 0.05$ for combined 10- to 40-Hz data, as determined by *t* test. (**B**) Optomotor responses (±SEM) to a 6-Hz green-and-black grating in the same strains and treatments as in (A) ($n = 8$ runs of ~30 flies for each). *, $P < 0.05$, as determined by *t* test.

maze. Attention-like behavior in dnc^1 was addressed more directly by adding a competing visual object to the optomotor paradigm (Fig. 3D). In wild-type flies, a static bar placed to one side of the transparent maze abolishes responsiveness to the moving grating, presumably by acting as a visual distractor (*18*) (black bars in Fig. 3E). The effect of competing visual stimuli on optomotor responsiveness has also been previously observed in tethered flight experiments, where it has been described as evidence of limited perceptual resources (i.e., attention) partitioned among visual stimuli (*1*, *20*). In the walking analog of this paradigm, I found that dnc^1 animals were not distracted by the competing visual stimulus (unlike wild-type flies), even though dnc^1 flies clearly perceived the distractor alone (gray bars in Fig. 3E). The rut^{2080} brain-response defects were also matched by behavioral anomalies: The *rut* mutant was unresponsive to the distractor and responded more strongly than did the wild type, throughout the maze, to the grating presented alone without an initial delay (fig. S5). Subtle differences between *rut* and *dnc* mutants [also observed in habituation (*21*) and socialization (*13*) experiments] suggest that common performance defects in these memory mutants may conceal differences at the level of short-term behavioral and brain processes.

Finally, I investigated whether the conditionally expressed *dnc* gene product (cAMP phosphodiesterase) could modulate the corresponding electrophysiological and behavioral phenotypes described here, by expressing wild-type DUNCE protein in a dnc^1 mutant background by using RU486-induced gene activation of a functional *dnc* transgene (*22*). When wild-type DUNCE protein was expressed throughout the brain [via ElavGAL4 GeneSwitch (*23*)] in adult mutant animals (by feeding adult flies RU486 for 24 hours), optomotor responsiveness remained high and brain responsiveness to novelty remained correspondingly insignificant, resembling dnc^1 flies (Fig. 4, A and B, + RU486, adult). When the same construct was activated throughout development (by growing transgenic flies on RU486-laced food), optomotor responsiveness decreased to wild-type levels, and brain responsiveness to novelty was correspondingly increased to wild-type levels (Fig. 4, A and B, + RU486, chronic). A temporal examination of 20- to 30-Hz responses in the brain (as in Fig. 2A) revealed that extinction dynamics were rescued as well, with the strong selective response persisting for at least 9 s in RU486-grown flies (fig. S6). The constitutive requirement of DUNCE suggests that short-term plasticity for visual responsiveness in *Drosophila* adults is dependent on cAMP effects in the brain during its growth and development (see fig. S7 for additional supporting experiments).

Why should animals defective in visual selective attention, such as dnc^1 and rut^{2080}

flies, display stronger responses in optomotor assays? This paradox may be resolved by recalling that optomotor "reflexes" are normally suppressible (*1*) and by proposing that excessive optomotor responsiveness indicates defective short-term plasticity. Such plasticity may be required for optimal performance in a visual environment, so a strong and nondistractible optomotor response, as seen in *dnc* and *rut* mutants, may reflect failure of an interacting attention-like mechanism designed to periodically alternate among competing percepts of variable salience. Distinct behavioral processes among mutants in the optomotor maze might thus be predictive of defects at the level of selective attention in the brain. Because the ability to shift selective attention appropriately among competing visuals is likely to be crucial for learning, it is probable that the visual attention defects uncovered here in *Drosophila* short-term memory mutants contribute to their eventual learning and memory deficits in visual paradigms (*16*, *24*, *25*).

References and Notes

1. M. Heisenberg, R. Wolf, *Vision in Drosophila. Studies of Brain Function* (Springer-Verlag, Berlin, 1984).
2. B. van Swinderen, *Bioessays* **27**, 321 (2005).
3. S. Tang, A. Guo, *Science* **294**, 1543 (2001).
4. L. Liu, R. Wolf, R. Ernst, M. Heisenberg, *Nature* **400**, 753 (1999).
5. B. Brembs, J. Wiener, *Learn. Mem.* **13**, 618 (2006).
6. J. Guo, A. Guo, *Science* **309**, 307 (2005).
7. S. Tang, R. Wolf, S. Xu, M. Heisenberg, *Science* **305**, 1020 (2004).
8. B. van Swinderen, R. J. Greenspan, *Nat. Neurosci.* **6**, 579 (2003).
9. B. van Swinderen, *J. Neurobiol.* **66**, 1195 (2006).
10. R. Andretic, B. van Swinderen, R. J. Greenspan, *Curr. Biol.* **15**, 1165 (2005).
11. T. Tully, W. G. Quinn, *J. Comp. Physiol.* **157**, 263 (1985).
12. R. L. Davis, *Annu. Rev. Neurosci.* **28**, 275 (2005).
13. I. Ganguly-Fitzgerald, J. Donlea, P. J. Shaw, *Science* **313**, 1775 (2006).
14. Y. Dudai, Y. N. Jan, D. Byers, W. G. Quinn, S. Benzer, *Proc. Natl. Acad. Sci. U.S.A.* **73**, 1684 (1976).
15. R. L. Davis, J. Cherry, B. Dauwalder, P. L. Han, E. Skoulakis, *Mol. Cell. Biochem.* **149–150**, 271 (1995).
16. Z. Gong, S. Xia, L. Liu, C. Feng, A. Guo, *J. Insect Physiol.* **44**, 1149 (1998).
17. Materials and methods are available as supporting material on *Science* Online.
18. B. van Swinderen, K. A. Flores, *J. Neurobiol.*; published online 7 December 2006 (10.1002/neu.20334).
19. T. Tully, T. Preat, S. C. Boynton, M. Del Vecchio, *Cell* **79**, 35 (1994).
20. R. Wolf, M. Heisenberg, *J. Comp. Physiol.* **140**, 69 (1980).
21. J. E. Engel, C. F. Wu, *J. Neurosci.* **16**, 3486 (1996).
22. B. Dauwalder, R. L. Davis, *J. Neurosci.* **15**, 3490 (1995).
23. G. Roman, K. Endo, L. Zong, R. L. Davis, *Proc. Natl. Acad. Sci. U.S.A.* **98**, 12602 (2001).
24. E. Folkers, *J. Insect Physiol.* **28**, 535 (1982).
25. G. Liu *et al.*, *Nature* **439**, 551 (2006).

26. I thank A. McCartney and K. Flores for excellent technical assistance; H. Dierick, G. Miklos, and R. Andretic for suggestions on the manuscript; and S. Waddell and R. Greenspan for materials and helpful criticism. This material is based on work supported by NSF under grant no. 052326 and by the Neurosciences Research Foundation.

Supporting Online Material

www.sciencemag.org/cgi/content/full/315/5818/1590/DC1
Materials and Methods
Figs. S1 to S7
References

27 November 2006; accepted 9 February 2007
10.1126/science.1137931

GENOMICS:

FROM CHEMISTRY KIT TO TOOL BOX

Numerous tools have been developed recently that exploit breakthroughs in the understanding of genomic chemistries. From improved sequencing technologies to microRNA detection, advances in basic chemistry – impacting a diverse array of research fields – have been translated into viable products that can aid scientists in achieving their research and clinical goals. Now, as cross-disciplinary communication continues to grow and mature, research at the intersection of chemistry and biology is increasingly exploited to solve fundamental questions in science and medicine. **By David Bradley**

Frederick Sanger's original sequencing method is fast approaching middle age and despite instrumentation advances that allow parallel sequencing of several hundred bases, it is the young upstart technologies that promise to fulfill the increasingly demanding requirements of today's research scientists.

All Fired Up

Among the novel approaches currently being developed to do this are sequencing-by-synthesis, which includes pyrosequencing and so-called FISSEQ (fluorescent in situ sequencing), and sequencing-by-hybridization (SBH). The first of these new chemistries to be commercialized was pyrosequencing, by the Branford, Connecticut, company **454 Life Sciences**. In 2005, 454 and **Roche** entered into an exclusive five-year development and distribution agreement for their Genome Sequencing Systems product. A cyclical sequence of reactions is employed, involving sequential addition of deoxynucleotide triphosphates and the generation of a light signal through luciferin that is proportional to the number of bases added. This system is advantageous since no gels or fluorescent molecules are needed and hundreds of thousands of DNA fragments in parallel can be analyzed, making it ideal for whole genome sequencing or identification of single nucleotide polymorphisms (SNPs) in DNA samples from multiple sources.

Timothy Harkins, marketing manager for genome sequencing at Roche Applied Science, believes that the 454 Genome Sequencer is changing science by allowing previously unanswered questions to be addressed, and "at a speed that was unimaginable just a few years ago." Harkins continues, "This has enabled breakthroughs in several sciences from whole genome analysis to transcriptome analysis to gene regulation studies," adding, "It's not just the sequencing that has been transformed, but also the front end with regard to sample preparation." Indeed, the 454/Roche pyrosequencing technology has already been applied successfully to the sequencing of the Neanderthal genome published recently in *Science*.

Another player in this arena, Solexa, Inc. (recently acquired by **Illumina** to round out its sequencing portfolio), has been focusing on driving down costs. Its approach to sequencing-by-synthesis extends Sanger's original four-color tagging but adds a twist that allows massively parallel sequencing to be carried out with novel reversible terminator chemistry, achieving a claimed 99.995 percent accuracy.

In contrast, the FISSEQ technique was developed to enable the localized amplification of single DNA molecules using an acrylamide gel, creating colonies of PCR product called "polonies" which could subsequently be sequenced in situ. It has now been improved and extended by researchers in George Church's lab at **Harvard Medical School** in Boston. Also known as bead-based polony sequencing, this technology – licensed in the US to Agencourt Biosciences, now a part of **Beckman Coulter** – could have significant implications for personalized medicine and low-cost genome analysis. "Our contributions to commercial, next-generation technologies have been focused on interfacing polonies with single-

continued ›

> "This has enabled breakthroughs in several sciences from whole genome analysis to transcriptome analysis to gene regulation studies. It's not just the sequencing that has been transformed, but also the front end with regard to sample preparation."

Look for these **Upcoming** Articles
Cell Signaling — April 6
Stem Cells — April 20
RNAi — June 1

"As companies are looking for novel ways to discover the function of their gene targets, fluorescent chemistries will increase in importance."

tube capture of human exons, yielding an affordable $3,000 direct assay for causative alleles rather than depending on linkage to noncoding common SNPs," Church says.

Getting Together

Another approach that could accelerate genomic research is so-called sequencing-by-hybridization. First suggested in the 1990s, it has taken a decade or so to reach commercial reality with Affymetrix and Illumina at the forefront. The process uses differential hybridization of sequence-specific probes on microfabricated arrays to known or unknown DNA samples in order to determine the sequence of the target DNA, technology predominantly used for SNP detection.

Affymetrix spin-out company **Perlegen**, for instance, has produced SBH technology which allows for the simultaneous sequencing of hundreds of millions of individual DNA fragments. The company explains that the driver for this technology is to allow them to quickly identify SNPs for the purposes of understanding genetic disorders and defining the pharmacogenomics of drug reactions in individuals with specific SNPs. While the Perlegen technology has not yet been widely adopted, its biggest advantage is its larger wafer size, meaning more DNAs per chip.

Illumina is also pushing the boundaries of chip density with its latest 1M BeadChip for SNP profiling and detection, an array containing up to 1 million unique probes. Carsten Rosenow, marketing manager for DNA analysis products at Illumina, explains that this new technology "allows researchers to look beyond standard SNPs, giving them the ability to interrogate the so-called unSNPable parts of the genome where we don't have a uniform probe design." The 1M BeadChip, elaborates Rosenow, allows integrated analysis of SNPs and novel copy number variations using uniform probe distribution, giving unprecedented whole genome coverage.

Assembly Line Sequencing Goes with the Flow

Cambridge, UK's **genapta Limited** is exploiting recent advances in microfluidics and single molecule fluorescent detection to allow the company to pursue an alternative to conventional single strand sequencing systems. "It is possible that up to 30 percent of the fluorophores remain invisible if fixed down to a solid surface," says genapta's Julian White. "As a result, so are the molecules to which they are attached." He suggests that a better approach is to leave the DNA suspended in a flowing medium, allowing the fluorophores more chance to fluoresce and measurements to be carried out continuously. This system is more suited to high throughput methodologies than the inherent batch mode of solid support systems.

"It's early days," concedes White, "but despite the simplicity of optics, the technology gives near single molecule sensitivity, which makes us cautiously optimistic that we're on the right track." This is an allusion to one of the holy grails of this field: single molecule sequencing. Although undeniably still in its infancy, much effort and financial resources are being applied to the problem.

Small, Smaller, Smallest

One of the approaches attempting to directly address the single molecule conundrum involves the use of protein channels or synthetic nanopores. Hypothetically, strands of DNA can wriggle through such pores and their sequences can be read as they emerge.

The concept was first patented more than a decade ago by Church and colleagues John Kasianowicz, Eric Brandin, Daniel Branton, and David Deamer. They demonstrated that individual polynucleotide molecules could be driven through a 2.6 nanometer protein ion channel in a lipid membrane bilayer using an electric field. The passage of each molecule inhibits the ionic current across the channel and its duration correlates with polynucleotide length. The next stage would be to identify exactly how that current fluctuates as each base passes through the channel; each of the four DNA bases being slightly different in size should produce a characteristic measurable fluctuation.

Gregory Timp and his colleagues at the **University of Illinois at Urbana-Champaign** are working on a similar process, in which they punch nanoscopic holes in an inorganic semiconductor material, such as silicon nitride, to create the requisite nanopores rather than relying on biological channels. Timp is confident that with improved control of the transport of DNA through such nanopores they will be able to apply sensing technology at the single molecule scale to obtain the strand's sequence.

Seeing the Light

An important component of many genomic technologies is a method for detecting the presence or modification of DNA targets. The conventional labeling molecules used in sequencing have several drawbacks, including photobleaching and interference. David Smoller of **Sigma-Aldrich** in St Louis, Missouri, explains that modern organic chemistry is getting around such problems, enabling the function of genes to be revealed and applications such as drug discovery to be developed. "As companies are looking for novel ways to discover the function of their gene targets, fluorescent chemistries will increase in importance," he says.

Sigma-Aldrich has worked with **Panomics** (formerly Genospectra) in Fremont, California, to bring together recombinant technology, fluorescent organic molecules, and a novel nanoparticle cell delivery system. This particular combination of technologies allows them to produce biosensors that, once delivered into the cell, can measure the amount, the activity, and the location of endogenous proteins in living cells, Smoller explains. "These biosensors will have great value and application in the fields of high content screening and cell-based assays."

The system is being developed with David Lawrence and colleagues at Albert Einstein College of Medicine and with Klaus Hahn of the University of North Carolina, Chapel Hill. "There has been wonderful synergy between both companies and our respective research groups," Lawrence says of the collaboration.

Please SERS

Taking a different approach, nanotech-based chemistries that can detect the tiniest quantities of mononucleotide are continued ›

being used to develop label-free assays. This according to scientists at **Queen's University Belfast** who have collaborated with **Avalon Instruments** (now part of **PerkinElmer Life and Analytical Sciences**).

Steven Bell, director of the innovative molecular materials group at QUB and his colleagues, are exploiting novel silver colloid nanoparticle chemistry to help them obtain surface-enhanced Raman spectra (SERS) of DNA and RNA mononucleotides with high sensitivity. "The main advantage of our SERS approach is that it allows direct, label-free identification in aqueous solution," Bell explains. His approach, which challenges the traditional fluorescence paradigm, can produce spectra at tens of nanograms per milliliter and less. "We are working with large samples, but reducing the sampling volume to a few microliters, which would move the sample down to tens of picograms," he adds. "The ability to skip the labeling steps entirely seems like a significant advantage that could lead to entirely new protocols."

Pushing Microarray Limits

DNA microarrays have already become widespread, improving expression screening, sequencing, and drug discovery, by virtue of parallel detection. E.M. LeProust, genomics chemistry manager at **Agilent**, comments, "Recent advances in surface chemistry, synthesis fidelity, uniformity and robustness of array manufacture, and inkjet printing technologies have enabled the development of products with sensitivity and specificity not imagined before." In real terms, this means the ability to print designer chips with over 240,000 unique oligonucleotides of any sequence desired, with unparalleled speed and fidelity. "The flexibility of the system combined with the high performance is what makes it unique and powerful," observes L.K. Bruhn, a project manager at Agilent. "This allows researchers to answer questions they previously could not," she continues, "ranging from surveying the whole genome for small deletions with custom designed large arrays to effectively profiling all known human miRNAs using subarrays."

Charles Cantor and colleagues at **Boston University** suggest that microarray use might be extended still further by advances in spectral self-interference fluorescence microscopy. They recently demonstrated that this interferometric technique can provide precise data on the average location of a fluorescent label relative to a surface and so offer specific information about the conformation of a bound DNA molecule.

The team studied the conformation of both single-stranded (ssDNA) and double-stranded DNA (dsDNA) on glass surfaces using 50- and 21-nt oligonucleotides. The first strand of the DNA was bound to an oxide-coated silicon surface. Applying the interference technique allowed them to estimate the shape of coiled ssDNA, the average tilt of dsDNA, and the degree of hybridization. The research offers a proof of principle for the approach and, says Cantor, offers the possibility of utilizing array technologies to obtain conformation information that would be useful but has not previously been accessible. Applications promise to be widespread and might include both clinical and diagnostic uses.

To Interference... and Beyond

New chemical technologies are enabling much more than studies on just DNA. Peter Roberts of Danish company **Exiqon** comments that "the postgenomic world is focusing very much on noncoding RNA, what some call the 'dark matter' of the genome." The means of action of this dark matter is RNA interference (RNAi), a mere curiosity for many years, but the subject of the 2006 Nobel Prize in Physiology or Medicine and a phenomenon with dramatic implications for understanding cellular regulation and treating disease. Understanding RNAi is gradually being facilitated by the new technologies, one of which is locked nucleic acids (LNAs).

"Our LNA is a high-affinity nucleic acid analog that provides higher binding affinities for targets such as microRNAs," Exiqon's Roberts says. LNAs are nucleic acid analogs in which the ribose ring is "locked" by a methylene bridge connecting the 2'-O atom to the 4'-C atom allowing them to discriminate very effectively between short RNA and DNA targets. Roberts suggests that LNAs, properly incorporated into oligonucleotides, provide a powerful alternative for detection of small RNA targets. "It turns out that LNA-based probes are the perfect basis for studying these short RNA targets, for in situ detection, microarrays, and knockdown," he says. "In situ detection of miRNA on this scale of sensitivity and specificity in this field was entirely enabled by the use of LNA probes," Roberts continues. "It just was not possible previously."

So where are all these diverse new chemical tools taking genomic science? Sigma-Aldrich's Smoller puts it quite succinctly. "Combining the disciplines of chemistry and biology has provided a wealth of innovation," he says. "The innovation has opened many doors into the understanding of human health, biology, and gene function."

Jeffery Schloss, program director for technology development coordination at the **National Human Genome Research Institute** of the NIH, agrees, pointing out that the new genomic and postgenomic chemistries will enable the much-vaunted personalized medicine. "A key factor in the eventual success of these technology development and implementation programs," he says, "is the collaboration among chemists, biologists, physicists, engineers, and computer scientists, to conceive and realize technologies that can be commercialized and produce information of biomedical utility."

David Bradley is a freelance science writer based in Cambridge, UK.

Featured Participants

454 Life Sciences
www.454.com

Affymetrix
www.affymetrix.com

Agilent
www.agilent.com

Avalon Instruments
www.avaloninst.com

Beckman Coulter
www.beckmancoulter.com

Boston University
www.bu.edu

› **Exiqon**
www.exiqon.com

genapta Limited
www.genapta.com

Harvard Medical School
hms.harvard.edu

Illumina
www.illumina.com

National Human Genome Research Institute
www.genome.gov

Panomics
www.panomics.com

PerkinElemer Life and Analytical Sciences
las.perkinelmer.com

Perlegen
www.perlegen.com

Queen's University Belfast
www.qub.ac.uk

Roche
www.roche-applied-science.com

Sigma-Aldrich
www.sigmaaldrich.com

University of Illinois at Urbana–Champaign
www.uiuc.edu

› *featured advertiser*

New Products

Gel Band Excision

The GelX tips are a new range of disposable gel excision tips designed to provide a cleaner, simpler, and quicker method for removing bands from agarose and protein gels without the need for scalpels. GelX tips allow complete single-handed operation throughout the gel excision process through "Press and Go" gel band excision, push-button gel release, and push-button tip release. Users simply fit the GelX tip to a 1000 µl pipette, select the gel band, then press the tip into the gel. The gel slice is neatly extracted into the tip, and from there injected into a tube or other container. The used tip can then be ejected and disposed of. GelX tips are autoclavable and free of deoxyribonuclease and ribonuclease.

Cleaver Scientific
For information +44 (0) 1788 565 300
www.cleaverscientific.com

Horizontal Gel Electrophoresis Unit

The HU15 standard horizontal gel electrophoresis unit features the popular gel tray size of 15 cm by 15 cm with additional casting options for versatility. Comb options range from 1 to 30 samples and four comb slots at 3.5-cm intervals provide fast separation of up to 120 samples. The HU15 system consists of the standard horizontal gel unit with a removable casting tray, casting gates, two 1-mm thick 16-sample combs, colored loading strips, and buffer recirculation ports. HU15 casting options are provided by the casting gates with integral silicone seals or 15-cm long Scie-Plas Super Seals, which enable the gel length to be tailored to particular requirements. The choice of 30 different combs includes multichannel pipette-compatible combs with a maximum 30-sample throughput and preparatory combs for scaling up nucleic acids for cloning.

Scie-Plas
For information +44 (0) 1926 814093
www.scie-plas.com

Faster Real-Time PCR

The QuantiFast product line features a novel, proprietary technology that significantly reduces processing times of real-time polymerase chain reaction (PCR). The kits feature faster results with time savings of up to 60 percent; one procedure for all standard and fast cyclers; specific and sensitive detection of low-copy targets; accurate detection of a wide range of template amounts; and optimized master mixes and protocols. The kits are compatible with all commercially available thermocyclers and existing PCR assays without requiring complex adaptations. Kits include SYBR Green PCR Kit, available in one-step, two-step reverse transcription (RT) PCR, and one-step RT-PCR formats, and Probe PCR Kits, available in one-step and two-step RT-PCR formats.

Qiagen
For information +49 (0) 21033-16410
www.qiagen.com

Multiplex Toxicity Screening

The GenomeLab GeXP Rat MultitoxPlex Kit for preclinical drug research screening contains 25 genes involved in key toxicological pathways, including toxicity, stress, DNA damage, and apoptosis. It also includes three reference genes and one internal standard. Designed for use with the GenomeLab GeXP Genetic Analysis System, the kit delivers multiplexed quantitative analysis from hundreds of samples at one time. The assays run in a 96-well plate format, providing a quick way to screen large compound libraries, and with up to 30 genes analyzed in one reaction. Researchers can add their own genes of interest to the panel. The GeXP technology is designed to fill the gap between whole genome microarrays and single-gene real-time PCR. The kit contains a control RNA to verify the accuracy of the assay and is used with a Start Kit containing all the necessary buffers and reagents.

Beckman Coulter
For information 714-993-8955
www.beckman.com

AdenoSilence Vectors

A new line of adenoviral small-hairpin (sh) RNA expression vector reagents target the human druggable genome. The new release includes all the major protein classes amenable to small molecule intervention, including kinases, G protein-coupled receptors, ion channels, proteases, nuclear hormone receptors, secreted proteins, and receptors. Available in three sequence variants, the vectors allow single-step delivery of shRNA through the direct application of the virus supernatants into a primary cell culture, thereby making additional transfection reagents or complex transfection protocols unnecessary. A replication-incompetent version of the human adenovirus is used to introduce shRNA into a broad range of primary cells that decrease the expression of the targeted genes, with the gene of interest typically silenced for more than 10 days. This extended knockdown duration supports longer term assay protocols, such as differentiation assays.

Millipore
For information 800-548-7853
www.millipore.com

Biomarker Discovery Software

Genedata Expressionist Pro 4.0 is a fully scalable data management and analysis platform for biomarker discovery. The program integrates data from a variety of applications, such as genomics and proteomics, which Genedata refers to as "cross-omics" technologies, into a single computational system. A major challenge in biomarker discovery is integrating a variety of "-omics" data, including transcript profiles generated from different microarray technologies and protein and metabolite profiles obtained from mass spectrometry. These data must be combined to understand the biological processes at different functional levels, and the Expressionist platform automates this integration process and standardizes the way results are placed in context.

Genedata
For information +41 61 697 8510
www.genedata.com

POSITIONS OPEN

ASSISTANT PROFESSOR
Insect Ecology, University of Kentucky

The Department of Entomology **(website: http://www.uky.edu/Ag/Entomology)** at the University of Kentucky invites applications for a tenure-track faculty position in insect ecology. This is primarily a research position; the individual will also have extension responsibilities. The successful candidate will develop a nationally recognized research program in the ecology and management of arthropod species in agricultural, forest, or urban environments. Areas of research emphasis could include: landscape ecology, spatial dynamics, arthropod dispersal, population, behavioral, evolutionary or molecular ecology, or the influence of invasive species on biodiversity. The individual will be expected to compete successfully for extramural research funding and mentor graduate students. The individual will coordinate the Cooperative Agricultural Pest Survey (CAPS) program for Kentucky, which is administered within the Department of Entomology.

Applicants must have a Ph.D. in entomology, ecology, or a closely related field, with experience and/or training in applied entomology and ecology. Postdoctoral experience is desired. Demonstrated potential as both an independent researcher and as a member of a multidisciplinary team is desirable. Interest in outreach and extension is essential, and experience interacting with clientele, stakeholders, and/or the general public is expected.

Applicants should submit curriculum vitae, list of publications with up to (five) selected reprints, names and addresses of four individuals who can be contacted for letters of reference, copies of undergraduate and graduate transcripts, and an application letter describing their background and expertise specifically related to this research/extension position at the University of Kentucky. Application deadline is May 1, 2007, or until a suitable applicant is identified.

Submit applications to: **Dr. Lynne Rieske-Kinney, Chair, Insect Ecology Search Committee, University of Kentucky, Department of Entomology, S-225 Agriculture Science North, Lexington, KY 40546-0091, e-mail: lrieske@uky.edu. Website: http:// www.uky.edu.**

The University of Kentucky is an Equal Opportunity Employer and encourages applications from minorities and females.

ASSISTANT PROFESSOR
Microbiology and Cell Science
DIRECTOR
Electron Microscopy and Bioimaging Laboratory
University of Florida

The Microbiology and Cell Science Department and the Interdisciplinary Center for Biotechnology Research (ICBR) at the University of Florida invite applications for an Assistant Professor tenure-track position to develop an externally funded research program in bioimaging and direct ICBR microscopy core facility.

Technical support staff will be provided to perform the daily service tasks of this ICBR research facility. As Director, the incumbent will be charged with setting the vision and acquiring the resources necessary to make this ICBR facility among the best in the nation. Candidates with interests in applying modern bioimaging technology, including electron microscopy, to important problems in cellular and/or molecular biology are especially encouraged to apply.

Applicants must have a Ph.D., postdoctoral experience, and a strong publication record. The successful candidate is expected to participate in our undergraduate and graduate programs. A very competitive startup package and salary are available to the successful candidate. Details of the Department and ICBR may be found at **websites: http://microcell.ufl.edu** and **http://www.biotech.ufl.edu.** Submit applications as a single PDF file containing a cover letter, curriculum vitae, and summary of research interests to **Dr. Peter Kima (e-mail: pkima@ufl.edu).** Three letters of reference should also be sent directly to **e-mail: pkima@ufl.edu.** Review of applications will begin on April 2, 2007. *The University of Florida is an Equal Opportunity Employer.*

POSITIONS OPEN

CHAIR
Department of Molecular Genetics
Lerner Research Institute
The Cleveland Clinic

We are seeking a Chair for the Department of Molecular Genetics which occupies over 20,000 square feet in the Lerner Research Institute (LRI). An Endowed Chair accompanies this position. The Department currently consists of 12 faculty with well-funded research programs in the areas of signal transduction, cell and viral gene expression, nucleic acid biochemistry, cell cycle regulation, oncogenesis and aging. The ideal applicant for this position will have an outstanding national reputation in an area that complements the strengths of the Department. The Lerner Research Institute (LRI) with over 160 independent investigators in nine departments and an annual budget of over $140 million ($83 million from NIH in 2005) has a commitment to excellence in basic and translational biomedical research. Medical and graduate students from the Cleveland Clinic Lerner College of Medicine and multiple other universities train in LRI laboratories. We are seeking candidates with the vision and energy to recruit other talented scientists who will synergize with current faculty. The Chair will be provided with a highly competitive salary, generous space and startup support, and recruitment packages for new faculty.

A letter of interest, curriculum vitae, and names and addresses of three references should be sent to:

Martha K. Cathcart, Ph.D.
Search Committee for the Chair of Molecular Genetics
Department of Cell Biology, NC10
Cleveland Clinic Research Institute
9500 Euclid Avenue
Cleveland, OH 44195

On the web, see **website: http://www.lerner.ccf.org/, e-mail: cathcam@ccf.org.** *The Cleveland Clinic Foundation is an Equal Opportunity Employer.*

RESEARCH ASSOCIATE PROFESSOR
Stony Brook University

The Mineral Physics Institute (MPI) of Stony Brook University and the National Synchrotron Light Source (NSLS) of Brookhaven National Laboratory seek applicants for a Research Associate Professor in high-pressure material physics. The successful candidate will develop and lead an HP research program at the NSLS. The candidate should have experience and interests in: laser-heated diamond-anvil cell, x-ray diffraction, and spectroscopy at high pressure. Required: Ph.D. in physics, geoscience, or related fields. Preference will be given to candidates with research experience involving synchrotron-based HP research and demonstrated ability to obtain external funding. Applicants should send curriculum vitae, list of publications, research statement, and three letters of recommendation to: **Ms. Samantha Lin, Mineral Physics Institute, ESS Building, Stony Brook University, Stony Brook, NY 11794-2100 U.S.A.** Visit **website: http://www.stonybrook.edu/cjo** for employment information. *Equal Opportunity/Affirmative Action Employer.*

POSTDOCTORAL POSITION, NIH Training Grant, Department of Orthopaedics, University of Rochester, New York. M.D. or Ph.D. degree *as well as U.S. citizenship or green card* required. Applicants interested in basic or translational research related to bone and joints should send a letter indicating research interests, curriculum vitae, and the names of three references to: **Dr. Regis O'Keefe, Department of Orthopaedics, University of Rochester, 601 Elmwood Avenue, P.O. Box 665, Rochester, NY 14642.** *University of Rochester is an Equal Opportunity/Affirmative Action Employer.*

CO-DIRECTOR, CENTER OF CARDIOVASCULAR TRANSLATIONAL BIOMEDICINE

The University of Utah Health Sciences Center (UUHSC) invites nominations or applications for the Co-Director of a newly created Center of Excellence in Cardiovascular Translational Biomedicine. The Co-Director will spearhead the creation of a vibrant, cutting-edge research program with emphasis on stem and cell-based therapies, therapeutic angiogenesis, model systems (e.g., zebrafish), and innovative technologies (e.g., molecular imaging). Applicants should hold a doctoral degree (M.D., Ph.D., or equivalent). Preference will be given to candidates with experience in bioinformatics, small molecule screening, and modeling of complex biological systems. In addition to a generous start-up package, the Co-Director will fill the Nora Eccles Harrison Presidential Endowed Chair for Cardiovascular Research. Applications are encouraged from candidates with an outstanding record of sustained, extramural research program and a commitment to take a lead role in program project grant and other multi-disciplinary grants. There is no mandatory teaching requirement. The successful candidate, however, will be key administrative and scientific partner with the current Christi T. Smith Professor and Division Chief of Cardiology for the Center. The Co-Director will spearhead the recruitment of two additional junior and experienced investigators at the assistant and associate professor levels.

Review of applications will begin, **April 1, 2007**. The application must include a letter of interest, curriculum vitae, and names of three references. Salary is commensurate with qualifications and experience.

ASSISTANT/ASSOCIATE PROFESSOR POSITIONS

The University of Utah Cardiology Division and Department of Medicine University of Utah School of Medicine invite nominations or applications for positions in a newly created Center of Excellence in Cardiovascular Translational Biomedicine. The Cardiology Division will undergo significant rebuilding, and several faculty will be recruited over the next few years. Applications will be considered in any area of cardiovascular biology and molecular physiology; however, the ideal candidate will have a research interest that is focused on stem and cell-based therapies, therapeutic angiogenesis, model systems (e.g., zebrafish) with an emphasis on disease mechanisms and/or translational medicine. Applicants should hold a doctoral degree (M.D., Ph.D., or equivalent), have a strong research record, and prior experience and evidence of extramural grant support. Candidates at the level of Assistant Professor and/or Associate Professor will be considered. Ample start-up packages are available.

Send curriculum vitae, a statement of teaching experience and research background and interest, and the names of three potential references to: **Dr. Ivor J. Benjamin, Christi T. Smith Professor of Medicine, c/o Ms. Lori Kaumans, Division of Cardiology, Univ. of Utah HSC, Salt Lake City, UT 84132-2401.** Email: **lori.kaumans@hsc.utah.edu**.

The review of applications will begin immediately, and applications will be considered until the positions are filled.

The University of Utah provides excellent benefits. Utah offers tremendous outdoor activities for all seasons, and Salt Lake City has outstanding cultural programs in a safe environment with a reasonable cost-of-living.

The University of Utah is an OEO/AA Employer and encourages applications from women and minorities.

Ludwig Institute for Cancer Research
the global cancer institute

Group Leaders in Cancer Biology

The establishment of a new Branch of the Ludwig Institute for Cancer Research (LICR) in Oxford University will focus its research endeavours on cancer biology including suppressing tumour growth and preventing cancer metastasis. We are actively recruiting Research Group Leaders at the Assistant Member (Assistant Professor/Lecturer), Associate Member (Associate Professor/Senior Lecturer/Reader) and Member (Professor) levels.

The LICR Oxford Branch will be housed in a new state of the art building in the Institute of Cancer Medicine and be affiliated to the Nuffield Department of Clinical Medicine (NDM); part of the Medical Sciences Division, University of Oxford. The LICR is a global non-profit organization with nine Branches and numerous Affiliates worldwide.

As an LICR faculty member, you will enjoy the benefits of being a distinctive part of a dynamic local environment at a world-class university, and also of belonging to an internationally recognized Institute that is actively pursuing the translation of its research discoveries into applications for human benefit.

For further details about these positions and how to apply, please email Sarah Barnsley, **sbarnsley@ludwig.ucl.ac.uk**, quoting ref – oxf-sci. The closing date is Monday 30th April 2007.

LUDWIG INSTITUTE FOR CANCER RESEARCH

www.licr.org

The Ludwig Institute for Cancer Research is an Equal Opportunity Employer. All qualified applicants will receive consideration for employment without regard to race, color, religion, sex or national origin.

President and Director

Woods Hole Oceanographic Institution

Woods Hole, Massachusetts

Woods Hole Oceanographic Institution (WHOI), the world's largest private institution dedicated to research and education at the frontiers of oceanography, seeks a dynamic new President and Director. The Institution supports world-class research and education with vessels and instruments that enable unmatched access to the sea and with premier shore-based laboratories and other facilities. With an annual budget of $136 million, the WHOI community includes some 500 scientific and technical staff, nearly 400 operating, administrative, and support staff, and approximately 200 students and postdoctoral scholars.

This is a rare opportunity to lead an institution with a remarkable history of achievement and the resources to continue to expand understanding of the oceans and their central influence on Earth systems and human society. The new President and Director will be a person of exceptional intellectual vision and scientific judgment, a proven leader who listens well and communicates persuasively, and a person who embraces the pressing scientific work of the Institution with passion.

WHOI is working with a national executive search firm, Isaacson, Miller, on this recruitment. For a detailed position announcement or to apply, please email 3350@imsearch.com. All inquiries will be held in strict confidence.

WHOI is an Affirmative Action/ Equal Opportunity Employer.

WOODS HOLE OCEANOGRAPHIC INSTITUTION 1930

Life. Enhanced.

New Breakthroughs, New Opportunities.

If you're looking for an exciting place to work with a future full of opportunities, consider Bristol-Myers Squibb. We recently launched four major medicines in just over two years. And we have a robust pipeline of investigational products to treat serious diseases with unmet medical needs. Help us fulfill our mission to extend and enhance human life. You'll not only help enrich the lives of others, but also have the opportunity for a rewarding career with personal and professional advancement in a high-caliber, team-oriented environment.

We are actively recruiting individuals at all levels interested in joining a winning team who are dedicated to extending and enhancing human life.

Senior Research Investigator I/II- Hopewell, New Jersey

We are seeking an individual with a Ph. D (equivalent experience) and at least 5 years of industrial or genome center level experience in the fields of Genome Sciences or molecular biology who has demonstrated clear leadership and the ability to direct large genomic scale projects. Board understanding of human genetics and human genome and the manipulation of gene expression via RNAi to find and validated new targets for drug discovery considered essential. The ideal candidate would have direct hands on experience with lentiviral transduction systems, RNAi and cDNA over-expression screens as well as developing and implementing various primary and secondary cellular assays.. Must have proven managerial experience and be able to reduce to practice established protocols as well as develop and trouble shoot new and novel applications.. Must be comfortable with high-through-put genomic methodologies and basic liquid handling automation. Must be highly proficient in project and laboratory information management system and principals. Must possess strong organizational/multi-tasking abilities and communication skills and be willing to work in a highly collaborative production environment.

The individual will lead the mammalian genetic screening group and will be responsible for the planning and execution of whole genome size screens using lentiviral based approaches as well as smaller scale efforts using focused gene sets. The successful candidate will also ensure that resources are appropriately utilized for maximum efficiency. The individual will also oversee the development and implementation of various assay platforms, including ELISA, qPCR and reporter based assays and will work closely with our High Content Screening group to ensure seamless collaboration. **Requisition Number: 18896**

Senior Research Investigator- Wallingford, Connecticut

Degree in Biology, Biochemistry, Biotechnology or related field. Ph.D. with 3 years experience or B.S. or M.S. with 10 years experience including significant effort in Neuroscience.

Applies genomic technologies to design and execute experiments that provide critical information to the drug discovery pipeline for Neuroscience and Infectious Disease therapeutic areas in Wallingford, CT. Genomic technologies available in Wallingford include DNA sequencing, Affymetrix expression profiling, target class mammalian genetic screens using RNAi or over expression constructs, high content assay development, and high throughput qPCR. Collaborates with the Hopewell Applied Genomics facility for additional experiments as appropriate. Supervise laboratory tasks of two research associates. Acquires and maintains knowledge of drug discovery programs at the site and identifies opportunities for collaborations. Organizes and maintains experimental documentation.

Knowledge of neuroanatomy. Preference for industrial experience. Knowledge of experimental design theory and statistical analysis. Facility with data analysis software. Ability to work independently in a highly collaborative, team focused environment. Excellent written and verbal communication and presentation skills. This position requires work or contact with chemical or biological agents which may pose health or safety hazards if improperly handled. **Requisition Number: 18448**

Senior Research Investigator I- Wallingford, Connecticut

Head of HIV cell culture laboratory. PhD with demonstrated ability to plan, execute and interpret results from critical cell based antiviral assays. Preference for scientists having experience working with HIV. **Requisition Number: 19101**

Research Investigator- Wallingford, Connecticut

The Lead Discovery department is seeking an Assay Design Scientist for high throughput screening. Candidates will possess experience with cell based and biochemical assays using various screening formats. The assay design scientist will be expected to have a fundamental understanding of pharmacological assessment of test compounds in assays including generation and interpretation of concentration response relationships. Ideally, the candidate will have a demonstrated ability in statistical analysis of assay robustness and Quality Control. Experience in high throughput screening automation, as well as low volume microtiter plate assays is required.

Ph.D. in appropriate discipline or Bachelor Master of Science with appropriate experience. At least 3 years of pharmaceutical or biotechnology industry experience. Complete responsibility for running HTS assays from de novo assay design, through assay validation, robotic validation, screening and data analysis. Will be responsible for communication of results to research teams in therapeutic areas, lead profiling and lead evaluation groups. Must be able to critically assess HTS processes and work with a dynamic group of biologists, biochemists, engineers and IT specialists to develop new procedures and enhance the Lead Discovery environment. **Requisition Number: 19062**

You can visit our career website to apply for a specific position or express general interestat http://www.bms.com/career/data

Bristol-Myers Squibb, P.O. Box 4000, Princeton, NJ 08543-40005
Bristol-Myers Squibb, 5 Research Parkway, Wallingford, CT 06492
Bristol-Myers Squibb is an equal opportunity employer.

Bristol-Myers Squibb

Life. Enhanced.

New Breakthroughs, New Opportunities.

If you're looking for an exciting place to work with a future full of opportunities, consider Bristol-Myers Squibb. We recently launched four major medicines in just over two years. And we have a robust pipeline of investigational products to treat serious diseases with unmet medical needs. Help us fulfill our mission to extend and enhance human life. You'll not only help enrich the lives of others, but also have the opportunity for a rewarding career with personal and professional advancement in a high-caliber, team-oriented environment.

We are actively recruiting individuals at all levels interested in joining a winning team who are dedicated to extending and enhancing human life.

Molecular Genetics Screening and Library Management Associate- Hopewell, New Jersey
We are seeking an individual with a BS/MS and at least 2-4 years of industrial or genome center level experience in the fields of Molecular Biology and/or Genome Sciences. Broad understanding of human genetics, human genome and the regulation of gene expression required. Must possess a solid understanding of the basic scientific principles underlying techniques such as DNA isolation, RNAi, mammalian cell culture and lenti-viral transduction systems. Must be able to reduce standard operating procedures to practice as well as to trouble shoot technical issues. Familiarity with high-throughput genomic methodologies and the use of automated liquid handling and related robotics essential. .Also required is basic project and laboratory information management principles and skills. Must be comfortable with various computer programs such as Windows, Microsoft Project and Excel. Must possess strong organizational/multi-tasking abilities, communication skills and be willing to work in a highly collaborative production environment.

The individual will be a key participant in Applied Genomics efforts to build comprehensive lenti-viral shRNAi clone sets and virus to support target discovery and drug development. The individual will be responsible for maintaining a large collection of shRNAi clones, replicating and re-arraying clones on demand, making DNA and producing high titer virus. The individual will also oversee and/or participate in clone sequencing and verification, inventory, distribution and help to curate and manage the collection. **Requisition Number: 18692**

Research Scientist I/II- Hopewell, New Jersey
The successful candidate will have a B.S. or M.S. degree in a Biological science plus a minimum of 7-9 years (B.S.) or 4-6 years (M.S.) of experience. He or she will have excellent working knowledge of cell and molecular biology and experience in at least two of the following areas: RNA interference, viral expression systems and High Content cell-based assays. Familiarity with functional genomics, target identification and validation, laboratory automation, and data analysis is highly desirable. Pharmaceutical or biotech industry experience is preferred but not required. The candidate must be able to work in a collaborative, team-oriented environment. He or she will be self-motivated, results-oriented, well-organized and have excellent written and spoken communication skills.

Assist in carrying out target identification and validation projects in close collaboration with Disease Area scientists and Applied Genomics staff. These projects will focus on the use of collections of RNAi reagents and small molecules in High Content cell-based assays to identify and/or prioritize candidate drug targets. Will design assays and conduct screens and participate in analysis of data and interpretation of results. Will also present findings in team meeting. **Requisition Number: 18702**

Senior Research Investigator I/II- Hopewell, New Jersey
The successful candidate will have a Ph.D. degree in a Biological science, with a minimum of 4 years of post-doctoral research experience. He or she will have expert knowledge of cell and molecular biology and functional genomic technologies including RNA interference (siRNA and shRNA), viral expression systems (especially lentivirus) and High Content cell-based assays. The candidate must have working knowledge of target identification and validation processes in drug discovery. Familiarity with laboratory automation, analysis of complex data sets and statistical methods is also highly desirable. Pharmaceutical or biotech industry experience is strongly preferred. The candidate must have a proven track record of success in scientific research as demonstrated by publications in high quality, peer-reviewed journals. He or she must be able to work in a collaborative, team-oriented environment. They will be self-motivated, results-oriented, well-organized and have excellent written and spoken communication skills and strong leadership skills. Experience leading teams and managing direct reports is a plus.

Initiate and carry out target identification and validation projects in close collaboration with Disease Area scientists and Applied Genomics staff. These projects will focus on the use of collections of RNAi reagents and small molecules in High Content cell-based assays to identify and/or prioritize candidate drug targets. Design assays and conduct screens, analyze data and interpret results, present findings to teams and working group meetings and write summary documents. Become familiar with one or more Disease Area and identify opportunities for collaboration. Develop and manage portfolio of projects aligned with Disease Area and Applied Genomics goals. Oversee activities and provide career development for one or two research staff. Publish results in peer-reviewed journals. Contribute to technology development and group and departmental strategy. **Requisition Number: 18695**

You can visit our career website to apply for a specific position or express general interest at http://www.bms.com/career/data

Bristol-Myers Squibb, P.O. Box 4000, Princeton, NJ 08543-40005
Bristol-Myers Squibb, 5 Research Parkway, Wallingford, CT 06492

Bristol-Myers Squibb

Research Scientist I/II- Hopewell, New Jersey
We are seeking a highly motivated, energetic, results-oriented research scientist to work in the area of RNA interference. The candidate must have a B.S./M.S. degree in biology or a related field, with a minimum of 3 years of research experience, and a multi-disciplinary skill set. Practical experience and a solid theoretical understanding of molecular biology and cell biology techniques – RNA isolation, qPCR, culturing and transfection of continuous cell lines and primary cells, is essential. Familiarity with in situ hybridization techniques, ELISAs and other methods of protein quantitation are desirable. The candidate should also possess experience or be willing to work with animals – conducting various animal dosing procedures and animal dissections. The ability to translate standard operating procedures to practice, trouble-shoot and think critically and analytically are important for success. The individual must have good oral and written communication skills

The individual will work on multiple RNAi projects simultaneously. A primary responsibility will be to screen for active siRNA/antisense oligos which meet criteria required for in vivo experiments. This will involve transfecting into cell culture systems then evaluating activities by measuring mRNA or protein levels. The candidate will also be expected to assist in the design of negative control oligos and support the in vivo efforts of the laboratory. He/she will interact with Applied Genomics bioinformatics scientists to evaluate the sequence specificity of our active and control sequences. He/she will also analyze target mRNA or protein levels in tissue samples from experimental animals. **Requisition Number 18691**

Research Scientist I- Wallingford, Connecticut
Applies genomic technologies to design and execute experiments that provide critical information to the drug discovery pipeline for Neuroscience and Infectious Disease therapeutic areas in Wallingford, CT. Genomic technologies available in Wallingford include DNA sequencing, Affymetrix expression profiling, target class mammalian genetic screens using RNAi or over expression constructs, high content assay development, and high throughput qPCR. Collaborates with the Hopewell NJ Applied Genomics facility for additional experiments as appropriate. Organizes and maintains experimental documentation.

Degree in Biology, Biochemistry, Biotechnology or related field. B.S. or M.S. with 10 years experience. Preference for previous experience in Neuroscience. Preference for industrial experience. Experience with at least three of the genomic technologies listed above. Facility with data analysis software. Ability to work independently in a highly collaborative, team focused environment. Excellent written and verbal communication and presentation skills. This position requires work or contact with chemical or biological agents which may pose health or safety hazards if improperly handled. **Requisition Number: 19174**

Senior Research Investigator- Wallingford, Connecticut
Lead a group of scientists for de novo assay design, assay validation and screening of enzyme based targets. Integral member of a leadership team responsible for overseeing the strategy and operations of an industry leading HTS department. Communication with discovery working groups, chemistry and other discovery based organizations across three sites. Sourcing and evaluation of bio assay technologies appropriate for HTS.

Ph.D. in appropriate discipline or Bachelor, Master of Science with appropriate discipline. At least 5 years of pharmaceutical or biotechnology industry experience. This is a team leader position for a group of experienced assay designers responsible for a variety of challenging enzyme based targets. The ideal candidate will have a strong background in enzymology with an extensive track record of success in assay design for high throughput screens. Supervisory experience is essential. A clear understanding of high throughput assay technologies and instrumentation, together with data analysis and statistical techniques is very important. Working as part of highly talented and motivated team means that strong communication and outstanding team building behaviors are vital. **Requisition Number: 19172**

Senior Research Investigator- Wallingford, Connecticut
We are seeking a biochemical pharmacologist to join an established Neuroscience group with a focus on drug discovery in the broad area of psychiatry. The successful candidate will be challenged to develop and employ assays using both cellular and in vitro approaches. Responsibilities also include target identification and evaluation as well as support for ongoing programs.

Ph.D. in biochemistry, pharmacology, or neuroscience with at least 3 years of relevant post doctoral and or industry experience. Candidates should have a research and publication record demonstrating experience in pharmacological evaluation of cellular signaling molecules. Preferred candidates will have experience deorphaning and developing functional assays for novel targets. Demonstrated understanding of neuropharmacology and psychiatric disease is desired. Strong oral and written communication skills, flexibility, and a desire to work and contribute in a team environment are essential. **Requisition Number: 18971**

Research Investigator- Wallingford, Connecticut
The successful candidate will join a multidisciplinary team engaged in high throughput ion channel screening to discover small molecule modulators of therapeutically relevant ion channel targets. The successful candidate will combine high throughput optical and binding techniques, as well as electrophysiological approaches, to design and execute experiments to support target based drug discovery and ion channel liability assessment. The candidate will be responsible for communicating results to collaborators in discovery working groups.

Ph.D., at least 3 years of pharmaceutical or biotechnology industry experience. Demonstrated skills in ion channel pharmacology, electrophysiology, and live cell imaging techniques in a high throughput industrial setting strongly preferred. Experienced patch clamping of heterologous expression systems, primary cells and hands on knowledge of HT instrumentation including automated patch clamping, e.g. PatchXpress, would be preferred. Proficiency in ion channel receptor binding techniques would also be valuable. Excellent verbal and written communication skills and ability to interact with scientists throughout the discovery organization is also required. This candidate must have a strong desire to succeed in a team setting, proven ability to meet goals working in a group of peers, proven innovative thinking as demonstrated by a record of publications in top journals that publish ion channel work. Ability and desire to master new skills, methods and technologies in a high throughput environment is a must. Experience using data analysis tools and computer fluency is required. **Requisition Number: 19051**

You can visit our career website to apply for a specific position or express general interest at http://www.bms.com/career/data

Bristol-Myers Squibb, P.O. Box 4000, Princeton, NJ 08543-40005
Bristol-Myers Squibb, 5 Research Parkway, Wallingford, CT 06492

Bristol-Myers Squibb

LSU Health Sciences Center
NEW ORLEANS

Dean
LSUHSC School of Medicine

The Louisiana State University Health Sciences Center School of Medicine in New Orleans invites applications and nominations for the position of Dean of the School of Medicine. The successful candidate will be responsible for all facets of activity in the school, including undergraduate medical education, resident and fellow program accreditation, continuing medical education, faculty recruitment and retention, clinical practice development in public and private venues, and nurturing and development of basic science, clinical science and translational research programs. The successful candidate will also be responsible for the finances of the School of Medicine. The successful candidate will work with the Chancellor's Office and Dean's Office administrations, provide oversight and leadership to the faculty group practice (LSU HealthCare Network), and interface with various hospital entities and their administrations. The successful candidate must be capable of representing the School of Medicine to various diverse agencies and constituencies. The successful candidate will have a MD, PhD or MD/PhD and will also be board-certified in his or her specialty and eligible for or licensed to practice in Louisiana, if relevant. He or she must demonstrate leadership ability, a proven commitment to education and clinical service, and the ability to provide vision for the school that builds on its historic strengths. Achievements in teaching, multi-disciplinary collaborative research, mentorship, and administration that promote an inclusive environment are essential. The successful candidate must be qualified to be appointed at the professorial rank in accordance with School of Medicine and LSU System criteria; the compensation package will be competitive.

Candidates should provide a Curriculum Vitae including a full list of administrative accomplishments and scientific publications, and a brief statement of educational, research, service, and administrative interests, skills and strengths. These materials should be forwarded electronically or by conventional mail to: **Kurt Varner, PhD, Professor and Interim Head, Department of Pharmacology, LSUHSC School of Medicine, 1900 Perdido St., New Orleans, LA 70112; kvarne@lsuhsc.edu.**

Review of applications will commence immediately and will continue until the position is filled.

LSUHSC is an Equal Opportunity/Affirmative Action Employer.

Federal (GS)
Neurotrauma Research
Position

The Department of Applied Neurobiology and the Combat Casualty Care Research Program in Brain Trauma and Neuroprotection at the Walter Reed Army Institute of Research (WRAIR) is seeking a Ph.D. level neuroscientist/neurobiologist with experience in experimental brain trauma and neuroprotection studies. Ongoing research projects involve the pre-clinical evaluation of novel neuroprotection strategies (including drug, brain cooling and stem cell applications) to treat brain injury resulting from penetrating ballistic-like brain trauma and/or cerebrovascular insults.

The successful applicant will be joining a dynamic, internationally recognized team of researchers dedicated to advancing the field of brain trauma and developing improved diagnostic and treatment strategies for military medicine. The position is offered as a Civilian Federal Government (General Schedule (GS) Equivalent), Term-Hire (maximum 5 years/full benefits) at a salary offered commensurate with qualifications and experience. U.S. citizenship and ability to obtain security clearance required.

To learn more about the Walter Reed Army Institute of Research, please visit our website: **http://wrair-www.army.mil**

Applicants should send their C.V., a written summary of their accomplishments and the email addresses of 3 references to **Dr. Frank Tortella** at **FRANK.C.TORTELLA@US.ARMY.MIL**.

YALE UNIVERSITY
School of Forestry & Environmental Studies
School of Architecture

Junior Faculty Position in Sustainable Design and Development

Yale University's School of Forestry & Environmental Studies and School of Architecture seek applicants for an unprecedented joint ladder level Assistant Professorship in Sustainable Design and Development, with an emphasis on the urban environment. More specifically, we seek individuals who have expertise, or the potential to establish this expertise, in the management and design of urban environmental systems and urban ecological infrastructures with a focus on the neighborhood and community scale rather than the building and site scale. Candidates should not only demonstrate an interest in minimizing adverse environmental impacts of urban development but also in enhancing beneficial human connections to natural systems in urban areas. The successful candidate will be expected to advise, supervise and instruct both environmental studies and architecture students, offering lecture, seminar and/or project-based courses in areas such as sustainable design and development, urban design, urban ecology, landscape ecology and design, and restoration of urban environmental systems. This person will be expected to assume a leadership role in the recently established School of Forestry & Environmental Studies and School of Architecture joint Master's Degree program. We prefer a candidate with advanced training in any of the following fields: sustainable design and development, urban design, landscape ecology and design, urban ecology, architecture, or allied fields.

Applicants should send a curriculum vitae; statement of research, teaching, and/or professional practice interests; two representative examples of research or professional publications and/or design work; and a list of three references to: **Professor Stephen R. Kellert, Yale University, School of Forestry & Environmental Studies, 205 Prospect Street, New Haven, CT 06511, USA. AND Professor James Axley, Yale University, School of Architecture, 180 York Street, New Haven, CT 06511, USA**. The deadline for applications is **April 1, 2007**.

Yale University is an Affirmative Action/Equal Opportunity Employer. Men and women of diverse racial/ethnic backgrounds and cultures are encouraged to apply.

OSU
Oregon State University

Environmental and Molecular Toxicology Department Head

Oregon State University is seeking an exceptional candidate to provide progressive, innovative administrative leadership. The primary mission of the Environmental and Molecular Toxicology Department is to increase understanding of mechanisms and consequences of chemical uses through quality education, research, outreach, and service. The department offers specialized training in Environmental Chemistry and Ecotoxicology, Molecular and Cellular Toxicology, and Neurotoxicology – and the collegial character of our faculty is demonstrated by extensive collaborative research and teaching. The Department Head will lead and coordinate the research, extension, outreach, and teaching activities of the unit, and will take the initiative in working with the faculty to develop and periodically revise a strategic plan that will identify program priorities. Research programs depend on extramural funding, so managing state funds to facilitate independent investigator success in securing competitive grants is a high priority. The Department Head must also foster relationships with the public and policy-makers who look to the department for science-based information in making critical decisions that influence human health and environmental quality.

Applicants must have a national or international reputation for excellence in Toxicology or a closely related field; superior leadership qualities and administrative ability (preferably in the university environment), an active research program, and a history of external grant support. For a complete announcement see:
http://jobs.oregonstate.edu/applicants/Central?quickFind=50872

Department of Environmental and Molecular Toxicology
Oregon State University
1007 Agriculture and Life Sciences Building
Corvallis, Oregon 97331-7301
T 541-737-3791 | F 541-737-0497 | http://emt.oregonstate.edu

WWW.NIH.GOV

Positions @ NIH

THE NATIONAL INSTITUTES OF HEALTH

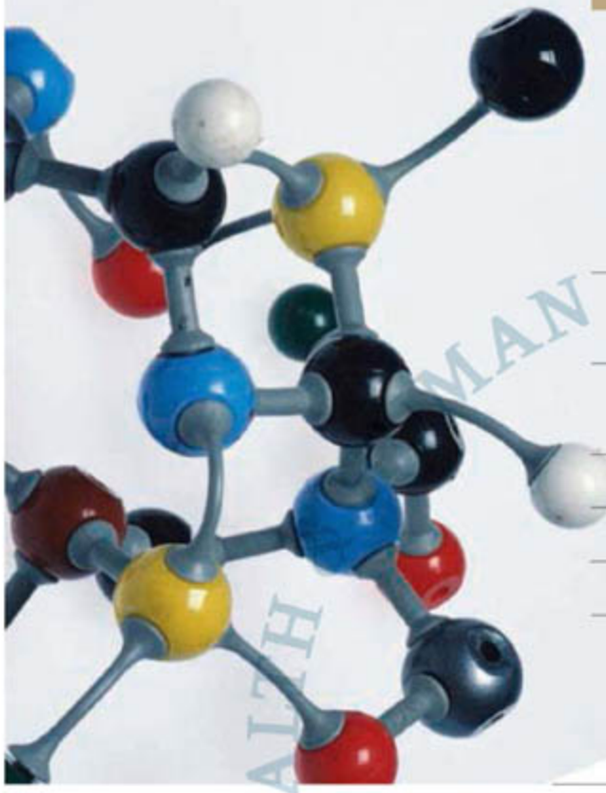

Postdoctoral Research Training at NIH

Launch a career to improve human health

Work in one of 1250 of the most innovative and well-equipped biomedical research laboratories in the world

Explore new options in interdisciplinary and bench-to-bedside research

Develop the professional skills essential for success

Earn an excellent stipend and benefits

Click on www.training.nih.gov

Office of Intramural Training and Education

Postdoctoral, Research and Clinical Fellowships at the National Institutes of Health

www.training.nih.gov/pdopenings

www.training.nih.gov/clinopenings

Train at the bench, the bedside, or both

Office of Intramural Training and Education
Bethesda, Maryland 20892-0240
800.445.8283

NIDDK

Staff Scientist Position
Genetics & Biochemistry Branch

The National Institute of Diabetes and Digestive and Kidney Diseases, a major research component of the National Institutes of Health and the Dept. of Health and Human Services, is recruiting a Staff Scientist within the Genetics & Biochemistry Branch to join a group of investigators whose research focus is the study of genome instability, DNA repair, and cellular responses to DNA damage. Experience in molecular or cell biology, biochemistry, or protein chemistry is a prerequisite. Familiarity with DNA repair, cell signaling, or the characterization of macromolecular complexes is desirable.

The successful individual will be a PhD or MD scientist with at least three years postdoctoral research experience and a very strong publication record in top peer-reviewed journals. The position requires a highly motivated scientist with the ability to work independently as well as in collaboration with others.

Applicants should submit a curriculum vitae, a brief statement of research experience, and the names and addresses of three references to: **Peggy Hsieh, PhD, Bldg. 5, Rm. 324, 5 Memorial Dr. MSC 0538, NIH, Bethesda, MD 20892-0538; or use e-mail: <ph52x@nih.gov>; or FAX: 301-496-9878.**

http://intramural.niddk.nih.gov/research/faculty.asp?People_ID=1616

THE NIH IS DEDICATED TO BUILDING A DIVERSE COMMUNITY IN ITS TRAINING AND EMPLOYMENT PROGRAMS

LSU Health Sciences Center
NEW ORLEANS

Professor and Head
Department of Pharmacology
Louisiana State University Health Sciences Center, School of Medicine, New Orleans

The Louisiana State University Health Sciences Center School of Medicine in New Orleans invites applications and nominations for Professor and Head of the Department of Pharmacology. The School is renewing a period of extraordinary expansion with unprecedented investments by the state of Louisiana in the further development of biomedical sciences in collaborations between the School of Medicine and internal and external agencies. The position presents the opportunity to create a new level of interdisciplinary research and collaboration in a department with complementary and diverse areas of expertise that include cardiovascular, CNS, respiratory and gastrointestinal pharmacology, drug metabolism, and cellular and molecular signaling. The Department currently lists 24 full time faculty, 5 faculty with adjunct appointments, and 17 students in Ph.D. or M.D./Ph.D. programs. Many of the full-time faculty members hold joint appointments in the Cancer Center, Neuroscience Center of Excellence, Cardiovascular Center, Alcohol Research Center and Center for Oral and Craniofacial Biology. The Department participates in Interdisciplinary and Departmental graduate programs leading to a doctorate in Pharmacology. The Department also currently holds an NIH COBRE grant, "Mentoring in Cardiovascular Biology," to train junior faculty. The successful candidate will have a Ph.D. and/or M.D. degree, demonstrable leadership ability, a well-funded and internationally recognized research program, a proven commitment to education and research, and the ability to provide vision for the Department that builds on its historic strengths. Achievements in teaching, multi-disciplinary collaborative research, mentorship, and administration that promote an inclusive environment are essential. Additional information regarding the Department and Health Sciences Center can be obtained at **http://www.medschool.lsuhsc.edu/pharmacology/**.

Candidates should provide a *curriculum vitae* including a full list of publications, past and current research support, and a brief statement of educational, research, service, and administrative interests. These materials should be forwarded electronically to: **Dr. Arthur L. Haas, Chair, Pharmacology Search Committee, LSUHSC School of Medicine, Department of Biochemistry, 1901 Perdido Street, New Orleans, LA 70112; PharmacologySearch@lsuhsc.edu.**

LSUHSC is an Equal Opportunity/Affirmative Action Employer.

VCU
Virginia Commonwealth University

FACULTY POSITION IN MEDICINAL CHEMISTRY
Medical College of Virginia Campus

The Department of Medicinal Chemistry, School of Pharmacy, VCU, invites qualified candidates to apply for a tenure-track position at the Assistant or Associate Professor level available immediately. Preference will be given to those with research programs in the general area of CNS medicinal chemistry. The most successful candidate will have a funded program and publications in the design and synthesis (and preferably computational and QSAR aspects) of centrally acting small molecules or agents that influence neurotransmitter systems. Also preferred is experience in classroom teaching of medicinal chemistry at the professional and graduate levels.

The position will remain open until filled, and applications must include a detailed curriculum vitae, a description of research achievements, a statement of future research objectives, funding history, and the names (and contact information) of four references.

Applications should be submitted to:
Dr. Richard B. Westkaemper, Search Committee Chair, Department of Medicinal Chemistry, School of Pharmacy, Box 980540, VCU, Richmond, VA 23298.
Email: **richard.westkaemper@vcu.edu.**

VCU is an Equal Opportunity, Affirmative Action Employer. Women, minorities and persons with disabilities are encouraged to apply.

Lighting the Flame of Knowledge.

Faculty Positions - Assistant Professor (Associate considered)-Georgia Campus

Georgia Campus – PCOM is seeking Full Time candidates for its Division of Basic Sciences. GA-PCOM teaches an integrated medical curriculum to osteopathic medical students & has an evolving graduate program in biomedical sciences. Candidates for these positions will be expected to make contributions to the teaching of Master's level candidates and will be expected to engage in research activities supporting graduate program development. Must have an earned PhD degree in the respective field or closely related area, 3 years postdoctoral experience required.

Anatomy- Will teach medical gross anatomy, including dissection instruction in a cadaver-based laboratory. Preference will be given to individuals who can contribute to teaching in other sub disciplines of anatomy.

Biochemistry- Must have ability to teach in the area of medical biochemistry and/or molecular biology. Preference will be given to candidates in the areas of molecular biology/genetics and nutritional biochemistry.

Cell Biology- Should be trained in an area of cellular and molecular biology to teach medical students in an integrated curriculum as well as molecular biology/genetics in a Graduate Program in Biomedical Sciences. As a new program we are looking for candidates to complement our growing strength in cell signaling. Candidates with an interest in cellular aspects of aging will be given preference but all candidates will be given consideration.

Microbiology- Prefer training in bacteriology but will consider other areas. Major teaching areas will be in bacteriology and mycology. Broad experience in other areas a plus.

The Georgia Campus of PCOM is located in beautiful Suwanee, Georgia, just 38 miles from the airport and 33 miles to downtown Atlanta. Candidates should send letter of interest and curriculum vitae to:
Philadelphia College of Osteopathic Medicine
Human Resources Department
4190 City Avenue, Philadelphia, PA 19131,
Fax: 215-871-6505 or email: hr@pcom.edu. EOE.

PHILADELPHIA COLLEGE OF OSTEOPATHIC MEDICINE
PCOM
WWW.PCOM.EDU

Top 100 Hospital expanding in Central Texas

Endowed Chair in Pediatric Research
Scott & White Health System
Texas A&M System Health Science Center College of Medicine

The Children's Hospital at Scott & White and The Texas A&M System Health Science Center College of Medicine are seeking a nationally recognized research scientist as the first holder of the Josephine Ballard Endowed Chair in pediatric research. Applicants should be accomplished investigators (Ph.D., M.D. or M.D./Ph.D.) at the associate or professor level with current federal grants and a proven track record in basic, clinical, and/or translational research. The successful candidate will join an expanding faculty within a large academic healthcare system. The chair holder will play a critical role in directing and expanding research activities in pediatric disease, in close collaboration with investigators in local, national and international experts in cell biology, genomics and proteomics.

The Children's Hospital at Scott & White serves a large clinical base throughout Central Texas. There are outstanding clinical practice and laboratory facilities on campus that perform state of the art molecular and cellular biology techniques, flow cytometry, proteomics and genomics as well as biostatistical support services. Animal laboratory facilities include areas to perform medical and surgical procedures. Laboratory space and an appropriate start-up package for the chair holder will be provided. The Scott & White Healthcare system is one of the largest multi-specialty integrated delivery systems in the nation. Scott & White is the primary clinical and hospital teaching campus for the College of Medicine. Academic appointments at the associate and professor level through the College of Medicine are commensurate with qualifications and experience.

Interested candidates should send a copy of their curriculum vitae, letter addressing their qualifications and a list of 3 individuals who can provide references to: **Don P. Wilson, M.D., Chair, Search Committee for Josephine Ballard Centennial Chair in Pediatric Research; Chairman, Department of Pediatrics, 2401 South 31st Street, Temple, Texas 76508, 254-724-4363, fax 254-724-1938, email: dwilson@swmail.sw.org.**

Scott & White is an equal opportunity employer. For more information regarding Scott & White and The Texas A&M System Health Science Center College of Medicine, please log onto: www.tamu.edu and www.sw.org.

The Children's Hospital at SCOTT & WHITE

TEXAS A&M HEALTH SCIENCE CENTER COLLEGE OF MEDICINE

Research Opportunities

Virginia Bioinformatics Institute

Assistant, Associate and Full Professorships at the Virginia Bioinformatics Institute: Laboratory-Centered and Computationally-Centered

State-of-the-art facilities. The Virginia Bioinformatics Institute (VBI) at Virginia Tech has faculty openings for assistant, associate and full professorship levels. VBI is a world-class research institute in the life sciences, integrating theory, modeling, simulation and wet laboratories in a transdisciplinary, team research model. Areas of strength among the 18 research groups at VBI include infectious diseases, ranging from the molecular to the population scale, systems biology approaches to study stress response in several organisms, modeling and simulation of biological networks, functional genomics, metabolomics, proteomics and bioinformatics/computational/synthetic biology. Successful candidates at all levels are expected to have an established research program and a strong track record of substantial extramural research funding.

About VBI. Established in 2000 by the Commonwealth of Virginia, the Institute is a part of Virginia Tech (VT) and has its own 130,000 sq ft research facility with state-of-the-art core laboratory and computational facilities as well as new facilities in the Washington, D.C. area (in Alexandria, VA). VBI strongly emphasizes team science and organizes research outside of boundaries of academic disciplines. Research programs represented at VBI assemble to meet the specific needs of those programs; it is a flexible environment that rewards the notion of a problem-solving capability on the move. Extensive national and international collaborations complement the expertise of the faculty, including strong interactions with several biomedical research centers. Faculty entrepreneurial activities are strongly encouraged and the university provides support for the establishment of commercial ventures.

VBI's facility in Alexandria is an integral part of Virginia Tech's expansion into that region. Faculty members whose programs will not require proximity to their own laboratory facilities will have the option of basing their primary research efforts there while still accessing VBI's state-of-the-art wet laboratory facilities in Blacksburg. VBI strongly encourages candidates requiring wet-laboratory facilities to apply. Exceptional new faculty may also have the option of joint affiliations with other departments at Virginia Tech and two prominent medical schools on the East Coast. Reference posting 061384.

Along with a strong research environment, the Institute actively participates in "Genetics, Bioinformatics, and Computational Biology" (GBCB), an interdepartmental Ph.D. program that emphasizes both computational and experimental sciences, and which attracts outstanding students from diverse disciplinary backgrounds.

Other Research Opportunities at VBI:

- Genetical Genomics Analyst, posting 060988
- Micro- and Molecular Biologist, posting 061418
- Postdoctoral Associate: Nucleotide Metabolism Modeler, posting 061331
- Systems Administrator (multiple openings), posting 060434
- Training, Education and Outreach Program Manager, posting 061188
- Whole Genome Sequencer, posting 061332

For more Information:

To apply, visit www.jobs.vt.edu and search by posting number.
To learn more about VBI and our research, please visit us at www.vbi.vt.edu

To learn more about the Interdisciplinary PhD program in Genetics, Bioinformatics, and Computational Biology (GBCB), visit http://www.grads.vt.edu/academics/programs/gbcb/index.html

VBI
VirginiaTech
Invent the Future

Director of Research Complex

Diamond Light Source and Rutherford Appleton Laboratory

Harwell Science and Innovation Campus, Oxfordshire

Excellent Package

A Director is required to lead the new £30M Research Complex at the Harwell Science and Innovation Campus. This Research Complex is to be built adjacent to the new Diamond Light Source at the Rutherford Appleton Laboratory. The Director will be employed by the Medical Research Council (MRC). The Harwell Science and Innovation Campus is home to several major research facilities including the ISIS neutron source and the Central Laser Facility at the Rutherford Appleton Laboratory and the Diamond Light Source as well as MRC and other research units. The Research Complex will have laboratories and shared facilities for research teams funded from multiple sources with the aim of advancing the UK's standing as a global leader in life sciences and physical sciences research.

- The Director will provide leadership and direction for the Research Complex.
- The Director will report to a Management Board. Together they will be responsible for ensuring the Complex meets the needs of the scientific community, and satisfies all stakeholders.
- The Director has a unique opportunity to foster a multi-disciplinary culture and create synergy within the Research Complex and across the major facilities on the Harwell Science and Innovation Campus.
- The candidate should be of international research standing in a relevant discipline, and be committed to translating research into practical applications.
- The candidate should give evidence of shaping and implementing a vision in a multi-team research operation where there are many challenges.
- The candidates should have strong leadership skills and be an effective communicator with the ability to build positive networks and collaborations and to operate in a multi-stakeholder environment.

Please reply in confidence, with full career and current salary details, quoting reference CRG/12262S

selection
odgers search
interim

Odgers Ray & Berndtson, 11 Hanover Square, London W1S 1JJ
t 020 7529 1111 **e** response.manager@odgers.com
www.odgers.com

CONFERENCE

MDC MAX DELBRUECK CENTER FOR MOLECULAR MEDICINE BERLIN-BUCH
in the HELMHOLTZ-GEMEINSCHAFT e.V.

Wnt 2007 - September 12 - 15, 2007 Berlin, Germany
2nd Max Delbrueck Center (MDC) Conference
„Wnt Signaling in Development and Disease"

Sessions

- Wnt Signaling at the Plasma Membrane
- Wnt Signaling in the Cytoplasm
- Wnt Signaling in the Nucleus
- Wnt Signaling in Development - Stem Cells
- Wnt Signaling in Disease
- Wnt Signaling and Drug Targets

Organizers

- Walter Birchmeier
- Thomas Holstein

Scientific Advisory Board

- Christof Niehrs
- Hans Clevers
- Konrad Basler
- Mariann Bienz
- Rolf Kemler
- Rudi Grosschedl

Confirmed speakers

- Akiyama, Tetsu - Tokyo, Japan
- Axelrod, J. D. - Stanford, USA
- Basler, Konrad - Zürich, Switzerland
- Bienz, Mariann - Cambridge, UK
- Bowerman, Bruce - Eugene, USA
- Cadigan, Ken - Ann Arbor, USA
- Clevers, Hans - Utrecht, The Netherlands
- Dale, Trevor - Cardiff, UK
- Rolf Kemler - Freiburg, Germany
- Fodde, Riccardo - Rotterdam, The Netherl.
- Grosschedl, Rudolf - Freiburg, Germany
- Gumbiner, Barry - Charlottesville, USA
- He, Xi - Boston, USA
- Herrmann, Bernhard G. - Berlin, Germany
- Kikuchi, Akira - Hiroshima, Japan
- McCrea, Pierre - Houston Texas, USA
- Mlodzik, Marek - New York, USA
- Moon, Randall - Seattle, USA
- Niehrs, Christof - Heidelberg, Germany
- Nusse, Roel - Stanford, USA
- Peifer, Mark - Chapel Hill, USA
- Perrimon, Norbert - Boston, USA
- Polakis, Paul - San Francisco, USA
- Sokol, Sergei - New York, USA
- Steinbeisser, Herbert - Heidelberg, Germany
- Taketo, Makoto - Kyoto, Japan
- Wedlich, Doris - Karlsruhe, Germany
- Weis, Bill - Stanford, USA
- Wynshaw-Boris, Tony - La Jolla, USA
- Yamaguchi, Terry - Frederick, USA

For further information please contact the conference secretariat:
Michaela Langer / Irmgard Wiznerowicz
Max Delbrück Centrum für Molekulare Medizin (MDC) Berlin-Buch
Robert-Rössle-Straße 10 • 13125 Berlin
phone: +49 30 94 06 37 20/38 00 • fax: +49 30 94 06 22 06/26 56
email: langer@mdc-berlin.de / wbirch@mdc-berlin.de
All information concerning the symposium is available on:
https://www.wnt-2007-berlin.de

AWARDS

Damon Runyon Cancer Research Foundation — Innovation Award

New Award Announcement
Damon Runyon – Rachleff Innovation Award

Securing funding for unproven ideas represents a major challenge for independent junior scientists. The **Damon Runyon – Rachleff Innovation Award** has been developed to help address this challenge by providing support for the next generation of exceptionally creative thinkers with "high risk/high reward" ideas. Research supported by this award must be novel, exceptionally creative and, if successful, have the strong potential to significantly impact our understanding of and/or approaches to cancer prevention, diagnosis or treatment.

Funds Available: A maximum of 5 awards will be granted each year. The awards will provide $450,000 in direct costs over three years.

Eligibility Requirements

- Applications will be accepted from newly appointed assistant professors, clinical instructors, senior clinical fellows, senior postdoctoral fellows, and highly motivated recent PhD and MD graduates – **all conducting independent research**.
- Applicants (including non-U.S. citizens) must be working at a U.S. institution.
- Institutional nominations are not required.
- Basic and translational/clinical projects will be considered.
- Individuals with a background in multiple disciplines are especially encouraged to apply.

PRE-PROPOSAL DEADLINE: June 1, 2007
ELIGIBILITY AND APPLICATION GUIDELINES ARE AVAILABLE AT: WWW.DRCRF.ORG

Summit on Systems Biology 2007

Integrative Basic, Clinical and Translational Research

June 5-7, 2007

The second annual Summit on Systems Biology at the historic five diamond Jefferson Hotel in Richmond, Virginia, will provide an interactive, highly interdisciplinary program that offers strategic presentations by leaders in the field. Dr. Leroy Hood, honorary co-chair of the summit and director of the Institute for Systems Biology in Seattle, will lead a panel of academic, industrial and government leaders in a discussion of the future of systems-based approaches to biological and biomedical research. Six scientific sessions will discuss systems approaches to basic, clinical and translational research.

For information and registration: http://www.vcu.edu/csbc/systemsbiologysummit/

Speakers include:

Leroy Hood (Institute for Systems Biology)
Claire Fraser-Liggett (The Institute for Genomic Research)
Rita Colwell (Former Director, National Science Foundation)
René Thomas (Universite Libre de Bruxelles)
Masaru Tomita (Keio University)
Christoph Adami (California Institute of Technology)
Bernhard Palsson (University of California – San Diego)
George Church (Harvard University)
Michael Savageau (University of California – Davis)
Marc Vidal (Harvard University)
James Bassingthwaighte (University of Washington)
Joe Loscalzo (Harvard University)
Gilles Clermont (University of Pittsburgh)
Thomas E. Johnson (University of Colorado)
Joseph Nevins (Duke University)
Alan Perelson (Los Alamos National Laboratory)

Program

Monday, June 4

Welcome Reception and Networking Conference

Tuesday, June 5

Session I: The Systems Biology Challenge in 21st Century Biomedical Research – discussion moderated by Dr. Leroy Hood and including academic, industrial and government decision-makers in systems biology research.

Session II: Complexity in Cellular and Sub-Cellular Systems – applications of systems approaches from chemical biology to cellular modeling.

Reception / Special Event.

Wednesday, June 6

Joint Keynote for Sessions III and IV: Systems Biology and Medicine

Session III: Pathways and Networks in Basic Research (concurrent with Session IV) – metabolic modeling, protein-protein interaction networks, synthetic biology.

Session IV: Systems Biology in Clinical and Translational Research I (concurrent with Session III) – applications of systems approaches in modeling normal and disease organ function.

Session V: Systems Biology in Clinical and Translational Research II – applications of systems approaches in normal and disease states in humans.

Gala Banquet at the Virginia Museum of Fine Arts.

Thursday, June 7

Session VI: Perspectives on the future of systems biology in biological and biomedical research.

Close of main Summit events/Opening of modeling workshops

Opening of Modeling Workshop: Lectures on Modeling in Systems Biology (open to all) – applications of modeling in basic, clinical and translational research.

Hands-on Modeling Workshops (separate registration)

Workshop I: Fast Start Modeling and Simulation Tools for Basic Research – modeling applications, biomedical systems simulation, and image processing/scientific visualization in basic systems-based research.

Workshop II: Modeling and Simulation in Clinical Research – mathematical and computational modeling/simulation methods for modeling individual organ and organ system dynamics.

Venue and Accommodations:

The Summit will be held for the second year at the Jefferson Hotel, a national landmark in downtown Richmond. While here, visit other cultural and historical landmarks – Richmond, Jamestown, Colonial Williamsburg, Skyline Drive, the James River Plantations, etc.

This activity has been approved for AMA PRA Credit.
For information regarding continuing education, contact:

CPDE, Virginia Commonwealth University.
Tel: 800-413-2872; Email: cmeinfo@vcu.edu

For program information:
Gregory A. Buck, Ph.D.; Chair,
Steering Committee
Center for the Study of Biological Complexity,
Virginia Commonwealth University.
Tel: 804-827-0026;

Email: sysbiosummit@vcu.edu
http://www.vcu.edu/csbc/systemsbiologysummit/

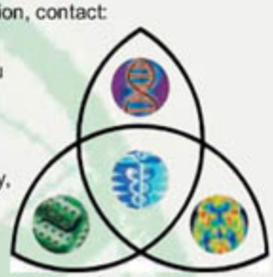

Virginia Commonwealth University

POSITIONS OPEN

CHAIRPERSON
Department of Physiology
Temple University School of Medicine

Tenure-track **PROFESSOR** level academic scientist to lead the Department of Physiology. The successful candidate will provide innovative academic and administrative leadership for all research and teaching programs of the Department of Physiology and will guide the Department's overall contribution to the service functions of the School of Medicine and to the University. Members of the Department of Physiology are actively engaged in research in the areas of cardiovascular physiology, cell signaling, immunology, neurophysiology, pulmonary physiology and education.

Minimum qualifications: the Ph.D. and/or M.D. degree, outstanding academic experience, excellence in scholarship, proven ability to secure and sustain independent and collaborative extramural funding, effective interpersonal skills, demonstrable leadership, and a vision for the sustained development of the Department.

Temple University offers a competitive compensation and comprehensive benefits package. Letters nominating qualified candidates are requested and may be sent to:

Joanne M. Orth, Ph.D.
Chairperson, Physiology Chair Search Committee
c/o Patricia Pileggi, Office of Faculty Affairs
Temple University School of Medicine
3420 N. Broad Street, Room 108 MRB
Philadelphia, PA 19140
E-mail: patricia.pileggi@temple.edu

Interested individuals are invited to submit a cover letter and current curriculum vitae to **e-mail: patricia.pileggi@temple.edu. Website: http://www.temple.edu/medicine.**

Temple University is an Equal Employment Opportunity/Affirmative Action Employer and strongly encourages applications from women and minorities.

FACULTY POSITION, BIOLOGY

The Biology Department at Fairfield University invites applications for a one-year appointment at the **INSTRUCTOR** level for the 2007-2008 academic year. This position requires a Ph.D. in any specialty within the biological sciences, however, preference will be given to individuals with expertise in developmental genetics. Primary responsibilities for the fall semester will be to participate in the teaching of the molecular biology and development portions of the introductory general biology sequence for majors. This will include team-taught classroom lectures as well as laboratory instruction. A spring sophomore-level genetics course is also expected.

Fairfield University is a small comprehensive university located in southwestern Connecticut with easy access to Long Island Sound and New York City. Applicants should send curriculum vitae which includes prior teaching experience and the names of three references by April 15, 2007, to: **Biology Search Committee, Biology Department, Fairfield University, Fairfield, CT 06824.**

Fairfield University is an Affirmative Action/Equal Opportunity Employer. Women, minorities, and persons with disabilities are strongly encouraged to apply.

Two **POSTDOCTORAL FELLOW POSITIONS** are available to study DNA damage-induced hematopoietic stem cell (HSC) injury at the Department of Pathology, Medical University of South Carolina, Charleston, South Carolina. This is an excellent opportunity for career development to Staff Scientist or Junior Research Faculty appointment. Candidates with Ph.D. and/or M.D. and experience in experimental hematology and HSC research and gene therapy should send their curriculum vitae and names of three references to **Dr. Daohong Zhou** by **e-mail: zhoud@musc.edu.**

POSITIONS OPEN

RUSH UNIVERSITY MEDICAL CENTER

RADIATION ONCOLOGY INVESTIGATOR
Chicago

Rush University Medical Center is seeking a mid to senior-level, funded, laboratory-based Oncology Investigator/Faculty Member for the Department of Radiation Oncology. The successful candidate will be expected to collaborate with other oncology investigators and clinicians, and to pursue translational issues appropriate to radiation oncology. Opportunity includes academic faculty position with tenure; joint appointment with appropriate basic science department; participation in Radiation Therapy Oncology Group translational studies; collegial environment with seven senior faculty members; and competitive salary and benefits. Ideal candidate will possess either a Ph.D. degree or M.D./Ph.D. degrees and will have a demonstrated track record of success in translational, oncological investigations. Program building is an essential component of this position.

Please contact: **Ross Abrams, M.D., Chairman and Hendrickson Professor, Department of Radiation Oncology, Rush University Medical Center, 500 S. Paulina, 013 Atrium Building, Chicago, IL 60612-3833. Telephone: 312-942-5771** or **312-942-5751. E-mail: ross_a_abrams@rush.edu.**

The Department of Otolaryngology at the New York University (NYU) School of Medicine, in conjunction with Dr. Steven Burakoff, Director of the NYU Cancer Institute, has an opening for a full-time **POSTDOCTORAL RESEARCH FELLOW** position. Our research interests include the development and study of mouse models of head and neck cancer and the anti-tumor immune response. Join a small and exciting research environment that is committed to answer the unresolved questions in head and neck cancer.

Highly motivated individuals with an enthusiastic interest in our research program are invited to apply. Applicants should possess a Ph.D.. and/or M.D. degree obtained within the last three years in the biological sciences with experience in cancer genetics/animal models of disease and molecular/cellular biology. Previous experience with head and neck cancer is helpful, but not required. If interested please send a cover letter, curriculum vitae, and references to:

Theresa Tran, M.D.
160 East 34th Street, 9th Floor
New York, NY 10016

FACULTY POSITION
University of Wisconsin, Madison
Veterinary Pharmacology

The Department of Comparative Biosciences, School of Veterinary Medicine invites applications for a tenure-track faculty position **(ASSISTANT or ASSOCIATE PROFESSOR)**. Qualifications include Ph.D. or equivalent, postdoctoral experience, commitment to excellent teaching, and ability to develop an extramurally funded research program. Preference will be given to research areas complementing existing departmental strengths. Teaching responsibilities include participation in veterinary pharmacology instruction. To apply, send curriculum vitae, brief statements of research interests and teaching philosophies, and three letters of reference to: **Gordon S. Mitchell, Chair, Department of Comparative Biosciences, University of Wisconsin, 2015 Linden Drive, Madison, WI 53706.** Apply by April 30, 2007. For additional information, see **website: http://www.vetmed.wisc.edu/jobs.html.** *Equal Opportunity/Affirmative Action Employer.*

POSITIONS OPEN

TENURE FACULTY POSITION
University of Rochester
School of Medicine and Dentistry

The Department of Surgery/Division of Plastic Surgery and the Center for Musculoskeletal Research invites applications for a tenure-track faculty position in stem cell biology and soft tissue engineering. The successful candidate will develop independent translational research programs within a research center that is focused upon understanding molecular, cellular, structural, and functional issues related to skeletal tissues. Potential areas of focus are broad and include research related to peripheral nerve, wound healing, soft tissue injury and repair, tissue regeneration, peripheral nerve, and the role of aging and other pathologic processes. Applicants should have interests in molecular and stem cell biology and the interface of stem cells with tissue engineering and regeneration.

Applicants should have a M.D. or Ph.D. degree and postdoctoral research training. Candidates may be at either the **ASSISTANT or ASSOCIATE PROFESSOR** level. Prospective candidates should mail a letter of intent indicating research interest, curriculum vitae, and contact information for three references to:

Regis J. O'Keefe, M.D., Ph.D., Director
Center for Musculoskeletal Research
University of Rochester
601 Elmwood Avenue, P.O. Box 665
Rochester, NY 14642

The University of Rochester is an Equal Opportunity Employer.

USDA, Animal and Plant Health Inspection Service (APHIS), Plant Protection and Quarantine (PPQ), in Raleigh, North Carolina, is recruiting for a Senior Executive Service (SES) position, **DIRECTOR, CENTER for PLANT HEALTH SCIENCE and TECHNOLOGY.**

In this position, you will represent the Deputy Administrator with responsibility for the overall planning, coordination, and direction of development and transfer of technology used in APHIS plant health programs.

In addition, you will provide national leadership in developing and delivering new science and technology into operational program activities.

You will lead a complex and diverse organization of professional, technical, and administrative staff of 250 employees assigned to headquarters and eight laboratories. You must possess a degree in biological sciences, agriculture, natural resource management, chemistry, or related disciplines appropriate to the position, and must have supervisory/managerial experience which demonstrates the ability to provide leadership to a complex, service-oriented organization and its resources.

The salary range for this position is $111,676 to $154,600.

To apply, contact **Jocelyn White** at **telephone: 202- 720-3010** for information about the position and instructions on how to apply.

Please reference vacancy announcement number APHIS-SES-07-02A, and note the closing date of April 16, 2007. Only complete applications received by the closing date will be accepted.

POSTDOCTORAL POSITION available for studying the molecular mechanisms of sHSP/α-crystallin chaperone function using animal modeling. Experience in molecular biology, cell culture, and protein characterization is essential. Submit electronically curriculum vitae to: **Dr. Edathara C. Abraham, Professor of Department of Biochemistry and Molecular Biology, University of Arkansas for Medical Sciences. E-mail: ecabraham@uams.edu.** *An Equal Opportunity/Affirmative Action Employer.*

POSITIONS OPEN

CAREER OPPORTUNITY

The Veterans Affairs San Diego Healthcare System is currently seeking **PHYSICIAN** applications for the Chief of Pathology and Laboratory Service. Assignment is approximately 50 percent administrative and supervisory and 45 percent clinical and teaching, in this University of California San Diego School of Medicine affiliate. Responsibilities include oversight and direction of a clinical laboratory performing 2.5 million tests annually, anatomic pathology, and cytopathology; pre-analytical, analytical, and post-analytical procedures for clinical and anatomic pathology departments; accountability for the training of residents in the graduate medical education program; coordination of teaching and patient care conferences; and leadership to a Department of over 100 full-time employees, contract employees, and students, including direct supervision of nine staff, five physicians, and four administrative/technical personnel. We offer excellent education, teaching, research, and clinical practice opportunities in an interdisciplinary collaborative setting. Academic appointment with the affiliate is an expectation. Comprehensive benefits package. *Must be U.S. citizen.* Recruitment/relocation incentive may be authorized. Education Debt Reduction Program funding may be available. Send curriculum vitae and direct questions to: **Jan Stock, Human Resources Specialist, telephone: 858-552-8585, ext. 7859, Veterans Affaris San Diego Healthcare System, 3350 La Jolla Village Drive, San Diego, CA 92161.** *Equal Opportunity Employer.*

Veterans Affairs San Diego Healthcare System, a progressive, state-of-the-art university-affiliated teaching facility, is seeking Anatomic Pathology/Clincial Pathology Board-certified **PATHOLOGIST.** The Department of Pathology, in this College of American Pathologists-accredited clinical laboratory, is recruiting for a **CHIEF OF ANATOMIC PATHOLOGY**. Candidate will possess excellent clinical and organization skills. Responsible for all surgical pathology, autopsies, cytological examinations of the body fluids, exudates, and aspirates; responsible for coordination of all elements of anatomic pathology; and training of anatomic pathology residents. Maintains expertise for consultation and guidance in matters pertaining to anatomic pathology and cytopathology and is responsible for ensuring all activities meet requirements for accrediting agencies. Candidate should qualify for appointment as faculty to the Pathology Department of University of California San Diego School of Medicine. Salary/rank commensurate with experience and established Veterans Affairs salary scales. Medical license in any state. *Non-U.S. citizens will only be considered if this search yields no qualified candidates.* Recruitment/relocation incentive may be authorized. Education Debt Reduction Program funding may be available. Send curriculum vitae to: **Lorraine Conn, Mail Code 113, Veterans Affairs San Diego Healthcare System, 3350 La Jolla Village Drive, San Diego, CA 92161 (telephone: 858-518-7259).** *Affirmative Action/Equal Opportunity Employer.*

ASSOCIATE RESEARCH SCIENTIST and/or **POSTDOCTORAL RESEARCH SCIENTIST** positions available immediately in Department of Pharmacology at Columbia University. Opportunity to join interdisciplinary team investigating molecular basis of inherited mutation-induced rhythm disturbances in heart. Candidates must have either Ph.D. or M.D. degrees and must have experience appropriate for positions. Expertise in protein chemistry and/or biochemistry of membrane and signaling molecule proteins required. Send curriculum vitae to: **Dr. Robert S. Kass, Ph.D., Department of Pharmacology, Columbia University College of Physicians and Surgeons, 630 West 168th Street, New York, NY 10032.**

We are an Affirmative Action/Equal Opportunity Institution.

POSITIONS OPEN

FACULTY POSITION
Department of Microbiology and Immunology
University of Rochester

The University of Rochester School of Medicine and Dentistry and the Department of Microbiology and Immunology is expanding their existing scientific and research program in virology. The Department wishes to recruit a tenure-track **VIROLOGIST** at the **ASSISTANT, ASSOCIATE, or FULL PROFESSOR** level. The candidate will be expected to develop an independent research program that will complement existing programs. The successful candidate will be joining a highly interactive faculty **(website: http://www.urmc.rochester.edu/smd/mbi/)** housed in a new research building with state-of-the-art core facilities. An attractive salary, competitive startup package and new laboratory space adjacent to the other virologists in the Department are available.

Interested individuals should submit a letter of application, curriculum vitae, a statement of research interests and goals, and the names, addresses, and telephone numbers of three referees. These materials should be sent to:

Dr. Steve Dewhurst
Chair, Search Committee
Department of Microbiology and Immunology
P.O.Box 672
601 Elmwood Avenue
Rochester, NY 14642
E-mail: stephen_dewhurst@urmc.rochester.edu

POSTDOCTORAL POSITIONS are available to study the molecular and cellular mechanisms involved in brain immune responses and the formation and function of immunological synapses in vivo and their impact on the development of novel immunotherapeutics for brain cancer. (See: *Journal of Experimental Medicine,* **203**:2095-107, 2006; *Cancer Res.,* **65**:7194-7204, 2005; *Nature Biotechnol.,* **19**:582-585, 2001; *Proc. Natl. Acad. Sci.,* **97**:7482-7, 2000; *Nature Med.,* **5**:1256-1263, 1999). A strong background in immunology, cell biology, virology, neuroanatomy, image analysis, and confocal microscopy techniques is desired.

Our Institute is located at the Cedars-Sinai Medical Center campus and is part of the Departments of Medicine and Molecular and Medical Pharmacology, UCLA. It offers state-of-the-art facilities in an exciting research environment. Applicants should have a Ph.D. and/or an M.D. and under five years of postdoctoral experience. Salary is dependent on education and research experience; range: $36,000 to $45,000. E-mail cover letter, curriculum vitae, summary of research experiences, and contact information of three references to: **Pedro R. Lowenstein, M.D., Ph.D. (e-mail: lowensteinp@cshs.org)** or **Maria G. Castro, Ph.D. (e-mail: castromg@cshs.org), Department of Medicine, Cedars-Sinai Medical Center, 8700 Beverly Boulevard, Davis Building, Room 5090, Los Angeles, CA 90048.**

SENIOR POSTDOCTORAL FELLOW/INSTRUCTOR POSITION

An excellent opportunity for career development with conversion to a Junior Faculty appointment, this position will study signal transduction, transformation, and apoptosis in cancer. Ongoing projects areas include regulation of prostate cancer growth and development using mouse and tissue culture models, transformation by the Pim protooncogene, and the molecular functioning of AML1 and AML/ETO in human leukemia. Individuals should possess a strong background in molecular, cellular biology, protein chemistry or hematopoiesis. Candidates should forward curriculum vitae and the names of three references to: **Andrew S. Kraft, M.D., Director, Hollings Cancer Center, 86 Jonathan Lucas Street, P.O. Box 250955, Charleston, SC 29425. E-mail: hccjobs@musc.edu.** Reference ad number 105.

COURSES

COURSE ANNOUNCEMENT
Biomechanics, Physiology, and Genetics of Intertidal Communities

Intertidal communities have been used as a model system in ecological interaction for decades and are a sensitive bellwether of climate change. Fundamental factors responsible for structuring these communities include abiotic variables such as wave exposure, temperature, wind speed, and light, primarily through an interaction between environment and individual fitness. The physical and biological environments also set the geographic scale for dispersal, adaptation and gene flow. This four-week summer course offers experimental ecologists theoretical and hands-on instruction in cutting-edge methods in biomechanics, physiology/biochemistry/molecular biology, and genetic investigations of dispersal and local adaptation, as applied to questions in community ecology and environmental adaptation.

Instructors: **Drs. Mark Denny, Steve Palumbi, and George Somero.** Dates: June 18 through July 13, 2007. Independent research following the course is possible. Location: Hopkins Marine Station, Stanford University, Pacific Grove, California 93950-3094. For additional information, including a course prospectus and instructions for application, see **website: http://hms.stanford.edu/HMSweb/mech.html** or contact the instructors **(e-mail: mwdenny@stanford.edu, e-mail: spalumbi@stanford.edu,** or **e-mail: somero@stanford.edu).** Deadline for receipt of all application materials is April 1, 2007.

MARKETPLACE

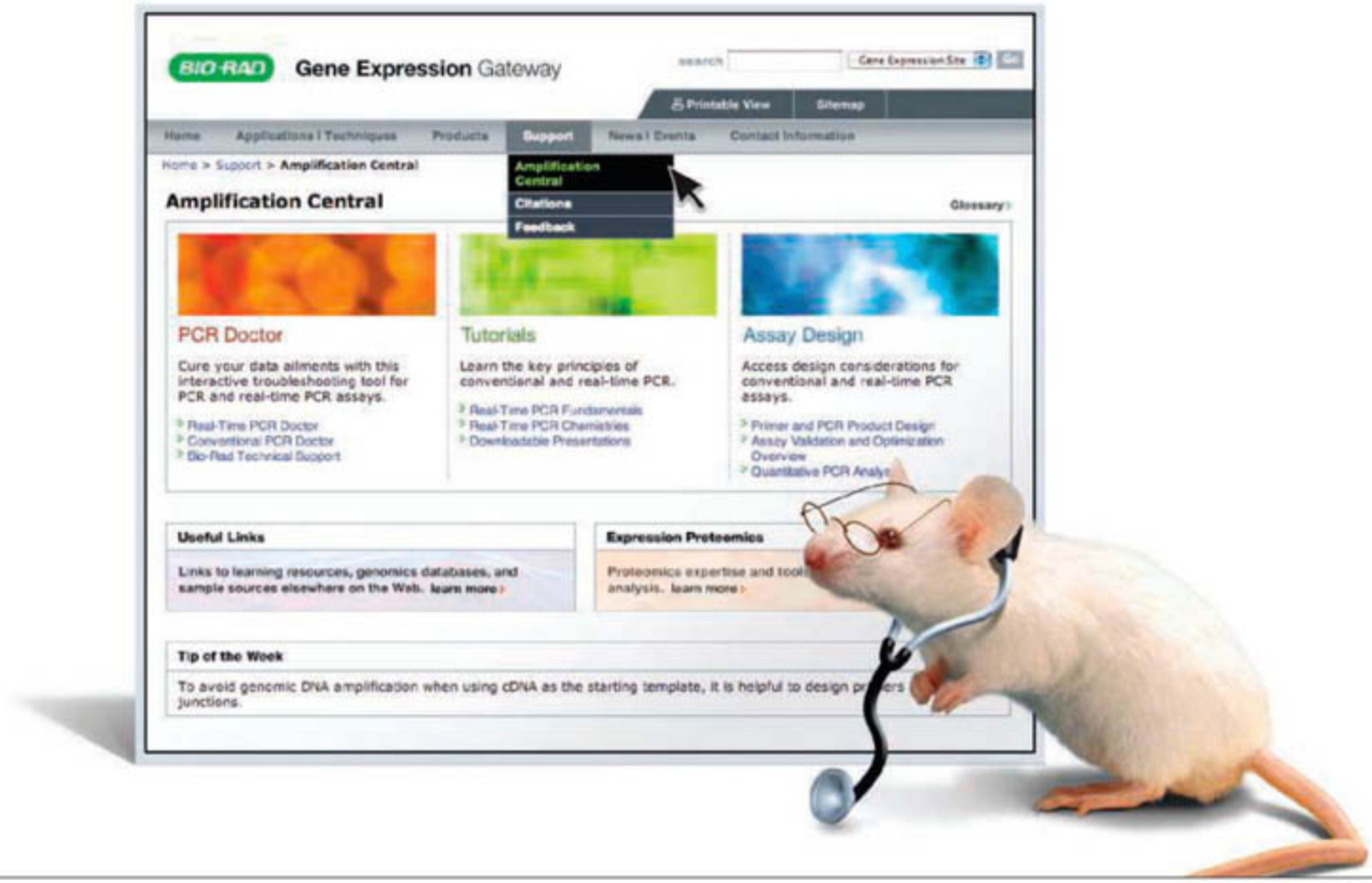

Amplification Central — Just what the PCR Doctor ordered.

Now there are even more reasons to mouse on over to Bio-Rad's Gene Expression Gateway:

- Educational tutorials and slide presentations
- Troubleshooting and solutions for problems commonly found in PCR data
- Guidelines for experimental design, optimization, and validation
- Weekly tips for improving PCR design and laboratory practices
- Abstracts of the most-cited PCR and real-time PCR articles

Your gateway to Bio-Rad's extensive genomics expertise is just a click away. Visit us on the Web at **www.bio-rad.com/genomics/pcrsupport/**

PCR Doctor, assay designs, and a host of guided tutorials will help you achieve successful research results.

Practice of the polymerase chain reaction (PCR) may require a license.

Visit us on the Web at **discover.bio-rad.com**
Call toll free at 1-800-4BIORAD (1-800-424-6723); outside the US, contact your local sales office.

BIO-RAD